Vol. 64 December, 1960 No. 12

THE JOURNAL OF PHYSICAL CHEMISTRY

(Registered in U. S. Patent Office)

CONTENTS

THE JOURNAL OF PHYSICAL CHEMISTRY

(Registered in U. S. Patent Office)

Published monthly by the American Chemical Society at 20th and Northampton Sts., Easton, Pa.

Second-class mail privileges authorized at Easton, Pa. This publication is authorized to be mailed at the special rates of postage prescribed by Section 131.122.

The *Journal of Physical Chemistry* is devoted to the publication of selected symposia in the broad field of physical chemistry and to other contributed papers.

Manuscripts originating in the British Isles, Europe and Africa should be sent to F. C. Tompkins, The Faraday Society, 6 Gray's Inn Square, London W. C. 1, England.

Manuscripts originating elsewhere should be sent to W. Albert Noyes, Jr., Department of Chemistry, University of Rochester, Rochester 20, N. Y.

Correspondence regarding accepted copy, proofs and reprints should be directed to Assistant Editor, Allen D. Bliss, Department of Chemistry, Simmons College, 300 The Fenway, Boston 15, Mass.

Business Office: Alden H. Emery, Executive Secretary, American Chemical Society, 1155 Sixteenth St., N. W., Washington 6, D. C.

Advertising Office: Reinhold Publishing Corporation, 430 Park Avenue, New York 22, N. Y.

Articles must be submitted in duplicate, typed and double spaced. They should have at the beginning a brief Abstract, in no case exceeding 300 words. Original drawings should accompany the manuscript. Lettering at the sides of graphs (black on white or blue) may be pencilled in and will be typeset. Figures and tables should be held to a minimum consistent with adequate presentation of information. Photographs will not be printed on glossy paper except by special arrangement. All footnotes and references to the literature should be numbered consecutively and placed in the manuscript at the proper places. Initials of authors referred to in citations should be given. Nomenclature should conform to that used in *Chemical Abstracts*, mathematical characters be marked for italic, Greek letters carefully made or annotated, and subscripts and superscripts clearly shown. Articles should be written as briefly as possible consistent with clarity and should avoid historical background unnecessary for specialists.

Notes describe fragmentary or incomplete studies but do not otherwise differ fundamentally from articles and are subjected to the same editorial appraisal as are articles. In their preparation particular attention should be paid to brevity and conciseness. Material included in Notes must be definitive and may not be republished subsequently.

Communications to the Editor are designed to afford prompt preliminary publication of observations or discoveries whose value to science is so great that immediate publication is imperative. The appearance of related work from other laboratories is in itself not considered sufficient justification for the publication of a Communication, which must in addition meet special requirements of timeliness and significance. Their total length may in no case exceed 500 words or their equivalent. They differ from Articles and Notes in that their subject matter may be republished.

Symposium papers should be sent in all cases to Secretaries of Divisions sponsoring the symposium, who will be responsible for their transmittal to the Editor. The Secretary of the Division by agreement with the Editor will specify a time after which symposium papers cannot be accepted. The Editor reserves the right to refuse to publish symposium articles, for valid scientific reasons. Each symposium paper may not exceed four printed pages (about sixteen double spaced typewritten pages) in length except by prior arrangement with the Editor.

Remittances and orders for subscriptions and for single copies, notices of changes of address and new professional connections, and claims for missing numbers should be sent to the American Chemical Society, 1155 Sixteenth St., N. W., Washington 6, D. C. Changes of address for the *Journal of Physical Chemistry* must be received on or before the 30th of the preceding month.

Claims for missing numbers will not be allowed (1) if received more than sixty days from date of issue (because of delivery hazards, no claims can be honored from subscribers in Central Europe, Asia, or Pacific Islands other than Hawaii), (2) if loss was due to failure of notice of change of address to be received before the date specified in the preceding paragraph, or (3) if the reason for the claim is "missing from files."

Subscription Rates (1960): members of American Chemical Society, $12.00 for 1 year; to non-members, $24.00 for 1 year. Postage to countries in the Pan American Union $0.80; Canada, $0.40; all other countries, $1.20. Single copies, current volume, $2.50; foreign postage, $0.15; Canadian postage $0.05; Pan-American Union, $0.05. Back volumes (Vol. 56–59) $25.00 per volume; (starting with Vol. 60) $30.00 per volume; foreign postage, per volume $1.20, Canadian, $0.15; Pan-American Union, $0.25. Single copies: back issues, $3.00; for current year, $2.50; postage, single copies: foreign, $0.15; Canadian, $0.05; Pan American Union, $0.05.

The American Chemical Society and the Editors of the *Journal of Physical Chemistry* assume no responsibility for the statements and opinions advanced by contributors to THIS JOURNAL.

The American Chemical Society also publishes *Journal of the American Chemical Society, Chemical Abstracts, Industrial and Engineering Chemistry*, International Edition of *Industrial and Engineering Chemistry, Chemical and Engineering News, Analytical Chemistry, Journal of Agricultural and Food Chemistry, Journal of Organic Chemistry, Journal of Chemical and Engineering Data* and *Chemical Reviews*. Rates on request.

THE JOURNAL OF PHYSICAL CHEMISTRY

(Registered in U. S. Patent Office)

VOLUME 64 JANUARY 4, 1961 NUMBER 12

THE ANALYSIS OF MOLECULAR WAVE FUNCTIONS BY NUCLEAR MAGNETIC RESONANCE SPECTROSCOPY[1a]

BY MARTIN KARPLUS[1b,2]

Noyes Chemical Laboratory, University of Illinois, Urbana, Illinois

Received January 27, 1960

A valence-bond formulation is presented for the relationship between molecular wave functions and the electron-coupled nuclear spin interactions observed by nuclear magnetic resonance spectroscopy. For non-bonded atoms, the magnitude of the coupling is shown to depend on the deviations from perfect pairing in the wave function. This result makes it possible to use the measured coupling constants in testing models for hyperconjugation. An application to the second-order hyperconjugation in ethane is given. For directly-bonded atoms, the coupling constant depends on parameters, such as orbital hybridization and bond polarization, in localized electron-pair functions. Use of this dependence is made to determine the bond polarization in several tetrahedral molecules.

A knowledge of the wave functions of atoms and molecules is of fundamental importance for the determination and interpretation of chemical properties. Since the techniques available at present are not sufficient for the calculation of exact wave functions for most systems of chemical interest, approximation methods have had to be introduced. The inaccuracies in these approximate treatments are such that experimental comparisons are necessary to justify or supplement the theory. In this paper we wish to discuss two approaches to the use of the results from nuclear magnetic resonance spectroscopy (n.m.r.) in the study of molecular wave functions. One example is concerned with the determination of the validity of a theoretical model for hyperconjugation and the other with the evaluation of coefficients in a parametrized electron-pair function for molecules.

In n.m.r. one is concerned with measurement of the energy levels of a system of nuclear spin magnetic moments in an external magnetic field. If we briefly consider the simplest case of a bare proton in a magnetic field H_0 of 10^4 gauss, we obtain the energy levels shown in Fig. 1b relative to an arbitrary zero in the absence of a field (Fig. 1a). Since the proton has spin $I_H = {}^1/_2$, there are two energy levels ($M_H = \pm {}^1/_2$), which are separated by an energy ΔE given by the equation

$$\Delta E = g_H \beta_N H_0 \qquad (1)$$

Here g_H is the g factor for the proton ($g_H = 5.586$), β_N is the nuclear magneton ($\beta_N = 0.50504 \times 10^{-23}$ ergs gauss^{-1}). For $H_0 = 10^4$ gauss, the resulting ΔE value is 1.420×10^{-3} cm.$^{-1}$. By the application of a radiation field of the appropriate frequency (42.6 Mc.), transitions between the two levels are induced and the resonance absorption can be observed.

If what has been described were the entire scope of n.m.r., the technique would be of considerable utility to the physicist for the measurement of nuclear g-factors, but of very little interest to the chemist. Since the protons commonly studied are in molecules surrounded by electrons and neighbored by other nuclei, the energy level scheme is modified significantly from that pictured in Fig. 1b for the isolated proton. The electrons that are present shield the proton moment from the external field with the result that the energy level spacing is altered. For the field H_0, we now have

$$\Delta E = g_H \beta_N (1 - \sigma_H) H_0 \qquad (2)$$

as shown in Fig. 1c. The quantity σ_H is the proton shielding parameter, which varies from $\sim 0.9 \times 10^{-5}$ to $\sim 4.5 \times 10^{-5}$ in different molecules (σ_H in H_2 is 2.66×10^{-5}). If other nuclei with magnetic moments are present, they also interact

(1) (a) Work supported in part by a grant from the University of Illinois Graduate Research Board. (b) Alfred P. Sloan Foundation Fellow.

(2) Department of Chemistry, Columbia University, New York 27, N. Y.

with the proton. In HD, the deuteron has a spin $I_D = 1$ with three components ($M_D = -1$, 0, +1) with respect to an external field. The interaction energy of the proton and deuteron moments depends on their relative orientation with the result pictured in Fig. 1d. The energy level diagram for the proton in the presence of the deuteron, as well as the two electrons, is given approximately by the equation

$$E = g_H\beta_N(1 - \sigma_H)H_0M_H + hA_{HD}M_HM_D \qquad \begin{matrix} M_H = \pm 1/2 \\ M_D = 0, \pm 1 \end{matrix} \quad (3)$$

where A_{HD} is the coupling constant. As is evident from Fig. 1d and eq. 3, there are now three proton transitions with ΔE equal to

$$\Delta E = g_H\beta_N(1 - \sigma_H)\,H_0 \begin{cases} +A_{HD} \\ 0 \\ -A_{HD} \end{cases} \quad (4)$$

from which the absolute value of A_{HD} can be determined ($|A_{HD}|$ in HD is 40.3 c.p.s.).

Since the shielding parameter and coupling constant for protons and other nuclei vary from one molecule to another, their values should provide chemically useful information. The evident connection between the electrons and the shielding parameter suggests that its magnitude can be utilized for the study of electronic wave functions. Although considerable research has been done in this field, we do not concern ourselves with the results.[3] For the coupling constants, the connection with electronic properties is not self-evident. The direct dipole–dipole interaction between nuclear moments, which is important in solids, averages to zero in the rapidly tumbling molecules found in solution. The residual coupling that is observed in solution arises from the interaction between electrons and the nuclei. In the simple example of HD, the proton p and the deuteron d have their magnetic moments oriented in the local fields generated by the magnetic moments of the electrons in the atomic orbitals ψ_H and ψ_D, respectively. Since the electronic moments are coupled in an anti-parallel orientation by the electrostatic interaction which comprises the chemical bond, the proton spins have an indirect interaction of the form (p spin : ψ_H spin : ψ_D spin : d spin) or, diagrammatically, (p $\uparrow$: ψ_H $\downarrow$: ψ_D $\uparrow$: d $\downarrow$). This electronic interaction mechanism suggests that the coupling constant, like the shielding parameter, can serve to increase our understanding of molecular wave functions.

For a molecule containing several nuclei with non-zero magnetic moments, the observed spectrum and its analysis can be considerably more complicated than in the HD example discussed above. The effective Hamiltonian for the nuclear spin wave functions has the form

$$\mathcal{H} = \beta_N H_0 \sum_n g_n(1 - \sigma_n)I_z + h \sum_{n>n'} A_{nn'}\mathbf{I}_n\cdot\mathbf{I}_{n'} \quad (5)$$

where g_n is the g-factor for nucleus n, $\mathbf{I}_n$, $\mathbf{I}_{n'}$ are the spin operators for nucleus n,n′ and I_{nz} is the z-component spin operator for nucleus n. The quantity $A_{nn'}$, the coupling constant between nucleus n and n′, is usually expressed in cycles per second (c.p.s.) and is defined as positive if the anti-parallel orientation of $\mathbf{I}_n$ and $\mathbf{I}_{n'}$ is of lower energy than the parallel orientation. Techniques have been developed[4] for obtaining unambiguous values of σ_n and $A_{nn'}$ from the observed spectra. For some relatively complicated cases, it has been possible to determine not only the magnitude but also the relative signs of the coupling constants.[5] In the treatment given in the body of this paper, we make use of the fact that the magnetic resonance spectra have been analyzed and the coupling constants determined experimentally for the molecules considered.

Hyperconjugation in Ethane

Although the concept of hyperconjugative interactions has long been utilized for rationalizing certain molecular properties,[6] there is still considerable disagreement concerning its importance.[7] One cause of this uncertainty is that many of the effects ascribed to hyperconjugation represent relatively small variations in molecular properties (heats of hydrogenation, bond lengths, dipole moments, reaction rates, etc.).[6] Since there are several different explanations for the observed changes, their relation to hyperconjugation is not always clear.

We here employ the coupling constants $A_{HH'}$ between vicinal protons to elucidate the contribution made by hyperconjugation to the ground state energies and wave functions of molecules (especially ethane). Although all semi-quantitative attempts to study hyperconjugation have been in terms of the molecular orbital method (L.C.A.O. approximation),[8] we base our treatment on a valence-bond approach and include σ-type terms, as well as the usual π-orbital contributions. In terms of the valence bond model, hyperconjugation arises from presence in the ground state wave function of structures other than the one with perfect pairing. Correspondingly, the decrease in energy resulting from the inclusion of these additional structures is the hyperconjugation energy. Because the errors in the valence-bond model, as in most of the theory of many-electron systems, are difficult to assess by direct calculation, we employ an experimental criterion for the validity of our approach. Since the vicinal proton coupling constant $A_{HH'}$ is a sensitive function of the contribution of structures with deviations from perfect pairing, a comparison of calculated and experimental $A_{HH'}$ values

(3) For a relatively up-to-date review, see J. A. Pople, W. G. Schneider and H. J. Bernstein, "High Resolution Nuclear Magnetic Resonance," McGraw-Hill Book Co., Inc., New York, 1959, especially Chapts. 7, 11 and 12.

(4) Pople, *et al.*, ref. 3, Chapt. 6 and references therein.

(5) H. S. Gutowsky, C. H. Holm, A. Saika and G. A. Williams, *J. Am. Chem. Soc.*, **79**, 4596 (1957).

(6) R. S. Mulliken, *J. Chem. Phys.*, **7**, 339 (1939). See V. A. Crawford, *Quart. Rev.*, **3**, 226 (1949) for a general survey; also J. W. Baker, "Hyperconjugation," The Clarendon Press, Oxford, 1952.

(7) A good sample of the varied views maintained by different workers can be found in the papers of the Conference on Hyperconjugation held at Indiana University, June, 1958, and published in *Tetrahedron*, **5**, No. 2/3 (January, 1959). See also R. S. Mulliken, *ibid.*, **6**, 68 (1959).

(8) R. S. Mulliken, C. A. Rieke and W. G. Brown, *J. Am. Chem. Soc.*, **63**, 41 (1941). Also see N. Muller and R. S. Mulliken, *ibid.*, **80**, 3489 (1958) for references to recent calculations and slight modifications of the approach of Mulliken, Rieke and Brown.

is used to test the applicability of the valence-bond model to the hyperconjugation problem.

To express the coupling constants in terms of valence-bond theory,[9] we require the details of the electron-nuclear interactions that are involved. For protons it has been shown[10] that the dominant terms in the Hamiltonian are given by the expression

$$\mathcal{H} = -\frac{h^2}{2m}\sum_k \nabla_k^2 + V + \frac{8\beta_e\beta_N}{3}\sum_{k,n} g_n\delta(\mathbf{r}_{kn})\mathbf{S}_k\cdot\mathbf{I}_n \quad (6)$$

where β_e is the electronic g-factor, $\mathbf{S}_k$ the electron spin operator, and $\delta(\mathbf{r}_{kn})$ a Dirac delta function centered on nucleus n. The first two terms represent the usual kinetic and potential energy of the k electrons in the molecule and the third term is the Fermi contact interaction between the electron and nuclear spins. Treating the Fermi term as a perturbation, we can use approximate second-order perturbation theory to write the isotropic contribution to the interaction energy $\Delta E_{nn'}$ between nucleus n and n′ in the form

$$\Delta E_{nn'} = \frac{2}{3\Delta}\left(\frac{16\pi\beta_e\beta_N}{3}\right)^2 g_n g_{n'} \left(\Psi_0\left|\sum_{k,k'}\delta(\mathbf{r}_{kn})\delta(\mathbf{r}_{k'n'})\mathbf{S}_k\cdot\mathbf{S}_{k'}\right|\Psi_0\right)\mathbf{I}_n\cdot\mathbf{I}_{n'} \quad (7)$$

where Ψ_0 is the unperturbed ground state wave function and Δ the appropriate average excitation energy.[11] Comparison of eq. 5 and 7 shows that $A_{nn'}$ can be written

$$A_{nn'} = \frac{2}{3h\Delta}\left(\frac{16\pi\beta_e\beta_N}{3}\right)^2 g_n g_{n'} \left(\Psi_0\left|\sum_{k,k'}\delta(\mathbf{r}_{kn})\,\delta(\mathbf{r}_{k'n'})\mathbf{S}_k\cdot\mathbf{S}_{k'}\right|\Psi_0\right) \quad (8)$$

Equation 8 provides the required relationship between the coupling constant and the ground state wave function Ψ_0. We now introduce the valence-bond model for Ψ_0, which can be expressed in the form

$$\Psi_0 = \sum_j c_j\psi_j \quad (9)$$

where the ψ_j are the non-ionic canonical valence-bond structures and the c_j are constant coefficients obtained by a variational procedure. Substitution of eq. 9 into eq. 8 specialized for protons leads to the equation[9]

$$A_{HH'} = \frac{1.395\times10^3}{\Delta(\text{e.v.})}\sum_{j,l} c_j c_l\left(\frac{1}{2^{n-i_{j,l}}}\right)[1 + 2f_{j,l}(p_{HH'})] \quad (10)$$

where, for the superposition diagram of ψ_j and ψ_j, $i_{j,l}$ is the number of islands and $f_{j,l}(p_{HH'})$ is the exchange coefficient between the 1s orbitals on H and H′.

From the form of eq. 10 and the meaning of the exchange factor in valence-bond theory,[12] we can see the relation between $A_{HH'}$ and hyperconjugation. If ψ_0 is the perfect-pairing structure and there is no hyperconjugation (*i.e.*, $c_j = 0$ for $j > 0$), $A_{HH'}$ is zero for H and H′ vicinal protons [$f_{00}(p_{HH'}) = -1/2$).[13] Conversely, a non-zero $A_{HH'}$ value implies that hyperconjugation is present in the ground state.

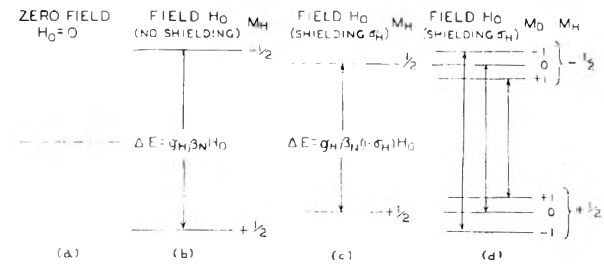

Fig. 1.—Diagram of proton energy levels: (a) no field (arbitrary zero of energy); (b) external field H_0, but no electronic shielding; (c) external field H_0 and electronic shielding σ_H; (d) external field H_0, electronic shielding σ_H, and coupling with deuteron in HD.

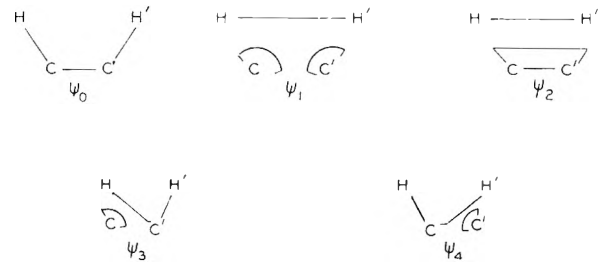

Fig. 2.—Diagrams of the five valence-bond structures for an HCC′H′ six-electron fragment. ψ_0 is the structure with perfect pairing.

To illustrate the formulation, we apply it to ethylenic compounds, for which the somewhat surprising result has been found[14] that the *trans*-proton coupling is always considerably larger than that for the *cis*-protons ($|A^{cis}_{HH'}|\sim$5–12 c.p.s., $|A^{trans}_{HH'}|\sim$12–18 c.p.s.). Approximating the molecule by a six-electron fragment with appropriately hybridized orbitals,[15] we can write five valence-bond structures for the ground state. These are diagrammed in Fig. 2. With coefficients c_j determined by the variational calculation and Δ set equal to the value of 9 e.v. used in methane,[9] one finds that $A^{cis}_{HH'} = +6.1$ c.p.s. and $A^{trans}_{HH'} = +11.9$ c.p.s. The relative values of the *cis* and *trans* coupling are in excellent agreement with the measured results. Also, in some cases, it has been possible to find indications that the two constants have the same relative sign, which corresponds to the theory.[16] The somewhat smaller magnitude of the theoretical values, as compared with the experimental ones, may indicate that the true ground state wave function has larger contributions from ψ_j ($j > 0$) than those calculated here. Also, the compounds in which $A_{HH'}$ was measured

(9) M. Karplus and D. H. Anderson, *J. Chem. Phys.*, **30**, 6 (1959).

(10) N. F. Ramsey, *Phys. Rev.*, **91**, 303 (1953); M. J. Stephens, *Proc. Roy. Soc.* (*London*), **A243**, 274 (1957).

(11) See Ramsey, ref. 10. There are a number of alternatives to the somewhat complex average excitation energy approach. Some of these are discussed in M. Karplus, *Rev. Mod. Phys.*, **32**, 455 (1960).

(12) L. Pauling, *J. Chem. Phys.*, **1**, 280 (1933).

(13) In eq. 10 and this argument we have neglected direct electronic interactions, which can yield a contribution to $A_{HH'}$, on the order of 0.1 c.p.s.

(14) S. Alexander, *J. Chem. Phys.*, **28**, 358 (1958); H. S. Gutowsky, M. Karplus and D. M. Grant, *ibid.*, **31**, 1278 (1959), lists a number of compounds.

(15) See M. Karplus, *ibid.*, **30**, 11 (1959), where the details of the calculations are presented.

(16) C. N. Banwell, A. D. Cohen, N. Sheppard and J. J. Turner, *Proc. Chem. Soc.*, 266 (1959). Also A. D. Cohen and N. Sheppard, *Proc. Roy. Soc.* (*London*), **A252**, 488 (1959); N. Sheppard and J. J. Turner, *ibid.*, **A252**, 506 (1959).

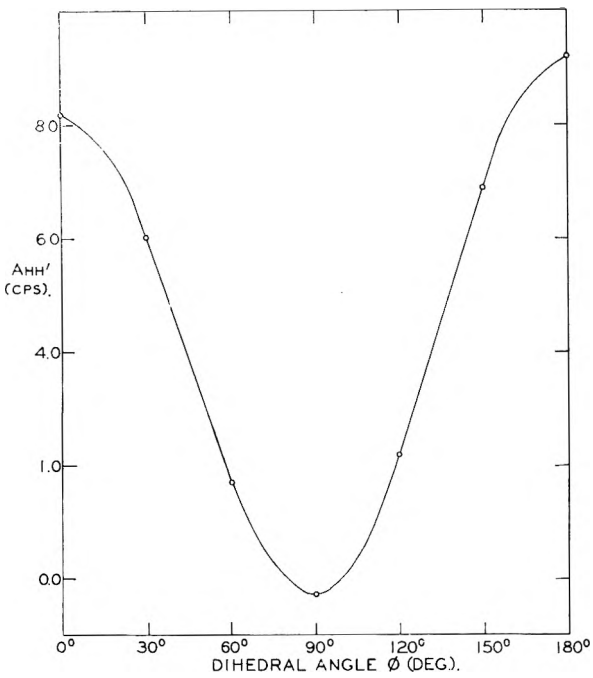

Fig. 3.—The vicinal proton coupling constant $A_{HH'}$ in ethane as a function of the dihedral angle ϕ. The open circles correspond to the values of ϕ for which $A_{HH'}$ was calculated and the curve is drawn through the points on the assumption of a $\cos^2\phi$ dependence.

contained various substituents, whose effect is neglected in the model.

We now apply the corresponding model to ethane-like systems, which can be treated also as six-electron problems. Here we consider the vicinal proton coupling as a function of the HCC'/CC'H' dihedral angle ϕ. The results obtained are plotted in Fig. 3, which shows that $A_{HH'}$ is a sensitive function of the angle ϕ. To determine the accuracy of the theoretical curve, it would be necessary to have experimental coupling constants for a series of compounds with known dihedral angle. Unfortunately there does not appear to be a single ethane derivative in which the required angle has been measured. In spite of this lack of structural data, there are comparisons that can be made. For a number of compounds the known conformations are such that estimates of the dihedral angle can be made, with pairs of axial hydrogens corresponding to $\phi\sim180°$, and one equatorial and one axial hydrogen corresponding to $\phi\sim60°$ (see Table I). Recently, Banwell, *et al.*,[16] have been able to determine the *trans* ($\phi\sim180°$) and *gauche* ($\phi\sim60°$) coupling constants in substituted ethanes by using solvents of different dielectric constants to vary the proportions of rotational isomers (see Table I). These results, as well as the extensive measurements of Lemieux, *et al.*, on acetylated sugars,[17] confirm the theory in the finding that $|A_{HH'}^{trans}| > |A_{HH'}^{gauche}|$. The experimental data also suggest that, as in the ethylene case, the calculated couplings are somewhat low, *i.e.*, that $A_{HH'}$ ($\phi = 60°$)$\sim$3–6 c.p.s. and $A_{HH'}$ ($\phi = 180°$)$\sim$10–18 c.p.s. Such a correction would be in agreement with the rotational average of vicinal coupling constants, which in substituted ethanes is found to be in the range 6.0–7.4 c.p.s.[18]

TABLE I

COUPLING CONSTANTS $A_{HH'}$ (C.P.S.) FOR VICINAL PROTONS

	"Estimated" angle ϕ	$A_{HH'}$ (calcd.)	$A_{HH'}$ (expt.)
2-Bromo-4,4-dimethylcyclohexanone[a]			
(Axial-axial)	$\sim180°$	+9.2	12.2
(Axial-equat.)	$\sim 60°$	+1.7	7.0
2-α-Bromocholestan-3-one[a]			
(Axial-axial)	$\sim180°$	+9.2	13.1
(Axial-equat.)	$\sim 60°$	+1.7	6.3
Substituted ethanes[b]			
(*trans*)	$\sim180°$	+9.2	10–18
(*gauche*)	$\sim 60°$	+1.7	1–3.5

[a] E. J. Corey, private communication. [b] C. H. Banwell, A. D. Cohen, N. Sheppard and J. J. Turner, *Proc. Chem. Soc.*, 266 (1959).

Having seen that the contributions of deviations from perfect pairing obtained by a variational calculation lead to approximately correct values for the vicinal coupling constants, we can now attempt to employ the valence-bond model for an estimate of the hyperconjugation energy of ethane. Table II gives the results for the HCCH fragment as a function of the angle ϕ. It is evident that ψ_0, the perfect pairing structure (see Fig. 2) has a coefficient on the order of unity. The other structures, ψ_i (i = 1,2,3,4), which involve deviations from perfect pairing and the loss of effective bonds, make only a small contribution, with the sum of the absolute values of their coefficients between 0.025 and 0.063. Correspondingly, the stabilization energy E_h arising from these structures is also small (<0.5 kcal.). If one assumes that all the contributions are additive,[19] one finds that for staggered ethane the total extra stabilization energy is 3.2 kcal.,[20] with a somewhat larger value indicated by the coupling constant measurements.

The figure of $\sim$3 kcal. for the second-order hyperconjugation energy[8] is not directly comparable with those obtained in other calculations. Following in the path of Mulliken, all workers have restricted their considerations to the hypercon-

TABLE II

ETHANE FRAGMENT WAVE FUNCTION AND ENERGY

Dihedral angle ϕ	0°	60°	120°	180°
c_0[a]	1.013	1.020	1.019	1.011
$\sum_i \lvert c_i \rvert$[b]	0.061	0.048	0.049	0.063
E_h (kcal.)[c]	.3950	.3187	.3210	.4160

[a] Coefficient of ψ_0. [b] Sum of absolute value of the coefficients of ψ_i. [c] E_h (kcal.) is the hyperconjugation energy difference between the energy of ψ_0 and the five structure function.

(17) Lemieux, Kullnig, Bernstein and Schneider, *J. Am. Chem. Soc.*, **80**, 6098 (1958). We do not list the values because the lack of rigidity of the structures is such as to fix the angle ϕ with even less accuracy than those given in Table I.

(18) R. E. Glick and A. A. Bothner-By, *J. Chem. Phys.*, **25**, 362 (1956).

(19) This is exactly the approximation of perturbation theory, which should be accurate for this case.

(20) The evident implications of these results for the theory of the rotational barrier in ethane are discussed in another paper (M. Karplus, *J. Chem. Phys.*, **33**, 316 (1960)).

jugation arising from the π-system of the molecule. Contributions from σ-π or σ terms were not included. Within these limitations, the second-order energy has ranged from the value 5.25 kcal. obtained by Roberts and Skinner[21] (zero overlap approximation), to the value of 1.3 kcal. found by Lofthus[22] (overlap included). The results of other calculations,[8,23] each involving somewhat different empirical parameters, fall between these two extremes. In the valence-bond model used here, none of the structures ψ_j ($j > 0$) correspond to pure π-type hyperconjugation. The structure ψ_5, in which the C–C σ-bond is not broken and the major term involves π-orbital interactions, contribute only 0.3 kcal. to the hyperconjugation energy. Although an exact separation of the energy arising from the ψ_1, ψ_3 and ψ_4 into π, σ and σ-π terms is difficult, it is evident that a considerable fraction comes from non-π interactions. This suggests that, although the M.O. calculations of Lofthus[22] for the π-type hyperconjugation energy yield results of the same order as those found here, consideration must be given to the σ and σ-π contributions.

Since most of the chemical effects of hyperconjugation have been assumed to result from the variation in first-order interactions, it would be of interest to have a valence-bond model and coupling constants for appropriate systems. Although some qualitative arguments along these lines have already been made,[24] no semi-quantitative results are available. Another approach, which is outside the scope of this paper, would utilize the hyperfine splitting observed in the electron spin resonance of hydrocarbon radicals.[25] It is to be hoped that by combining these modern experimental techniques with valence theory a clearer understanding of hyperconjugation can be obtained.

Bond Polarization in Tetrahedral Molecules

Because of the difficulty of an accurate calculation of the charge distribution in a molecule, it has been found useful to introduce bond polarization parameters which can be evaluated by means of experimental data. Typical of this procedure is the use of molecular dipole moments[26] and nuclear quadrupole coupling constants[27] for determining bond polarization. In what follows, we show how the coupling constant between directly-bonded atoms can be utilized in a corresponding manner, especially for molecules to which other criteria are not applicable.

We consider the coupling constant A_{XH} between a pair of atoms, one of which is a proton. Since terms other than the Fermi contact interaction are still relatively small,[28] eq. 8 is a good approximation. For the coupling constant between directly-bonded atoms in saturated molecules, deviations from perfect pairing are not important and the ground state wave function Ψ_0 can be expressed in terms of antisymmetrical products of localized electron-pair functions[29] of the form

$$\psi_{(i,j)} = \frac{1}{\sqrt{2}}\eta\{\phi_x(i)\phi_y(j) + \phi_x(j)\phi_y(i) + \lambda_x\phi_x(i)\phi_x(j) + \lambda_y\phi_y(i)\phi_y(j)\} \cdot \{\alpha(i)\beta(j) - \beta(i)\alpha(j)\} \quad (11)$$

where ϕ_x and ϕ_y are hybrid orbitals on nucleus x and y, respectively, λ_x and λ_y are the bond polarization parameters, η is the normalizing factor (including overlap), and α,β represent the usual spin functions. By substituting this form for Ψ_0 into eq. 8 and neglecting contributions from other bonds, one obtains an expression for the coupling constant which is a function of only the hybridization of ϕ_x,ϕ_y and the bond polarization λ_x,λ_y.[30] For an X–H bond, which is of interest here, ϕ_y reduces to a hydrogenic ls orbital.

It is obviously impossible to evaluate all three parameters (ϕ_x hybridization, λ_x, λ_H) from a knowledge of the experimental value of A_{XH}. Rather than attempting to introduce the results of a number of different measurements to completely determine the wave function, we consider a series of molecules for which all but one of the parameters can be estimated with resonable confidence. These are the tetrahedral species BH_4^-, CH_4, NH_4^+. The central atom x (x = B,C,N) can be assumed to contribute tetrahedral hybrids of the form $\phi_x = (1/2)s + (\sqrt{3/2})p\sigma_x$ to each localized X–H bond. Further, the parameter λ_H in eq. 11, which corresponds to the ionic term $\phi_H(i)\phi_H(j)$, is likely to be very small[31] and can be set equal to zero. With these assumptions, λ_x is the only undetermined parameter. Introducing a mean Δ of 9 e.v., equal to that used in the hydrocarbon calculations, we obtain the values of A_{XH} as a function of λ_x. From the computed results given in Table III, it can be seen that A_{XH} is a sensitive function of λ_x^2 for the three molecules. In Table IV are listed the experimental A_{XH} values, as well as the λ_x^2 parameters for which A_{XH}(calcd.) equals A_{XH}(expt.). We also include the "normalized" parameters $\eta^2\lambda_x^2$, which correspond more closely to the usual ionic character, and the electronegativity differences ($X_X - X_H$) between X and H.[32] Since there are no quantitative formulas for the relationships between the $\eta^2\lambda_x^2$ parameters, which include overlap, and electronegativity differences, only a qualitative comparison is possible. It is evident that the values obtained for $\eta^2\lambda_x^2$ are reasonable, with their ratio for CH_4 and NH_4^+ about the same as the corresponding X_x–X_H ratio. The BH_4^- result suggests that neglected $\phi_H(i)\phi_H(j)$ terms might

(21) J. S. Roberts and H. A. Skinner, *Trans. Faraday Soc.*, **45**, 339 (1949).

(22) A. Loftus, *J. Am. Chem. Soc.*, **79**, 24 (1957).

(23) C. A. Coulson and V. A. Crawford, *J. Chem. Soc.*, 2052 (1953); Y. I'Haya, *J. Chem. Phys.*, **23**, 1171 (1955).

(24) E. B. Whipple, J. H. Goldstein and L. Mandell, *ibid.*, **30**, 1109 (1959); R. A. Hoffman, *Mol. Phys.*, **1**, 326 (1958); M. Kreevoy, private communication.

(25) R. Bersohn, *J. Chem. Phys.*, **24**, 1066 (1956); D. B. Chesnut, *ibid.*, **29**, 43 (1958); A. D. McLachlan, *Mol. Phys.*, **1**, 233 (1958).

(26) C. A. Coulson, "Valence," Oxford University Press, Oxford, 1952; D. Z. Robinson, *J. Chem. Phys.*, **17**, 1022 (1949).

(27) B. P. Dailey and C. H. Townes, *ibid.*, **23**, 118 (1955).

(28) D. M. Grant and M. Karplus, unpublished calculations.

(29) A. C. Hurley, J. E. Lennard-Jones and J. A. Pople, *Proc. Roy. Soc.* (*London*), **A220**, 446 (1953); J. M. Parks and R. G. Parr, *J. Chem. Phys.*, **28**, 335 (1958).

(30) M. Karplus and D. H. Grant, *Proc. Nat. Acad. Sci.*, **45**, 1269 (1959).

(31) C. A. Coulson, *Trans. Faraday Soc.*, **38**, 433 (1942).

(32) L. Pauling, "The Nature of the Chemical Bond," Cornell University Press, Ithaca, N. Y., 1960. No change in values has been introduced to take account of the charged species.

TABLE III

COUPLING CONSTANT A_{XH} (C.P.S.) FOR TETRAHEDRAL MOLECULES

Molecule	A_{XH} (calcd.) $\lambda_X^2 = 0$	$\lambda_X^2 = 0.05$	$\lambda_X^2 = 0.1$	$\lambda_X^2 = 0.2$	$\lambda_X^2 = 0.3$
BH_4^-	105	84.7	77.3	67.2	..
CH_4	181	147	134	117	..
NH_4^+	89.3	72.9	66.6	57.2	51.2

TABLE IV

"EXPERIMENTAL" BOND POLARIZATION

Molecule	A_{XH} (expt.)[a]	λ_X^2 (expt.)	$[\eta^2\lambda_X^2]$	$(X_X - X_H)$[b]
BH_4^-	80.5	0.07	0.021	−0.1
CH_4	124–125	.14	.047	+ .4
NH_4^+	53.5	.27	.096	+ .9

[a] P. C. Lauterbur, private communication; also N. Muller and D. E. Pritchard, *J. Chem. Phys.*, **31**, 768 (1959), for CH_4. [b] Electronegativity difference between X and H from ref. 32.

make a contribution of the same order as the $\phi_B(i)\phi_B(j)$ product.

Another parameter to which the coupling constant is very sensitive is the orbital hybridization. Since the contact term depends on the electron density at the nucleus, only s-orbitals make a contribution. Consequently, the magnitude of the coupling is directly related to the square of hybridization parameter a in the expression $\phi_x = as + bp\sigma_x$. With the assumption of orbital following, relatively good correlations between hybridization and the observed coupling have been obtained.[33]

Acknowledgment.—The author wishes to thank Dr. D. E. Applequist for cogent comments on the hyperconjugation section of the manuscript.

(33) See ref. 30. Also N. Muller and D. E. Pritchard, *J. Chem. Phys.*, **31**, 768 (1959); W. D. Phillips, H. C. Miller and E. L. Muetterties, *J. Am. Chem. Soc.*, **81**, 4446 (1959); J. N. Shoolery, *J. Chem. Phys.*, **31**, 1427 (1959).

A MOLECULAR ORBITAL MODEL FOR INFRARED BAND INTENSITIES: FUNCTIONAL GROUP INTENSITIES IN AROMATIC COMPOUNDS[1]

BY THEODORE L. BROWN

Noyes Chemical Laboratory, University of Illinois, Urbana, Illinois

Received January 27, 1960

A simple molecular orbital model has been developed for infrared absorption intensities in aromatic compounds of the form XC_6H_4S where S contains the absorbing functional group and X is a *meta* or *para* substituent. For a given group S the intensity is related to the π electronic energy levels in the substituted benzene, C_6H_5X. On the basis of a simple electrostatic theory of substituent effects in chemical reactivities, it is shown that the appropriate set of substituent constants should be linearly related to the square root of the observed absorption intensity. This relationship is in fact found for a number of series, including substituted benzonitrile, phenols, anilines and N-methylanilines. The fact that correlations of this type are obtained is indication that the changes in electron distribution occurring in the molecule as a result of vibrational distortions are closely parallel to those occurring in the formation of the transition state during chemical reaction.

There has been considerable interest in recent years in the intensities of infrared absorption bands which are associated with functional group vibrations. The effect of structure upon the intensity of a functional group absorption which is common to a series of related molecules has been of particular interest. Attempts have been made to correlate the intensity variations in substituted benzonitriles,[2] phenols,[3,4] anilines,[5,6] etc., with the sigma constants[7] of the substituents. Correlations of intensity with substituent constants or other molecular properties have been hampered by the lack of a theoretical basis on which to choose the proper function of the intensity. The present paper deals with a simple molecular orbital model for infrared intensities in compounds of the form

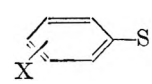

where S contains the absorbing functional group and X is a *meta* or *para* substituent. The model presented is useful in that it provides some basis for choosing a particular function of the intensity for correlations with substituent constants. In addition it clearly indicates the origin of the intensity variations as a function of substituent.

I. General Theory

The model chosen is one which has been employed by Nagakura and co-workers in connection with the electronic spectra of substituted benzenes.[8-10] In this initial discussion the group S will be limited to one which is *meta*-directing and which possesses a π-orbital of appropriate symmetry, *e.g.*, $-C{\equiv}N$, $-NO_2$ or $-COCH_3$. A second class of groups, which are *ortho–para*-directing, will be discussed in a later section.

The π-electronic interaction of S with the ring is assumed to consist in the formation of a molecular orbital from the highest filled orbital (or orbitals) in the ring and the lowest vacant orbital in S. The three occupied molecular orbitals (MO's) in benzene are

(1) Presented at the symposium on Electron Distributions in Organic Molecules, 136th National Meeting, American Chemical Society, Atlantic City, N. J., September 15, 1959.

(2) (a) T. L. Brown, *J. Am. Chem. Soc.*, **80**, 794 (1958); (b) P. J. Krueger and H. W. Thompson, *Proc. Roy. Soc.* (*London*), **A250**, 22 (1959).

(3) T. L. Brown, THIS JOURNAL, **61**, 820 (1957).

(4) P. J. Stone and H. W. Thompson, *Spectrochim. Acta*, **10**, 17 (1957).

(5) S. Califano and R. Moccia, *Gazz. chim. ital.*, **87**, 58 (1957).

(6) P. J. Krueger and H. W. Thompson, *Proc. Roy. Soc.* (*London*), **A243**, 143 (1957).

(7) H. H. Jaffe, *Chem. Revs.*, **53**, 221 (1953).

(8) S. Nagakura and J. Tanaka, *J. Chem. Phys.*, **22**, 236 (1954).

(9) S. Nagakura, *ibid.*, **23**, 1441 (1955).

(10) J. Tanaka, S. Nagakura and M. Kobayashi, *ibid.*, **24**, 311 (1956).

TABLE I

Substituent	H[b]	F[a]	Cl[b]	CH_3[a]	OH[b]	OCH_3[a]	CHO[a]	NH_2[b]	CN[a]	NO_2[a]
$-H_b$ (e.v.)[c]	9.24	9.19	9.07	8.82	8.50	8.20	9.51	7.70	9.67[d]	9.77[d]
c_b (*meta*)	0.289	.267	.267	.290	.283	.283	.264	.299	.262	.262
c_b (*para*)	0.577	.571	.571	.580	.586	.586	.579	.601	.565	.565

[a] Coefficients estimated. [b] Coefficients from H. H. Jaffe, *J. Chem. Phys.*, 20, 279 (1952). [c] The values used here for H_b are the photo-ionization values of K. Watanabe, *ibid.*, 26, 542 (1957). These are essentially the same as the spectroscopic values. [d] For NO_2 and CN, photo-ionization or spectroscopic values were not available. H_b for C_6H_5CN was estimated by taking the differences in the electron impact values for this compound and benzene (F. H. Field and J. L. Franklin, "Electron Impact Phenomena," Academic Press, Inc., New York, N. Y., 1957, p. 105 ff.) and adding to the photo-ionization value for benzene. H_b for nitrobenzene was estimated as being slightly larger than the value for C_6H_5CN.

C_{2v} Symmetry

$$\phi_1 = (\psi_1 + \psi_2 + \psi_3 + \psi_4 + \psi_5 + \psi_6)/\sqrt{6} \qquad B_2$$

$$\phi_2 = (\psi_2 + \psi_3 - \psi_5 - \psi_6)/\sqrt{4} \qquad A_2$$

$$\phi_3 = (2\psi_1 + \psi_2 - \psi_3 - 2\psi_4 - \psi_5 - \psi_6)/\sqrt{12} \qquad B_2$$

It is necessary to consider the effect of X on these benzene orbitals It will be assumed that of the two higher energy orbitals, which are degenerate in benzene, only ϕ_3 is perturbed by X.[11] The interaction of S with ϕ_2 and ϕ_3 depends on the orientation of S with respect to X. In *para* substitution S forms an MO only with ϕ_3. In *meta* substitution, however, both ϕ_2 and ϕ_3 interact with S. These conclusions follow from the symmetry properties of the benzene orbitals.

Figure 1 shows a simplified energy diagram of the orbitals involved. The vacant orbital in S, ϕ_s, is at an energy level V_S which is measured by the difference between the ionization potential and the energy of the n-π^* electronic transition energy of the alkyl derivative of S. H_b represents the energy of the highest occupied level in benzene or the substituted benzene. In benzene itself ϕ_2 and ϕ_3 are degenerate; H_b is set equal to the ionization potential, -9.24 e.v. In the substituted benzenes ϕ_2 and ϕ_3 are no longer degenerate. It will be assumed that the ionization potential of the compound C_6H_5X is a measure of the energy of ϕ_3, and that ϕ_2 remains at the same energy as in benzene itself.[12] The energies and atomic orbital coefficients for ϕ_3 for a number of substituted benzenes are listed in Table I.

Foregoing for the sake of clarity the distinction between *meta* and *para* substitution (see the Appendix) we write for the MO formed between the orbital in the ring, ϕ_b and orbital in S, ϕ_s

$$\Phi = a\phi_b + b\phi_s \qquad (1)$$

We employ the variation method to obtain the ratio of orbital coefficients $b/a = \lambda$

$$\lambda = \frac{V_s - H_b - [(H_b - V_s)^2 + 4c_s^2c_b^2\beta^2]^{1/2}}{2c_sc_b\beta} \qquad (2)$$

The integrals $\int \phi_s H \phi_s d\tau$ and $\int \phi_b H \phi_b \tau$ have been set equal to V_s and H_b, respectively. β is taken as -2.25 e.v.; c_s and c_b are the coefficients of the atomic orbitals in the MO's ϕ_s and ϕ_b for the two atoms which join S and the ring. The overlap integral $\int \phi_s \phi_b d\tau$ is set to equal zero.

It is true that the substituent affects λ largely through the variation in H_b, and that the change in c_b is of relatively minor importance. Therefore, although the values of c_b for many substituents had to be estimated, it is not a serious matter in the development which follows.

II. Application of the Model to the Calculation of Infrared Intensities

To illustrate the application of the above model for π-electron interaction between the ring and S to infrared intensities the substituted benzonitriles will be considered. The spectroscopic ionization potential of acetonitrile is reported as 11.96 e.v.[13] The n-π^* transition for alkyl cyanides is not observed below 160 mμ. We assume a value of 8.86 e.v. which leads to -3.10 e.v. for V_s. (It should be pointed out that the matter of principal concern in this paper is the *change* in intensity throughout a series of compounds. If V_s has been incorrectly estimated the relative order of calculated intensities is not affected.)

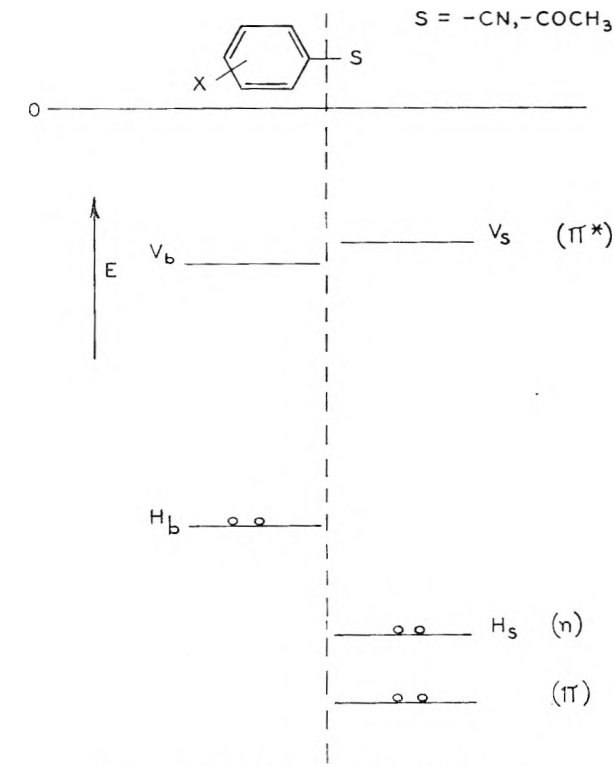

Fig. 1.—Simplified π-electronic energy diagram.

The vibrational transition which is of interest is that corresponding to the vibration of the C≡N group so that the vibrational coördinate is largely the carbon–nitrogen bond axis r. The intensity of the transition A is related to the first derivative of the dipole moment change by

$$\frac{\partial \mu}{\partial r} = \left(\frac{3000c^2mA}{N^2\pi}\right)^{1/2} = \frac{1}{\omega}A^{1/2} \qquad (3)$$

where c is the velocity of light, m is the reduced mass, N is Avogadro's number and intensity is expressed in units of mole^{-1} liter cm.$^{-2}$. The dipole moment of the molecule is approximated by

$$\mu = \mu_0 + 2b^2e\mathbf{x} \qquad (4)$$

The second term on the right represents the moment arising from migration of charge from ϕ_b to ϕ_s. This migration is related to the contribution from the ϕ_s orbital in (1) and is measured by b^2. $\mathbf{x}$ represents the distance separating the charge centers, here taken as 3.30 Å., the distance from the

(11) F. A. Matsen, "Chemical Applications of Spectroscopy," Interscience Publishers, Inc., New York, N. Y., 1956, p. 671.

(12) This assumption is only approximately correct, since the observed ionization potential is some kind of average of the energies of ϕ_2 and ϕ_3.

(13) J. A. Cutler, *J. Chem. Phys.*, **16**, 136 (1948).

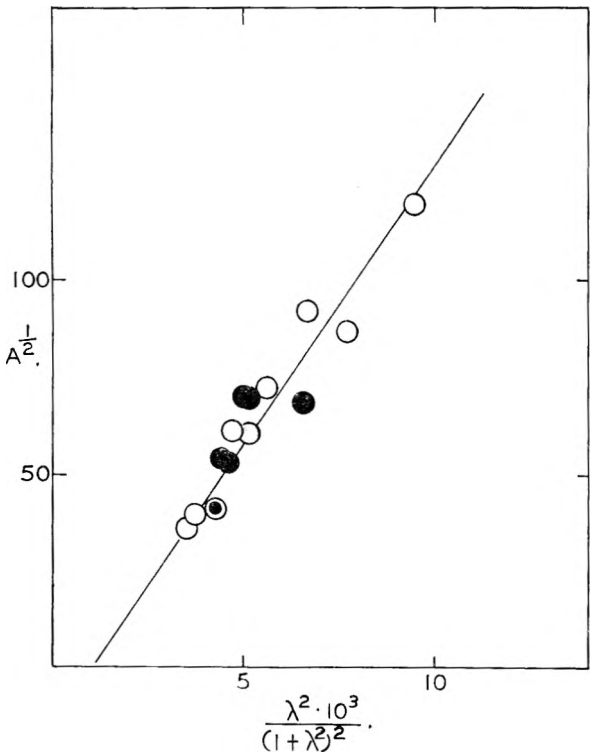

Fig. 2.—Square root of observed intensity in benzonitriles *vs.* calculated function. Closed circles represent *meta* substituents.

center of the ring to the center of the C≡N bond. μ_0 represents all other contributions to the moment. Then

$$\frac{\partial \mu}{\partial r} = \frac{\partial \mu_0}{\partial r} + 2b^2 e \frac{\partial \mathbf{x}}{\partial r} + 2e\mathbf{x} \frac{\partial b^2}{\partial r} \qquad (5)$$

It will be assumed that $\partial\mu_0/\partial r$ is a constant independent of the substituent. $\partial \mathbf{x}/\partial r$ is small,[14] and the term involving it can be dropped. b^2 can be evaluated from (2), since $b^2 = \lambda^2/(1 + \lambda^2)$. There remains the evaluation of $\partial b^2/\partial r$.

$$\frac{\partial b^2}{\partial r} = \frac{-2\lambda^2 \partial V_s/\partial r}{(1+\lambda^2)^2[(H_b - V_s)^2 + 4c_s^2 c_b^2 \beta^2]^{1/2}} \qquad (6)$$

From (3), (5) and (6)

$$A^{1/2} = \omega \frac{\partial \mu_0}{\partial r} - \frac{4\omega e \mathbf{x} \lambda^2}{(1+\lambda^2)^2 \xi} \frac{\partial V_s}{\partial r} \qquad (7)$$

where

$$\xi = [(H_b - V_s)^2 + 4c_s^2 c_b^2 \beta^2]^{1/2}$$

If a value were available for $\partial V_s/\partial r$ in (7), the equation could be tested by comparing $A^{1/2}$ with the last term. Qualitatively, the level V_s should become more negative with increasing bond distance, so that $\partial V_s/\partial r$ is then negative in sign. Using the simple LCAO model for the C≡N bond, and setting the coulomb integral for nitrogen, α_N, equal to $\alpha_c + \beta$,[15] the energy of π^* level, $V_s = \alpha_c - 0.62\ \beta_{CN}$. Then, assuming that the coulomb integrals are unchanged as the C≡N bond stretches slightly

$$\frac{\partial V_s}{\partial r} = -0.62 \frac{\partial \beta_{CN}}{\partial r} \qquad (8)$$

On the basis of the values of β given for various carbon–carbon bonds[16] (in acetylene, ethylene and benzene) $\partial\beta_{CC}/\partial r$ is approximately linear, with a value of 6.25 e.v./Å. Taking β_{CN} to be 1.2 β_{CC}, a value of −4.65 e.v./Å. is obtained for $\partial V_s/\partial r$. Inserting this value into (7) one obtains

$$A^{1/2} = K_1 + 0.61 \times 10^4 \chi \qquad (9)$$

$$\chi = \frac{\lambda^2}{(1+\lambda^2)^2 \xi}$$

In Table II, χ for each substituent is listed along with the observed values of $A^{1/2}$ for the compounds in chloroform solution.[2] The relationship is graphed in Fig. 2; it is satisfactorily linear over a wide range of substituents.

The observed slope is 1.5×10^4, as compared with the calculated value of 0.61×10^4. But the observed intensities were determined in chloroform solution in which the intensities are higher by an unknown factor—perhaps four to six—than they would be in the vapor state.[17] If this is accounted for in (9), the calculated slope is about $1.2–1.5 \times 10^4$, in good agreement with the observed value. In view of the simplicity of the model agreement to this degree is quite satisfactory. The intercepts lead to quite small values of $\partial\mu/\partial r$, which indicates only that most of the change in charge distribution has been accounted for by the other terms in equation 5. In view of the good accord between the observed and calculated quantities it must be concluded that the model, in spite of its simplicity and many inherent uncertainties, is a reasonable one in accounting for the C≡N intensities in benzonitriles.

III. Extension of the Model to Correlations with Substituent Constants

The electrostatic theory of substituent effects[18–20] has in general accounted for the over-all behavior of systems obeying the Hammett equation[7,21] $\log k/k_0 = \sigma\rho$. We can write the activation energy for a process involving electrophilic attack at a side chain as

$$E_a = E_a^0 + E_a'$$

where E_a' is the contribution from electrostatic effects and E_a^0 that due to all other factors. It will be assumed that the latter term remains constant as the substituent *meta* or *para* to the side chain is varied. Then

$$(E_a)_x - (E_a)_H = (E_a')_x - (E_a')_H$$

From the usual linear free energy assumption[21] it follows that

$$\log k_x - \log k_H = \frac{-[(E_a')_x - (E_a')_H]}{RT} = \sigma\rho \qquad (10)$$

(14) Consideration of the normal vibration involved, (assuming F_{CC} = 5md/Å., F_{CN} = 17 md./Å., treating the benzene ring as a single mass of 78) leads to an estimate of 0.15 for $\partial \mathbf{x}/\partial r$. Dropping this term leads to about a 2–3% error in the values for the coefficient of the variable term in equation (9).

(15) L. E. Orgel, T. L. Cottrell, W. Dick and L. E. Sutton, *Trans. Faraday Soc.*, **47**, 113 (1951).

(16) (a) R. Pariser and R. G. Parr, *J. Chem. Phys.*, **21**, 767 (1953); (b) R. S. Mulliken, *J. chim. phys.*, **46**, 497 (1949).

(17) J. P. Jessup and H. W. Thompson, *Spectrochim. Acta*, **13**, 217 (1958). The ratio of chloroform solution to vapor intensities for a number of *alkyl* cyanides averages about 6.

(18) C. C. Price, *Chem. Revs.*, **29**, 61 (1941).

(19) F. L. J. Sixma, *Rec. trav. chim.*, **72**, 673 (1953).

(20) T. Ri and H. Eyring, *J. Chem. Phys.*, **8**, 433 (1940).

(21) L. P. Hammett, "Physical Organic Chemistry," McGraw-Hill Book Co., Inc., New York, N. Y., 1941, p. 184.

Table II

Substituent	NH_2	OH	OCH_3	CH_3	F	Cl	H	CHO	CN	NO_2
$\lambda^2 \times 10^2$ (*meta*)[a]	4.16	3.54	3.67	3.53	3.30	3.31	3.35	3.18	3.15	3.12
$\chi \times 10^3$[b]	6.67	5.22	5.52	5.08	4.70	4.74	4.76	4.46	4.39	4.34
$A^{1/2}$ (*meta*)[c]	69	69	...	70[d]	...	52	59	54	41	41
$\lambda^2 \times 10^2$ (*para*)	5.46	4.31	4.74	3.76	3.30	3.46	3.35	2.98	2.81	2.73
$\chi \times 10^3$ (*para*)	9.49	6.74	7.72	5.68	4.75	5.25	4.76	4.15	3.84	3.67
$A^{1/2}$ (*para*)[c]	120	92	87	72	61	60	59	...	39	36

[a] λ^2 given here is the total for interaction of C≡N with both orbitals on benzene. [b] Corrected to give same value for H; see Appendix. [c] Intensities in units of mole^{-1} liter cm.$^{-2}$, in chloroform solution.[2] [d] Recently determined in the author's laboratory.

where σ is a constant characteristic of the substituent X and ρ is a constant characteristic of the side chain, attacking reagent and reaction medium. E_a' arises from the interaction of the electrophile with the partial charge on the side chain, and is an electrostatic potential of the form

$$E_a' = \frac{-2(b^2 + \delta b^2)(S)}{r^n} \qquad (11)$$

r represents the distance separating the interacting centers in the transition state. (S) and the value for n in (11) depend on the nature of the electrophile (ion, dipole, etc.). By way of example, the protonation of the nitrile group in benzonitriles would be a reaction of the type envisaged here.

δb^2 represents the change in the fractional charge in the side chain in the transition state from that in the molecule in the equilibrium condition, b^2. Because of the strongly polarizing character of the electrophile, δb^2 is quite likely to be large in comparison with b^2. In terms of the molecular orbital model developed earlier, δb^2 arises from a change in the V_s level in forming the transition state. This change in V_s can be considered to arise from two effects: (a) the change in the π-bond length in forming the transition state and (b) the coulombic effect of the electrophile in proximity to the π-bond. Both of these effects probably serve to lower V_s. Then

$$\delta b^2 = \frac{-2\lambda^2 \delta V_s}{(1 + \lambda^2)^2 \xi} \qquad (12)$$

On substituting (12) into (11)

$$E_a' = \frac{-(S)2\lambda^2}{r^n(1 + \lambda^2)^2\xi}[(1 + \lambda^2)\xi - 2\delta V_s] \qquad (13)$$

The similarity between this expression and equation 7 is evident. In contrast with $\partial V_s/\partial r$, however, δV_s cannot be considered to remain constant as the substituent X is varied. This is because it is determined by the total interaction between the electrophile and the side-chain. Therefore, as b^2 increases (electron-releasing substituents), δV_s also increases. The variation in δV_s with substituent is in the opposite direction from that for the term $(1 + \lambda^2)\xi$, since the latter term is smallest for the most electron-releasing groups.

We will optimistically assume that these two effects cancel one another, and that the term in brackets in equation 13 is a constant. The change in $(1 + \lambda^2)\xi$ in comparing the most electron-releasing (p — NH_2) with the most electron-withdrawing (p-NO_2) substituent is about 2.4 e.v. It is not at all unreasonable that δV_s should vary over half this wide a range, at least for an ionic electrophile. Then

$$E_a' = G\chi \qquad (14)$$

$$G = \frac{-2(S)}{r^n}[(1 + \lambda^2)\xi - 2\delta V_s] \approx \text{constant}$$

On comparing equations 14 and 9 it is clear that the variation in activation energy and—through equation 10—the substituent constants is linearly related to $A^{1/2}$. A graph of $A^{1/2}$ *vs.* σ^+, the electrophilic substituent constants,[22] is shown in Fig. 3

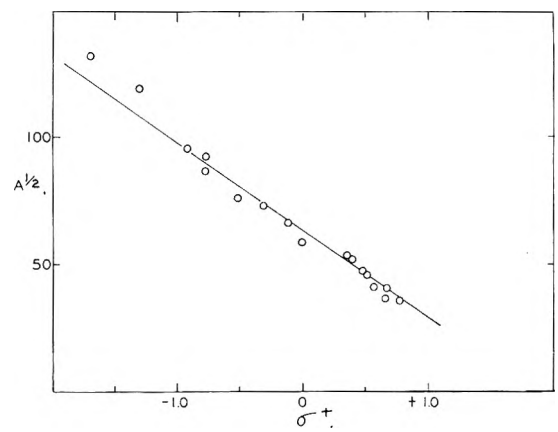

Fig. 3.—Square root of the observed intensity in benzonitriles *vs.* the electrophilic substituent constants.

for the substituted benzonitriles. A good correlation is obtained for a large number of substituents. It is appropriate to use the σ^+ constants here rather than the Hammett constants because of the similar natures of the rate process for which the σ^+ values are determined and the vibrational transition under consideration (insofar as their effect on the electron distribution is concerned).

A procedure entirely analogous to that used for the benzonitriles can be applied to substituted acetophenones for which a few intensity data are available.[23] A graph of $A^{1/2}$ of the carbonyl stretching bond *vs.* σ^+ for these compounds is shown in Fig. 4, and for some ethyl benzoates[23] in Fig. 5. The intensity is not very sensitive to substituents in these compounds as it is in benzonitriles, possibly because the carbonyl group is capable of rotation out of the plane of the ring.

It should be pointed out that one of the assumptions made in the derivation of equation 7 is that the distance **x**, which separates the partial charges, is a constant as a function of substituent. For a few substituents such as phenyl or other spatially extended groups which are capable of resonance in-

(22) H. C. Brown and Y. Okamoto, *J. Am. Chem. Soc.*, **80**, 4979 (1958).

(23) H. W. Thompson, R. W. Needham and J. Jameson, *Spectrochim. Acta*, **9**, 208 (1957).

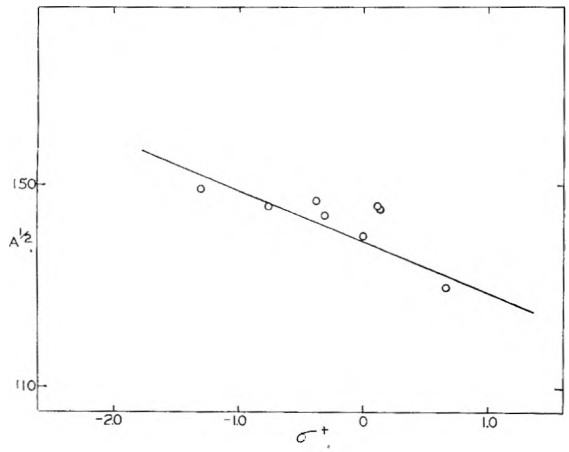

Fig. 4.—Square root of the observed carbonyl intensity in acetophenones *vs.* the electrophilic substituent constants.

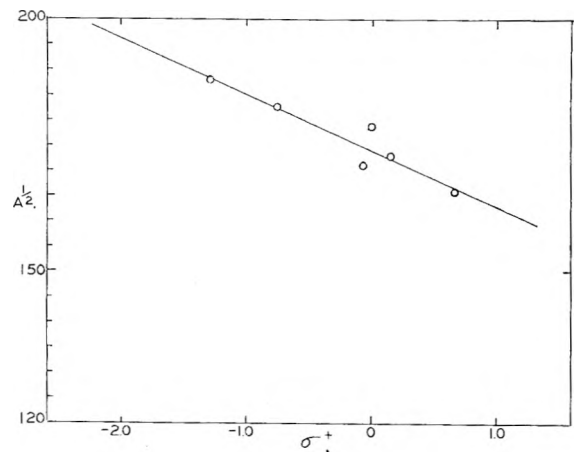

Fig. 5.—Square root of the observed carbonyl intensity in substituted ethyl acetates *vs.* the electrophilic substituent constants.

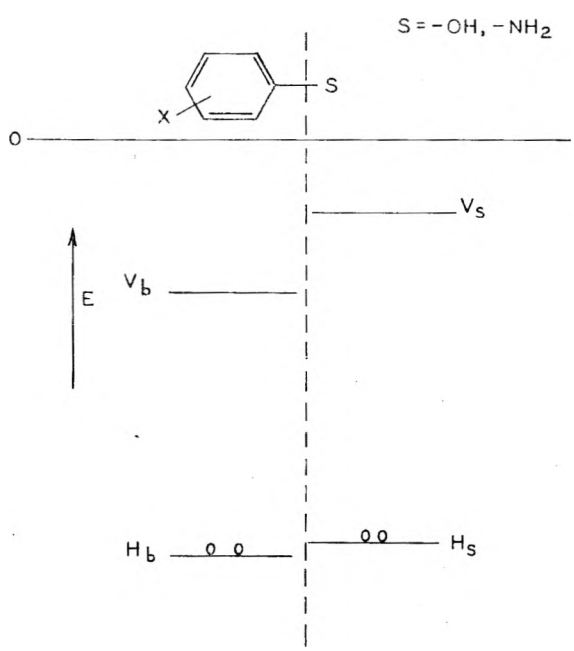

Fig. 6.—Simplified π-electronic energy level diagram.

teraction with the ring, this is a particularly poor assumption: for these, since the effective x is larger than otherwise, the intensity should appear to be abnormally high.

IV. Extension to Other Aromatic Compounds

A simplified energy diagram for compounds typified by phenols and anilines is shown in Fig. 6. The π-electronic interaction between S and the ring in this class of compounds consists in the formation of an MO from the highest occupied orbital (non-bonding electrons) on S, of energy H_s, and the lowest vacant orbital in the ring, of energy V_b. The substituent X located *meta* or *para* to S may cause a change in V_b. An electron-releasing substituent causes a raising of V_b, thus increasing the energy separation between V_b and H_s, and decreasing the π-electronic interaction.

The vibrational band of interest in, for example, the phenols corresponds to the OH stretching vibration. As the OH bond distance increases the bond becomes more ionic, structure b.

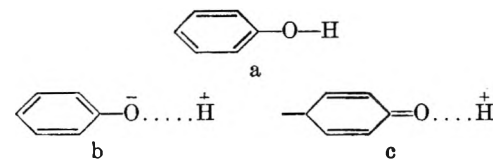

The added charge on oxygen results in a raising of H_s, and an increased π-electronic interaction with the ring. Proceeding as before we write

$$\Phi = a\phi_b + b\phi_s$$

$$\lambda = \frac{b}{a} = \frac{H_s - V_b - [(V_b - H_s)^2 + 4c_s^2c_b^2\beta^2)]^{1/2}}{2c_sc_b\beta} \quad (15)$$

In this class of compounds, $b > a$.

The dipole moment of a phenol may be written as

$$\mu = \mu_0 + 2a^2ex + \alpha er \quad (16)$$

The second term on the right expresses the contribution to the moment arising from migration of charge from the OH side-chain into the ring. The third term represents the moment arising from the partial ionic character of the OH bond.[24] μ_0 again represents all other contributions to the moment. The change in dipole moment as a function of the OH bond distance is

$$\frac{\partial\mu}{\partial r} = \frac{\partial\mu_0}{\partial r} + 2ex\frac{\partial a^2}{\partial r} + e\alpha + er\frac{\partial\alpha}{\partial r} \quad (17)$$

The matter of principal interest is the effect of the substituent X on the terms in equation 17. $\partial a^2/\partial r$ represents the increased migration of charge from the oxygen atom into the ring as the OH bond stretches. $\partial\alpha/\partial r$ is the change in the ionic character of the OH bond as a function of OH distance. This term should, if it varies at all as a function of substituent, change in the same way as $\partial a^2/\partial r$. This is because the change in ionic character is facilitated by removal of formal negative charge from the oxygen, measured by a^2 and $\partial a^2/\partial r$. We assume that the change in $\partial\alpha/\partial r$ with substituent is proportional to the variation in $\partial a^2/\partial r$. $\partial\mu_0/\partial r$ and αe are assumed constant. Then

(24) G. M. Barrow, THIS JOURNAL, 59, 1129 (1955).

$$\frac{\partial \mu}{\partial r} = K + k\frac{\partial a^2}{\partial r}$$

$$a^2 = \frac{1}{1+\lambda^2}$$

$$\frac{\partial \mu}{\partial r} = K + k\chi\frac{\partial H_s}{\partial r} \qquad (18)$$

Where

$$\chi = \frac{\lambda^2}{(1+\lambda^2)^2\xi'}$$

$$\xi' = [(H_s - V_b)^2 + 4c_s^2c_b^2\beta^2]^{1/2}$$

From (3) and (18)

$$A^{1/2} = K' + k'\chi\frac{\partial H_s}{\partial r} \qquad (19)$$

No attempt will be made to compare $A^{1/2}$ with χ as was done for the benzonitriles. The necessary values for V_b in the substituted phenols are not known; there is also some doubt that $\partial H_s/\partial r$, which represents the variation of the energy of the occupied orbital on the oxygen with the OH distance, is a constant independent of substituent. It is possible, however, to proceed to a correlation of the OH band intensities with the substituent constants for X.

The reaction which is used to determine the substituent constants for substituted phenols is the ionization of the phenol

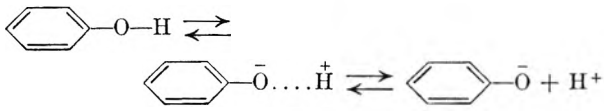

Again adopting the electrostatic model one has

$$\log K_X - \log K_H = \frac{-[(E_a')_X - (E_a')_H]}{RT} = \sigma\rho$$

where the K's represent the ionization constants of the substituted (K_X) and unsubstituted (K_H) phenols, and the E_a's represent the electrostatic energy contribution to the free energy difference. This contribution can be written as

$$E_a' = E_t' - E_g' + E_f'$$

where E_t' and E_g' represent the electrostatic energies of the OH bond in the transition and ground states, respectively, and E_f' the electrostatic energy difference in the transition and final states. This latter term is assumed to be a constant as a function of the substituent X. Then

$$E_g' = \frac{-k_g e^2(1-2a^2)}{r_g}$$

$$E_t' = \frac{-k_t e^2(1-2a^2-2\delta a^2)}{r_t}$$

$$E_a' = L - 2e^2a^2\left(\frac{k_g}{r_g} - \frac{k_t}{r_t}\right) + \frac{2k_te^2\delta a^2}{r_t}$$

δa^2 represents the change in the π-electronic interaction of the side-chain with the ring in the transition state from that in the ground state, a^2. It results from the increase in the value of H_s as the formal negative charge on oxygen increases. L is a constant, k_g and k_t represent the fractional contribution of the ionic form to the OH bond in the ground and transition states, respectively; r_g and r_t represent the corresponding OH bond distances. The term $(k_g/r_g - k_t/r_t)$ can be expressed approximately as $-0.8\ (k_t/r_t)$. There is no need for the present purposes to know this term very precisely. Using $a^2 = 1/(1+\lambda^2)$

$$E_a' = L + \frac{2e^2k_t}{r_t}\left(\frac{0.8}{1+\lambda^2} + \frac{2\lambda^2\delta H_s}{(1+\lambda^2)^2\xi'}\right)$$

$$E_a' = L + L'\frac{\lambda^2}{(1+\lambda^2)^2\xi'}\left(\frac{0.8(1+\lambda^2)\xi'}{\lambda^2} + 2\delta H_s\right)$$

For phenol, for which the requisite energy levels are known, λ^2 is about 31, so that to a good approximation

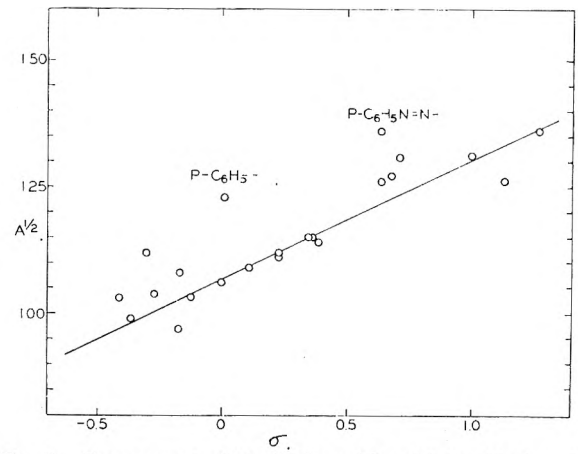

Fig. 7.—Square root of the hydroxyl band intensity in substituted phenols *vs.* the Hammett substituent constants.

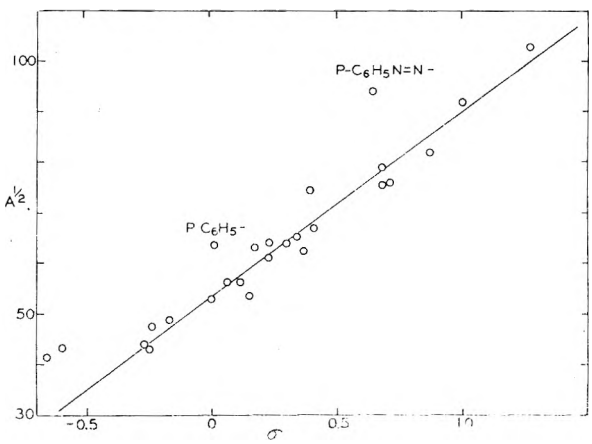

Fig. 8.—Square root of the symmetric NH_2 band intensity in anilines *vs.* the Hammett substituent constants.

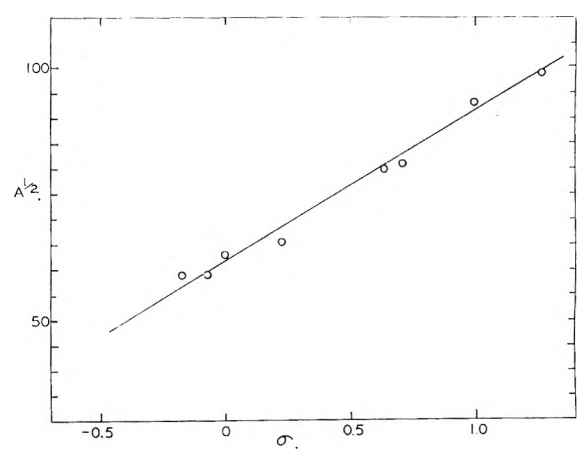

Fig. 9.—Square root of the NH band intensity in N-methylanilines *vs.* the Hammett substituent constants.

$$E_a' = L + L'\chi(0.8\,\xi' + 2\delta H_s) \qquad (20)$$

A comparison of (20) with (19) shows that E_a' is linearly related to $A^{1/2}$, provided the terms $\partial H_s/\partial r$ and $(0.8\,\xi' + 2\,\delta\,H_s)$ are either both constant or vary in proportion. The latter assumption would seem to be relatively safe, since if these terms do vary with substituent, they must have the same qualitative dependence on this variable. The result is then that $A^{1/2}$ for the OH stretching band in substituted phenols should vary linearly with the appropriate substituent constants. A similar conclusion applies to the symmetric N–H stretching band for substituted anilines. Figure 7 shows $A^{1/2}$ for phenols measured in carbon tetrachloride solution[3,4] *vs.* the substituent constants determined from ionization of phenols.[7] Figures 8 and 9 show a similar relationship for the symmetric NH_2 band in anilines and the NH band of N-methylanilines, respectively.[6]

Although the scatter is rather large for the phenols, the relationship appears in all cases to be linear, and is particularly good for the anilines. The points corresponding to substituents which are spatially extended and capable of resonance interaction with the ring are identified on the figures. For these the intensity is higher than the value of σ for the substituent would suggest. The reason for this is clear, and was discussed in the last paragraph of section III. The marked enhancement of the intensity in these cases, since it is just what is predicted from the theory, may be taken as further evidence that the change in dipole moment during vibration has been accounted for correctly.

V. Discussion

Empirical correlations of substituent constants with intensities in compounds of the type discussed here have been made by various workers.[1–6] H. W. Thompson and his co-workers have used log A in such correlations, while the present writer has used simply the intensity, A. The square root of the intensity correlates with substituent constants as well as log A, and far better than A. It appears, therefore, that from an empirical point of view as well as on the basis of the model presented here, it is the correct function to use.

It is interesting to note the analogy which can be drawn between the change in electron distribution in the molecule resulting from vibrational distortion and that which results from distortion of the molecule under the influence of an attacking reagent. This analogy is the basis for the derivation of a relationship between the intensity variations and substituent constants. The vibrational transition represents a relatively small perturbation of the molecule in comparison with the changes it undergoes in forming the transition state during chemical reaction. From the fact that the intensity variations do correlate well with substituent constants, however, it would appear that infrared band intensities will be useful in attempts to understand the changes in electron distribution occurring in molecules during chemical reaction.

VI. Appendix

For compounds in which a *meta*-directing S is located *para* to X the interaction with the ring involves only ϕ_3. The energy of this orbital is set equal to the ionization potential of C_6H_5X; λ is calculated from equation 2 using the values of H_b and c_b for the *para* carbon atomic orbital listed in Table I.

For compounds in which S is *meta* to X the total interaction of S with the ring is taken to be the sum of the interactions with both ϕ_2 and ϕ_3. ϕ_2 is assumed to be unperturbed by X so the energy of this orbital is set equal to the ionization potential of benzene and the coefficient of the *meta* carbon atomic orbital is assumed to be the same as in benzene, 0.5. The contribution to λ from this orbital is then the same for all X. The contribution to λ from interaction of S with ϕ_3 is computed from equation 2 using the values of H_b and c_b for the *meta* carbon atomic orbital given in Table I. A separate value of χ (equation 9) is then calculated for each of the two values of λ, and these are then added to give the total χ for *meta* substitution. (The same values of $\mathbf{x}$ and $\partial\mathbf{x}/\partial r$ are used for *meta* and *para* compounds.)

When the calculations are carried out for benzonitrile, it develops that the total χ from the "*meta* calculations" is 5.02×10^{-3}, whereas for the "*para* calculations" it is 4.76×10^{-3}. They should, of course be the same if the two calculations were entirely equivalent; the difference, which is not large, results from the approximate character of the model. In order to put the values of χ calculated for the *meta* compounds on the same scale as those for the *para* compounds, each total χ for the *meta* derivatives in the benzonitriles was multiplied by the ratio 4.76/5.02.

The essential feature of the calculations for the *meta* compounds is that the effects associated with a particular substituent are of smaller magnitude than for the *para* compounds, because of the smaller influence of ϕ_3 on S at the *meta* carbon atom. This point is made evident by the results obtained using the procedure given above.

For phenols, anilines and similar compounds the same considerations apply, except that one is dealing with the two lowest vacant orbitals in the ring.

SIGMA VALUES FROM REACTIVITIES[1]

BY ROBERT W. TAFT, JR.

College of Chemistry and Physics, The Pennsylvania State University, University Park, Penna.

Received January 27, 1960

Generalized reactivity parameters provide an important source of information on electronic distributions in organic molecules. The schematics for classification and treatment of reactivities of *m*- and *p*-substituted derivatives of benzene in terms of $\sigma\rho$ correlations are presented. The limitations on precise Hammett linear free energy relationships which are imposed by reaction type and solvent conditions are emphasized and recently proposed modifications of the relationship are shown to be intelligible in terms of electronic distribution effects. The bi-section of τ values to contributing inductive and resonance effects adds insight into the electronic effects of substituent groups. The relationships observed support the classical notion that the resonating substituent localizes charge alternately on the ortho and para positions of the ring. Deductions based upon reactivity relationships are shown to be powerfully confirmed by F^{19} n.m.r. shielding parameters for *m*- and *p*-substituted fluorobenzenes.

A. Introduction

In principle the effect of structure on reactivity may be quite complex. The effect of changing structure from R_0 (an arbitrary standard of comparison) to R (a general substituent) on a reaction equilibrium or rate is given by[2,3a]

For equilibria: $\Delta F^0 = RT \ln (k/k_0) = \Delta E_0^0 - RT \ln (\pi Q)$ (1a)

For rates: $\Delta F^{\ddagger} = RT \ln (k/k_0) = \Delta E_0^{\ddagger} - RT \ln (\pi Q^{\ddagger})$ (1b)

for the generalized process

$$R\text{-}Y + R_0\text{-}Y' \rightleftharpoons R_0\text{-}Y + R\text{-}Y' \qquad (2)$$

where Y and Y′ are functional groups (reaction centers) in the reactant state and the product state (for equilibria) or the transition state (for rates), respectively.

The ΔE_0^0 (or $\Delta E_0^{\ddagger}$) term measures the change in potential energy accompanying the reaction process, a quantity which in appropriate cases can presumably be discussed in terms of the effect of electronic distribution. The πQ term involves a quotient of partition functions which is determined by molecular motions. This term may be very complex, especially since most of the systematic reactivity studies have been carried out in solution and motions of the solvent are in some way included in this term. An exact analysis of the contribution of potential and kinetic energy terms to the measured free energy change is unknown. It is apparent, however, in the instance that $\pi Q \cong 1$, $\Delta F^0 \cong \Delta E_0^0$ (or $\Delta F^{\ddagger} \cong \Delta E_0^{\ddagger}$). This simple result can be expected to apply, approximately, in special circumstances.[2,4]

In spite of the potential complexity of the free energy changes of the kind in question, it is possible experimentally to make such determinations with rather good precision. It is further possible to make extremely systematic investigations of the effect of structure on ΔF^0 (or $\Delta F^{\ddagger}$). A very extensive literature of such determinations exists. For these reasons (and those given below), reactivity data in part militate against their potential complexity and provide an important source of information on electronic distributions in organic molecules.

It is a matter of empirical fact that in especially suited reactivity systems, the measured free energy changes are simply and systematically related. Relationships of this kind are known which have broad scopes of applicability. It is difficult to imagine how results of this character could be obtained unless the measured free energy changes are in fact direct measures of (equal or proportional to) the potential energy changes resulting from electronic distribution effects.[2,3b] Hammett first applied this reasoning to the class of reactivities involving *meta* and *para* substituted side-chain derivatives of benzene.[5,6] The present paper will be concerned principally with the knowledge of electronic distributions as deduced from reactivities of this type. Brief consideration will also be given to the empirical confirmation of these deductions based upon powerful new physical techniques for obtaining detailed information on electronic distributions.

B. The Hammett Linear Free Energy Relationship

The linear free energy relationship of Hammett is illustrated in Fig. 1. The approximately quantitative linear relationship between the effects of corresponding *m*- and *p*-substituents on the rates of saponification of ethyl benzoates and on the ionization of benzoic acids in water is shown. A σ-value is defined as log (K/K_0) for the latter reaction, and is presumed to be a substituent parameter independent of reaction type or conditions. Hammett selected the benzoic acid ionization as the standard reaction series because of the availability of accurate data. The slope of the plot in Fig. 1 is the reaction constant, ρ. It is a susceptibility factor reflecting the change in electron density at the reaction center.[7a] A great many reactivities follow this relationship with rather comparable precision. Jaffé in 1953 summarized the fit of available reactivities to the relationship.[7]

C. Limited Linear Free Energy Relationships

(1) **Deviations from the Hammett Relationship.**—Certain reactivities do not correlate at all well with the benzoic acid ionization. These are reactivities aside from those of *ortho* substituted

(1) This work was supported in part by the Office of Naval Research.

(2) L. P. Hammett, "Physical Organic Chemistry," McGraw-Hill Book Co., Inc., New York, N. Y., 1940, pp. 76.

(3) R. W. Taft, Jr., in M. S. Newman, "Steric Effects in Organic Chemistry," John Wiley and Sons, Inc., New York, N. Y., 1956, (a) pp. 563–570; (b) pp. 660–665.

(4) (a) K. J. Laidler, *Trans. Faraday Soc.*, **55**, 1725 (1959). (b) R. P. Bell, "The Proton in Chemistry," Cornell Univ. Press, Ithaca, N. Y., 1959, pp. 69–73.

(5) L. P. Hammett, *Chem. Revs.*, **17**, 125 (1935).

(6) Ref. 2, pp. 184–187.

(7) H. H. Jaffé, *Chem. Revs.*, **53**, 191 (1953); *cf.* also *J. Am. Chem. Soc.*, **81**, 3020 (1959); (7a) *cf.* reference 2f.

derivatives of benzene which frequently deviate because of steric effects.[3,6] For example, Hammett noted that in reactions of the derivatives of phenols and anilines the p-NO_2 and p-CN substituents have correspondingly exalted effects. Recently, H. C. Brown has demonstrated the existence of linear free energy relationships for certain electrophilic reactivities, in which *para* substituents such as CH_3O and CH_3 show substantially exalted effects.[8] Figure 2 illustrates the limited linear free energy relationship obtained for the ionization of phenols in water, 25°. Figure 3 illustrates the rather complete breakdown of the relationship for the rates of decomposition of diazonium salts in water, 29°. Deviations such as those illustrated in Fig. 2 and 3 call for modification of the original Hammett linear free energy relationship, especially if precise correlations and predictions of reactivities are to be achieved. The modifications, which still permit in similar terms certain precise descriptions of broad ranges of reactivity, are quite intelligible in terms of electronic distributions.

(2) Formulation and Classification of the Problem.—The reactivities of m- and p-substituted derivatives of benzene may be considered from either of two points of view. Since both points of view may have distinct advantages depending upon the problem in question, it is essential to distinguish clearly the particular viewpoint. First, one may consider, in the generalized reaction 2, the substituent, R, as the m- or p-X-C_6H_4 group, the standard substituent, R_0, as the unsubstituted phenyl group, and the side-chain reaction centers as the functional groups, Y and Y′. Alternately, one may look upon the variation of structure as involving for the group, R, the m- or p-substituent, X, with the standard substituent, R_0, the H atom. Let us, for the present, pursue the former viewpoint.

If, in reaction 2, there is a change in energy of a particular type of interaction between R and Y (of R–Y) and R and Y′ (of R–Y′) as compared with that between R_0 and Y′ (of R_0–Y′) and R_0 and Y (of R_0–Y), there will result an effect on reactivity attributable to this kind of interaction. Thus a change in resonance interactions is said to produce a resonance effect on ΔF^0 (or $\Delta F^{\ddagger}$) and so on.[3] In the discussion which follows, the generally accepted assumption will be made that the reactivities (ΔF^0 or log (k/k_0) values) of m- and p-substituted derivatives of benzene can be treated as the sum of inductive and resonance effects.[3,6,7]

Quite apparently many of the deviations from precise Hammett linear free energy relationships (*cf.* Figs. 2 and 3) involve systems in which a change in resonance interactions in reaction 2 is expected for p-X-C_6H_4 substituents which are strongly conjugated with either Y or Y′ (hereafter referred to as an Ar–Y resonance effect).[9]

(3) Precise Hammett Relationships for Select *Meta* Substituents.—Taft and Lewis recently have completed a critical examination of the data for eighty-eight reaction series in which substituents effects are relatively large and for which, in general, at least four *meta* substituents had been investigated.[10] While this paper was in preparation, Professor B. M. Wepster kindly provided the author with a manuscript by himself and co-workers in which a similar examination was carried out along

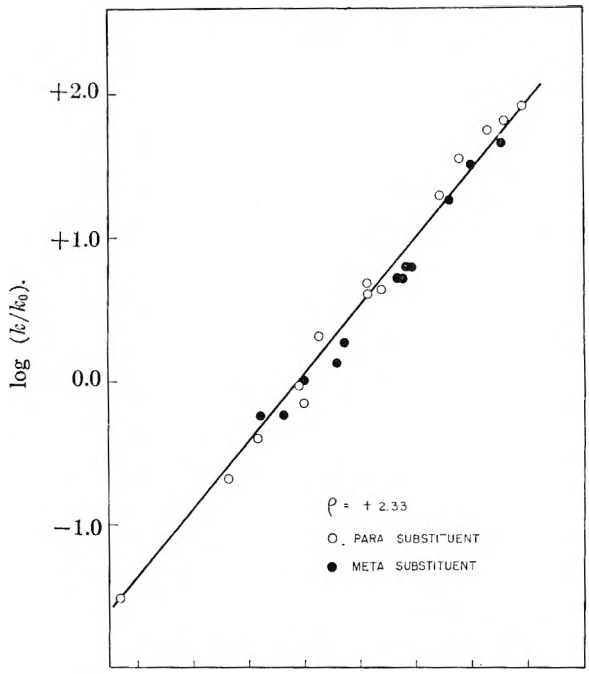

Fig. 1.—Hammett linear free energy relationship, log (k/k_0) = $\sigma\rho$, for the rates of saponification of ethyl benzoates, 60% aq. acetone, 25°. *Cf.* reaction A.15, ref. 10.

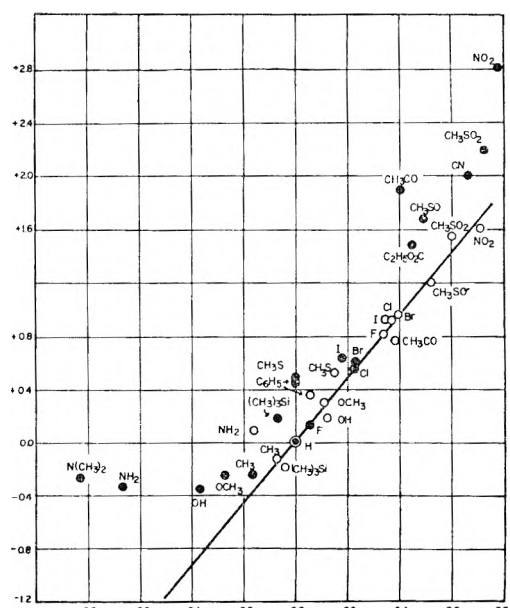

Fig. 2.—Limited linear free energy relationship for ionization of m- and p-substituted phenols and benzoic acids, H_2O, 25°: ordinate gives log (K/K_0) values for phenols and abscissa corresponding values for benzoic acids. Closed circles are for *para* substituents, open circles for *meta*.

(8) H. C. Brown and Y. Okamoto, *ibid.*, **79**, 1913 (1957); **80**, 4979 (1958); *cf.* also N. C. Deno and A. Schriesheim, *ibid.*, **77**, 3051 (1955); and N. C. Deno and W. L. Evans, *ibid.*, **79**, 5804 (1957).

(9) G. E. K. Branch and M. Calvin, "The Theory of Organic Chemistry," Prentice-Hall, Inc., New York, N. Y., 1941, pp. 246–257, 416–419.

(10) R. W. Taft, Jr., and I. C. Lewis, *J. Am. Chem. Soc.*, **81**, 5343 (1959).

somewhat different lines. On nearly all major points, their conclusions are similar to those of Taft and Lewis.[11]

A select group of *m*-X-C_6H_4 substituents exhibit precise linear free energy relationships with much more generality than for other substituents. The mean sigma values for this group are listed in Table I and are designated as σ^0 values. In general, about 90% of the available data for each substituent follow the Hammett equation to a precision of a standard error of ± 0.03 in the sigma value.[10] In no case does the mean value differ from that originally given by Hammett by more than this standard error. Within the standard error of ±0.03 the linear free energy relationships for these substituents are independent of whether the process is rate or equilibrium, the solvents or the temperature. The solvent variation is from non-hydroxylic solvents such as benzene to aqueous solutions. However, for the several substituents indicated in Table I, this degree of precision was achieved only by restriction to the indicated solvent classes. The maximum temperature variation involved is from 273 to 470°K. Each σ^0 value encompasses extremely wide variations in reactivity type.

In contrast to the results for the select group of *meta* substituted phenyl groups, no *para* substituted phenyl substituent was found which meets the same generality and precision criterion. Using the linear free energy relationships for the select group of *meta* substituted phenyl substituents to determine the value of ρ, the reaction constant, effective sigma values, $\bar{\sigma}$, may be obtained for comparison purposes, $\bar{\sigma} = {}^1/_\rho (\log k/k_0)$. The values of $\bar{\sigma}$ obtained for *para* substituted phenyl substituents cover quite substantial ranges, even for series of rather similar reactivities (including the ionization of benzoic acids in various media). In some cases $\bar{\sigma}$ values are actually of opposite sign.[10]

(4) **Interpretation.**—The precise and general linear free energy relationships observed only for the select group of *meta* substituted phenyl substituents are inherently reasonable in terms of the classical qualitative theory of electronic distribution in benzene derivatives, namely, that there is localization of π-electronic charge alternately about a benzene ring in the positions *ortho* and *para* to a resonating substituent, X.[12] In fact, the relationships described above to some extent were anticipated on this basis by Branch and Calvin almost twenty years ago.[9]

The precise and highly general linear free energy relationships for the select group of *meta* substituted phenyl substituents are ascribed to the fact that in general substituents in the *meta* position are not directly conjugated with the side-chain reaction centers, Y and Y′, and thus specific Ar–Y resonance effects do not contribute. The substituent effect

(11) H. Van Bekkum, P. E. Verkade and B. M. Wepster, *Rec. trav. chim.*, **78**, 815 (1959). These authors use the symbol σ^n instead of σ^0 used in the present paper. In general, corresponding values of σ^0 and σ^n do not differ significantly. However, for the *m*- and *p*-$N(CH_3)_3$ and NH_3 substituents and the *p*-F substituent there are, for example, significant differences. In these instances, the author prefers σ^0 values for the reasons set forth in reference 10 and in C-5, C-6, and E-4 of this paper.

(12) C. K. Ingold, *Chem. Revs.*, **15**, 225 (1934); G. W. Wheland and L. Pauling, *J. Am. Chem. Soc.*, **57**, 2086 (1935).

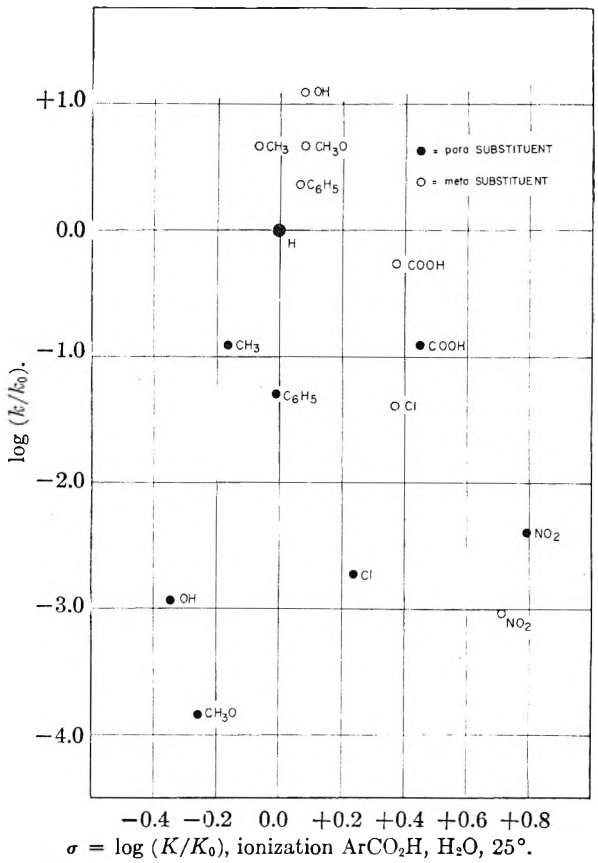

Fig. 3.—Failure of linear free energy relationship for decomposition of benzenediazonium chlorides, H_2O, 29°, *cf.* reaction E.4, ref. 10.

measured is considered to result formally from the inductive transmission (by field or internal bond polarity effects) of charge across the Ar–Y bond. Consequently, if viewed at this position, the reactivity effects described by log $(k/k_0) = \sigma^0\rho$ are appropriately regarded as following an inductive effect relationship (hereafter referred to as Ar–Y inductive effects).

The σ^0-values represent inductive constants for the substituted phenyl groups (R) relative to the unsubstituted phenyl group (R_0). The σ^0-values include contributions, of course, from the resonance interaction of the *meta* substituent, X, with the ring (*i.e.*, conjugative X–Ar interaction in the general system X–Ar–Y) which are considered in detail in section E. It is important to note at this point, however, that substantial evidence is available[10] indicating that the quantitative inductive order for X-C_6H_4 groups can be altered appreciably (especially for the easily polarizable NH_2 and SCH_3 groups) by polarization induced by highly polarizing functional groups, Y and Y′. A formal charge on the first atom of the functional group appears especially effective in this regard. The polarization effect apparently results from the effect on the resonance interaction of the *meta* substituent, X, with the benzene ring.[10]

The rather infrequent deviations from the relationship log $(k/k_0) = \sigma^0\rho$ for *meta* substituted phenyl groups (those exceeding 0.1 sigma unit) are in part due to this cause, although in very

special reactivities the effect of direct conjugation between the *meta* substituent, X, and the side-chain functional group, Y, can lead to deviations.[13] Specific interactions (especially H-bonding) between solvent and the substituent, X, can also alter the Ar–Y inductive order.[7,14] These solvent effects can be taken into account by assigning a σ^0-value characteristic of a particular solvent class (as given in Table I for the several pertinent substituents).

(5) **Precise Linear Ar–Y Inductive Effect Relationships for *Para* Substituents.**—In order to obtain Ar–Y inductive constants (σ^0-values) for *p*-substituted phenyl substituents, Taft and coworkers selected reactivities in which a methylene group is interposed between the benzene ring and the reaction center.[15] It was assumed that the Ar–"Y" resonance effect would be essentially constant for such a reaction series. The reaction series of this class for which data were available are listed in Table II. The linear free energy relationships for these reactivities appear to be as precise for *para*- as for *meta*-substituted phenyl substituents (with all sigma values precise to a standard error of approximately ±0.03). The σ^0-values so obtained for the *para* substituted phenyl groups are listed in Table I.

TABLE I

INDUCTIVE CONSTANTS FOR THE *meta*- AND *para*-SUBSTITUTED PHENYL SUBSTITUENTS: σ^0-VALUES

Substituent	Position: *meta*[a]	Position: *para*
$-C_6H_4N(CH_3)_2$	−0.15	−0.44
$-C_6H_4NH_2$	− .14	− .38
$-C_6H_4OCH_3$	+ *.13*[b] (+0.06)[c]	−0.12[b] (−0.16)[c]
$-C_6H_4OH$	[d] (+0.04)[e]	[d] (−0.13)[e]
$-C_6H_4F$	+ *.35*	+ .17
$-C_6H_4Cl$	+ *.37*	+ .27
$-C_6H_4Br$	+ *.38*	+ .26
$-C_6H_4I$	+ *.35*	+ .27
$-C_6H_4CH_3$	− *.07*	− .15
$-C_6H_5$	*.00*	.00
$-C_6H_4CN$	+ .62	+ .69[f] (+0.63)[e]
$-C_6H_4CO_2R$	+ .36	+ .46[f] (?)
$-C_6H_4COCH_3$	+ *.34*	+ .46[f] (+0.40)[e]
$-C_6H_4NO_2$	+ *.70*	+ .82[f] (+0.73)[e]

[a] Italicized values indicate the select group of *meta* substituents given in ref. 10. [b] Value for pure aqueous solutions only. [c] Value for non-hydroxylic media and most mixed aqueous organic solvents. [d] Value strongly dependent upon hydroxylic solvent. [e] Value for non-hydroxylic solvents only. [f] Value for pure aqueous and most mixed aqueous organic solvents.

In Table I the substituted phenyl groups listed above the standard phenyl group contain −R *meta* or *para* substituents by Wheland's classification,[16,17] *i.e.*, the substituents, X, release charge by resonance interaction with the ring. The substituted phenyl groups appearing below the phenyl group contain substituents, X, which are +R in character. A negative sign of σ^0 indicates a net charge releasing effect relative to the standard, and a positive sign a net charge accepting effect. It is significant to note for the −R substituted groups that the value of σ^0 is in each case more negative for the *para* than the *meta* substitution. In turn, for the +R substituted groups the value of σ^0 is more positive for the *para* than the *meta* substitution.

TABLE II

p-X–C_6H_4–CH_2–Y REACTIVITIES USED TO DEFINE σ^0 VALUES FOR *p*-SUBSTITUTED PHENYL GROUPS

Reaction[a]		ρ
B.1	Ionization, $ArCH_2CO_2H$, H_2O, 25°	+0.46
B.2	Rate of saponification, $ArCH_2CO_2Et$, 88% aq. EtOH, 30°	+1.00
B.3	Ionization $ArCH_2CH_2CO_2H$, H_2O, 25°	+0.24
B.14	Rate of saponification, $ArCH_2OCOCH_3$, 60% aq. acetone, 25°	+0.73

[a] Reaction designations refer to those given in ref. 10.

The σ^0-values for groups containing +R *para* substituents (but not those with −R *para* substituents, *cf.* section C6) apparently are not distinguishable from those obtained by Hammett within a standard error of ± 0.03. Consequently, the σ^0-values listed for these substituents in Table I (and III) are the average values obtained from all reactivities except those with nucleophilic character.[10] In obtaining these averages it was apparent that the σ^0-values for the +R substituents show a dependence on solvent. The values given in the main column of Table I pertain to aqueous solution and those listed in parentheses pertain to reactivities in the designated media. If no value is given in parentheses, the σ^0-value apparently holds generally independent of solvent.

If the σ^0-values for *para* substituted phenyl groups applied only to precise correlations of reactivities of specifically the $ArCH_2Y$ type, their utility would be so limited as to be of little value. However, a substantial number of other reactivities are correlated by σ^0-values to a precision of ± 0.03 sigma units.[15] Two typical examples are given in Figs. 4 and 5. The crossed circles in these figures designate points for sigma values based upon the ionization of benzoic acids in water (original Hammett σ-values).

(6) **Evaluation of Specific Ar–Y Resonance and Polarization Effects.**—A number of authors have expressed the belief that the sigma value which Hammett derived from the ionization of *p*-methoxybenzoic acid in water, for example, has a measurable contribution from an Ar–Y resonance effect.[18]

(13) Evidence of effects of this kind has been obtained from the polarographic potentials for oxidation of *m*- and *p*-substituted anilines to corresponding radical-ions, I. Fox, R. W. Taft, Jr., and J. M. Schemf, abstracts of papers, Am. Chem. Soc. Meeting, Atlantic City, N. J., Sept., 1959, p. 72-P.

(14) H. K. Hall, Jr., *J. Am. Chem. Soc.*, **79**, 5441 (1957).

(15) R. W. Taft, Jr., S. Ehrenson, I. C. Lewis and R. E. Glick, *ibid.*, **81**, 5352 (1959).

(16) G. W. Wheland, "Resonance in Organic Chemistry," John Wiley and Sons, Inc., New York, N. Y., 1955, pp. 429.

(17) The Wheland classification of a −R effect is equivalent to the +T effect, in Ingold's classification (C. K. Ingold, "Structure and Mechanism in Organic Chemistry," Cornell University Press, Ithaca, N. Y., 1953, p. 64). The conformity of both rate and equilibrium processes to the linear free energy relationships provides no evidence for the necessity to distinguish the T-effects for the former processes as E-effects and those for the latter as M-effects.

(18) *Cf.*, for example (a) ref. 9; (b) F. G. Bordwell and P. J. Boutan, *J. Am. Chem. Soc.*, **78**, 854 (1956); **79**, 719 (1957); (c) ref. 3, p. 576–578; (d) ref. 11, p. 842.

Such a contribution will result if the isovalent conjugation in the acid

is more important than that in the anion (as is reasonable on several grounds)

In accord with this expectation the σ-values obtained from the ionization of benzoic acids in water are distinctly exalted compared to the corresponding σ^0-values for the *para* substituted phenyl groups containing strong $-$R substituents. The two sets of sigma values (for aqueous solutions) are compared in Table III. The difference, $\sigma-\sigma^0$, is the Ar–Y resonance effect for ionization of benzoic acids in water.[19]

TABLE III

COMPARISON OF σ^0 AND HAMMETT σ-VALUES FOR *para* SUBSTITUTED PHENYL GROUPS

Subst.	σ^0	σ
$-C_6H_4N(CH_3)$	-0.44	-0.82
$-C_6H_4NH_2$	$-.38$	$-.76$
$-C_6H_4OCH_3$	$-.12$	$-.27$
$-C_6H_4F$	$+.17$	$+.06$
$-C_6H_4Cl$	$+.27$	$+.23$
$-C_6H_4Br$	$+.26$	$+.23$
$-C_6H_4I$	$+.27$	$+.28$
$-C_6H_4CH_3$	$-.15$	$-.17$
$-C_6H_5$	.00	.00
$-C_6H_4CN$	$+.69$	.66
$-C_6H_4CO_2R$	$+.46$	.45
$-C_6H_4COCH_3$	$+.46$	$+.50$
$-C_6H_4NO_2$	$+.82$	$+.78$

It is apparent from Table III that the σ^0-values for the groups containing the weak $-$R *para* substituents such as, Cl, Br, CH_3, are not really distinguishable from the Hammett σ-values.

The precise correlation (Fig. 5) of the data of Davis and Hetzer[20] on ion-pair formation of benzoic acids in benzene by σ^0- values is especially noteworthy. The correlation implies that there is essentially no Ar–Y resonance effect (for strong $-$R *para* substituted phenyl groups) as in the ionization of benzoic acids in water. The absence of Ar–Y resonance effects for this reaction does not require that isovalent conjugation in *p*-methoxybenzoic acid, for example, be frozen out in benzene solution. Dipole moment analysis of Rogers[21] indicates that such an interaction exists under these conditions. The correlation implies only that such interaction takes place to the same extent in the ion-pair product as in the reactant benzoic acid.

(19) Several attempts have been made to estimate quantitatively the Ar–Y resonance effects in the ionization of benzoic acids from calculations of the Ar–Y inductive effects by field electrostatic theory, *cf.*, for example, J. N. Sarmousakis, *J. Chem. Phys.*, **12**, 277 (1944). In general agreement between this method and the empirical σ^0-method is poor. However, in the case of the four *para* halogen substituted phenyl groups the agreement between the values given by Sarmousakis and the $\sigma-\sigma^0$ values is reasonably quantitative.

(20) M. M. Davis and H. B. Hetzer, *J. Research Natl. Bur. Standards*, **60**, 569 (1958).

(21) M. T. Rogers, *J. Am. Chem. Soc.*, **77**, 3681 (1955).

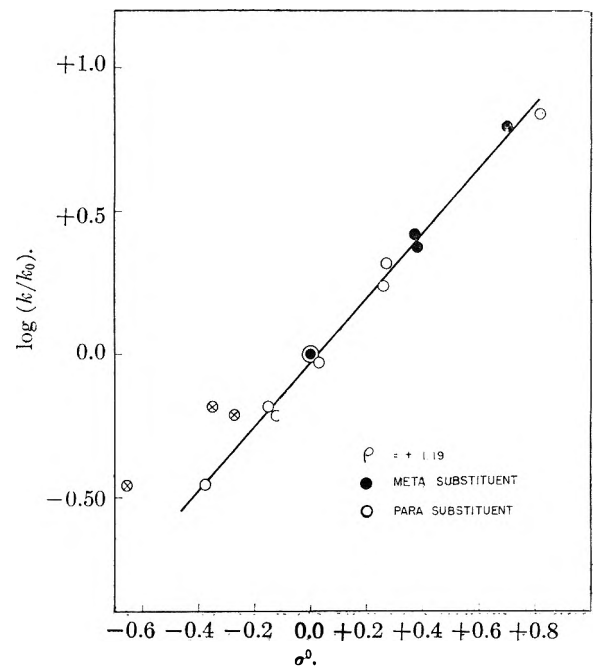

Fig. 4.—Ionization of $ArPO_2(OH^-)$, H_2O, 25°, correlated by σ^0 values. *Cf.* reaction B.6, ref. 10. The crossed circles designate points based upon original Hammett σ-values where these differ in a significant way (*cf.* Table III) from the σ^0 values.

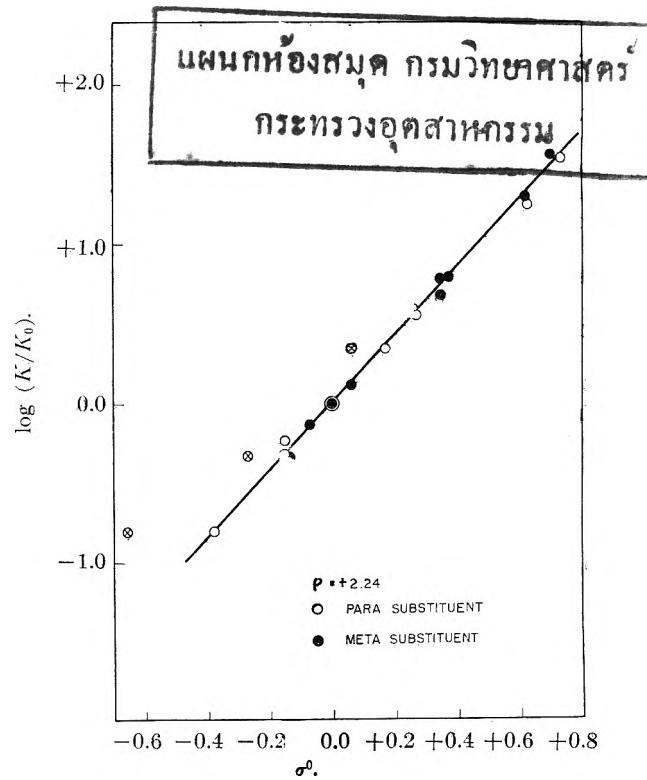

Fig. 5.—Ion-pair equilibria, $ArCO_2H$ with 1,3-diphenylguanidine, benzene, 25°, correlated by σ^0 values. *Cf.* reaction A.13, ref. 10. The crossed circles designate points based upon original Hammett σ-values where these differ in a significant way from the σ^0 values.

It is highly probable, however, that such a condition arises as a consequence of the fact that the fractional contribution of the dipolar isovalent resonance form (above) to the resonance hybrid of

the substituted benzoic acid does make a substantially smaller contribution in benzene solution than in the more ionizing aqueous solution. Solvent effects of this kind have been proposed earlier by Gutbezahl and Grunwald[22] and have been considered by Davis and Hetzer in interpretation of their results.

It is of interest in this connection that unequivocal evidence has been reported based upon the shielding parameters from the F^{19} nuclear magnetic resonance spectra of *m*- and *p*-substituted fluorobenzenes which shows that dipolar resonance structures, *e.g.*

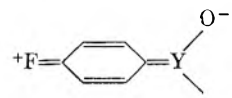

make increasingly greater contributions to the resonance hybrid in more ionizing media.[23]

The σ^0-values have general utility in the identification and study of specific polarization and Ar–Y resonance effects which are dependent upon both solvent conditions and reaction type. Deviations from the relationship $\log (k/k_0) = \sigma^0\rho$ provide a measure of such effects. This use of σ^0-values has been illustrated.[10,11] The Ar–Y resonance effects obtained by this procedure have been represented[3] by the symbol ψ.

D. Concerning ρ-Values

The reaction constants, ρ, obtained from the precise linear free energy relationship for the select group of *meta* substituted phenyl substituents in acid ionization equilibria in aqueous solution are instructive. All of the available values conform to the relationship $\rho = (2.8 \pm 0.5)^{1-i}$, where i = the number of "saturated" links intervening between the benzene ring and the atom at which there is a unit decrease in formal charge on ionization of the proton.[24] This relationship is followed in a manner roughly independent of the charge type of the acid or the kind of atoms involved. It represents a special case of the Branch and Calvin scheme for treating inductive effects in acid ionization equilibria.[25] This relationship, besides having value as a useful empirical tool, serves to show that ρ is a measure of the change (for the reaction process) of the electron density at the reaction center.

Hine has proposed[26] that the value of ρ can be obtained from the σ-values of substituent groups involved at the functional centers, Y and Y′. Evidently, the change in formal charge of an atom can be represented approximately by a substituent parameter (about 0.75 sigma unit for each unit increase in formal charge of the first atom of the functional center).

E. The Separation of Log (k/k_0) Values to Contributing X–Ar Inductive and Resonance Effects

(1) Linear Inductive Effect Relationships in the Aliphatic Series.

—It is useful now to consider the alternate viewpoint of the effect of structure on the reactivity of *m*- and *p*-substituted derivations of benzene. That is, the substituent (R) of eq. 2 is now to be regarded as the *m*- or *p*-substituent, X, and the functional group (Y or Y′) is a side-chain substituted phenyl group. By adopting this point of view we turn attention to the effects on reactivity which result from interactions taking place (formally) through the X–Ar bond (instead of the Ar–Y bond which we have been considering to this point). Such an empirical analysis is permitted by results obtained from the consideration of reactivity effects in the aliphatic series.

The inductive effects of substituent groups in reactions in the aliphatic series (*i.e.*, R in R–Y) are correlated by an equation of the same form as Hammett's $\sigma\rho$ relationship (*i.e.*, $\sigma^*\rho^*$).[27] Although reactivities in the aliphatic series are frequently complicated by specific steric, resonance and other effects, an appreciable variety of reactivity types has been found in which these effects are apparently constant and the relationship, $\log (k/k_0) = \sigma^*\rho^*$, holds. These inductive effect correlations have been reviewed recently.[28]

(2) Parameters Applicable to X–Ar Inductive Effects.

—The generality of the correlations of inductive effects in the aliphatic series leads to the hypothesis that the same inductive order holds for substituents bonded to an aromatic as to an aliphatic carbon atom.[27,28]

The aliphatic series inductive sigma values (for the substituent, X) on a scale for direct comparison with aromatic sigma values, can be obtained by the defining equation[27]

$$\sigma_I \equiv \left(\frac{1}{6.23}\right)[\log (k/k_0)_{OH} - \log (k/k_0)_{H^+}]$$

where k's refer to rate constants for the ester hydrolysis reactions

$$XCH_2CO_2Et + H_2O \xrightarrow[k_{H^+}]{k_{OH^-}} XCH_2CO_2H + EtOH$$

The logarithmic difference on the right-hand side of this equation is a measure of the substituent effect on the free energy difference between two transitions states of closely identical steric requirements but of opposite charge types. Ingold had suggested previously that such a quantity would provide a good experimental measure of the inductive effect.[29] The basis for the 1/6.23 factor has been discussed.[28] For present purposes, suffice it to say that it is essentially equal to (coincidentally) an empirical fall-off factor for the inductive effect of the substituent X, acting through an interposed benzene ring.

Table IV shows the periodic relationship of the σ_I parameters. Comparison is made between the values of σ_I and the relative electronegativities of

(22) B. Gutbezahl and E. Grunwald, *J. Am. Chem. Soc.*, **75**, 559 (1953).

(23) R. W. Taft, Jr., R. E. Glick, I. C. Lewis, I. Fox and S. Ehrenson, *ibid.*, **82**, 756 (1960).

(24) R. W. Taft, Jr., and I. C. Lewis, *ibid.*, **80**, 2436 (1958); *cf.* also ref. 10 and additional examples provided in Table II of this reference.

(25) Reference 9a, pp. 201–225.

(26) J. Hine, *J. Am. Chem. Soc.*, **81**, 1126 (1959).

(27) (a) R. W. Taft, Jr., *ibid.*, **75**, 4231 (1953); (b) ref. 3, Chapter 13; (c) R. W. Taft, Jr., *J. Chem. Phys.*, **26**, 93 (1957).

(28) R. W. Taft, Jr., N. C. Deno and P. S. Skell, *Anal. Rev. Phys. Chem.*, **9**, 292 (1958).

(29) C. K. Ingold, *J. Chem. Soc.*, 1032 (1930).

Pauling,[30] and the inductive constants, I_A, of Branch and Calvin.[25] The latter were obtained from acidities of X–OH compounds in water. Although there is generally a satisfactory qualitative correlation of σ_I and electronegativity, the relationship is by no means quantitative. The reasons for the lack of a better quantitative correlation are not fully understood at present.[31] On the other hand, the correlation with Branch and Calvin constants is satisfactorily quantitative, as shown in Fig. 6.

The order of σ_I-values is in general distinctly different from the order of observed effects of *meta* and *para* substituents in any known reactivity. This unique character has been previously illustrated,[32] for example, by the wide scattering of points in a plot of log (K/K_0) values for the ionization of benzoic acids in water *vs.* corresponding σ_I-values. Values of σ_I are tabulated in reference 24.

TABLE IV

PERIODIC RELATIONSHIP OF THE INDUCTIVE CONSTANTS, σ_I AND I_a, AND PAULING'S ELECTRONEGATIVITIES, X

	CH_3	NH_2	OH	F
σ_I	−0.05	+0.10	+0.25	+0.52
I_a	−0.4	+1.3	+4	+9
$X - X_H$	+0.4	+0.9	+1.4	+1.9
	SiH_3	PH_2	SH	Cl
σ_I	−0.10	+0.06	+0.25	+0.47
I_a	...	+1.1	+3.4	+8.5
$X - X_H$	−0.3	0.0	+0.4	+0.9
		AsH_2	SeH	Br
σ_I		+0.06	+0.16	+0.45
I_a		+1.0	+2.7	+7.5
$X - X_H$		−0.1	+0.3	+0.7
			TeH	I
σ_I			+0.14	+0.38
I_a			+2.4	+6
$X - X_H$			...	+0.4

Two independent direct lines of evidence have been obtained which support the hypothesis that σ_I-values are acceptable empirical measures of the inductive order of substituent groups bonded to aromatic carbon, *i.e.*, of X–Ar inductive effects. In both cases physical property–reactivity correlations are involved.

Wepster[33] has reported a linear relationship (Fig. 7) between the effects on the ultraviolet extinction coefficient and on the base strength produced by the introduction of groups which sterically inhibit the resonance interaction of the nitro group in substituted *p*-nitroanilines. If it is assumed that complete steric inhibition of resonance of the nitro group will reduce the extinction coefficient to approximately zero, then by a very short extrapolation of this relationship it may be estimated that the effect on base strength (which must now be due to the inductive effect only) is 1.8 log units. This value divided by the reaction constant, ρ, gives the "aromatic" σ_I-value for the nitro group, *i.e.*, a value of + 0.62. The σ_I-value from aliphatic

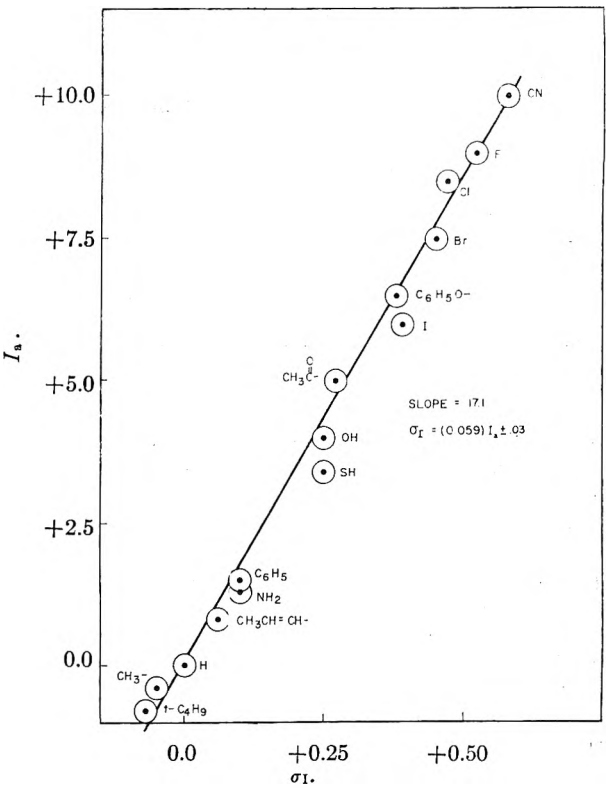

Fig. 6.—Relationship between Branch and Calvin inductive constant, I_a, and σ_I-values.

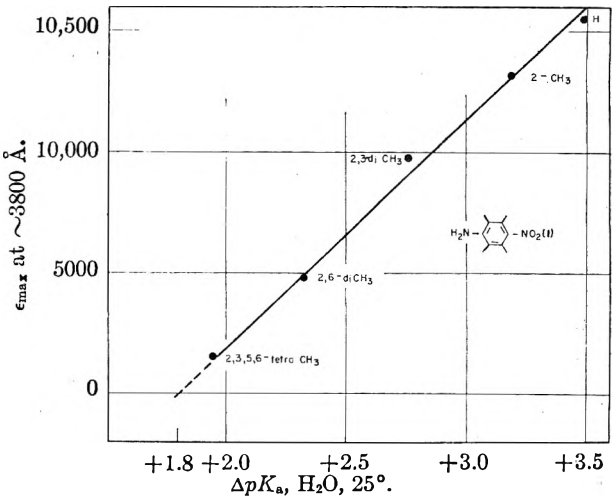

Fig. 7.—Wepster's correlation of the effects of steric inhibition of resonance of the nitro group in methyl substituted *p*-nitroanilines on ultraviolet absorption and base strength.

series reactivities is +0.63, an altogether satisfactory agreement. By a similar means Taft and Evans[34] have shown that complete steric inhibition of resonance of the OCH_3 and $N(CH_3)_2$ groups give sigma values equal to σ_I.

The second line of direct evidence is the correlation of the shielding parameters for *meta* substituents in the F^{19} nuclear magnetic resonance spectra of fluorobenzenes by σ_I-values. This correlation is

(30) L. Pauling, "Nature of the Chemical Bond," Cornell University Press, Ithaca, N. Y., 1944, p. 60.

(31) *Cf.* discussion of ref. 27.

(32) R. W. Taft, Jr., and I. C. Lewis, *Tetrahedron*, **5**, 213 (1959).

(33) B. M. Wepster, *Rec. trav. chim.*, **76**, 335, 357 (1957).

(34) R. W. Taft, Jr., and H. D. Evans, *J. Chem. Phys.*, **27**, 1427 (1957).

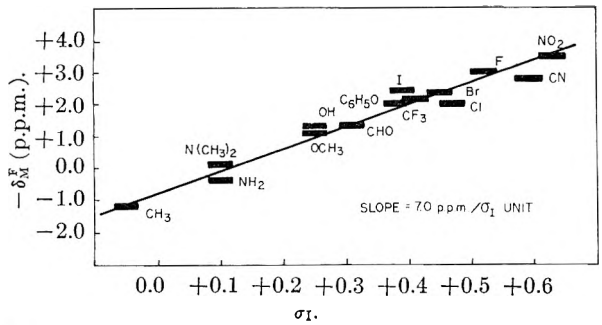

Fig. 8.—Correlation of n.m.r. shielding parameter, δ_M^F, for *meta*-substituted fluorobenzenes with inductive parameter, σ_I.

shown in Fig. 8. The shielding parameters (in p.p.m.) shown in Fig. 8 have been obtained in very dilute carbon tetrachloride solutions.[15,35] Nearly equivalent results have been obtained for very dilute methanol and aqueous methanol solutions.[35] The correlation is remarkable in view of the wide range of resonance capacities of the substituents included in the relationship, a point to be considered further in section G. The relationship of Fig. 8 is particularly significant since the n.m.r. parameters are apparently measures of the inductive perturbations of the *meta* substituents on the charge density in the immediate vicinity of the fluorine atom. These parameters therefore are measures of the inductive order in a single state (the fluorobenzene) rather than in the difference between two states as is always involved in reactivities.

For these and reasons which follow, it is considered a satisfactory and useful approximation to treat generally the effects of *m*- and *p*-substituents on the reactivities of benzene derivatives according to the additive relationships[10,24]

$$\log (k^m/k_0) = I + R^m = \sigma_I\rho + R^m$$

and

$$\log (k^p/k_0) = I + R^p = \sigma_I\rho + R^p$$

The term $\sigma_I\rho$ is the estimated effect (hereafter called the X–Ar inductive effect) on log (k/k_0) values resulting formally from inductive interaction through the X–Ar bond for the hypothetical molecule which involves no resonance interactions through this bond. The R value is the total effect on the log (k/k_0) value resulting from resonance (or additional) interactions which take place through the X–Ar bond. It is the sense of this proposed separation that any inductive effects which arise as a consequence of the resonance interaction are included in the R values.[10]

In further support of the hypothesis that σ_I-values are applicable to aromatic reactivities in general, Taft and Lewis have shown that the assumption of a roughly linear relationship between corresponding R^m and R^p values for a *given reaction series* permits an approximate evaluation of "aromatic" σ_I-values.[10,24] The method has been somewhat modified by Roberts and Jaffé,[36] who show statistically its wide applicability. In Table V are shown some typical "aromatic" σ_I-values obtained in the manner of Roberts and Jaffé from the log (k/k_0) values for the indicated reaction series. The agreement between the σ_I-values is of a precision closely on the order of a standard error of ± 0.03.

It follows consequently that the dispersion (especially of *para* substituents) in linear free energy plots of aromatic series reactivities (*e.g.*, Fig. 2 and 3) is attributable to good approximation to the dependence of R values on reaction type and conditions.[10]

(3) The Evaluation of X–Ar Resonance Effects (R Values).—The use of the $\sigma_I\rho$-term to evaluate resonance contributions (R values), *i.e.*, R = log $(k/k_0) - \sigma_I\rho$, offers two generally promising avenues of attack on reactivity problems.

TABLE V

"AROMATIC" σ_I-VALUES DERIVED FROM VALUES OF LOG (k^m/k_0) AND LOG (k^p/k_0) BY METHOD OF ROBERTS AND JAFFÉ[a]

Subst.	A.1 Ioniz. $ArCO_2H$ H_2O, 25°	C.9 Ioniz. $ArNH_3^+$ H_2O, 25°	E.4 Decomp. ArN_2^+ H_2O, 29°	C.4 Ioniz. ArSH 48% aq. EtOH, 35°	F.2 $ArCH_3$ $+Cl_2$ 70°	"Aliphatic" σ_I
CH_3	−0.03	−0.02	−0.01	−0.04	−0.06	−0.05
NH_2	+ .04	+ .11		+ .10		+ .10
C_6H_5	+ .09	+ .14	+ .07		+ .09	+ .10
OCH_3	+ .28	+ .27	+ .26	+ .32		+ .29
CH_3CO	+ .32	+ .27		+ .27		+ .28
CF_3	+ .38	+ .32				+ .41
Br	+ .45	+ .42		+ .44		+ .45
Cl	+ .42	+ .43	+ .45	+ .46	+ .48	+ .47
F	+ .45	+ .55				+ .52
CN	+ .52	+ .56			+ .50	+ .58
NO_2	+ .68	+ .60	+ .66	+ .66		+ .63

[a] Reaction designation refer to those as listed in Table II of ref. 10.

First, precise empirical relationships between R values for similar reactivities provide a means of making accurate predictions and correlations of reactivities. These empirical relationships *and their limitations* provide a means of studying the factors which determine R values. The specific nature of R values offers a valuable tool in establishing the nature of transition states in mechanism studies. Secondly, the empirical evaluation of R values provides an "observable" which may be given theoretical consideration, for example, by the π-electron model. An example of such a treatment is given brief comment in later discussion related to Fig. 10.

(4) X–Ar Resonance Effect Parameters.—At the considerable risk of vulnerability in the matter of discussing the perplexities of nature in terms of a profusion of symbols, it is frequently convenient to express R values in sigma units.[10] This may be done by dividing through the above relationship by the ρ-value. Thus, in general, the "effective" $\bar{\sigma}_R$-value is obtained from the "effective" $\bar{\sigma}$-value by subtracting the value of σ_I: $\bar{\sigma}_R = {}^1/_\rho[\log (k/k_0) - \sigma_I\rho] = \bar{\sigma} - \sigma_I$. If the value belongs to one of the various classes having limited generality, a resonance parameter characteristic of that class of reactivity is obtained. If used within its appropriate reactivity class, this resonance parameter is capable of giving precise correlations and predictions.

For example, an X–Ar resonance effect parameter is obtained for the limited group of "electrophilic"

(35) Unpublished results.

(36) J. L. Roberts and H. H. Jaffé, *J. Am. Chem. Soc.*, **81**, 1635 (1959).

reaction series which are correlated by the σ^+ parameter,[8] *i.e.*, $\sigma_R^+ = \sigma^+ - \sigma_I$. Similarly, for the limited group of "nucleophilic" reaction series which are correlated by σ^--values,[7,28] one obtains the X-Ar resonance effect parameter $\sigma_R^- = \sigma^- - \sigma_I$. Sigma values corresponding to what has been called the resonance polar effect[3] are obtained from the Ar–Y inductive constants, σ^0, *i.e.*, $\sigma_R^0 = \sigma_0 - \sigma_I$.

Since the σ_R^0 parameters for the select group of *meta* substituents have very great general applicability, it is of especial interest to examine these X–Ar resonance effect parameters. This may be done by reference to Fig. 9 in which σ_R^0 values for *meta* substituents, X, are plotted *vs.* σ_R^0 values for corresponding *para* substituents. Values of σ_R^0 are tabulated in ref. 10. The order of substituents along the correlation line in Fig. 9 is Ingold's well-known mesomeric order.[37] The $-$R substituents (*meta* or *para*) have negative resonance parameters and those for the $+$R substituents are positive. The relatively highly precise correlation of these two resonance parameters[10] (which is exact within the precision of the parameters or their solvent dependence) is of interest. This result is reasonable on the basis of conclusions reached earlier[10,11] concerning the parent sigma values, namely, that neither of the parameters is affected by direct specific interactions between the substituent, X, and side-chain reaction centers, Y and Y′. A similar plot of corresponding σ^0-values leads to a wide scattering of points indicating that the separation to σ_R^0 and σ_I-values is essential to achieving the simple relationship of Fig. 9.

Both the non-zero values of σ_R^0 for *meta* substituents and the slope (α) of ~ 0.5 obtained in Fig. 9 may be accounted for by classical valence bond structures and an empirical inductive effect fall-off per bond. This is illustrated below by the structures in which equal charges are shown localized in the positions *ortho* and *para* to the substituent, X. If the usual fall-off factor per bond of approximately $^1/_3$ is employed,[25] it follows that the net charge accumulated on Y is six-tenths as great when the substituent, X, is in the *meta* as in the *para* position. While this relationship undoubtedly is over-simplified, it appears to deal adequately with the approximate empirical relationship of Fig. 9

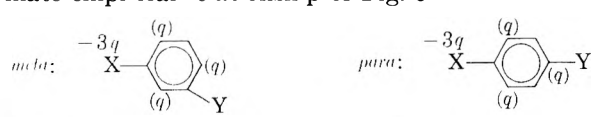

$$\text{“}\alpha\text{”} = \frac{\text{“effective charge” from } meta \text{ X}}{\text{“effective charge” from } para \text{ X}} = \frac{2q(1/3) + 2q(1/3)^3}{q + 2q(1/3)^2} \cong 0.6$$

(5) Further Remarks on Specific Character of X–Ar Resonance Effects.—In general, it is found that precise correlations of "effective" $\bar{\sigma}_R$ parameters are limited to closely related reactivities and reaction conditions.[10] An example of the dispersion which may appear in plots of X–Ar resonance effects is illustrated by a plot of σ_R^+ *vs.* σ_R^0 for $-$R substituents, as shown in Fig. 10. In this plot only a limited precise linear relationship is found.

(37) C. K. Ingold, "Structure and Mechanism in Organic Chemistry," Cornell University Press, Ithaca, N. Y., 1953, Chapter VI.

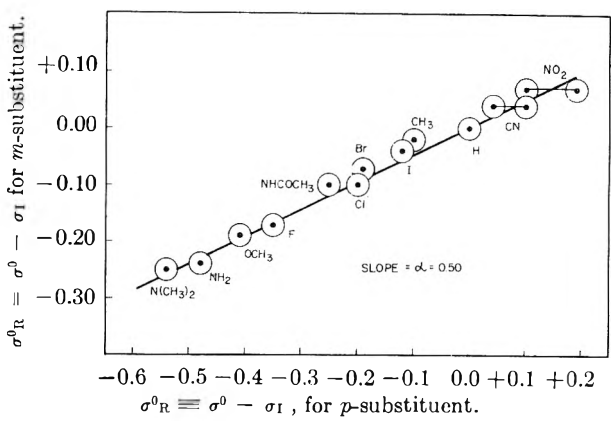

Fig. 9.—Resonance effect fall-off factor, α, between *meta* and *para*-positions for the σ^0 scale.

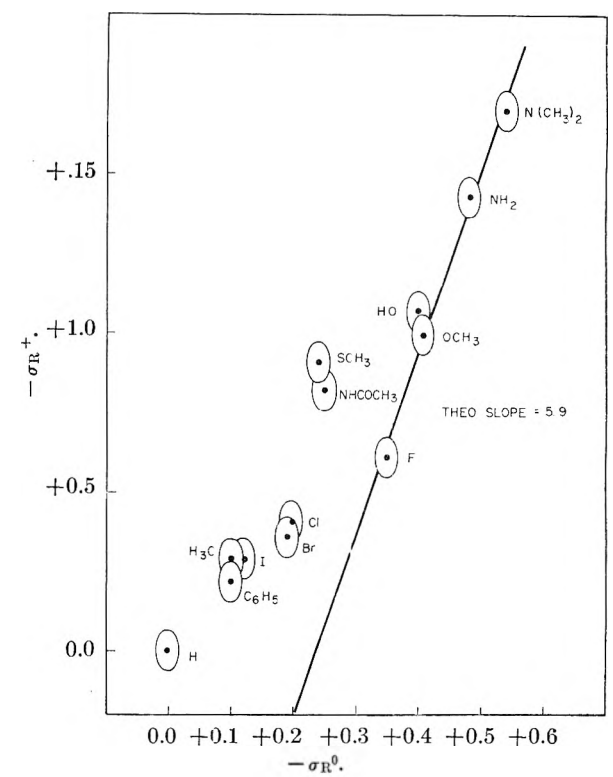

Fig. 10.—Resonance effect exaltation factor for $-$R *para*-substituents in σ^+ and σ^0 reactivities.

In unpublished work Ehrenson, Goodman and Taft have derived models for consideration by the naive LCAO–MO method of the exalted resonance effects of $-$R *para* substituents in σ^+ as compared to σ^0 reactivities. The method makes the basic assumption that the σ_R^+ and σ_R^0 parameters are proportional to the change in the total π-electronic energy accompanying the reaction process. The exaltation factor for the former parameters predicted by the treatment is that shown as the theoretical slope in Fig. 10. The theory anticipates that the linear relationship of Fig. 10 should not pass through the origin and that it should include the five substituents shown. Only these five substituents involve simple π(p-p)-conjugation of the first atom of the substituent with the benzene ring, for which conjugative electron-release decreases regularly with increasing effective electronegativity (or

TABLE VI

SCHEMATICS FOR TREATMENT OF LOG (k/k_0) VALUES FOR REACTIVITIES OF *m*- AND *p*-SUBSTITUTED DERIVATIVES OF BENZENE

Point of view: X–Ar–Y General substituent: X–C_6H_5– Standard substituent: C_6H_5– (log (k/k_0)		Point of view: X–Ar–Y General substituent: X– Standard substituent: H– log (k/k_0)	
Resonance effects (Ar–Y)	Inductive effects (Ar–Y)	Resonance effects (X–Ar)	Inductive effects (X–Ar)
Frequently estimated by $\psi \equiv \log (k/k_0) - \sigma^0\rho$. In general ψ values are specific to the nature of Y and reaction conditions. However, for a correlation of ψ values for electrophilic reactivities, *cf.* Yukawa and Eaborn[b]	Frequently represented by σ^0; relationship followed: log $(k/k_0) = \sigma^0\rho$	Represented by $\bar{\sigma}_R \equiv \bar{\sigma} - \sigma_I$. In general, $\bar{\sigma}_R$ values show a considerable degree of specificity to reaction type and conditions. Represented in appropriate special cases by σ_R^0, σ_R^-, σ_R^+. Limited relationships followed: $R = \rho'\sigma_R^{(0,+,-)}$	Represented by σ_I; relationship followed: $I = \sigma_I\rho$

[a] Y. Yukawa and Y. Tsuno, *Bull. Chem. Soc. Japan*, **32**, 971 (1959). [b] J. D. Dickinson and C. Eaborn, *J. Chem. Soc.*, 3036 (1959).

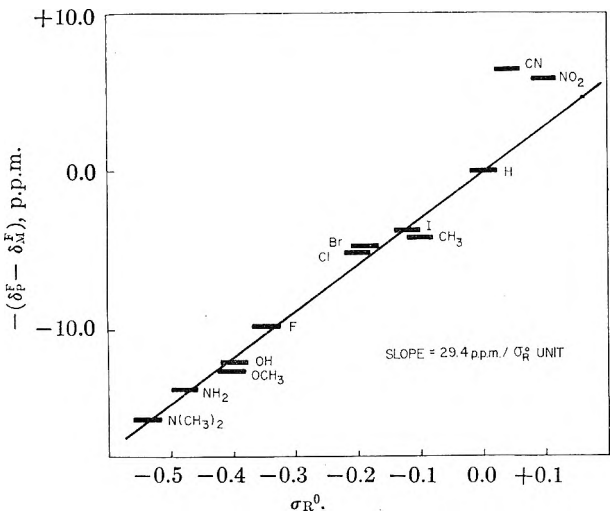

Fig. 11.—Correlation of resonance contribution to the n.m.r. shielding parameter for *para*-substituted fluorobenzenes, $-(\delta_P^F - \delta_M^F)$, with the resonance parameter, σ_R^0.

σ_I value). The deviating substituents all have available open orbitals which undoubtedly are involved in additional conjugation, *e.g.*

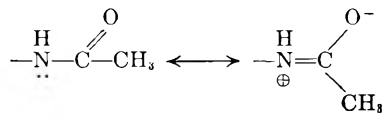

The halogen atoms, Cl, Br and I, have d orbitals of their valence shell which may exert acceptor action in π(p-d) conjugation. This possibility was first pointed out to the author several years ago by Professor J. G. Aston, and is strongly supported by the theoretical calculations reported in his symposium paper by Goodman.[38]

F. Summary of Schematics for Classification and Treatment of Reactivities

In Table VI the schematics for the treatment of the log (k/k_0) values for the reactivities of *m*- and *p*-substituted derivatives of benzene as discussed herein have been summarized.

G. Correlation of Electronic Distribution Parameters from Reactivities with Those Obtained by Physical Means

In conclusion, brief consideration will be made of how empirical physical property–reactivity relationships greatly add to our confidence that both measured properties do provide useful information on electronic distributions. The shielding parameters for *m*- and *p*-substituents in the F^{19} nuclear magnetic resonance spectra of fluorobenzene have found especial utility and may be regarded as illustrative in this connection. These shielding parameters were first investigated by Gutowsky and his students.[39] Their work in the present connection has been so valuable[40] that additional investigations have been initiated and are being further pursued in our laboratory.

Table VII lists values of shielding parameters (in p.p.m.) for some typical *meta* and *para* substituents obtained in "infinitely dilute" carbon tetrachloride solution.[15,36] Positive values of f^F indicate that resonance occurs at a higher field than for unsubstituted fluorobenzene and, accordingly, that the F^{19} nucleus "sees" a greater density of electronic charge.[41] It is immediately apparent that all of the substituents of Table VII exert very different effects from the *para* than the *meta* position. Figure 8 shows that the f_M^F values are quite

(38) (a) L. Goodman, THIS JOURNAL, **64**, 1816 (1960); (b) the order of net charge *release* by conjugation through the X–Ar bond is F > Cl > Br > I > H = 0 (*cf.* Fig. 11). The order expected for π-(p-p) conjugation (based upon ionization potentials) is F < Cl < Br < I. The π(p-d) conjugation is expected to give the following order of charge *withdrawal:* Cl < Br < I. Consequently, a combination of π(p-p) and π(p-d) conjugation in which the former predominates can explain both the net charge releasing effect and the observed halogen order. Apparently, the relative contributions of π(p-p) and π(p-d) conjugation for a given halogen are not strongly dependent upon the side-chain functional group (Y, of X–Ar–Y). This conclusion is dictated by the σ^0 and σ_R^0 correlations (*e.g.*, Fig. 11). The interpretation given here receives additional support from nuclear quadrupole coupling studies of BX_3 compounds. In these compounds π(p-d) acceptor action is not possible and the % double bond character of the B–X bond increases in the order expected for increasing π(p-p) conjugation, *i.e.*, Cl < Br < I *cf.* W. G. Laurita and W. S. Koski, *J. Am. Chem. Soc.*, **81**, 3179 (1959).

(39) H. S. Gutowsky, D. W. McCall, B. R. McGarvey and L. H. Meyer, *ibid.*, **74**, 4809 (1952).

(40) R. W. Taft, Jr., *ibid.*, **79**, 1045 (1957).

(41) J. A. Pople, W. G. Schneider and H. J. Bernstein, "High-resolution Nuclear Magnetic Resonance," McGraw-Hill Book Co., Inc., New York, N. Y., 1959.

precisely correlated by the inductive constants, σ_I (*meta* σ^0-values give a considerably poorer correlation).

TABLE VII

F^{19} SHIELDING PARAMETERS FOR *m*- AND *p*-SUBSTITUTED FLUOROBENZENES IN INFINITELY DILUTE CARBON TETRACHLORIDE SOLUTION (EXP. ERROR = ±0.1 P.P.M.)

para		*meta*	
Subst.	f_{F^P} (p.p.m.)	Subst.	f_{F^M} (p.p.m.)
NMe_2	+15.6	CH_3	+1.2
NH_2	+14.2	NH_2	+0.4
OCH_3	+11.5	NMe_2	−0.1
OH	+10.8	CO_2H	−0.9
OC_6H_5	+ 7.4	OCH_3	−1.1
F	+ 6.8	OH	−1.3
CH_3	+ 5.4	CHO	−1.3
C_6H_5	+ 2.9	CH_3OCO	−1.5
Cl	+ 3.1	C_6H_5O	−2.0
Br	+ 2.5	Cl	−2.0
I	+ 1.5	CF_3	−2.1
H	0.0	COCl	−2.1
CF_3	− 5.1	Br	−2.3
CH_3CO	− 6.6	I	−2.4
CN	− 9.2	CN	−2.8
NO_2	− 9.3	F	−3.0
CHO	− 9.4	NO_2	−3.5

The quantity $-(f_P{}^F - f_M{}^F)$ may be considered an accurate measure of the perturbations in electron density detected by the F^{19} nucleus as the result of resonance interaction of the *para* substituent with the fluorobenzene system.[15,39,40]

It is expected according to classical valence bond theory that the −R *para* substituents cannot conjugate with the fluorine atom of the fluorobenzene so that the charge released by resonance interaction of these substituents must be inductively transmitted to the F^{19} nucleus through the Ar–F bond. Support for this theory is provided by the precise correlation shown in Fig. 11 between values of $-(f_P{}^F - f_M{}^F)$ and the appropriate reactivity resonance parameters, $\sigma_R{}^0$ values (any of the other classes of resonance parameters of section E.4 give poorer correlations).

Conjugation between +R *para* substituents and the fluorine atom of fluorobenzene is anticipated by valence bond theory, and in accord with this theory these substituents shield the F^{19} nucleus substantially less than expected by correlation with the $\sigma_R{}^0$ parameter.[15,40] This relationship is indicated in Fig. 11 by the deviations for the NO_2 and CN substituents (the extent of deviation is substantially greater in hydroxylic solvents[23]).

The correlations of Figs. 8 and 11 cannot be reasonably explained unless the classical notion[12] that the resonating substituent localizes charge alternately on the *ortho* and *para* positions of the ring is a remarkably exact relationship. These correlations demonstrate that the shielding parameters and the reactivities which follow the σ^0-scale are both determined to good approximation by the same generalized quantitative orders of charge-release through the X–Ar bond by the inductive and resonance mechanisms. Further, the separation of the X-Ar inductive and resonance contributions shows that the susceptibilities of the two observables to these factors are very appreciably different.

This is illustrated by the relationships which summarize the several correlations:

For *para* substituents: $\sigma^0 = \sigma_R{}^0 + \sigma_I$

$$-f_P{}^F = (29.7)\,\sigma_R{}^0 + (6.1)(\sigma_I) + c$$

For *meta* substituents: $\sigma^0 = \sigma_R{}^0 + \sigma_I = (0.5)\sigma_R{}^0{}_{(para)} + \sigma_I$

$$-f_M{}^F = (6.1)\,\sigma_I + c$$

By definition, the relative susceptibility of σ^0-values for *para* substituents to $\sigma_R{}^0$ and σ_I is unity. However, the shielding parameters for *para* substituents are *five* times more susceptible to $\sigma_R{}^0$ than σ_I. For *meta* substituents, σ^0-values are, in contrast, 0.5 as susceptible to $\sigma_R{}^0$ (for *para* substituents) as σ_I, whereas the shielding parameters show no measurable dependence upon $\sigma_R{}^0$.

It is puzzling that the shielding parameters for *meta* substituents show a dependence upon σ_I but no detectable dependence upon $\sigma_R{}^0$. Nevertheless it is clear that the grossly different behavior must arise as a consequence of different susceptibilities of the physical observable to the total electronic distribution. The shielding parameter depends upon electron density in the very close vicinity of the F^{19} nucleus (perhaps the electron density localized on the F atom). The reactivities apparently depend upon charges localized more widely throughout the substituted benzene ring (as discussed in connection with Fig. 9).

These relationships point up the urgent need for knowledge of accurate detailed electronic distributions in molecules. Only when this information becomes available will it be possible to develop rigorous theories of structural effects on the electronic distribution in molecules and of the effects of these electronic distributions on various observables.

BONDING IN CONJUGATED HALOGEN COMPOUNDS[1]

BY J. R. HOYLAND[2] AND LIONEL GOODMAN

Whitmore Chemical Laboratory, The Pennsylvania State University, University Park, Pa.

Received March 24, 1960

The effect of inclusion of $d\pi$ orbitals in halogen conjugation is considered. The resulting p-d hybridization yields a considerable increase, ~2 e.v., in bonding energy (greater than that found in Cl_2 through $p\pi$-$d\pi$ hybridization). For conjugated C–Cl bonds the valence state of the chlorine atom is estimated at $p\pi^{1.90}d\pi^{.10}$. The greatly increased C–Cl bond order indicates considerable triple bond character. The factors determining the conditions for $d\pi$-$p\pi$ hybridization are analyzed, and V.B. structures are proposed. In particular, $Y^+ = R = X^-$, where Y is a strong electron donating group, seems to be important. It is suggested that dipole moments, resonance energies and intensities in the ultraviolet spectra of halogen compounds (in particular chloro-, bromo- and iodobenzenes) need reinterpretation in the light of the above.

Introduction

The halogen compounds have been an enigma in the theory of bonding of simply conjugated derivatives of olefinic and aromatic systems. In the interpretation of reactivity data, a mesomeric release of electrons in the order[3] F > Cl > Br > I usually has been utilized for conjugated halogen compounds. However, in the ultraviolet spectra of aromatic halogen compounds, red shifts of the 2600 Å. benzene analog transition are in the order[4]: I > Br > Cl > F, indicating a mesomeric order exactly opposite to that obtained from reactivity considerations. Other sources of electron density information, such as asymmetry parameters and coupling constants[5a] obtained from nuclear quadrupole resonance spectra, solvent effects on reactivities[3] and ultraviolet spectra,[5b] and intensities of halobenzene spectra,[5c] yield one or the other of these mesomeric orderings, seemingly dependent upon the nature of the system bonded to the halogen.

Several authors, notably Mulliken, have pointed out that the halogen atoms, Cl, Br and I, have d-orbitals available in the valence shell for acceptor action[6] suggesting the possibility that the net charge release in conjugated systems is controlled by competition between the donor action of $p\pi$ and the accepter action of $d\pi$ orbitals.

The purpose of this paper is to investigate whether halogen d-orbital participation in conjugation in olefinic and aromatic halogen derivatives is feasible, and whether the apparent paradox in the mesomeric behavior of the halogens can be reasonably understood through d-p hybridization.

Mulliken[6] has demonstrated that the greater strength of the Cl–Cl bond in Cl_2 compared to the F–F bond in F_2 is due largely to the participation of the $3d\pi$ orbitals of chlorine, which are normally unoccupied in the ground state of atomic chlorine, and are usually not taken into account in the LCAO–MO scheme. The inclusion of $3d\pi$ orbitals in the bonding scheme of the Cl_2 molecule was shown by Mulliken to lead to pronounced multiple-bond character because of the increased overlap of the π-orbitals between the two Cl atomic centers. (Presumably the same result should be true for Br_2 and I_2.) Mulliken further concluded that only a small amount of $d\pi$ character is needed for a pronounced increase in double bond character. It was estimated that only 5% $d\pi$ character leads to 20% double bond character in Cl_2.

The participation of d-orbitals in carbon–halogen π-conjugation differs from that in X_2 in four major ways.

(1) The "size" of the carbon $2p\pi$ atomic orbital is considerably smaller than that of a $3p\pi$ chlorine orbital. This causes the overlap between the "natural"[7] Cl $3d\pi$ AO and a "natural" C $2p\pi$ AO in the C–Cl bond to be very much smaller than the overlap between $3p\pi$ and $3d\pi$ Cl orbitals on adjacent centers. The net effect of the small "size" of the carbon $2p\pi$ orbital is to require greater contraction[8] of the 3d Cl orbital for effective overlap and thus the promotion energy is increased relative to that required in Cl_2. Thus this factor will decrease d-orbital participation in the carbon–chlorine resonance relative to that in Cl_2, the same presumably being true for bromine and iodine.

(2) Because of the equivalence degeneracy of the AO on each center, a resonance condition exists in Cl_2 regardless of hybridization. This is not true in the case of the C–Cl bond where this ordering of orbital term values holds: Cl_{3p} (−13 e.v.) < C_{2p} (−11 e.v.) < Cl_{3d} (−1 e.v.). The term value for Cl_{3d} is for the natural orbital (Z = 1.1). Formation of a $p\pi$-$d\pi$ hybrid orbital of the form

$$\pi_{Cl} = \alpha 3p\pi + \beta 3d\pi \qquad (1)$$

causes the resonance condition to be approached, thus making the energy factor more favorable for $p\pi$-$d\pi$ hybridization in the C–Cl bond than in Cl_2.

(3) In any parent conjugated hydrocarbon, the individual orbitals in the Π-MO scheme (Φ_i) differ in their mixing with the Cl $d\pi$-orbital. Because of energetic considerations, the frontier and antibonding MO's in the parent hydrocarbon will in general interact more strongly with the halogen $d\pi$ orbital than the lowest-lying hydrocarbon bonding MO's. In addition to the energy factor the charge order at the substituted carbon atom ($c^2_{i\mu}$) in the

(1) Presented at the Symposium on Electronic Distributions in Organic Molecules at the Atlantic City Meeting of the American Chemical Society, September, 1959.

(2) National Science Foundation, Predoctoral Fellow, 1959–1960.

(3) R. W. Taft, Jr., THIS JOURNAL, **64**, 1805 (1960), and references therein.

(4) F. A. Matsen, *J. Am. Chem. Soc.*, **72**, 5248 (1950).

(5) (a) W. G. Laurita and W. S. Koski, *ibid.*, **81**, 3179 (1959); (b) W. M. Schubert and J. M. Craven, *ibid.*, **82**, 1353 (1960); (c) L. Goodman and L. J. Frolen, *J. Chem. Phys.*, **30**, 1361 (1959).

(6) R. S. Mulliken, *J. Am. Chem. Soc.*, **77**, 884 (1955); R. W. Taft, Jr., *J. Chem. Phys.*, **26**, 93 (1957) and references therein; also private communication with Professor J. G. Aston.

(7) A natural AO here refers to an AO with an effective nuclear charge appropriate to the free atom (Z_{nat}). The term is not to be confused with that of Löwdin and Shull pertaining to spin density considerations (P. O. Löwdin and H. Shull, *Phys. Rev.*, **101**, 1730 (1956)).

(8) The smaller C–Cl internuclear distance (1.69 Å.) compared to the Cl–Cl internuclear distance (1.99 Å.) only partially mitigates this effect.

parent hydrocarbon governs the mixing of Cl $d\pi$ with any given MO

$$\Phi_i' \sim \Phi_i + \frac{C_{i\mu}\beta}{\epsilon_i - \epsilon_{(d)}}\phi_{d\pi} \qquad (2)$$

Since both the charge orders and energies of frontier MO's undergo a variation in a series of parent hydrocarbons, considerable variation in the importance of $d\pi$ interaction is expected.

In addition to the above factors, because of orthogonality considerations, a process of forced mixing takes place in which some of the Cl $d\pi$ character in the antibonding orbitals is transmitted into the bonding (and occupied) orbitals. In Cl_2, mixing of the π_u and π_g MO's is prevented by symmetry considerations, so that the forced mixing referred to above, along with its resulting stabilization, is absent. This latter factor is not as important as the charge-order and energy considerations.

(4) The Π-MO configuration of R–Cl, where R is an alternate hydrocarbon, may be written as

$$\Phi_1'^2\Phi_2'^2 \ldots\ldots \Phi_n'^2\Phi_{Cl}'^2 \qquad (3)$$

where the electron configuration of the parent hydrocarbon is $\Phi_1^2\Phi_2^2$ --- Φ_n^2, Φ_1 --- Φ_n being bonding or non-bonding for alternate hydrocarbons. The π-electron configuration of Cl_2 is, in Mulliken's notation

$$\ldots\ldots(2\pi_u)^4\,(2\pi_g)^4$$

where π_u is bonding and π_g antibonding. The effect of $d\pi$–$p\pi$ hybridization on π_g is to reduce its antibonding nature, whereas no such possibility exists for molecules having configuration (3).

Thus one is led to the conclusion that the key factors which cause $d\pi$–$p\pi$ hybridization to yield a large net bonding effect in Cl_2 differ sufficiently in R–Cl to prevent an analogous argument from being used in these latter molecules. If $d\pi$–$p\pi$ hybridization is to be significant in R–Cl, factor (2) and a favorable factor (3) must overcome the unfavorable factors (1) and (4).

Mention should be made of two additional differences in the interaction of a halogen with a hydrocarbon from the interactions in X_2.

(5) The $d\pi$ AO may interact with $2p\pi$ orbitals centered on non-nearest neighbor atoms. This effect may be considered as quite small.

(6) Donation of charge from the Cl $3p\pi$ orbital into the Π-system of the hydrocarbon leaves the chlorine atom with a formal positive charge, reducing the promotion energy required for hybridization.

Neither factor (5) nor (6) was investigated in any detail in this study.

Π-Bonding in Vinyl Chloride.—The Π-electron wave function for the ground state of vinyl chloride may be written as[9]

$$\Phi'^2_1\Phi'^2_{Cl} \qquad (4)$$

To determine Φ_1' and Φ_{Cl}', along with the corresponding eigenvalues, a secular equation of rank 4 was solved. The evaluation of the matrix elements was carried out in the following manner.

(1) The exchange integral, β_{CX}, for a C–X bond was assumed proportional to the overlap integral

(9) Φ_{Cl} is the delocalized Cl function. $\Sigma a_i\Phi_i + b\pi_{Cl}$.

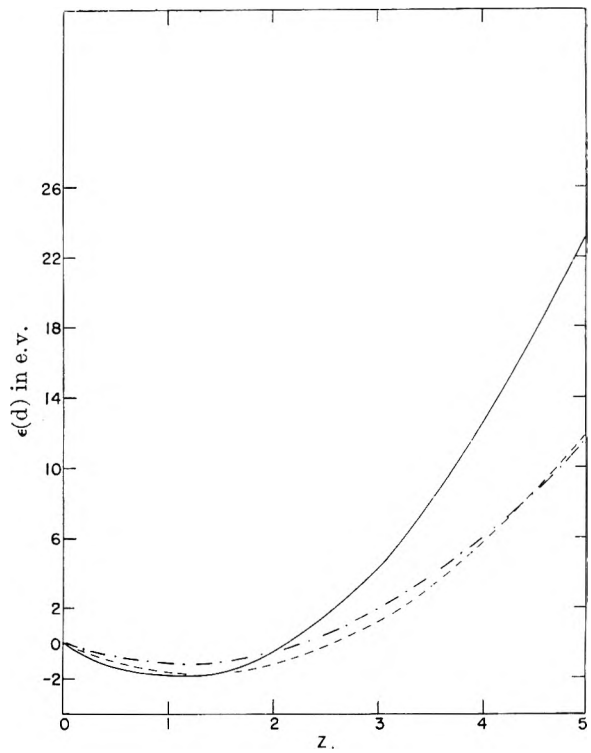

Fig. 1.—Variation of E(nd) in e.v. with Z for the halogens as given by the Virial Theorem: —— Cl; – – –, Br; — · —, I.

S_{CX} (all β_{st} for s,t not nearest neighbors are taken to be zero). Thus β_{CX} is given by the expression

$$\beta_{CX} = \beta_{CC}S_{CX}/S_{CC} \qquad (5)$$

(2) The coulomb integral for a halogen orbital was set equal to the expression

$$\alpha_X = \alpha^0 + E(C) - E(X) \qquad (6)$$

where α^0 is the coulomb integral for a carbon 2 p_z orbital and E(C) amd E(X) are the energies before interaction of a carbon $2p_z$ orbital and an orbital (d or p) of the halogen, respectively. For carbon 2p, E(C) was taken to be −10 e.v. while for the halogen n p orbital, E(X) was set equal to the negative of the observed ionization potential. A numerical value of −3 e.v. was assigned to β_{CC}. This procedure should give reasonable values to the parameters in question.

The energy values E(d), for the d-orbital before interaction with the hydrocarbon were obtained by applying the Virial Theorem as follows. The Virial Theorem states that in a conservative central field system

$$\bar{U} = -2\bar{T} \qquad (7)$$

Here $\bar{U}$ is the average potential energy and $\bar{T}$ the average kinetic energy. The kinetic energy of an electron in an orbital of effective nuclear charge Z depends on Z^2 whereas the potential energy is proportional to Z. Thus we may write

$$E(d) = aZ^2 + bZ \qquad (8)$$

But by the Virial Theorem

$$2aZ^2 \text{ natural} = -bZ \text{ natural} \qquad (9)$$

So that

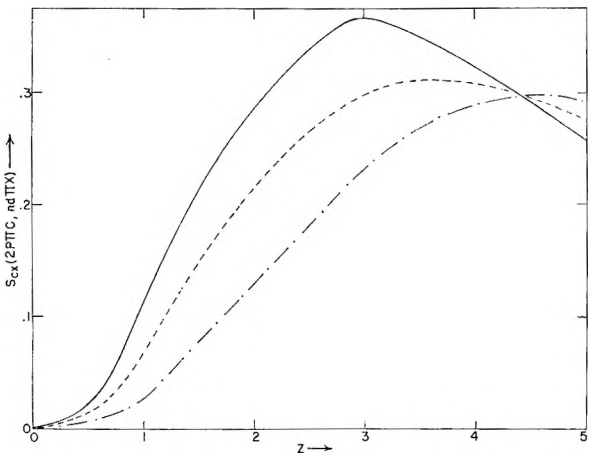

Fig. 2.—Variation of S_{CX} ($2p\pi$, $nd\pi$) with Z for the halogens: ——, S_{CCl} ($2p\pi$, $3d\pi$); – – –, S_{CBr} ($2p\pi$, $4d\pi$); —·—, S_{CI} ($2p\pi$, $5d\pi$).

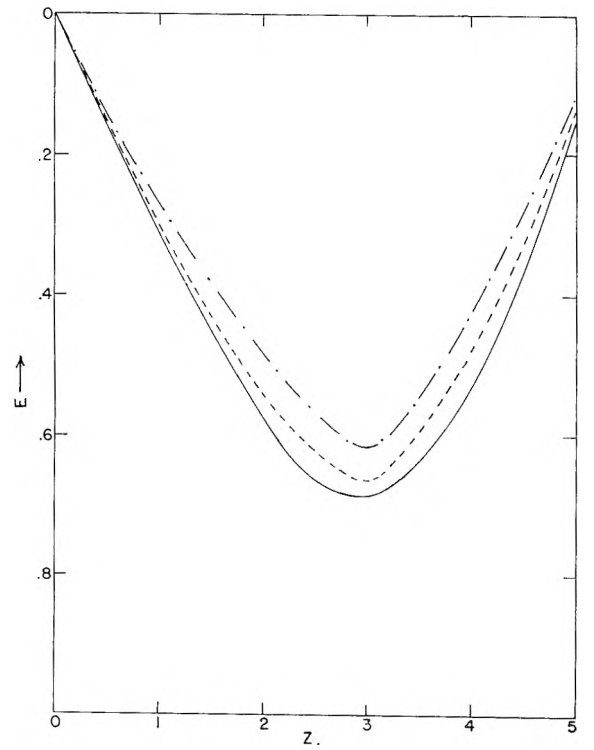

Fig. 3.—Variation of ground state energy (in units of $\beta = -3.0$ e.v.) with Z for some conjugated chloro compounds: ——, vinyl chloride; – – –, *p*-chloroanisole; —·—, chlorobenzene.

$$a = -E(\mathrm{d})\ \text{observed}/Z^2\ \text{natural}$$

Figure 1 shows the variation of the Cl 3d orbital energy as a function of Z. Also shown are the corresponding variations of the 4d and 5d orbital energies of Br and I, respectively.

The contraction of the halogen orbital with increasing Z causes a corresponding increase in the C $2p\pi$-Cl $3d\pi$ overlap integral, S_{CCl} ($2p\pi$, $3d\pi$). The variation of S_{CCl} ($2p\pi$, $3d\pi$) with Z, computed using Slater-orbitals,[10] is shown in Fig. 2. Overlap integrals for the C–Br bond ($2p\pi$, $4d\pi$) and the C–I bond ($2p\pi$, $5d\pi$) are also included for comparison. Because of the increasing uncertainty of the validity of Slater orbitals for these higher shells, however, the Br and I overlap integrals should be regarded as schematic only.

In accord with the Variation Theorem, the value of Z_{3d} was varied until the minimum ground state energy for the molecule was obtained. The problem was programmed for calculation on a digital computor (Pennstac) in the Pennsylvania State University Computing Center.[11] The variation of the ground state energy of vinyl chloride with Z is shown in Fig. 3, the magnitude of the depression of the energy is about 2 e.v. which is somewhat larger than the gain in bonding through $d\pi$-$p\pi$ hybridization in Cl_2.[6] The major portion of the depression in ground state energy (Table I) with $p\pi$-$d\pi$ hybridization occurs because of an increase in the C–Cl bond strength. The remaining and smaller part is due to increased delocalization of the R π-electrons. Some notion of the degree of $d\pi$-$p\pi$ hybridization may be obtained from the computed atomic population (Table I). The atomic population $Cl:3p^{1.92}3d^{0.11}$ corresponds to 5.4% $p\pi$–$d\pi$ hybridization or 4% promotion ($p^2\pi \rightarrow p\pi d\pi$). The excess C–Cl bond order (Table I) corresponds to a 90% increase in double bond character (or to 20% triple bond character,)[12] largely a result of the contribution of the VB structure

$$+\mathrm{C{-}C{=}Cl{-}}$$

(borne out by the computed charge density changes engendered by $d\pi$–$p\pi$ hybridization). At $Z = Z_{min} \sim 3$ these are (sign convention: excess electron density is negative)

$$\begin{array}{ccc} & & \mathrm{Cl}\ -0.13 \\ & \diagup & \\ \mathrm{C{-}C} & & \\ +0.33 & -0.20 & \end{array}$$

The effect of the inclusion of the originally unoccupied Cl $3d\pi$ orbital in the conjugation scheme is to compete with the chlorine mesomeric release of the $3p\pi$ electrons. Thus there is considerably less *net* release to the vinyl group.

Since the charge densities are governed by the competition of the vinyl group orbitals and the Cl $3d\pi$ orbital for the Cl $3p\pi$-electrons, accurate vinyl chloride charge densities will be governed by accurate values for the chlorine coulomb integrals, $\alpha_{3p\pi}$ and $\alpha_{3d\pi}$. In the extremely simplified treatment carried out here these are only roughly obtained and hence no reliance whatsoever should be placed on absolute charge densities calculated by this scheme

Π-Bonding in Chlorobenzene.—The ground state Π-electron configuration of chlorobenzene is

$$\Phi_0'^2\Phi_T'^2\Phi_1'^2\Phi_{Cl}'^2 \qquad (10)$$

where Φ_0', Φ_T', Φ_1', are perturbed benzene orbitals in order of increasing energy.[13] Orbitals of B_2 (C_{2v}) symmetry (Φ_0, Φ_1 plus excited MO's Φ_2, Φ_3) may interact with Cl $3d\pi$ which is also of B_2 sym-

(10) Interpolated from tables given by H. H. Jaffé, *J. Chem. Phys.* **21**, 258 (1953).

(11) The authors gratefully acknowledge the help of Mr. Franklin P. Prosser of this Laboratory and the members of the computer group at the Pennsylvania State University for their assistance and guidance in carrying out the computations.

(12) This corresponds to the contribution of $p_{C\text{-}Cl}$ ($2p\pi$, $3d\pi$) to the total bond order.

(13) M. Goeppert-Mayer and A. L. Sklar, *J. Chem. Phys.*, **6**, 645 (1938).

metry. Orbital $\Phi_{\bar{1}}$ is of A_2 symmetry and hence does not interact with Cl $3d\pi$ but is of proper symmetry to mix with Cl $3d\pi'$. However the leading term in this latter interaction involves overlap with the $2p_z$ functions on the *ortho* carbon atoms of the ring, and hence in practice $\Phi_{\bar{1}}$ (and $\Phi_{\bar{2}}$) are nearly unperturbed.

The variation of the ground state energy with Z of chlorobenzene is shown in Fig. 3 and of bromobenzene is shown in Fig. 4. The Cl orbital population, hybridization values and excess C–Cl bond order are given in Table I. Charge density changes at various atomic centers due to $d\pi$-$p\pi$ hybridization are

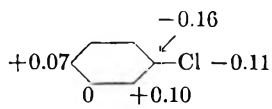

The stabilization energy due to $d\pi$-p-hybridization is slightly less for chlorobenzene than for vinyl chloride reflecting the smaller $d\pi$-$p\pi$ hybridization shown in Table I.

The important contributing V.B. structures in chlorobenzene in addition to the usual ones are

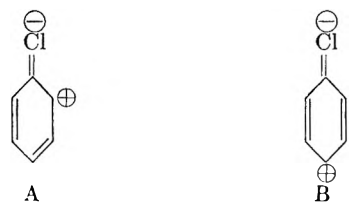

Π-Bonding in *p*-Chloroanisole.—In conjugated chlorine compounds where there is a strongly electron-donating substituent there is the possibility of the Cl-$3d\pi$ orbital acting as an electron acceptor so that cross conjugation can take place. A favorable case should be *p*-chloroanisole, since the $-OCH_3$ group is strongly electron releasing. Structure C, and also less strongly structure D, should be the principal contributing structures for such cross conjugation.

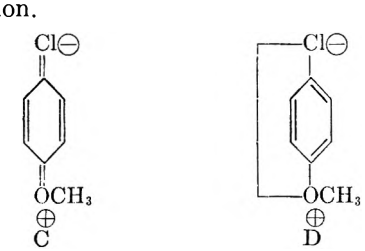

The change in charge density brought about by the inclusion of Cl $3d\pi$ orbitals in the bonding scheme is

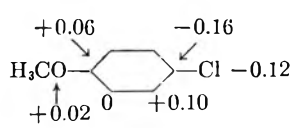

Since the oxygen charge density decreases and the chlorine charge density is greater than 2, we conclude that structure C and possibly structure D are important in the ground state. Other important structures are of course the analogs of A and B (preceding section).

The increased stabilization energy of > 2 kcal. (Table I) compared to chlorobenzene, bears out the importance of these additional structures.

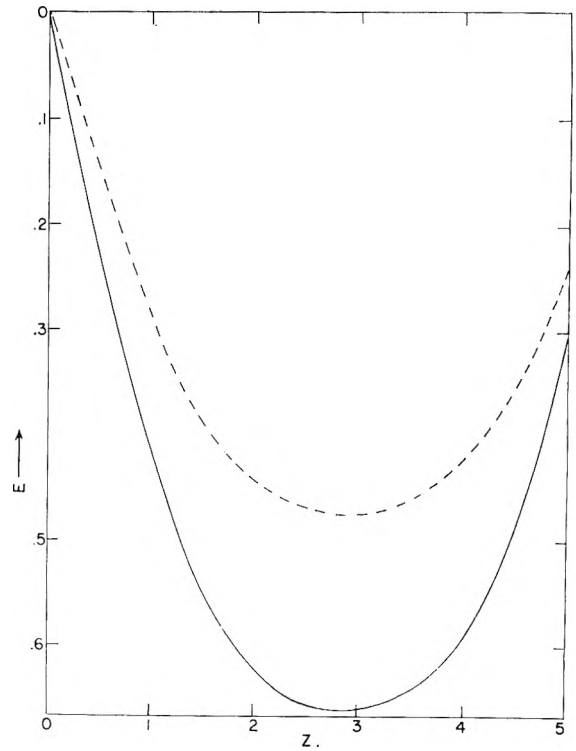

Fig. 4.—Variation of the ground state energy (in units of $\beta = -3.0$ e.v.) with Z for bromobenzene (– – – –) and *p*-bromoanisole (——).

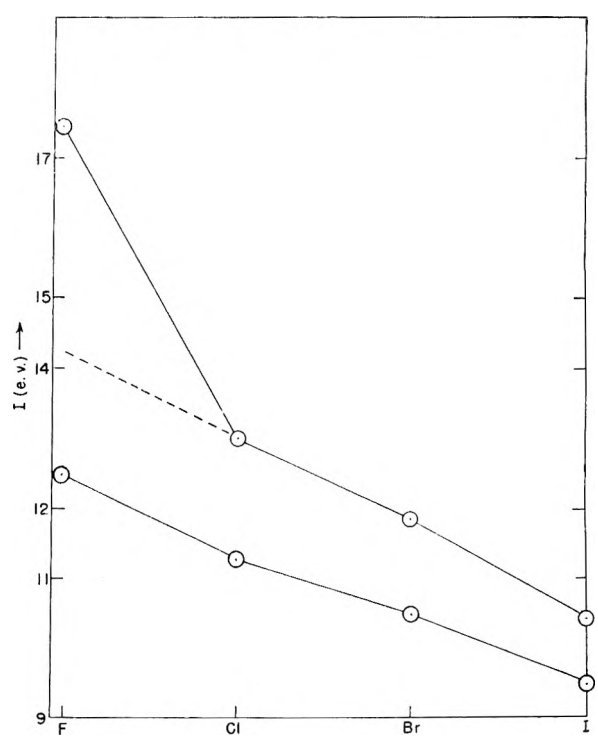

Fig. 5.—Ionization energies of the free halogens and the methyl halides. The upper plot is that for the free halogens.

Remarks on Electronic Structure of Conjugated Fluorine Compounds.—Account must be taken of Factor (6) in applying the preceding calculations

to R-F because of the extremely large electronegativity of F. Figure 5 shows a plot of the ionization potentials of atomic halogens and also of the methyl halides. In all cases except F, a fairly constant interval is maintained between the ionization potentials of the atomic halogen and that of the methyl halide. Maintenance of this constant interval would require the ionization potential of F to be 14.25 e.v. rather than the observed value of 17.52 e.v. It is reasonable to assume that this discrepancy of over 3 e.v. occurs in CH_3F due to the extreme inductive effect of F pulling charge from the carbon atom through the σ framework. The resulting increased shielding lowers the ionization potential. This effect will be important in estimating the effect of d-orbitals on π-bonding in conjugated fluorine compounds, inasmuch as a major increase in shielding of the d-orbitals will result in a large increase in promotion energy. One might be tempted to make a crude estimation. Using Slater rules, the postulated decrease in the ionization potential of over 3 e.v. in CH_3F corresponds to an increased F-electronic charge of approximately 0.6e assuming that the sole effect is an increase in the F 2p population. Therefore a "Natural" $3d\pi$ F orbital is acted upon by a much smaller effective nuclear charge ($Z_{eff} \sim 0.4$) than if there were no F inductive effect. Promotion of $2p\pi$ F to natural $3d\pi$ F ($Z_{eff} = 0.4$) costs only about 13–14 e.v.; however, the overlap is vanishingly small. Promotion to $3d\pi$ F with Z_{eff} increased to maximize S_{CF} ($2p\pi$, $3d\pi$) ($Z_{eff} \sim 3$) costs well over 50 e.v. This high promotion energy is prohibitive as far as obtaining any appreciable gain in bond energy through $p\pi$–$d\pi$ hybridization. (For comparison promotion of $3p\pi$ Cl to $3d\pi$ Cl ($Z_{min} = 3$) costs roughly 15 e.v. and $4p\pi$ Br to $4d\pi$ Br ($Z_{eff} = 3$) perhaps 10 e.v.) In the case where no shielding can be brought about by the F inductive effect (*e.g.*, F_2) promotion of $2p\pi$ F to natural $3d\pi$ ($Z_{eff} = 1.0$) costs about 16 e.v., and promotion with $Z_{eff} = 3$ costs only about 30 e.v. It is thus clear that the large inductive effect of F acting on a carbon skeleton[14] is strongly inimical to $d\pi$-$p\pi$ hybridization.

Conclusions

On the basis of the preceding results $d\pi$–$p\pi$ hybridization appears to be important in conjugated Cl compounds. Presumably this also is true in conjugated Br and I compounds. Some additional points should be mentioned, however.

The Cl $4p\pi$ orbital has approximately the same energy as Cl $3d\pi$ and the overlap integral S_{CX} ($2p\pi$, $4p\pi$) varies with Z in much the same way as does S_{CX} ($2p\pi$, $3d\pi$). Thus in the naive framework the $4p\pi$ orbital produces effects similar to those brought about by the $3d\pi$ orbitals. However, no essential orthogonality exists between the $3p\pi$ and $4p\pi$ orbitals. With increasing Z, causing contraction of the $4p\pi$ orbital, strong forced mixing takes place opposing any stabilization gained by spontaneous $3p\pi$–$4p\pi$ mixing. This effect precludes any appreciable stabilization from mixing of 2p and 3p orbitals in the second-row diatomics.[15] The essential $3p\pi$-$3d\pi$ orthogonality is thus an important prerequisite to carrying out the naive calculations reported here.

A more difficult question to answer is whether a flexibility has been introduced in the Cl $3d\pi$ orbital which is, in part, compensating for the deficiencies of the Cl $3p\pi$ and C $2p\pi$ orbitals. Orthogonality restrictions preclude strong inter-dependence between the scale factors of the Cl $3p\pi$ and $3d\pi$ orbitals. Therefore variation of Z_{eff} for Cl 3p may only change the Cl 3p energy level, thus affecting the promotion energy in a fairly minor way. Although the overlap integral S_{CCl} ($2p\pi$, $3d\pi$) will be affected by deficiencies in the C $2p\pi$ orbitals, it is highly unlikely that any essential changes in the conclusions can be obtained by variation of Z_{eff} for C 2p. It should be emphasized that the magnitudes listed in Table I will be dependent upon S_{CCl} ($2p\pi$, $3d\pi$) and must be regarded as schematic only.

Examination of Table I shows that Cl $d\pi$-$p\pi$ hybridization for the three parent conjugated systems considered causes considerably greater increased stabilization energy than in Cl_2[6] ($\sim$ 2 e.v. *vs.* 1 e.v.). This appears to be due mainly to the favorable factor (2) mentioned in the Introduction, since the atomic population and degree of hybridization in every case is approximately constant and comparable to that predicted for Cl_2. (We again mention that no reliance should be placed on the actual magnitudes of the atomic population (see Vinyl Chloride Section), but only in their relative values.)

The considerable variation in stabilization energy arises from the variation in the energy level and charge order scheme of the parent part of the molecule (factor 3 of the Introduction). The additional depression of over 0.5 e.v. for the ground state energy listed in Table I of the 3π-electron system $\cdot CH_2Cl$ (chloromethyl radical) provides verification of this statement since in this case the energy of the single parent MO is much higher than in any other case considered. In addition the charge order is unity, so that this according to factor 3 should be an unusually favorable case.[16] The increased stabilization energy of *p*-chloroanisole is tied up with factor 3 since the introduction of the

TABLE I

ATOMIC POPULATIONS, BOND ORDERS AND STABILIZATION ENERGIES OF SOME CONJUGATED CHLORO COMPOUNDS

Molecule	Cl orbital population	ΔE,[b] e.v.	% $d\pi$–$p\pi$ hybridization	(c) ΔP_{CCl}
Vinyl chloride	$3p^{1.92}3d^{0.11}$	−2.07	5.4	0.29
Chlorobenzene	$3p^{1.93}3d^{0.10}$	−1.86	4.9	.29
p-Chloroanisole	$3p^{1.94}3d^{0.11}$	−2.00	5.4	.29
Chloromethyl radical[a]	$3p^{1.63}3d^{0.15}$	−2.64	8.4	.50

[a] The planar species CH_2Cl. [b] Depression of the total ground state energy as solved by the variation theorem as a function of d-orbital interaction (see Fig. 3). [c] Increase in C–Cl bond order due to Cl $p\pi - d\pi$ hybridization.

(14) The above estimates would yield a small amount of $p\pi$-$d\pi$ hybridization in F_2 however.

(15) R. S. Mulliken, "Laboratory of Molecular Structure and Spectra," Technical Report 1957–1959, Part II (p. 25–27).

(16) Thus the C–Cl bond in the unprepared species Cl–C_3–H (chloropropargylene)[17] is predicted to show unusual stability.

(17) P. S. Skell and K. Klohe, *J. Am. Chem. Soc.*, **82**, 247 (1960).

OCH_3 group onto the benzene ring both raises the frontier level and increases its charge order. This allows the somewhat tentative prediction that the effect of d-orbital mixing on the stabilization energy should be most pronounced when there is a charge donor (Y) present *i.e.*, when the structure of type C

$$+ Y = R = X -$$

is important.[18] To paraphrase Mulliken, a little of structure C goes a long way!

Because of the lower energy differences between the d-orbital and that of "excited" π-electron orbitals, $d\pi$-$p\pi$ hybridization effects should be exhibited much more strongly in excited states. This is evidenced by considering the excited state wave function for the 2600 Å. benzene analog transition ($^1L_B \leftarrow {}^1A$) to a first-order CI approximation previously described.[20] Second-order CI with doubly excited configurations is neglected here. While not precisely correct[21] the first-order approximation gives the leading terms. Charge density changes are shown for bromobenzene in the excited state upon inclusion of $d\pi$-$p\pi$ hybridization.[22]

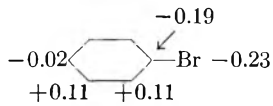

For the excited states of bromoanisole, the charge density changes upon inclusion of $d\pi$-$p\pi$ hybridization are

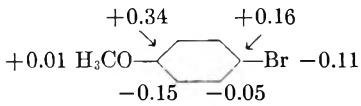

The excited state of wave functions for bromoanisole for these systems are (see ref. 18 for terminology)

$$\Psi_{Lb} = \cos(\Pi/4 - \Lambda_B)\,\chi_{12} - \sin(\Pi/4 - \Lambda_B)\,\chi_{\bar{1}z}$$

The transition moment integral for the ($^1L_b \leftarrow {}^1A$) band may be written as

$$\mathbf{M}_{Lb} = \cos\Lambda_B \mathbf{M}'_{B_{2u}} + \sin\Lambda_B \mathbf{M}'_{E_{1u}}$$

The larger the value of the E_{1u} mixing parameter Λ_B, the greater should be the intensity of the band, and conversely. In Table II the values of Λ_B for bromobenzene and *p*-bromoanisole are given. In these molecules two opposing effects occur. The mixing of the $d\pi$ halogen orbital tends to lower the value of Λ_B, thereby decreasing the intensity. However, mixing with the occupied $p\pi$ orbital tends to raise the value of Λ_B, and hence the intensity of the transition. The crude method of calculation employed cannot be expected to yield an accurate net result of these two effects. Three conclusions may be drawn, however.

TABLE II

VALUES OF E_{1u} MIXING PARAMETER Λ_B[c]

Molecule	Λ_B[a]	Λ_B[b]
Bromobenzene	−19°	− 5°
p-Bromoanisole	− 2.3°	+26°

[a] 4d orbital included in conjugation. [b] 4d orbital neglected. [c] See footnote 25 in text for discussion of magnitude and sign of Λ_B.

(1) The lowered intensities found in *p*-bromo- and iodoanisoles by Goodman and Frolen[5] can be explained reasonably by means of $p\pi$-$d\pi$ hybridization causing a change in the excited state wave function.[23]

(2) The low intensity of the 2600 Å. band in chloro- and bromobenzenes (and presumably iodobenzene) is due, at least in part, to d orbital effects (Table II).

(3) The mixing of the halogen $d\pi$ orbitals in the excited state causes a red shift of the 2600 Å. transition due to additional stabilization of the excited state relative to the ground state. Hence the red shift order: Br > Cl > F arises at least partially from $d\pi$-$p\pi$ mixing.

These effects indicate that halogen parameters obtained from spectroscopic data, intensities or frequencies, neglecting d-orbital effects, are likely to be in error. The same holds true for information taken from quadrupole moment and coupling data[24] since the d-orbital population should in general contribute to the moment in a different fashion (smaller) from the p-orbital populations.

Finally, it would appear that in the light of Table I, reinterpretation of dipole moments of conjugated Cl compounds may be needed, since the π-electron moment apparently is reduced strongly by $d\pi$-$p\pi$ hybridization.

Acknowledgment.—L. G. thanks Professor J. G. Astón for pointing out evidence of d-orbital participation in reactions involving the lower halogens. The authors gratefully acknowledge correspondence with Professor R. S. Mulliken, who pointed out that 4p mixing in Cl is mitigated by the non-orthogonality to 3p; and very helpful conversations with Professors C. A. Coulson and R. W. Taft, Jr.

(18) Factor (6) would tend to reduce the degree of $d\pi$-$p\pi$ hybridization because of the negative charge induced by structure C. However for Cl we estimate that an increase of 0.1e in 3d would tend to increase the promotion energy $3p^2 \rightarrow 3p3d$ by ~0.4 e.v. (at Z_{nat}) which corresponds to only ~1 e.v. at Z_{min}. Structures of type A and B involve a decrease in the 3p population and if important may lead to a major decrease in the promotion energy.[19]

(19) Craig, Maecoll, Nyholm, Orgel and Sutton, *J. Chem. Soc.*, 332 (1954). For a decrease of 0.1e in the 3p population we estimate a decrease of ~2 e.v. in the promotion energy $3p^2 \rightarrow 3p3d$.

(20) L. Goodman and H. Shull, *ibid.*, **27**, 1388 (1957).

(21) J. N. Murrell and K. L. McEwen, *ibid.*, **25**, 1143 (1956).

(22) These values given above for charge density changes in the excited state are subject to even greater error than for the ground state. These values are not only sensitive to the coulomb integral both for X $np\pi$ and X $nd\pi$, but also to the approximations in finding the excited state wave function,[20] so that these values must be regarded with extreme caution.

(23) The effect of $d\pi$-$p\pi$ hybridization on $\mathbf{M}'_{B_{2u}}$ and $\mathbf{M}'_{E_{1u}}$ is minor compared to the effect on Λ_B, hence the reduction in intensity arises almost entirely from the change in E1u mixing.

(24) J. H. Goldstein, *J. Chem. Phys.*, **24**, 106 (1956).

(25) The enhancement in intensity is dependent upon $\sin^2\Lambda_B$, Λ_B in turn, is dependent upon the magnitude of $[(\epsilon_1'-\epsilon_1') + (\epsilon_2'-\epsilon_2')]$. Including d-orbitals in the conjugation scheme causes ϵ_2' to be depressed so that $(\epsilon_2'-\epsilon_2') < 0$. The halogen np-orbital forces $(\epsilon_1{}^1-\epsilon_1{}^1)^2 > 0$ if $|\alpha_X| > |\alpha_c + \beta|$, but $(\epsilon_1'-\epsilon_1') < 0$ for $|\alpha_X| < |\alpha_c + \beta|$. *Thus Λ_B decreases for the case $|\alpha_X| > |\alpha_c + \beta|$.* Our method of choosing parameters yields α_X (np) ~ $\alpha_c + \beta$. Therefore the magnitude and sign of Λ_B is strongly dependent upon the initial parameter α_X (np), and a small variation in the magnitude of α_X (np) can reverse the direction of the effect of d-orbitals upon Λ_B. The values listed in Table II should in no way be regarded as correct. They have been included only for the purpose of showing that d-orbital effects will in general be large in considering the excited states of conjugated halogen compounds.

THE THEORY OF THE DISTILLATION COLUMN

BY ANDRZEJ WITKOWSKI[1]

Department of Chemistry, Harvard University, Cambridge, Massachusetts

Received December 29, 1958

It will be shown that concentration in a simple distillation column obeys the differential equation $\mu \frac{\partial c}{\partial t} + \alpha \frac{\partial c(1-c)}{\partial z} + \beta \frac{\partial c}{\partial z} - \gamma \frac{\partial^2 c}{\partial z^2} = 0$, where constant coefficients of the equation are explicitly expressed by diffusion constants and relative volatility. In particular one can get the time of the equilibrium establishment in the column and can expect the existence of a phenomenon similar to Debye's effect in the thermogravitational column.

Many papers[2] have been written in connection with the theories of distillation but most of these have been concerned only with equilibrium separation. The well known theory of Westhaver[3] involving the equilibrium separation generally agrees favorably with experiment. Recently a complete analysis of the hydraulics of the problem has been given by Michalik.[4]

The problem of approaching to equilibrium especially for the columns without packing has not been studied in as great detail as the equilibrium case. On the other hand it has been stressed[5] that this problem is very important in the separation by the distillation of isotopes and other components with only slightly different boiling points. Thus we will make an attempt to formulate a theory of the distillation column with particular concern for the time dependence and which is valid for the problem of the separation of such components.

We will apply the analysis to the simple type of column composed of an opened tube with a thin film of liquid flowing down the wall around the vapor streaming up. Separation is obtained by virtue of the existence of a concentration difference between the liquid and the vapor together with relative motion; the changes of concentration are governed by the continuity equation in which diffusion plays an important role. Usually the problem must be formulated using 3 variables: time, coördinate along and across the column, with specific boundary conditions for the contact between vapor and liquid. This problem as stated is too complicated for the exact treatment; however, we will make certain approximations which enable solution to a very good degree of approximation. Owing to the fact that changes of the concentration across the column are usually small compared to changes along the column, it will be shown that it is possible to include the "horizontal problem" in a vertical one. Thus, we may transform a linear 3-dimensional differential equation with non-linear boundary conditions at interface to a 2-dimensional "vertical" non-linear differential equation with known solution with only a small percentage error later to be determined.

2. Consider an open tube distillation column. Consider a two component mixture. Define the cylindrical coördinate system with Z-axis vertically upwards corresponding to the axis of the cylinder. We denote by ξ the coördinate of the surface of the liquid and by a the inner radius of the tube. Denoting by J_r radial and by J_z vertical components, at once for both phases, of the vector of the mass flux J we have

$$J_r = -D\zeta \frac{\partial c}{\partial r} \tag{1}$$

$$J_z = -D\zeta \frac{\partial c}{\partial z} + V\zeta c \tag{2}$$

where D denotes the diffusion coefficient, δ density, v velocity and where concentration c is measured in fractional molar units, thus $c_1 + c_2 = 1$. For simplicity we will denote $c_1 = c$, thus $c_2 = 1 - c$. Writing equation 1 we are concerned with the isothermal distillation problem. The problem of the distillation in a system where a horizontal temperature gradient exists, thus when distillation combines with thermal diffusion, was considered by the author elsewhere.[6]

We have continuity equation for the concentration

$$\frac{\partial(\zeta c)}{\partial t} + \operatorname{div} J = 0 \tag{3}$$

with boundary conditions

$$(J_r)_{r=0} < \infty \tag{4}$$

$$(J_r)_{r=a} = 0 \tag{5}$$

Because we do not have any positive or negative sources on the surface of the liquid, thus

$$\lim_{r \to \xi^-} J_r = \lim_{r \to \xi^+} J_r \tag{6}$$

We make the following assumptions: (a) We assume that on the phase boundary there exists an equilibrium between vapor and liquid. This assumption is reasonable owing to the fact that above some given pressure (several cm.) the rate of the interphase mass transfer is considerably greater than the rate of diffusion in the gas phase.[2,3] Thus for example Westhaver's theory of the distillation column based on this assumption is well confirmed by experiment.[7] Also direct calculations of Kuhn[8] show that the non-equilibrium state on the phase boundary implies the existence on this boundary of a gas membrane; but of the thickness which for the pressures higher than a few cm. can be usually neglected as compared with the thickness of the gas phase. (b) We assume that in

(1) Department of Theoretical Chemistry, Jagellonian University, Kraków, Poland.

(2) A. Rose, *et al.*, "Distillation," Interscience Publ. Inc., New York, N. Y., 1951.

(3) J. W. Westhaver, *Ind. Eng. Chem.*, **34**, 126 (1942).

(4) Michalik, *Am. Inst. Chem. Eng.*, **3**, 276 (1957).

(5) Ref. 2, p. 94.

(6) A. Witkowski, *Acta Phys. Polon.*, **16**, 79 (1957).

(7) A. Rose, *Ind. Eng. Chem.*, **28**, 1210 (1936).

(8) W. Kuhn, *Helv. Chim. Acta*, **37**, 1407 (1954).

the liquid film flowing along the wall the concentration is uniform in the direction perpendicular to the surface of the liquid. The theory of the distillation column based on this assumption[3] has been well confirmed by experiment.[7] Moreover, the direct calculations of Kuhn[8] show that in columns without packing one can neglect the diffusional "resistance" of the liquid as compared with that of the gas phase.

Owing to assumed equilibrium on the phase boundary and uniform concentration in the liquid phase along the radial coördinate, we can write instead of (6)

$$\lim_{r\to\xi^-} \frac{c}{1-c} = \epsilon \frac{c_v}{1-c_v} \qquad (7)$$

In (7) we denote by ϵ the relative volatility and by c_v—more explicitly than in (1), (2)—concentration in the liquid phase. The boundary conditions (7) may be written in another mathematical form more convenient for the calculations. It can be shown[2] that for $1.0 \leqslant \epsilon \leqslant 1.1$ instead of condition (7) one can write with an error smaller than 5% that

$$\lim_{r\to\xi^-} c - c_v = \ln \epsilon \lim_{r\to\xi^-} c(1-c) \qquad (8)$$

We write the equation 3 in cylindrical coördinates, taking into account the angular symmetry

$$\frac{\partial(\zeta c)}{\partial t} + \frac{1}{r}\frac{\partial}{\partial r}(rJ_r) + \frac{\partial J_z}{\partial z} = 0 \qquad (9)$$

If we multiply (9) by r, integrate and use the boundary conditions (4), (5) we obtain

$$\int_0^a \frac{\partial(\zeta c)}{\partial t} r\mathrm{d}r - \frac{\partial}{\partial z}\int_0^a D\zeta \frac{\partial c}{\partial z} r\mathrm{d}r + \frac{\partial}{\partial z}\int_0^a v\zeta c r\mathrm{d}r = 0 \qquad (10)$$

We introduce the function H defined by the equation

$$H = \int_0^r \zeta v r\mathrm{d}r \text{ for } 0 \leqslant r \leqslant \xi \qquad (11)$$

if we assume that ζ, v are independent of z, we have

$$\frac{\mathrm{d}H}{\mathrm{d}r} = \zeta v r$$

Evaluating

$$\frac{\partial}{\partial z}\int_0^\xi v\zeta c r\mathrm{d}r$$

by parts and using H we obtain

$$\frac{\partial}{\partial z}\int_0^\xi v\zeta c r\mathrm{d}r = \left(\frac{\partial c}{\partial z}\right)_{\xi^-} H(\xi-) - \int_0^\xi H \frac{\partial^2 c}{\partial z \partial r}\,\mathrm{d}r \qquad (12)$$

The second integral in equation 12, equal

$$\frac{\partial}{\partial z}\int_0^\xi H \frac{\partial c}{\partial r}\,\mathrm{d}r$$

gives the separation caused by the radial variation of the concentration in the gas phase. To obtain this radial variation we use the continuity equation for $0 \leqslant r \leqslant \xi$, from which we have

$$\frac{\partial^2 c}{\partial z \partial r} = \frac{1}{D\zeta r}\int_0^r r' \frac{\partial^2(\zeta' c')}{\partial z \partial t}\,\mathrm{d}r' + \frac{1}{D\zeta r}\int_0^r \frac{\partial^2 J_z'}{\partial z^2} r'\mathrm{d}r' \qquad (13)$$

where we introduced the prime in order to distinguish the integration coördinate.

If we define

$$I(r) = \int_r^\xi \frac{H'}{D\zeta' r'}\,\mathrm{d}r'; \quad J = r\left(\frac{\partial(\zeta c)}{\partial z \partial t} + \zeta v \frac{\partial^2 c}{\partial z^2} - D\zeta \frac{\partial^2 c}{\partial z^2}\right)$$

then using Dirichlet's transformation we can obtain

$$\int_0^a \frac{\partial(c\zeta)}{\partial t} r\mathrm{d}r - \frac{\partial}{\partial z}\int_0^a D\zeta \frac{\partial c}{\partial z} r\mathrm{d}r - \int_0^\xi I(r) J\mathrm{d}r + \left(\frac{\partial c}{\partial z}\right)_{\xi^-} H(\xi^-) + \frac{\partial c_v}{\partial z}\int_\xi^a \zeta v r\mathrm{d}r = 0 \qquad (14)$$

The last integral in (14) gives the separation caused by the movement of the liquid phase. Because c in the liquid phase denoted c_v, does not, owing to assumption b, depend on coördinate r, we do not have for the liquid phase in (14) terms similar to $\int I J\mathrm{d}r$. Terms $\int I J\mathrm{d}r$ are derived from the integral $\frac{\partial}{\partial z}\int H\frac{\partial c}{\partial r}\mathrm{d}r$, equal zero for the liquid phase; origin of this integral is clearly caused by the radial dependence of c in the given phase.

If we denote by

$$\int_\xi^a v\zeta r\mathrm{d}r = -\delta_0; \quad \int_0^a v\zeta r\mathrm{d}r = \delta_1$$

then taking into account assumption b and using boundary condition (8) we obtain from (14)

$$\int_0^\xi \zeta\left(\frac{\partial}{\partial t} - D\frac{\partial^2}{\partial z^2}\right)\left(1 - I(r)\frac{\partial}{\partial z}\right) c r\mathrm{d}r + \int_\xi^a \zeta\left(\frac{\partial c}{\partial t} - D\frac{\partial^2 c}{\partial z^2}\right) r\mathrm{d}r + \frac{\partial}{\partial z}\{\delta_0 \ln \epsilon\,[c(1-c)]_{\xi^-}\} + \delta_1\left(\frac{\partial c}{\partial z}\right)_{\xi^-} - \int_0^\xi \frac{\partial^2 c}{\partial z^2} v\zeta r \int_r^\xi \frac{H'}{D\zeta' r'}\,\mathrm{d}r'\mathrm{d}r' = 0 \qquad (15)$$

Let us observe that from (8) follows that the relative change of the concentration across the column is of the order of $\ln \epsilon$. Thus, if we solve (15) for z,t dependence of the concentration using mean across the column value of the concentration, error for c will be of this order. Also substitution of mean value of coördinate r (*i.e.*, value of r corresponding to mean value of c) instead of ξ- must give lesser error than $\ln \epsilon$, because $\ln \epsilon$ gives total (relative) change of concentration across the column. In other word, solving (15) (for z,t dependence) we obtain c depending parametrically on ξ-; if we put instead of ξ- the mean value of r from $0 \leqslant r \leqslant \xi$, it must give smaller error for c than $\ln \epsilon$, which is total change of c across the column. For an actual operation in separation of closely boiling mixtures ($\epsilon \leqslant 1{,}1$), this error for c is of some per cent.

Let us neglect for a moment the vertical static diffusion which decreases the difference of the concentration between the top and the bottom. Let us consider the vertical equilibrium and hence the state when we have the maximal separation. Then for the concentration mean across the column applying the Dirichlet's transformation to the last integral in (15) we can write

$$\delta_0 c(1-c)\ln \epsilon + c\delta_1 = \frac{\mathrm{d}c}{\mathrm{d}z}\int_0^\xi \frac{H^2}{D\zeta r}\,\mathrm{d}r = A\frac{\mathrm{d}c}{\mathrm{d}z}$$

Thus

$$A\frac{1}{c}\frac{\partial c}{\partial z} \leqslant A\frac{1}{c}\frac{\mathrm{d}c}{\mathrm{d}z} = \delta_0(1-c)\ln \epsilon + \delta_1 \leqslant \delta_0 \ln \epsilon + \delta_1$$

Let us investigate now the expression

$$\Delta = \int_0^\xi I(r)\frac{\partial c}{\partial r} r\mathrm{d}r \Big\backslash \int_0^\xi c r\mathrm{d}r$$

We can see that

$$\Delta \leqslant 2\frac{\delta_0 \ln \epsilon + \delta_1}{A\xi^2}\int_0^\xi I(r)r\mathrm{d}r = \frac{2(\delta_0 \ln \epsilon + \delta_1)}{\xi^2\int_0^\xi \frac{H^2}{D\zeta r}\,\mathrm{d}r}\int_0^r r\int_r^\xi \frac{H'}{D\zeta' r'}\,\mathrm{d}r'\mathrm{d}r = \frac{2(\delta_0 \ln \epsilon + \delta_1)}{\xi^2\int_0^\xi \frac{H^2}{D\zeta r}\,\mathrm{d}r}\int_0^\xi \frac{H'}{D\zeta' r'}\int_0^{r'} r\mathrm{d}r\mathrm{d}r' = \frac{\delta_0 \ln \epsilon + \delta_1}{\xi^2\int_0^\xi \frac{H^2}{D\zeta r}\,\mathrm{d}r}\int_0^\xi \frac{Hr}{D\zeta}\,\mathrm{d}r$$

where in the last step but one we used the Dirichlet transformation. Thus

$$\Delta = \tilde{f}\frac{\delta_0 \ln \epsilon + \delta_1}{\xi^2\int_0^\xi \frac{H^2}{D\zeta r}\,\mathrm{d}r}\int_0^\xi \frac{Hr}{D\zeta}\,\mathrm{d}r, \text{ where } |\tilde{f}| \leqslant 1 \quad (16)$$

3. To calculate the integrals which are included in (15) we must know the velocity of gas phase. The equation of the laminar, viscous flow is

$$\eta\frac{1}{r}\frac{\mathrm{d}}{\mathrm{d}r}r\frac{\mathrm{d}v}{\mathrm{d}r} = \zeta g + \frac{\mathrm{d}p(z)}{\mathrm{d}z} \quad (17)$$

where η denotes viscosity, ζ density, g acceleration of gravity, p pressure. The boundary condition for (17) is

$$v(0) < \infty$$

and because of slow velocity of the liquid phase as compared with the gas one we assume for simplicity that

$$v(\xi) = 0$$

After the integration one obtains

$$v = \frac{4H(\xi)}{\bar{\zeta}\xi^2}\left(1 - \frac{r^2}{\xi^2}\right) \quad (18)$$

Using v, after the evaluation of the integrals we obtain

$$\Delta = f\frac{\delta_0 \ln \epsilon + \delta_1}{H(\xi)}, \text{ where } |f| = \frac{24}{33}|\tilde{f}| \leqslant 1$$

So with this error we can neglect Δc in the solution of the (15). When $\delta_1 = 0$ the error is not greater than $\ln \epsilon$ and increases with increasing flow δ_1 through the column.

Finally, after the multiplication of (15) by 2π we have the result that with an error for c of Δ order we have obtained the following equation for the concentration c

$$2\pi\left(\frac{\partial c}{\partial t} - D\frac{\partial^2 c}{\partial z^2}\right)\int_0^a \zeta r\mathrm{d}r + 2\pi\left[\frac{\partial}{\partial z}\{\delta_0 \ln \epsilon\, c(1-c) + c\delta_1\} - 2\pi\frac{\partial^2 c}{\partial z^2}\int_0^\xi \frac{H^2}{D\zeta r}\,\mathrm{d}r = 0\right.$$

Denoting by

$$2\pi\delta_0 \ln \epsilon = \alpha$$

$$2\pi\delta_1 = \beta$$

$$\gamma' = 2\pi\int_0^\xi \frac{H^2}{D\zeta r}\,\mathrm{d}r = \frac{22\pi H^2(\xi)}{24D\bar{\zeta}}$$

$$2\pi\int_0^\xi \zeta r\mathrm{d}r = \mu'$$

$$2\pi\int_\xi^a \zeta r\mathrm{d}r = \mu_v$$

$$\mu' + \mu_v = \mu$$

$$\gamma' + D\mu' + D_v\mu_v = \gamma$$

we obtain the final form

$$\mu\frac{\partial c}{\partial t} + \alpha\frac{\partial c(1-c)}{\partial z} + \beta\frac{\partial c}{\partial z} - \gamma\frac{\partial^2 c}{\partial z^2} = 0 \quad (19)$$

4. The non-linear equation 19 was recently solved.[9] The boundary condition for the distillation for either infinite or finite bottom containers and closed tube at the top may be satisfied by this solution. The detailed discussion of the equation 19 was given in ref. 9. It should be noticed that an equation similar to (19) was obtained in the theory of the thermogravitational column.[10] In some ways our treatment is analogous to Bardeen's[10b] treatment of thermal diffusion.

Let us investigate a little more carefully the linear case of (19) *i.e.* when $c^2 << 1$. Then for an infinite container at the bottom and for a closed tube at the top the solution of (19) may be found by the usual superposition. It can be shown[11,12] that for

$$\beta = 0, \frac{\alpha L}{2\gamma} << 1$$

where L denotes the length of the column, and when time of the experiment t is small compared with the time of the equilibrium establishment of the column t_1

$$t << t_1 = \frac{4\mu L^2}{\pi^2\gamma}$$

the ratio of concentration at the top to that at the bottom is equal to

$$\frac{c_t}{c_b} = 1 + 2\alpha\left(\frac{t}{\pi\mu\gamma}\right)^{1/2} + \ldots \quad (20)$$

Consequently, we obtain from (20) two general conclusions: (1) (that initial ratio of the concentration will vary as the square root of the time and 2) that the initial increase of this ratio is independent of the height of the column. Thus, in a distillation column one may expect the existence of a phenomenon similar to Debye's effect in the thermogravitational column.

Let us consider finally the equilibrium separation of general non-linear case.

We assume that: (a) we have equilibrium, thus

$$\frac{\partial c}{\partial t} = 0$$

(b) no net flow of the mixture through the horizontal section takes place, so

$$\beta = 0$$

(c) one can neglect the diffusion in the liquid phase, so that

$$D_v\frac{\partial^2 c}{\partial z^2} = 0$$

then from (19) we obtain after the integration

$$\frac{c}{1-c} : \frac{c_b}{1-c_b} = e^{(\alpha/\gamma)z}$$

Now using the definition of the height equivalent to the theoretical plate l we obtain from the last equation

(9) S. D. Majumdar, *Phys. Rev.*, **81**, 844 (1951).

(10) (a) W. H. Furry, R. C. Jones and L. Onsager, *ibid.*, **55**, 1083 (1939); (b) J. Bardeen, *ibid.*, **58**, 94 (1940).

(11) P. Debye, *Ann. Phys.*, **36**, 284 (1939).

(12) W. H. Furry and R. C. Jones, *Rev. Mod. Phys.*, **18**, 151 (1946).

$$l = \frac{1}{\delta_0}\left(\frac{1}{2}\xi^2\zeta D + \frac{11\delta_0^2}{24D\zeta}\right)$$

Because

$$\delta_0 = \frac{v\zeta}{2}\xi^2$$

we have finally

$$l = \frac{11}{48}\frac{v\xi^2}{D} + \frac{D}{v} \qquad (21)$$

Thus, as the limiting case, under the assumptions a,b,c follows from our theory the well known equilibrium separation theory of Westhaver.[2,3]

Let us, at the end, list the assumptions we have made in this theory. The following assumptions were involved: (a) equilibrium on the phase boundary between vapor and liquid, (b) uniform radial concentration in the liquid film, (c) two component mixture is closely boiling: $1.0 \leqslant \epsilon \leqslant 1.1$ (d) the motion of vapor is laminar, (e) velocity v, density ζ are independent on the height z, (f) diffusion coefficient D, viscosity η are constant, (g) average velocity of vapor is much greater than that of the liquid: $v(\xi\text{-}) = 0$.

Author wishes to express his gratitude to Professor W. H. Furry and Dr. Reed Howald from Harvard University for reading the manuscript and for valuable comments.

MECHANISM AND KINETICS OF THE UNCATALYZED MERCURY(I)–CERIUM(IV) REACTION

BY W. H. MCCURDY, JR., AND

University of Delaware, Newark, Delaware

G. G. GUILBAULT

Princeton University, Princeton, New Jersey

Received January 11, 1960

The rate of oxidation of mercury(I) perchlorate by cerium(IV) sulfate in perchloric acid media has been found to follow the rate expression: $-d[Ce(IV)]/dt = 8.5\,[Ce(IV)][Hg_2^{+2}]$ at 50.0°, in which the concentrations are moles per liter and time is in minutes. The dependence of the reaction rate on sulfuric and perchloric acids is discussed in terms of the cerium(IV) species in solution. A reaction mechanism is proposed in which the rate-determining step is believed to involve concomitant breaking of the $(Hg–Hg)^{+2}$ bond and electron transfer. The activation energy of this reaction was found to be 14.4 kcal./mole.

In a previous paper[1] it was reported that the slow oxidation of mercury(I) perchlorate by cerium(IV) sulfate in perchloric acid is catalyzed by silver(I) and manganese(II) salts. Further details on the mechanism of the catalyzed reaction will be presented in the near future. This study describes the mechanism and kinetics of the uncatalyzed mercury(I)–cerium(IV) reaction.

Experimental

All solutions were prepared from distilled water and reagent grade chemicals.

Reagents. Mercury(I) Solution, 0.025 *F*.—Mercury(I) nitrate monohydrate (7.025 g.) was dissolved in one liter of 1.0 *F* perchloric acid. This solution was standardized gravimetrically by precipitation of mercury(I) chloride and titrimetrically with standard ferric alum in the presence of thiocyanate.

Cerium(IV) Reagent, 0.025 *F*.—A solution was prepared by treating 13.2 g. of $Ce(HSO_4)_4$ (G. F. Smith Chemical Co.) with 5.0 ml. of 98% sulfuric acid. The resulting paste was heated with stirring for five minutes and gradually diluted to one liter with distilled water containing 82.5 ml. of 72% perchloric acid. The solution was standardized against arsenious acid.

Mercury(II) Solution, 0.050 *F*.—Dry mercury(II) oxide (10.8305 g.) was dissolved in 91 ml. of 72% perchloric acid and diluted to one liter.

Rate Measurements.—The rate of the reaction

$$2Ce^{+4} + Hg_2^{+2} \longrightarrow 2Ce^{+3} + 2Hg^{+2}$$

was followed by titrimetric evaluation of unreacted cerium (IV) in the reaction mixture with standard iron(II) sulfate at definite time intervals. All solutions were thermostated in a constant temperature bath (50.0 ± 0.1° for most measurements) before mixing and during the reaction. Suitable amounts of cerium(IV) reagent and mercury(I) perchlorate in perchloric acid were placed in a 500-ml. three-neck flask and the resulting solution stirred continuously. Samples were taken from the reaction flask by pipet, the time being recorded by a stop watch at the moment the sample solution reached the index mark of a calibrated 25.0-ml. pipet. Further reaction was rapidly quenched by mixing the sample with cold 6 *F* sulfuric acid.

The initial rate of the reaction was calculated graphically from concentration *versus* time curves by extrapolation to zero time and determining the slope of the curve at this point.

Results and Discussion

Effect of Acid Concentration.—The oxidation of mercury(I) sulfate by cerium(IV) sulfate proceeds slowly in boiling 2 *F* sulfuric acid.[2] As shown by data in Table I (A), there is considerable dependence of the rate upon the nature of the acid and the acid concentration. The rate is 3.6 times faster in 2.0 *F* perchloric acid than in 1.0 *F* sulfuric acid, indicating that sulfate ion hinders the oxidation. It is also evident that the rate of oxidation increases with first-order dependence on perchloric acid at low acid concentration, reaches a maximum in 4 *F* acid, then decreases.

Wadsworth, Duke and Goetz[3] have summarized the present status of information concerning cerium(IV)–cerium(III) potentials as well as the formation constants of $Ce(OH)^{+3}$, $CeOCe^{+6}$ ion species

(1) W. H. McCurdy, Jr., and G. G. Guilbault, *Anal. Chem.*, **32**, 647 (1960).

(2) H. H. Willard and P. J. Young, *J. Am. Chem. Soc.*, **52**, 557 (1930).

(3) E. Wadsworth, F. R. Duke and C. A. Goetz, *Anal. Chem.*, **29**, 1824 (1957).

in perchloric acid and $Ce(SO_4)^{+2}$, $Ce(SO_4)_2$ and $Ce(SO_4)_3^{-2}$ species in sulfuric acid. Suitable equilibrium calculations from these data indicate that $Ce(SO_4)^{+2}$ will be the predominate ion species in 1.0 *F* $HClO_4$–0.10 *F* H_2SO_4 containing 0.025 *F* total cerium(IV) concentration.

Table I

Initial Rate of Cerium(IV)–Mercury(I) Reaction as a Function of Initial Mercury(I), Cerium(IV) and Acid Concentration

$-\frac{d[Ce(IV)]}{dt} \times 10^5$, mole l.$^{-1}$ min.$^{-1}$	$[Ce(IV)]_0 \times 10^3$, mole l.$^{-1}$	$[Hg_2^{+2}]_0 \times 10^3$, mole l.$^{-1}$	Acid
	Part (A)		
0.42	2.50	0.91	0.5 *F* $HClO_4$
0.86	2.50	.91	1.0 *F* $HClO_4$
1.81	2.50	.91	2.0 *F* $HClO_4$
2.16	2.50	.91	4.0 *F* $HClO_4$
0.905	2.50	.91	6.0 *F* $HClO_4$
0.50	2.50	.91	1.0 *F* H_2SO_4
0.31	2.50	.91	2.0 *F* H_2SO_4
	Part (B)		
0.127	1.88	0.081	2.0 *F* $HClO_4$
.257	1.88	.161	2.0 *F* $HClO_4$
.510	1.88	.320	2.0 *F* $HClO_4$
.220	0.143	1.82	2.0 *F* $HClO_4$
.438	.284	1.82	2.0 *F* $HClO_4$
.870	.562	1.82	2.0 *F* $HClO_4$
1.70	1.10	1.82	2.0 *F* $HClO_4$

A prior equilibrium reaction of the type

$$Ce(SO_4)_x^{4-2x} + H^+ \xrightarrow{K_{eq}} Ce(SO_4)_{(x-1)}^{6-2x} + HSO_4^-$$

may be invoked to explain the data of Table I. The increase in rate of mercury(I) oxidation by cerium(IV) with increasing perchloric acid (0.5–2.0 *F*) is attributed to formation of a less complexed and hence kinetically more reactive cerium(IV) ion species. Addition of sulfate inhibits the reaction by shifting the equilibrium in the reverse direction. At concentrations of perchloric acid above 2 *F*, precipitation of cerium(IV) salts begins to occur, forming a heterogeneous system and a decreasing rate.

It was found that either addition of 6 *F* perchloric acid to a sulfuric acid solution of cerium(IV) sulfate, or addition of sulfuric acid to a 6 *F* perchloric acid solution of cerium(IV) perchlorate produces a heavy precipitate of a mixed cerium(IV) sulfate–perchlorate salt. The [sulfate]/[cerium(IV)] and [perchlorate]/[cerium(IV)] mole ratios were determined on several of these (vacuum dried) precipitates by chemical analysis.[4] These results are summarized in Table II.

Table II

Analysis of Mixed Cerium(IV) Sulfate–Perchlorate Salts

$HClO_4$ concn.,[a] *F*	Mole ratio [Sulfate]/[Ce(IV)]	Mole ratio [Perchlorate]/[Ce(IV)]
2.0	1.92, 2.06	Very small
4.0	1.53	0.95
6.0	1.35, 1.34	1.64
8.0	1.29	..

[a] Concentration of acid from which salt was precipitated.

The fact that sulfate is retained in precipitates formed in very strong perchloric acid suggests that it is also bound to cerium(IV) in solution. These precipitates are quite insoluble in 6 *F* perchloric acid but readily soluble in dilute sulfuric acid.

Some further evidence in support of the proposed prior equilibrium step is obtained by graphical treatment of data similar to Table I in a manner described by Duke.[5] Constructing a plot of the rate constant^{-1} *vs.* the $[HSO_4^-]/[H^+]$ concentration ratio permits calculation of an equilibrium constant for the prior equilibrium step. A value of 0.0085 obtained at 25° is of the correct magnitude to indicate $Ce(SO_4)^{+2}$ (K_{eq} = 0.005 at 25°)[3] as the reactive species in this oxidation.

Since all further rate measurements were made in 2.0 *F* perchloric acid, the notation [Ce(IV)] will be used to indicate the total cerium(IV) concentration.

Effect of Cerium(IV) Concentration.—The rate of mercury(I) oxidation as a function of the cerium(IV) concentration was determined at a constant mercury(I) concentration of 1.82×10^{-3} *M* in 2.0 *F* perchloric acid at 50.0°. The rate was found to be first order in cerium(IV) over the range $0.143–1.10 \times 10^{-3}$ *M* employed (Table I, Part B). A plot of $\ln[Ce(IV)]_0/[Ce(IV)]$ *vs.* time at an initial cerium(IV) concentration of 0.143×10^{-3} *M*, yielded a straight line indicating a first-order relationship

$$\frac{-d[Ce(IV)]}{dt} = k_1[Ce(IV)]$$

which is integrated to

$$\ln \frac{[Ce(IV)]_0}{[Ce(IV)]} = k_1 t$$

Effect of Mercury(I) Concentration.—The effect of mercury(I) concentration on the reaction rate was obtained at a constant cerium(IV) concentration of 1.88×10^{-3} *M* in 2.0 *F* perchloric acid at 50.0°. As shown by data in Table I, Part B, a variation in concentration of mercury(I) in the range $0.081–0.320 \times 10^{-3}$ *M* produces a linear increase in the rate of oxidation, indicating a first-order reaction.

Effect of Mercury(II) and Cerium(III) Concentrations.—The effect of these ions on the rate was tested in a solution which contained 0.182×10^{-3} *M* mercury(I), 0.40×10^{-3} *M* cerium(IV) and 2.0 *F* perchloric acid. The rate of oxidation proved to be independent of mercury(II) and cerium(III) perchlorate over the range of concentrations tested: 0–0.20 *M*.

Mechanism and Rate of Reaction as a Function of Cerium(IV) and Mercury(I) Concentrations.—The mechanism proposed to account for the observed first-order rate in cerium(IV) and mercury(I) is

(4) W. W. Scott, "Standard Methods of Chemical Analysis," N. H. Furman, ed., Vol. 1, D. Van Nostrand Co., New York, N. Y., 1939, p. 215; A. B. Lamb and J. W. Marden, *J. Am. Chem. Soc.*, **34**, 812 (1912).

(5) F. R. Duke, M. Kolthoff and P. J. Elving, eds., "Treatise on Analytical Chemistry," Vol. 1, Interscience Publ., New York, N. Y. 1959, Chapter 15.

$$Ce^{+4} + (Hg - Hg)^{+2} \xrightarrow[\text{slow}]{k_1} Ce^{+3} + Hg^{+1} + Hg^{+2}$$

$$Ce^{+4} + Hg^{+1} \xrightarrow[\text{fast}]{k_2} Ce^{+3} + Hg^{+2}$$

The rate-determining step in this proposed mechanism is the breaking of the $(Hg–Hg)^{+2}$ bond, concomitant with transfer of an electron; the Hg^{+1} formed reacts with cerium(IV) in a fast step to form Hg^{+2}. The kinetic expression is

$$\frac{-d[Ce(IV)]}{dt} = k_1[Ce(IV)][Hg_2^{+2}]$$

From the slope of a plot of (Initial Rate)/$[Ce(IV)]_0$ *vs.* $[Hg_2^{+2}]_0$, the constant k_1 was found to have the value 8.5 l. moles^{-1} min.$^{-1}$ at 50.0°. This rate constant becomes approximately 3.8 l.^{2} moles^{-2} min.$^{-1}$ when the effect of perchloric acid over the concentration range 0.5–2.0 F is included. The rate expression then becomes

$$\frac{-d[Ce(IV)]}{dt} = k_1'[Ce(IV)][Hg_2^{+2}][HClO_4]$$

Energy of Activation.—The effect of temperature on the rate of mercury(I) oxidation at a constant initial cerium concentration of 2.05×10^{-3} M in 2.0 F perchloric acid is shown in Table III.

TABLE III

VARIATION OF RATE CONSTANT WITH TEMPERATURE

$[Ce(IV)]_0 = 2.05 \times 10^{-3}$ M, $[Hg_2^{+2}]_0 = 0.80 \times 10^{-3}$ M, $[HClO_4] = 2.0$ F

Temp., °C.	K_1, l. moles^{-1} min.$^{-1}$
50.0	8.5
60.0	18.2
70.0	30.0

Calculation of the activation energy from the slope of an Arrhenius plot of ln k_1 *vs.* $1/T$ yielded a value of 14.4 ± 0.2 kcal. It is interesting to note that this value is in close agreement with activation energy values for other uncatalyzed cerium(IV) oxidation reactions studied under somewhat different conditions.[6,7]

Acknowledgments.—We wish to thank Dr. David Garvin for helpful suggestions, and one of us (G) wishes to express appreciation to the National Science Foundation for financial support under which this work was accomplished.

(6) V. F. Stefanovskii and M. S. Gaukham, *J. Gen. Chem. U. S. S. R.*, **11**, 970 (1941).

(7) F. B. Baker, T. W. Newton and Milton Kahn, THIS JOURNAL, **64**, 109 (1960).

ADSORPTION FROM BINARY SOLUTIONS OF NON-ELECTROLYTES

BY G. DELMAS AND D. PATTERSON

Department of Chemistry, University of Montreal, Montreal, Canada

Received January 11, 1960

A treatment of adsorption of binary regular solutions is presented using the Grand Partition Function and the Bragg–Williams approximation. Explicit solutions of the problem are found (1) when the surface makes a small perturbation of the solution composition (2) at the critical point for phase separation and (3) when adsorption is confined to the 1st or surface layer of the solution. The effect of the surface falls off exponentially and rapidly on entering the solution except near the critical point where a very slow fall-off is found. Case (3) is thus usually found experimentally; published experimental isotherms for the adsorption of benzene–cyclohexane on carbon blacks are analyzed, showing the degree of heterogeneity of these surfaces.

Introduction

Experimental isotherms for the adsorption of non-electrolyte solutions on solid surfaces[1,2] have often been interpreted from the point of view of classical thermodynamics or by supposing that each separate component is related to its concentration through a Freundlich or Langmuir isotherm. Statistical mechanical discussions of the analogous problem of the surface tension of binary solutions have been given using the cell model.[3–6]

Adsorption has also been considered,[7] the surface of the liquid being taken to be a particular lattice plane and the equilibrium equations discussed to give the composition of the solution near the surface. In the following, we present similar general equilibrium equations using an extension of previous work,[3–5] and give particular solutions of the equations to yield adsorption isotherms. We apply the results in a particular case to typical experimental isotherms reported in the literature.

(1) J. J. Kipling, *Quart. Revs.*, **5**, 60 (1951).

(2) C. G. Gosser and J. J. Kipling, THIS JOURNAL, **64**, 710 (1960).

(3) E. A. Guggenheim and N. K. Adam, *Proc. Roy. Soc. (London)*, **A139**, 218 (1933).

(4) E. A. Guggenheim, "Mixtures," Oxford University Press, 1952, Chapter XIX.

(5) R. Defay and I. Prigogine, *Trans. Faraday Soc.*, **46**, 199 (1950).

(6) F. Murakami, S. Ono, M. Tamura and M. Kurata, *J. Phys. Soc. Japan*, **6**, 309 (1951).

(7) S. Ono, *Mem. of the Faculty of Eng. Kyushu University*, **12**, 19 (1950).

Adsorption Using the Grand Partition Function

Following the cell model of Guggenheim and Adam,[3,4] the solution contains N_A and N_B molecules of types A and B; at the surface each molecule loses a fraction m of its z nearest neighbors, interacting instead with the solid surface with an adsorption energy E_{ads}^A or E_{ads}^B; the mole fraction of B in the surface molecular layer is x_1, that in the ith layer x_i which tends to x in the bulk solution. Molecules A and B are assumed to each take up the same area in a molecular plane. The total number of molecules in each molecular plane is n.

The following expression for the energy of the system may be written as an extension of the results in ref. 3 and 4 where the composition x_i is taken equal to x for $i > 1$ and for $i > 2$, respec-

tively. Regular solution theory and the Bragg–Williams approximation are used.

$$E = -\frac{1}{2}N_A z\epsilon_{AA} - \frac{1}{2}N_B z\epsilon_{BB} + \frac{1}{2}nx_1\{mz(\epsilon_{BB} - E^B_{ads})\} + \frac{1}{2}n(1 - x_1)\{mz(\epsilon_{AA} - E^A_{ads})\} + \Sigma W_i \quad (1)$$

where

$$W_1 = n[wx_1(1 - x_1) + \frac{1}{2}mw(x_1 - x_2)^2 - mwx_1(1 - x_1)] \quad (2)$$

and for $i > 1$

$$W_i = n[wx_i(1 - x_i) + \frac{1}{2}mw\{(x_i - x_{i+1})^2 + (x_i - x_{i-1})^2\}] \quad (3)$$

The symbols have the usual significance accorded them by regular solution theory.

The partition function for the solution may be written as usual

$$Q = \prod_i [n!/(nx_i)!\{n(1 - x_i)\}!\, q_{A,i}{}^{n(1-x_i)}\, q_{B,i}{}^{nx_i} \exp(-W_i/RT)] \quad (4)$$

Here

$$q_{A,i} \equiv q_A = a_{A,i}\exp\left\{\frac{1}{2}\epsilon_{AA}z/kT\right\} \quad (5)$$

$$q_{A,1} \equiv q_A' = a_{A,1}\exp\left\{-\frac{1}{2}mz(\epsilon_{AA} - E^A_{ads})/kT\right\} \times \exp\left\{\frac{1}{2}\epsilon_{AA}z/kT\right\} \quad (6)$$

$a_{A,i}$ and $a_{A,1}$ are the usual non-configurational parts of the partition functions of the A and B molecules in the different layers. Minimizing the Grand Partition Function[4] with respect to x_i leads to the following set of equilibrium equations

$$\ln(\lambda_B q_B'/\lambda_A q_A') - \ln(x_1/(1 - x_1)) - w/kT\left[(1 - 2x_1) - 2m\left(x_2 + \frac{1}{2} - 2x_1\right)\right] = 0 \quad (7)$$

$$\ln(\lambda_B q_B/\lambda_A q_A) - \ln(x_i(1 - x_i)) - w/kT[(1 - 2x_i) - 2m(x_{i-1} + x_{i+1} - 2x_i)] = 0 \quad (8)$$

The activities may be eliminated from these equations by subtraction of the equilibrium equation for the bulk equation[4] giving

$$\ln x_1/(1 - x_1) - \ln x/(1 - x) = \ln q_B'q_A/q_Bq_A' + 2w/kT\left[(x_1 - x) + m\left(\frac{1}{2} + x_2 - 2x_1\right)\right]; \quad (9)$$

for $i > 1$

$$\ln x_i/(1 - x_i) - \ln x/(1 - x) = 2w/kT[(x_i - x) + m(x_{i-1} + x_{i+1} - 2x_i)] \quad (10)$$

These equations are formally the same, on the introduction of x_0 into (9), as

$$x_0 = \frac{1}{2} + \Delta E/2mw$$
$$\Delta E = E^B_{ads} - E^A_{ads} - m(E^B_{vap} - E^A_{vap}) = kT\ln(q_B'q_A/q_A'q_B) \quad (11)$$

Here we suppose the entropic part of the partition function of the molecules to be the same at the surface as in the interior. This assumption, however, is not essential and $\ln q_B'q_A/q_Bq_A'$ may be considered to be a free energy term. A solution of the equilibrium equations for the x_i will give the adsorption from the solution on the surface, and the interfacial tension.

Solution of the Equilibrium Equations

It is of interest to discuss various particular cases in which analytical solutions of the equilibrium equations may be obtained. The first occurs for small adsorption or a small perturbation of the composition in each molecular layer, and as seen later, the solution not too near the critical point, $x_c = {}^1/_2$, $w/kT_c = 2$. The second case occurs at the critical point, and the third, although rather trivial, is nevertheless the one usually encountered in experiments. Here, although the effect of the surface may be large, it is nevertheless confined to the first molecular layer. The condition that this occurs is that $w/kT < \sim 0.7$.

(1) **A Small Perturbation of the Solution by the Surface.**—We put

$$y_i = x_i - x = Ae^{-\beta i} \quad (12)$$

Expanding equation 10 in powers of y_i

$$y_i\{1/x + 1/(1 - x) - 2w/kT\} + \frac{1}{2}y_i^2\{1/(1 - x_i)^2 - 1/x^2\} + \frac{1}{3}y_i^3\{1/(1 - x)^3 + 1/x^3\} + \ldots 2mw/kT(2y_i - y_{i+1} - y_{i-1}) = 0 \quad (13)$$

Retaining only the first power of y_i, (12) is found to be a solution of the equilibrium difference equations with a value of β given by

$$1/x(1 - x) - 2w/kT\{1 - 2m(1 - \cosh\beta)\} = 0 \quad (14)$$

When $w > 0$, β has real values, and there is thus a monotonic exponential decrease of the x_i toward x as $i \to \infty$. For $w < 0$, imaginary values of β are obtained, and this case is dealt with below. Employing eq. 12 as a boundary condition

$$A = \left(\frac{1}{2} - x\right) + \ln q_B'q_A/q_A'q_B\,(kT/2mw) = x_0 - x \quad (15)$$

and the adsorption on the surface is given by

$$n\Sigma y_i = nA\exp(-\beta)/1 - \exp(-\beta) \quad (16)$$

which is the quantity designated by Gibbs as Γ_2, when expressed per unit surface. Equation 14 shows that unless the system is quite near the critical point the effect of the surface falls off rapidly on entering the solution and the surface region may be taken as only one molecular layer thick as assumed by Guggenheim and Adam. Cosh β may then be replaced by ${}^1/_2\exp\beta$ in (13) whence the adsorption is given by

$$y_1 = 2Am\text{-}vkT\,x(1 - x)$$

It is evident that curves of adsorption *vs.* concentration will display the characteristic S-shape found experimentally, and that this shape is due to nonideality of the mixture as suggested by Jones and Mill.[8]

When $w < 0$, solutions of (9) and (10) are sought which have the form

$$y_i = A\exp[-(a + bj)i] \quad (17)$$

where a and bj are real and imaginary parts of the constant β. Placing (17) in (9) and (10), one finds that

(8) D. C. Jones and G. S. Mill, *J. Chem. Soc.*, 213 (1957).

$$y_i = (-1)^i A \exp(-ai) \quad (18)$$

a being given by the equation

$$1/x(1-x) - 2w/kT[1 - 2m(1 + \cosh a)] \quad (19)$$

Thus in this case, values of x_i oscillate about the limiting value of x. The physical reason for this oscillation of x_i rather than the monotonic change as with $w>0$ seems to be the following. Suppose one component, say A, to be adsorbed at the surface in the layer $i = 1$. Since $w<0$, there will be an accumulation of molecules of type B in the layer $i=2$, followed by an accumulation of type A molecules in the layer $i = 3$, and so on.

The above treatment becomes inaccurate when terms higher than the first power of y_i must be taken into account, thus when the coefficient of the first term of (3) tends to zero, or when the system approaches the unstable region[7] lying below the curve

$$1/x + 1/(1-x) - 2w/kT = 0 \quad (20)$$

in the usual phase diagram. The coexistence curve lies above this line except for the critical point common to both curves, and which is therefore the only point on (20) attainable by the stable solution; adsorption at this point is discussed below. When $\Delta E = 0$, in eq. 14 the temperature may be as low as 1.05 T_c without destroying the validity of the approximation; this temperature is raised to $\sim 1.4T_c$ when $\Delta E/2mw = 4$ to take a particular case.

(2) **Adsorption at the Critical Point.**—It has been seen that as the critical temperature is approached an analytical expression for the adsorption becomes unobtainable. At T_c, however, an analytical solution is again possible. By expanding y_{i+1} and y_{i-1} around y_i in a Taylor series we put

$$y_{i+1} + y_{i-1} - 2y_i = \partial^2 y/\partial i^2 + 2/4!\, \partial^4 y/\partial i^4 + 2/6!\, \partial^6 y/\partial i^6 + \ldots \quad (21)$$

$\partial^4 y/\partial i^4$ and higher orders may be neglected to a good approximation. (21) is used in (13) and the resulting differential equation integrated.

In the equation, the coefficients of y^2 and all odd powers of y disappear at the critical point. Neglecting coefficients of y^6 and higher powers (a good approximation at the critical point) we have

$$(\partial y/\partial i)^2 = 2y^4/3m \quad (22)$$

whence by integration

$$1/y = 1/A + (3m/2)^{1/2} i \quad (23)$$

using the boundary condition that $y = A$ when $i = 0$. It may be seen that in this approximation the effect of the surface falls off very slowly at the critical temperature, the total adsorption apparently diverging for an infinitely large solution. The effect of the surface on the critical temperature of thin films will be discussed at a later date.

(3) **Adsorption in First Layer Only.**—In almost all experimental results to be found in the literature, the temperature is so far above the critical temperature as to effectively confine adsorption to the first layer of the solution. In this case, $x_i = x$ when $i > 1$, and equation 9 may be written

$$\ln x_1/(1-x_1) - \ln x/(1-x) - 2w/kT[(x_1 - x) - m\left(2x_1 - x - \frac{1}{2}\right)] = \ln q_B' q_A/q_B q_A' = \Delta E/kT \quad (24)$$

Most experiments are performed with surfaces for which either A or B is strongly adsorbed in order to produce an easily measurable adsorption. Thus, $|\Delta E| \gg W$, and the term is brackets in (24) may be neglected also, to give what is essentially the analog of the Langmuir isotherm for the monomolecular adsorption of a gas on a solid surface, *viz.*

$$\ln x_1/(1-x_1) - \ln x/(1-x) = \Delta E/kT \quad (25)$$

Application to Experiments

Equation 26 has been applied to the experimental results of Blackburn, Kipling and Tester[8] for the adsorption of benzene–cyclohexane on two non-porous solids, Spheron-6 and artificial graphite, and also to the results of Kiselev and Platova[9] for the adsorption of toluene–heptane on oxidized and graphitized carbon black. In the first set of results, the benzene is preferentially adsorbed on the Spheron-6 at all concentrations, while for the graphite, an S-shaped curve is found with preferential adsorption of benzene below a benzene mole fraction of 0.93. The Russian results are qualitatively similar, the toluene being adsorbed preferentially up to mole fractions of 0.87 and 0.43 on the oxidized and graphitized carbon blacks, respectively. Values of x_1 may be obtained by comparing the adsorption of benzene or toluene with the amount adsorbed from the pure benzene or toluene vapor to form a monolayer. We have calculated values of ΔE as a function of the mole fraction of aromatic hydrocarbon using equation 25; ΔE is quite constant for the results obtained by Kipling and collaborators using Spheron-6 as adsorbent suggesting this surface to be fairly homogeneous. With graphite, however, the values of ΔE fall continuously as shown in Table I. Visual inspection of isotherms for other systems shows that such a decrease of ΔE with increasing x, *i.e.*, decrease of the surface's affinity for the component with increasing concentration of the component, is commonly found.

TABLE I

VALUES OF $\Delta E/kT$ FOR ADSORPTION OF BENZENE–CYCLOHEXANE ON ARTIFICIAL GRAPHITE (RESULTS OF BLACKBURN, TESTER AND KIPLING)

x	$\Delta E/kT$ expt.	$\Delta E/kT$ calcd.
0.05	1.67	1.78
.1	1.63	1.65
.3	1.47	1.40
.5	1.26	1.26
.9	0.91	0.97
.90	.23	.23
.95	− .08	− .08

Changes of ΔE with concentration may be produced in at least two ways: (1) a heterogeneity of the surface and (2) specific orientations of the ad-

(7) I. Prigogine and R. Defay, "Chemical Thermodynamics," Longmans, Green and Co. Ltd., London, 1954, p. 248.

(8) A. Blackburn, D. A. Tester and J. J. Kipling, *J. Chem. Soc.*, 2373 (1957).

(9) A. V. Kiselev and V. V. Platova, "Proceedings of the Second International Congress of Surface Activity," vol. III, Butterworths, London, 1957, p. 526.

sorbed molecules at the surface rather than the random orientation which we have assumed. The second effect can produce an increase or fall of ΔE with x, and hence cannot explain the generally observed fall of ΔE. The effect of surface heterogeneity, however, is always such as to produce a decrease of ΔE with increasing x. We have assumed the "graphite" surface to be composed of only two groups of sites, for simplicity, comprising 90 and 10% of the surface with values of $\Delta E/kT = 1.8$ and -2.8, respectively. The adsorption on each group of sites was calculated using equation 25 and the total adsorption then used to give mean values of $\Delta E/kT$. These are presented in Table I and show a reasonable fit with the experimental values. A similar analysis of the results of Kiselev and Platova for the graphitized carbon black showed 52% of the sites favoring the aromatic hydrocarbon, $\Delta E/kT = 2.6$, the rest with $\Delta E/kT = -3.2$. The isotherm is not very sensitive to the choice of energies and hence these values must be considered rather approximate.

Adsorption from binary non-electrolyte solutions has been used to characterize in a qualitative way the surface of carbon black[10] and other pigments.[11] It is possible that such problems might be treated quantitatively as described above.

(10) C. W. Sweitzer, L. J. Venuto and R. K. Estebu, *Paint, Oil and Chem. Rev.*, **115**, 22 (1952).

(11) L. Dintenfoss, *Chemistry and Industry*, 560 (1957).

It is known that the whole surface of the Spheron-6 is probably oxidized, thus presenting a fairly homogeneous surface. The artificial graphite is certainly less oxidized (see the analyses of Blackburn, Kipling and Tester) and the 10% of sites with $\Delta E/kT = -2.8$ may be associated with bare graphite sites. Observations[12] that graphon (a practically pure graphite surface) adsorbs cyclohexane vapor more strongly than benzene would seem to be in accord with the above assignment.

Such an adsorption of benzene and other aromatic hydrocarbons in preference to non-aromatic hydrocarbons of about the same molecular weight is also to be found for hydrated silica gel as adsorbent[9] where there is a well-established donor–acceptor interaction between the acidic surface hydroxyls and the π-electrons of the aromatic nucleus. Both hydroxyl and carbonyl groups[1] are present on the surface of the oxidized carbon black, and various possibilities exist for obtaining a donor–acceptor interaction between the surface and the aromatic nucleus. A fuller discussion of this problem has been given elsewhere.[13]

Acknowledgments.—We acknowledge with gratitude the support of the Paint Research Institute of the Federation of Paint and Varnish Production Clubs which has made this work possible.

(12) R. N. Smith, C. Pierce and H. Cordes, *J. Am. Chem. Soc.*, **72**, 5595 (1950).

(13) G. Delmas and D. Patterson, *Offic. Dig. Federation Paint & Varnish Production Clubs*, **31**, 1129 (1959).

THE STUDY OF LIMITED MOLECULAR WEIGHT DISTRIBUTIONS BY THE USE OF EQUILIBRIUM ULTRACENTRIFUGATION[1]

BY THOMAS H. DONNELLY

Swift & Company Research Laboratories, Chicago, Illinois

Received January 29, 1960

In the investigation of heterodisperse systems, the technique of equilibrium ultracentrifugation offers the advantage of ability to evaluate more than one moment, of known form, of the weight distribution function. Unique specification of such a distribution function from these moments alone is possible only in the case of paucidisperse systems, such as might be obtained from fractionated small polymers. The present work recasts the equations of Goldberg and of Johnson, Kraus and Scatchard in a form more suitable for use with such paucidisperse systems, incorporating a simple correction adequate as a first-order approximation of pressure effects. The measurable moments of the distribution are defined in terms of measurements at infinite dilution. Calculations of the averages related to these moments are illustrated by application to a sample of linoleic acid polymers. The precision necessary in measuring these averages is made apparent by a consideration of the mathematics by which such a distribution function may be evaluated from its moments.

Introduction

The advantages of the use of short columns for rapid attainment of ultracentrifugal equilibrium, as pointed out by Van Holde and Baldwin,[2] have served to refocus attention on the capabilities of this technique for molecular weight studies. In simple, relatively ideal systems, attainment of equilibrium in the ultracentrifuge has the advantage of simpler calculations than those associated with the Archibald principle[3,4] for rapid measurement of molecular weights. With complex systems, the simple relationship of the molecular weight averages measured by equilibrium ultracentrifugation to the moments of mass of the molecular weight distribution will often outweigh any advantage gained by the use of the Archibald principle.[5]

(1) Presented in part before the Division of Polymer Chemistry at the 136th meeting of the American Chemical Society, Atlantic City, New Jersey, September, 1959.

(2) K. E. Van Holde and R. L. Baldwin, THIS JOURNAL, **62**, 734 (1958).

(3) W. J. Archibald, *ibid.*, **51**, 1204 (1947).

(4) S. M. Klainer and G. Kegeles, *ibid.*, **59**, 952 (1955).

(5) The types of averages evaluated by equilibrium ultracentrifugation have been described by Lansing and Kraemer.[6] The relationship of these averages to the moments of mass of the distribution is given, for example, by Goldberg.[7] The possibility of evaluating more than

Equilibrium ultracentrifugation has been employed as a method for studying distributions since Rinde's[10] studies of particle size distributions in gold sols. Methods for the calculation of distributions directly from the technique are given by Rinde,[10] Wales, Adler and Van Holde,[11] and Herdan.[12] These authors have often found that the distributions obtained are unsatisfactory, especially since they often indicate that certain size ranges are present in negative amounts. This is probably due to many general causes, one of which is the failure of the technique to afford sufficiently precise measurements, while another is the use of continuous rather than discrete distributions.

The present study is concerned with discrete distributions, especially those obtained in systems of very small polymers. For such systems, it is seen that compressibility corrections are of the order of the reciprocal molecular weight, while variations of partial specific volume with molecular weight may be far more important.

Theory

The thermodynamic description of the equilibrium state attained during ultracentrifugation has been given by Pedersen.[13] A more detailed treatment applicable to multi-component systems is given by Goldberg[7] in an extension of the classical thermodynamics of solutions in gravitational fields as given by Guggenheim.[14] A further refinement has been added by Young, Kraus and Johnson,[15] who have considered the effects of activity coefficients and compressibilities in simple systems. The studies of Fujita[16] and Cheng and Schachman[17] suggest methods of incorporating compressibility corrections, although these studies are not concerned with equilibrium measurements.

The basic equation of the equilibrium ultracentrifuge, essentially as given by Pedersen,[13] is

$$\mathrm{d} \ln N_i = M_i (1 - \bar{v}_i \rho) \frac{\omega^2 x \, \mathrm{d}x}{RT} - \sum_{j=1}^{n} \left(\frac{\partial \ln f'_i}{\partial N_j} \right) \mathrm{d}N_j \quad (1)$$

where the symbols are as used by Pedersen except for the representation of the partial specific volume by $\bar{v}_i$.

Further evaluation of this equation may be made by considering the equation

$$\mathrm{d}V_i = \left(\frac{\partial V_i}{\partial T} \right)_{P,N_j} \mathrm{d}T + \left(\frac{\partial V_i}{\partial P} \right)_{T,N_j} \mathrm{d}P + \sum_{j=1}^{n} \left(\frac{\partial V_i}{\partial N_j} \right) \mathrm{d}N_i \quad (2)$$

At constant temperature, eq. 2 is reduced to the same variables as those of eq. 1 by using the definition of the isothermal compressibility.

$$\beta_i = -\frac{1}{V_i} \left(\frac{\partial V_i}{\partial P} \right)_{T,N_j} = -\frac{1}{\bar{v}_i} \left(\frac{\partial \bar{v}_i}{\partial P} \right)_{T,N_j} \quad (3)$$

Combining the condition of hydrostatic equilibrium with the definition of the ultracentrifugal potential gives

$$\mathrm{d}P = -\rho \mathrm{d}\phi = \rho \omega^2 x \, \mathrm{d}x \quad (4)$$

Also

$$\left(\frac{\partial V_i}{\partial N_j} \right) = \frac{\partial}{\partial N_j} \left(\frac{\partial \mu_i}{\partial P} \right) = \frac{\partial}{\partial P} \left(\frac{\partial \mu_i}{\partial N_j} \right) = RT \frac{\partial}{\partial P} \left(\frac{\partial \ln f'_i}{\partial N_j} \right) \quad (5)$$

which has been used by Young, Kraus and Johnson[15] in a previous study of simple compressible systems. Using these substitutions, eq. 2 becomes, at constant temperature

$$\mathrm{d} \ln \bar{v}_i = -\beta_i \rho \omega^2 x \, \mathrm{d}x + \frac{RT}{V_i} \sum_{j=1}^{n} \frac{\partial}{\partial P} \left(\frac{\partial \ln f_i'}{\partial N_j} \right) \mathrm{d}N_j \quad (6)$$

A completely general description of the mole fraction distribution in a solution column in which ultracentrifugal equilibrium is established may be obtained by combining eq. 1 and 6 with the definition

$$\rho = \frac{\sum_{i=0}^{n} N_i M_i}{\sum_{i=0}^{n} N_i M_i \bar{v}_i} = \frac{N_0 M_0 + \sum_{i=1}^{n} N_i M_i}{N_0 M_0 \bar{v}_0 + \sum_{i=1}^{n} N_i M_i \bar{v}_i} = \frac{1}{\bar{v}_0} \left(1 + \frac{\sum_{i=1}^{n} N_i M_i (1 - \bar{v}_i/\bar{v}_0)}{N_0 M_0} - \ldots \right) \quad (7)$$

Because of the ambiguity[18] regarding the terms, $(\partial \ln f'_i / \partial N_j)$, in any case, little is gained by writing such an equation except in the simplest cases. It would seem to be more appropriate to investigate the behavior of ideal systems and to presume that ideality may be approached by real systems. Further, in order to simplify eq. 7, it would seem most appropriate to assume that ideality is obtained at infinite dilution. In order to simplify

one average molecular weight by the Archibald principle has been established by Erlander and Foster,[8] while the form of such averages has been investigated by Yphantis.[9]

(6) W. D. Lansing and E. O. Kraemer, *J. Am. Chem. Soc.*, **57**, 1369 (1935).

(7) R. J. Goldberg, THIS JOURNAL, **57**, 194 (1953).

(8) S. R. Erlander and J. F. Foster, *J. Poly. Sci.*, **37**, 103 (1959).

(9) D. A. Yphantis, THIS JOURNAL, **63**, 1742 (1959).

(10) H. Rinde, Dissertation, Uppsala, 1928.

(11) M. Wales, F. T. Adler and K. E. Van Holde, THIS JOURNAL, **55**, 145 (1951).

(12) G. Herdan, *Research*, **3**, Suppl. 35 (1950).

(13) K. O. Pedersen, in "The Ultracentrifuge," Svedberg and Pedersen, Clarendon Press, Oxford, 1940, p. 48 ff. Reprinted by Johnson Reprint Corp., New York, 1959.

(14) E. A. Guggenheim, "Thermodynamics," North Holland Publishing Co., Amsterdam, 1957, pp. 403 ff.

(15) T. F. Young, K. A. Kraus and J. S. Johnson, *J. Chem. Phys.*, **22**, 878 (1954).

(16) H. Fujita, *J. Am. Chem. Soc.*, **78**, 3598 (1956).

(17) P. Y. Cheng and H. K. Schachman, *ibid.*, **77**, 1498 (1955).

(18) The theoretical form of these terms has been given by Krigbaum and Flory.[19] The complexity of these results, however, is such that no straightforward simplification results from their use. A more realistic approach is the use of systems with ideal behavior, as shown by Mandelkern, Williams and Weissberg,[20] although Fujita and his co-workers[21,22] have had some success with systems which are somewhat more non-ideal.

(19) W. R. Krigbaum and P. J. Flory, *J. Am. Chem. Soc.*, **75**, 1775 (1953).

(20) L. Mandelkern, L. C. Williams and J. G. Weissberg, THIS JOURNAL, **61**, 271 (1957).

(21) H. Fujita, *ibid.*, **63**, 1326 (1959).

(22) H. Fujita, A. M. Linklater and J. W. Williams, *J. Am. Chem. Soc.*, **82**, 379 (1960).

this and subsequent treatment, it will be convenient to introduce a variable, $u \equiv (x^2 - x_m^2)/(x_b^2 - x_m^2)$, where x_b is the value of the outer radius of rotation of the column, while x_m is that for the inner radius. Equation 1 may now be written as

$$dN_i = N_i M_i (1 - \bar{v}_i\rho) A \, du \tag{8}$$

where A is defined by the equation

$$A = \frac{\omega^2(x_b^2 - x_m^2)}{2RT} \tag{9}$$

Under these same conditions, eq. 6 becomes

$$d \ln \bar{v}_i = - \beta_i \rho \, RTA \, du \tag{10}$$

and eq. 7 is merely $\rho = 1/\bar{v}_0$.

$$d\bar{v}_0 = - \beta_0 \, RTA \, du \tag{11}$$

If it is now assumed that β_0 is a constant,[23] eq. 11 may be directly integrated to give

$$\bar{v}_0 = \bar{v}_0^{(0)} - \beta_0 \, RTAu \tag{12}$$

where the superscript (0) denotes that the value is taken at $u = 0$, or $x = x_m$. Equation 10 thus becomes, for the species $i = 1$ to n

$$d \ln \bar{v}_i = - \frac{\beta_i \, RTA}{\bar{v}_0^{(u)}} \, du \tag{13}$$

When eq. 12 is valid, and β_i is constant, this may be integrated to give

$$\bar{v}_i = \bar{v}_i^{(0)}(1 - \beta_0\rho_0^0 RTAu)^{\beta_i/\beta_0} \tag{14}$$

if $1/\bar{v}_0^{(0)}$ is written as ρ_0^0. Equation 8 may then be written as

$$dN_i = N_i M_i \{1 - \bar{v}_i^{(0)}\rho_0^0(1 - \beta_0\rho_0^0 RTAu)^{(\beta_i/\beta_0)}\} A \, du \tag{15}$$

by substituting eq. 12 and 14.

Equation 15 may then be expanded by the binomial theorem to give

$$dN_i = N_i M_i \left\{1 - \bar{v}_i^{(0)}\rho_0^0(1 - (\beta_i - \beta_0)\rho_0^0 RTAu + \frac{(\beta_i - \beta_0)(\beta_i - 2\beta_0)}{2} (\rho_0^0 \, RTAu)^2 + \ldots.)\right\} A \, du \tag{16}$$

This may be rewritten as

$$dN_i = N_i \left\{W_i + M_i\bar{v}_i^{(0)}(\rho_0^0)^2(\beta_i - \beta_0)RTAu \left(1 - \frac{(\beta_i - 2\beta_0)}{2} (\rho_0^0 \, RTAu) + \ldots\right)\right\} A \, du \tag{17}$$

if W_i is defined as

$$W_i = M_i (1 - \bar{v}_i^{(0)}\rho_0^0) \tag{18}[25]$$

While it may be useful to treat systems of few components or those in which all solute species are equally compressible by eq. 17 or its equivalent, this equation immediately suggests that, as should be expected, an appropriate approximation of compressibility effects might be obtained by considering all solute species to have compressibilities equal to the solvent, or $\beta_i = \beta_0 = \beta$. Under these conditions, eq. 17 becomes

$$dN_i = N_i W_i A \, du \tag{19}$$

Such a system may be related to one at laboratory conditions through the usual conservation of mass condition, *i.e.*

$$\int_m^b x c_i^{(x)} dx = \frac{(x_b^2 - x_m^2)}{2} \int_0^1 c_i^{(u)} \, du \tag{20}$$

This is just the analog of eq. 4 of Ginsburg, Appel and Schachman,[27] and $c_i^{(x)}$ is similar to their c. $c_i^{(u)}$ is the same value as $c_i^{(x)}$, but x is now expressed as the corresponding value of u. In the system considered in eq. 19, $c_i^{(u)}$ is given by

$$c_i^{(u)} = \frac{N_i^{(u)} M_i}{M_0 \bar{v}_0^{(u)}} = \frac{N_i^{(u)} M_i}{M_0 \bar{v}_0^{(0)} (1 - Yu)} \tag{21}$$

if we define Y by the expression

$$Y = \beta\rho_0^0 \, RTA \tag{22}$$

A system at laboratory conditions may be related to one at ultracentrifugal equilibrium by evaluating eq. 20 using eq. 21 before and after redistribution of species. This process is equivalent to the equation

$$(N_i)_0 \int_0^1 \frac{du}{(1 - Yu)} = N_i^{(0)} \int_0^1 \frac{e^{AW_i u} \, du}{(1 - Yu)} \tag{23}$$

where $(N_i)_0$ is the original mole-fraction of the ith species and is independent of compression. While the integral on the left is easily evaluated, that on the right has no simple evaluation. For the purposes of this work, a satisfactory evaluation may be made by expanding the denominator in the usual series and dropping terms in Y^2. Since Y is of the order of 0.02 or less in the systems dealt with here, this will usually be adequate. Using such a treatment, $N_i^{(0)}$ may be related to $(N_i)_0$ by the expression

$$N_i^{(0)} = (N_i)_0 \frac{AW_i (1 + Y/2)}{\left((e^{AW_i} - 1)\left(1 - \frac{Y}{AW_i}\right) + Ye^{AW_i}\right)} \tag{24}$$

This may be used to evaluate the constant in the integrated form of eq. 19, giving the result that

$$N_i^{(u)} = \frac{(N_i)_0 AW_i(1 + Y/2)e^{AW_i u}}{\left((e^{AW_i} - 1)\left(1 - \frac{Y}{AW_i}\right) + Ye^{AW_i}\right)} \tag{25}$$

Refractive increments may be defined so that

$$(n - n_0) = \frac{\sum_{i=1}^{n} R_i N_i M_i}{\sum_{i=0}^{n} N_i M_i} \tag{26}$$

which, for constant and equal R_i, would mean that the difference between the refractive index of the solution and that of the solvent is propor-

(23) This assumption will usually describe amply well the sort of system which is likely to be encountered in the use of this procedure. Use of the technique of Van Holde and Baldwin[2] make such an assumption even more realistic. When such an assumption is not adequate, it is possible to resort to an equation of state such as the Tait equation.[24] The mathematics of this procedure are far more cumbersome than those encountered here, and such a procedure apparently adds little to the understanding of present day experiments.

(24) See, for example, H. S. Harned and B. B. Owen, "The Physical Chemistry of Electrolytic Solutions," Rheinhold Publ. Corp., New York, N. Y., 1958, p. 379 ff.

(25) W_i is used here, rather than the similar L_i of Johnson, Kraus and Scatchard[26] or the M_i^* of Yphantis,[9] since ρ is not usually equal to ρ_0^0.

(26) J. S. Johnson, K. A. Kraus and G. Scatchard, THIS JOURNAL, **58**, 1034 (1954).

(27) A. Ginsburg, P. Appel and H. K. Schachman, *Arch. Biochem. Biophys.*, **65**, 545 (1956).

tional to the percentage by weight of solute. These R_i are related to the $\bar{R}_i$ of Van Holde and Baldwin[2] by the relationship

$$R_i = \rho_0 B_i \tag{27}$$

where the B_i are the $\bar{R}_i$ of Van Holde and Baldwin[2] evaluated at infinite dilution.[28] If $(n - n_0)$ is abbreviated as n_c, as suggested by Van Holde and Baldwin,[2] eq. 25 and 26 may be combined to give

$$n_c = \frac{A\left(1 + \frac{Y}{2}\right)\sum_{i=1}^{n} \frac{R_i(N_i)_0 M_i W_i e^{AW_i u}}{\left((e^{AW_i} - 1)\left(1 - \frac{Y}{AW_i}\right) + Ye^{AW_i}\right)}}{\sum_{i=0}^{n} N_i M_i} \tag{28}$$

Equation 28 and succeeding results will be considerably simplified by defining W_i' by the expression

$$W_i' = \frac{W_i}{\left(1 - \frac{Y}{AW_i} + \frac{Ye^{AW_i}}{e^{AW_i} - 1}\right)} \tag{29}$$

and A' by the expression

$$A' = A\left(1 + \frac{Y}{2}\right) \tag{30}$$

Equation 28 thus becomes

$$n_c^{(u)} = \frac{A' \sum_{i=1}^{n} R_i (N_i)_0 M_i W_i' e^{AW_i u}/(e^{AW_i} - 1)}{\sum_{i=0}^{n} N_i M_i} \tag{31}$$

Equation 26 may be written as

$$(n_c)_0 = \frac{\sum_{i=1}^{n} R_i (N_i)_0 M_i}{\sum_{i=0}^{n} N_i M_i} \tag{32}$$

where $(n_c)_0$ is the value of $(n - n_0)$ measured before redistribution of species. Equation 32 may now be combined with eq. 31 to give

$$\lim_{N_0 \to 1}\left(\frac{(n_c)^{(u)}}{(n_c)_0}\right) = A' \frac{\sum_{i=1}^{n} R_i(N_i)_0 M_i W_i' e^{AW_i u}/(e^{AW_i} - 1)}{\sum_{i=1}^{n} R_i(N_i)_0 M_i} \tag{33}$$

By combining the derivative of eq. 33 with that equation, there results

$$\lim_{N_0 \to 1}\left(\frac{\mathrm{d} \ln (n_c)}{\mathrm{d}u}\right) = A \frac{\sum_{i=1}^{n} R_i(N_i)_0 M_i W_i' W_i e^{AW_i u}/(e^{AW_i} - 1)}{\sum_{i=1}^{n} R_i(N_i)_0 M_i W_i' e^{AW_i u}/(e^{AW_i} - 1)} \tag{34}$$

Equation 34 defines a quantity which is proportional to the quantity, M_{wz}, ordinarily defined. Extrapolation of the reciprocal of M_{wz} has usually been taken as valid, although there is some question as to the reliability of any such procedure.[20] When such a procedure is valid, one may extrapolate the reciprocal of the quantity on the left of eq. 34 and use the function so obtained to evaluate the quantity on the right. In order that this procedure be strictly valid, the values of A should be constant in all experiments. This usually means that the value of $(x_b^2 - x_m^2)$ should be constant. As a first-order correction, values of $(x_b^2 - x_m^2)_{\text{ref.}}/(\mathrm{d} \ln (n_c)/\mathrm{d}u)$ may be extrapolated to zero concentration.[29] This procedure will define $(\mathrm{d} \ln (n_c)/\mathrm{d}u)$ as a function of u only. This function is then used to define the various molecular weight averages as well as they can be defined by the use of equilibrium ultracentrifugation. The evaluation of such molecular weight averages is by an extension of the classical methods of Lansing and Kraemer[6] and Wales.[30] By such a procedure, it may be shown, for example, that

$$\frac{\left(\frac{n_c^{(1)}}{n_c^{(0)}} - 1\right)}{A\int_0^1 \left(\frac{n_c^{(u)}}{n_c^{(0)}}\right) \mathrm{d}u} = \frac{\sum_{i=1}^{n} R_i(N_i)_0 M_i W_i'}{\sum_{i=1}^{n} R_i(N_i)_0 M_i \left(\frac{W_i'}{W_i}\right)} \tag{35-a}[31]$$

$$\frac{\left(\frac{\mathrm{d} \ln n_c}{\mathrm{d}u}\right)^{(1)}\left(\frac{n_c^{(1)}}{n_c^{(0)}}\right) - \left(\frac{\mathrm{d} \ln n_c}{\mathrm{d}u}\right)^{(0)}}{A\left(\frac{n_c^{(1)}}{n_c^{(0)}} - 1\right)} = \frac{\sum_{i=1}^{n} R_i(N_i)_0 M_i W_i' W_i}{\sum_{i=1}^{n} R_i(N_i)_0 M_i W_i'} \tag{35-b}$$

$$\frac{\left(\frac{n_c^{(1)}}{n_c^{(0)}}\right)\left\{\left(\frac{\mathrm{d}^2 \ln n_c}{\mathrm{d}u^2}\right)^{(1)} + \left(\left(\frac{\mathrm{d} \ln n_c}{\mathrm{d}u}\right)^{(1)}\right)^2\right\} - \left\{\left(\frac{\mathrm{d}^2 \ln n_c}{\mathrm{d}u^2}\right)^{(0)} + \left(\left(\frac{\mathrm{d} \ln n_c}{\mathrm{d}u}\right)^{(0)}\right)^2\right\}}{A\left\{\left(\frac{\mathrm{d} \ln n_c}{\mathrm{d}u}\right)^{(1)}\left(\frac{n_c^{(1)}}{n_c^{(0)}}\right) - \left(\frac{\mathrm{d} \ln n_c}{\mathrm{d}u}\right)^{(0)}\right\}} = \frac{\sum_{i=1}^{n} R_i(N_i)_0 M_i W_i' W_i^2}{\sum_{i=1}^{n} R_i(N_i)_0 M_i W_i' W_i} \tag{35-c}$$

and so forth. The quantities on the right in eq. 35 are related to the usual weight, z and $z + 1$ molecular weights.

As in the cases described, for example, by Wales,[30] the accuracy of the higher averages produced by further differentiation is determined by the accuracy with which the derivatives of the function, $(\mathrm{d} \ln n_c/\mathrm{d}u)$, may be evaluated at the end-points.

(28) In fact, the B_i are identical to the $\bar{R}_i$ of Van Holde and Baldwin,[2] since their R_i are constants independent of concentration. It should be emphasized that the R_i used in the present work are also taken as independent of pressure.

(29) Here $(x_b^2 - x_m^2)_{\text{ref}}$ is a reference value of $(x_b^2 - x_m^2)$ and determines the value of A for the set of values to be extrapolated. It should, therefore, be that value of A which minimizes the values of ΔA, the variation of the value of A for each set of data from this value.

(30) M. Wales, THIS JOURNAL, **52**, 235 (1948).

(31) This equation may be evaluated by a procedure equivalent to that of Johnson, Scatchard and Kraus[32] involving the use of interference optics. It should also be emphasized that studies such as the present should be interpreted in the light of second-order effects such as those which are pointed out by these authors.

(32) J. S. Johnson, G. Scatchard and K. A. Kraus, THIS JOURNAL, **63**, 787 (1959).

The problem of evaluability of higher molecular weight averages is therefore directly related to the problem of evaluation of the derivatives of a function from the function itself. This is the inverse of the problem of evaluating the Taylor's series for (d ln (n_c)/du) in the interval, u = 0 to u = 1. It is apparent from eq. 33 that the Taylor's series is usually an infinite series in u whose derivatives do not vanish. Thus, it cannot be accurately represented by a finite polynomial. Further, representation of (d ln n_c/du) by any polynomial other than this exact Taylor's series will lead to incorrect evaluation of the higher molecular weight averages. Since it is usually possible to represent this function by a polynomial other than exact, such interpretation of equilibrium ultracentrifugation data will not usually determine uniquely the exact molecular weight distribution in polydisperse systems. However, other methods of molecular weight determination are even less attractive than equilibrium ultracentrifugation as regards accurate determination of this distribution. It should be apparent that only fractionating procedures have this possibility, and that present fractionation techniques leave much to be desired. Therefore, the failure of equilibrium ultracentrifugation to provide accurate distribution functions should not be surprising.

Despite its present inability to produce exact molecular distribution functions, the technique of equilibrium ultracentrifugation is valuable in such studies since it is virtually the only technique which provides an indication and a measure of polydispersity in a single experiment. While it is true that vapor phase chromatography is a superior technique for volatile, low-molecular weight samples, and that liquid phase chromatography and electrophoresis are superior for certain medium to high molecular weight samples, neither of these techniques is as generally applicable as equilibrium ultracentrifugation. This is especially true when general applicability is judged on a molecular weight basis. Thus, it is of interest to determine how well a molecular weight distribution function may be characterized by the technique of equilibrium ultracentrifugation.

It is, of course, obvious that a system composed of one, two, or three components of known partial specific volume and molecular weight may be directly specified by equilibrium ultracentrifugation to within the limits of experimental error. This may be raised to four components in light of the suggestion by Wales[30] that derivatives corresponding to the $(z + 1)$ molecular weight average can be roughly evaluated.

As Goldberg[7] has pointed out, further information regarding the shape of molecular weight distribution curves is often available, especially if the system consists of polymeric species condensing according to some statistical rule. By virtue of the fact that it measures the first three moments of a molecular weight distribution, equilibrium ultracentrifugation may be used to verify that a system follows such a rule.

The worst case is that cited by Williams, Van Holde, Baldwin and Fujita[33] in which the distribution is specified by giving its measurable moments. To picture such a distribution, one may use the Chebychev inequality.[34] This states that, if one has a distribution whose mean is M_w and whose standard deviation is $M_w(M_z/M_w - 1)^{1/2}$, then the fraction of the distribution lying within the range $M_w(1 \pm k\,(M_z/M_w - 1)^{1/2})$ is greater than or equal to $(1 - 1/k^2)$. If a molecular weight distribution is specified in terms of weight fractions, then it is such a distribution, as is pointed out by Williams, *et al.*[33]

Experimental

This procedure was applied to samples isolated from the materials formed during the thermal polymerization of "winterized" cottonseed oil. The preparation and isolation of the sample was based on the procedure of Chang and Kummerow[35] and will be described elsewhere. Essentially it consisted of heating the oil under controlled conditions, and fractionation of the product by saponification, acidification, urea-adduct formation, and selective extraction with solvent mixtures.

A portion of this material was used for analysis of the methyl esters by gas–liquid partition chromatography. The methylation was carried out by refluxing with absolute methanol. A 50-microliter sample of the methyl esters was then analyzed using a column of Reoplex 400 on Celite 545. The Reoplex 400 was kindly supplied by the Geigy Chemical Company. This column was held at 220° in a Perkin–Elmer Model 154-B "Vapor Fractometer," and helium was used as the carrier gas. A similar determination was carried out using methyl oleate as a reference standard.

The sample for ultracentrifugal analysis was dissolved in absolute methanol. The centrifuge runs were made using a Spinco Model E ultracentrifuge, in conjunction with an analytical An-D rotor and two plain window analytical cells, Spinco No. 1190. (It was necessary to use two cells rather than one double sector cell due to the high speeds used.) One-tenth ml. of Fluorochemical FC-43,[36] produced by Minnesota Mining and Manufacturing Co., was placed in each cell using a small volume hypodermic syringe.[37] A 0.1-ml. portion of the sample dissolved in methanol was then added to one cell, while the same amount of methanol was placed in the other cell. The two cells were then placed opposite each other in the rotor, and the run carried out in accordance with the procedure of Van Holde and Baldwin.[2] Other concentrations of sample were studied similarly.

The runs were followed using the schlieren pattern as observed with a phase-plate.[38] The attainment of equilibrium was verified by failure of this pattern to change within one hour after apparent attainment. The resulting pattern was photographed, and calculations were made from enlarged tracings of the photographs. These calculations were done using a tabular scheme similar to that employed by Schachman.[39] The values of $d(n_c)/dx$ were obtained by measurement of the difference between the schlieren pattern of the solvent and that of the solution.

(33) J. W. Williams, K. E. Van Holde, R. L. Baldwin and H. Fujita, *Chem. Revs.*, **58**, 715 (1958).

(34) See, for example, H. Cramer, "Mathematical Methods of Statistics," Princeton University Press, Princeton, N. J., 1946, p. 182–183.

(35) S. S. Chang and F. A. Kummerow, *J. Am. Oil Chem. Soc.*, **30**, 403 (1953).

(36) This material has been found to have a satisfactorily high degree of insolubility in water, alcohols, ketones, aldehydes, tetrahydrofuran and ethylenediamine. In fact, studies of solutions in these solvents are limited, when using this technique, primarily by the solvent resistance of the components of boundary-forming cells. The material, however, is not satisfactory for use with hexane and benzene, and also cannot be used with the halogenated hydrocarbons.

(37) Although the volumes used here could be measured with a syringe such as a B-D Yale, 1/4-cc. capacity, it has been found to be more generally satisfactory to use one such as the Hamilton 100 microliter syringe. The Hamilton syringe is far superior in measuring, reproducibly, amounts of less than 0.1 ml.

(38) R. Trautman and V. W. Burns, *Biochim. et Biophys. Acta*, **14**, 26 (1954).

(39) H. K. Schachman, "Methods in Enzymology," IV, Academic Press, New York, N. Y., 1957, p. 32 ff.

These were tabulated *versus* x, the radius of rotation at which they were observed. Values of u and $1/x(\mathrm{d}(n_c)/\mathrm{d}x)$ were also tabulated. The quantity

$$(n_c)\Big/\frac{1}{x}\left(\frac{\mathrm{d}(n_c)}{\mathrm{d}x}\right), \text{ which is just } (x_b^2 - x_m^2)\Big/2\left(\frac{\mathrm{d}\ln(n_c)}{\mathrm{d}u}\right),$$

was determined, at various selected values of u for each dilution, by interpolation of the $1/x(\mathrm{d}(n_c)/\mathrm{d}x)$ data, and integration of the same data from $u = 0$, after determining (n_c) at $u = 0$. It may be seen that $(n_c)^{(u)} = (n_c)^{(0)} + (x_b^2 - x_m^2)/2\int_0^u 1/x(\mathrm{d}(n_c)/\mathrm{d}x)\mathrm{d}u$ in analogy to the similar equation by Ginsburg, Appel and Schachman.[27] In the work here reported, the interpolation has been done graphically from a smoothed plot, and the integration has been done with an Ott-Type 22 planimeter using the same plot. The value of (n_c) at $u = 0$ has been determined by using the relationship

$$(n_c)^{(0)} = (n_c)_0 - \frac{(x_b^2 - x_m^2)}{2}\int_0^1 (1 - u)\frac{1}{x}\left(\frac{\mathrm{d}(n_c)}{\mathrm{d}x}\right)\mathrm{d}u$$

which may be seen to be completely analogous to the comparable equation used by Ginsburg, Appel and Schachman.[27] $(n_c)_0$ is evaluated using the synthetic boundary cell, although this is run at a speed such that the solution below the synthetic boundary is as compressed as the solution in the column in which equilibrium is established. Such a speed may be determined from eq. 12, 20 and 21. For our conditions, it is approximately

$$\omega_B = 0.4\ \omega_E \qquad (36)$$

if ω_B is the speed used during the synthetic boundary run, while ω_E is used during the equilibrium run. Values of $n_c/1/x(\mathrm{d}\ n_c/\mathrm{d}x)$ have been multiplied by $(x_b^2 - x_m^2)_{ref}/(x_b^2 - x_m^2)$ to provide the first-order correction described above.[29] They are thus equal to $(x_b^2 - x_m^2)_{ref}/2(\mathrm{d}\ln n_c/\mathrm{d}u)$. These values were then plotted *vs.* $(n_c) + u$ and extrapolated, at constant u, to give $(x_b^2 - x_m^2)_{ref}/2(\mathrm{d}\ln(n_c)/\mathrm{d}u)_{N_0=1}$. From this, values of $(\mathrm{d}\ln(n_c)/\mathrm{d}u)_{N_0=1}$ were obtained as a function of u. From these latter values, a table was drawn up and the functions $(\mathrm{d}\ln(n_c)/\mathrm{d}u)_{N_0=1}$, $(\ln((n_c)^{(u)}))/n_c^{(0)})_{N_0=1}$, and $\left(\int_0^1 (n_c^{(u)}/n_c^{(0)})\mathrm{d}u\right)_{N_0=1}$ tabulated *vs.* u. These were used to evaluate the moments defined here, and the value of A was determined using the value of $(x_b^2 - x_m^2)_{ref}$. Calculation of the appropriate distribution function is based on these moments.[40]

Throughout this work, it has been assumed that the errors involved were similar to those reported by Van Holde and Baldwin,[2] and that the results could be treated accordingly. Thus, we would expect that the error of measurement of the moment defined by eq. 35-b is about 1%. This has perhaps been verified by standardization with sucrose, for which we have measured, by Method II of Van Holde and Baldwin,[2] a value of 345 for the molecular weight. It should also be pointed out that runs using solvent only in both cells do not show measurably different schlieren patterns for similarly filled cells.

Results and Discussion

Characterization of the equilibrium state attained during ultracentrifugation in terms of the equations presented here, and the appropriate calculations, is shown in Tables I, II and III. Table I presents the actual experimental data, at points close to the chosen values of u, from the run of the most concentrated example. Table II is calculated from Table I and is used for the extrapolation. Tables similar to Tables I and II are drawn up for each dilution of sample. Figure 1 illustrates the extrapolation of the data from Table II for the sample reported here. Table III is set

(40) With the help of Mr. Richard Clinite, of the Comptroller's Office, Swift & Company, we have recently developed a program for carrying out these calculations using the IBM 650 digital computer. When such a computer is not available, it is advantageous to employ a desk calculator similar to that recommended by Trautman.[41]

(41) R. Trautman, *Biochim. Biophys. Acta*, **28**, 417 (1958).

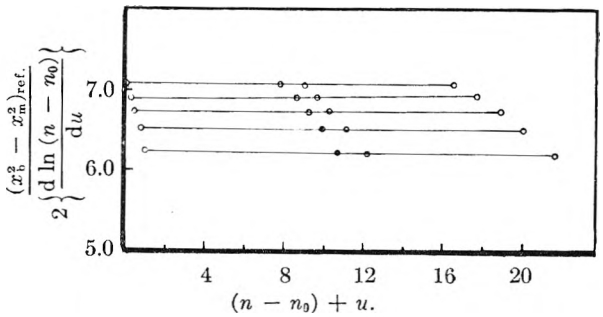

Fig. 1—An illustration of the method of extrapolation of data to infinite dilution to obtain the function from which the moments of the molecular weight distribution are evaluated.

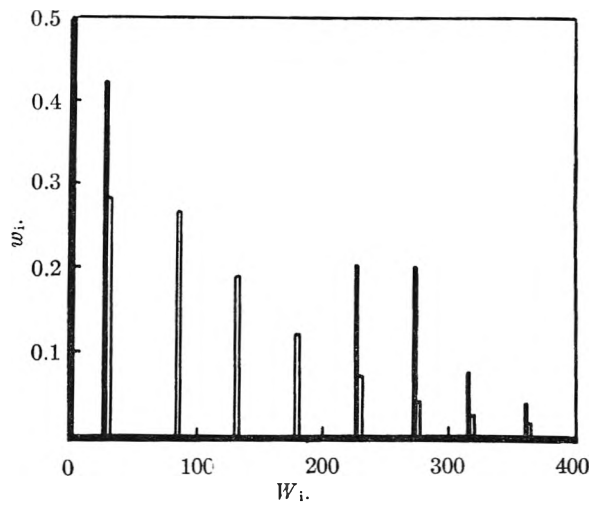

Fig. 2.—Crude representations of the spread of the molecular weight distribution based on the evaluation of the first two moments of the weight distribution as determined by these measurements, | using the Chebychev inequality, and [] using a distribution equivalent to the "most probable distribution in linear open chain molecules" as described by Flory.

up using the extrapolated data, and is used to evaluate the measurable moments of the molecular weight distribution.

For the sample reported here, the averages defined by eq. 35-a (I) and 35-b (II) are, respectively,

$$\mathrm{I} = \frac{1.284 - 1.000}{1.133(2.08 \times 10^{-3})} = 120$$

$$\mathrm{II} = \frac{(1.284)(0.238) - (0.211)}{(1.284 - 1.000)(2.08 \times 10^{-3})} = 155$$

To compute the average based on eq. 35-c, we shall resort to fitting the data by an analytic function which is an infinite polynomial whose derivatives constantly increase. The simplest such function is $\exp\{a + bu/c - u\}$. In the case at hand, the constants can be evaluated to give

$$f(u) = \exp\left\{-1.556 + \frac{0.297u}{3.47 - u}\right\}$$

This agrees with the values listed in second column of Table III to well within the experimental error, as shown in Table IV.

Differentiating this function may be used to evaluate the average defined by eq. 35-c (III). This derivative is

TABLE I

EVALUATION OF u AND $(1 - u)\frac{1}{x}\left(\frac{d(n_c)}{dx}\right)$ FROM EXPERIMENTAL DATA

x, cm.	$\left(\frac{d(n_c)}{dx}\right)$, mm.[a]	$\frac{1}{x}\left(\frac{d(n_c)}{dx}\right)$, mm./cm.	x^2, cm.^{2}	u	$(1 - u)$	$(1 - u)\times\frac{1}{x}\left(\frac{d(n_c)}{dx}\right)$, mm.[a]/cm.
6.773	16.95	2.50	45.874	0.000	1.000	2.50
6.820	18.25	2.68	46.512	.229	0.771	2.06
6.873	19.85	2.89	47.238	.489	.511	1.48
6.927	22.30	3.22	47.983	.756	.244	0.79
6.976	25.45	3.65	48.665	1.000	.000	0.00

$$\frac{(x_b^2 - x_m^2)}{2}\int_0^1 (1 - u)\frac{1}{x}\left(\frac{d(n_c)}{dx}\right) du = 1.99 \text{ mm.}^a\text{-cm.}$$

$$(n_c)_0 = 18.48 \text{ mm.}^a\text{-cm.}$$

$$(n_c)^{(0)} = 16.49 \text{ mm.}^a\text{-cm.}$$

[a] These numbers were measured on enlarged tracings using a viewing table and an accurate scale. Their actual magnitude is determined, of course, by the magnification factors, bar angle, etc., all of which have been held constant throughout these experiments. Use of different methods of measuring the refractive index gradient at x will, of course, lead to different magnitudes. Units are immaterial, since they cancel out in forming the quotients to be extrapolated.

TABLE II

EVALUATION OF QUANTITIES FOR EXTRAPOLATION

u	$\frac{1}{x}\left(\frac{d(n_c)}{dx}\right)$	(n_c)	$\frac{(x_b^2 - x_m^2)}{2\left(\frac{d \ln (n_c)}{du}\right)}$	$\frac{(x_b^2 - x_m^2)_{ref}}{2\left(\frac{d \ln (n_c)}{du}\right)}$	$\frac{(n_c) + }{u}$
0.0	2.50	16.49	6.59	7.06	16.49
0.25	2.68	17.41	6.50	6.96	17.66
.5	2.90	18.41	6.34	6.79	18.91
.75	3.22	19.55	6.07	6.51	20.30
1.0	3.65	20.69	5.69	6.09	21.69

TABLE III

EXTRAPOLATED RESULTS AND CALCULATIONS THEREON

u	$\left(\frac{d \ln (n_c)}{du}\right)_{N_0=1}$	$\left(\ln\frac{n_c(u)}{n_c(0)}\right)_{N_0=1}$	$\left(\frac{n_c(u)}{n_c(0)}\right)_{N_0=1}$
0.0	0.211	0.000	1.000
.25	.217	.059	1.061
.5	.221	.120	1.128
.75	.229	.182	1.200
1.0	.238	.250	1.284

$$\left(\int_0^1 \left(\frac{n_c^{(u)}}{n_c^{(0)}}\right) du\right)_{N_0=1} = 1.133$$

TABLE IV

FIT OF EXPERIMENTAL RESULTS TO INFINITE POLYNOMIAL

u	$\left(\frac{d \ln (n_c)}{du}\right)_{N_0=1}$	$\exp\left\{-1.556 + \frac{0.297\ u}{3.47 - u}\right\}$
0.0	0.211	0.211
.25	.217	.216
.5	.221	.222
.75	.229	.229
1.0	.238	.238

$f'(u) = \left(\frac{(0.297)(3.47)}{(3.47 - u)^2}\right) f(u)$. Thus

$f'(0) = (0.0856)(f(0))$ and $f'(1) = (0.169)(f(1))$, or

$f'(0) = (0.0181)$ and $f'(1) = (0.0402)$. Therefore,

$$III = \left(\frac{(1.284)(0.0567 + 0.0402) - (0.0181 + 0.0446)}{(1.284)(0.238) - (0.211)}\right)\frac{1}{2.08 \times 10} - 3 = 308$$

The distribution of which these measurements give the moments is not actually a molecular weight distribution, but is a distribution over R_iW_i' since

$$w_i = \frac{(N_i)_0 M_i}{\sum_{i=1}^{n} (N_i)_0 M_i} \qquad (37)$$

where w_i is the weight-fraction of the ith species. The R_iW_i' may be evaluated for each species and listed as in Table V. In so doing it is necessary to draw on all available information regarding the parameters characteristic of each molecular species which may be present. In the sample presented here, it was assumed that oxidative polymers are essentially absent, and that the variation of $\bar{v}_i^{(0)}$ with i may be predicted on the basis of parachor data.[42,43] For this calculation, values of $(\gamma_i)^{1/4}$ have been assumed constant. Values of R_i have been taken as constant based on computation from estimated molar refractions.[44]

TABLE V

EVALUATION OF ALLOWED VALUES OF MOLECULAR WEIGHT AND RELATED FUNCTIONS

i	M_i	$\bar{v}_i^{(0)}$[a]	$(1 - \bar{v}_i^{(0)}\rho_0^0)$	W_i	W_i'[b]
1	280	1.107	0.125	34.7	34.6
2	561	1.076	.149	83.6	83.4
3	841	1.067	.156	131	130.7
4	1122	1.061	.160	181	181
5	1402	1.060	.161	226	225
6	1682	1.059	.162	273	272
7	1963	1.059	.162	319	318
8	2243	1.059	.162	364	363
9	2524	1.059	.162	410	409
10	2804	1.059	.162	454	453

[a] Computed from the equation

$$\bar{v}_{i+1}^{(0)} = \bar{v}_i^{(0)}\left(\frac{i}{i + 1}\right)\left(\frac{694\ (i + 1) + 40}{694i + 40}\right)$$

derived on the basis of parachlor data, assuming $(\gamma_i)^{1/4}$ is constant. $\bar{v}_1^{(0)}$ is estimated as 1/0.903 at 20°.[45] Values of $(1 - \bar{v}_i^{(0)}\rho_0^0)$ are computed at 20°, and taken as independent of temperature, using the density of methanol as 0.791.[46] [b] β for methanol is taken from Gibson[47] as 1.25×10^{-10} cm.^{2}/dyne at 25°. $\bar{v}_0^{(0)}$ is taken as 1/0.786 by interpolation.[46] Thus $\beta RT/\bar{v}_0^{(0)}$ is 2.43 g. A is 2.08×10^{-5} (g.)$^{-1}$ for this particular run.

Calculation of the best distribution from the averages measured here is done by the most suitable available method. If the sample can be adequately represented by a finite distribution, a

(42) See, for example, G. W. Thompson, in A. Weissberger, "Physical Methods of Organic Chemistry," Vol. I, Interscience Publ. Co., New York, N. Y., 1946, p. 202 ff.

(43) This procedure has been checked approximately by using the second estimated molecular weight distribution given here to predict the value of $\bar{v}$ which should be observed for this sample. The agreement was satisfactory, but it should be emphasized that this value of $\bar{v}$ is primarily determined by the paucimeric species in this particular sample. Thus, it is not very different from $\bar{v}$ for the monomer in methanol, and the apparent check is not adequate. A further verification is given by comparison with the density data of Chang and Kummerow[35] for their analogous fractions. The values of Table V are thus seen to be quite reasonable and far more reliable than those obtained by neglecting the dependence of $\bar{v}_i^{(0)}$ on i.

(44) See, for example, K. Fajans, in A. Weissberger, "Physical Methods of Organic Chemistry," Vol. I, Interscience Publ. Co., New York, N. Y., 1946, p. 672 ff.

(45) K. S. Markley, "Fatty Acids," Interscience, New York, N. Y., 1947, p. 216.

(46) "International Critical Tables," Vol. III, McGraw-Hill Book Co., New York, N. Y., 1933, p. 27.

(47) R. E. Gibson, *J. Am. Chem. Soc.*, **59**, 1525 (1937).

matrix method such as is developed in the Appendix might be employed. The spread of values of I, II and III may be used to indicate whether or not this is a good approximation. In the present case, the great disparity between II and III indicates that the actual distribution has a high molecular weight "tail" which must be accounted for. This is done using the most appropriate statistical rule.

When no such rule is appropriate, the spread of the distribution may be pictured using the Chebychev inequality[34] applied as an equality. The value of the mean, μ, I or 120, and the value of the standard deviation, σ, $I(II/I - 1)^{1/2}$, $120(155/120 - 1)^{1/2}$ or 64.8, are applied to those values of W_i' more than one standard deviation from the mean. One cannot, obviously, determine any properties of the distribution within $\mu \pm \sigma$ from this approach. Outside the interval $\mu \pm \sigma$, or $55 < W_i' < 185$, however, k_i may be computed for each value of W_i' as $(W_i' - 120)/64.8$ and the distribution constructed by assuming the weight percentage of i-mer to be equal to $100(1 - 1/k_i^2)$ less the percentage already accounted for by i-mers whose values of W_i' are closer to the mean. Thus, for this sample, the W_i' values 83.4, 130.7 and 181 lie with the 1 σ interval. The value of W_i' next closest to the mean is that for the monomer, 34.6. In this type of calculation, the minimum amount of material which could be in the range 34.6–205.4 is thus counted as monomer. It could, however, be spread over the four W_i' values, 34.6, 83.4, 130.7 and 181. Also, more material could be present in this range of W_i'. In addition, it may be recalled that the mean is often near the median and that one-half of the material is distributed on each side of the median. This might be used to improve the estimate of material present as monomer and dimer, for example. Subject to such inaccuracies, however, the distribution may be further delineated. The value of W_i' next furthest from the mean is 225, and the minimum weight-percentage of material within the range 15–225 is determined from the corresponding value of k_i. The increment between this weight percentage and the previous one is taken as the weight per cent. of 5-mer. Such a process is continued to give the distribution in the second column of Table VI. The hazards of such a procedure are apparent if one redetermines the averages of eq. 35 from the values of Table VI, since the values of I and II thus computed do not reproduce the values from which Table VI is determined. This is presumably due to the failure of the procedure near the mean.

In the present case, it is interesting to use the values of Table V to see how well the moments of the molecular weight distribution of the sample reported here agree with those predicted, for example, for a distribution of the simplest type described by Flory,[48] the most probable distribution in linear, open-chain molecules. This is the distribution in which the mole fraction of i-mer is equal to some constant, less than unity, times the mole fraction of (i − 1)mer. In Flory's terms, this is

(48) P. J. Flory, "Principles of Polymer Chemistry," Cornell University Press, Ithaca, N. Y., 1953, p. 318 ff.

TABLE VI

CRUDE APPROXIMATIONS OF DISTRIBUTION OVER ALLOWED VALUES OF W_i'

i	W_i'	w_i[a]	w_i[b]
1	34.6	0.424	0.281
2	83.4	...	.264
3	130.7	...	.186
4	181	...	.116
5	225	.195	.0684
6	272	.199	.0385
7	318	.075	.0211
8	363	.036	.0113
9	409	.0211	.00598
10	453	.0131	.00312

[a] Computed from Chebychev inequality as described in text. [b] Computed from most probable distribution in linear, open chain molecules as described in text.

$$N_i = p^{(i-1)}(1 - p) \tag{38}$$

and w_i is given as

$$w_i = ip^{(i-1)}(1 - p) \tag{39}$$

The moments defined by eq. 35-a, b, and c are seen to be

$$\sum_{i=1}^{n} w_i W_i' \Big/ \sum_{i=1}^{n} w_i \left(\frac{W_i'}{W_i}\right), \sum_{i=1}^{n} w_i W_i' W_i \Big/ \sum_{i=1}^{n} w_i W_i',$$

$$\sum_{i=1}^{n} w_i W_i' W_i^2 \Big/ \sum_{i=1}^{n} w_i W_i' W_i$$

respectively, for this system. Further, since $\sum_{i=1}^{n} w_i = 1$, $\sum_{i=1}^{n} w_i (W_i'/W_i)$ may be approximated as 0.997 based on the data of Table V. I, the moment described by eq. 35-a, is thus

$$I = \frac{(1 - p)^2 \sum_{i=1}^{\infty} ip^{(i-1)} W_i'}{0.997} \tag{40}$$

From the expression, p may be evaluated as 0.470. When applied to eq. 39, this gives the values in the third column of Table VI.

The higher moments measured by eq. 35-b and c may be predicted from this value of p. They are thus given as II = 183 and III = 245 for this distribution. Thus, this sample is an example of the case which will often be met, *i.e.*, one in which a good picture of the distribution is not immediately available. At present, there seems to be no generally satisfactory method for such samples, and the development of such a procedure is beyond the scope of the present work.

In an attempt to verify that the moments measured for this sample are in accord with the actual molecular weight distribution, the w_i's predicted from eq. 39 are used to compute a number-average molecular weight of 528. This may be compared with the value of 406 reported by Chang and Kummerow[34] for their equivalent sample. The distribution pictured by eq. 38 can be brought into agreement with this value only by the addition of more material on the low molecular weight side, especially in the range of monomer. A similar conclusion is reached using the technique of gas chromatography for monomer analysis. Such determinations were carried out on the methyl

esters of the sample used in the preceding studies. Only one peak was observed, and it was found to correspond to methyl linoleate. A calibration run was carried out using an equal amount of a sample of pure methyl oleate. As shown in Table VII, only half as much material was detected when the unknown methyl esters were analyzed. This indicates that monomeric linoleic acid makes up about half of the unknown sample on which the ultracentrifugation studies were carried out.

TABLE VII

MONOMER ANALYSIS BY GAS CHROMATOGRAPHY

Sample	Area of peak, cm.²
Unknown	39.0 ± 1.4
Me oleate	77.2 ± 2.8

From these results, we may legitimately conclude that the distribution computed using eq. 38 is in error. The actual distribution is probably richer in monomer, but not as broad in linear polymers, as this proposed distribution. However, the actual distribution probably contains, in addition, a broad distribution of oxidative polymers. Such a picture could agree with all these observations. In addition we may estimate that measurement of III by this technique is in error by as much as 50% since a distribution which will check the values of 120 and 155 for *I* and *II*, and will agree with the monomer analysis data, is not likely to give a value of 305 for III if it is a statistically predicted distribution, and a value about 200 would be more likely. However, it may be seen that the insight gained into the molecular distribution justifies the application of ultracentrifugation to even such low molecular weight samples as the one reported here.

Acknowledgments.—We are greatly indebted to the administrative staff of the Research Laboratories of Swift & Company as well as to many of our colleagues on the staff for advice and encouragement during the course of this work. Further, we would like to express appreciation to Dr. K. E. Van Holde and Dr. H. K. Schachman for enlightening discussions regarding the use of equilibrium ultracentrifugation.

In addition, we are greatly indebted to Dr. F. L. Kauffman and Mr. G. D. Lee, who carried out the gas chromatographic studies, Dr. E. E. Rice and Mr. W. D. Warner, who prepared the sample reported here, and Mr. J. M. Becktel, who pointed out some of the statistical considerations involved.

Appendix

In the case where the third measured average does not indicate great divergence from the first two, it may be possible to develop a finite distribution which will adequately picture the molecular weight distribution in some samples. In order to do this, it is first observed that

$$\lim_{j \to \infty} \frac{\Sigma w_i W_i' W_i^{j+1}}{\Sigma w_i W_i' W_i^{j}} = W_{max} \qquad \text{(A-1)}$$

in a system where W_{max} is the value of W_i for the highest molecular weight species present. The value of W_{max} is then estimated from the three measured averages. Values of averages between the third measured average and the value of W_{max} may then be estimated from the manner in which the first three averages approach W_{max}. These could then be used to compute moments of the distribution similar to those defined by Goldberg.[7] For any system, the equations

$$w_1 \frac{W_1'}{W_1} + w_2 \frac{W_2'}{W_2} + w_3 \frac{W_3'}{W_3} + \ldots w_{max} \frac{W_{max}'}{W_{max}} = (1 - \epsilon) \qquad \text{(A-2-a)}$$

$$w_1 W_1' + w_2 W_2' + w_3 W_3' + \ldots w_{max} W_{max}' = I \qquad \text{(b)}$$

$$w_1 W_1' W_1 + w_2 W_2' W_2 + w_3 W_3' W_3 + \ldots w_{max} W_{max}' W_{max} = I \times II \qquad \text{(c)}$$

etc., could then be written, and ϵ might be estimated as in the text. This family of equations could then be solved by determinants. An interesting case which has a fairly general solution is one in which $W_i = iW$ and $W_i' = iW'$. This will also illustrate the hazards and shortcomings of this procedure. In this case, eq. A-2 becomes

$$w_1 + w_2 + w_3 + \ldots w_{max} = W/W' \qquad \text{(A-3-a)}$$

$$w_1 + 2w_2 + 3w_3 + \ldots = I/W'$$

$$w_1 + 2^2 w_2 + 3^2 w_3^2 + \ldots = I \times II/W'W$$

These equations are then re-written in matrix notation as

$$\begin{Vmatrix} 1 & 1 & 1 & \cdot\cdot \\ 1 & 2 & 3 & \cdot\cdot \\ 1 & 2^2 & 3^2 & \cdot\cdot \\ 1 & 2^3 & 3^3 & \cdot\cdot \\ \cdot & \cdot & \cdot & \cdot \\ \cdot & \cdot & \cdot & \cdot \\ \cdot & \cdot & \cdot & \cdot \end{Vmatrix} \times \begin{vmatrix} w_1 \\ w_2 \\ w_3 \\ w_4 \\ \cdot \\ \cdot \\ \cdot \end{vmatrix} = \begin{vmatrix} W/W' \\ I/W' \\ I \times II/W' \times W \\ I \times II \times III/W' \times W^2 \\ \cdot \\ \cdot \\ \cdot \end{vmatrix} \qquad \text{(A-4)}$$

This equation can be solved by matrix inversion, and would give

$$\begin{vmatrix} w_1 \\ w_2 \\ w_3 \\ w_4 \\ \cdot \\ \cdot \\ \cdot \end{vmatrix} = \begin{Vmatrix} \text{INVERSE} \end{Vmatrix} \times \begin{vmatrix} W/W' \\ I/W' \\ I \times II/W' \times W \\ I \times II \times III/W' \times W^2 \\ \cdot \\ \cdot \\ \cdot \end{vmatrix} \qquad \text{(A-5)}$$

The inverse matrices of eq. A-5 can be determined using standard techniques of matrix algebra. However, for these $(m \times m)$ matrices of eq. A-4, it may be shown that the elements of the first and last columns of the inverses are given by

$$A_{im} = \frac{(-1)^{(i-m+2)}}{(m-i)!\,(i-1)!} \qquad \text{(A-6)}$$

and

$$A_{i1} = \frac{(-1)^{(i+1)}\,(m)!}{(m-i)!\,(i)!} \qquad \text{(A-7)}$$

Further, it may be seen empirically that the coefficients of the $(m+1) \times (m+1)$ inverse may be obtained from those of the $m \times m$ inverse by the relationship

$$(A'_{i,j})_{(m+1)\times(m+1)} = m\,(A'_{i,j})_{(m\times m)} + (A'_{i,j-1})_{(m\times m)} \qquad \text{(A-8)}$$

where $(A'_{i,j})$ is defined by

$$(A'_{i,j}) = A_{i,j} \times \frac{(m-1)!\,(i-1)!}{(-1)^{(i-m+2)}} \qquad \text{(A-9)}$$

The last row of the $(m+1) \times (m+1)$ inverse is then easily computed by the usual method, since it is not evaluated by this scheme. Inverses of the matrices of eq. A-4 can thus be produced from the

2×2 inverse, which can be evaluated by eq. A-6 and A-7. The first few inverses are thus

$$\begin{Vmatrix} 2 & -1 \\ -1 & 1 \end{Vmatrix} \quad \begin{Vmatrix} 3 & -\frac{5}{2} & \frac{1}{2} \\ -3 & 4 & -1 \\ 1 & -\frac{3}{2} & \frac{1}{2} \end{Vmatrix} \quad \begin{Vmatrix} 4 & -\frac{13}{3} & \frac{3}{2} & -\frac{1}{6} \\ -6 & \frac{19}{2} & -4 & \frac{1}{2} \\ 4 & -7 & \frac{7}{2} & -\frac{1}{2} \\ -1 & \frac{11}{6} & -1 & \frac{1}{6} \end{Vmatrix}$$

as may be verified by simple calculation. This scheme has been verified by calculation using the IBM 650 digital computer up to 10×10 matrices.

Inspection of these inverses shows that they produce convergent values of w_i only as small differences between large numbers of opposing signs. Thus, the accuracy with which the W averages should be observed increases as the number of components present increases, and is of an order which is not easily obtained even when only a few components are present. For example, the relative concentrations in a three component system of this type can usually be specified only to two places when the measured averages are accurate to three places. Since similar considerations would hold for any system to be studied by equilibrium ultracentrifugation, it is seen that the unequivocal determination of molecular weight distributions by this technique is usually a highly imaginative undertaking. An essentially equivalent conclusion has been reached by Goldberg[7] and by Williams, *et al.*[33]

THE RADIATION CHEMISTRY OF AQUEOUS PERMANGANATE SOLUTIONS[1]

BY MALCOLM DANIELS[2]

Chemistry Division, Argonne National Laboratory, Lemont, Illinois

Received March 9, 1960

The reduction of permanganate solutions, induced by Co^{60} γ-rays, has been investigated in acid, neutral and alkaline solution. In 0.8 N H_2SO_4 the major products are MnO_2 and O_2, and yields have been determined over a wide range of radiation intensity and permanganate concentration. A chain reaction has been found and the over-all rate of reduction can be represented by $G(-MnO_4^-) = G_0 + k_1(MnO_4^-)^{1/2} + k_2(MnO_4^-/I)^{1/2}$, where $G_0 = 2.3$, $k_1 = 10$ and $k_2 = 0.8 \times 10^{11}$ (G is defined as molecules/100 e.v., concentration units are M, and intensity units are e.v./l./min.) An explanation is offered involving intermediate formation of 0 atoms and MnO_5^-. Yields of hydrogen gas ("molecular yield") have been determined at various permanganate concentrations, and reactions of solutions saturated with H_2 have been investigated. Explanation in terms of MnO_5^- is suggested. At pH 5.6 colloidal Mn(IV) is produced but in 0.5 M OH^-, manganate is the initial product. In both neutral and alkaline solution curves of product yield *vs.* dose exhibit decrease in slope when the product accumulates; this is attributed to re-oxidizing reactions of OH radical with the products.

Introduction

Progress in the understanding of radiation chemistry of liquids has largely been based on detailed studies of chemical changes induced in reactive additives, usually termed "scavengers," as exemplified by ferrous ion, ceric ion and formic acid in aqueous solution, and I_2 in organic liquids.

The ability of permanganate ion to oxidize water (expressed by its high oxidation potential), coupled with its high solubility over a wide pH range, suggested investigation of its possible utility as such a scavenger. The possibility of clarifying the mechanisms of reduction of permanganate was a further factor.

Previous work was sparse, limited in scope, and contradictory in nature.[3-9] In the course of the present work results of more detailed investigations appeared,[10,11] and will be discussed later in the appropriate places.

Experimental

Irradiation Arrangements.—Irradiations were carried out with sources of Co^{60} γ-rays whose activities ranged from 80 to 4500 curies. Dosimetry was carried out using the standard ferrous sulfate dosimeter[12] [$G(Fe^{3+}) = 15.6$], together with the ferrous–cupric system[13] for the higher dose-rates. The range of dose-rates used were from 1.2×10^{18} e.v./l./min. to 3.0×10^{21} e.v./l./min.

Preparation of Solutions.—All solutions for irradiation were prepared with triply distilled water[14] using analytical grade H_2SO_4, NaOH and $KMnO_4$. The sodium salt, $NaMnO_4 \cdot 3H_2O$, was "purified" grade. It was noted that concentrated solutions of $NaMnO_4$ showed considerably less tendency to decompose heterogeneously than those of the potassium salt. Degassing procedure has been previously described[14] as have the cells used for the irradiation of degassed solutions[14] and the syringes used for hydrogen saturated solutions.[15] Cells and syringes were used in the "radiation-browned" condition rather than being furnace-treated at 550°, for the latter condition seemed to cause heterogeneous thermal decomposition of the permanganate.[16]

(1) Based on work performed under the auspices of the U. S. Atomic Energy Commission. Presented in part at the April 1958 ACS meeting held in San Francisco, California.

(2) Chemistry Department, U. College of West Indies, Kingston, Jamaica.

(3) K. Chamberlain, *Phys. Rev.*, **26**, 525 (1925).

(4) G. W. Clark and L. W. Pickett, *J. Am. Chem. Soc.*, **52**, 465 (1930).

(5) G. W. Clark and W. S. Coe, *J. Chem. Phys.*, **5**, 97 (1937).

(6) F. C. Lanning and S. C. Lind, THIS JOURNAL, **42**, 1229 (1938).

(7) L. Bloch-Frankenthal and G. Goldhaber, *Bull. Res. Council of Is-ael*, **1**, 117 (1951).

(8) V. I. Veselovsky, Ts. I. Zalkind, N. B. Miller, N. A. Aladzhalova, Symp. on Radiation Chem., Acad. Sci. U.S.S.R., Moscow, 1955, p. 36.

(9) E. L. Alexander, Dissertation, Vanderbilt Univ., 1956.

(10) B. A. Gvozdev and V. N. Shubin, Treatise of 1st All-Union Conf. on Radiation Chem., March 25–30th, 1957.

(11) G. Simonoff, *J. chim. phys.*, **55**, 547 (1958).

(12) C. J. Hochanadel and J. Ghormley, *J. Chem. Phys.*, **21**, 1080 (1953).

(13) E. J. Hart and P. D. Walsh, *Rad. Res.*, **1**, 342 (1954).

(14) E. J. Hart, *J. Am. Chem. Soc.*, **73**, 68 (1951).

(15) E. J. Hart, S. Gordon and D. A. Hutchinson, *ibid.*, **75**, 6165 (1953)

Cleaning of the cells was carried out with oxalic acid solution followed by rinsing with triply-distilled water and rinsing with permanganate solution before filling.

Analytical Methods.—(a) Loss of MnO_4^- was determined by centrifuging the solution for 10 min. to remove suspended particles of MnO_2, followed by suitable dilutions and measurement of the optical density at one of the visible peaks, λ 526 mμ (uncorrected), (on a Beckman DU spectrophotometer) $\epsilon = 2.43 \times 10^3$.

(b) The presence of Mn^{2+} was tested for by first determining the remaining MnO_4^- concentration as just described, then adding to the (acid) solution ~1 g. of sodium bismuthate, $NaBiO_3$, recentrifuging and determining any change in optical density at 526 mμ.

(c) Manganese dioxide precipitates were quantitatively analyzed as: after filtration, the precipitates were washed with 0.8 N H_2SO_4 until the filtrate was colorless, then five times with water and dried for 30 hr. under vacuum at room temperature. Total manganese was determined by reducing a weighed amount to Mn^{2+} with excess oxalic acid, then oxidizing to MnO_4^- with bismuthate and determining the MnO_4^- spectrophotometrically. Total oxidizing power was determined by titration of a weighed amount of precipitate with standard ferrous salt at 50° in the presence of 1 N H_2SO_4.

(d) The final reduction state attained in neutral solution was determined by oxidizing an excess of ferrous ammonium sulfate and back-titrating the excess with standard permanganate.

(e) In alkaline solution (0.5 M) the manganate ion, MnO_4^{2-}, was identified qualitatively by its green color. By following the absorption at 600 mμ it was observed that formation of the green product reached a maximum after 3.4×10^{22} e.v./l. and the ultraviolet and visible absorption spectrum at this close coincided with that of synthetic Na_2MnO_4 in 0.5 M NaOH. Na_2MnO_4 was prepared by heating 1.0 g. of $KMnO_4$ in 20 cc. of 8 M NaOH at 120° for 2 hr., filtering off the Na_2MnO_4 when cold and recrystallizing.

The yellow-brown precipitate obtained in strongly alkaline solution was analyzed in the manner just described for MnO_2. However washing was limited to 0.1 N NaOH.

(f) Gas analysis: the reactivity of pure and partially decomposed MnO_4^- with mercury prevented use of the Van Slyke apparatus, and two adaptors were designed to allow transfer to the gas-containing liquid to a high vacuum line. For collecting small amounts of gas from solutions originally degassed, the capillary outlet of the irradiation cell was frozen in liquid N_2, the whole cell then placed in a suitable flask and pumped down. When evacuated, the frozen construction was allowed to thaw, as a result of which the liquid spurted out into the vacuum and automatically degassed itself in doing so. For collecting larger volumes of gas, *e.g.*, from solutions originally saturated with H_2, a syringe cell was used. Solutions were weighed from it into an evacuated flask *via* a 5/20 joint (sealed with a small amount of degassed permanganate solution) and stopcock (lubricated with Dow silicone grease). After suitable drying, all gases were collected *via* an automatic toepler pump and analyzed mass-spectrometrically for H_2, O_2, N_2 and CO_2. The amount of thermal reaction of H_2 with MnO_4^- over the duration of the experiments was small (max. 10–12%) and was followed by simultaneous control experiments.

Results

Though experiments have been carried out in the neutral and alkaline region, the major portion of the work (described in sections 1–3 below) was restricted to solutions in 0.8 N H_2SO_4.

1. Products and Stoichiometry.—The visual change in permanganate solution upon irradiation is simply that of fading together with the formation of a dark brown-black granular precipitate. The absorption spectrum from 2100 to 5800 Å., determined after the precipitate had been removed by centrifuging showed that MnO_4^- had disappeared and that no other light absorbing species was formed.

(16) E. Richardson and C. D. Poucher, *Research*, **11**, 247 (1958); J. A. Waddams, *ibid.*, **11**, 370 (1958).

Analysis of the precipitates collected from solutions originally 1×10^{-4} M and 2×10^{-2} M in MnO_4^- are shown in Table I. It can be seen that the compositions correspond to hydrated manganese dioxides, formulas $MnO_{2.03}\cdot H_2O$ and $MnO_{2.10}\cdot H_2O$. As manganese dioxide often has a non-integral ratio, Mn/O,[17] closer agreement is perhaps not to be expected. Tests for Mn^{2+} during the initial stages of reduction of 1×10^{-3} M MnO_4 showed it to be only 4–7% of total permanganate loss, though at larger doses the proportion increased to ~30% when all the permanganate was consumed. It was accordingly concluded that in the region where initial rates were measured the major product of reduction of permanganate was MnO_2. The rate of loss of permanganate, designated hereafter as $G(-MnO_4^-)$ where G is defined in the conventional way as *molecules* reacted/100 e.v., was determined from changes in optical density with dose as described in Experimental. At all except the highest permanganate concentrations and lowest radiation intensities spontaneous heterogeneous decomposition was very small and was corrected for by control measurements. The rate of heterogeneous decomposition was not increased by irradiation, as shown by the absence of any post-irradiation changes—apparently under these conditions heterogeneous effects occur primarily at glass surfaces rather than on the MnO_2 produced by the radiation. In later work at high concentrations the sodium salt was used, and found to be more stable than the potassium salt.

TABLE I

ANALYSIS OF PRECIPITATES PRODUCED BY IRRADIATION OF ACID PERMANGANATE SOLUTIONS[a]

	% Mn	Equiv. wt.[b]	Oxid. equiv. G. atom Mn
1	51.48	52.44	2.03
2	52.25	50.07	2.10
3	52.38	52.50	2.00
4	63.31	43.50	2.00

[a] 1, precipitates collected from solution of initial concentration 2×10^{-2} M; 2, precipitates collected from solution of initial concentration 1×10^{-3} M; 3, calculated for $MnO_2\cdot H_2O$; 4, calculated for MnO_2. [b] Defined with respect to the reduction Mn^{2+}.

To determine proportions, analysis was carried out on the gaseous products of irradiation, and it was shown that under all conditions oxygen was the major product, hydrogen amounting to at most only a few per cent. of the total gas. Hydrogen yields are considered in detail later. Comparable values for the loss of MnO_4^- and formation of O_2 are shown in Table II. For all concentrations greater than 10^{-3} M, $G(O_2)/G(-MnO_4^-) \simeq 0.75$, in agreement with a reaction ratio such as

$$4MnO_4^- + 4H^+ \longrightarrow 2MnO_2 + 3O_2 + 2H_2O$$

The significance of these ratios, $G(O_2)/G(-MnO_4^-)$ will be discusssed later.

2. Concentration and Intensity Effects.—Preliminary experiments at 1×10^{-3} and 5×10^{-5} M indicated a dependence of $G(-MnO_4^-)$ on initial concentration of MnO_4^-. Further experiments then showed that the variation was too large to be

(17) J. P. Brenet and A. M. Briot, *Compt. rend.*, **232**, 726 (1956).

TABLE II

STOICHIOMETRY OF Co^{60} γ-RAY INDUCED REDUCTION OF PERMANGANATE IN 0.8 N H_2SO_4

$(MnO_4^-)_0$, M	I, e.v./l./min.	$G(-MnO_4^-)$	$G(O_2)$	$\frac{G(O_2)}{G(-MnO_4^-)}$
1×10^{-1}	2.0×10^{19}	9.8	7.2	0.73
	6.14×10^{19}	9.0	7.0	.78
	1.16×10^{20}	6.1	4.5	.74
2×10^{-2}	1.2×10^{18}	13.0 ± 0.7	9.5	0.73 ± 0.04
	2.0×10^{19}	6.2	4.6	0.74
	1.16×10^{20}	4.65	3.5	.76
5×10^{-3}	5.6×10^{19}	4.5	3.2	.71
1×10^{-3}	2.0×10^{19}	3.2	1.6	.50
	2.4×10^{20}	2.8	1.15	.41

attributed to competition with the primary radical recombination process

$$HO_2 + OH \longrightarrow H_2O + O_2$$

or with

$$2H \longrightarrow H_2$$

and that $G[MnO_4^-]$ did not reach a limiting value with increasing permanganate concentrations which might be expected in such cases. The results indicate a completely different functional dependence on initial permanganate concentration, which is actually a simple square root form similar to Fig. 2.

$$G(-MnO_4^-) = G' + a(MnO_4^-)^{1/2} \qquad (A)$$

Where $G' \simeq 2.4$ and $a = 26.2$ at 2.0×10^{19} e.v./l./min.

The effect of radiation intensity on reaction rate was investigated at a number of concentrations and Fig. 1 shows $G(-MnO_4^-)$ as a function of $I^{1/2}$ where I is radiation intensity (dose rate) in e.v./l./min. Obviously we can write in a general way

$$G(-MnO_4^-) = G' + k_2 \frac{(MnO_4^-)^{1/2}}{I^{1/2}} \qquad (B)$$

The relevant constants are summarized in Table III. Variation of rate with intensity is negligible at concentrations $< 10^{-3}$ M, thus accounting for the absence of intensity effects noted by Simonoff.[11] However it is apparent that G-values ex-

TABLE III

EXPERIMENTAL CONSTANTS FOR THE CONCURRENT INTENSITY AND CONCENTRATION DEPENDENT REDUCTION OF PERMANGANATE IN 0.8 N H_2SO_4

$(MnO_4^-)_0$, M	G'	b	$k_2 = \frac{b}{(MnO_4^-)^{1/2}}$
10^{-1}	5.6	2.27×10^{10}	0.7×10^{11}
2×10^{-2}	4.2	1.0×10^{10}	$.5 \times 10^{11}$
1×10^{-3}	2.6	0.26×10^{10}	$.8 \times 10^{11}$

trapolated to zero dependence on $I^{-1/2}$ still exhibit an increase with initial permanganate concentration. The G'-values of Table II were augmented by others at higher MnO_4^- concentrations obtained at one intensity, which was, however, high enough to almost eliminate effects due to this variable, (correction for chain reaction, calculated using k's determined at lower concentrations, never exceeded 10%); the dose rate used was 2.8×10^{21} e.v./l./min. It is a striking feature that the functional dependence of G' on the initial permanganate concentration is also a half power (Fig. 2)

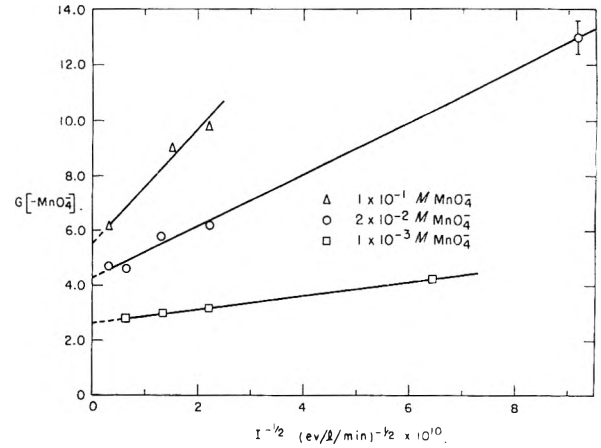

Fig. 1.—Intensity dependence of rate of loss of permanganate in 0.8 N H_2SO_4: Δ, 1×10^{-1} M MnO_4^-; ○, 2×10^{-2} M MnO_4^-; □, 1×10^{-3} M MnO_4^-.

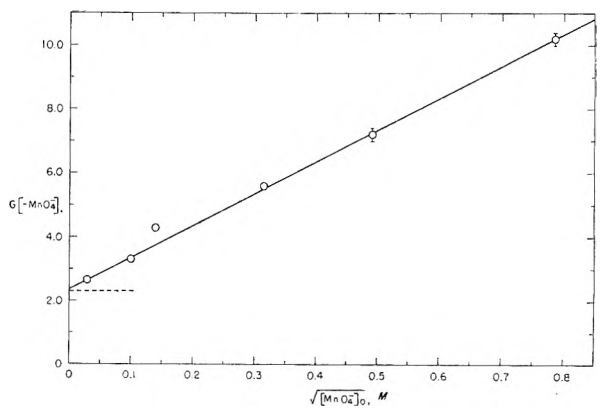

Fig. 2.—Dependence of G' on initial permanganate concentration in 0.8 N H_2SO_4.

$$G' = 2.3 + k_1(MnO_4^-)^{1/2} \qquad (C)$$

The results of Gvozdev and Shubin[8] using high intensity accelerated electrons can be similarly rectified.

Accordingly the over-all course of reduction of permanganate in 0.8 N H_2SO_4 at concentrations from 10^{-4} to 0.6 M and intensities from 1.2×10^{18} to 2.8×10^{21} e.v./l./min. can be empirically represented as

$$G(-MnO_4^-) = G_0 + k_1(MnO_4^-)^{1/2} + k_2 \frac{(MnO_4^-)^{1/2}}{I^{1/2}} \qquad (D)$$

where $G_0 \simeq 2.3$, $k_1 \simeq 10$, $k_2 \simeq 0.8 \times 10^{11}$.

3. Gas Formation and Consumption.—In view of its high oxidizing power, it was expected that permanganate would prove to be a good scavenger for H atoms and it was accordingly of great interest to determine the yields of hydrogen gas. Survey experiments of Rigg[18] using 200 kv. X-rays, indicated a G-value of 0.076, lower than that of other scavengers at a comparable concentration.

Hydrogen yields were therefore determined at high intensity for a number of concentrations. In all cases linear yield–dose curves were obtained as was found by Rigg, and G-values as a function of initial permanganate concentration are presented in Fig. 3. It can be seen that at concentrations of

(18) T. Rigg, *Disc. Faraday Soc.*, **12**, 119 (1952).

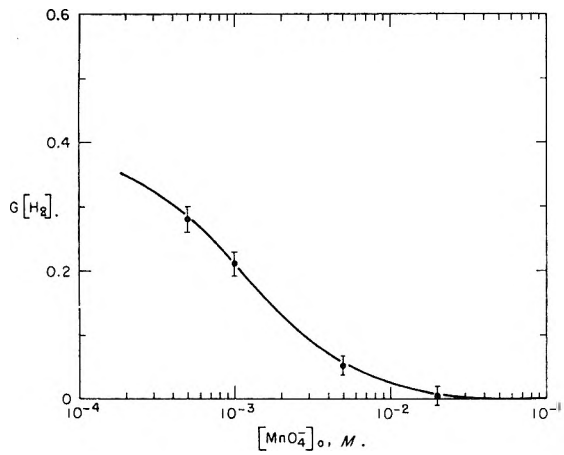

Fig. 3.—Dependence of hydrogen yield on initial permanganate concentration.

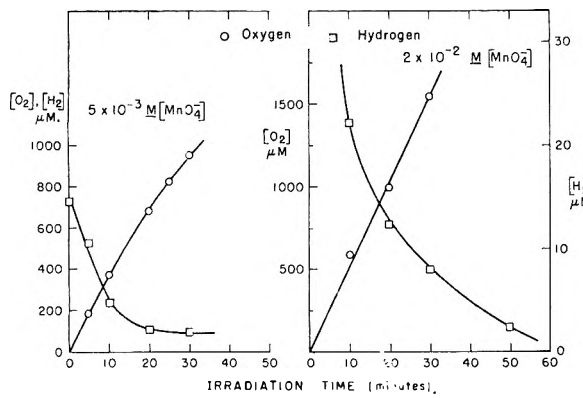

Fig. 4.—Oxygen yield and hydrogen consumption as a function of dose on irradiating hydrogen-saturated permanganate solutions in 0.8 N H_2SO_4.

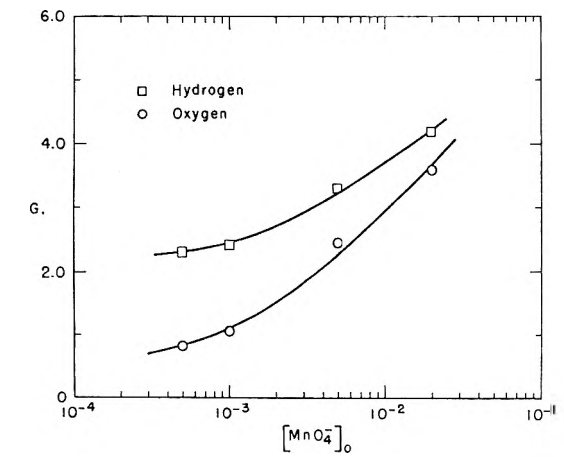

Fig. 5.—$G(O_2)$ and $G(-H_2)$ for H_2-saturated permanganate solutions as a function of initial permanganate concentration.

MnO_4^- greater than 10^{-2} M, formation of H_2 is practically negligible, but at concentrations lower than 10^{-3} M it appears to approach values considered normal for "molecular yield" products. In view of known thermal reduction of permanganate by H_2[19] it was decided to irradiate solutions of permanganate of varying concentration, saturated with hydrogen at atmospheric pressure, again at high intensities. As a result of this it was found that H_2 is indeed consumed during irradiation at a rate which depends on permanganate concentration. Typical yield-dose curves are shown in Fig. 4. Of particular interest is the fact that oxygen formation is not eliminated as might be expected if the properties in the reduction were simply

$$3H_2 + 2MnO_4^- + 2H^+ \longrightarrow 2MnO_2 + 4H_2O$$

as is the case for the thermal reaction but decreases to a value corresponding to "mol. yield" H_2O_2. The variation of $G(-H_2)$ and $G(O_2)$ determined in this way, with the initial permaganate concentration, is shown in Fig. 5.

Hydrogen consumption increases with increasing MnO_4^- concentration. Oxygen formation is an inverse function of the ratio, $(H_2)_0/[MnO_4^-]_0$

$$\frac{1}{G[O]_2 - 0.70} = 4.15 \frac{[H_2]_0}{[MnO_4^-]_0} \qquad (E)$$

4. Reduction in Neutral Solution.—When irradiated at pH 5.6, with or without O_2 present, permanganate solutions change color to varying shades of red-brown and develop a turbidity. The solution also exhibited a post-irradiation change whereby the absorption increased at about 10% hr. initially; this effect was independent of light and O_2 but was prevented by acidification or prevention of access of CO_2. The absorption spectrum taken immediately after irradiation is shown in Fig. 6.

Because of possible ambiguities due to colloidal scattering, investigation by spectrophotometry was curtained. The course of the reduction was followed by treating the irradiated solutions with standard ferrous ammonium sulfate as described in Experimental. It was found that reduction did not proceed beyond the Mn(IV) stage (Fig. 7), *i.e.*, the limiting yield corresponds to an oxidation of ferrous by Mn(IV) only. The product may perhaps be described as a hydrated colloidal manganite such as $HMnO_3^-$.

The yield-dose curve exhibits essentially two linear dependencies, paralleling the absorption changes; the initially linear section has G(Mn(IV) = 3.0, whilst for the second slope the G-value drops to 0.55.

5. Reduction in Alkaline Solution.—The reduction of permanganate to manganate in 0.5 M NaOH is shown in Fig. 8 as a function of dose. As in neutral solution the curve has two linear sections and the respective rates are, $G(MnO_4^{2-})$ = 3.0 and 1.30. However, complete conversion of MnO_4^- to MnO_4^{2-} is not found, for after ~70% conversion, a net loss of MnO_4^{2-} occurs and simultaneously a yellow-brown precipitate forms. Analysis of this precipitate gave equiv./g. atom Mn = 2.05 (*i.e.*, Mn(IV)) and % Mn = 19.8; this latter figure is close to that for sodium manganite, $Na_2Mn_2O_5$.

Discussion

In the discussion which follows an explanation will be attempted in terms of the current theory of γ-radiolysis of water[20] in which the net products of the complicated primary processes are presumed to be freely diffusing H and OH radicals in relatively

(19) A. H. Webster and J. Halpern, *Trans. Faraday Soc.*, **53**, 51 1957).

(20) A. O. Allen, Proceedings of the Int. Conf. Peaceful Uses Atomic Energy, **7**, 513 (1955), Geneva.

high yield together with smaller amounts of the radical recombination products H_2 and H_2O_2. The net yields of those products in 0.8 N H_2SO_4 (in the presence of reactive solutes) will be taken as $g(H) = 3.6$, $g(OH) = 2.9$, $g(H_2) = 0.4$ and $g(H_2O_2) = 0.7$.[21]

A resumé of simple manganese chemistry in aqueous solution is also necessary for the interpretation. Briefly, all oxidation states of manganese from VII to II are now known in aqueous solution. Of these, only Mn(VII) (MnO_4^-), Mn(IV) (MnO_2) and Mn(II) (Mn^{2+}) are stable in dilute acid; Mn (VI) (MnO_4^{2-}) and Mn(V) (MnO_3^- or MnO_4^{3-}) are stable in alkaline solution. Under suitable conditions (neutral, electrolyte-free solution) Mn(IV) can be prepared in a reactive colloidal form as $HMnO_3^-$ (manganite) and salts of this state can be formed in alkaline solution.

1. Products and Stoichiometry.—The nature of the reduction products in acid solution is one of the major points of contradiction in previous work. Veselovsky, *et al.*,[8] found that MnO_2 was not formed at acidities ≥ 2 N and at 0.8 N both MnO_2 and Mn^{2+} were found though the proportions were not estimated. Alexander[9] however found MnO_2 up to 3 N acid and no evidence for reduction of Mn^{2+}. Gvozdev and Shubin[10] found MnO_2 to be the major product in 0.8 N H_2S_4, together with small amounts of Mn^{2+}; Simonoff,[11] working in the range of $5 \times 10^{-4} - 5 \times 10^{-3}$ M MnO_4^- attributed a post-irradiation loss of MnO_4^- to the over-all reaction

$$3Mn^{2+} + 2MnO_4^- + 2H_2O \longrightarrow 5MnO_2 + 4H^+$$

which appears to have an inverse dependence on acidity, and hence inferred the presence of Mn^{2+}. In the present work it has not been possible to show the presence of more than minor amounts of Mn^{2+}. It is pertinent at this stage to consider the available chemical evidence concerning the conditions necessary for the formation of the various oxidation states of manganese in dilute acid solution. Arguments leading to the expectation of Mn^{2+} formation are twofold. In the first place the oxidation-reduction potential for the over-all change Mn(VII) -Mn(II) is very favorable in acid solution.[22] ($E_0 = -1.51$). However, feasibility is not synonymous with facility for such a complicated reaction as this which involves a change of five equivalents and loss of four oxygen atoms, and reduction to the Mn(II) stage only occurs with excess of reducing agent.[22] Secondly it is suggested that Mn^{2+} is formed by the reduction of permanganate by hydrogen peroxide according to the reaction

$$2MnO_4^- + 5H_2O_2 + 6H^+ \longrightarrow 2Mn^{2+} + 5O_2 + 8H_2O$$

In actual practice, however, the above general remark applies and this relationship only holds under carefully controlled conditions such that there is always an excess of hydrogen peroxide present.[23] With excess of permanganate over hydrogen peroxide, MnO_2 forms[24] and the numerical relationship changes.[25]

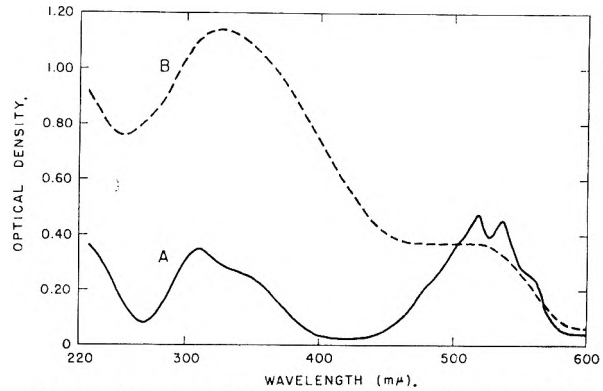

Fig. 6.—(A) absorption spectrum of $KMnO_4$, 2×10^{-4} M, pH 5.6; (B) absorption spectrum of $KMnO_4$, after 7.25 hours irradiation, dose rate 5.6×10^{19} e.v./l./min.

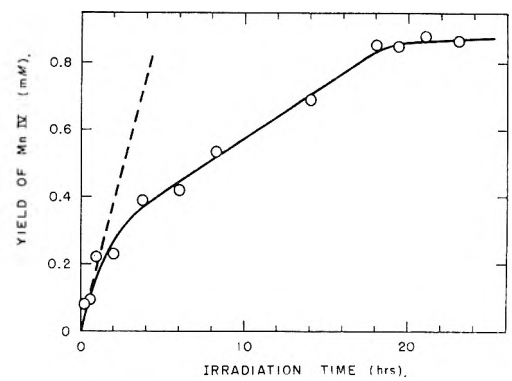

Fig. 7.—Reduction of 0.9×10^{-3} M $KMnO_4$ at pH 5.6, Co^{60} γ-rays, dose rate 5.6×10^{19} e.v./l./min.

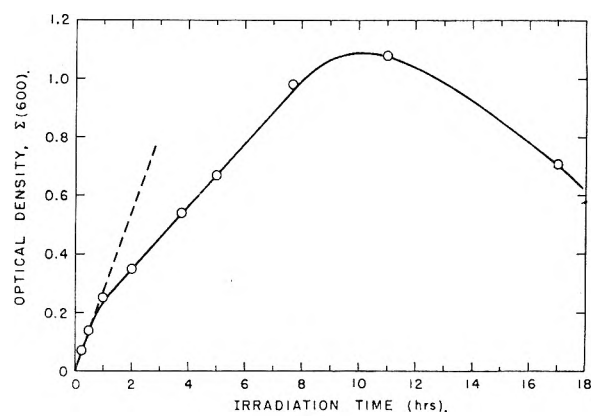

Fig. 8.—Irradiation of 1×10^{-3} M $KMnO_4$ in 0.5 N NaOH. Yield of MnO_4^- as a function of dose.

The application of these generalizations to the situation encountered in γ-radiolysis follows from the fact that the only reducing agent which may be locally or temporarily in excess over the permanganate is the molecular yield hydrogen peroxide. Consequently, it might be expected that $G(Mn^{2+}) \simeq 2/5\, g(H_2O_2) \simeq 0.28$.

The actual value found for 1×10^{-3} M MnO_4^- was 4-7% of total loss of MnO_4^-; at the dose rate employed $G(-MnO_4^-) = 3.2$, giving $G(Mn^{2+}) \sim 0.2$ in reasonable agreement with this expectation.

(21) E. Hart, *Proc. 2nd Int. Conf. Peaceful Uses Atomic Energy*, **29**, 5 (1958), Geneva.

(22) W. M. Latimer, "Oxidation Potentials," Prentice-Hall Book Co., New York, N. Y., 1952, p. 241.

(23) R. M. Fowler and H. A. Bright, *J. Research Natl. Bur. Standards*. **16**, 493 (1935).

(24) W. Ramsey, *J. Chem. Soc.*, 1324 (1901).

(25) M. I. Bowman, *J. Chem. Educ.*, **26**, 103 (1949).

All other reactive species in γ-irradiated solutions are at such a low concentration relative to the permanganate that reduction will not go to the manganese-II state but to the manganese-IV and be terminated by precipitation of MnO_2. It would seem then that the results found here are in accord with chemical experience.

The oxygen yields are also in agreement with the conclusion that MnO_2 is the major reduction product (see Table II) with the exception of the yields determined at the lowest concentration (1×10^{-3} M). No simple explanation can be offered for this discrepancy, for the precipitate analyzes clearly as MnO_2, and the loss of MnO_4^- and formation of Mn^{2+} have been determined. The only possibility is that during precipitation at such low concentrations O_2 is occluded on or in the precipitate, but is lost during drying and does not titrate. Further speculation is not warranted and there are no other published determinations of gas yields to offer comparison.

In the discussion which follows values for the loss of permanganate $G[-MnO_4^-]$ will be interpreted as requiring 3 reducing equiv./molecule, corresponding to the reduction Mn(VII) → Mn(IV) so that the experimental rate of reduction in molecules/100 e.v. will be related to rate of radical production by expressions of the type

$$G[-MnO_4^-] = 1/3 \text{ f } [g(H), g(OH)]$$

2. Mechanism of Reduction in Acid Solution.— The essential features of the reduction which any mechanism will have to account for have been described in Results and may be summarized as (a) the generally high reduction yield, $G(-MnO_4^-)$ which extrapolates to 2.3; (b) the chain-reaction type dependence of $G(-MnO_4^-)$ and $G(O_2)$ on intensity and concentration of MnO_4^-; (c) the intensity-independent variation of $G_0(-MnO_4^-)$ with permanganate concentration.

Having noted that "molecular yield" H_2O_2 probably reduces MnO_4^- to Mn^{2+} the reaction of the radicals, H and OH, produced in larger amounts, can be considered. There seems to be no reason to doubt that H atoms can rapidly reduce permanganate to manganate.

$$H + MnO_4^- \longrightarrow H^+ + MnO_4^{2-} \qquad (1)$$

The mode of reaction of the OH radicals is more unusual. From work on the thermal decomposition of permanganate in alkaline solution it has been suggested[26] that OH radicals can oxidize manganate ion to permanganate *via* the equilibrium

$$MnO_4^{2-} + OH \rightleftharpoons MnO_4^- + OH^- \qquad (2)$$

Such a reaction however is unlikely in acid solution where the lifetime of the manganate and the concentration of OH^- are very small. Furthermore, such a "back-reaction" would lead to a low net reduction yield by radicals and will not account for the experimental facts. It is therefore necessary to conclude that the reaction of the OH radical leads to reduction of the permanganate, in contrast to its more usual oxidizing role, and due to the instability and low concentration of Mn(VI) and Mn(V) species in acid solution it seems that this reaction must be with the permanganate ion. This general conclusion has also been reached by other workers,[10,11] who have suggested as mechanistic steps the reactions

$$OH + MnO_4^- + H_2O \longrightarrow MnO_4^{2-} + H_2O_2 + H^+ \qquad \Delta F = 3.7 \text{ kcal.}$$

(which in effect involves oxidation of OH to H_2O_2)

$$OH + MnO_4^- \longrightarrow MnO_2 + O_2 + OH^- \qquad \Delta F = -44.8 \text{ kcal.}$$

Although the former reaction seems to be energetically unfavorable and the latter seems mechanistically impossible, in that a single one-step reaction cannot produce monomeric MnO_2, these reactions are discounted on the grounds that (a) both reactions lead to 3 equiv. reduced/OH radical, which in turn gives a $G[-MnO_4^-]$ by radical reactions of $1/3\ [g(H) + 3g(OH)] = 4.1$, much higher than the limiting values of equation (D); (*b*) neither of these reactions leads to a product capable, under suitable conditions, of initiating a chain reaction. A reaction sequence which overcomes both of these objections would be one leading to the formation of an O atom. This could proceed in either of two ways.

$$OH + MnO_4^- \longrightarrow MnO_4^{2-} + H^+ + O \qquad \Delta F = 34 \text{ kcal.} \quad (3a)$$

or

$$OH + MnO_4^- \longrightarrow OH^- + MnO_4$$
$$MnO_4 \longrightarrow MnO_3(MnVI) + O \qquad (3b)$$

Using the data of Latimer[22] the former is energetically impossible, and the latter involving transient oxidation to Mn(VIII) will be preferred here. If the fate of the oxygen atoms is to produce molecular oxygen by simple recombination

$$2O \longrightarrow O_2 \qquad (4)$$

and the manganate ions are presumed to disproportionate rapidly by the reaction

$$3MnO_4^{2} + 4H^+ \longrightarrow 2MnO_4^- + MnO_2 + 2H_2O \qquad (5)$$

(discussion of the mechanism of this reaction is beyond the scope of this paper), then the net limiting reduction yield of permanganate will be given by $G[-MnO_4^-] = 1/3\ [g[H] + g(OH)] = 2.16$; taking into account the reduction by H_2O_2 discussed above we have an over-all $G[-MnO_4^-] \simeq 2.16 + 0.2 \simeq 2.36$, in good agreement with the extrapolated experimental value 2.3. It seems then that reaction, 1, 3 and 4 can adequately account for the non-chain, reduction of permanganate at low concentrations (in a later part of the discussion it will be seen that (4) may be written slightly differently).

As the initial concentration of permanganate is increased, a chain reaction sets in at low intensities. Such behavior is not surprising if the O atom formed *via* reaction 3 can further undergo reaction with permanganate

$$O + MnO_4^- \longrightarrow O_2 + MnO_3^-, \quad \Delta F = -80 \text{ kcal.} \quad (6)$$

to give an ion of Mn(V), followed by regeneration of the initiating OH radical by a reaction such as

$$H\ MnO_3 + H_2O \longrightarrow H_2MnO_3\ (Mn(IV)) + OH \qquad (7)$$

Evidence for the transient existence of the ion of Mn(V) in permanganate oxidations has recently been brought forward[27] but little is known of its

(26) M. C. R. Symons, *J. Chem. Soc.*, 3956 (1953).

(27) W. A. Waters, *Quart. Revs.*, **12**, 277 (1958).

reactions beyond its extreme instability in other than strongly alkaline solution; reaction 7 has been invoked in the thermal reduction of permanganate in alkaline solution.[28] The sequence of reactions thus outlined, which essentially is comprised of a competition between reactions 6 and 4, does not fully satisfy the requirements, for application of the stationary state approximation to the kinetics leads to the expression.

$$G[-MnO_4] = 1/3\,[g(H) + g(OH)] + 4/3\left[g(OH)\frac{k_6^2}{2k_4}\right]^{1/2}\frac{[MnO_4^-]}{I^{1/2}}$$

with only a linear dependence on permanganate concentration. A square root dependence is obtained if the termination reaction involves permanganate in a termolecular reaction, such as

$$O + O + MnO_4^- \longrightarrow O_2 + MnO_4^- \qquad (8)$$

A completely satisfactory formal description of the chain kinetics can thus be given by reactions 1, 3, 6, 7 and 8, which lead to the expression

$$G[-MnO_4^-] = 1/2[gH + gOH] + \frac{4}{3}\left(\frac{gOH \times k_6^2}{2k_8}\right)^{1/2}\frac{[MnO_4^-]^{1/2}}{I^{1/2}}$$

Although termolecular reactions are traditionally held to be improbable, the situation has been reviewed by Hart and Matheson[29] in work demonstrating a half-power concentration dependence in the γ-ray induced decomposition of hydrogen peroxide. The role of permanganate in the termination step is perhaps clarified by the following reaction sequence. Let it be supposed that reaction 6 does not occur immediately, but passes through an intermediate stage of significant lifetime

$$O + MnO_4^- \rightleftharpoons MnO_5^- \qquad (9)$$

whose structure can be suggested as

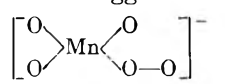

This product can decompose to oxygen and hypomanganate, giving a chain

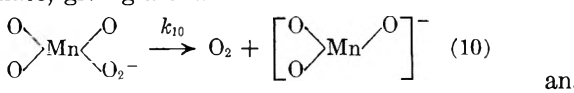

(10)

On the other hand, termination can occur by

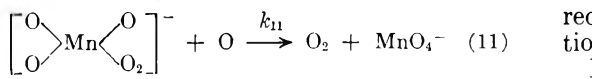

(11)

Reactions 9 and 11 together are effectively a third-order termination step.

A brief discussion of other mechanisms seems warranted.

Alternative reactions of the chain carriers are of course possible, but do not appear to lead to a suitable rate expression. The Mn(V) can possibly react

$$2MnO_3^- + 2H^+ \longrightarrow H_2Mn_2O_5(Mn(IV)) + O$$

but this is a rapidly degenerating chain as well as being less probable than (5). Termination by a one-radical reaction could occur by

$$MnO_3^- + MnO_4^- + H_2O \longrightarrow 2MnO^{2-}{}_4 + 2H^+$$

but this of course does not give a square root dependence on intensity. Termination by

$$2MnO_3^- + H_2O \longrightarrow HMnO_3^- + HMnO_4^-$$

does not lead to a term including MnO_4^- in the rate expression and due to the extreme reactivity of Mn(V), is again thought to be less probable than (7). The other termination possibility

$$2[MnO_5^-] \longrightarrow 2MnO_4^- + O_2$$

also leads to an expression with no term in $[MnO_4]$.

A reaction sequence entirely analogous to that suggested above, but not involving O atoms in the rate-determining steps, can be set up; the requirements are simply a bimolecular propagation step involving MnO_4^- and a termolecular termination step (bimolecular in radicals) involving MnO_4^-. Such a sequence could possibly be written for MnO_5^- *e.g.*

$$MnO_5^- - MnO_4^- \longrightarrow \text{Propagation}$$
$$2MnO_5^- + MnO_4^- \longrightarrow \text{Termination}$$

However this mechanism requires complex transition states and cannot be extended to include the kinetics in concentrated solution as can the simple mechanism involving O atoms. It is concluded then that the best explanation that can currently be given is as previously suggested, *i.e.*, the sequence 1, 3, 9, 10, 7 and 11, which lead to the expression

$$G[-MnO_4^-] = 1/3\,(gH + gOH) + \frac{4}{3}\left(g(OH)\frac{K_9k_{10}^2}{2k_{11}}\right)^{1/2}\left(\frac{MnO_4^-}{I}\right)^{1/2}$$

where K_9 is the pseudo equilibrium constant for reaction 9 and all the other symbols have their usual significance.

Further evidence in support of the feasibility of intermediate peroxy complex formation is found in the work of Scholder and Kolb[30] who, by reaction of concentrated H_2O_2 with manganate in cold alkali were able to isolate crystalline compounds with structures

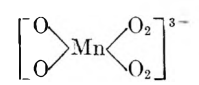

analogous to those posulated here in reaction 9. The existence of the intermediate MnO_2^- is also required to account for the radiation-induced reaction of H_2 and MnO_4^- (see below).

It remains now to consider the intensity-independent increase of $G[-MnO_4^-]$ with permanganate concentration. This cannot be accounted for on the basis of the above considerations which indicate that at high intensity, where the chain reaction is presumably eliminated, $G(-MnO_4^-)$ should approach $1/3[g(OH)+g(OH)] \simeq 2.1$; this is only true at low permanganate concentrations. Even if it were possible for the mechanism to change to include a 3 equiv./OH radical reaction such as were discussed above, or a sequence such as

$$OH + MnO_4^- \longrightarrow HMnO_5^- \longrightarrow O_2 + HMnO_3^-\,(Mn(IV))$$

this would give a limiting $G[-MnO_4^-]$ of $1/3[g$

(28) B. Jezowska-Trzebiatowaka, J. Nawojska and M. Wronska' *Bull. de l'Acad. Polon. Sci.*, C1 III, *II*, 447 (1954).

(29) E. J. Hart and M. Matheson, *Disc. Faraday Soc.*, **12**, 169 (1952).

(30) R. Scholder and A. Kolb, *Z. anorg. allgem. Chem.*, **260**, 41 (1949–1950).

(H) + 3g (OH)] $\simeq$ 4.1 whereas in practice G-[$-MnO_4^-$] increases to values exceeding 10. The variation of G' with permanganate concentration is continuous, apparently without limit, and attains values which far exceed those which could possibly be attributed to increased effective radical yields (which might arise from competition with radical recombination within the spurs or capture of excited water species). This behavior has also been observed by Gvozdev and Shubin,[10] who unfortunately offered no explanation. It seems most likely that these results are due to the operation of an intensity-independent chain reaction, and this can readily be visualized in general terms by simple changes in the mechanism suggested above. Thus at high permanganate concentrations, the second-order, radical-radical termination step 11, may be replaced by a first-order radical-molecule reaction such as

$$MnO_5^- + MnO_4^- \longrightarrow O_2 + MnO_3\,(Mn(IV)) + MnO_4^{2-}$$

or

$$MnO_5^- + MnO_4^- \longrightarrow MnO_2\,(Mn(VI)) + MnO_4^{2-}$$

Such a change immediately eliminates the intensity dependence from the rate expression, but introduces a $1/[MnO_4]$ term. If the rate-determining propagation step is also modified to include reaction with MnO_4^- a rate expression independent of MnO_4^- is obtained. However with the assumption that permanganate exists in concentrated solution predominantly in a dimeric form, and that for termination simple MnO_4^- ions are necessary while for propagation any permanganate species will suffice, then the rate expression becomes

$$G[\text{-}MnO_4^-] = G_0 + \tfrac{4}{3}\,g(OH)\,\frac{k_{prop}}{k_{term}}\,\frac{[Mn(VII)]}{\sqrt{\overline{Mn(VII)}/K}}$$

where K is the dimerization content. This reduces to

$$G[\text{-}MnO_4^-] = G_0 + \tfrac{4}{3}\,g(OH)\,\frac{k_{prop}}{k_{term}}\,K^{1/2}\,[Mn(VII)]^{1/2}$$

in agreement with experiment. The present state of permanganate chemistry does not allow a choice to be made between the various propagation and termination steps which can be suggested. Neither can any evidence be found concerning dimerization in concentrated permanganate solution. However, an entirely analogous situation is found in kinetics of reaction of cobaltic ion with water and hydrogen peroxide[31] and other cases involving dimeric species are well known.

3. Mechanism of Reaction with H_2.—Experiments described here have shown the existence of a radiation-induced reaction between hydrogen gas and permanganate which is most probably responsible for the abnormally low values obtained for "molecular yield" hydrogen. The salient features of this effect are as follows: Hydrogen consumption increases with permanganate concentration; consequently the simple competition for OH radicals of reactions

$$OH + MnO_4^- \longrightarrow MnO_3 + O + OH^- \quad (12)$$

and

$$OH + H_2 \longrightarrow H_2O + H$$

cannot be solely responsible, suggesting incidentally that $k_{OH + MnO_4^-} > k_{OH + H_2}$; furthermore, oxygen formation, while not eliminated, decreases with the ratio $[H_2]_0/[MnO_4^-]_0$ until a yield corresponding to that of the molecular yield hydrogen peroxide is obtained. It therefore seems justifiable to conclude that hydrogen gas interferes with radical reactions leading to O_2 formation; in support of this is the "competition plot" giving equation (E). On the basis of the previous discussion of the formal reaction mechanism it can be seen that all the oxygen would be expected to originate in reactions of O atoms and a pair of competing reactions which have to be considered in attempting to account for this behavior are

$$O + MnO_4^- \longrightarrow O_2 + MnO_3^-$$
$$O + H_2 \longrightarrow OH + H \text{ (or } H_2O?) \quad (13)$$

However, one of the consequences of this is that H_2 consumption would again be expected to decrease with increasing concentration of permanganate. To account for the behavior of simultaneously increasing oxygen formation and increasing hydrogen consumption, a reactant is needed which will evolve O_2 in the process of reacting with hydrogen. It is suggested that the relatively stable intermediate complex of reaction 9 can in fact react with H_2

$$MnO_5^- + H_2 \longrightarrow H + H\,MnO_5^- \left[\begin{array}{c} O \\ \diagup \\ O \end{array}\!\!>\!Mn<\!\!\begin{array}{c} O^- \\ \diagdown \\ O_2H \end{array}\right] \quad (14)$$

subsequently decomposing to Mn(V) and a product giving rise to oxygen (HO_2)

$$HMnO_5^- \longrightarrow MnO_3^- + HO_2 \quad (15)$$
$$HO_2 + MnO_4^- \longrightarrow MnO_4^{2-} + H^+ + O_2 \quad (16)$$

The net effect being that H_2 is consumed and O_2 evolved, without appreciably affecting the original reaction sequence.

The experimental findings seem to be best accommodated by a combination of reactions 14–16 with either (12) or (13). Reaction 12 is preferred over (13) because, among other things, it predicts $G(-H_2) \sim g(OH)$ for high values of $[H_2]_0/[MnO_4^-]_0$ whereas (13) constitutes a chain sequence with reaction 3; experimentally $G(-H_2) \rightarrow 2.3$ at high values of $[H_2]_0/[MnO_4^-]_0$ and $g(OH) - g(H_2) = 2.5$.

In the limit, when all the hydrogen is being consumed in reaction 14, then it would be expected that $G(-H_2) \sim G(O_2)$ when due allowance is made for "molecular yield" H_2 and oxygen originating in "molecular yield" hydrogen peroxide. It can be seen that this limit is almost reached in the present work.

4. Reaction in Neutral Solutions.—The essential feature of the reduction in neutral solution is the shape of the yield–dose curve, which is completely different from that in acid solution. However the initial yield of Mn(IV) is the same as is found in acid solution at the same concentration and intensity, and it is justifiable to assume that substantially the same mechanism is occurring. But when the concentration of Mn(IV) (which probably

(31) J. H. Baxendale and C. F. Wells, *Trans. Faraday Soc.*, **53**, 800 (1957).

exists in a colloidal state as a reactive polymeric form of the ion $HMnO_3^-$ with general formula $[Mn_xO_{2x-1}]^{2-}$ reaches about 200 μM, its rate of formation decreases considerably, indicating participation of the product in an oxidizing back reaction

$$Mn(IV) + OH \longrightarrow Mn(V) + H_2O$$
$$(HMnO_3^-) + OH \longrightarrow MnO_3^- + H_2O)$$

When all OH radicals are consumed in this reaction, as indicated in the second linear section of the yield–dose curve, then the small amount of chain reaction initially occurring at this concentration will be eliminated, and all the H atoms will reduce to Mn(IV) *via* reactions 1 and 5. Consequently the net radical reduction yield becomes $g(H)-g(OH)$ The true course of the reaction of hydrogen peroxide with permanganate is not known in neutral solution but we shall simply assume that it reduces 2 equivalents, which eventually become stabilized as Mn(IV). The total yield is then the sum of the radical and hydrogen peroxide yields. $G(-MnO_4^-) = 1/3\,[g(H) - g(OH) + 2g(H_2O_2)]$. Exact values for the radical and molecular product yields in neutral solution are still uncertain;[21] if $g(H) \sim g(OH)$ and $g(H_2O_2) = 0.75$ (substantially the same as in acid solution) then the anticipated value of $G[-MnO_4^-]$ would be 0.5. If $g[H_5O_5] \sim 0.5$ as indicated by the work of Senvar and Hart[32] and Adams,[33] then the experimental value of $G[-MnO_4^-]$ would indicate $g(H) - g(OH) \sim 0.6$.

(32) C. B. Senvar and E. J. Hart (unpublished results).
(33) G. E. Adams, private communication.

5. Reduction in Alkaline Solution.—The qualitative features of the reduction in strongly alkaline solution are similar to those of neutral solution, but the quantitative aspects merit some discussion. The stable reduction product here is manganate ion (Mn (VI)) and consequently the decrease in slope of the yield–dose (Fig. 12) when manganate accumulates is attributed to reaction 2.

$$MnO_4^{2-} + OH \longrightarrow MnO_4^- + OH^-$$

For the over-all 1 equivalent reduction we have for the initial yield $G[-MnO_4^-] = G[MnO_4^{2-}] = g(H) + g(OH) + 2g(H_2O_2) = 3.0$. For the secondary slope $G[MnO_4^{2-}] = g(H) - g(OH) + 2g(H_2O_2) = 1.30$, so that $g(OH) \simeq 0.8$. It is apparent that determination of $G(O)_2$ would give a value for $g(H_2O_2)$ and allow determination of $g(H)$. Consequently this system may well allow the determination of all the primary chemical products $g(H_2)$, $g(H_2O_2)$, $g(H)$ and $g(OH)$ over the range of alkalinity in which manganate is stable, and further work is anticipated.

Acknowledgments.—This work was commenced at King's College, Newcastle-on-Tyne, England on the suggestion of Prof. Joseph Weiss. Thanks are due to the Director of A.E.R.E. (Harwell) for support of this part of the investigation and permission to publish at Argonne. Thanks are due to Miss Vicki R. Meyers for experimental assistance, and to Dr. E. J. Hart for constant encouragement and critical discussion.

THE PHOTOLYSIS OF ACETONE

BY B. DEB. DARWENT, M. J. ALLARD, M. F. HARTMAN AND L. J. LANGE

Department of Chemistry, The Catholic University of America, Washington 17, D. C.

Received April 1, 1960

The effects of pressure, intensity and surface/volume ratio on $R_{CH_4}/R^{1/2}_{C_2H_6} = \gamma$ have been investigated between 217 and 327°. The plot of γ *vs.* p, the concentration of acetone, are linear but with positive intercepts, the magnitude of which increases with intensity and temperature. This indicates that CH_4 is formed by the reaction of CH_3 with a substance, possibly CH_3COCH_2, whose concentration varies as $I^{1/2}$ and is approximately independent of p, in addition to the accepted reaction of CH_3 with acetone.

I. Introduction

Although the kinetics of the photolysis of acetone are complex below 100° and above 350°, within that interval they appear to be simple and to be adequately represented, at least as far as the formation of methane and ethane are concerned, by the mechanism

$$(CH_3)_2CO + h\nu \longrightarrow CH_3 + CH_3CO \quad (0)$$
$$CH_3CO \longrightarrow CH_3 + CO \quad (1)$$
$$CH_3 + (CH_3)_2CO \longrightarrow CH_4 + CH_2COCH_3 \quad (2)$$
$$2CH_3 \longrightarrow C_2H_6 \quad (3)$$

which leads to the relationship

$$\gamma = R_{CH_4}/R^{1/2}_{C_2H_6} = (k_2/k_3^{1/2})p \quad (A)$$

where R is the rate of formation of the product and p the concentration of acetone.

Some preliminary results[1] showed that, although a linear relationship existed between γ and p at 280°, a distinct positive intercept was obtained which is not in accordance with equation A. In addition, previously published results[2] are not inconsistent with the presence of such an intercept. The results of the present investigation provide further data concerning the reality of the intercept and the effects of temperature, intensity and surface/volume ratio on its magnitude.

II. Experimental

The reaction vessel was a cylindrical Pyrex cell, 5 cm. × 10 cm., fitted with a corex window, transparent to $\lambda \gg 2800$ Å., connected to a trap and to conventional storage, vacuum and analytical systems. The cell was surrounded by a cylindrical furnace, the temperature of which was manually controlled and did not vary by more than 1° along the length of the cell or between experiments at a constant stated temperature. The volumes of the reaction cell and of the total

(1) B. deB. Darwent and J. E. Schingh, unpublished results.

(2) (a) A. F. Trotman-Dickenson and E. W. R. Steacie, *J. Chem. Phys.*, **73**, 3986 (1951); (b) R. H. Linnell and W. A. Noyes, *J. Am. Chem. Soc.*, **18**, 1097 (1950).

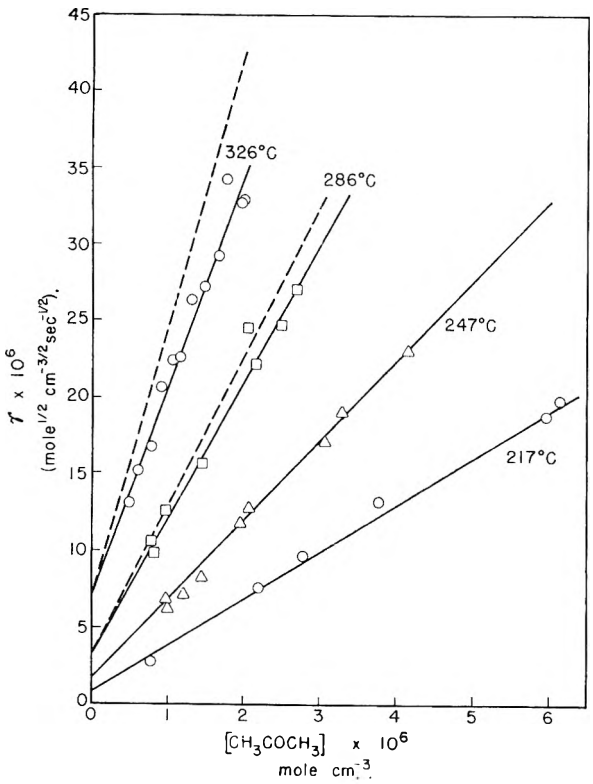

Fig. 1.—The relationship between γ and p. The temperatures are as indicated. The broken lines represent the relationship corrected for C_2H_4.

reaction system were 180 cm.^{3} and 335 cm.^{3}, respectively. Spectroscopically pure acetone was used after purification by trap-to-trap distillation *in vacuo*. The active light was obtained from a Hanovia Type S medium pressure mercury arc; the unfiltered light was approximately collimated by a quartz lens and completely filled the reaction cell.

At completion of the photolysis, the acetone was condensed at −80° in a trap in the reaction system and the products separated into two fractions, CH_4 + CO at −196° and C_2 hydrocarbons at −160°. The CH_4 + CO fraction was analyzed by hot CuO oxidation and this was checked occasionally by mass spectrometric analysis. The following values are representative of the percentage of CH_4 as measured by the two procedures

	I	II	III	IV	V
Mass spectrometer	48.4	64.1	61.1	57.9	60.7
CuO	49.4	64.7	61.2	59.0	60.5

No significant amount of C_2 hydrocarbon was ever found in this fraction.

The C_2 hydrocarbon fraction was usually much less than the CH_4 + CO. In fact, the volumes of C_2 obtained, although large enough for accurate measurement, were too small for reliable mass spectrometric analysis. Such analyses showed that the C_2 fraction occasionally contained small amounts of acetone, always less than 5%, but it was not possible to obtain a reliable estimate of the amount of ethylene present.

In some experiments the surface/volume ratio was increased, approximately 12-fold, by nearly filling the reaction cell with thin walled Pyrex tubing of 6 mm. diameter. This increased the surface area 8-fold and decreased the volume from 180 to 120 cm.^{3}; it also resulted in a decrease in the incident intensity.

III. Results

The experimental results obtained in this investigation are presented in Table I together with the estimated production of C_2H_6 from the measured amounts of the C_2 fraction. As mentioned previously, the C_2 fraction was too small for accurate mass spectrometric analysis and Mandelcorn and Steacie[3] have shown that ethylene becomes of some importance at temperatures in the

TABLE I

THE PHOTOLYSIS OF ACETONE

Reaction cell, 180 cm.^{3}; reaction system, 335 cm.^{3}

$[CH_3COCH_3]$ (moles cm.$^{-3}$ × 10^6)	Duration (sec.)	Products (moles × 10^6) CO	CH_4	C_2	C_2H_6
		Temp. = 217°			
0.79	1950	4.4	2.4	2.14	2.14
2.19	1207	8.1	6.0	2.92	2.92
2.78	920	7.2	6.0	2.31	2.31
3.74	640	7.1	6.4	2.04	2.04
5.93	630	8.8	8.8	1.91	1.91
6.11	660	9.3	9.4	2.08	2.08
		Temp. = 246°			
0.96	2400	7.2	6.3	2.05	2.05
0.99	3195	8.2	7.1	2.23	2.23
1.10	3300	9.4	8.6	2.41	2.41
1.20	3370	10.4	10.3	2.57	2.57
1.92	2400	12.5	12.8	2.65	2.65
2.05	2475	13.0	13.7	2.60	2.60
3.01	1555	11.9	11.9	1.74	1.74
3.27	1200	9.9	11.5	1.71	1.71
4.13	1505	12.2	14.9	1.54	1.54
		Temp. = 285°			
0.78	6240	15.0	17.4	2.29	2.29
0.79	4290	8.4	11.6	1.75	1.75
0.95	4135	12.2	13.7	1.59	1.44
1.41	1800	7.8	8.6	0.92	0.85
2.08	1500	8.8	11.8	0.85	0.75
2.14	2445	12.6	15.6	1.13	1.00
2.49	1825	12.2	16.5	1.33	1.15
2.67	1770	12.7	16.2	1.11	0.96
		Temp. = 327°; full intensity			
0.48	4880	7.6	11.8	0.91	0.64
0.59	2400	4.9	5.9	.35	.26
0.75	2330	6.7	8.1	.54	.39
0.88	2390	6.6	10.0	.54	.38
1.05	4845	19.0	23.4	1.25	.90
1.14	2400	9.2	11.3	0.58	.41
1.27	2395	10.4	14.4	0.68	.47
1.42	4820	24.0	31.6	1.54	1.08
1.63	1380	6.7	9.6	0.43	0.29
1.74	4680	31.6	34.1	1.17	.83
1.93	1200	7.1	9.6	0.40	.26
1.97	1200	6.8	10.0	0.43	.28
		Temp. = 327°; packed cell[a]; intermediate intensity			
0.70	4440	4.2	5.7	0.37	0.23
0.90	4080	5.0	7.0	.41	.25
1.67	3000	6.4	9.3	.37	.22
2.04	2400	5.8	8.6	.35	.18
		Temp. = 327°; low intensity			
0.48	25200	3.7	5.5	0.16	0.099
0.50	30000	4.5	6.5	.22	.113
1.26	21600	8.6	13.3	.48	.131
1.66	21720	10.5	16.1	.50	.121
1.85	20400	9.8	15.2	.44	.099
2.10	18780	11.0	17.0	.50	.104

[a] Reaction cell = 120 cm.^{3}.

(3) L. Mandelcorn and E. W. R. Steacie, *Can. J. Chem.*, **32**, 331 (1954).

vicinity of 300°. Since they measured the effects of temperature, concentration and intensity on the rates of formation of C_2H_6 and C_2H_4 it was possible, by interpolation within the temperature range covered, to obtain the ratio C_2H_4/C_2H_6 at two concentrations and two intensities at the temperatures used in the present investigation, thus permitting the amount of ethane produced to be calculated. The relationships derived from Mandelcorn and Steacie's data and used for correcting the present results were

$$C_2H_4/C_2H_6 = 1.13 \times 10^{-3}\, pI_a^{-0.8} \text{ at } 327°$$
$$= 6.1 \times 10^{-4}\, p \text{ at } 285°$$

where p is the concentration of acetone (moles cm.$^{-3}$) and I_a the rate of formation of CO (moles cm.$^{-3}$ sec.$^{-1}$). The ratio was quite negligible at the lower temperatures but was large at 327° and especially so at the lower intensities.

The relationship between γ and p is shown, for the high intensity experiments, in Fig. 1. The corrected values are also shown, as broken lines, for the two highest temperatures. The effect of intensity on that relationship, using the "corrected" values of γ, at 327° is shown in Fig. 2. Those data demonstrate quite clearly that positive intercepts are required if γ is assumed to be a linear function of p. The effect of intensity on the slopes and intercepts obtained at 327° (Fig. 2) is shown in Fig. 3. The intercepts are seen to be dependent on $I^{0.54}$ and the slopes on $I^{0.15}$, *i.e.*, the intercepts vary approximately as $\sqrt{I}$ and the slopes are approximately independent of the intensity.

The relationships between γ and p at three lowest temperatures are at least reasonably sound. However, at 327° and especially at the lowest intensity the corrections for C_2H_4 were large and those data should be accepted only with reservation.

IV. Discussion

The data obtained in this investigation demonstrate the following facts:

(a) The quantity γ is a linear function of p but positive intercepts are obtained.

(b) The slopes and intercepts of the γ *vs.* p plots increase with increasing temperature and, at 327°, the intercepts increase with intensity.

(c) The rate of formation of CO (identified with I_a) is a linear function of p. This requires the fraction of the incident light absorbed to be small. Hence the intensity was approximately constant throughout the cell, indicating that diffusion of the radicals was not an important consideration.

(d) The rate of formation of CO is independent of temperature, at constant p and I, so that there was no significant contribution from chains.

(e) In the experiments with the packed cell the values of γ are just about as expected from the change in intensity resulting from the packing. Accordingly the change in surface/volume ratio, by a factor of 12, did not have any detectable effect on γ. Hence surface effects are probably not important.

The relationship between γ and p is of the type

$$\gamma = ap + bI_a^{1/2} \qquad \text{(B)}$$

where a and b are constants independent of pressure,

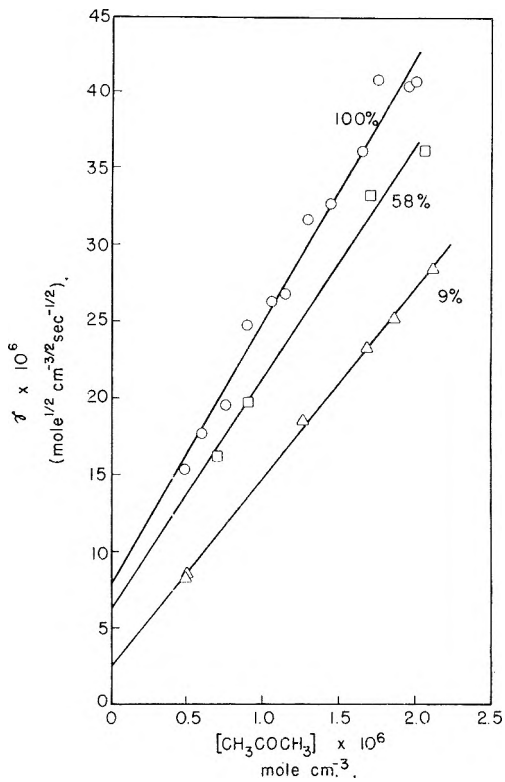

Fig. 2.—The effect of intensity at 327°. Relative percentage intensities as indicated.

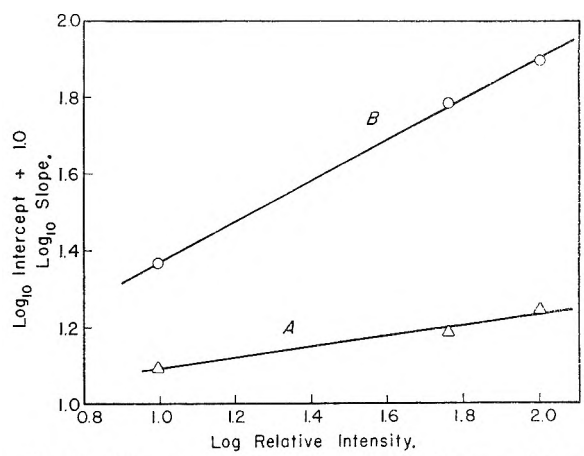

Fig. 3.—The effect of intensity on the slopes and intercepts of the γ *vs.* p plots at 327°: line A, slopes; line B, intercepts.

intensity and surface/volume ratio; they are presumably ratios and products of rate constants. The results also show that the term $bI_a^{1/2}$ is by no means negligible compared with ap at temperatures in excess of about 250° and at pressures and intensities commonly used in studies of the photolysis of acetone. Hence, the previously adopted relationship (A) is erroneous and data derived on that basis are questionable.

It is possible that the constant a is, actually, the ratio $(k_2/k_3^{1/2})$ and b includes the rate constant for a reaction

$$CH_3 + HX \longrightarrow CH_4 + X$$

between CH_3 and some substance (HX), whose con-

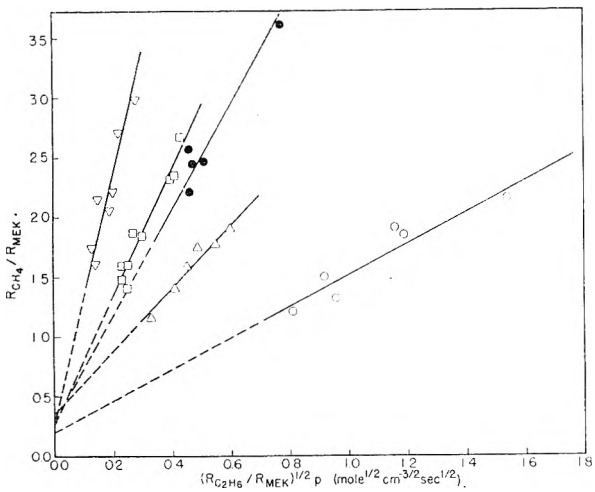

Fig. 4.—Test of suggested mechanism: ○, 184° (Mandelcorn and Steacie); △, 217°; ●, 241° (Mandelcorn and Steacie); □, 246°; ▽, 285°.

centration is independent of the concentration of acetone, or approximately so, and varies as $\sqrt{I_a}$.

The results appear to preclude the possibility of HX being absorbed acetone. Also CH_3CO is too unstable at the temperatures under consideration for its stationary concentration to be at all appreciable. Hence it is not likely that CH_3CO contributes to the formation of CH_4 in a reaction of the type suggested.

An alternative explanation, based on the third body restriction to the combination of CH_3, does yield an equation of the correct type for the relationship between γ and p. However it is inadequate since (a) it requires γ to be independent of I_a at constant p and T; (b) the effect should not be at all detectable over the range of pressures involved.

The suggestion that HX is the acetonyl radical is much more plausible. That radical is stable and disappears by combination with either methyl radicals[4] of itself. The suggested methane-producing reaction

$$CH_3 + CH_3COCH_2 \longrightarrow CH_4 + CH_2COCH_2 \quad (4)$$

is actually a disproportionation of free radicals which is considered to be of low activation energy and of comparable rate to the combination of radicals. In the present case reaction 4 will be in competition with

$$CH_3 + CH_3COCH_2 \longrightarrow CH_3COC_2H_5 \quad (5)$$
$$2CH_3COCH_2 \longrightarrow CH_3COCH_2CH_2COCH_3 \quad (6)$$

Accordingly, the rate of formation of CH_4 by reaction 4 should be of the same magnitude as that of the formation of methyl ethyl ketone (MEK) and Mandelcorn and Steacie have shown[4] that the rate of formation of MEK is not much lower than R_{CH_4} over a wide range of temperatures. Hence, it is likely that reaction 4 will contribute significantly to the formation of CH_4 in the photolysis of acetone.

The introduction of reaction 4 leads to the relationship

$$\gamma = \frac{k_2}{k_3^{1/2}} p + \frac{k_4}{k_3^{1/2}} r$$

Since r is a function of p, the slope of the γ *vs.* p plots will not necessarily provide a correct value of the ratio $k_2/k_3^{1/2}$. Accordingly, r should be eliminated from the above relationship.

Attempts to eliminate r by the use of steady-state equations have not been successful because of the complexity of the equations. One alternative is to obtain an expression for r in terms of a measurable quantity, *e.g.*, the rate of formation of methyl ethyl ketone or diacetonyl.

If ethane and methyl ethyl ketone are produced only by reactions 3 and 5, respectively, and if they do not disappear after they have been formed, we have

$$r = \frac{k_3^{1/2}}{k_5} \frac{R_{MEK}}{R'^{1/2}_{C_2H_6}} \quad (C)$$

This allows the γ *vs.* p relationship to be modified to

$$\frac{R_{CH_4}}{R_{MEK}} = \frac{k_2}{k_3^{1/2}} p \times \frac{R'^{1/2}_{C_2H_6}}{R_{MEK}} + \frac{k_4}{k_5} \quad (D)$$

The rate of formation of MEK was not measured in the present investigation and the published data are not sufficiently extensive to allow the suggested mechanism to be tested. However, it is possible to calculate R_{MEK} from the stoichiometry of the reaction and values thus obtained have been used.

The relationship between (R_{CH_4}/R_{MEK}) and $(R'^{1/2}_{C_2H_6}/R_{MEK})p$ is shown, in Fig. 4, for our experiments at 217, 246 and 285° and for the experimentally determined values of Mandelcorn and Steacie at 184 and 241°. Our data at 326° were much too scattered to be of any significance.

The results are not in disagreement with equation D but the data do not extend over a wide enough range to provide a strict test of that equation. The intercepts (k_4/k_5) are subject to a considerable uncertainty but a value of 0.25 ± 0.25 is not unreasonable; there does not appear to be any consistent effect of temperature on the intercept so that $E_4 \approx E_5 \approx 0$.

The following values have been obtained for the slopes

T (°C.)	184	217	241	246	285
Slope	1.35 ± 0.15	2.6 ± 0.4	4.5	5.4 ± 0.6	9.5 ± 1.0

The uncertainty appears to be approximately ± 10% over the range of temperature investigated. The Arrhenius plot of the slopes is not inconsistent with a straight line, the slope of which suggests an activation energy $(E_2 - {}^1/_2 E_2)$ of 10.0 ± 1.0 kcal. mole^{-1}. Assuming $P_3 \approx 1.0$ and collision frequencies of 10^{14} mole^{-1} cm.^{3} sec.$^{-1}$ we find $P_2 = 7 \times 10^{-3}$ with an uncertainty of a factor of about 10.

The values of E_2 and P_2 obtained do not differ significantly from those based on equation A. However, our results are based on calculated and corrected data and so can be only approximately correct. The reaction should be reinvestigated under conditions such that ethane and methyl ethyl ketone may be accurately measured.

(4) L. Mandelcorn and E. W. R. Steacie, *ibid.*, **32**, 79 (1954).

CONDITIONS FOR A STEADY STATE IN CHEMICAL KINETICS[1]

By O. K. Rice

Department of Chemistry, University of North Carolina, Chapel Hill, North Carolina

Received April 1, 1960

A general set of inequalities involving kinetic quantities is derived, whose validity is necessary for the establishment of a steady state in a reaction involving transient species. The *stability* of the steady state requires further that all the roots of a certain determinantal equation be negative (or, if complex, have a negative real portion). These criteria are applied to a number of examples, including branching chain reactions, the hydrogen bromide reaction, an oscillating reaction, a set of consecutive reactions, and a mechanism of interest in the consideration of flow processes, and the various factors affecting their application are elucidated.

It is customary in the discussion of chain reactions to make use of the Bodenstein method, in which it is assumed that certain transient species, commonly free radicals, come rapidly to a stationary concentration, which can be calculated by setting the rate of production of the radicals equal to the rate at which they are destroyed. Usually one's intuition in following this procedure leads to valid results, but difficulties can arise, and in some cases a better justification may be desired.

Some work has, indeed, been done in attempting to elucidate the conditions under which Bodenstein's assumption is valid. One method is to discuss the kinetic equations in detail, finding how the various concentrations change with time; it can then be ascertained whether the concentrations of intermediates tend to come to a steady state within a time which is small compared to the time required for appreciable changes in other substances. Semenov[2] discussed a number of reaction mechanisms from this point of view. More recently Benson[3] has considered a number of chain reactions on this basis, and has shown that in some cases the steady-state hypothesis is not valid. The problem has been treated by Hirschfelder,[4] by showing that the steady-state equation is the zeroth approximation to the solution of a set of differential equations involving the time. In a particular case he showed that, on the basis of the relative values of the rate constants involved, this approximation would be a very good one. However, in the general case the relationships become quite involved.

If one is interested in following the concentrations as a function of time there is no alternative to solving the set of differential equations involving the time supplied by the kinetic equations. From the point of view of investigating the steady state itself, there are advantages in considering principally conditions in the immediate neighborhood of the steady state (assuming it exists), and we shall see that many questions can be answered in this way. Apparently the paper which comes nearest to the present work is one by Frank-Kamenetsky,[5] who took this point of view, though his development is somewhat different from ours.

(1) Work assisted by the National Science Foundation.

(2) N. N. Semenov, *Acta Physicochim. U.R.S.S.*, **18**, 433 (1943).

(3) (a) S. W. Benson, *J. Chem. Phys.*, **20**, 1605 (1952); (b) S. W. Benson and J. H. Buss, *ibid.*, **28**, 301 (1958).

(4) J. O. Hirschfelder, *ibid.*, **26**, 271 (1957).

(5) (a) D. A. Frank-Kamenetsky, *Zhur. Fiz. Khim.*, **14** 695 (1940); (b) "Diffusion and Heat Exchange in Chemical Kinetics" (trans. by N. Thon), Princeton University Press, Princeton, N. J., 1955. Chapter X.

1. Case with Only One Intermediate.—Let us first consider the case where there is a single transient species whose concentration is c. The over-all rate per unit time and per unit volume at which this entity is formed we shall call R_f, and the rate at which it is being destroyed by other processes we shall call R_d. Then

$$dc/dt = R_f - R_d \tag{1.1}$$

Differentiating this

$$\frac{d^2c}{dt^2} = \left(\frac{\partial R_f}{\partial t}\right)_c - \left(\frac{\partial R_d}{\partial t}\right)_c + \left[\left(\frac{\partial R_f}{\partial c}\right)_t - \left(\frac{\partial R_d}{\partial c}\right)_t\right]\frac{dc}{dt} \tag{1.2}$$

At a steady state dc/dt must vanish, or nearly vanish, and, in order that it shall stay at zero, d^2c/dt^2 must vanish also. Necessary conditions for this are

$$\begin{aligned} |R_f^{-1}(\partial R_f/\partial t)_c| &\ll |(\partial R_f/\partial c)_t - (\partial R_d/\partial c)_t| \\ |R_d^{-1}(\partial R_d/\partial t)_c| &\ll |(\partial R_f/\partial c)_t - (\partial R_d/\partial c)_t| \end{aligned} \tag{1.3}$$

If these conditions hold, then it can be seen, bearing eq. 1.1 in mind, that, except when R_f is very close to R_d, the first term of eq. 1.2 is small compared to the second, so we write

$$d^2c/dt^2 \cong [(\partial R_f/\partial c)_t - (\partial R_d/\partial c)_t]\, dc/dt \tag{1.4}$$

In general, then, when dc/dt is very small, d^2c/dt^2 will be very small also (not greater than the order of magnitude of the neglected terms), and a steady state is possible. We can then set

$$R_f - R_d = 0 \tag{1.5}$$

and use this equation to calculate the value c_0 of c at the steady state.

However, if the stationary condition is to be approached if the system is somewhat removed from it, that is, if the steady state is to be stable, the sign of d^2c/dt^2 must be opposite to that of dc/dt. This gives rise to the additional condition

$$(\partial R_f/\partial c)_t - (\partial R_d/\partial c)_t < 0 \tag{1.6}$$

In general we will find the value of c given by eq. 1.5, and will test whether this gives a valid steady state by finding whether substituting the value so obtained causes the inequalities 1.3 and 1.6 to hold.

We may now consider the significance of the conditions (1.3). In the first place, we will usually not expect R_f to depend upon the concentration of the radical being formed, so most often $(\partial R_f/\partial c)_t$ will be zero. Since the reactions which destroy the intermediate will depend upon a small power of its concentration, we will have $(\partial R_d/\partial c)_t \sim R_d/c$, which will clearly be closely related to the inverse of the half-life, τ_d of the radical. On the

other hand, the change of R_f and R_d with time will depend upon the rate of change of other substances than the radical, and $R_f^{-1}(\partial R_f/\partial t)_c$ and $R_d^{-1}(\partial R_d/\partial t)_c$ will be rough measures of the inverse of the half-life, τ_r, of the reactants. It is thus seen that (1.3) is equivalent to $\tau_r >> \tau_d$. This is the condition usually assumed for the validity of the Bodenstein hypothesis, and is essentially similar to the conclusion reached by Frank-Kamenetsky.

It will be noted from eq. 1.4 that τ_d is very closely related to the time required to establish the steady state. The condition for a steady state to be possible, then, is essentially equivalent to the condition that the induction period for its establishment be small compared to the time for the over-all reaction. Though we shall not mention it again explicitly, similar conditions hold, also, in more complex mechanisms.

2. Case with Several Intermediates.—In general we may expect there to be several different kinds of transient species, M_1, M_2, . . . and their rates of appearance, R_{f1}, R_{f2} . . . and their rates of disappearance, R_{d1}, R_{d2}, . . . will depend upon their concentrations c_1, c_2, . . . in an involved way. We will have an equation like eq. 1.1 for each of the species.

$$dc_i/dt = R_{fi} - R_{di} = \Delta R_i \qquad (2.1)$$

and in place of (1.2)

$$d^2c_i/dt^2 = \partial\Delta R_i/\partial t + \Sigma_j(\partial\Delta R_i/\partial c_j)dc_j/dt \qquad (2.2)$$

where i and j can take on any one of the index numbers, 1, 2, ... In a partial derivative all variables (t, c_1, c_2, . . .) are held constant except the one specifically used in the differentiation.

We can now consider a set of inequalities

$$\begin{aligned} |R_{fj}^{-1}(\partial R_{fi}/\partial t)| &\ll |\partial\Delta R_i/\partial c_j| \\ |R_{dj}^{-1}(\partial R_{di}/\partial t)| &\ll |\partial\Delta R_i/\partial c_j| \end{aligned} \qquad (2.3)$$

Since we will in general test these inequalities at or near the steady state we can always substitute R_{fj} for R_{dj}, or *vice versa*, outside the derivative in the left-hand side of the inequalities. There are several remarks to be made about the right-hand members of these inequalities. Sometimes ΔR_i will not be a function of c_j at all, in which case the corresponding inequality is simply to be omitted. On the other hand, $\partial\Delta R_i/\partial c_j$ may be a sum of several terms. If certain steady-state relationships are established more rapidly than others, some of these terms in (2.2) may cancel against others in the sum in (2.2). In this case, they do not effectively contribute to the sum as far as other steady-state conditions are concerned, and the terms in (2.3) derived from them should be omitted. If the modified inequalities (2.3) still hold we can write

$$d^2c_i/dt^2 \leqq \Sigma_j(\partial\Delta R_i/\partial c_j)\, dc_j/dt \qquad (2.4)$$

whence, if all the dc_i/dt vanish, the d^2c_i/dt^2 will also, so we again have the steady-state conditions satisfied. The condition for the stability of such a steady state will not be as simple as (1.6), however, for away from the steady state the various dc_i/dt may have different signs.

Let us set up a new function c' which is a linear combination of the c_i, thus

$$c' = \Sigma_i a_i c_i \qquad (2.5)$$

where the a_i are constants. Then, by eq. 2.4

$$d^2c'/dt^2 = \Sigma_i a_i d^2c_i/dt^2 = \Sigma_{ij} a_i(\partial\Delta R_i/\partial c_j)dc_j/dt \qquad (2.6)$$

If we determine the coefficients so that

$$\beta a_j = \Sigma_i a_i(\partial\Delta R_i/\partial c_j) \qquad (2.7)$$

where β is another constant, the partial derivatives being given the values they have at the steady state, then near the steady state we have approximately

$$d^2c'/dt^2 = \Sigma_j \beta a_j dc_j/dt = \beta dc'/dt \qquad (2.8)$$

The steady state will be stable for the particular linear combination c' if $\beta < 0$. Since eq. 2.7 constitutes a linear system there will be values of a_i other than zero only if the determinant of the coefficients vanishes

$$\begin{vmatrix} \frac{\partial\Delta R_1}{\partial c_1} - \beta & \frac{\partial\Delta R_2}{\partial c_1} & \cdots \\ \frac{\partial\Delta R_1}{\partial c_2} & \frac{\partial\Delta R_2}{\partial c_2} - \beta & \cdots \\ \cdots & \cdots & \cdots \end{vmatrix} = 0 \qquad (2.9)$$

If there are n concentrations c_i there will in general be n eigenvalues β of this determinant and, correspondingly, n linear combinations c'. If all the eigenvalues are negative there will be n combinations of the concentrations which will tend toward their steady-state values; hence the n concentrations must tend toward their steady-state values and the system will be stable.

This determinant is not entirely new. It appears when one attempts to solve for the concentrations as a function of time, in cases in which all its elements are constant in time, that is cases in which all the reactions are first order with respect to the transient species. In such cases, Semenov[2] has indeed used the sign of the eigenvalues to indicate whether a steady state is possible.

If we set in the determinant values of the derivatives attained at the steady state (*i.e.*, found by setting eq. 2.1 equal to zero), which of course we shall do, this amounts to an approximate linearization of the problem for the region near the steady state. This has also been achieved by Frank-Kamenetsky,[5b] who derived the determinant by integrating the kinetic equations 2.1 after introducing approximations valid near the steady state.

Our instinct tells us that a steady state, if attained, will be stable unless there are branching-chain reactions. This can, indeed, be verified by considering the properties of the determinant. If there is no branching chain reaction any set of reactions in which a given radical, j, takes part must result in net destruction of that radical; thus $\partial\Delta R_j/\partial c_j$ must be negative. Further the stoichiometry must be such that the rate of production of other radicals due to reactions involving the radical j cannot exceed the rate of destruction of the radical j. This means that, always

$$|\partial\Delta R_j/\partial c_j| \geq \Sigma_i{}' \partial\Delta R_i/\partial c_j \qquad (2.10)$$

where the accent on the summation sign means that the term $i = j$ is not included in the sum. If ΔR_j involves separate reactions of the radical j the inequality must, indeed, hold for each reaction separately. Thus it will not be upset by the presence of reactions of different orders.

If all the sums $\Sigma_i'\partial\Delta R_i/\partial c_j$ were zero the roots, β, would be equal to the terms $\partial\Delta R_j/\partial c_j$, *i.e.*, to negative real numbers; call these numbers $\beta_{0,j}$. It can be shown[6] that, in general, all the roots will lie in circles in the complex plane which have centers at the points $\beta_{0,j}$ and radii equal to the respective sums $\Sigma_i'\partial\Delta R_i/\partial c_j$. Thus, if (2.10) holds, there will be no roots with positive real parts. Complex roots are possible; this results in oscillating concentrations, but as will become clear from an example (Section 5), the steady state will still be stable. Zero roots may also be possible in some instances. These represent a rather special case, in which the equality of (2.10) holds. For a zero root, the left-hand side of eq. 2.7 vanishes, and since the complete sum $\Sigma_i\partial\Delta R_i/\partial c_j = 0$ for some j by (2.10) ($\partial\Delta R_j/\partial c_j$ being negative) all the a_i must be equal. Since they are all equal, the equality of (2.10) must, by eq. 2.7, hold for *all* j. Therefore, the case of a zero root can occur only if all the sums $\Sigma_i\partial\Delta R_i/\partial c_j$ vanish.

As a result of these considerations, we see that we do not need to take (2.9) into account, except for branching-chain reactions, or unless we wish to consider the possibility of complex roots.

We shall now consider examples which bring out the use of the various criteria. The last two examples (sections 6 and 7), do not bring out any new features, but they are of sufficient intrinsic interest to warrent a more rigorous treatment than the usual considerations provide.

3. A Branching-chain Reaction.—The following mechanism has been suggested to explain the upper explosion limit in the oxidation of carbon monoxide.[7]

$$CO + O_2 \xrightarrow{k_1} CO_2 + O$$

$$O + O_2 + Y \xrightarrow{k_2} O_3 + Y$$

$$O_3 + CO \xrightarrow{k_3} CO_2 + 2O$$

$$O_3 + CO + Y \xrightarrow{k_4} CO_2 + O_2 + Y$$

Y is any molecule which takes part in a given reaction only to the extent of supplying or removing energy. We have (using parentheses to indicate concentrations)

$$\Delta R_O = k_1(CO)(O_2) + 2k_3(O_3)(CO) - k_2(O)(O_2)(Y) \quad (3.1)$$

$$\Delta R_{O_3} = k_2(O)(O_2)(Y) - k_3(O_3)(CO) - k_4(O_3)(CO)(Y) \quad (3.2)$$

If we assume that O_3 and O come to steady-state concentrations, we have

$$(O_3) = k_1(O_2)/[k_4(Y) - k_3] \quad (3.3)$$

and

$$(O) = \frac{k_1(CO)[k_4(Y) + k_3]}{k_2(Y)[k_4(Y) - k_3]} \quad (3.4)$$

If (Y) is decreased, the concentrations of O_3 and O eventually become infinite and change sign. With (Y) below this critical value there is no steady-state solution and an explosion results.

Let us now consider the inequalities (2.3) applied, say to (O). Since the rate of reaction 1, the chain initiating step, will be relatively slow, we may write

$$\begin{aligned} |R_{O,f}^{-1}\,\partial R_{O,f}/\partial t| &= |(CO)^{-1}\mathrm{d}(CO)/\mathrm{d}t| \\ &= (O_3)[k_3 + k_4(Y)] \\ &= k_1(O_2)[k_3 + k_4(Y)]/[k_4(Y) - k_3] \end{aligned} \quad (3.5)$$

The last relation, of course, uses eq. 3.3, which is legitimate, since we wish to test the steady state. Assuming inert molecules are present in excess, so that (Y) does not change rapidly (if Y is chiefly O_2 and CO then the results will be changed only in detail),

$$\begin{aligned} |R_{O,d}^{-1}\,\partial R_{O,d}/\partial t| &= |(O_2)^{-1}\,\mathrm{d}(O_2)/\mathrm{d}t| \\ &\cong k_2(O)(Y) \\ &= k_1(CO)[k_3 + k_4(Y)]/[k_4(Y) - k_3] \end{aligned} \quad (3.6)$$

On the other hand

$$|\partial\Delta R_O/\partial(O)| = k_2(O_2)(Y) \quad (3.7)$$

We may now compare eq. 3.7 with eq. 3.5 and 3.6. Since (O_2) is, under normal experimental conditions in a quiet reaction, much greater than (O), and since $k_2(Y)(O)$ will be comparable with $[k_3 + k_4(Y)](O_3)$ we see that the inequality will be valid. In a sense, this is putting the matter backwards. The reason that (O) is small compared to (O_2), for example, is that k_1 is small compared to $k_2(Y)$, which gives the inequality directly, and which expresses the fact that O is a reactive intermediate. Of course, just when the explosion limit is approached, the steady-state concentrations of O and O_3 approach the concentrations of O_2 and CO and so the inequalities (2.3) and with them the validity of the steady state breaks down just before the explosion limit is reached.

The other inequalities (2.3) can be tested in similar fashion. If we again recall that the chain-carrying steps (2) and (3) go rapidly compared to reaction 1, and assume $(O_2) \sim (CO)$, we may write

$$\begin{aligned} |R_{O_2,f}^{-1}\,\partial R_{O,f}/\partial t| &\cong |2(k_3/k_2)[(O_3)/(O)](O_2)^{-1}(Y)^{-1} \\ &\qquad \mathrm{d}(CO)/\mathrm{d}t| \\ &\cong 2k_3(O_3) \end{aligned} \quad (3.8)$$

and

$$\begin{aligned} |R_{O_3,d}^{-1}\,\partial R_{O,d}/\partial t| &= \left|\frac{k_2(O)(Y)\,\mathrm{d}(O_2)/\mathrm{d}t}{k_3(O_3)(CO) + k_4(O_3)(CO)(Y)}\right| \\ &\cong k_2(O)(Y) \cong 2k_3(O_3) \end{aligned} \quad (3.9)$$

It is once again seen that in each case we are essentially comparing the concentration of a reactive intermediate with that of one of the more stable molecules, so again the inequalities hold. We will not go through the other cases, but they work out in much the same way.

The determinant (2.9) is easily set up and solved for β in this case, since it contains only two rows and two columns. One obtains

$$\beta = -\tfrac{1}{2}b \pm \tfrac{1}{2}(b^2 - 4c)^{1/2} \quad (3.10)$$

with $b = k_2(O_2)(Y) + k_3(CO) + k_4(CO)(Y)$

and $c = -k_2k_3(CO)(O_2)(Y) + k_2k_4(O_2)(CO)(Y)^2$

It is easily verified that the roots will always be real, but if c becomes negative, *i.e.*, if $k_3 > k_4$ (Y),

(6) A. Brauer, *Duke Math. J.*, **13**, 387 (1946) (Theorem 1). I am indebted to Professor Brauer for a discussion of this problem.

(7) K. J. Laidler, "Chemical Kinetics," McGraw-Hill Book Co., New York, N. Y., 1950, p. 327. We have left out some reactions which account for the production of light, but which are of minor importance chemically.

one of the roots will be positive. It is seen that this occurs just at the point at which the other conditions for the establishment of a steady state break down. Thus, if a steady state is possible it will always be stable.

We will now consider a conceivable modification of this mechanism

$$CO + O_2 \xrightarrow{k_1} CO_2 + O$$

$$O + O_2 + Y \xrightarrow{k_2} O_3 + Y$$

$$2O_3 + CO \xrightarrow{k_3} CO_2 + 3O + O_2$$

$$O_3 + CO \xrightarrow{k_4} CO_2 + O_2$$

We do not wish to imply that this is a possible alternative to the previously considered mechanism as an explanation of the experimental facts. We merely wish to consider it as a conceivable mechanism with certain peculiar properties. We have

$$\Delta R_O = k_1(CO)(O_2) + 3k_3(O_3)^2(CO) - k_2(O)(O_2)(Y) \quad (3.11)$$

$$\Delta R_{O_3} = k_2(O)(O_2)(Y) - 2k_3(O_3)^2(CO) - k_4(O_3)(CO) \quad (3.12)$$

At the steady state we have for the O_3 concentration

$$2k_3(O_3) = k_4 \pm [k_4^2 - 4k_1k_3(O_2)]^{1/2} \quad (3.13)$$

It is seen that according to this mechanism, there will be no real solution if $(O_2) > k_4^2/4k_1k_3$. If $(O_2) < k_4^2/4k_1k_3$ two solutions appear possible. Clearly if one starts with no O_3 present, one will not expect to reach the higher solution, but one might expect to be able to reach it by adding O_3. However, it may readily be seen that the higher solution will not be stable. The determinant, eq. 2.9, is again readily set up and solved, and we find

$$\beta = -{}^1/_2 b \pm {}^1/_2(b^2 - 4c)^{1/2} \quad (3.14)$$

where

$$b = k_2(O_2)(Y) + 4k_3(CO)(O_3) + k_4(CO)$$
$$c = -2k_2k_3(O_2)(O_3)(CO)(Y) + k_2k_4(CO)(O_2)(Y)$$

The roots are always real, but one is positive if c is negative, *i.e.*, if $2k_3(O_3) > k_4$. It is seen that this is exactly the situation for the larger root of eq. 3.13. This higher concentration of O_3 will, therefore, not result in a stable steady state.

Thus we could increase (O_3) by adding O_2, until $(O_2) = k_4^2/4k_1k_3$ and $(O_3) = k_4/2k_3$. Beyond this point further addition of O_2 would at first increase the rate of production of O_3, and since no steady state can be reached we must presume that the concentration would increase indefinitely and an explosion would result.

The validity of the inequalities (2.3) may be tested in much the same ways as for the other mechanism, and it does not seem worthwhile to give the details. It is found that these inequalities hold if $(CO) >> (O_3)$ and $(O_2) >> (O_3)$. Depending on the concentration of CO and the value of k_4/k_3, this inequality might break down before O_3 had reached its maximum concentration.

It is rather unlikely that a mechanism of this type will be found, for it has, as a chain propagating reaction, one in which two molecules of the same unstable intermediate are involved, but it is not impossible. We see from this example that, with such a reaction scheme, a satisfactory understanding would involve consideration of all the inequalities in some detail. It is true that, the determinant being of the second rank only, the condition of stability could be handled otherwise. It is necessary, however, to take it into account, and the use of (2.9) seems the most expeditious way.

4. The Hydrogen-Bromide Reaction.—In the examples considered, the inequalities (2.3) hold when the concentration of an intermediate is small compared to those of the main reactants present. In some cases, however, this is not sufficient and in this section we will analyze one of these situations. Benson[3] has considered the mechanism of the hydrogen bromide reaction and other similar reactions in some detail, and has shown that some of them may have long induction periods and may not be amenable to the steady-state treatment.

The mechanism of the hydrogen bromide reaction is essentially

$$Y + Br_2 \underset{k_2}{\overset{k_1}{\rightleftarrows}} 2Br + Y$$

$$Br + H_2 \xrightarrow{k_3} HBr + H$$

$$H + Br_2 \xrightarrow{k_4} HBr + Br$$

We have then

$$\Delta R_{Br} = k_1(Y)(Br_2) + k_4(H)(Br_2) - k_2(Br)^2(Y) - k_3(Br)(H_2) \quad (4.1)$$

$$\Delta R_H = k_3(Br)(H_2) - k_4(H)(Br_2) \quad (4.2)$$

In this case it will be advisable to write down all the quantities which are involved in the consideration of (2.3). We have

$$|R_{f,Br}^{-1}(\partial R_{f,Br}/\partial t)| = |(Br_2)^{-1}\, d(Br_2)/dt| \cong k_4(H) \quad (4.3)$$

$$|R_{d,Br}^{-1}\,\partial(R_{d,Br}/\partial t)| = |[k_2(Br)^2(Y) + k_3(Br)(H_2)]^{-1}\, k_3(Br)d(H_2)/dt| \cong (k_3^2/k_2)(H_2)/(Y) \text{ or } \cong k_3(Br) \quad (4.4)$$

$$|R_{f,H}^{-1}(\partial R_{f,Br}/\partial t)| = |[k_3(Br)(H_2)]^{-1}[k_1(Y) + k_4(H)]d(Br_2)/dt| \cong k_1(Y) \text{ or } \cong k_4(H) \quad (4.5)$$

$$|R_{d,H}^{-1}(\partial R_{d,Br}/\partial t)| = |[k_4(H)Br_2]^{-1}\, k_3(Br)\, d(H_2)/dt| = k_3(Br) \quad (4.6)$$

$$|R_{f,H}^{-1}(\partial R_{f,H}/\partial t)| = |(H_2)^{-1}\, d(H_2)/dt| = k_3(Br) \quad (4.7)$$

$$|R_{d,H}^{-1}(\partial R_{d,H}/\partial t)| = |(Br_2)^{-1}\, d(Br_2)/dt| \cong k_4(H) \quad (4.8)$$

$$|R_{f,Br}^{-1}(\partial R_{f,H}/\partial t)| = |[k_1(Y)(Br_2) + k_4(H)(Br_2)]^{-1}\, k_3(Br)\, d(H_2)/dt)| \cong (k_3^2/k_1)(Br)^2(H_2)(Br_2)^{-1}(Y)^{-1} \text{ or } \cong k_3(Br) \quad (4.9)$$

$$|R_{d,Br}^{-1}(\partial R_{d,H}/\partial t)| = |[k_2(Br)^2(Y) + k_3(Br)(H_2)]^{-1} k_4(H)\, d(Br_2)/dt| \cong (k_3^2/k_2)(H_2)^2(Y)^{-1}(Br_2)^{-1} \text{ or } \cong k_4(H) \quad (4.10)$$

In evaluating $d(Br_2)/dt$ and $d(H_2)/dt$ we have used rate expressions from the chemical reactions, assuming, as would be true near the steady state, that the rate of disappearance of Br_2 is principally controlled by the fourth reaction, and we have used the steady-state conditions as convenient. We have assumed that (Y) does not change with time. The alternate expressions come from as-

suming that one or the other of the terms in the brackets predominates. For comparison we have

$$|\partial\Delta R_{Br}/\partial(Br)| = 2k_2(Br)(Y) + k_3(H_2) \quad (4.11)$$

$$|\partial\Delta R_{Br}/\partial(H)| = k_4(Br_2) \quad (4.12)$$

$$|\partial\Delta R_{H}/\partial(H)| = k_4(Br_2) \quad (4.13)$$

$$|\partial\Delta R_{H}/\partial(Br)| = k_3(H_2) \quad (4.14)$$

First we may compare (4.13) with (4.7) and (4.8) and (4.14) with (4.9) and (4.10). Since in the two latter cases, either of the two alternative expressions is larger than the true expression we may compare $k_3(H_2)$ with $k_3(Br)$ and $k_4(H)$. If the free atoms are present in small concentrations compared to stable molecules, $k_3(H_2)$ will be large compared to $k_3(Br)$. Since at a steady state $k_4(H) = k_3(Br)(H_2)/(Br_2)$, we see that $k_3(H_2)$ will also be large compared to $k_4(H)$ unless (H_2) is in very great excess. Similarly (4.13) may be supposed to be large compared with (4.7) and (4.8). From this we may suppose that there is no hindrance to the setting up of a steady state for H. Indeed we may apply the inequalities to H alone, treating Br as a substance whose concentration does not change rapidly, in which case we have only to consider

$$R_{f,H}^{-1}\,\partial R_{f,H}/\partial t = (Br)^{-1}\,d(Br)/dt + (H_2)^{-1}\,d(H_2)/dt \cong (Br)^{-1}\,k_1(Y)(Br_2) - 2k_2(Br)(Y) \quad (4.15)$$

$$R_{d,H}^{-1}\,\partial R_{d,H}/\partial t = (Br_2)^{-1}\,d(Br_2)/dt \cong k_4(H) \quad (4.16)$$

In evaluating (4.15) we neglected the last term, and found $d(Br)/dt$ from (4.1), assuming $\Delta R_H = 0$. The condition for a steady state involving H, then, is found by comparing (4.13) with (4.15) and (4.16). It is seen that such a steady state can be set up if

$$k_4(Br) \gg k_1(Y) \quad (4.17)$$

even though a steady state with respect to Br may not have been achieved.

Let us now return to a consideration of the steady state involving Br. We see that the condition that (4.12) be much greater than (4.5) and (4.6) will in general be fulfilled.[7a] Finally we have to compare (4.11) with (4.3) and (4.4). If (4.17) holds, we should, following the warning after (2.3), strike out the term $k_3(H_2)$ in (4.11). We must then compare $k_2(Br)$ (Y) with $k_4(H)$, or $k_3(Br)$, which is essentially the same thing. In order for a steady concentration of Br to be attained we must have $k_2(Y) >> k_3$. This is just the condition found by Benson by integrating the kinetic equations. The set of inequalities which we have written down avoids the necessity of the integration. As Benson noted, the condition is fulfilled for the hydrogen bromine reaction, but for analogous reactions it may not be.

There being no branching chain, the steady state will be stable.

5. An Oscillating Reaction.—We will now turn to a mechanism suggested by Christiansen[8] and discussed by Bak,[9] which gives rise to a damped periodic or oscillating reaction.

$$A_1 + M_1 \xrightarrow{k_1} M_2 + B_2$$

$$A_2 + M_2 \xrightarrow{k_2} M_3 + B_3$$

$$A_3 + M_3 \xrightarrow{k_3} M_1 + B_1$$

Actually the scheme proposed by Christiansen allowed the reactions to proceed in either direction. This is not necessary for the purposes of our illustration. While some fairly detailed discussions of oscillating reactions have been given[5b,9] it seems worthwhile to discuss this particularly simple case, and to see how the result fits in with the discussion of (2.9) given in Section 2.

In this mechanism $M_1 + M_2 + M_2$ (using here italicized letters to represent concentrations) cannot change. If M_1, M_2, and M_3 are small the M's will function as catalysts, but they will not appear if not present at the start.

We have

$$\Delta R_{M_1} = k_3A_3M_3 - k_1A_1M_1 \quad (5.1)$$

$$\Delta R_{M_2} = k_1A_1M_1 - k_2A_2M_2 \quad (5.2)$$

$$\Delta R_{M_3} = k_2A_2M_2 - k_3A_3M_3 \quad (5.3)$$

At the steady state we have three equations of which only two are independent. We can only find the ratios of the steady-state concentrations. Thus

$$M_1 = [k_3A_3/k_1A_1]M_3 \quad (5.4)$$

$$M_2 = [k_3A_3/k_2A_2]M_3 \quad (5.5)$$

Examining the validity of the inequalities (2.3), we find, for example

$$|R_{d,M_i}^{-1}\,\partial R_{d,M_i}/\partial t| = (k_j/k_i)(M_j/M_i)A_i^{-1}dA_j/dt \quad (5.6)$$

where i precedes j in the cyclic order (1, 2, 3, 1, . . .), and

$$|\partial\Delta R_{M_i}/\partial M_i| = k_iA_i \quad (5.7)$$

Thus if M_j and M_i, and k_i and k_j, are of the same order of magnitude we must have

$$dA_j/dt \ll k_iA_i^2 \quad (5.8)$$

These inequalities and similar ones from the R_f's will clearly hold if the concentrations of the M's are much smaller than those of the A's.

The determinant in this case has the form

$$\begin{vmatrix} -k_1A_1 - \beta & k_1A_1 & 0 \\ 0 & -k_2A_2 - \beta & k_2A_2 \\ k_3A_3 & 0 & -k_3A_3 - \beta \end{vmatrix} = 0 \quad (5.9)$$

which may be written

$$(\beta + k_1A_1)(\beta + k_2A_2)(\beta + k_3A_3) - k_1k_2k_3A_1A_2A_3 = 0 \quad (5.10)$$

It will be noted that this determinant is an example of the case in which (2.10) has the equality sign for each j. It does, indeed, have a zero root, as may be seen by inspection. This root corresponds to $c' = M_1 + M_2 + M_3$, for which combination dc'/dt always vanishes.

To investigate the other roots we may without loss of generality take $k_1A_1 > k_2A_2 > k_3A_3$. It will be noted that the first term in (5.10) is zero when $\beta = -k_2A_1$, $-k_2A_2$, or $-k_3A_3$, and has a maximum between $-k_2A_1$ and $-k_2A_2$. If $k_1k_2k_3A_1A_2A_3$ is greater than the value of the first term at the maximum, (which must be the case if k_1A_1 is close enough to k_2A_2), then two of the roots of the determinant become complex. This means that the linear combination c' of M_1, M_2, and M_3 (which will itself be complex), corresponding to one of these

(7a) If H is always in a steady state, this condition is really not of interest.

(8) J. A. Christiansen, "Advances in Catalysis," Vol. 5, 1953, p. 311.

(9) T. A. Bak, Thesis, University of Copenhagen, 1959, pp. 40ff.

values of β, will have a value of dc'/dt which, in the complex plane, spirals around the point $dc'/dt = 0$. Since the real part of β will always be negative it will spiral toward $dc'/dt = 0$, corresponding to the steady state, so the latter will be stable, as was noted by Bak.

6. A Set of Consecutive Bimolecular Reactions.—Another example of some general interest is furnished by the reaction scheme

$$2A \underset{k_{-0}}{\overset{k_0}{\rightleftharpoons}} M_1 + A$$

$$A + M_1 \underset{k_{-1}}{\overset{k_1}{\rightleftharpoons}} M_2 + A$$

$$A + M_2 \underset{k_{-2}}{\overset{k_2}{\rightleftharpoons}} M_3 + A$$

. . . . . .

$$\begin{vmatrix} -(k_{-0}+k_1)A-\beta & k_1A & 0 & \cdots \\ k_{-1}A & -(k_{-1}+k_2A)-\beta & k_2A & \cdots \\ 0 & k_{-2}A & -(k_{-2}+k_2)A-\beta & \cdots \\ \cdots & \cdots & \cdots & \cdots \\ \cdots & -(k_{-(n-2)}+k_{n-1})A-\beta & k_{n-1}A & \\ \cdots & k_{-(n-1)}A & -(k_{-(n-1)}+k_n)A-\beta & \end{vmatrix} = 0$$

$$A + M_{n-1} \underset{k_{-(n-1)}}{\overset{k_{n-1}}{\rightleftharpoons}} M_n + A$$

$$A + M_n \xrightarrow{k_n} M_{n+1} + A$$

If M_1, M_2, . . M_n be considered to be successive energy states and M_{n+1} a reaction product, this is the type of mechanism which has been considered in discussing the departure from equilibrium caused by a reaction process[10]

We have

$$\Delta R_{M_1} = k_0A^2 + k_{-1}AM_2 - -k_{-0}AM_1 - k_1AM_1$$
$$\Delta R_{M_2} = k_1AM_1 + k_{-2}AM_3 - k_{-1}AM_2 - k_2AM_2 \quad (6.1)$$
. . . . . .
$$\Delta R_{Mn} = k_{n-1}AM_{n-1} - k_{-(n-1)}AM_n - k_nAM_n$$

It can be easily seen that these expressions can be set equal to zero and the resulting equations solved for the steady state concentrations. The last equation can be used to get M_n in terms of M_{n-1}. This expression for M_n can be substituted in the next to the last equation, and the latter then solved for M_{n-1} in terms of M_{n-2}. This process can be repeated and the first equation finally used to obtain M_1 in terms of A.

In order to test the inequalities (2.3) we note that (except for R_{f,M_1}, which will not differ in order of magnitude)

$$|R_{f,M_i}{}^{-1}\,\partial R_{f,M_i}/\partial t| = |R_{d,M_i}{}^{-1}\,\partial R_{d,M_i}/\partial t| = A^{-1}\,dA/dt$$
$$= |k_0A - k_{-0}M_1| \quad (6.2)$$

the last relation arising from consideration of reaction zero which is the only one which results in a change in A. We have

$$\partial\Delta R_{M_i}/\partial M_i = -(k_{-(i-1)} + k_i)A \quad (6.3)$$

Comparing these we see that (2.3) requires that

$$|k_0A - k_{-0}M_1| \ll |k_{-(i-1)} + k_i|A \quad (6.4)$$

We see that this will be fulfilled if $A >> M_i$ and if k_0 is much smaller than the other k_i, all of which are assumed to be of the same order of magnitude. It is especially well fulfilled if M_1 is nearly in equilibrium with A; *i.e.*, if some energy level can be found such $M_1 << A$ and yet M_1 is sufficiently removed from the product M_{n+1}, so that M_1 can be considered to be in equilibrium. A similar effect of an equilibrium was noted in a series of consecutive reactions by Benson.[3a]

The case of the inequalities of (2.3) for which $i \neq j$ would involve factors of the order of magnitude $k_{\pm i}M_i/k_{\pm(i+1)}M_{i+}$, which, if all the k_i and k_{-i} are of the same order of magnitude, should not upset the inequalities.

The determinant in this case takes the form

This determinant has zeros except on the diagonal and in the positions next to the diagonal. It has appeared before in connection with finding the solution of the differential equations which give the concentrations as functions of the time.[10] It conforms to (2.10), so the system is stable, and it can be shown to have no complex roots. The value of the determinant is unaltered by multiplying any row by a given number and dividing the corresponding column by the same number. Doing this with the first row and column, the second, the third, etc., we choose the successive numbers so that the affected non-diagonal elements are changed in such a way that the determinant becomes symmetric; this may be readily seen to be possible, since all the non-diagonal terms are positive. The diagonal elements, of course, remain unchanged. A symmetric determinant is known to have all real roots.[11] Thus we see that this problem, involving the effect of a reaction in causing departure from equilibrium, can be handled by a steady-state method.

7. A Mechanism of Interest in Flow Processes.—In a following paper[12] we shall describe certain flow process by the mechanism

$$S + A_+ \underset{k_{-1}}{\overset{k_1}{\rightleftharpoons}} M_+ \underset{\lambda}{\overset{\lambda}{\rightleftharpoons}} M_- \underset{k_{-2}}{\overset{k_2}{\rightleftharpoons}} S + A_-$$

Here M_+ and M_- are intermediates whose concentrations are small compared to those of S, A_+ and A_-, and which are nearly in equilibrium with S and A_+ and with S and A_-, respectively; also k_1 and k_{-2} are of the same order of magnitude, as are k_{-1} and k_2. We have

$$\Delta R_{M_+} = k_1SA_+ + \lambda M_- - (k_{-1} + \lambda)M_+ \quad (7.1)$$
$$\Delta R_{M_-} = k_{-2}SA_- - \lambda M_+ - (k_2 + \lambda)M_- \quad (7.2)$$

(10) E. W. Montroll and K. E. Shuler in "Advances in Chemical Physics," Vol. I (I. Prigogine, Ed.) Interscience Publishers, Inc., New York, 1958, p. 361; E. E. Nikitin and N. D. Sokolov, *J. Chem. Phys.*, **31**, 1371 (1959).

(11) I am indebted to Professor Alfred T. Brauer for suggesting this proof.

(12) O. K. Rice, THIS JOURNAL, **64**, 1857 (1960).

and, as S is the symbol for a substrate which does not change rapidly

$$|R_{f,M_+}{}^{-1}\,\partial R_{f,M_+}/\partial t| < A_+{}^{-1}\,\mathrm{d}A_+/\mathrm{d}t \quad (7.3)$$

$$|R_{f,M_-}{}^{-1}\,\partial R_{f,M_+}/\partial t| < A_-{}^{-1}\,(k_1/k_{-2})\mathrm{d}A_+/\mathrm{d}t \sim A_-{}^{-1}\,\mathrm{d}A_+/\mathrm{d}t \quad (7.4)$$

$$|R_{f,M_-}{}^{-1}\,\partial R_{f,M_-}/\partial t| < A_-{}^{-1}\,\mathrm{d}A_-/\mathrm{d}t \quad (7.5)$$

$$|R_{f,M_+}{}^{-1}\,\partial R_{f,M_-}/\partial t| < A_+{}^{-1}(k_{-2}/k_1)\mathrm{d}A_-/\mathrm{d}t \sim A_+{}^{-1}\,\mathrm{d}A_-/\mathrm{d}t \quad (7.6)$$

$$\partial R_{d,M_+}/\partial t = \partial R_{d,M_-}/\partial t = 0 \quad (7.7)$$

also

$$|\partial \Delta R_{M_+}/\partial M_+| = k_{-1} + \lambda \quad (7.8)$$

$$|\partial \Delta R_{M_+}/\partial M_-| = |\partial \Delta R_{M_-}/\partial M_+| = \lambda \quad (7.9)$$

$$|\partial \Delta R_{M_-}/\partial M_-| = k_2 + \lambda \quad (7.10)$$

Typically, we must show that

$$\lambda A_- \gg |\mathrm{d}A_+/\mathrm{d}t| \quad (7.11)$$

But

$$|\mathrm{d}A_+/\mathrm{d}t| = |k_{-1}M_+ - k_1 S A^+| \quad (7.12)$$

At a steady state, from (7.1)

$$k_{-1}M_+ - k_1 S A_+ = \lambda[M_- - M_+] \quad (7.13)$$

If M_- and M_+ are intermediates which are present in small concentrations this is clearly much smaller than the left-hand side of (7.11), and again we see that the more nearly equilibrium is established between M_+ and A_+ the more valid is the inequality.

Since no branching chains are involved the steady state is stable.

Conclusions

We have illustrated the application of the general set of inequalities derived in Section 2 by a sufficient number of examples to demonstrate its power in indicating the conditions necessary for a steady state. Usually it is found that the requirement for a steady state reduces to the necessity for the concentrations of reactive intermediates to be small compared to those of other species. However, even in rather unusual situations, it is found that the inequalities, if properly applied, are adequate to disentangle the various factors involved, and can serve as a guide to the conditions under which a steady state can occur, without the necessity of integrating kinetic equations. When many reactions are involved the process may become rather tedious, but it resolves by a systematic procedure all questions concerning the existence and stability of a steady state.

I am indebted to Dr. W. Forst for reading and commenting upon portions of this paper and for a translation of the paper by Frank-Kamenetsky, and to the referee for a criticism which resulted in an improvement in the discussion of (2.9).

THE PRINCIPLE OF MINIMUM ENTROPY PRODUCTION AND THE KINETIC APPROACH TO IRREVERSIBLE THERMODYNAMICS[1]

BY O. K. RICE

Department of Chemistry, University of North Carolina, Chapel Hill, North Carolina

Received April 1, 1960

A distinction is made between a steady state in detail, in which certain reactive intermediates come to a steady state, and a steady state in the large, in which substances in larger concentrations come to a steady state under certain restraints. It is shown very generally that in either case a state is reached in which the rate of entropy production is a minimum consistent with the constraints imposed, provided the system is not far removed from equilibrium. A mechanism is considered which may be applied to the consideration of flow processes. The relation of these ideas to the general principles of irreversible thermodynamics is considered, and it shows that the laws of irreversible thermodynamics follow from the minimum-entropy principle. The article closes with a discussion of the assumptions involved in this deduction and their significance.

It is well known that when a steady state becomes established in a system which is only slightly displaced from equilibrium the rate of production of entropy is a minimum. This condition as it applies to chemical reactions has been examined in some detail by Prigogine[2] and by Bak.[3] These considerations involve the usual methods of irreversible thermodynamics in which the entropy production is expressed in terms of forces and fluxes. While Prigogine has considered some cases which do not directly involve Onsager's reciprocal relations, the particular types of steady state considered were not too close to those of interest to chemists, and the principal interest seems to have been in the relation between the reciprocal relations and the law of microscopic reversibility. It is, however, possible to introduce this subject by a direct consideration of steady states in which short-lived intermediates are involved, as, indeed, they are, in one way or another, in most reactions. The principle of minimum entropy production can be established in a very general fashion on the basis of the assumptions usual in chemical kinetics, including, indeed, the law of microscopic reversibility, without any direct reference to the reciprocal relations. It is then possible to obtain the formalism of irreversible thermodynamics using the minimum entropy principle as a basis. A number of interesting points emerge when this exercise is carried out.

A short-lived intermediate comes quickly to a steady state,[4] and the concentrations of the substances which are present in larger amounts change slowly. Under certain circumstances these

(1) Work assisted by the National Science Foundation.

(2) See I. Prigogine, "Introduction to Thermodynamics of Irreversible Processes," Charles C. Thomas, Springfield, Ill., 1955, Chap. VI.

(3) T. A. Bak Thesis, University of Copenhagen, 1959, Chap. 2.

(4) See O. K. Rice, THIS JOURNAL, **65**, 1851 (1961) (preceding article) and D. A. Frank-Kamenetsky, *Zhur. Fis. Khim.*, **14**, 695 (1940).

concentrations can also reach a steady state. Thus we have two types of steady state, the first type involving the intermediates which we may call the steady state in detail, and the second type involving the substances present in measurable concentrations, which we call the steady state in the large.

1. Minimum Entropy Production and the Steady State.—An intermediate, which we shall call M, may be involved in a series of reactions of varying complexity, which may be written in the generalized form (the subscript i characterizing a particular reaction).

$$a_iA_i + b_iB_i + \ldots + m_iM + n_iN_i + \ldots \underset{k_{-i}}{\overset{k_i}{\rightleftharpoons}} q_iQ_i + r_iR_i + \ldots m_i'M + p_iP_i + \ldots$$

Here the large letters represent chemical substances, $A_i,B_i, \ldots Q_i,R_i, \ldots$ present in large quantities, $N_i, \ldots P_i, \ldots$ being other intermediates, and the small letters representing stoichiometric constants. The subscript i is used since different substances may be involved in the various reactions.[5]

A steady state for M will occur when

$$\Sigma_i(m_i' - m_i)[k_i(A_i^{a_i}B_i^{b_i} \ldots M^{m_i}N^{n_i} \ldots) - k_{-i}(Q_i^{q_i}R_i^{r_i} \ldots M^{m_i'}P_i^{p_i} \ldots)] = 0 \quad (1.1)$$

the italic letters representing concentrations (or activities), and the summation being over all reactions in which M is involved. We now let ΔS_i be the entropy when the reaction proceeds by one unit in a large *isolated* system. The rate of entropy production $dS/dt = \Phi$ will be given by

$$\Phi = \Sigma_i[k_i(A_i^{a_i}B_i^{b_i} \ldots M^{m_i}N_i^{n_i} \ldots) - k_{-i}(Q_i^{q_i}R_i^{r_i} \ldots M^{m_i'}P_i^{p_i} \ldots)]\Delta S_i \quad (1.2)$$

We could have followed Prigogine and others in expressing the rate of entropy production in terms of the affinities and degree of advancement of the various reactions, using the ideas of de Donder, instead of expressing the rate in terms of entropy production in an isolated system, but the latter method seems somewhat simplier for our purposes.

For the entropy production to be a minimum a necessary condition is $\partial\Phi/\partial M = 0$. To evaluate this we must first find out something about the ΔS_i. We note in the first place that we assume that none of the reactions are far displaced from equilibrium. If any given reaction i is in equilibrium $\Delta S_i = 0$. Furthermore, we see that a change of M will change all the ΔS_i in related ways. Thus we may write[5a]

$$\partial\Delta S_i/\partial M = (m_i' - m_i)\Delta S_M \quad (1.3)$$

where ΔS_M is a factor which is common to all the reactions. Also we can express ΔS_i by taking the first term in a Taylor's expansion about the concentration $M_{e,i}$ of M which is necessary to bring the particular reaction into equilibrium. Thus

$$\Delta S_i = (M - M_{e,i})(\partial\Delta S_i/\partial M) = (M - M_{e,i})(m_i' - m_i)\Delta S_M \quad (1.4)$$

Using eq. 1.2 and 1.4, we see that $\partial\Phi/\partial M = 0$ gives

$$\Sigma_i[m_ik_i(A_i^{a_i}B_i^{b_i} \ldots M^{m_i-1}N_i^{n_i} \ldots) - m_i'k_{-i}(Q_i^{q_i}R_i^{r_i} \ldots M^{m_i'-1}P_i^{p_i} \ldots)](M - M_{e,i})(m_i' - m_i)\Delta S_M + \Sigma_i[k_i(A_i^{a_i}B_i^{b_i} \ldots M^{m_i}N_i^{n_i} \ldots) - k_{-i}(Q_i^{q_i}R_i^{r_i} \ldots M^{m_i'}P_i^{p_i} \ldots)](m_i' - m_i)\Delta S_M = 0 \quad (1.5)$$

Now we can write

$$k_iA_i^{a_i}B_i^{b_i} \ldots M_{e,i}^{m_i}N_i^{n_i} \ldots = k_{-i}Q_i^{q_i}R_i^{r_i} \ldots M_{e,i}^{m_i'}P_i^{p_i} \ldots \quad (1.6)$$

by the definition of $M_{e,i}$. Hence the ith bracketed quantity under the second summation of (1.5) can be written

$$k_i(A_i^{a_i}B_i^{b_i} \ldots N_i^{n_i} \ldots)(M^{m_i} - M_{e,i}^{m_i}) - k_{-i}(Q_i^{q_i}R_i^{r_i} \ldots P_i^{p_i} \ldots)(M^{m_i'} - M_{e,i}^{m_i'})$$

which, since M is close to $M_{e,i}$, is equivalent to

$$m_ik_i(A_i^{a_i}B_i^{b_i} \ldots N_i^{n_i} \ldots)M^{m_i-1}(M - M_{e,i}) - m_i'k_i(Q_i^{q_i}R_i^{r_i} \ldots P_i^{p_i} \ldots)M^{m_i'-1}(M - M_{e,i})$$

and hence is equal to the corresponding quantity in the first summation sign.

Thus

$$\partial\Phi/\partial M = 2\Sigma_i[k_i(A_i^{a_i}B_i^{b_i} \ldots M^{m_i}N_i^{n_i} \ldots) - k_{-i}(Q_i^{q_i}R_i^{r_i} \ldots M^{m_i'}P_i^{p_i} \ldots)](m_i' - m_i)\Delta S_M \quad (1.7)$$

Comparing eq. 1.1 and 1.7 we see that the condition of minimum entropy production is the same as the condition for the steady state.

It remains to be verified that the rate of entropy production is a minimum rather than a maximum. From eq. 1.7

$$\partial^2\Phi/\partial M^2 = 2\Sigma_i[k_im_i(A_i^{a_i}B_i^{b_i} \ldots M^{m_i}N^{n_i} \ldots) - k_{-i}m_i'(Q_i^{q_i}R_i^{r_i} \ldots M^{m_i'}P_i^{p_i} \ldots)]M^{-1}(m_i' - m_i)\Delta S_M \quad (1.8)$$

Since we are never far from equilibrium, eq. 1.6 will be nearly fulfulled for the value of M actually existing. Hence we may see that the right-hand side of eq. 1.8 will have a sign opposite to that of ΔS_M. Since eq. 1.3 exhibits ΔS_M as the change with concentration of the entropy increment per unit M introduced by a process into the system, it is clear that ΔS_M will be negative, for the entropy increment per unit M is less the greater M is. Therefore, $\partial^2(dS/dt)/\partial M^2$ is positive, which shows that dS/dt is a minimum.

One can carry out similar differentiations for any one of the short lived intermediates. Indeed, it is also possible to carry them out for the other substances, also. The lowest minimum will be obtained when the derivative of Φ with respect to the concentrations of all possible substances is zero. However, this lowest minimum will naturally occur

(5) It may be noted that by putting the substance M on both sides of the equation, and allowing m_i' and m_i to take on non-integral values, and by allowing the possibility that some of the other substances appear on both sides (*e.g.*, A_i and Q_i might be identical) we allow sufficient generality to deal with any situation that may arise. Because the equilibrium constant must be expressible as a simple quotient in terms of activities, a difference like $m_i' - m_i$ must be an integer. We might, in general, expect the rate constants in either direction to be rather complex functions of all the activities, but a function which would be the same for k_i and k_{-i} and which would thus divide out of the equilibrium constant to leave it a combination of simple powers. For very small shifts from a given state of equilibrium such a function can be sufficiently well approximated by a product of single powers of the various variables, the power in each case being determined to give the correct value of the first partial derivative.

(5a) ΔS_M might be different for different reactions if concentrations are used, since the thermodynamic functions for one substance might be changed by changing the concentration of another, but all difficulties of this sort are avoided by replacing concentrations by activities, (which is, strictly, also necessary in eq. 1.1 and 1.2).

at $\Phi = 0$, when all substances are in mutual equilibrium. It is possible to set up conditions such that the concentrations of some of the species $A_i, B_i, \ldots Q_i, R_i, \ldots$, *i.e.*, the substances present in large concentration, are held fixed by some artificial means, by introducing or removing some of this material. The system will then come to a steady state with respect to all of the unconstrained concentrations, the steady-state equations for any particular species being of the general type (1.1), regardless of whether it is a short-lived intermediate or not, and this will be the situation of minimum entropy production under the constraints applied.

The difference between the short-lived intermediates and the other substances lies in the fact that the former come to their steady state very quickly; that is, the steady state in detail is rapidly attained. The other concentrations then change slowly, and the system eventually drifts toward the steady state in the large, which is, if the system is close to equilibrium, a state of minimum entropy production. Of course, if the system is close to equilibrium, this drift time may be small, but it will in any case be long compared to the time required to establish the steady state in detail.

2. Application to Flow Processes.—The reactions which we have considered can be of a rather general type. We can imagine, for example, that we have constraints on the system, so that some of the substances involved could be at a different pressure from others. Pressure differences and differences in concentration may be maintained by semipermeable membranes and pistons, in a way which requires no gain or loss of entropy. But if temperature gradients are present we are in immediate trouble, because transfer of material cannot occur without transfer of heat, so the temperature difference cannot be maintained in an isolated system. Thus one cannot be certain that equality of the rates of forward and back reactions really implies a state where $\Delta S = 0$, a condition which is quite essential for the deductions we have given. If semipermeable membranes are not allowed, similar situations may occur with concentration gradients.

In situations of this sort, I have proposed[6] that we consider a "transference unit," or "transfer complex." A transference unit, which we will now designate as M_+, is a group of molecules, the outside regions of which blend in with the surroundings, but which contains some portion which is in a special configuration which can go over to another state in which transfer of material and heat has occurred. The latter state is the inverse unit, which we will call M_-. It can go back to M_+, with the same probability that holds for the direct reaction. In a simple case, a transference complex is striving to come to equilibrium with some particular substance A (the substance transferred) at some particular point in space, where the activity of A is, say, A_+. This inverse unit will be trying to come to equilibrium at a slightly displaced position where the activity is A_-. Also, the effective temperatures for the unit and its inverse will be slightly different. We can write a representative reaction scheme for this situation as

$$S + A_+ \underset{k_{-1}}{\overset{k_1}{\rightleftharpoons}} M_+ \overset{\lambda}{\underset{\lambda}{\rightleftharpoons}} M_- \underset{k_{-2}}{\overset{k_2}{\rightleftharpoons}} S + A_-$$

S represents the rest of the substrate which, in the light of the above description, since in a simple case the transference unit transfers only A, will be the same for M_+ and M_-. The rate constant for $M_+ \rightarrow M_-$, which is designated as λ, will, as already noted, be the same as that for $M_- \rightarrow M_+$. Since different temperatures are involved, we will have $k_1 \neq k_{-2}$ and $k_{-1} \neq k_2$, and, in fact, $k_1/k_{-1} \neq k_{-2}/k_2$. Because an energy level of M_+ can go over into a corresponding one of M_- and *vice versa*, for the reaction $M_+ \rightarrow M_-$ we can write $\Delta S_\lambda = 0$ if $M_+ = M_-$. In general

$$\Delta S_\lambda = (M_- - M_+)\Delta S_M \qquad (2.1)$$

where

$$\Delta S_M = \partial \Delta S_\lambda / \partial M_- = -\partial \Delta S_\lambda / \partial M_+ \qquad (2.2)$$

Since M_+ and M_- are, respectively, capable of coming into equilibrium with $S + A_+$ and $S + A_-$ we can write

$$\Delta S_1 = -(M_+ - M_{+,e})\Delta S_M \qquad (2.3)$$

and

$$\Delta S_2 = (M_- - M_{-,e})\Delta S_M \qquad (2.4)$$

The assumption here, of course, is that one can get a true equilibrium even when there are temperature and concentration gradients. As I have previously remarked,[6] this seems inherent in the assumption that such a system has definable thermodynamic functions. It is equivalent to the Kelvin principle, applied to elementary processes.

It is now seen that by the device of introducing the transference units we have reduced the mechanism to one in which all the reactions involved can come to an equilibrium in which the ΔS vanishes. So the same calculations can be made, and the steady state will be a state of minimum entropy production. This will be true for the steady state for M_+ and M_- if S, A_+ and A_- are held fixed. It will also be true for the steady state for A_+ if A_- is held fixed. The first situation, of course, represents the steady state in detail. If, say, A_- is held fixed we will eventually approach the steady state in the large, in which A_+ is determined by A_-. Of course, if k_+ were equal to k_-, then by obvious symmetry $A_+ = A_-$. However, in general, k_+ and k_- are not equal on account of the temperature gradient, and A_+ and A_- come to a steady relationship, with a difference in A_+ and A_- which corresponds roughly to the Soret effect. By considering this somewhat oversimplified example, we see the relationship between the steady state in detail and the steady state in the large in the usual problems of irreversible thermodynamics.

3. Irreversible Thermodynamics.—In irreversible thermodynamics, certain "fluxes" J_i are expressed in terms of "forces" X_i by a linear relationship

$$J_i = \Sigma_j L_{ij} X_j \qquad (3.1)$$

and the entropy production is given by

(6) O. K. Rice, THIS JOURNAL, 61, 622 (1957).

$$\Phi = \Sigma_i J_i X_i = \Sigma_{i,j} L_{ij} X_i X_j \quad (3.2)$$

If certain of the X_i are assigned specific values then the system comes eventually to a steady state in which the *other* J_i are equal to zero if none of the component involved is added to or removed from the system. The J_i corresponding to a fixed X_i cannot be zero, for material of type i must be added at one end of the system and removed at the other in order to keep the X_i constant.

In general the number of indices i or j involved will be very much less than the number of reactions involved in our discussion in Sections 1 and 2. The implication is that most of the reactions are already in a steady state (essentially the steady state in detail is already established) even when the J_i are not in a steady state. When the final steady state is reached, the steady state is established in detail and in the large. This must be a situation of minimum entropy production under whatever restraints are assumed to exist.

The reciprocal relations follow from the minimum entropy production for a steady state, as well as the reverse. Suppose, for example, we fix all the X_i at zero except X_1, which is fixed at a definite non-zero value, and X_2, which is free. Then for the entropy production to be a minimum with respect to variation of X_2

$$2L_{22}X_2 + (L_{12} + L_{21})X_1 = 0 \quad (3.3)$$

But for J_2 to be equal to zero, *i.e.*, for a steady state to exist under these circumstances, we see from (3.1) that

$$L_{21}X_1 + L_{22}X_2 = 0 \quad (3.4)$$

It then follows from eq. 3.3 and 3.4 that

$$L_{12} = L_{21} \quad (3.5)$$

and so for the other pairs. If X_2 were fixed and X_1 free, the same thing could have been proved, but it is not necessary to prove it twice. This is fortunate, for one of the forces can be associated with the temperature gradient. As we have noted in Section 2, the case of a fixed temperature gradient can be satisfactorily handled. On the other hand, while it is possible to leave the temperature free and reach a steady state with other gradients fixed, it may not be possible to describe such a steady state in terms of chemical equations. So such a steady state would have a somewhat different basis. But once we have the reciprocal relations it can also be shown to be a state of minimum entropy production.

From the above discussion, it can be seen that the laws of irreversible thermodynamics follow from the assumptions we have made, through the vehicle of the law of minimum entropy production.

4. Analysis of the Assumptions Made.—As we have remarked, a detailed consideration of the system involves a great many more variables than are ordinarily included in equations like (3.1) and (3.2). We can, however, as in Section 1, imagine the entropy production expressed in terms of all the chemical reactions, plus a term due to that part of the conduction of heat which does not involve reaction or transfer of material. All these processes occur independently of each other, if we use activities in our equations and consider the generalization noted in footnote 5. Thus we have avoided cross terms like $L_{ij}(i \neq j)$ in our formulation of the entropy production. If we assume that the reciprocal relations hold, it will always be possible to diagonalize the matrix of the coefficients, L_{ij}, and so arrive at a formulation of the type we have considered.[7] This point was noted by Bak,[3] who stated that it formed the basis for the use of transference units. He also stated that the reciprocal relations cannot be proved from transference units. Whether one states that the reciprocal relations cannot be proved by the use of transference units is certainly to a large extent a question of semantics. One cannot prove them without making certain assumptions, the most important one being, in the present formulation, that ΔS_1 and ΔS_2 of eq. 2.3 and 2.4 are zero when M_+ and M_- are in "equilibrium" with the substrate. It may be that one would prefer the assumption made by Onsager, namely that the rate of regression of fluctuations is given by the macroscopic equations, but whichever assumption one prefers, it is of interest that they lead to the same results. Of course, either treatment involves the law of microscopic reversibility. This is involved in the present treatment because of the consideration of the direct and reverse reactions in the individual equilibria.

It was further stated by Bak that the chief interest in the use of transference units lies in the fact that one may sometimes imagine what their nature might be. This is certainly a point of some importance, but a more profound interest lies in the possibility of interpreting the macroscopic phenomena in terms of independent elementary processes in a rather direct and pictorial manner. In order to do this, it is not necessary to specify the nature of a transference unit in anything but the broadest outline.

(7) Actually, of course, the steady-state conditions of Sections 1 and 2 are somewhat involved and cannot be formulated in terms of having certain of the J's constant. Indeed this would give nothing of interest in the diagonal representation.

ELECTROMOTIVE FORCE STUDIES IN AQUEOUS SOLUTIONS AT ELEVATED TEMPERATURES. III. THE STANDARD POTENTIAL OF THE SILVER–SILVER BROMIDE ELECTRODE AND THE MEAN IONIC ACTIVITY COEFFICIENT OF HYDROBROMIC ACID[1]

BY MICHAEL B. TOWNS,[2] RICHARD S. GREELEY AND M. H. LIETZKE

Chemistry Division, Oak Ridge National Laboratory, Oak Ridge, Tennessee

Received April 9, 1960

The e.m.f. of the cell Pt–$H_2(p)$ |HBr(m)| AgBr–Ag was measured from 25 to 200° using hydrogen pressures of about 1 atm. and HBr concentrations from 0.005 to 0.5 m. Additional measurements were made on 1.0 m HBr from 25 to 150°. The standard potential of the cell was determined and found to fit the following equation with a standard error of fit of 1.1 mv. $E^0 = 0.08289 - 4.0647 \times 10^{-4}t - 2.3986 \times 10^{-6}t^2$ volts. The mean ionic activity coefficients of HBr were calculated for several concentrations from an extended Debye-Hückel equation, the linear (B) parameter of which was obtained from a least squares treatment of the e.m.f. data.

Introduction

The standard potential of the silver–silver bromide electrode has been determined from 0 to 60° by Harned, Keston and Donelson[3] from measurements of the cell

Pt–$H_2(p)$ |HBr(m)| AgBr–Ag (A)

but no measurements at higher temperatures have been reported. In connection with a general program on the properties of aqueous solutions at elevated temperatures and, in particular, following a study of the chloride cell analogous to (A) at temperatures to 275°,[4,5] it was of interest to extend the measurements of cell (A) to as high a temperature as possible. Therefore cell (A) was investigated over the concentration range 0.005 to 0.5 m HBr, the temperature range 25 to 200°, and at hydrogen pressures of about one atmosphere. Additional measurements were made on 1.0 m HBr to 150°.

Experimental

The Apparatus.—The experimental apparatus has been described previously[4] and was used without modification.

The electrodes.—The hydrogen electrode was a length of platinum wire platinized prior to each run according to the procedure given by Bates.[6] The silver bromide electrodes were of the thermal type made by decomposing a 7:1 mixture by weight of silver oxide and silver bromate on a platinum wire at 650° in a manner similar to the method of Keston.[7] Enough silver bromide was deposited on the wire to provide an excess over the amount estimated to be dissolved by the solution at 200°. In addition, excess silver bromide was added to the cell to ensure saturation. The platinum base wire of each type of electrode was long enough to pass through the bomb head, obviating the necessity of crimping the electrodes to a lead wire. The same pair of silver–silver bromide electrodes was used for the entire set of experiments. They were checked at 25° prior to each run by comparing the cell e.m.f. with that given by Harned, Keston and Donelson[3] for the particular solution in use. Agreement was always within ±0.3 mv.

The Solutions and Materials.—All solutions were made from conductivity water, all apparatus was given final rinsings with the same, and all chemicals were recrystallized or washed in conductivity water as deemed necessary. The hydrobromic acid solutions were made up by weight dilutions from twice-distilled constant boiling hydrobromic acid which had been analyzed gravimetrically and found to agree with literature values.[8] The silver oxide was that made previously for the chloride work.[4] Silver bromate was made according to the procedure given by Keston.[7] Electrolytic hydrogen obtained in commercial cylinders was passed over Ascarite, Drierite, and a platinized catalyst bed before passing through two bubble towers containing solutions identical to that under test and then into the autoclave.

General Procedure.—The procedure for each test was essentially the same as that for the chloride work.[4]

Results and Calculations

E.m.f. measurements were made on 0.005, 0.01, 0.02, 0.05, 0.075, 0.1 and 0.5 m HBr at 25, 60, 90, 125, 150, 175 and 200° and on 1.0 m HBr at the above temperatures to 150°. Duplicate tests were made with each solution and the e.m.f. values taken at the same temperature were reproducible to within about ± 0.3 mv. at 25°, ± 0.5 mv. at 60 and 90° and ± 1 mv. above 90°. Measurements were made only during ascending temperatures except for a final measurement at room temperature. Agreement between initial and final values at 25° averaged 1 mv.

No drift of e.m.f. with time as observed in the chloride work[4] was encountered. Limiting the temperature to 200° (150° for 1.0 m HBr) and limiting the time at each temperature to the minimum necessary to reach thermal equilibrium resulted in negligible errors due to corrosion of the autoclave head or reaction between hydrogen and silver bromide. No silver was detected on the hydrogen electrode after any run.

In the calculations, the solubility of AgBr was neglected and the mean molality and ionic strength was taken to be equal to the HBr molality. It was assumed that the ratio of solubility of AgBr to AgCl at 100 to 200° was roughly the same as at 25 to 100° (*viz.*, about 1:10), which would make a contribution to the ionic strength of less than 1% for all molalities of HBr studied to 200°. No correction was made for the loss of water or of HBr to the vapor space.

The hydrogen pressure was obtained as previously[4] by subtracting the corrected steam pressure from the observed total pressure. Each e.m.f. value was then corrected to 1.00 atm. H_2 by subtracting $(RT/2F)$ ln f_{H_2} where the fugacity f_{H_2} was taken to be equal to the hydrogen pressure.

(1) This paper is based upon work performed for the United States Atomic Energy Commission at the Oak Ridge National Laboratory operated by Union Carbide Corporation.

(2) (a) Oak Ridge Institute of Nuclear Studies summer participant. (b) Department of Chemistry, Tennessee A. and I. College, Nashville, Tennessee.

(3) H. S. Harned, A. S. Keston and J. G. Donelson, *J. Am. Chem. Soc.*, **58**, 989 (1936).

(4) R. S. Greeley, *et al.*, THIS JOURNAL, **64**, 652 (1960).

(5) R. S. Greeley, *et al.*, to be published.

(6) R. G. Bates, "Electrometric pH Determinations," John Wiley and Sons, Inc., New York, N. Y., 1954, p. 167.

(7) A. S. Keston, *J. Am. Chem. Soc.*, **57**, 1571 (1935).

(8) "International Critical Tables," First Ed., Vol. III, McGraw-Hill Book Co., Inc., New York, N. Y., p. 323.

The e.m.f. values, taken at temperatures slightly different from the exact values listed above, were corrected to those nominal values by fitting the values at each molality to a cubic equation in the centigrade temperature by the method of least squares and solving the equations at the temperatures desired. The standard errors of fit of the cubic equations representing the data were all about 1 mv. or less.

The further treatment of the data involved the computation of $E^{0\prime\prime}$ for each e.m.f. value

$$E^{0\prime\prime} = E + \frac{2RT}{\mathfrak{F}} \ln m - \frac{4.606RT}{\mathfrak{F}} \left[\frac{S\sqrt{m}}{1 + A\sqrt{m}} \right] \quad (1)$$

where

E = e.m.f. at 1.00 atm. H_2 and nominal temp.
S = Debye–Hückel limiting slope
A = denominator coefficient = $50.29\ (DT)^{-1/2} \mathring{a} \rho_0^{1/2}$
D = dieletric constant of water[9]
$\mathring{a}$ = ion-size parameter
ρ_0 = density of water[10]
and m, R, $\mathfrak{F}$, and T have their usual meaning

The values of A were calculated using values of $\mathring{a}$ taken from the previous work on HCl at each temperature[4] for the reason discussed below. Then $E^{0\prime\prime}$ was fitted by the method of least squares for 12 cells over the range 0.005 to 0.1 m HBr to

$$E^{0\prime\prime} = E^0 - \frac{4.606RT}{\mathfrak{F}} Bm \quad (2)$$

where E^0 = the standard potential of the silver–silver bromide electrode. Values of E^0, B, their standard errors, and the standard errors of fit of equation 2 to the data are listed in Table I. The values of E^0 were fitted to a quadratic function of the centigrade temperature by the method of least squares to yield

$$E^0 = 0.08289 - 4.0647 \times 10^{-4} t - 2.3986 \times 10^{-6} t^2 \text{ volts} \quad (3)$$

with a standard error of fit of 1.1 mv. Values of E^0 calculated from equation 3 are listed in the final column of Table I.

Table I

Values of E^0, B and the Standard Error of Fit of Equation 2

Temp., °C.	E^0, v.	σ_{E^0}, v.	B, m^{-1}	σ_B, m^{-1}	σ_{fit}, v.	E^0,[a] v.
25	+0.0716	0.00067	+0.112	0.096	0.00079	+0.0712
60	+ .0501	.00084	+ .0323	.160	.0012	+ .0499
90	+ .0251	.0012	− .012	.180	.0012	+ .0269
125	− .0048	.00077	+ .060	.089	.0013	− .0054
150	− .0312	.00048	− .056	.053	.00081	− .0320
175	− .0612	.00067	− .145	.067	.0010	− .0617
200	− .0951	.0011	− .277	.106	.0017	− .0943

[a] $E^0 = 0.08289 - 4.0647 \times 10^{-4} t - 2.3986 \times 10^{-6} t^2$ volts.

The mean ionic activity coefficients of hydrobromic acid from 0.001 to 0.1 m were calculated from the Debye–Hückel extended equation

$$\log \gamma\pm = - \frac{S\sqrt{m}}{1 + A\sqrt{m}} + Bm \quad (4)$$

using the above values of A and B. The activity coefficients for 0.5, and 1.0 m HBr were calculated from

$$\log \gamma\pm = \frac{\mathfrak{F}}{4.606RT} (E - E^0) - \log m \quad (5)$$

where values of E were available. All of these values are listed in Table II.

Finally smooth values of the e.m.f. of cell (A) at round molalities from 0.001 to 0.1 m were calculated for several temperatures from

Table II

Mean Ionic Activity Coefficients of Hydrobromic Acid

m	25°	60°	90°	125°	150°	175°	200°
0.001	0.965	0.963	0.960	0.956	0.953	0.949	0.945
.005	.929	.925	.919	.913	.906	.900	.894
.01	.905	.901	.896	.886	.878	.870	.863
.02	.875	.871	.865	.854	.844	.834	.826
.05	.830	.826	.82	.808	.792	.779	.769
.075	.809	.804	.798	.787	.768	.752	.739
.1	.794	.789	.78	.773	.750	.731	.715
.5	.808	.819	.75	.708	.662	.618	.580
1.0	.873	.852	.774	.717	.653	...	...

$$E_{smooth} = E^0 - \frac{2RT}{\mathfrak{F}} \ln m \gamma\pm \quad (6)$$

These values are given in Table III. Also listed in Table III are the average experimental values of the e.m.f. for the 0.5 and 1.0 m HBr solutions.

Discussion

Values of $E^{0\prime\prime}$ were calculated using six values for the denominator parameter, A, from 0 to 5 for each e.m.f. measurement and these were plotted *vs.* concentration at each temperature. It was observed that good straight lines were obtained for extrapolation to infinite dilution when the A values corresponding to those used in the chloride work[4] were used. E.m.f. values of sufficient precision were not obtained to allow the use of the statistical procedure of minimizing the standard error of fit of equation 2 to determine A, as in the chloride work. The values of E^0 obtained at 25 and 60° agree with those of Harned, Keston and Donelson[2] within 0.3 and 0.5 mv., respectively. The values of E^0 obtained from 25 to 200° fitted a quadratic function of the temperature within experimental error (see equation 3). However a cubic equation was required to fit the experimental e.m.f. values to a function of the temperature.

The decrease with temperature in the value of E^0 for the Ag–AgBr electrode is slightly greater than the decrease of E^0 for the Ag–AgCl electrode. Upon subtracting the E^0 for the former from the E^0 for the latter at each temperature it is found that the E^0 for the metathetical reaction

$$AgCl + HBr = AgBr + HCl \quad (7)$$

decreases from 0.150 volts at 25° to 0.130 volts at 200°.

The mean ionic activity coefficients of HBr decrease with temperature at each molality in a very similar way to $\gamma\pm$ for HCl. However the activity coefficients for HBr are generally slightly higher than for HCl, becoming one to two per cent, higher at 200°. Agreement with the values listed by Harned, Keston and Donelson[3] at 25 and 60° was within one per cent. As with the chloride work, the Debye–Hückel extended equation with a linear, Bm, term was found to be entirely applicable. The extended terms of Gronwell, LaMer and Sandved[11] were neglected, as was the correction from the rational to the practical activity coefficient scale, since these terms were essentially within the experimental error and since the empirically determined parameters included such corrections.

The experimental error in this work was substantially larger than in the chloride work, *viz.*, ±1

(9) G. C. Åkerlof and H. I. Oshry, *J. Am. Chem. Soc.*, **72**, 2844 (1950).

(10) N. A. Lange, Ed., "Handbook of Chemistry," Seventh Ed. Handbook Publishers, Inc., Sandusky, Ohio, 1949.

(11) T. H. Gronwell, V. K. LaMer and K. Sandved, *Physik. Z.*, **29**, 358 (1928).

TABLE III

SMOOTHED VALUES OF THE E.M.F. FOR THE CELL

$Pt-H_2(p)\,|HBr(m)|\,AgBr-Ag$

Temp., °C.	m_{HBr} 0.005	0.01	0.02	0.05	0.075	0.1	0.5	1.0
25	0.3476	0.3133	0.2795	0.2351	0.2156	0.2018	0.1180	0.0784
60	.3588	.3205	.2826	.2331	.2113	.1959	.1012	.0591
90	.3620	.3202	.2791	.2249	.2013	.1847	.0862	.0178
125	.3650	.3195	.2745	.2154	.1894	.1709	.0662	− .0004
150	.3623	.3141	.2664	.2043	.1769	.1577	.0492	− .0020
175	.3561	.3052	.2549	.1894	.1608	.1408	.0293	.....
200	.3462	.2923	.2396	.1707	.1408	.1201	.0057	.....

and ±0.4 mv., respectively. For this reason the change of $\gamma \pm$ with temperature and the relative partial molal heat content and heat capacity were not calculated.

Acknowledgment.—We wish to thank Professor W. T. Smith, Jr., and Dr. R. W. Stoughton for many helpful discussions during the course of the work. We also wish to thank Mrs. Marjorie Lietzke for carrying out the computer calculations, Mrs. Laura Meers for assistance with the hand calculations, and Mr. Raymond Jensen for preparing the HBr solutions.

EFFECTS OF STRUCTURE OF N,N-DISUBSTITUTED AMIDES ON THEIR EXTRACTION OF ACTINIDE AND ZIRCONIUM NITRATES AND OF NITRIC ACID[1]

BY T. H. SIDDALL, III

Savannah River Laboratory, E. I. du Pont de Nemours & Co., Aiken, South Carolina

Received April 18, 1960

The effects of changes in the structure of 21 N,N-disubstituted amides on the extraction of actinide and zirconium nitrates and of nitric acid are given. Successive alkyl substitution on the α-carbon atom greatly decreases the extraction of quadrivalent actinides and of zirconium, but only moderately decreases the extraction of hexavalent actinides and nitric acid. The extraction mechanisms for the extraction of uranyl nitrate and nitric acid are very similar to the mechanisms of extraction by trialkyl phosphates and dialkyl alkylphosphonates. However, the extraction mechanisms for the quadrivalent species by amides appear to be quite different from the mechanisms with the phosphorus compounds. A connection between the stretching frequency of the carbonyl bond in the amides and their power as extractants is substantiated in a general and qualitative way, but an exception is noted.

Introduction

It is to be expected that the disubstituted amides should be strong extractants. The carbonyl stretching frequency of these amides is considerably lower than that for ketones. The lower frequency has been ascribed to resonance[2]

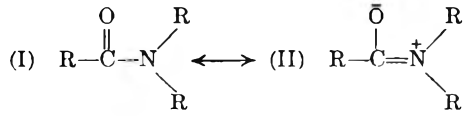

The contribution of II should not only weaken the carbonyl bond, but should also increase the availability of the electrons of the oxygen atom for bond formation. As a consequence amides should be somewhat stronger extractants than ketones, ketones being only moderately strong extractants. Feder[3] confirmed this prediction by showing that N,N-dibutylacetamide is roughly comparable to tributyl phosphate as an extractant for uranyl nitrate. In this work Feder's investigations were extended, with emphasis on the effects of altering the hydrocarbon substituents in the amide molecule on the extraction of the nitrates of quadrivalent and hexavalent actinides, zirconium nitrate and nitric acid.

Experimental

Most of the disubstituted amides were prepared by combining equimolar quantities of the desired acid anhydride and disubstituted amine. The reaction was completed by letting the solution stand overnight, or by warming the solution to 50–60° for a few hours. When the acid anhydride was not available it was prepared by exchange of the carboxylic acid with acetic anhydride at 140–170°. The acid anhydride and residual acetic anhydride were then separated by fractional distillation. The formamides were prepared by dehydration of the amine salts of formic acid at 190–200° for 4–6 hours. As a matter of interest, only very small yields of amide were obtained when the dehydration procedure rather than the anhydride procedure was attempted with pivalic acid. N,N-Dibutylacetamide and N,N-diethyldecanamide were purchased from Distillations Products Industries, Eastman Kodak Co.

In all cases the crude reaction mixtures of the amides were given preliminary purification by washing with aqueous caustic, hydrochloric acid and water. Most of the amides were given final purification by crystallizing the solid adducts formed with uranyl nitrate. After crystallization the uranyl nitrate was removed by washing with water and aqueous sodium carbonate. Solvent and water were removed under vacuum.

Solid adducts were formed with uranyl nitrate more or less readily by all the amides investigated. In order to get

(1) The information contained in this article was developed during the course of work under contract AT(07-2)-1 with the U. S. Atomic Energy Commission.

(2) A. Weissberger, "Technique of Organic Chemistry," Vol. IX, Interscience Publishers, New York, N. Y., 1949, p. 523.

(3) H. M. Feder, Argonne National Laboratory, ANL 4675, pp. 66–69, July 30, 1951 (Classified Report).

TABLE I

EFFECT OF STRUCTURE OF AMIDES ON EXTRACTION COEFFICIENT[a] AT 30°

	3.0 *M* HNO_3 in the aqueous phase						6.0 *M* HNO_3 in the aqueous phase					
Amide[b]	U(VI)	Pu-(IV)	Pu-(VI)	Np(IV)	Np-(VI)	HNO_3	U-(VI)	Pu(IV)	Np-(IV)	Th	Zr	HNO_3
N,N-Dihexylformamide	4.1	2.4				0.119	3.6	4.0		0.10	0.54	0.090
N,N-Dibutylacetamide	9.9	21				.138	6.4	38		.74	.21	.102
N,N-Dibutylpropionamide	4.5	3.5				.112	4.5	7.2		.11	.044	.094
N,N-Dibutylisobutyramide	2.4	0.080	0.23	0.024	1.2	.103	3.3	0.21	0.070	.0040	.0026	.083
N,N-Dibutylpivalamide	0.60	0.0009	.051		0.33	.057	1.4	0.0048		.0001	< .001	.060
N,N-Dibutylbutyramide	5.3	4.0	.63	1.0	3.4	.114	4.7	8.7	2.2	.095	.039	.095
N,N-Di-isobutylbutyramide	5.1	3.5	.48	0.62	3.0	.108	4.8	7.1	1.6	.028	.046	.088
N,N-Di-isobutylisobutyramide	2.0	0.057		0.0070		.100	3.1	0.11	0.037	.0010	.0012	.085
N,N-Dicyclohexylformamide	9.4	9.9				.150	4.8	11		.21	1.1	.100
N,N-Dicyclohexylaeetamide	14	11		2.2		.142	6.3	16		.68	0.026	.091
N,N-Dicyelohexylbutyramide	7.9	1.7				.148	5.1	5.9		.16	.010	.103
N,N-Dibutyl-2-ethylhexanamide	4.0	0.19				.125	4.1	0.29		.0043	.0022	.094
N,N-Dimethyldecanamide	4.9	10				.115	4.4	39		.63	.096	.091
N,N-Diethyldecanamide	5.1	6.9				.120	5.0	16		.34	.049	.096
1-Hexanoylpiperidine	7.2	8.7				.115	5.8	20		.32	.077	.096
1-(2-Ethylhexanoyl)-piperidine	2.8	0.60				.087	4.2	1.5		.025	.011	.080
N,N-Di-*sec*-butylhexanamide	5.5	0.90				.120	4.0	3.9		.092	.0092	.094
N,N-Dibutylcyclohexanecarboxamide	3.1	0.19				.103	4.1	1.0		.0040	.0034	.090
N-Butyl-N-phenylbutyramide	1.4	0.23				.088	2.4	1.3		.0033	.0099	.085
N,N-Dibutylbenzamide	0.86	0.34				.105	1.2	0.69		.0099	.0070	.088
N,N-Dibenzylacetamide	3.3	0.22				.077	4.3	1.0		.014	.021	.077

[a] Extraction coefficient is defined as moles/liter in the organic phase divided by moles/liter in aqueous phase. [b] All 0.50 *M* in toluene.

a desirable dependence of solubility of the adducts on temperature, it was usually necessary to use mixed solvents such as hexane–toluene, hexane–dichloromethane, or hexane-diethyl ketone. In all common solvents the adducts of the cyclohexyl substituted amides were too insoluble for convenient crystallization. Fortunately these amides are solids themselves and were readily crystallized from hexane. Neither N,N-dihexylformamide nor its adduct with uranyl nitrate could be crystallized in a satisfactory manner. This amide was purified by molecular distillation.

Toluene was used as a diluent for the amides. With an aliphatic diluent the amides generally form a three-phase system when contacted with even moderate concentrations of nitric acid. A concentration of 0.5 *M* amide in diluent was most commonly used. This concentration was the compromise arrived at to give extraction coefficients of conveniently measurable magnitude.

U^{233}, Pu^{239}, Np^{237}, Th^{234} and Zr^{95} were used as tracers without the addition of stable or longer-lived isotopes. The techniques used in purifying tracer stocks have been described elsewhere.[4] Pu(IV) was stabilized with 0.01 *M* nitrous acid, Np(IV) with 0.005 *M* ferrous sulfamate, and Pu(VI) and Np(VI) with 0.01 *M* ceric nitrate.

The technique of mixing phases in the extraction experiments, and the methods for measurement of radioactivities and hydrogen ion concentrations are described elsewhere.[4a] In the cases of N,N-dibutylacetamide and propionamide the aqueous phase was always pre-equilibrated with organic phase. The acetamide, in particular, has an appreciable solubility in aqueous systems.

The thermodynamic data in Table II were obtained by the technique described previously.[5]

Results and Discussion

Table I shows the effects of altering the hydrocarbon substituents in amide molecules. Extraction coefficients are reported for U(VI), Pu(IV) and nitric acid with 3.0 *M* nitric acid in the aqueous phase at equilibrium. Extraction coefficients for these as well as for Th and Zr are also given for 6.0 *M* nitric acid. Complete data were not obtained for Np(IV), Np(VI) and Pu(VI), since the behavior of these species parallels that of Pu(IV) or U(VI).

The most outstanding effect is obtained by methyl substitution on the carbon atom (the α-carbon atom) adjacent to the carbonyl group. In going from acetamide with no methyl substitution to pivalamide with complete methyl substitution, the extraction of U(VI) is only decreased moderately. However, the extraction of Pu(IV) and Th is reduced by factors of 10^3 to 10^4, and that of Zr at least by several hundred. Furthermore, the separation between the extraction of U(VI) and the quadrivalent species increases in a regular manner for the series: acetamide < propionamide < isobutyramide < pivalamide.

Substitution of ethyl or even longer chains does not appear to have any enhanced effect over that obtained by methyl substitution. N,N-Dibutylbutyramide is quite similar in its behavior to N,N-dibutylpropionamide. The behavior of N,N-dibutyl-2-ethylhexanamide is also quite similar to that of N,N-dibutylisobutyramide.

It might be expected that elimination of the α-carbon atom would lead to a superextractant for the quadrivalent species, but the data for the formamides show that it does not. The extraction of Zr increases but that of Pu(IV) and Th decreases.

Branching or bulkiness of the amine substituents has the same general effect as branching at the α-carbon atom, but to a much smaller extent and with some exceptions. Of the amides with one alkyl substituent on the α-carbon atom, N,N-dimethyldecanamide is the strongest extractant for the quadrivalent species. N,N-Di-*sec*-butylhexanamide is the poorest extractant in this category for Pu(IV) and Zr, although normal for Th. Both piperidines show equivalent or better extraction for quadrivalent species as compared with the appropriate amides. N,N-Dicyclohexylacetamide and butyramide follow closely the same pattern for the quadrivalent species as that of N,N-di-*sec*-butylhexanamide, but the formamide does not. When attached to the nitrogen, cyclohexyl groups increased the extraction of both U(VI) and HNO_3.

The data in Figs. 1 and 2 show that the mechanisms of extraction of U(VI) and HNO_3 are very similar to the types observed with phosphorus

(4) (a) T. H. Siddall, III, *Ind. Eng. Chem.*, **51**, 41 (1959); (b) T. H. Siddall, III, and E. K. Dukes, *J. Am. Chem. Soc.*, **81**, 790 (1959).

(5) T. H. Siddall, III, *ibid.*, **81**, 4176 (1959).

compounds. The slopes for U(VI) are equal to two, except at the highest concentrations. As with the phosphorus compounds the slope decreases at high concentrations of extractant in a manner that suggests interaction between extractant molecules. The slopes for HNO_3 are equal to or very nearly equal to unity over the entire range of extractant concentration. Evidently U(VI) requires two extractant molecules in its coördination sphere. With 3.0 *M* HNO_3 in the aqueous phase the major extraction mechanism involves one molecule of amide for each acid molecule. However, it can be seen from the data in Table I that at higher acidity, as with the phosphorus compounds more than one mole of HNO_3 is extracted for each mole of extractant.

By analogy with the behavior of trialkyl phosphates[6] it might have been expected that bulkiness in the amides would decrease the extraction of Th, but not of Np(IV), Pu(IV) and of Zr. Thorium nitrate is associated with three molecules of trialkyl phosphate in its major extraction mechanism. As a consequence the extraction of Th is quite easily hindered sterically. On the other hand the other quadrivalent species combine with only two molecules of trialkyl phosphate and their extraction is not noticeably more subject to steric effects than that of the hexavalent actinides.

The data in Figs. 1 and 2 show that Np(IV) has a behavior similar to that of Th with the amides. This contrasts with the fact that the behavior of Np(IV) is similar to that of U(VI) with the phosphorus compounds. The slopes of the curves for Np(IV) and Th indicate that a small cluster of more than two amide molecules are involved in the extraction of each metal atom. The slopes approach two only at low concentrations of the amides.

Because of the difficulty in obtaining Pu that approaches 100% Pu(IV), reproducible results could not be obtained at high amide concentration and no data are shown for Pu(IV). It appears, however, that the extraction of Pu(IV) follows the same pattern as that of Np(IV) and Th.

The effect of extractant bulk is easily explained by the fact that Np(IV), Pu(IV) and Th require more than two amide molecules for extraction, which is contrary to the case with U(VI). It is more difficult to crowd a cluster of bulky extractant molecules in addition to four nitrate ions around the central ion. On the other hand, since each U(VI) ion is bound to only two amide molecules, there is not too much crowding.

The extraction of zirconium probably involves two amide molecules per zirconium molecule. The slopes (1.6 with the acetamide and 1.8 with the butyramide) are closer to two than any other whole number. On this basis it might be erroneously assumed that zirconium has grossly the same extraction mechanism with amides as it does with phosphorus compounds.

However, the data in Fig. 3 show that the mechanism of Zr extraction with amides, whatever it may be, involves something different than that with phosphorus compounds. With the butyramide the extraction of Zr passes through a maximum at about 6 *M* HNO_3 in the aqueous phase. With tributyl phosphate as an example, the extraction of Zr is a monotone, increasing to very large values at high acidity.

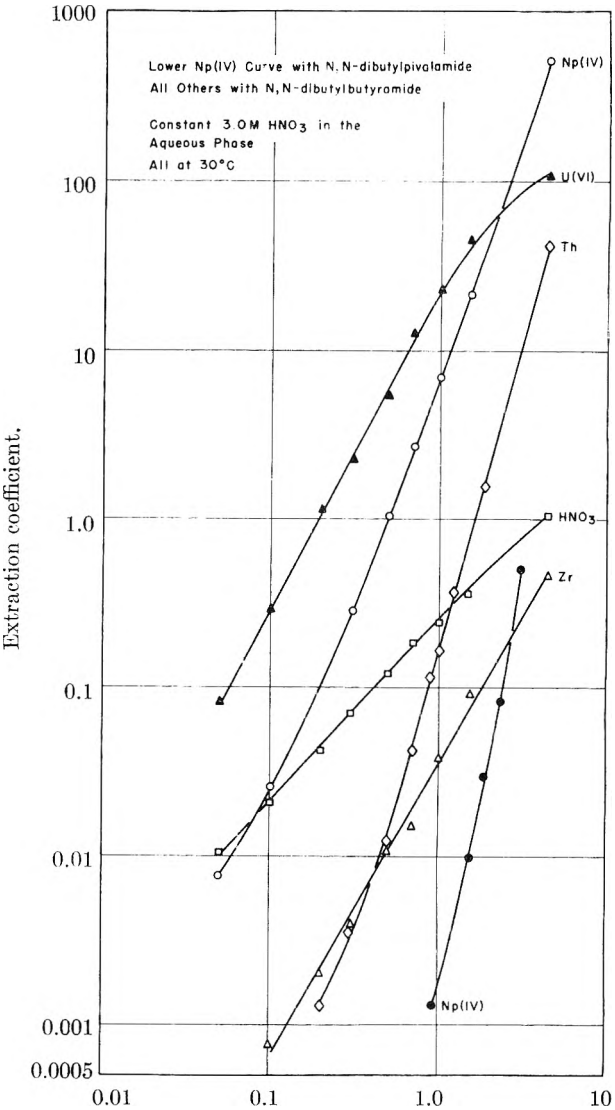

Fig. 1.—Extraction mechanisms.

Although substitution on the α-carbon has a relatively small effect on the extraction of U(VI) as compared to that of the quadrivalent species, the data in Table II show that the effect with U(VI) is still quite significant. A difference of more than two kilocalories is found between ΔF of extraction of uranyl nitrate by N,N-dibutylbutyramide and by N,N-dibutylpivalamide. The lesser extraction of HNO_3 by the pivalamide makes the difference smaller in the extraction coefficients of the two compounds for U(VI) than might otherwise be the case. Especially at higher acidities there is much less competition by nitric acid for extractant molecules with the pivalamide. Intrinsically the effects of structural change are greater than would be realized from a superficial glance at extraction coefficients. This argument applies with even greater force to the extraction of

(6) T. H. Siddall, III, *J. Inorg. Nuclear Chem.*, **13**, 151-155 (1960).

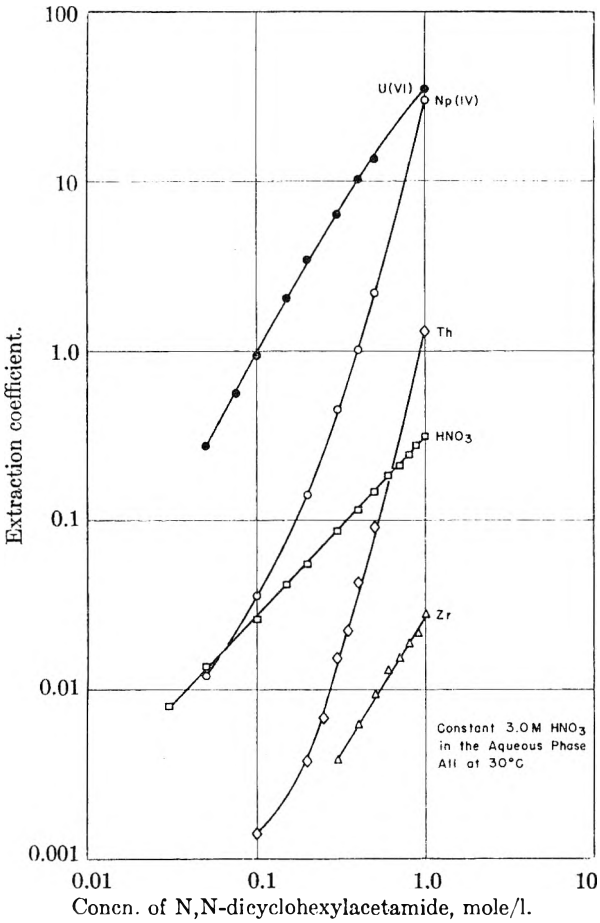

Fig. 2.—Extraction mechanisms with N,N-dicyclohexylacetamide.

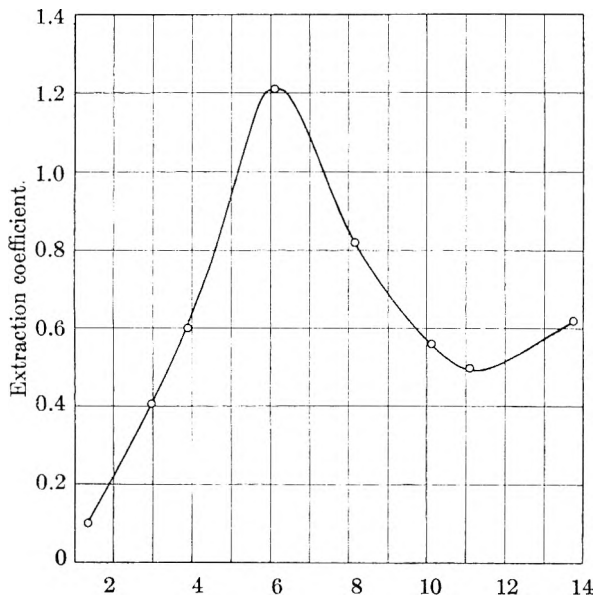

Fig. 3.—Extraction of zirconium by 100% N,N-dibutylbutyramide at 30°.

actinides(IV), which depends on higher powers of the concentration of extractant.

There is no obvious reason why substitution on the α-carbon atom should particularly affect the extraction of uranium. Molecular models, even of the pivalamide, do not indicate that there should be crowding when only two extractant molecules are coördinated. Certainly no such effect is observed with phosphorus compounds. The author has recently synthesized and tested di-2-butyl 2-butylphosphonate and 2-butyl di-2-butylphosphinate in addition to earlier work.[6] The branched phosphonate and phosphinate show perfectly normal or even superior uranium extraction, yet these molecules should occupy a much larger solid angle than even the pivalamide.

TABLE II

THERMODYNAMIC QUANTITIES[a] FOR EXTRACTION BY AMIDES

Amide	For the extraction of $UO_2(NO_3)_2$ ΔH_{25}	ΔS_{25}	ΔF_{25}	For the extraction of HNO_3 ΔF_{25}
N,N-Dibutylbutyramide	−6500	−18.4	− 998	+1180
N,N-Dibutylisobutyramide	−7000	−22.7	− 215	+1400
N,N-Dibutylcyclohexanecarboxamide	−7500	−23.6	− 482	+1300
N N-Dibutylpivalamide	−6000	−24.2	+1147	+2050
N,N-Dibutylbenzamide	−5200	−19.1	+ 531	+1510
N-Butyl-N-phenylbutyramide	−4400	−18.0	+ 924	+1900

[a] Calculated on the basis: Amide + $HNO_3 \leftrightarrows HNO_3 \cdot$ Amide. 2 Amide + $UO_2(NO_3)_2 \leftrightarrows UO_2(NO_3)_2 \cdot 2$ Amide.

The data in Table II show that, contrary to expectation, N,N-dibutylbenzamide is a poorer extractant than most of the completely alkyl substituted amides. Conjugation with the benzene ring ought to increase the availability of electrons for bond formation. In fact, conjugation has been employed to explain the low carbonyl stretching frequency of benzamides as compared to that of other amides.[7] The failure of these considerations to predict extractant strength in this case suggests that the line of reasoning given in the introduction must be used with caution when applied in detail.

On the other hand, N-butyl-N-phenylbutyramide is a poor extractant, as is expected. Conjugation of the phenyl ring with the nitrogen atom should decrease the single bond character of the carbonyl group and the ability of the amide molecule to donate electrons. This conjugation has been used to explain the higher carbonyl frequency of amides with a phenyl group on the nitrogen atom.[7]

The data given in Table II tend to eliminate steric considerations as an explanation for the failure of the benzamide to be a superior extractant. As compared to N,N-dibutylbutyramide the relative weakness of the benzamide as an extractant for U(VI) is entirely due to the smaller value of ΔH. The straightforward interpretation is that the benzamide is simply a poorer electron donor. The only point to the contary is the fact that, relatively speaking, the benzamide is a better extractant for nitric acid than might have been expected from its extraction of U(VI).

(7) A. Weissburger, ref. 2, p. 525.

ACTIVITY COEFFICIENTS OF SILICOTUNGSTIC ACID; ULTRACENTRIFUGATION AND LIGHT SCATTERING[1]

BY JAMES S. JOHNSON, KURT A. KRAUS AND GEORGE SCATCHARD[2]

Contribution from the Oak Ridge National Laboratory, Chemistry Division, Oak Ridge, Tenn.

Received May 20, 1960

Activity coefficients of silicotungstic acid (0.0004–0.04 *M*) in aqueous solution were measured by equilibrium ultracentrifugation. The results agree with the Debye–Hückel theory for a 1–4 electrolyte, with a distance of closest approach parameter of 7.6 Å. A few ultracentrifugations of sodium silicotungstate indicate that the activity coefficients of this solute are similar. Turbidities of silicotungstic acid solutions are reported; they agree with the values predicted from ultracentrifugation results. Turbidities expected for two-component electrolyte–water systems at low concentration are discussed. Densities and refractive indices of silicotungstic acid solutions are presented.

The class of compounds designated as heteropoly acids has attracted increasing interest in the past few years as a bridge between the solution chemistry of simple salts and that of large molecules. Silicotungstic acid ($H_4SiW_{12}O_{40}$) has received special attention, since diffusion measurements[3] and equilibrium ultracentrifugations[4] in supporting electrolytes have indicated that it is essentially monodisperse; molecular weight determinations by velocity ultracentrifugation,[3] by light scattering in supporting electrolytes,[4,5] and by equilibrium ultracentrifugation in supporting electrolytes,[4] have indicated that the formula of the anion in solution (except, of course, for water of hydration) is written correctly as $SiW_{12}O_{40}^{-4}$. The charge given for the ion (−4) indicates that four protons are ionized. This was established by acidity measurements here[6] and elsewhere.[4,5] Further, X-ray scattering studies of concentrated solutions,[7] carred out in this Laboratory, have shown that the structure of the species in solution is the same as that in the crystal. The relative wealth of information concerning silicotungstic acid makes it an interesting "known" with which to test techniques developed for large aggregates.

In this paper, a correlation of light scattering results with ultracentrifugation is presented. Activity coefficients of silicotungstic acid in aqueous solution (two-component system) were computed from the equilibrium ultracentrifugations. Since few determinations of activity coefficients of 1–4 electrolytes have been reported,[8] these results perhaps have interest over and above possible value in the use of silicotungstic acid as a model for high molecular weight solutes.

Theoretical

The similarity between the information obtained by light scattering and by equilibrium ultracentrifugations has been noted.[9] The pertinent equations for ionized solutes will be discussed here.

1. Equilibrium Ultracentrifugation.—When equilibrium distribution in a gravitational field is attained, all components have constant partial molal free energy at all radii, free energy here being considered a function of position, as well as of concentration and pressure. Measurement of the concentration distribution in a two-component system allows computation of activity coefficient ratios by the equation

$$\left(\frac{\partial \ln a}{\partial \ln m}\right)_{P,x} \mathrm{d} \ln m = [M(1 - \bar{v}\rho)\,\omega^2/2RT]\,\mathrm{d}(x^2) \quad (1)$$

in its integrated form[10]

$$\frac{1}{\nu} \ln \frac{a_\beta}{a_\alpha} = \ln \frac{m_\beta}{m_\alpha} + \ln \frac{\gamma_{\pm\beta}}{\gamma_{\pm\alpha}} = \frac{M\omega^2}{2\nu RT}(x_\beta^2 - x_\alpha^2) - \frac{M}{\nu RT}\int_{P_\alpha}^{P_\beta} \bar{v}_\beta \,\mathrm{d}P \quad (1a)$$

where

$$\mathrm{d}P = \rho\omega^2 x \,\mathrm{d}x \quad (2)$$

In these equations, $a = a_\pm^\nu$ is the activity of the solute; m is its concentration in moles/1000 g. H_2O; $\gamma_\pm$ is the mean (molal) ionic activity coefficient; M is molecular weight of the solute; ν is number of moles of ions per mole solute; R, gas constant; T, absolute temperature; x, radius; ω, angular velocity (2π times revolutions/sec.); P is pressure; ρ, solution density; subscripts α and β indicate quantities at radii x_α and x_β; and $\bar{v}_\beta$ is the partial specific volume of the solute at m_β.[10] For an exact solution, the partial volume should be known as a function of pressure. If this information is available or if values measured at one atmosphere pressure are an acceptable approximation, activity coefficient ratios may be computed from the equilibrium concentration distribution. If x_α is the radius of the meniscus, the activity coefficient ratios will be for "bench-top" conditions.

As infinite dilution is approached, the activity

(1) This document is based on work performed for the U. S. Atomic Energy Commission at the Oak Ridge National Laboratory, Oak Ridge, Tennessee, operated by the Union Carbide Corporation. A preliminary report on this work was presented at the 138th American Chemical Society Meeting, New York, September, 1960.

(2) Department of Chemistry, Massachusetts Institute of Technology, Cambridge, Massachusetts. Consultant, Chemistry Division, Oak Ridge National Laboratory.

(3) M. C. Baker, P. A. Lyons and S. J. Singer, *J. Am. Chem. Soc.*, **77**, 2011 (1955).

(4) J. S. Johnson and K. A. Kraus, Chemistry Division Annual Reports, ORNL-2386, 1957, p. 99; ORNL-2584, 1958, p. 56.

(5) M. J. Kronman and S. N. Timasheff, THIS JOURNAL, **63**, 629 (1959).

(6) T. A. Carlson, unpublished results.

(7) H. A. Levy, P. A. Agron and M. D. Danford, *J. Chem. Phys.*, **30**, 1486 (1959).

(8) H. S. Harned and B. B. Owen, "The Physical Chemistry of Electrolytic Solutions," 3rd Edition, Reinhold Publ. Corp., New York, N. Y., 1958, Appendix A; R. A. Robinson and R. H. Stokes, "Electrolyte Solutions," Butterworths, London (1955); R. A. Robinson *J. Am. Chem. Soc.* **77**, 6200 (1955); C. H. Brubaker, *ibid.*, **78**, 5762 (1956); **79**, 4274 (1957); K. O. Groves, J. L. Dye and C. H. Brubaker, *ibid.*, **82**, 4445 (1956).

(9) See *e.g.*, R. J. Goldberg, THIS JOURNAL, **57**, 194 (1953).

(10) T. F. Young, K. A. Kraus and J. S. Johnson, *J. Chem. Phys.*, **22**, 878 (1954).

coefficient term disappears and measurement of the concentration distribution gives M/ν, the number average molecular weight of the ions.

2. Light Scattering.—For a two-component system, showing no dissymmetry in scattering, the turbidity $\Delta\tau$ (in excess of solvent scattering) may be written[11]

$$\Delta\tau = \frac{H'V(\partial n/\partial m)^2 m}{(\partial \ln a/\partial \ln m)} \quad (3)$$

where

$$H' = (32\pi^3 n^2/3N\lambda^4)$$

In equation 3, n is refractive index; V, volume of solution containing 1000 grams of solvent; N, Avogadro's number; and λ is the wave length of light. In these partial derivatives, pressure and temperature are constant; with this restriction, partial derivatives with respect to molality are, in a two-component system, equivalent to total derivatives.

For an electrolyte, it is customary to write the activity as an ion product, and hence

$$(\partial \ln a/\partial \ln m) = (\partial \ln m_{\pm}^{\nu}\gamma_{\pm}^{\nu}/\partial \ln m) = \nu[1 + (\partial \ln \gamma_{\pm}/\partial \ln m)] \quad (4)$$

If the correct value of ν is selected, the activity coefficient term will approach zero as the concentration is lowered. From Equations 3 and 4 we obtain

$$\Delta\tau = \frac{H'V(\partial n/\partial m)^2 m}{\nu[1 + (\partial \ln \gamma_{\pm}/\partial \ln m)]} \quad (5)$$

or

$$\frac{Hw}{\Delta\tau} = \frac{\nu}{M}[1 + (\partial \ln \gamma_{\pm}/\partial \ln w)] \quad (6)$$

where $H = H'V(\partial n/\partial w)^2/1000$, and $w = Mm/1000$ is the weight of solute per gram of solvent.

Equation 5 may also be written

$$\left(\frac{\partial \ln \gamma_{\pm}}{\partial \ln m}\right) = \frac{\mathrm{d} \ln \gamma_{\pm}}{\mathrm{d} \ln m} = \frac{H'V(\partial n/\partial m)^2 m}{\nu \Delta\tau} - 1 \quad (7)$$

Thus, one obtains from light scattering of a solute of known molecular weight (with supplementary measurements of refractive index increments) the slopes, d ln $\gamma_{\pm}$/d ln m, which can, after appropriate integration, be used to obtain activity coefficients, just as with the ultracentrifuge.

A direct experimental comparison between light scattering and ultracentrifugation results may be made if $(\partial n/\partial m)$ is independent of pressure and if the terms $(\partial \ln a/\partial \ln m)$ of Equations 1 and 3 are equal (*i.e.*, if $\bar{v}$ does not vary under the conditions of the experiment). One then obtains from these equations

$$\Delta\tau = \frac{H'V(\partial n/\partial m)}{2Ax}\frac{\mathrm{d}n}{\mathrm{d}x} = \frac{H'V(\partial n/\partial w)RT\mathrm{d}n}{1000(1 - \bar{v}\rho)\omega^2 \mathrm{d}x} \quad (8)$$

where $A = M(1 - \bar{v}\rho)\omega^2/2RT$. The comparison is particularly straightforward when the ultracentrifugation is carried out with schlieren optics, in which case the experimentally obtained quantity is directly proportional to $\mathrm{d}n/\mathrm{d}x$. If different wave lengths of light are used in the two methods, comparison may nevertheless be made by multiplying the right side of Equation 8 by the appropriate ratio of refractive index increments.

(11) W. H. Stockmayer, *J. Chem. Phys.*, **18**, 58 (1950).

As the concentration is lowered, the term $(\partial \ln \gamma_{\pm}/\partial \ln m) = (\partial \ln \gamma_{\pm}/\partial \ln w)$ in Equation 6 becomes smaller, and a number average weight of the ions, M/ν, is approached,[12] *i.e.*, the same result which is found by ultracentrifugation without supporting electrolyte.

The equations given here for the light scattering of electrolytes are valid only as long as electroneutrality "is seriously violated only for regions with dimensions small compared to the wavelength of light."[11] In solutions so dilute that electroneutrality is violated for dimensions large relative to the wave length of the light, one expects the term ν in the equations to be replaced by unity if scattering by the small ions is negligible. The matter has been treated quantitatively by Hermans[13] on the basis of interference scattering theory. In his equations, the distances in question enter in terms of the ratio $(\kappa^2/\sigma^2) = (m/q)$, in which κ is the Debye–Hückel reciprocal length and $\sigma = (4\pi/\lambda)\sin(\theta/2)$, θ being the angle between incident and deflected light. From his equations 10 and 11, we obtain for ν', the apparent number of moles of ions/mole of solute, with neglect of scattering contributions by small ions

$$\nu' = \frac{1 + (m/q)}{1 + (m/\nu q)} \quad (9)$$

For a 1–4 electrolyte and wave length 436 mμ, $\nu = 5$ and $q \approx 4 \times 10^{-6}$. Although the equation is somewhat approximate, it should allow a good estimate of the lower concentration limit for the light scattering equations presented here.

Experimental

Ultracentrifugations were carried out at 25.0 ± 0.1° with a Spinco Model E Ultracentrifuge, equipped with the temperature control standard with the machine. In the low concentration range, interference optics and a five cell Analytical G rotor (cells 12 mm. thick in light path) were used; higher concentrations were followed by schlieren optics with a two cell (30 mm. in light path) Analytical E rotor. Light of 546 mμ, isolated with a Baird interference filter, was employed. Details of experimental procedure have been given previously.[14,15]

A Brice–Phoenix photometer was used in light scattering measurements, with dissymmetry cells standard with this instrument. Calibration was effected by use of the opal glass diffuser provided with the instrument. The constants for the diffuser given by the manufacturer had been earlier checked with Cornell Standard polymer in toluene.[16] Solutions were clarified by filtration through ultrafine sintered glass. Freedom from dust was checked by visual inspection of a Tyndall beam and by dissymmetry in scattering. Two measurements of the scattering of each solution were made, with a second filtration intervening, and the average of these is reported.

Densities were measured with a 25-cc. pycnometer, and refractive indices with a Brice–Phoenix differential refractometer. Chemicals were reagent or C.P. grade. Distilled

(12) Confusion on this point seems to have crept into the literature, perhaps in part because Doty and Edsall (P. Doty and J. T. Edsall, *Advances in Protein Chemistry*, Volume VI, 35 (1951)) tacitly limit the discussion of two component systems (p. 61) to un-ionized solutes, for which ν is equal to unity.

(13) J. J. Hermans, *Rec. trav. chim.*, **68**, 859 (1949). In this discussion, possible supporting electrolyte effects arising from impurities or ionization of solvent are neglected.

(14) J. S. Johnson, K. A. Kraus and T. F. Young, *J. Am. Chem. Soc.*, **76**, 1436 (1954); J. S. Johnson, G. Scatchard and K. A. Kraus, *J. Phys. Chem.* **63**, 787 (1959).

(15) Performed by Dr. E. W. Anacker Montana State College, Oak Ridge National Laboratory Summer Participant, 1957.

water deionized by passage through a mixed bed ion exchanger was used in preparation of solutions.

Concentrations of all but two of the solutions used in centrifugation were determined by gravimetric analysis or computed from weight dilution of an analyzed stock (uncertainty of composition, about ±0.3%). In the two exceptions, poor checks between separate analyses were obtained, and an average concentration based on density, refractive index, and analyses was used. (Volumes and refractive indices of these two solutions are not reported in Table I, because of uncertainties in the composition, about 1%). Analysis of silicotungstic acid (the solid contains a variable quantity of water) was usually by precipitation with cinchonine,[16] followed by ignition, expulsion of silica with HF, and weighing as WO_3. In some cases, a simple evaporation of solvent was substituted for precipitation by cinchonine; in some, SiO_2 was not expelled, and the analysis was based on the weight of oxide as $SiO_2 \cdot 12WO_3$. Neither of these modifications of the procedure affected the results significantly. Concentrations of solutions employed in light scattering were computed from their densities.

Computations of the ultracentrifuge results were performed with the ORACLE, the ORNL digital computer. Corrections were made for the effect of differences in pressure on the refractive indices of solution and solvent.[14] These corrections amounted to about 0.3% in ratios of activity coefficients. Possible changes of the apparent molal volumes of the solutes with pressure were neglected. The maximum pressure in the centrifugations was 60 atmospheres.

TABLE I

VOLUMES AND REFRACTIVE INDEX INCREMENTS

Moles/l.	Apparent specific volume	$(\Delta n/c)_{436}$	$(\Delta n/c)_{546}$
	$H_4SiW_{12}O_{40}$		
0.03216	0.1448	0.305	0.287
.02511	.1455	.304	.289
.02002	.1447	.307	.289
.01604	.1444	.306	.286
.01255	.1445	.308	.289
.00774	.142	.305	.289
.00500	.142	.307	.287
.00386	.140	.307	.287
.00251	.147	.306	.288
.00249	.143	.314	.289
Weighted av.	.1444	.306	.288
	$Na_{3.8}H_{0.2}SiW_{12}O_{40}$		
0.01000	0.135	0.312	0.294
.005997	.138	.313	.294
.00200	.144	.314	.298
Weighted av.	.137	.313	.294

Results

1. Molal Volumes and Refractive Index Increments.—Results of measurements of apparent specific volumes and refractive index increments are summarized in Table I. Measurements on solutions at concentrations lower than 0.002 M are not included; their precision is low. Since no significant change was found in apparent specific volumes of silicotungstic acid over more than a ten fold range of concentration, an average value weighted according to concentration was used for the partial volume in computations with Equations 1 and 8. This was 0.144 cc./g. (or 414 cc./mole) and compares well with 0.141 cc./g. earlier reported for $H_4SiW_{12}O_{40}$ in acetate buffer.[3]

(16) W. F. Hillebrand, G. E. F. Lundell, H. A. Bright and J. I. Hoffman, "Applied Inorganic Analysis," John Wiley and Sons, Inc., New York, N. Y., 2nd Ed., 1953, p. 689.

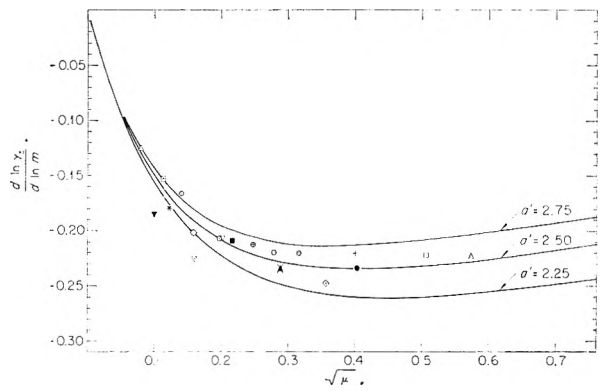

Fig. 1.—Experimental slopes from ultracentrifugation. Solid curves computed from Debye–Hückel theory (equation 10) with indicated values of a'. ⊕⊖, sodium silicotungstate; other symbols, silicotungstic acid. Symbols refer to same centrifugations as in Fig. 2 and 3.

Some measurements also are reported for the sodium salt of silicotungstic acid, obtained by neutralization of the acid. To avoid difficulties from possible decomposition of the silicotungstate ion at low acidities,[17] neutralization was carried only to the composition $Na_{3.8}H_{0.2}W_{12}O_{40}$. The average values 0.137 cc./g. obtained for the apparent specific volume and 406 cc./mole for the apparent molal volume are considered less certain than the corresponding values for the acid since fewer experiments were carried out and since solution composition was not known with as high a degree of accuracy. As with the acid, the apparent volumes for the sodium salt were sufficiently independent of concentration to permit their use as partial volumes.

Solution densities are needed in Equation 1 and for conversion between moles/l. (c scale) and moles/1000 g. H_2O (m scale). Densities at the concentrations in question here could be represented within ±0.00005 (average deviation, 0.00003) by the relationship

$$\rho = \rho_s + kc$$

where ρ_s is the density of solvent; c, concentration in moles/l.; and $k = 2.463$ for $H_4SiW_{12}O_{40}$ and 2.559 for $Na_{3.8}H_{0.2}SiW_{12}O_{40}$.

The refractive index increments (on a c scale) also show no significant change with concentration. Average values of $\Delta n/c = 0.288$ at 546 mμ and 0.306 at 436 mμ were obtained for the acid by weighting the individual values according to concentration; for the sodium salt, the corresponding values are 0.294 and 0.313, respectively. These values may be compared with the increment 0.3065 ± 0.0040 (436 mμ) reported by Kronman and Timasheff,[5] presumably for the acid. Increments were converted to the appropriate quantities on the m scale through the density data.

2. Activity Coefficients by Ultracentrifugation.—We have carried out seventeen centrifugations of silicotungstic acid involving fifteen solutions of concentrations from 0.0006 to 0.032 mole/liter, at speeds from 16,200 to 24,630 r.p.m. Activity coefficients were computed with Equation 1a ($\nu = 5$). Average values for the slopes, d ln $\gamma_\pm$/d

(17) L. Malaprade, *Ann. chim.* (*Paris*), [10] **11**, 159 (1929).

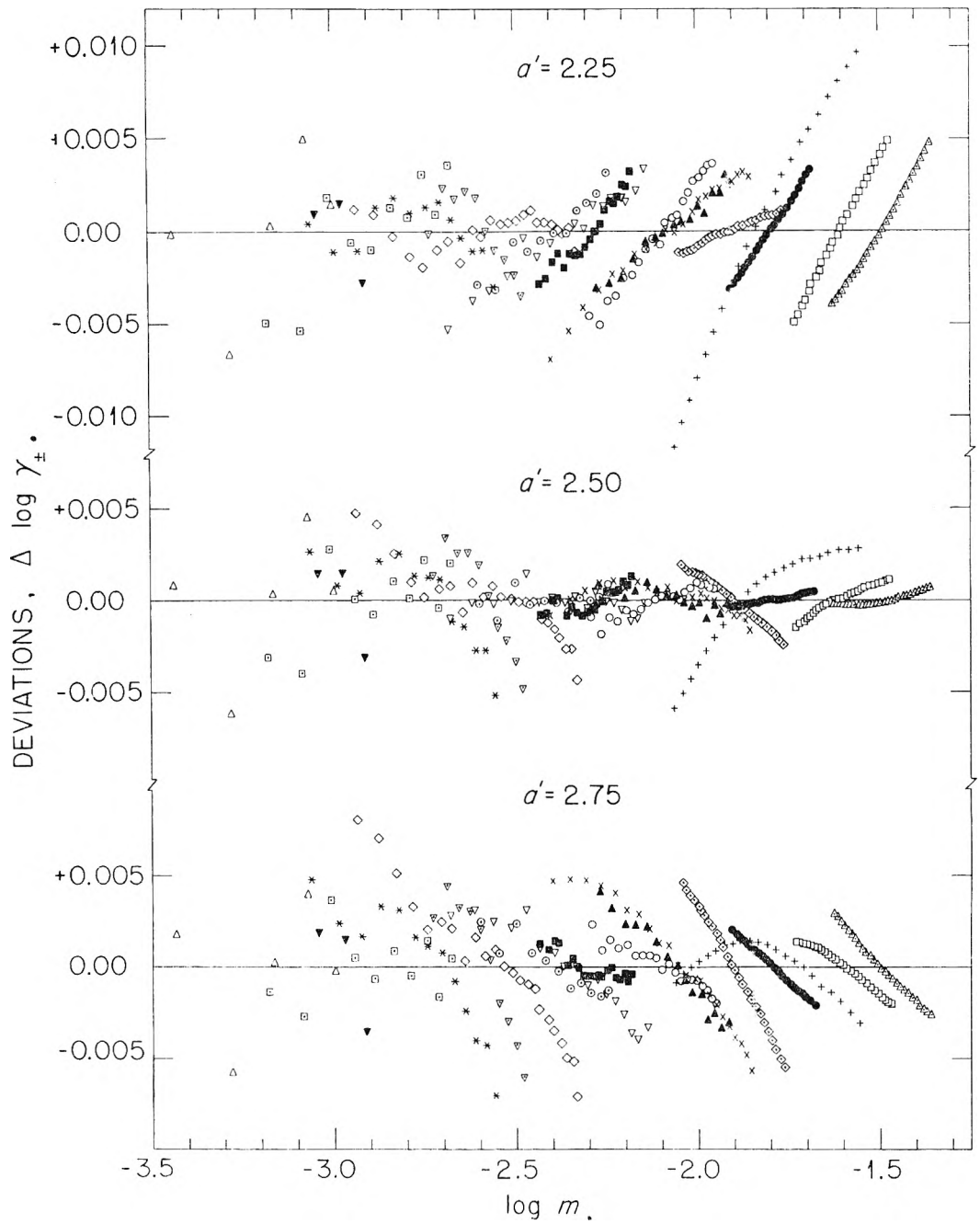

Fig. 2.—Deviations of experimental activity coefficients of silicotungstic acid from values computed with Debye–Hückel theory (equation 11). Approximate speeds of rotation (r.p.m.): 24,630, △, ⊡, ◇, *, +, ▽ (every 2nd fringe), × (every 3rd fringe); 19,160, ○ (every 2nd fringe), ○ (every 2nd fringe), ▲ (every 3rd fringe, same solution as ×); 16,200, ▼, ▽, □, ◈, ■, ◬, ● (same solution as +), □, ◈, ◬, +, ● Schlieren; all others, interference.

ln m, were estimated for the individual experiments and are presented in Fig. 1. Curves for the derivative

$$\frac{\mathrm{d} \ln \gamma_{\pm}}{\mathrm{d} \ln m} = \frac{-(4)(2.303)(0.5097)\sqrt{\mu}}{2(1 + a'\sqrt{\mu})^2} \qquad (10)$$

of the slightly modified Debye–Hückel equation

$$-\log \gamma_{\pm} = \frac{4(0.5097)\sqrt{\mu}}{1 + a'\sqrt{\mu}} \qquad (11)$$

for $a' = 2.25$, 2.50 and 2.75 are also exhibited in this figure, where μ is the ionic strength, $\Sigma m_i z_i^2/2$ (here $\mu = 10\ m$); and a' is a parameter proportional to the distance of closest approach $\mathring{a}$.

The curve for $a' = 2.50$ ($\mathring{a} = 7.6$ Å.) fits the measurements with reasonable precision. It should be emphasized that neither the determination of the experimental slopes, d ln $\gamma_{\pm}$/d ln m, from the individual ultracentrifugations nor the use of Equation 10 for computation of this quantity depend in any way on extrapolation to zero concentration.

Figure 2 shows the detailed deviations of experimental activity coefficient ratios

$$\Delta \log \gamma_{\pm} = \log (\gamma_{\pm}/\gamma_{\pm\,\mathrm{Men}})_{\mathrm{exp.}} - \log (\gamma_{\pm}/\gamma_{\pm\,\mathrm{Men}})_{\mathrm{comp.}} + \epsilon$$

from values computed with the Debye–Hückel

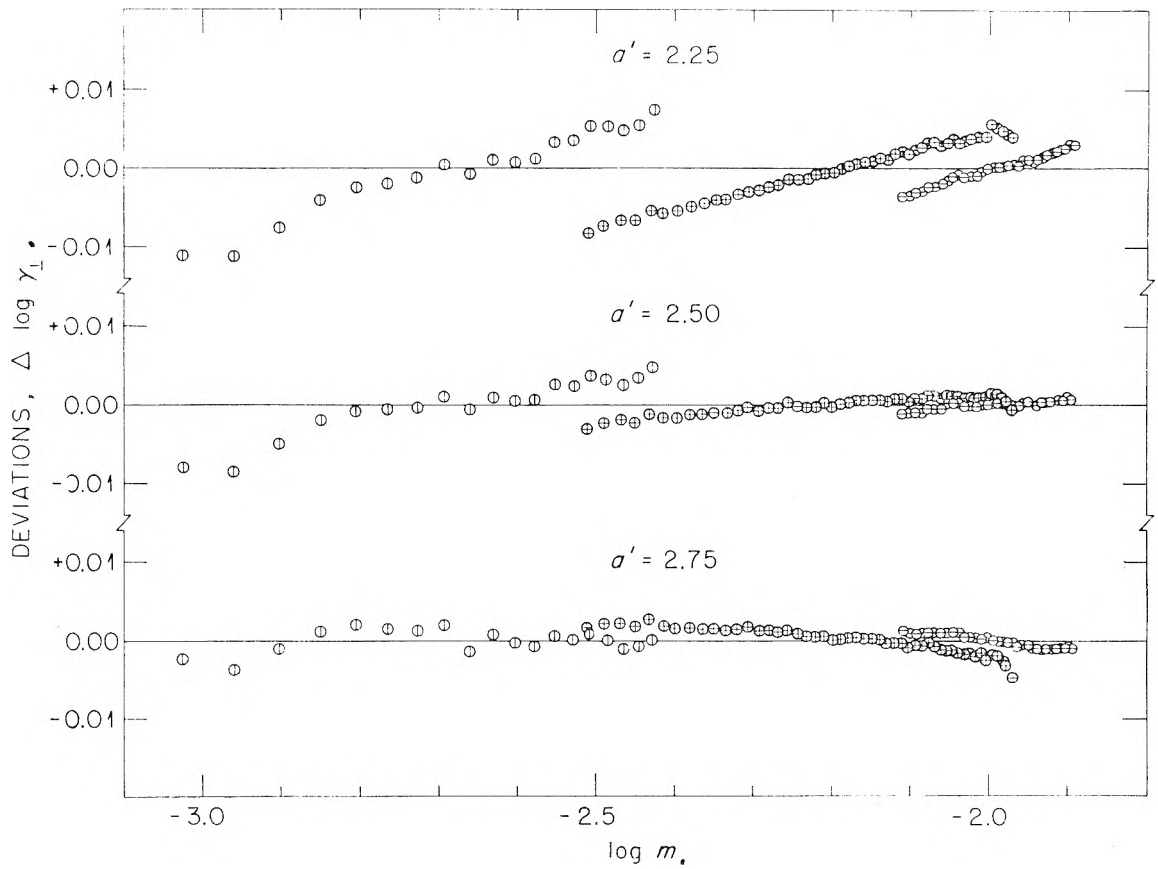

Fig. 3.—Deviations of experimental activity coefficients of sodium silicotungstate from values computed with Debye–Hückel theory (equation 11). All centrifugations with interference optics. Approximate speed of rotation (r.p.m.): 24,630, ⊙ ⊕; 14,290, ⊖.

equation 11, where the subscript "Men" refers to the meniscus, and ϵ is so selected that the sum of average deviations for a given run is zero. The individual points represent fringe positions in the experiments carried out with interference optics (only every second or third point is plotted in some cases to avoid excessive crowding) or readings at 0.05 cm. radial intervals with schlieren optics. If agreement were perfect, all points for a given experiment would lie on a horizontal line, of zero ordinate. From this figure, the lower precision of the results at low concentrations is evident; the values of the slopes, d ln $\gamma_{\pm}$/d ln m, given in Fig. 1, for this range are correspondingly uncertain. The insensitivity of these slopes to changes in a' at low concentration is also illustrated. No significant difference is noted between results for different speeds of rotation; this indicates that the assumption of constancy of $\bar{v}$ with pressure is valid within the accuracy of the present results.

We have also carried out a few activity coefficient measurements on the sodium salt of silicotungstic acid (neutralized with NaOH to an average formula $Na_{3.8}H_{0.2}SiW_{12}O_{40}$). The interpretation assumed a two-component system with solute having the average formula; differences in equilibrium distribution between the sodium salt and the small amount of acid present affect the results to only a minor extent. The results are shown in Fig. 1, and the deviation plots in Fig. 3. Equations 10 and 11 with $a' = 2.50$ also represent these results satisfactorily. Within experimental uncertainty, the activity coefficients of the acid and of the sodium salt appear to be the same.

3. Light Scattering.—Turbidity measurements have been made on silicotungstic acid solutions in the concentration range $c = 0.005$ to 0.04, and the results are recorded in Table II.

TABLE II

COMPARISON OF EXPERIMENTAL TURBIDITIES WITH TURBIDITIES COMPUTED FROM ULTRACENTRIFUGATIONS WITH SCHLIEREN OPTICS

m	λ	$10^4\Delta\tau_{exp.}$	$10^4\Delta\tau_{comp.(Eq. 8)}$
0.0404	436	2.51	2.63
	546	0.90	0.93
.0310	436	1.92	1.89
	546	0.71	0.67
.0196	436	1.25	1.28
	546	0.45	0.46
.00973	436	0.60	0.62
	546	0.21	0.22
.00494	436	0.31	[a]
	546	0.10	[a]

[a] No centrifugations with schlieren optics carried out at this concentration.

A direct comparison is also presented in this table with turbidities computed from values of dn/dx obtained by ultracentrifugations with schlieren optics (Equation 8). The agreement is particularly gratifying since in this comparison

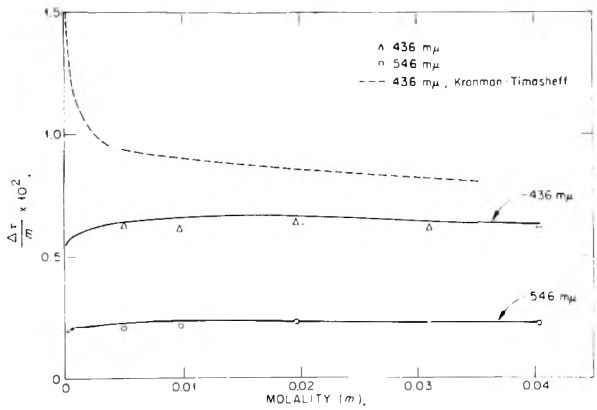

Fig. 4.—Comparison of experimental and computed turbidities. Solid curve computed with equations 5 and 10; $a' = 2.50$.

only experimental quantities are used, and, in particular, no estimates of activity coefficients or their derivatives are necessary.

In Fig. 4 the light scattering results at 436 and 546 mμ are compared with turbidities computed by Equation 5. The activity coefficient term was evaluated from Equation 10, with the value $a' = 2.50$, estimated from ultracentrifugation. Again, the agreement is fairly good. Equation 5 is applicable, since at our lowest concentration, ν' (computed by Equation 9) is 4.98, or negligibly different from 5.

In summary, the activity coefficients of silicotungstic acid are consistent with the Debye–Hückel equation for a 1–4 electrolyte with $a' = 2.5$.

Discussion

1. Comparison with Values of Turbidity in the Literature.—Kronman and Timasheff have studied the light scattering of two component sodium silicotungstate solutions at 436 mμ.[18] We compare their turbidities, obtained from their curve of Hc/τ *vs.* c, (their Fig. 2) with our results in our Fig. 4. The comparison should be with the computed curve for 436 mμ raised by about 5%; although the activity coefficient term for the acid and the sodium salt in Equation 5 should be the same, the refractive index increment of the sodium salt is higher. The agreement is not good; in the concentration range for which we have measured turbidities, their values are about 15–25% higher than those computed for the sodium salt. (Larger discrepancies between their experimental and our computed results at lower concentration will be discussed later.)

Reasons for the discrepancy are not clear. Differences in calibration of photometers seem ruled out, since both laboratories obtained essentially the same molecular weight for the solute by light scattering in the presence of supporting electrolyte. Either low or high molecular weight impurities could cause high turbidities, the former by acting as supporting electrolyte. It seems doubtful that low molecular weight impurities in the salt or water used could account for the discrepancies, except perhaps at the low concentration end, since the molal concentration of a 1–1 electrolytic impurity would have to be about one-half that of the silicotungstate to give an increment of twenty per cent. Decomposition of part of the solute into a high molecular weight species could explain high turbidities. If one per cent., for example, attained a molecular weight of 10^5, the weight average molecular weight, and consequently the turbidity, would be about 30% higher. We do not believe that acid solutions decompose in this manner; turbidities of a 0.03 M silicotungstic acid solution measured over a period of five weeks agreed within ±3% with the turbidity of the freshly prepared solution at both wave lengths (see Table III). In any case, the turbidities we report were measured on the day of preparation of each solution. Kronman and Timasheff's measurements were also on freshly prepared solutions,[18] but there could have been decomposition occurring in their neutralization or in their dilution procedure. However, it would seem that any products of decomposition causing trouble of this magnitude must be non-equilibrium species, since the tungstate species, at least, reported in the pH range of 4–4.5 are neither large enough nor small enough to account for the discrepancy.[19]

TABLE III

LIGHT SCATTERING OF 0.03 M M $H_4SiW_{12}O_{40}$ AS FUNCTION OF TIME

Age, weeks	$\tau_{436} \times 10^4$ [a]	$\tau_{546} \times 10^5$ [a]
<0.1	2.52	9.9
1	2.56	9.8
3	2.54	9.8
5	2.57	10.0
5[b]	2.53	9.6

[a] Solvent scattering not subtracted. [b] This measurement upon separate sample of aged stock. Other measurements all on same sample, filtered just before each measurement.

Because of the agreement between our ultracentrifugation and light scattering measurements, we believe our turbidities to be more nearly correct than those of Kronman and Timasheff.

In order to explain their observations that scattering is much lower in the two component system than in the presence of supporting electrolyte, Kronman and Timasheff postulate a Kirkwood–Mazur[20] ordering of solute molecules, brought about by repulsive forces between the ions. To explain our results, in which the scattering is lower yet, by this hypothesis would require even greater ordering. Our findings indicate that silicotungstic acid is a normal 1–4 electrolyte, and it does not seem necessary to invoke ordering other than implied in ordinary Debye–Hückel behavior. Kronman and Timasheff,[5] in their argument for ordering, state that the lower values of turbidity in absence of supporting electrolyte, on the basis of their equation 3, indicates a high value for the gradient of excess free energy of solute with concentration. It seems to us that they find the latter quantity unexpectedly high because they do not consider the activity of their solute in the terms one usually

(18) S. N. Timasheff, private communication. The title of their paper (ref. 5) refers to silicotungstic acid, but their measurements were actually on the acid neutralized to the sodium salt (pH 4.5–5).

(19) G. Jander and K. F. Jahr, *Kolloid-Beih.*, **41**, 1 (1935).

(20) J. G. Kirkwood and J. Mazur, *J. Polymer Sci.*, **9**, 519 (1952).

deals with electrolytes; that is, they neglect the quantity ν. Neglect of ν also leads them to conclude that they should, in a standard $Hw/\Delta\tau$ graph, approach the reciprocal of the molecular weight of silicotungstic acid with decrease in concentration. Their observations support this. We did not feel that our light scattering measurements were accurate enough to check them in this region but, on the basis of our ultracentrifugation results, such an increase in turbidity should not be observed unless the solutions are so dilute that departures from electroneutrality are occurring in dimensions comparable to the wave length. Their lowest concentration appears to be about 3×10^{-4} mole/liter. Here ν' computed by Equation 9 is within 10% of 5. Their results in the low concentration range cannot be understood on this basis.

2. Silicotungstic Acid in Calibration of Photometers.—Two component solutions of silicotungstic acid have possible usefulness as primary light scattering calibration standards for aqueous solutions. The material is inexpensive and obtainable in adequate purity. Although, because of variation in water content of the salt, one would need analysis to establish concentration, a density or perhaps a refractive index measurement should suffice. Scattering by this solute is sufficient to allow calibration at concentrations for which the refractive index of the solution would not be greatly different from those of usual "unknown" aqueous solutions. The activity coefficients and refractive index increments presented here should be accurate enough to allow computation of excess turbidities to about 3% (based on an uncertainty of 0.15 in a' and of 0.3% in refractive index increments) in the concentration range 0.01–0.04 moles/liter.

Ludox has been used as a calibration standard but its properties have been criticized. Recently, sucrose[21] also has been used for this purpose. At concentrations which scatter desirable levels of light, however, the refractive indices of sucrose solutions are somewhat higher than those of the usual aqueous solutions of interest, and the possibility of differences in apparatus constants is thus introduced. In addition, recent recomputations of the expected turbidity with exact equations by Stigter[22] have not given quite as good agreement between experimental and computed values as previously reported.[23] Further, there is an impurity (or impurities) apparently present in even the best sucrose samples, which must be eliminated by charcoal treatment. Finally, agreement[22,23] of computed with experimental turbidities has been obtained with use of a substantial depolarization correction, the magnitude of which may be questionable with an optically active solute. There thus still seems to be a need for a convenient aqueous standard.

Silicotungstate turbidities in the presence of supporting electrolyte could be used for secondary standards, although the requisite activity coefficient derivatives are not available for computation of turbidities for a given solution. The scattering would, however, be less sensitive to interference by low molecular weight impurities than with the two component system.

Acknowledgment.—We wish to acknowledge indebtedness to Dr. W. R. Busing for advice concerning programming of computations both in this work and, belatedly, in an earlier study.[14] We are indebted to Dr. E. W. Anacker for helpful comments on the paper, and to Miss Neva Harrison for technical assistance.

(21) K. J. Mysels and L. H. Princen, *J. Phys. Chem.*, **63**, 1696 (1959).
(22) D. Stigter, *J. Phys. Chem.*, **64**, 114 (1960).
(23) S. H. Maron and R. L. H. Lou, *ibid.*, **59**, 231 (1955).

SOME OBSERVATIONS ON THE ELECTRON PARAMAGNETIC RESONANCE SPECTRA OF GASEOUS FREE RADICALS

BY C. J. ULTEE*

Research Laboratory, Linde Company, Division of Union Carbide Corporation, Tonawanda, New York

Received May 5, 1960

The e.p.r. spectra of atomic nitrogen, oxygen and hydrogen have been observed over a wide pressure range. Relaxation and pressure broadening effects complicate the spectra and have limited the present study to qualitative observations. It seems quite feasible, however, to adopt e.p.r. methods for kinetic studies of free radical reactions in the gas phase. In the case of atomic nitrogen an unexpected effect of oxygen was observed which may have some bearing on the theory of active nitrogen.

Introduction

Electron paramagnetic resonance (e.p.r.) studies of gases have been limited mainly to the determination of spectroscopic parameters for a number of paramagnetic species. There seems to have been no application of e.p.r. spectroscopy to the study of the chemical properties of gaseous free radicals, although this technique would seem ideally suited to enlarge the present knowledge and understanding of gas-phase free-radical reactions. This study was undertaken to explore the use of e.p.r. spectroscopy in the investigation of gas-phase kinetics, using a commercially available instrument without extensive modifications. A survey of our observations on atomic nitrogen, oxygen and hydrogen is given below. Since the spectra of these species have been reported recently,[1-3] the discussion is limited to

* AVCO Research and Advanced Development Division, 201 Lowell Street, Wilmington, Mass.

(1) E. R. Rawson and R. Beringer, *Phys. Rev.*, **88**, 677 (1952).
(2) M. A. Heald and R. Beringer, *ibid.*, **96**, 645 (1954).
(3) R. Beringer and M. A. Heald, *ibid.*, **95**, 1474 (1954).

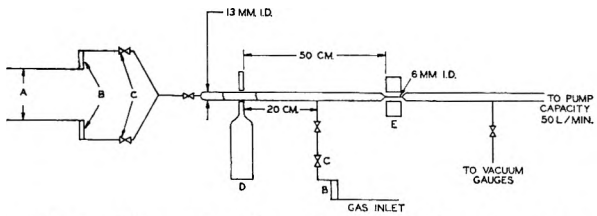

Fig. 1.—Flow system for activation of the gases: A, gas inlet; B, flowmeters; C, needle valves; D, exitation cavity; E, spectrometer cavity.

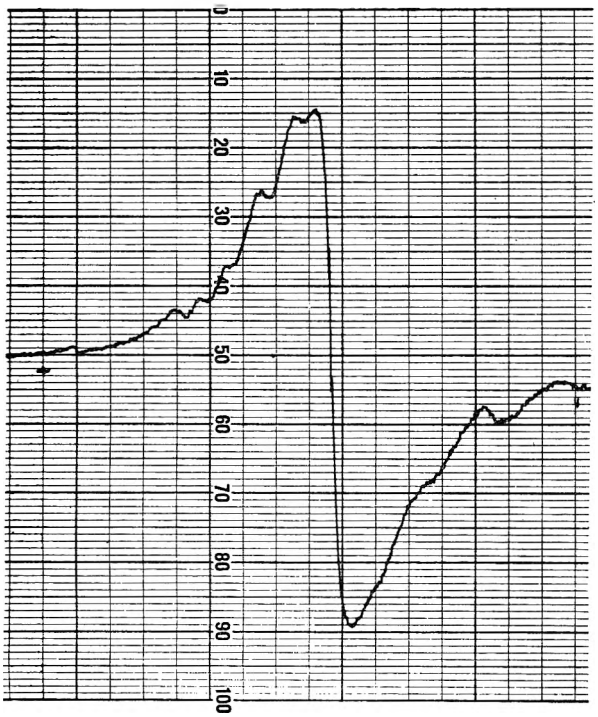

Fig. 2.—The cyclotron resonance signal in active nitrogen.

specific experimental details and to the effects of some variables not previously reported.

Experimental

The general principles and instrumental techniques of e.p.r. spectroscopy have been the subject of recent reviews[4,5] and will not be discussed here. The e.p.r. spectrometer used in this work is a Varian Associates Model V-4500 e.p.r. spectrometer operating at a nominal frequency of 9.4 kMc./sec. A rectangular cavity operating in the TE_{012} mode is used, with sample openings in the center of the narrow face such that the sample is positioned in a region of maximum microwave magnetic field. The only modification made in the cavity was an increase in the diameter of the sample openings to 11 mm. Modulation of the magnetic field is provided by two small coils attached to the side of the cavity. The coils are driven by a 400 c./sec. audiooscillator. Resonance absorption in the cavity appears as audio modulation at a MA 408A crystal used as a detector. The signal is amplified, demodulated and recorded by conventional techniques. With low modulation amplitudes the recorder tracing approximates the derivative of the resonance absorption curve.

Magnetic field strengths were determined by measuring corresponding proton resonance frequencies. Microwave frequencies were measured with a heterodyne frequency meter. The accuracy of the frequency measurements is estimated at 0.005%.

Modulating amplitudes were generally adjusted for optimum signal presentation,[6] *i.e.* $H_m = 2\Delta H_{1/2}$, except during line width measurements for which the lowest feasible amplitudes were used.

The vacuum line and flow system are shown in Fig. 1. The electrodeless discharge is excited in a quartz section of the line which passes through a slot in a resonant cavity. A 2450 Mc./sec., 125-watt Raytheon diathermy unit is used to supply the discharge power. Commercial high purity cylinder gases were used without further purification.

Results and Discussions

Nitrogen.—Nitrogen, after passing through the discharge, showed the characteristic yellow afterglow. The e.p.r. spectrum of this active nitrogen consists of a group of three narrow, evenly spaced lines of equal intensity which are superimposed on a very broad and intense line. Both signals are centered about $g = 2.0$. However, under experimental conditions that are optimum for the observation of the spectrum of atomic nitrogen, *i.e.*, low modulation amplitude, low microwave power and slow scanning over a narrow magnetic field region, the broad line is not observed. The width of this broad line varies with pressure and microwave power. At 15 mm. pressure its width (between maximum and minimum points on the derivative curve) is about 200 gauss. The line shows considerable structure (Fig. 2) which is, however, not readily resolved. When oxygen is added to the nitrogen prior to its passage through the discharge, this signal increases sharply in amplitude, reaches a maximum at 0.2 volume % (total pressure 10 mm.), then slowly decreases, reaching zero at 2.5% oxygen.

Several investigators have demonstrated the presence of free electrons in active nitrogen by probe and microwave methods.[7-10] The present data may be correlated closely with the microwave electron density measurements in active nitrogen reported by Kunkel and Gardner[10] who observed a maximum at about 0.2 volume % oxygen. The broad line can therefore be explained as a cyclotron resonance signal from free electrons in active nitrogen. The transition probability for cyclotron resonance is proportional to the square of the electric dipole moment; for fields of the same order of magnitude it is about 10^{12} times the transition probability for spin resonance. The higher probability accounts for the intensity of the line, which is too high to interpret it as an e.p.r. line of an impurity in the nitrogen. A similar line observed in gas discharges has been assigned to cyclotron resonance by Ingram and Tapley.[11] If it is assumed that the electrons have their origin in the ionization of NO by the reaction $N + N + NO \rightarrow N_2 + NO^+ + e^-$,[10] than the effect of oxygen is readily explained. The addition of oxygen leads to the formation of nitric oxide. As long as nitrogen atoms are present in excess, the ionization step will take place. However, at high oxygen concentrations the reaction of oxygen with atomic nitrogen will decrease the concentration of the latter. Consequently the concentration of free electrons will also decrease.

The three narrow lines (Fig. 3) form the spectrum of $^4S_{3/2}$ (ground state) nitrogen atoms. At

(4) J. E. Wertz, *Chem. Revs.*, **55**, 829 (1955).
(5) G. Feher, *Bell System Techn. J.*, **34**, 449 (1957).
(6) R. Beringer and J. G. Castle, Jr., *Phys. Rev.*, **78**, 581 (1950).
(7) Rayleigh, *Proc. Roy. Soc.* (*London*), **A180**, 140 (1952).
(8) J. M. Benson, *J. Appl. Phys.*, **23**, 757 (1952).
(9) A. L. Gardner, *Phys. Rev.*, **98**, 263 A (1955).
(10) W. B. Kunkel and A. L. Gardner, *ibid.*, **98**, 558 A (1955).
(11) D. J. E. Ingram and J. A. Tapley, *ibid.*, **97**, 238 (1955).

20 mm. total pressure, the observed spacing of 3.8 gauss, line width of 0.09 gauss, and g-factor of 2.0021 are identical with those reported by Heald and Beringer.[2]

The atomic nitrogen spectrum was observed over the range of 0.5 to 80 mm. total pressure. Atomic nitrogen concentrations as determined by "titration" with NO[12] varied from 1% (volume) at 20 mm. to 4% at 1 mm. From 5 to 20 mm. the partial pressure of atomic nitrogen remained essentially constant.

If we use the Van Vleck–Weisskopf theory[13] of pressure broadening and identify the lifetime τ of a spin state with the time t, between collisions of atomic species, the half-width at half height on a frequency scale is given by $\Delta\nu \sim 1/2\pi\tau$. Using a kinetic theory cross section and making the appropriate conversions to magnetic field units, the calculated line width for atomic nitrogen at a partial pressure of 0.2 mm. (total pressure 10 mm.) is ~ 0.1 gauss, in good agreement with the observed width under these conditions.

A study of the reaction between atomic nitrogen and molecular oxygen showed that addition of oxygen affects the atomic nitrogen signal to a considerable extent. Figure 4 shows the effect of oxygen on the signal amplitude at various power levels. The initial parts of the curves are difficult to explain on the basis of any plausible reaction mechanism. The curve at lower power levels show a less prominent maximum, suggesting that the phenomenon is related to saturation at high power levels. Figure 5 shows the effect of microwave power on nitrogen containing varying amounts of oxygen. These results were obtained by decreasing the power level in the cavity with a variable attenuater, keeping bias and signal amplification constant. Under these conditions, the signal amplitude varies as the square root of the power. The signal amplitudes are therefore normalized by dividing by $\sqrt{P}$. At high oxygen concentrations the curves show no evidence of saturation, but as the oxygen content becomes less, saturation does occur. The difference in signal amplitude levels for these curves is caused by the fact that the oxygen reacts with part of the atomic nitrogen before it reaches the microwave cavity. In essence, the curves correspond to different amounts of atomic nitrogen, although pressure and initial concentration remained the same. Thus, it appears that the oxygen decreases the relaxation time and allows the nitrogen signal to approach its full, unsaturated amplitude. Qualitatively this effect is readily accounted for. In monatomic gases there are no intramolecular magnetic fields which can lead to relaxation processes as in polyatomic molecules. Indeed, neglecting quadrupole effects, the only relaxation mechanism available is through collisions or near-collisions with other magnetic species. The addition of a paramagnetic gas increases the number of these collisions and is thus capable of shortening the relaxation time. This effect is well recognized and has been used in nuclear magnetic resonance studies of gases. However, the lack of detailed knowledge of the relaxation processes in the gas phase, make it difficult to calculate the relaxation time for the above system, while the present equipment does not permit their measurements either. We are unable

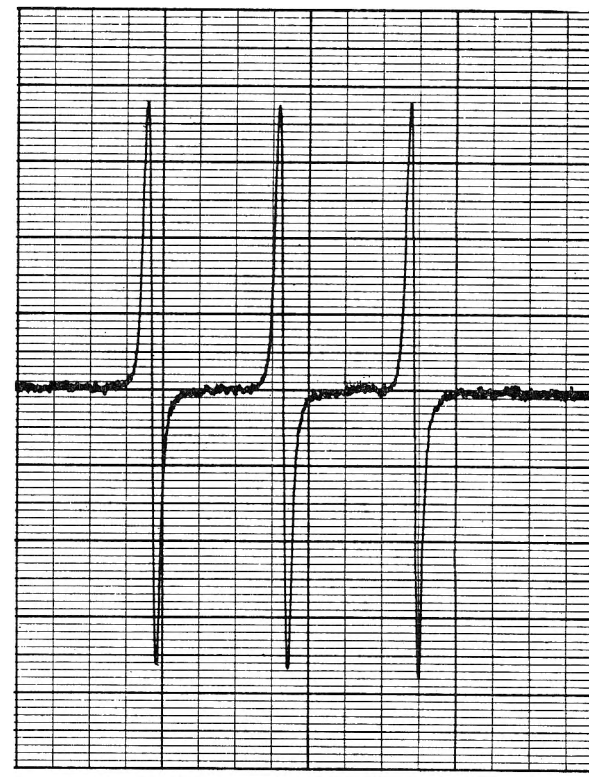

Fig. 3.—E.p.r. spectrum of atomic nitrogen.

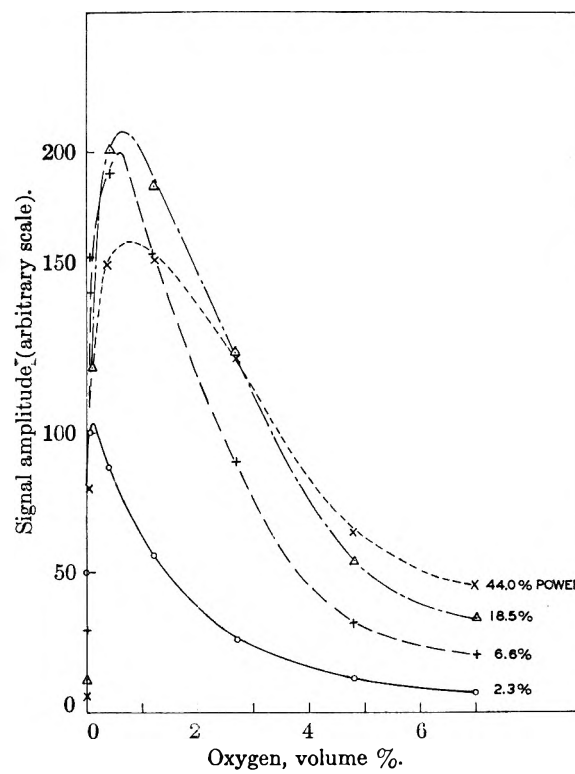

Fig. 4.—The effect of oxygen on the atomic nitrogen signa amplitude.

(12) F. Kaufman and J. R. Kelso, *J. Chem. Phys.*, **27**, 1209 (1957).
(13) J. H. Van Vleck and V. F. Weisskopf, *Revs. Mod. Phys.*, **17**, 227 (1945).

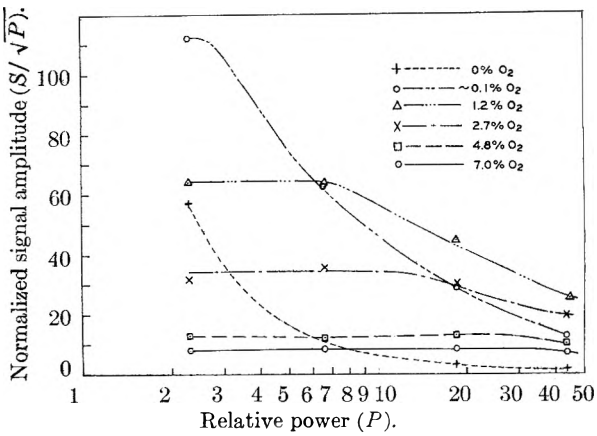

Fig. 5.—Effect of microwave power on the atomic nitrogen signal.

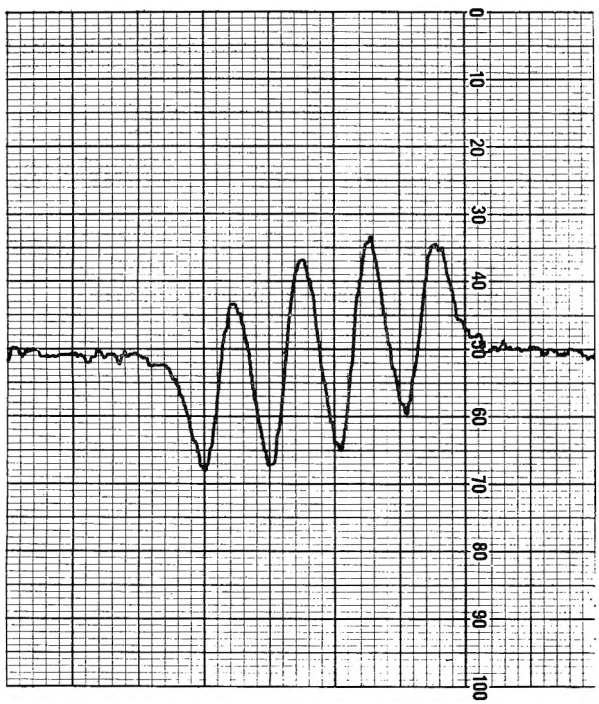

Fig. 6.—The atomic oxygen ($^3P_2$) spectrum (low pressure).

therefore, to decide at this time, whether such a mechanism can account for the observed results.

Another possible explanation is to assume a collision time for $N–O_2$ collisions which is long compared to the spin precession period. Such a collision complex would in essence provide a relaxation mechanism similar to that of polyatomic molecules. Reinecke[14] has postulated an essentially similar effect to explain the afterglow duration and the intensity distribution among the vibrational levels of the first positive system in the afterglow spectrum. Many investigators have claimed that absolutely pure nitrogen does not give an afterglow.[15–17] The recent data of Anderson, *et al.*,[16,17] are quite convincing and seem to exclude the possibility that the effect is due to wall poisoning alone.

(14) L. H. Reinecke, *Z. Phys.*, **135**, 361 (1953).

(15) Rayleigh, *Proc. Roy. Soc. (London)*, **A151**, 567 (1935).

(16) J. M. Anderson, A. K. Kavadas and R. W. McKay, *Proc. Phys. Soc.*, **A71**, 877 (1957).

(17) J. M. Anderson, *ibid.*, **A71**, 887 (1957).

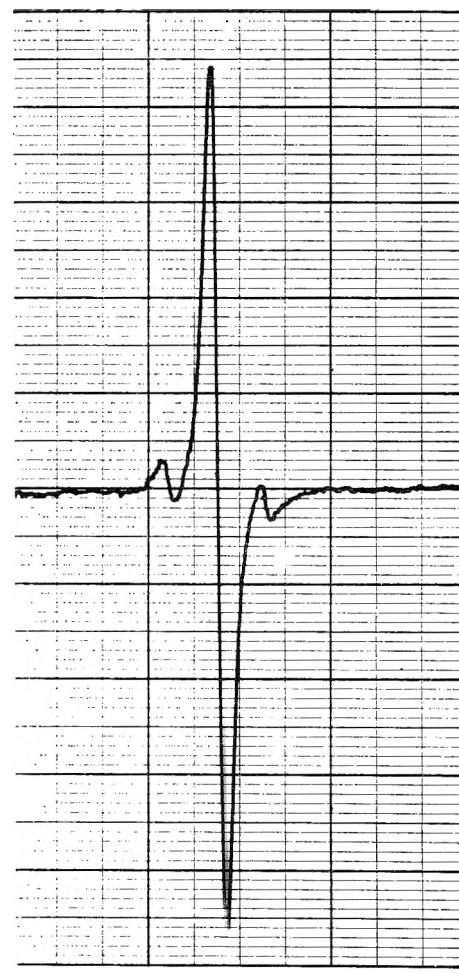

Fig. 7.—The atomic oxygen ($^3P_2$ and $^3P_1$) spectrum (high pressure).

Unless the long-lived nitrogen atoms are exclusively in the form of $(N–O_2)$ complexes, one would expect some difference between the N and $(N–O_2)$ e.p.r. spectra. We have been unable to detect any changes in g-value of the nitrogen spectrum on the addition of oxygen, but this point requires further investigation. Line shape and more accurate line width measurements would also be informative, but are at present complicated by saturation effects. Such data in addition to quantitative relaxation time measurements should shed more light on these questions.

Oxygen.—The atomic oxygen spectrum has been reported by Rawson and Beringer,[1] who reported nine lines, centered about $g = 1.5$. Two of these were assigned to transitions of $^3P_1$ atoms, and four to $^3P_2$ (ground state) atom transitions; the remaining three lines were unexplained. Hughes and Geiger[18] have recently shown that these three lines are due to two-quantum transitions between the magnetic sub-levels of $^3P_2$ oxygen atoms.

At total pressures below 0.1 mm. our spectra are essentially in agreement with those reported by Beringer. Observations on the variation of the spectrum with changes in microwave power support the assignment by Hughes and Geiger. At high power levels three strong and four weak lines are

(18) V. W. Hughes and J. S. Geiger, *Phys. Rev.*, **99**, 1842 (1955).

observed. As the power is decreased the four weak lines increase in amplitude, while the three strong lines decrease. At about 10 mw. only the four, single-quantum transition lines remain (Fig. 6). These transitions are more easily saturated and as a result are observed with low amplitudes at high power levels; consequently, a decrease in power effects mainly the two-quantum transitions. At pressures above 0.20 mm. the spectrum consists of only three lines; the two $^3P_1$ oxygen transitions and a strong, single line instead of the four (or seven lines, depending on the microwave power) lines observed at low pressures (Fig. 7). This dependence of the spectrum on pressure was further investigated. From 0.020 to 0.120 mm. the width of the resolved single-quantum transitions shows a linear increase from 0.05 to 0.25 gauss. These values are in reasonable agreement with the Van Vleck–Weisskopf theory. In the pressure range from 0.20 to 9.0 mm., where the four lines are broadened into a single line, the width of this line increases again linearly from 2.5 to 6.2 gauss. From about 0.120 to 0.20 mm. there is a smooth transition from the four lines to a single line. Thus the appearance of the spectrum at high pressures is apparently the result of pressure broadening of the closely spaced individual lines.

At low pressures a single broad line may also be obtained by over-modulating. Using this technique, which makes the detection somewhat easier, the atomic oxygen was observed down to a pressure of 0.005 mm. (total pressure in the flow system). Above 10 mm. total pressure detection becomes difficult due to the width of this line.

Atomic oxygen, in contrast with atomic nitrogen is readily detected when air is passed through the discharge, demonstrating the longer lifetime of atomic oxygen under these conditions.

Hydrogen.[19]—The spectrum of atomic hydrogen consists of two lines centered at about $g = 2.003$, with a separation of approximately 1420 Mc./sec.[3] This spectrum was observed over the pressure range of 3.0 to 8.0 mm. Optimum pressure in our case was about 3 mm. The intensity was low, saturation was noticed even at low microwave power and the over-all reproducibility was poor. It seems likely that these results are due to a low and poorly reproducible production of hydrogen atoms in the 2450 Mc./sec. discharge.

Acknowledgments.—The author wishes to acknowledge the assistance of Mr. C. A. Hauck, Mr. B. M. Shields, and Mr. J. Saia in the various experimental phases of this work.

(19) After this work was completed, Hildebrandt, Booth and Barth [*J. Chem. Phys.*, **31**, 273 (1959)] in a Letter to the Editor, reported their observations on the e.p.r. spectrum of atomic hydrogen. The effect of pressure on the line width for the atomic hydrogen lines is covered in more detail, with results similar to those reported here.

THE COMPARATIVE ROLES OF OXYGEN AND INHIBITORS IN THE PASSIVATION OF IRON. I. NON-OXIDIZING INHIBITORS

BY G. H. CARTLEDGE

Chemistry Division, Oak Ridge National Laboratory, Operated by Union Carbide Corporation for the U. S. Atomic Energy Commission, Oak Ridge, Tennessee

Received May 7, 1960

Conflicting views are held as to the respective roles of oxidizing agent and inhibitor in the passivation of iron in aerated solutions of certain inhibitors. In the first paper of this series, experiments with inhibitors having no oxidizing properties are presented. It was found that passivation at a noble potential may be achieved under conditions in which oxygen is necessarily the oxidizing agent, though without the inhibitor it leads to corrosion. It was found also that the passive potential is destroyed by low concentrations of sulfate ions, and thus exhibits the same behavior as that previously observed with oxidizing inhibitors. By means of cathodic polarization measurements, the magnitude of the cathodic current density in the reduction of oxygen on passive iron at potentials above or somewhat below the Flade potential was determined. It was found, further, that addition of sulfate ions in low concentration sensitizes the system to activation under cathodic polarization. The results are interpreted as further evidence that the inhibitor's essential function is related to its adsorption, in competition with other ions or molecules.

Introduction

In most of the earlier work on the passive state of iron, passivation was produced either by anodic polarization or by use of a vigorous oxidizing agent such as nitric acid. Recently, several studies have been concerned with passivation in aerated solutions of certain compounds commonly referred to as inhibitors.[1-3] Stern discussed the polarization curves of iron and stainless steel and superimposed upon them schematic polarization curves for an added oxidation–reduction couple to show how its normal electrode potential, exchange current, polarization characteristics and concentration enter into its ability to passivate the metal by its own reduction. Uhlig considers the passive film to consist of chemisorbed oxygen,[4] and Uhlig and King[5] have suggested that oxidizing agents like chromate and pertechnetate ions passivate iron by being reduced on large, discrete cathodic areas, thereby producing a sufficiently large local-cell current density on small anodic areas for passivation to result. A similar explanation is inherent in the treatment by Stern.[2] These interpretations are obviously of an entirely different type from the strictly chemical point of view proposed by

(1) G. H. Cartledge, *Z. Elektrochem.*, **62**, 684 (1958). Contains references to several prior papers.

(2) Milton Stern, *J. Electrochem. Soc.*, **105**, 638 (1958).

(3) M. Cohen and A. F. Beck, *Z. Elektrochem.*, **62**, 696 (1958).

(4) H. H. Uhlig, *ibid.*, **62**, 626 (1958).

(5) H. H. Uhlig and P. F. King, *J. Electrochem. Soc.*, **106**, 1 (1959).

(6) T. P. Hoar and U. R. Evans, *ibid.*, **99**, 212 (1952).

Hoar and Evans,[6] Evans,[7] and Cohen and Beck.[3]

It is generally recognized that oxidation of iron by some means is involved in passivation processes, that is, processes in which both a low corrosion rate and a noble electrode potential result. If a reducible inhibitor is used in aerated solutions, experiments show that it may be reduced along with oxygen during passivation under certain conditions, but it remains to be demonstrated whether its function in the maintenance of passivity depends primarily upon such oxidizing and precipitating properties. The alternative view has been expressed that the inhibiting substance, without which passivation in aerated solutions does not occur, is adsorbed as such and that the adsorbed ions in some way alter the kinetics of one or more of the reactions involved in the corrosion and passivation processes. Cartledge[8,9] proposed the hypothesis that a special kind of interfacial electrostatic field arises by adsorption of XO_4^{n-} particles when X has a high formal positive charge and the X–O bonds have considerable polar character. For short distances from the interface within the solid substrate, this field was calculated to be opposite in sign from the image charge due to the negative ion considered as a unit.[1] The adsorption of such ions was therefore assumed to alter specifically the kinetics of one or more processes involved in the corrosion reactions in such a way as to permit passivation. A related view was proposed by Kabanov and Leikis.[10]

It is obvious that an adequate interpretation of the passivation reaction presupposes an understanding of the process to be inhibited. In a recent paper, Heusler[11] has given convincing evidence that the dissolution of iron involves an initial step by which a catalytic intermediate is formed electrochemically from iron and a hydroxide ion and remains adsorbed on the surface. The effect of competitive adsorption of inhibiting species on the surface then becomes understandable. This effect has been studied quantitatively for the anodic dissolution of iron in sulfuric acid with carbon monoxide or iodide ions as inhibitor.[12]

In whatever way an inhibitor may affect the polarization characteristics of the electrode processes of iron and protons in the active region, however, it is also necessary to know specifically what cathodic processes are effective in producing and maintaining the higher potentials of the passive state, and what the relation of inhibitors to these processes is. Previous experiments[13] showed that passivation of iron may be effected in an aerated solution of pertechnetate ions with consumption of so little TcO_4^- by reduction that oxygen is clearly the chief oxidizing agent. Yet without the pertechnetate at sufficient concentration corrosion proceeds rapidly under otherwise similar conditions. It is also known that both CrO_4^{--} and TcO_4^- may react with iron to form a film of insoluble oxides, but even in aerated solution this film does not long retard corrosion in the absence of the unreduced ions. According to Hoar and Evans,[6] this excess of inhibitor is needed to precipitate *in situ* any iron (II) ions emerging through faults in the protective film. The data of Brasher and co-workers[14–16] do, indeed, show that the amount of Cr^{51} on a passive surface increases slowly on long exposure to solutions containing $Cr^{51}O_4^{--}$. Yet the fact[17,18] that a variety of ions, such as SO_4^{--} and ReO_4^-, may destroy the inhibiting action of TcO_4^-, CrO_4^{--}, etc., apparently supports the suggestion that adsorption of the inhibitor in competition with other anions is an important, if not dominant, factor in its action. It is therefore an experimental problem to determine whether such reduction of a reducible inhibitor as actually occurs is really the essential part of its action in the passivation process. The experiments to be described constitute the first of a series of studies directed to an attempt to determine definitely the respective roles of oxygen and a variety of inhibitors in producing and maintaining the passivity of iron. The first portion of the study deals with the combined action of oxygen and inhibitors which are unable, of themselves, to oxidize iron or ferrous ions to the state found in the passive film. The action of certain potentially oxidizing inhibitors will be considered in subsequent papers.

Passivation in the Presence of Non-oxidizing Inhibitors.—As non-oxidizing inhibitors, benzoate, phthalate and phosphate ions were chosen. It has been reported previously that neither benzoate[19] nor phosphate[20] inhibits in the absence of oxygen. Measurements were therefore made to determine (a) whether these three inhibitors in the presence of oxygen lead to an electrode potential that is more noble than the Flade potential, (b) whether the noble potential, if attained, is sensitive to low concentrations of added foreign ions, as was previously found with the reducible XO_4^{n-} inhibitors,[18] and (c) the behavior of electrodes passivated in such systems when polarized cathodically.

Experimental

Phthalate was used at concentrations of 5×10^{-3} to 5×10^{-2} *f* and acidities corresponding to *p*H values between 5.40 and 7.05. (Passivation was not achieved in an oxygenated 1.0×10^{-2} *f* solution at *p*H 5.4.) The electrodes were made of electrolytic iron; they were abraded with 2/0 emery and cleaned in acetone and water. A stream of air or oxygen bubbled rapidly through the cell. The electrode was connected to a saturated calomel half-cell (S.C.E.) through a Haber–Luggin capillary and bridge leading to another compartment. A Vibrating Reed Electrometer and Brown Recorder were used in measuring the e.m.f.'s. The potentials recorded were the essentially

(7) U. R. Evans, *Z. Elektrochem.*, **62**, 619 (1958).
(8) G. H. Cartledge, *J. Am. Chem. Soc.*, **77**, 2658 (1955).
(9) G. H. Cartledge, *Corrosion*, **11**, 335t (1955).
(10) B. N. Kabanov and D. I. Leikis, *Z. Elektrochem.*, **62**, 660 (1958).
(11) K. E. Heusler, *ibid.*, **62**, 582 (1958).
(12) K. E. Heusler and G. H. Cartledge, in process of publication.
(13) G. H. Cartledge, THIS JOURNAL, **59**, 979 (1955).
(14) D. M. Brasher, A. H. Kingsbury and A. D. Mercer, *Nature*, **180**, 27 (1957).
(15) D. M. Brasher and C. P. De, *ibid.*, **180**, 28 (1957).
(16) D. M. Brasher and A. H. Kingsbury, *Trans. Faraday Soc.*, **54**, 1214 (1958).
(17) G. H. Cartledge, THIS JOURNAL, **60**, 28 (1956).
(18) R. F. Sympson and G. H Cartledge, *ibid.*, **60**, 1037 (1956).
(19) D. M. Brasher, "Chemistry Research" 1954, Her Majesty's Stationery Office, London, 1955 p. 12 (Personal Communication). *Cf.* also F. Wormwell and A. D. Mercer, *J. Appl. Chem.*, **2**, 150 (1952).
(20) M. J. Pryor and M. Cohen, *J. Electrochem. Soc.*, **98**, 263 (1951); M. J. Pryor, M. Cohen and F. Brown, *ibid.*, **99**, 542 (1952).

stable values attained after an exposure to the environment lasting 13 hr. or longer.

As shown in Table I, potentials more noble than the Flade potential were obtained; the potentials varied somewhat for different specimens and with the conditions of passivation. The most noble potentials were achieved when the solution was allowed to accumulate the iron ions that passed into solution during the passivation process, as in the experiment with footnote reference *e* in Table I. If the solution was replaced with fresh electrolyte before complete passivation, the electrode potential became noble to the calculated Flade potential,[21] but without the appearance of visible film or of coloration in the solution. Potassium sulfate was subsequently added to certain of the solutions to determine whether the nobility is sensitive to the presence of foreign ions. It was observed that the potential remained stable in the 5.0×10^{-2} *f* phthalate solution at *p*H 7.05 until the sulfate-ion concentration reached 3.3×10^{-2} *f*, when instability developed. In the similar test with phthalate 5.0×10^{-3} *f* at a *p*H of 6.08, addition of sulfate to a concentration of 4×10^{-3} *f* caused immediate debasing. The fall of potential in phthalate solutions was so irregular as to make it uncertain whether a halt sometimes observed in the vicinity of the calculated Flade potential was significant. In any event, complete passivation was achieved under the conditions indicated.

TABLE I

PASSIVATION IN SOLUTIONS OF NON-OXIDIZING INHIBITORS, 20–23°

Inhibitor	*p*H	Potential mv. (S.C.E.)	Flade potential calcd. mv. (S.C.E.), 20°
Phthalate, 5.0×10^{-3} *f*	6.08[a]	+10	−16
Phthalate, 1.0×10^{-2} *f*	5.80[b]	[c]	0
Phthalate, 1.0×10^{-2} *f*	6.20[a]	−55[d]	−22
Phthalate, 1.0×10^{-2} *f*	6.22[b]	+115	−23
Phthalate, 2.5×10^{-2} *f*	5.92[b]	+81[e]	− 6
Phthalate, 5.0×10^{-2} *f*	7.05[a]	−17	−72
Benzoate, 1.05×10^{-2} *f*	5.60[a]	+35	+12
Benzoate, 1.05×10^{-2} *f*	5.60[a]	+40	+12
Benzoate, 1.00×10^{-2} *f*	5.35[b]	+71	+27
Benzoate, 1.16×10^{-2} *f*	5.13[a]	+102	+39
Benzoate, 1.16×10^{-2} *f*	5.13[a]	+116	+39
Benzoate, 1.25×10^{-2} *f*	4.80[a]	Active	..
Benzoate, 1.00×10^{-1} *f*	5.40[b]	+ 3	+24
Phosphate, 4.8×10^{-3} *f*	7.20[a]	−55	−81
Phosphate, 1.0×10^{-2} *f*	7.11[b]	−78	−76
Phosphate, 1.0×10^{-1} *f*	7.02[b]	−60	−69
Phosphate, 1.0×10^{-1} *f*	7.02[b]	− 9	−69

[a] Aerated; [b] Oxygenated. [c] In 90 min. potential rose to −10 mv., then fell to −70 mv., with formation of a slight turbidity in 3 days. [d] Stable and electrode remained bright, although the potential never reached the Flade potential; the solution was clear after 3 days. [e] Visible film and solution had perceptible brown coloration; weak test for Fe^{3+}.

With fully aerated and buffered benzoate solutions, as with the phthalate solutions, the range of concentrations and *p*H values within which complete passivation is possible is rather limited. Thus, a 1.25×10^{-2} *f* benzoate solution at *p*H 4.80 left the metal at an active potential in four tests. With 1.0×10^{-2} *f* benzoate solution in the *p*H range of 5.0 to 7.5 and thoroughly aerated or oxygenated, the potential in various experiments rose well above the Flade potential (Table I). The potentials again became unstable when a sufficient concentration of sulfate ions was present, and definite halts very close to the Flade potential were obtained during the activation, as seen for four experiments in Fig. 1, for *p*H values of 5.27, 5.60 and 5.70, respectively. These experiments supplement the results previously reported for inorganic inhibitors and extend the relationship between *p*H value and Flade potential in inhibited systems to slightly lower *p*H values.[22,23]

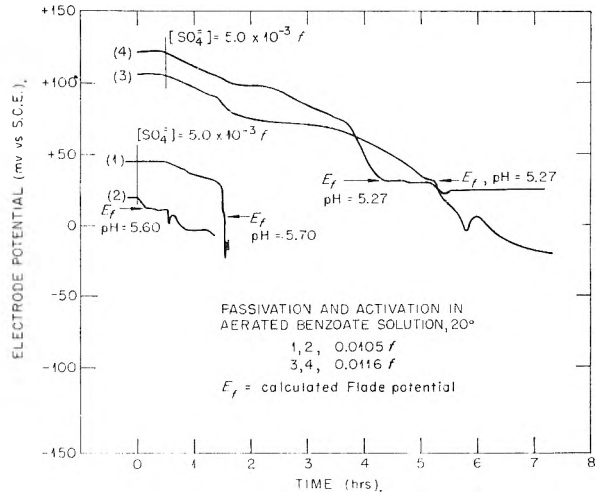

Fig. 1.—Potential-time curves for activation of iron passivated in aerated benzoate solutions. Flade potentials are calculated from $E_f = 338 - 59$ *p*H mv. *vs.* S.C.E.

For the phosphate solutions, phosphoric acid was diluted with triply distilled water and neutralized by sodium hydroxide to give solutions of various concentrations and *p*H values. With rapid oxygenation, passivation was not obtained in 5.0×10^{-2} *f* solutions at *p*H's of 5.68 or 6.61. Between 5×10^{-3} *f* and 1.0×10^{-1} *f*, passivation above the calculated Flade potential was usually attained when the *p*H value was 7 or somewhat higher. Certain data are shown in Table I. In a 4.8×10^{-3} *f* solution at *p*H 7.20, sensitivity to added sulfate ions was demonstrated. The passive potential (−55 mv.) was maintained only 12 min. after addition of potassium sulfate to a concentration of 1.4×10^{-2} *f*. There was no evidence of a halt at the Flade potential during the ensuing activation.

Discussion

These experiments demonstrate that the attainment of passive potentials does not require reduction of the inhibitor itself, since neither of the three inhibitors used is reducible under the conditions in effect. Furthermore, the passivity produced was shown to be destroyed by small concentrations of sulfate ions, as was previously shown for oxidizing inhibitors.[17,18] With benzoate, at least, there was an indication of a Flade potential, though, unfortunately, the *p*H range in which passivation may be attained barely extends into the region in which the inhibitor is well buffered, so that the experiments were necessarily limited to a narrow range of acidities. At any rate, it is clear that oxygen even at 0.2 atm. pressure can produce passivation very effectively without the help of an

(21) U. F. Franck, *Z. Naturforschg.*, **4a**, 378 (1949).

(22) G. H. Cartledge and R. F. Sympson, THIS JOURNAL, **61**, 973 (1957).

(23) The irregularities in certain of the curves of Fig. 1 would leave some doubt as to the significance of halts near the theoretical Flade potential were it not for the cumulative evidence of many previous experiments with four other inhibitors, as given in ref. 22. The experiments were necessarily conducted under marginal conditions between activation and passivation, and the curves clearly demonstrate the effects of the opposed processes in operation. At *p*H values of 6 or higher the reactions associated with the Flade potential are known to be sluggish and somewhat erratic, but use of the experimental relation between E_f and *p*H at the values of *p*H required for passivation in phthalate and phosphate solutions seems to be justified by the experiments on molybdate and tungstate[22] around *p*H 7, even though no reliable halts were observed with phthalate and phosphate solutions. According to these measurements, the Flade potential is a property of the iron-film-proton system, and not of the inhibitor, unless it be in a secondary effect.

oxidizing inhibitor, provided a non-oxidizing inhibitor is present under suitable conditions of concentration and acidity. Although the *p*H value is a crucial condition, the failure of the perrhenate ion[24] or most other anions to inhibit in the same range of acidities shows that the maintenance of a low acidity is not the sole reason for the effectiveness of the anions which do inhibit. The experiments do not of themselves show what the specific effect of the inhibitor is, but definitely eliminate the requirement that it shall contribute directly to the cathodic process by which the noble mixed potential is achieved. The results are consistent with the hypothesis that competing adsorption is involved.

Cathodic Processes on Passivated Iron.—Previous experiments have shown that passivation in a chromate solution in contact with air gives a film containing both iron and chromium, with the iron compound predominating.[3,25] If the specimen is first exposed to air, less chromium is taken up.[16] The amount of chromium in the film is also a function of the acidity, becoming less as the *p*H value increases.[16,26] The chromium taken up was shown by autoradiography to be rather uniformly distributed over the surface when an active specimen was passivated, except that higher concentrations of radioactivity were found at inclusions, scratches, or other active sites.[3] Similar observations were made when TcO_4^- was used as inhibitor.[9,13] It is unfortunate that, in the experiments with $Cr^{51}O_4^=$, no experimental differentiation between adsorbed $CrO_4^=$ and $Cr(OH)_3$ or Cr_2O_3 precipitated by reduction has been made, except that Brasher and De[15] considered that their data indicated approximately a monolayer of $CrO_4^=$ to be quickly adsorbed, while a slow reduction continues over long periods of time. Cohen and Beck[3] found a considerably larger uptake from Na_2CrO_4 (50 p.p.m.) within the first few minutes (up to 15 min.) on surfaces freshly reduced in hydrogen. Their data refer to the rapid initial action of some chromate species upon active iron or an iron(II) oxide when oxygen is either absent or limited by diffusion control from exerting its full effect. The situation is different after the fast initial reaction is ended and passivity is to be maintained at the more noble potential. The reported results therefore leave it somewhat uncertain to what extent the chromate ion is actually reduced in the maintenance of passivity, and, whatever the amount may be, they give no basis for deciding whether such reduction as actually occurs is the primary source of the continuing inhibitory action in the presence of oxygen.

The experiments of the preceding section demonstrated the ability of oxygen at atmospheric pressure or less to produce passivity in the presence of inhibitors that are unable of themselves to supplement the cathodic current available from reduction of oxygen. Further studies were therefore made to determine quantitatively the relative contributions of oxygen and a reducible inhibitor to the total cathodic current passing when a passivated iron electrode is cathodically polarized at potentials in the neighborhood of the Flade potential, under conditions of concentration and acidity that permit passivation before application of current. It was thought that such measurements should give results bearing on the role played by a reducible inhibitor in the maintenance of passivity, —that is, whether it actually adds significantly to the available cathodic current according to the proposal of references 2 and 5, or acts by some other mechanism, as is necessarily true of the inhibitors devoid of oxidizing properties. As a background for these studies, measurements of the cathodic polarization of iron electrodes passivated in oxygenated phthalate solutions were made. Here the possible cathodic processes are reduction of either oxygen (perhaps *via* HO_2 and H_2O_2) or the components of the passive film itself, with ensuing activation. The potentials used were too noble for reduction of protons to be a factor, and use of triply distilled water and pre-electrolyzed phthalate solutions eliminated significant concentrations of other reducible species.

Experimental

The galvanostatic procedure was used in making cathodic polarizations under conditions which preceding experiments showed to be requisite for maintenance of passivity. Polarizing current was drawn from a battery of up to 135 volts through high resistances, and the current was determined from the drop in potential across suitable precision resistors. Potentials were measured by use of a Vibrating Reed Electrometer or a Leeds and Northrup *p*H Indicator coupled to a Brown Recorder. Polarizations were made at the constant room temperature of 24°. The cathodes were strips of electrolytic iron having an area of approximately 1 cm.^{2}. Before use, they were abraded with 2/0 emery, scrubbed in water, and then degreased with acetone. Just before the start of an experiment, film formed during storage of the electrode in an oven at 110° was removed by treatment with 1 *N* H_2SO_4 until the surface brightened. A Haber–Luggin capillary and bridge led to a flask containing a solution of the same composition as that in the cell. A saturated calomel electrode dipped into the solution in the flask. The anode was platinum; to avoid changes in acidity, the electrodes were in the same cell.

The phthalate stock solution was prepared from buffer-grade potassium hydrogen phthalate, which was dissolved in triply distilled water from a silica duplex still. This solution was pre-electrolyzed in a stream of helium with platinum electrodes in a divided cell. In the first experiments, the catholyte from a 24–36 hr. electrolysis was again electrolyzed anodically. It was found, however, that if this electrolysis was conducted at too high a current density the product contained a trace of some reducible impurity which manifested itself by a distortion of the subsequent cathodic polarization curves at the lowest current densities used. Since the anodic pre-electrolysis was found not to change the general results of the polarization measurements, it was subsequently omitted. After cathodic pre-electrolysis, the solutions required very little sodium hydroxide to bring them to the desired *p*H values. During polarizations in oxygen, cylinder gas was passed successively through a long column of Ascarite, a tube packed with glass wool, and a water saturator.

Results

In preliminary measurements it was demonstrated that cathodic polarization of well-inhibited passive specimens in oxygen can usually be carried at least 150 mv. below the Flade potential without activation during the time required for the experiment. It was found also that the open-circuit

(24) G. H. Cartledge, THIS JOURNAL, **60**, 32 (1956).

(25) J. E. O. Mayne and M. J. Pryor, *J. Chem. Soc.*, 1831 (1949).

(26) R. A. Powers and N. Hackerman, *J. Electrochem. Soc.*, **100**, 314 (1953).

potential before polarization varied somewhat with the conditions of passivation, particularly with respect to the amount of iron that was allowed to accumulate in the solution before passivation was complete. If the *p*H value was much below 6 and the phthalate solution too concentrated, brown solutions and visible films on the electrodes resulted. In the measurements to be presented, the solutions were 0.0100 *f*, *p*H was close to 6.0, and the electrolyte in the cell was replaced with fresh solution at least once, and usually two or three times, before polarization of the passive electrode was started. Under these conditions the electrode remained bright and the solution was colorless.

Since passivation in phthalate solutions is achieved only at *p*H values as high as approximately 6, deviations from Tafel lines became apparent at current densities in the neighborhood of 10^{-5} amp./cm.^{2}, owing, presumably, to depletion of oxygen or hydrogen ions required for the reduction reaction. Further, the steady-state corrosion current density of passive iron in 0.05 *f* phthalate at *p*H 6 was reported by Weil and Bonhoeffer[27] to be approximately 2×10^{-7} amp./cm.^{2} and to be constant over a wide range of potentials. The present measurements indicated steady-state corrosion rates of the same order of magnitude or somewhat less, hence it was possible to utilize data obtained at the lowest current densities by correcting them, when necessary, for a constant anodic current density in the range of 10^{-7} – 10^{-8} amp./cm.^{2}, depending upon the conditions.

In Fig. 2, the curve marked IV-1 is representative of the polarization data obtained in numerous series of measurements on passivated electrodes. The Flade potential calculated for *p*H 6.0 (at 20°) is −11 mv. (S.C.E.), and it is clear that a normal polarization curve was obtained to as low as −140 mv. S.C.E. Curve V-A,3 shows the open-circuit potential, E_c, and three points determined potentiostatically on a different electrode in 0.0100 *f* phthalate, also at *p*H 6.0. When the polarizations were measured first with increasing cathodic current, the potential quickly returned to points on the curve upon diminishing the current. Such points are indicated on curve IV-1 by squares. Different electrodes passivated spontaneously to open-circuit potentials that ranged from approximately the Flade potential to +125 mv., S.C.E., with indicated steady-state corrosion rates that varied from about 10^{-8} to 3×10^{-7} amp./cm.^{2}. Tafel slopes averaged 70 ± 6 mv./decade in 14 polarizations with 5 electrodes variously treated in successive measurements. At −75 mv. S.C.E., the average current density for these 14 polarizations was $3.6 \pm 1.4 \times 10^{-7}$ amp./cm.^{2}. This value occasionally was as high as 2×10^{-6} amp./cm. when a specimen was first polarized.

For comparison, Fig. 2 shows a polarization curve for reduction of oxygen on a smooth platinum electrode in 0.011 *f* phthalate at *p*H 5.51. Before use, the electrode was cleaned in a mixture of HCl and H_2O_2. Rapid response to changes in

(27) K. G. Weil and K. F. Bonhoeffer, *Z. physik. Chem., N.F.*, **4**, 175 (1955).

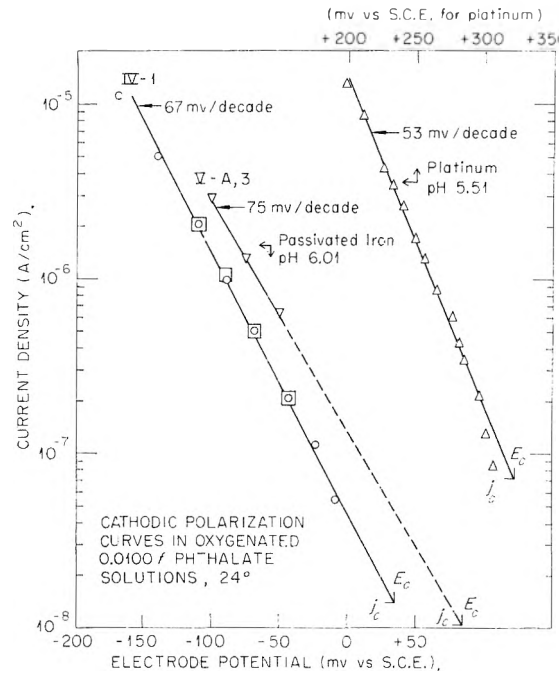

Fig. 2.—Cathodic polarization of passive iron or platinum electrodes in oxygenated phthalate solutions. Curves are extrapolated to E_c and j_c, which are the observed steady-state open-circuit potential and indicated current density, respectively. Current densities are in amperes per cm.^{2} of apparent surface. ▽, points established potentiostatically; ⊙, galvanostatic data for a different electrode; ⊡, points determined with decreasing current density.

current density and stable potentials were obtained when the electrode was first used. After standing overnight in the phthalate solution the electrode had lost some of its activity. The open-circuit potential and indicated pseudo-exchange current are most likely associated with the oxidation of some organic material, as mentioned in connection with anodic pre-electrolysis.

The deleterious effect of sulfate ions on the passivating inhibitors was clearly confirmed by addition of sodium sulfate during a polarization measurement. Thus, a passivated iron electrode was given a test polarization; it showed typical behavior from its corrosion potential of +60 mv. S.C.E. to −168 mv. at a current density of 5.05×10^{-6} amp./cm.^{2}. Current was then cut off and the electrode stabilized overnight to a potential of +89 mv. S.C.E. Potassium sulfate was added to make the phthalate solution 5×10^{-3} *f* in sulfate and a polarizing current density of 1.12×10^{-7} amp./cm.^{2} was applied. The potential fell rapidly at first, retarded at a value which fell near the Tafel line previously obtained, and then debased irregularly to an unsteady, oscillating value approximately −165 mv. S.C.E. The potential remained almost unchanged while the current density was increased to 5.02 to 10^{-6} amp./cm.^{2}, when activation set in. When the current was cut off, the specimen failed to become repassivated and subsequently corroded heavily.

Discussion

The rapid re-ennobling of the electrode potential on diminution of the applied cathodic current and the stability of the observed potentials at the cur-

rent densities used indicate that reduction of the passive film itself was unimportant kinetically by comparison with the reduction of oxygen. Incomplete studies in the benzoate system show that the general relationships are similar to those in the phthalate system, with some differences in detail.

For passivation to be maintained in the absence of an externally applied current it is necessary that the cathodic current density available from the effective passivator exceed the steady-state corrosion current density; that is, the polarization curve for reduction of the passivator must intersect the polarization curve of iron at a potential more noble than the Flade potential.[28] The steady-state corrosion rate varies with the nature and concentration of the electrolyte, as well as with *p*H, as may be seen by comparing the phthalate data of Weil and Bonhoeffer[27] with Vetter's data for sulfate solutions.[29] From the present experiments it is clear that at *p*H values appreciably below 6 in phthalate solutions of 5×10^{-3} to 5×10^{-2} *f* the oxygen current is inadequate for complete passivation, whereas it is ample at *p*H 6 or higher.

By extrapolation from Fig. 2 it is seen that, in the region of passive iron potentials, reduction of oxygen on the platinum electrode exceeded that on the iron electrode by a factor of about 10^4. This is a demonstration of an effect similar to that of platinum on the passivation of stainless steel, as discussed by Tomaschow,[30] and by Stern and Wissenberg[31] for platinum and titanium.

(28) This assumes the validity of Vetter s demonstration that the passive film is free of pores, so that both the anodic and cathodic processes operate over the same total area. *Cf.* K. J. Vetter, *Z. Elektrochem.*, **55**, 274 (1951).

(29) K. J. Vetter, *ibid.*, **59**, 67 (1955).

(30) N. D. Tomaschow, *ibid.*, **62**, 717 (1958).

(31) Milton Stern and Herman Wissenberg, *J. Electrochem. Soc.*, **106**, 759 (1959).

If the curves of Fig. 2 are extrapolated to the corresponding reversible oxygen electrode potentials, it may be estimated that the exchange currents are of the order of 10^{-14} amp./cm.^{2} on the platinum surface and 10^{-18} amp./cm.^{2} on passive iron. These numbers may be compared with 10^{-9} to 10^{-10} amp./cm.^{2} found by Bockris and Huq[32] for smooth platinum in sulfuric acid of *p*H 1.25, and 10^{-20} amp./cm.^{2} obtained by extrapolation of the data of Wade and Hackerman[33] on passive iron at 5° and at *p*H 4.

The present measurements therefore show that oxygen alone at 1 atm. or less is reduced rapidly enough on a passive iron electrode to maintain the mixed potential in the passive region in spite of a continuing corrosion current density, which is of the order of $10^{-7} - 10^{-8}$ amp./cm.^{2} in the phthalate system at *p*H 6. The non-oxidizing inhibitor is essential, however, and its effectiveness is disturbed by the addition of foreign ions such as the sulfate ion, which sensitize the system to activation. Since it is difficult to see how such ions enter directly into the electrochemical processes at the low concentrations involved, it seems most reasonable to assume that they compete with oxygen or inhibitor at sites that are active in the electrochemical reactions. In the following paper, the degree of participation of a reducible inhibitor in the total cathodic process will be examined.

Acknowledgment.—It is a pleasure to acknowledge helpful discussions with my colleagues, E. J. Kelly, R. E. Meyer and Franz A. Posey in connection with this series of studies.

(32) J. O'M. Bockris and A. K. M. S. Huq, *Proc. Roy. Soc.* (*London*), **A237**, 277 (1956).

(33) W. H. Wade and N. Hackerman, *Trans. Faraday Soc.*, **53**, 1 (1957).

THE COMPARATIVE ROLES OF OXYGEN AND INHIBITORS IN THE PASSIVATION OF IRON. II. THE PERTECHNETATE ION

BY G. H. CARTLEDGE

Chemistry Division, Oak Ridge National Laboratory, Operated by Union Carbide Corporation for the U. S. Atomic Energy Commission, Oak Ridge, Tennessee

Received May 7, 1960

Galvanostatic and potentiostatic polarizations of passive iron electrodes have been made in solutions of a phthalate or pertechnetate and mixtures of them. By measuring the polarizations both in oxygen and in essentially oxygen-free helium the relative contributions of oxygen and the reducible inhibitor to the total cathodic current have been determined. An acceleration of the cathodic processes by the reduction product of the pertechnetate ion was demonstrated. It was shown also that, in all cases, reduction of oxygen is the principal cathodic process at passive potentials.

The preceding paper in this series[1] demonstrated that passivation of iron can be achieved under the oxidizing action of oxygen alone at atmospheric pressure, provided a suitable non-oxidizing inhibitor is present. When a reducible inhibitor is available, it may supplement the cathodic current due to reduction of oxygen, and some reduction of such inhibitors is generally observed. The purpose of this study is to determine the extent to which the inhibitor itself is reduced under passivating conditions, in comparison with the reduction of oxygen under a total pressure (including water vapor) approximating 1 atm. For this purpose, the pertechnetate and chromate ions and osmium(VIII) oxide have been used as inhibitors.

The pertechnetate ion differs in important ways from the chromate ion with respect to properties that are important for theories of inhibition which assume oxidizing and precipitating power as the

(1) G. H. Cartledge, THIS JOURNAL, **64**, 1877 (1960).

essential requirement for an inhibitor. The pertechnetate ion, TcO_4^-, is univalent and derives from a strong acid. It therefore does not have the buffering action possessed by the chromate ion. The normal oxidation–reduction potential of the couple, $TcO_4^- + 4H^+ + 3e^- \rightleftarrows Tc(OH)_4$(ppt.), is 0.738 v. noble to the normal hydrogen electrode,[2] in comparison with a calculated value of 1.246 v. for the couple, $CrO_4^= + 5H^+ + 3e^- \rightleftarrows Cr(OH)_3 + H_2O$. For 10^{-3} *f* solutions at *p*H 6, the calculated reversible potentials for these couples are 0.20 and 0.59 v. for technetium and chromium, respectively. The chromate ion is therefore energetically a more vigorous oxidizing agent under conditions in which inhibition is very efficient. It also possesses good buffering action in the $CrO_4^= + H^+ \rightleftarrows HCrO_4^-$ equilibrium, and is therefore able to precipitate ferrous ions possibly arising from corrosion, as shown by Hoar and Evans.[3] Similar action by the pertechnetate ion is not possible thermodynamically under conditions which yet permit inhibition in aerated solutions.[4]

For an inhibitor to be effective in maintaining passivity by virtue of its own oxidizing action it is necessary that its reduction rate on the passive surface and at passive potentials be adequate to balance the corrosion still occurring. In the present experiments, therefore, cathodic polarizations of a passivated electrode have been made to establish the relative reduction rates of oxygen and the inhibitors mentioned.

Experimental

The measurements involved essentially the establishment of cathodic polarization curves for passive iron electrodes in inhibited systems when fully oxygenated and again when oxygen was reduced to a very low concentration by passage of a rapid stream of "oxygen-free" helium through the closed cell. In view of the results of the preceding paper,[1] 0.0100 *f* phthalate at about *p*H 6 was used as a medium for establishing the reliability of each electrode used. All phthalate solutions were pre-electrolyzed as previously described. The potassium or ammonium pertechnetate used had been repeatedly recrystallized and was very pure spectroscopically, but for obvious reasons could not be pre-electrolyzed. Solutions of these salts were prepared in triply distilled water. Measurements were made as in the previous work. The electrodes were from the same batch of electrolytic iron and the abraded and air-oxidized surfaces were activated by treatment with 1 *N* H_2SO_4 just before passivation. Polarizations were measured only in solutions that had been introduced to the cell after completion of passivation. The temperature was 23–24°. Helium, when used, was passed through freshly reduced copper turnings held at 425°, then through Ascarite, a cotton filter and a water saturator. Measurements were begun only when the electrode potential had become stable 16 hr. or more after the beginning of passivation. In most cases the galvanostatic procedure was used to establish the entire polarization curve, but in later series of experiments only the open-circuit potential and the steady-state current density at three suitable potentials were determined. As was pointed out in the preceding paper, galvanostatic measurements at the lowest current densities were corrected, when necessary, by taking account of a constant corrosion current density empirically determined to bring such points on a linear log $j - E$ curve in agreement with the values at the open-circuit potential. In the potentiostatic measurements, the chosen potentials obviated this necessity and also fell at current densities at which diffusion had not become a factor. For conven-

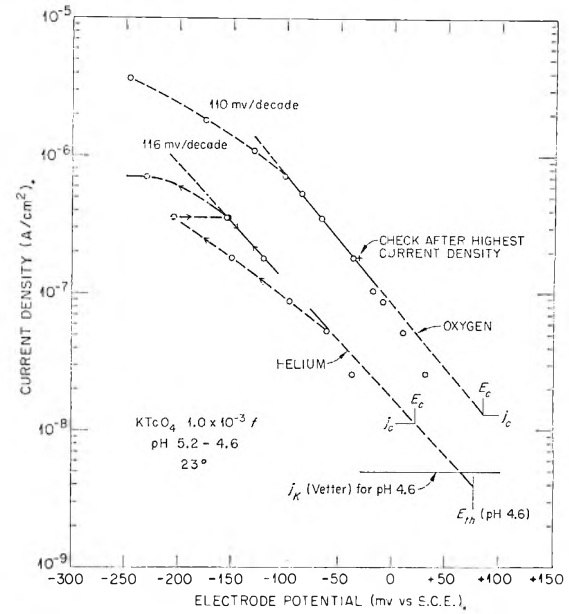

Fig. 1.—Cathodic polarization of passive iron in a pertechnetate solution in oxygen or in helium. E_o and j_c are the observed open-circuit potential and indicated corrosion current density, respectively. E_{th} is the calculated reversible potential of the Tc(VII)–(IV) couple for the conditions prevailing.

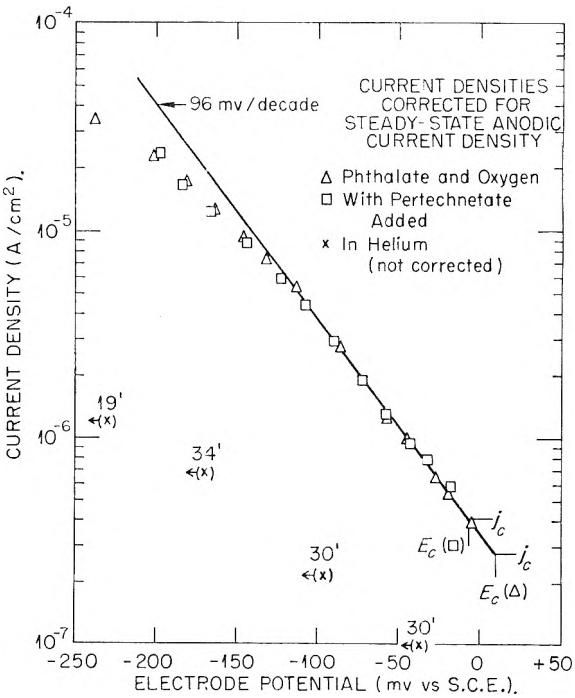

Fig. 2.—Cathodic polarization of passive iron in 1.00×10^{-2} *f* phthalate at *p*H 6.18, in oxygen, and in a mixture 1.00×10^{-2} *f* each in phthalate and pertechnetate at *p*H 6.13, in oxygen or in helium.

(2) G. H. Cartledge and Wm. T. Smith, Jr., *ibid.*, **59**, 1111 (1955).

(3) T. P. Hoar and U. R. Evans, *J. Chem. Soc.*, 2476 (1932).

(4) This conclusion was verified in an experiment for which the author is indebted to Dr. R. F. Sympson. The reactants were thoroughly deaerated and mixed in a vacuum system. No precipitate formed in five hours at room temperature, although the concentrations and *p*H value were such that corrosion of iron would have been inhibited. Slight precipitation occurred after opening the mixture to air for five days, but beta counting showed the well-washed precipitate to contain only of the order of 0.003% of the amount of technetium that would have been reduced had the total precipitate been due to reduction of pertechnetate ions. The experiment makes it clear that inhibition by the pertechnetate ion, which occurs at lower concentrations than are required in the case of chromate, cannot be ascribed to any power of precipitating ferrous ions.

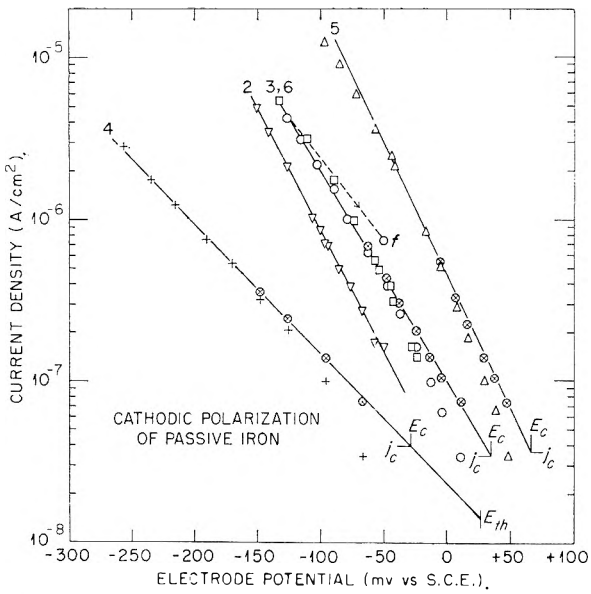

Fig. 3.—Cathode polarizations of Series II-A2-6: 2, ▽, oxygenated $1.00 \times 10^{-2} f$ phthalate, *p*H 6.00, second of duplicate measurements; 3, ⊙, oxygenated $1.00 \times 10^{-2} f$ pertechnetate, *p*H 5.95; 4, +, same in helium; 5, △, same in oxygen; 6, ⊡, same after removal of $Tc(OH)_4$ by anodic polarization. At low current densities, data points fall below the curves and points corrected by 4×10^{-8} amp./cm.² are indicated by ⊗'s.

ience in presenting the data, a potential of −75 mv. S.C.E. will be chiefly used.

When it became apparent that the reduction product from the pertechnetate ion influenced the rate of the reduction processes, several series of measurements were conducted with the design of establishing this effect definitely. The properties of technetium and its compounds make it eminently suitable for such a study, since the amount on an electrode may be determined from a count of beta activity, and cathodically deposited $Tc(OH)_4$ may be removed essentially quantitatively either by treatment with H_2O_2 or, more conveniently, by anodic oxidation to TcO_4^- without removal of the electrode from the cell.[5] One unfortunate property of a freshly reduced deposit of $Tc(OH)_4$ is its slow oxidation even by oxygen, so that it is not possible to keep an entirely constant quantity on an electrode during a polarization measurement in which amounts of a monolayer or less may be involved.

The following series of measurements were made: Series O: exploratory polarizations in $1.00 \times 10^{-3} f$ $KTcO_4$, first in oxygen, then in helium (Fig. 1); Series I: polarizations successively in oxygenated phthalate (Fig. 2, △); the same with $KTcO_4$ added (⊡); the same mixed electrolyte, but in helium (x); Series II: initial polarization in oxygenated phthalate (Fig. 3, curve 2); then in pertechnetate in oxygen (curve 3), in helium (curve 4), in oxygen (curve 5), and again in oxygen after removal of deposited $Tc(OH)_4$ by an anodic polarization (curve 6); Series III: polarizations in oxygenated phthalate only, before and after anodic treatment of the electrode; Series IV: polarization in confirmation of the effect of added sulfate ions[1]; Series V: potentiostatic measurements to establish (a) the comparative rates of the cathodic processes in a pertechnetate solution with and without oxygen, and (b) the accelerating effect of $Tc(OH)_4$ precipitated on the electrode.

Galvanostatic Measurements.—In Series O, the polarizations were made in potassium pertechnetate alone, first in oxygen and then in helium. Owing to scarcity of the material at the time, only a $1.0 \times 10^{-3} f$ solution at an initial *p*H of 5.2 could be used. Hence both iR drops and concentration polarization were encountered at current densities exceeding about 7×10^{-7} amp./cm.². Also, the solution being unbuffered, the *p*H value inevitably changed slightly during the measurements. Nevertheless, sufficient data were obtained to be significant and a typical set of data is shown in Fig. 1. In oxygen, the reproducibility was good and stable potentials were quickly established. The Tafel line had a slope of 110 mv./decade, the four points at lowest current density falling on the line if corrected by addition of the indicated corrosion current density of 1.5×10^{-8} amp./cm.².

When polarization was attempted in helium, the behavior of the system differed sharply from that in oxygen. After the two points at lowest current density had been obtained, the electrode showed incipient instability, but after a time at a current density of 3.6×10^{-7} amp./cm.² spontaneously ennobled to the point shown on the apparent Tafel line. (The probable reason for this behavior became evident from later results, as will be shown below.) The current density was reduced to 1.8×10^{-7} amp./cm.², giving another point on the curve. Upon increasing the current density again, the point at 3.6×10^{-7} amp./cm.² was closely duplicated. It was apparent that the system was initially very sluggish, in comparison with the oxygenated system. At the end of the measurements, *p*H had fallen to 4.6. Although oxygen was excluded as far as possible, it is certain that small traces were present, so that, considering the small currents involved, the curve shown for helium represents an upper limit for both the reduction current density of the pertechnetate ion and the indicated exchange current density of the Tc(VII)–(IV) couple. (E_{th} in Fig. 1 represents the calculated reversible potential of this couple at the conditions prevailing.[2]) It is evident that the corrosion current density, j_c at *p*H 4.6 is sufficient to produce an appreciable polarization of this couple potential.

In series I, the effect of displacing oxygen by helium was determined, the three requisite polarization curves being shown in Fig. 2. The curves plotted were obtained by using an anodic correction of 3×10^{-7} amp./cm.² for the phthalate solution and 5×10^{-7} amp./cm.² for the mixture. It was again observed that the helium system responded very slowly to changes in current density, non-steady states being shown for the observation times indicated. After the polarization in helium, the cell was left on open circuit in helium for 16 hr. and oxygen was then passed for 2 hr. The potential re-ennobled very rapidly. The electrode was subsequently washed and its technetium content was found by β-counting to be 0.27 μg. of Tc. This corresponds to 1.6×10^{15} atoms on an area of 0.90 cm.². The activity was reduced to 0.027 μg. by one washing with ammoniacal H_2O_2. Both the position of the non-steady potentials in helium and the rapid re-ennobling upon admission of oxygen indicate again that oxygen is the principal source of cathodic current when it is present along with phthalate and pertechnetate ions.

In Series II of the galvanostatic measurements an electrode was cathodically polarized in the sequence indicated by the legend of Fig. 3. In this figure the data for the first polarization are omitted, since they differed from the duplicate (2) by only a few millivolts at each current density. Corrections for anodic current were applied at the lowest current densities, as previously discussed. The total charge passed in the experiment with helium was approximately 4.0×10^{-3} coulomb. In the anodizing at the end of experiment (5) a charge of 5.7×10^{-3} coulomb was passed, and it is seen that the curve for experiment (6) then coincides rather closely with that of (3), which was conducted under the same conditions. As seen in the figure, the measurements in helium gave a good curve with satisfactory steady states, the duplicate polarizations in oxygenated pertechnetate (3) evidently having deposited sufficient $Tc(OH)_4$ to catalyze the reduction of pertechnetate ions. It is again evident that, with precipitated $Tc(OH)_4$ on the electrode in the amount here present, the current in oxygen exceeded that in helium by from 1 to 2 orders of magnitude (curves 5 *vs.* 4).

In Series III, it was determined that the anodic treatment of an electrode on which no $Tc(OH)_4$ was present produced no significant change in the polarization curve. For this purpose a new electrode was passivated in $1.00 \times 10^{-2} f$ oxygenated phthalate at *p*H 6.07. Duplicate determinations on successive days gave closely agreeing curves, the second polarization being shifted approximately 6 mv. negative to the first. After completion of the second polarization the electrode was made anode for 8 min., during which time 1.0×10^{-2} coulomb passed, the potential

(5) G. H. Cartledge, THIS JOURNAL, **59**, 979 (1955).

rising above 1 volt S.C.E. A third cathodic polarization was then applied after the potential became stable, and a Tafel curve was obtained which was no more than 5 mv. negative to the previous one. This demonstrates that the large negative shift observed in Series II (6 *vs.* 5) upon anodizing the electrode must have been due to the removal of the deposit of $Tc(OH)_4$.

Further demonstration of the activating effect of $Tc(OH)_4$ on the cathodic processes was furnished by the following observations. A series of galvanostatic polarizations was made in 2.5×10^{-3} *f* TcO_4^- at *p*H 5.87. The electrode was first freed of $Tc(OH)_4$ from previous use by an anodizing treatment, and after stabilization of the open-circuit potential gave a normal polarization curve in oxygenated solution (1.2×10^{-6} amp./cm.^{2} at −75 mv. S.C.E.). The electrode was again anodized briefly and an attempt was made to polarize it in helium. Even on open circuit the potential fell steadily from +25 mv. S.C.E. to −250 mv., and upon application of a cathodic polarization of 2.81×10^{-7} amp./cm.^{2} debased further to −380 mv. The current density was gradually increased to 1.98×10^{-5} amp./cm.^{2} over a period of 17 min., the potential reaching −480 mv. The potential rose at first only to −340 mv. when the current was shut off, but when oxygen was admitted repassivation to +27 mv. S.C.E. occurred in the next 22 min. and to +125 mv. overnight. In a polarization the following day in oxygen, the electrode was very active cathodically, the current density at −75 mv. S.C.E. being 2.5×10^{-6} amp./cm.^{2}, which is 21 times the value observed in the first polarization.

In another experiment, a freshly anodized electrode activated when polarized at a current density of 3.28×10^{-7} amp./em.^{2} in a pertechnetate solution under helium, the potential falling to −505 mv. S.C.E. The next polarization was conducted in oxygenated phthalate solution (1.00×10^{-2} *f*, *p*H 6.07) without removal of the $Tc(OH)_4$ formed while the electrode was active. The current density was carried as high as 2.5×10^{-4} amp./cm.^{2} without activation, and points falling within 2–3 mv. of the curve obtained with increasing current density resulted when the current density was reduced to 1.24×10^{-5} and 7.10×10^{-7} amp./cm.^{2}. It is evident from these observations also that reduced $Tc(OH)_4$ accelerates the reduction of both oxygen and the pertechnetate ion.

Final Potentiostatic Measurements.—The general results of the galvanostatic polarizations were (a) that the current required to polarize an electrode to a given potential is much less in helium than it is in oxygen and (b) that the activity of the electrode for the cathodic processes is modified by the presence of reduced $Tc(OH)_4$ on the surface. This made it difficult to obtain exact comparisons between the values for the cathodic current in different environments, since fairly long times are required to complete a galvanostatic polarization over a considerable range of current densities, during which time the amount of $Tc(OH)_4$ will be either increasing or decreasing, according to circumstances. For this reason the galvanostatic experiments were supplemented by a final series of potentiostatic polarizations at potentials of −50, −75 and −100 mv. S.C.E. This made it possible to change the electrolyte or the atmosphere rather quickly and consequently to measure the currents with minimum change in the state of the electrode.

Table I shows the sequence of potentiostatic polarizations and the results obtained in Series V-A. Initial measurements in the phthalate solution at −50, −75 and −100 mv. established the reliability of the electrode.

TABLE I

CURRENT DENSITIES AT −75 MV. S.C.E.—SERIES V-A

Electrolyte and conditions	j_{-75} (amp./cm.^{2})
(1) Oxygenated phthalate, 0.0100 *f*, *p*H 6.02[a]	1.33×10^{-6}
(2) TcO_4^- added, 0.010 *f*, *p*H 5.80	1.50×10^{-6}
(3) Same, three days later	1.48×10^{-6}
(4) Same, in helium	$<1.45 \times 10^{-7}$[b]
(5) Same, in oxygen	2.24×10^{-6}[c]

[a] Electrode freshly etched in 1 *N* H_2SO_4; electrolyte renewed after passivation; electrode surface bright, with no visible film. [b] Current fell from 1.48×10^{-6} amp./cm.^{2} to 2.40×10^{-7} amp./cm.^{2} in 14 min.; still falling slowly after 3.2 hr. [c] Current rose to stable value in ten min.

It is evident that addition of TcO_4^- in (2) increased the current density slightly in the oxygenated solution, that displacement of oxygen lowered the current density by more than an order of magnitude, and that subsequent polarization in oxygen gave a higher current density than was required before polarization in helium. This accelerating effect of the reduction product of TcO_4^- no doubt accounts for the behavior described in connection with Fig. 1. In that case, the electrode had been passivated initially in oxygenated pertechnetate, and evidently had sufficient surface activity to give reliable steady states at the lower current densities, but not, initially, at the high ones.

After completion of Series V-A, the electrode was anodized to remove precipitated $Tc(OH)_4$ and a new series, V-B, was started after re-passivation in phthalate and oxygen. The effect of precipitated $Tc(OH)_4$ was confirmed, and the increased current-carrying capacity of the electrode with increasing reduction of TcO_4^- made it apparent that any comparison of these values for different environments would have to be made with minimum passage of time and current. Hence in Series V-C the measurements summarized in Table II were made with this requirement in view.

TABLE II

CURRENT DENSITIES AT −75 MV. S.C.E.—SERIES V-C

Electrolyte and conditions	j_{-75} (amp./cm.^{2})
(1) Oxygenated phthalate 0.0100 *f*, *p*H 6.00	2.11×10^{-7}
(2a) TcO_4^- added, 0.010 *f*, *p*H 6.00	4.18×10^{-7}
(2b) Slow rise to	7.02×10^{-7}
(3) Oxygenated phthalate	3.92×10^{-7}
(4a) TcO_4^- added	5.49×10^{-7}
(4b) Slow rise to	6.65×10^{-7}
(5) Oxygenated phthalate	5.60×10^{-7}[a]

[a] At end of experiment Tc counted 1.5×10^{14} atoms/cm.^{2}.

Before the start of this series, the electrode had been passivated for three days in oxygenated 1.00×10^{-2} *f* phthalate at *p*H 6.00. The solution was changed before beginning the potentiostatic measurements from an open-circuit potential of +125 mv. S.C.E. After polarization in the phthalate solution, the solution in the cell was replaced by the mixture of phthalate and pertechnetate and polarizations were made in the sequence: −50, −75, −100, −75 mv. S.C.E. In Table II, the figure 4.18×10^{-7} amp./cm.^{2} for (2a) represents an essentially stable value for the first polarization at −75 mv. The figure 7.02×10^{-7} amp./cm.^{2} is the still slowly rising value on the second measurement at −75 mv., *i.e.*, after the electrode had been under a polarization of 1.02×10^{-6} amp./cm.^{2} at −100 mv. for 9 min. For the next measurement, the mixed electrolyte was removed, the cell was flushed three times with triply distilled water, and the phthalate solution was returned to the cell as quickly as possible (4 min. elapsed time).

Polarization was immediately resumed at −75 mv., followed by measurements at −50, −75, −100, −75 and −50 mv. S.C.E. The three successive and stable current densities at −75 mv. were 3.92, 3.94 and 3.97 $\times 10^{-7}$ amp./cm.^{2}, respectively. The mixed electrolyte was next quickly returned to the cell and polarized in the sequence: −50, −75, −100, −75 mv. The two values for −75 mv. are given in Table II. Finally, another polarization was made in the simple phthalate solution, after which the electrode was removed, thoroughly washed in running distilled water and counted, as indicated. The technetium found corresponds to about one third of the amount required to form a monomolecular layer if uniformly distributed over the projected area of the electrode.[6]

Discussion

The present experiments and previous related ones permit several conclusions to be drawn con-

(6) When oxygenated phthalate solutions were used after prolonged galvanostatic measurements in a pertechnetate solution, micromolar concentrations of TcO_4^- could be found in the phthalate solution, owing to re-oxidation of $Tc(OH)_4$. In the briefer potentiostatic measurements, this effect was minimized.

cerning passivity in the presence of oxygen and the pertechnetate ion.

(1) Maintenance of passivity by the pertechnetate ion is not caused by precipitation of ferrous ions emerging through imperfections in the film, since neither buffering action nor an adequate oxidation potential is available under conditions which nevertheless permit inhibition to occur. In this respect, the pertechnetate ion behaves even worse than the permanganate ion, which the experiments of Hoar and Evans[3] showed to be incapable of complete precipitation of ferrous ions without addition of alkali, in spite of its strong oxidizing power. Since the salts of pertechnetic acid, excepting the silver salt, are soluble, so far as is known, it is unlikely that a precipitation mechanism can be assumed to be operative in passivation by the pertechnetate ion, as has been done for the phosphate ion.[7]

(2) The polarization curves showed unmistakeably that the reduction of the pertechnetate ion under the conditions employed is at least an order of magnitude slower than that of oxygen, even though the pertechnetate ion was approximately eight times more concentrated. This may be seen in Figs. 1, 2 and 3 alike. In Fig. 3, the point marked f on curve 3 was taken at the end of that series of measurements and shows the activation of the cathodic processes by the precipitated $Tc(OH)_4$ formed during the experiment. This point represents closely the state of the electrode when the measurements were next begun in helium. If the current densities at -50 mv. on curves 4, 3f and 5 are compared, they are seen to be in the ratio of 1:15:50. Similar behavior was observed from the potentiostatic data and the accelerating effect of $Tc(OH)_4$ was confirmed. Thus, in Table II, it may be seen that, with the quickest change of environment and the minimum polarization time to ensure reasonably steady states, the addition of pertechnetate to oxygenated phthalate increased the current density by a factor of approximately 2 (V-C, 1 *vs.* 2a). The current density at -75 mv. in (2a) rose as a result of polarization at -100 mv., and then diminished by a factor of 1.8 when the mixed electrolyte was replaced by phthalate alone. In the final polarization in phthalate only, the current density was 2.6 times as great as the value obtained in the first polarization in the same environment, even though only a minute amount of $Tc(OH)_4$ was found on the electrode.

(3) The observed acceleration of the cathodic processes by a deposit of $Tc(OH)_4$ on the electrode means either that the effective surface is considerably increased by its presence or that a new reaction path of lowered activation energy is made available. Since an amount equivalent to less than a monolayer exerted a very appreciable effect, the first explanation could be valid only if a small fraction of the surface were normally active in the reduction processes. A similar acceleration has been observed to arise from deposition of the reduction product of OsO_4, but not from reduction of chromates.[8] It therefore seems more likely that the effect is to be ascribed to an increased specific reaction rate possibly associated with intermediates derived from two reactive electronic configurations of Tc–O or Os–O complexes at the surface.

(4) Since precipitated $Tc(OH)_4$ accelerates the cathodic reduction of both oxygen and the pertechnetate ion, and any reaction between the pertechnetate ion and active iron areas will form $Tc(OH)_4$, such a reaction provides a means for increasing the reduction rates of the oxidizing agents autocatalytically. This would be favorable to passivation by electrochemical action if the rate of the cathodic process were the limiting factor. In view of the results of the preceding paper,[1] however, including effects of non-oxidizing inhibitors and the activating effect of such foreign ions as sulfate, the oxidizing action of the inhibitor itself is not necessarily dominant in all cases. It was shown previously[9,10] that activation by low concentrations of sulfate or other anions characterizes the inhibition by the pertechnetate ion also. The effects were shown to be quickly reversed by removal of the sulfate ion, in support of the hypothesis that a labile, competitive adsorption is operative.

(5) In Figs. 1 and 3 (curve 3) the indicated corrosion rates in oxygenated pertechnetate are seen to be 1 and 4×10^{-8} amp./cm.^{2}, respectively. These rates are appreciably larger than values obtained by extrapolation of the curve of Vetter[11] for the steady-state corrosion rate in sulfate solutions of different *p*H's. It appears that the corrosion rate in a pertechnetate solution continues to decrease for a considerable time. Thus, a specimen of 0.1% carbon steel has been preserved for over six years in aerated 5×10^{-4} *f* $KTcO_4$ at *p*H *ca.* 6 with no visible change and with unchanged weight of 0.5727 g. It may be calculated that a constant corrosion current of 10^{-8} amp./cm.^{2} for six years should produce a film of Fe_2O_3 10^4 Å. thick. Since this is at least 25 times the thickness of a just-visible film, it is evident that the long-term corrosion rate in the inhibited system is, at most, 4×10^{-10} amp./cm.^{2}. This is just the value taken from the extrapolation of Vetter's curve to *p*H 6. From the β-activity of the specimen over the six-year period it is found that no continuing consumption of technetium has occurred. The specimen has had a count corresponding to 2×10^{14} atoms/cm.^{2}, for over six years, within the accuracy of the counting procedure.[12] The polarization curves for oxygenated phthalate solutions also indicate that the minimum corrosion rate is not attained within the first 24 hours of passivation if the electrolyte is renewed to remove iron compounds, although a passive potential and corrosion rates in the range of $10^{-7} - 10^{-8}$ amp./cm.^{2} are generally reached in an overnight exposure.[13]

(7) M. J. Pryor and M. Cohen, *J. Electrochem. Soc.*, **98**, 263 (1951).

(8) G. H. Cartledge, unpublished results.

(9) G. H. Cartledge, THIS JOURNAL, **60**, 28 (1956).

(10) R. F. Sympson and G. H. Cartledge, *ibid.*, **60**, 1037 (1956).

(11) K. J. Vetter, *Z. Elektrochem.*, **59**, 67 (1955).

(12) Approximately a third of this activity is concentrated in a tiny dark spot which developed around a flaw in the metal within the first six min. of exposure at 95°.

(13) The current densities at the points marked E_c and j_c in the figures cannot be regarded strictly as measures of the corrosion rate of the iron phase in the presence of the inhibitors. The total anodic cur-

(6) Two types of electrochemical action of reducible inhibitors need to be carefully distinguished. In the first, the inhibitor is reduced by reaction with bare (active) metal, a mixture of insoluble products being formed in most cases. The conditions under which such reactions are thermodynamically possible are clearly shown by the diagrams developed by Pourbaix.[14] The formation of such reaction products is not necessarily passivating, however, since the films may be non-protective and corrosion may continue with a mixed potential still in the active region. For passivity to be produced, it is necessary, secondly, that the mixed potential be raised appreciably above the normal corrosion potential, and the reducible inhibitor can achieve this only if its reduction rate on the passive surface at passive potentials is sufficiently high to overcompensate the continuing corrosion under those conditions. The present measurements show that oxygen is more effective than the pertechnetate ion in maintaining passivity at potentials above or somewhat below the Flade potential.

When a specimen of active iron is immersed in an aerated pertechnetate solution, diffusion control almost surely limits the reduction of oxygen at first, so that some pertechnetate is reduced. The same would be expected to occur with other reducible inhibitors. The long-term measurements of β-activity of specimens inhibited in a pertechnetate solution exposed to air do, in fact, show that the count comes quickly to a maximum (say, 2 hr. at 95°) and then diminishes somewhat as oxygen converts part of the $Tc(OH)_4$ back to TcO_4^-. After a week or so, specimens then have an essentially constant β-activity, oxygen being sufficient to maintain the passive potential, but only if a sufficient concentration of TcO_4^- remains in solution. The inhibitor must then be assumed to have still another function, which is most plausibly connected with its adsorption on the passivating surface.

The general conclusions from the experiments in phthalate and pertechnetate solutions are: (1) that oxygen alone at 1 atm. or less suffices to maintain the cathodic current density required for passivity in weakly acidic solutions, provided a suitable inhibitor is present; (2) that the reduction rate of the TcO_4^- ion under the conditions used is so much smaller than that of oxygen that reduction of oxygen in the principal cathodic process at passive potentials; (3) that the pertechnetate ion reacts with active iron areas, but the resulting film of mixed oxides does not lead to passivation unless some minimum concentration of pertechnetate remains in solution, even when oxygen is present; (4) that $Tc(OH)_4$ deposited on the surface catalyzes the reduction processes for both oxygen and pertechnetate ions; and (5) that the inhibitory properties are counteracted by low concentrations of anions which apparently act by competitive adsorption of a labile type.

Similar studies of passivation by the chromate ion and osmium(VIII) oxide will be presented in subsequent papers.

rent includes the dissolution of iron along with any other anodic processes deriving from oxygen or the inhibitors, such as electrochemical conversion of $Tc(OH)_4$ to TcO_4^-. Since the data show, however, that an essentially potential-independent correction for anodic current suffices to bring the points for lowest current densities onto a Tafel line, the indicated anodic currents must not differ greatly from the actual corrosion rates. This conclusion is supported, for the cases covered in the present paper, by observations made with heavier deposits of the easily re-oxidized reduction product from osmium(VIII) oxide, to be reported subsequently, namely, that a potential-dependent anodic correction is indicated in this system.

(14) M. Pourbaix, "Atlas d'Equilibres Electrochimiques," Centre Belge d'Etude de la Corrosion, Brussels, 1957.

A KINETIC STUDY OF THE COUPLING OF HEXACHLOROCYCLOPENTADIENE TO FORM BIS-(PENTACHLOROCYCLOPENTADIENYL)

BY CARLETON W. ROBERTS, DANIEL H. HAIGH AND W. G. LLOYD

Polymer Research Laboratory, The Dow Chemical Company, Midland, Michigan

Received May 23, 1960

By a suitable choice of solvent medium it has been possible to study the kinetics of the homogeneous bimolecular reductive coupling of hexachlorocyclopentadiene by cuprous chloride to yield bis-(pentachlorocyclopentadienyl). Rate constants for nine homogeneous runs yield an activation energy of 13.7 kcal. (s.d. $\pm$ 0.16). The pre-exponential factor, 9.7 ($\pm$0.5) $\times$ 10^9 l. mole^{-1} sec.$^{-1}$, is too large for a transition state involving two complex molecules. Evidence is advanced in support of a free radical mechanism.

The reductive coupling of hexachlorocyclopentadiene with itself under several reaction conditions has been reported to lead to bis-(pentachlorocyclopentadienyl) (I). Roedig and Hornig[1] report the heterogeneous coupling reaction using aluminum, magnesium, zinc or copper as reducing agents. Ladd reports the reduction with copper.[2] McBee, Idol and Roberts[3] report the use of either metallic copper or cuprous chloride as coupling agents, and present evidence that compound I has a preferred conformation Ia or Ib (Fig. 5). The latter also report the preparation of bis-(pentachlorocyclopentadienyl) from copper-bronze and by the passage of a stream of hydrogen[4] through a solution of

(1) A. Roedig and L. Hornig, *Angew. Chem.*, **67**, 302 (1955).

(2) E. L. Ladd, U. S. Patents 2,732,362 and 2,732,409 (January 24, (1956).

(3) E. T. McBee, J. D. Idol, Jr., and C. W. Roberts, *J. Am. Chem. Soc.*, **77**, 4375 (1955).

(4) J. T. Rucker, U. S. Patent 2,908,723 (October 13, 1959).

hexachlorocyclopentadiene in toluene with suspended palladium-on-carbon catalyst.

This paper reports the investigation of the kinetics of the coupling reaction of hexachlorocyclopentadiene with cuprous chloride under *homogeneous* reaction conditions.

Experimental

Reagents.—Hexachlorocyclopentadiene (Hooker Chemical Corporation) was dried over anhydrous magnesium sulfate and twice distilled under reduced pressure (nitrogen ebullition), b.p. 80° (1 mm.), $n^{25}D$ 1.5628. Cuprous chloride (Mallinckrodt Analytical Reagent—minimum 90% cuprous) was used as obtained, care being taken to prevent air oxidation during weighing and transfer operations. Concentrated hydrochloric acid (Baker Reagent), and ethanol 2B were used as obtained; tetrahydrofuran was dried over magnesium sulfate. Stock solutions of the reaction mixture were prepared by dissolving 43.0092 g. (0.4 mole based on 90% Cu(I)) of cuprous chloride in 1577 ml. of an 80% ethanol–water solution, 60 ml. of concentrated hydrochloric acid and 362 ml. of tetrahydrofuran (q.v. 2-1).

Reaction.—In a 1-l., five-necked, round-bottomed flask equipped with stirrer, dropping funnel, nitrogen inlet, reflux condenser and syringe-bottle stopper was placed 500 ml. of the above stock solution. The reaction flask was placed in a stirred, thermostated (±0.1°) water-bath for from 3 to 5 hr. to ensure equilibration. Two separate aliquots of 10 ml. each were withdrawn from the reaction flask by syringe, and each was titrated against a standard ceric sulfate solution to obtain a blank for the cuprous ion concentration. To the reaction mixture was then added an exactly weighed sample of hexachlorocyclopentadiene; this was washed in with enough tetrahydrofuran (15–20 ml.) to effect complete transfer and give a total known volume of reaction mixture. The time for the addition was noted; after predetermined times, 10-ml. aliquots of the reaction mixture were withdrawn and poured onto Dry Ice to prevent air oxidation. The resulting slurry was titrated for cuprous ion with ceric sulfate (0.082 *M*). In certain experiments the cuprous aliquots were quenched over Dry Ice with ferric sulfate solution, and the resultant ferrous sulfate titrated with ceric sulfate. Both titration methods gave substantially identical results. The times of sample withdrawal, the transfer times, and the equivalents of ceric sulfate used were recorded. As the reaction proceeded there was a tendency at high conversions (greater than 65–75%) to lose homogeneity. The results of ten experimental runs are shown in Table I.

The above reaction medium is a solvent for both of these dissimilar reactants, but its solvent power is limited to about 0.2 *M* C_5Cl_6. At high initial concentration of CuCl (above 0.2 *M*) the system very quickly becomes heterogeneous due to product insolubility. Further, at high ratios of C_5Cl_6 to CuCl we were unable to obtain clear endpoints for the ceric titration of cuprous ion (due, we believe, to complexing —v.i.). The usable kinetic data (Table I), therefore, are limited to a smaller range of reactant ratios than we would have liked. The indicated rate constants, however, are in good mutual agreement and show no drift.

In the absence of appreciable excesses of CuCl the crude reaction product is the sparingly soluble white crystalline $C_{10}Cl_{10}$, of quite high purity. With substantial excesses of CuCl the crude product is an intractable blackish semi-solid precipitate, rich in both copper and $C_{10}Cl_{10}$.

Discussion

Kinetics and Stoichiometry of the Coupling Reaction.—The reaction kinetics were followed by measuring the rate of consumption of cuprous ion. A preliminary inspection of the data indicated over-all second-order kinetics with, however, an unexpected variation with regard to reaction relationships. Runs with appreciable excesses of Cu(I) yielded data which provided good second-order fits only if the anomalous proportions of $2Cu(I):C_5Cl_6$ were assumed. For normal 1:1 proportions and with the rate proportional to the concentrations of each reactant, the expected relationship is

$$\int k\,dt = \frac{1}{(C_5Cl_6)_0 - (CuCl)_0} \ln\left[\frac{(CuCl)_0[(C_5Cl_6)_0 - x]}{(C_5Cl_6)_0[(CuCl)_0 - x]}\right] \quad (1)$$

where x is the reaction variable.[5] For the anomalous stoichiometry observed in the presence of excess Cu(I), the relationship becomes

$$\int k\,dt = \frac{1}{(CuCl)_0 - (C_5Cl_6)_0} \ln\left[\frac{(C_5Cl_6)_0((CuCl)_0 - 2x)}{(CuCl)_0((C_5Cl_6)_0 - x)}\right] \quad (2)$$

Plots of a typical run with excess Cu(I), showing conformity to equation 2, are shown in Fig. 1. That this is a real stoichiometric phenomenon, rather than a chance kinetic effect, may be seen by following a typical reaction to near-completion. The data (Fig. 2) clearly show consumption of Cu(I) far in excess of the demands of 1:1 proportions, and approaching asymptotically a 2:1 relationship.

This unusual dependency was not observed, however, in runs with little or no excess Cu(I). With C_5Cl_6 present in equivalent amounts or in excess, the observed data yielded second-order fits only if a normal 1:1 stoichiometry was assumed. A typical run of this type is illustrated in Fig. 3 (*cf.* Fig. 1).

An analysis of a series of ten coupling reaction runs is shown in Table I. One of these runs (5) was heterogeneous from the start, as the solubility of C_5Cl_6 in the solvent system was exceeded. The remaining nine runs, all homogeneous, may be compared for consistency of apparent rate constants. The four runs (1, 2, 3, 4) at 0.1°, all at different reactant ratios, show a high uniformity: the least-squares rate constant for each of these runs is close to the value 1×10^{-3} l. mole^{-1} sec.$^{-1}$. Again, there is a close check between the value calculated from run 7 (12.3×10^{-3} l. mole^{-1}

TABLE I

KINETICS OF THE REDUCTIVE COUPLING OF HEXACHLOROCYCLOPENTADIENE WITH CUPROUS CHLORIDE[a]

Run	Initial concn., *M* CuCl	Initial concn., *M* C_5Cl_6	Temp., °C.	Reaction proportions	Second-order rate constant[b]	S.d.[c]	D.F.[d]
1	0.1987	0.1905	0.1	1:1	1.04	0.013	7
2	.1916	.0967	.1	2:1	0.99	.016	6
3	.1774	.0487	.1	2:1	1.04	.030	6
4	.1612	.0246	.1	2:1	0.94	.021	4
5	.1913	.3697	.1	1:1	0.62[e]	.0064	6
6	.1891	.1905	20.5	1:1	5.32	.064	8
7	.1848	.1942	30.5	1:1	12.3	.257	4
8	.1840	.1942	30.9	1:1	12.5	.276	7
9	.1794	.1905	40.9	1:1	26.0	.651	6
10	.1834	.1905	50.3	1:1	54.0	1.24	4

[a] All reactions carried out in a medium consisting of 80% ethanol 78.2 parts, tetrahydrofuran 18.8 parts and concentrated hydrochloric acid 3.00 parts by volume. [b] In l. mole^{-1} sec.$^{-1}$, $\times 10^3$. [c] Standard deviation, in l. mole^{-1} sec.$^{-1}$ $\times 10^3$. [d] Degrees of freedom. [e] Run 5 was heterogeneous throughout.

(5) A. A. Frost and R. G. Pearson, "Kinetics and Mechanism," John Wiley and Sons, Inc., New York. N. Y., 1953, p. 9.

sec.$^{-1}$ at 30.5°) and run 8 (12.5 × 10^{-3} l. mole^{-1} sec.$^{-1}$ at 30.9°).

Taking the rate constants for the nine homogeneous runs summarized in Table I, conformity to the Arrhenius temperature dependency is shown in Fig. 4. These data permit a close estimate of the activation energy of the reaction: E_a = 13.7 kcal., s.d. ±0.16 kcal. The pre-exponential factor has a value of 9.7 (±0.5) × 10^9 l. mole^{-1} sec.$^{-1}$. This value is from two to four powers of ten too high for a normal transition state between two complex molecules, just as it is too low for an atom–atom transition state; it falls in the estimated range of magnitude for a non-linear transition state complex between an atom and a molecule.[6]

Thus the rate expression for the coupling reaction is:

$$k = 9.7 \times 10^9 \exp(-13{,}700/RT) \text{ l. mole}^{-1} \text{ sec.}^{-1}$$

which indicates a very small positive entropy of activation with reference to the standard state of 1 mole/cc.

$$\Delta S^{\ddagger} = 1 \text{ e.u.}$$

An Approach to Reaction Mechanism.—An adequate mechanism for the coupling reaction must account not only for the observed kinetics, but also for the two stoichiometries and for the sharp transition between them. Such a mechanism should also account for the formation of a sparingly soluble white precipitate of high purity $C_{10}Cl_{10}$ from coupling runs carried out with excess C_5Cl_6, and for the formation of a dark brown-black insoluble precipitate, rich in copper, from coupling runs carried out with excess CuCl.

Two mechanisms consistent with the above observations are outlined in the reactions

$$C_5Cl_6 + CuCl \rightleftarrows C_5Cl_6 \cdot CuCl \quad (1)$$

$$C_5Cl_6 \cdot CuCl \longrightarrow C_5Cl_5\cdot + CuCl_2 \quad (2)$$

$$2C_5Cl_5\cdot \longrightarrow C_{10}Cl_{10} \quad (3)$$

$$2C_5Cl_6 \cdot CuCl \longrightarrow C_{10}Cl_{10} + 2CuCl_2 \quad (4)$$

$$C_{10}Cl_{10} \rightleftarrows C_{10}Cl_{10}(\text{ppt.}) \quad (5)$$

$$C_{10}Cl_{10} + 2CuCl \rightleftarrows C_{10}Cl_{10} \cdot 2CuCl(\text{ppt.}) \quad (6)$$

Reactions 1 through 3 describe a free-radical mechanism in which step 1 is a rapid equilibration and step 3 a rapid coupling. The rate-determining step is the dissociation of the complex to yield the relatively stable and highly symmetrical $C_5Cl_5\cdot$ radical. Under this scheme the over-all reaction rate is

$$dx/dt = K_1k_2(C_5Cl_6)(CuCl) \quad (3)$$

Reactions 1 and 4 constitute another possible reaction route. The kinetic requirements demand that the complexing step of step 1 be a slow forward reaction with a negligible reverse reaction rate, and that the complex coupling step of reaction 4 be rapid. The rate-determining step here is complex formation, and the over-all reaction rate is

$$dx/dt = k_1(C_5Cl_6)(CuCl) \quad (4)$$

For either mechanism, the unusual stoichiometry and the abrupt transition in relationship and reagent proportions may be accounted for by a consideration of the properties of reactions 5 and 6.

(6) Ref. 5, p. 92.

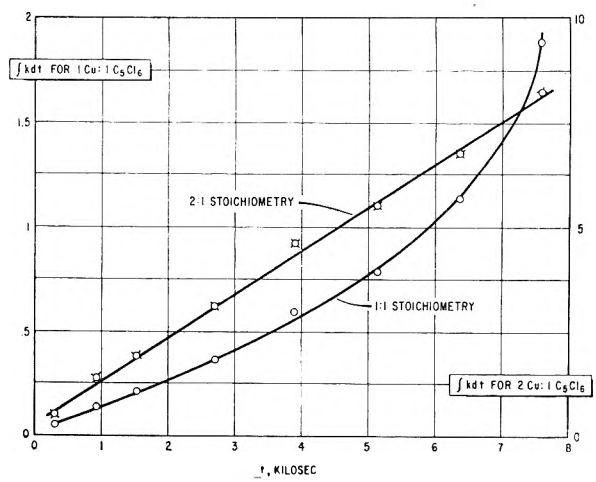

Fig. 1.—Second-order kinetics plot of data from run 3.

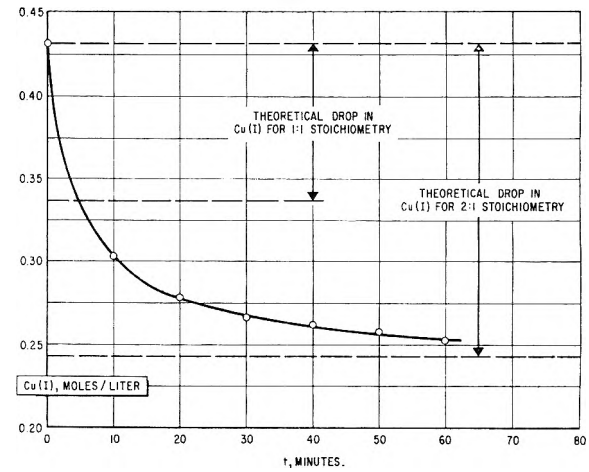

Fig. 2.—Consumption of Cu(I) by reaction with C_5Cl_6 at 30.2°; initial concentrations: Cu(I) 0.4310 *M*; C_5Cl_6 0.09409 *M*. Medium: 80% ethanol 50 parts plus concd. aq. HCl 3 parts.

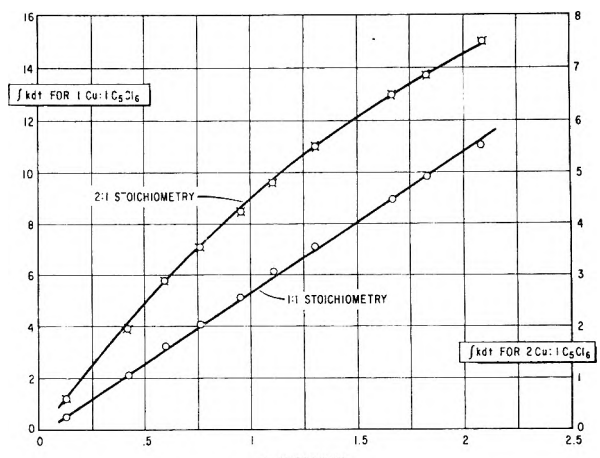

Fig. 3.—Second-order kinetics plot of data from run 6.

Considering the equilibrium reaction 5, and taking the activity of a solid phase as unity, the concentration of dissolved $C_{10}Cl_{10}$ in equilibrium with precipitated $C_{10}Cl_{10}$ must be

$$(C_{10}Cl_{10}) = 1/K_5 \quad (5)$$

Now considering reaction 6, the concentration of

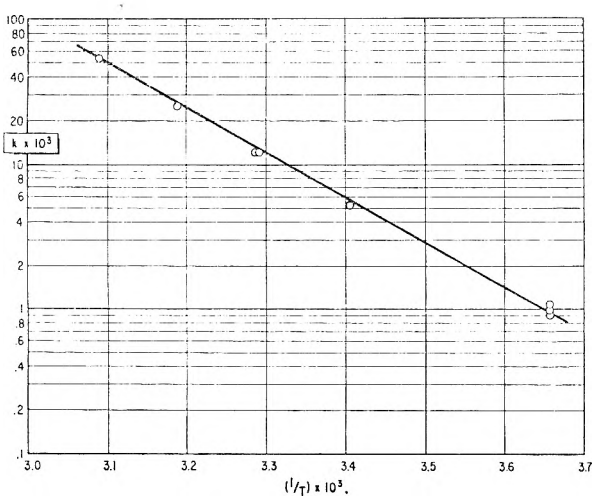

Fig. 4.—Arrhenius plot of second-order rate constants for the reductive coupling of hexachlorocyclopentadiene with cuprous chloride (conditions as specified in Table I).

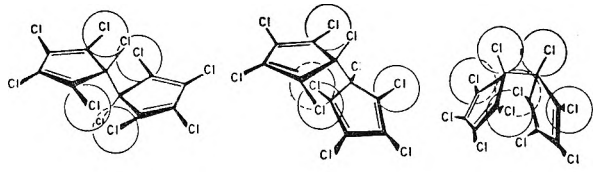

Ia Ib Ic

Fig. 5.—Conformations of bis-(pentachlorocyclopentadienyl) (after McBee, Idol and Roberts).

CuCl in equilibrium with the complexed precipitate must be

$$(CuCl) = K_6^{-1/2}(C_{10}Cl_{10})^{-1/2} \quad (6)$$

If both solid phases are present, then both equations 5 and 6 must obtain, and the concentration of CuCl must be

$$(CuCl)_c = (K_5/K_6)^{1/2} \quad (7)$$

The subscript c is used to designate the critical concentration of CuCl, for which both solid phases will be in equilibrium. If the actual concentration of CuCl is greater than $(CuCl)_c$, then more complexed precipitate will form and the uncomplexed precipitate will dissolve, until either the CuCl concentration has been reduced to the critical concentration or the $C_{10}Cl_{10}$ solid phase is all dissolved. Similarly, if the CuCl concentration is below the critical concentration, the requirements of the above equilibria will lead to the formation of precipitated $C_{10}Cl_{10}$ and to the dissolution of any complexed precipitate which may have been formed. Thus the tendency of the reacting system will be to form either the complexed or the uncomplexed $C_{10}Cl_{10}$ precipitate, but generally not both.

Both of these proposed mechanisms involve initial formation of a 1:1 complex between C_5Cl_6 and CuCl. There is considerable evidence of the formation of complexes between Cu(I) and conjugated dienes, and even with monoölefins. Thus, Moeller notes that "Ethylene and certain substituted ethylenes react with copper(I) chloride (or bromide) to give compounds of the type CuCl·Un (Un = C_2H_4, etc.)."[7] Andrews and Keefer have reported stable 1:1 complexes with a number of monoölefinic acids.[8] Diolefins such as isoprene and butadiene show a much greater affinity for cuprous chloride, to the extent that the latter is used for the selective absorption of diolefins from hydrocarbon streams.[9] A cyclopentadiene structure may be expected to complex with Cu(I) even more readily than with an acyclic diolefin, as the double bond system is fixed *cis* to enhance double complexing. Further, with hexachlorocyclopentadiene one of the non-coplanar allylic chlorine atoms may coördinate to fill the last valence orbital of Cu(I)

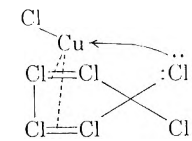

II

The tendency of chloro-compounds to complex with cuprous salts is indicated by the conductivity data obtained by Pospekhov[10] with solutions of cuprous halides in alkyl chloride solvents and various other organic solvents.

Reaction 5 is observed. Reaction 6 is strongly implied by the gross stoichiometry of the over-all reaction. We may therefore direct our attention to the relative likelihood of direct coupling of the complex (reaction 4) *vs.* complex decay followed by fast radical–radical coupling (reactions 2 and 3).

Stereochemical considerations argue against a direct frontal coupling; the four allylic chlorine atoms comprise a formidable barrier, considering the demands of a transition state for an easy, low-temperature reaction. Possible conformations of the coupled product are shown in Fig. 5. This problem could be avoided, however, by postulating an allylic S_E2' attack

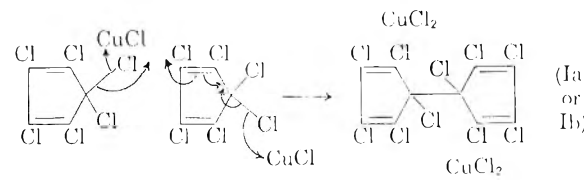

The argument for such an attack may be buttressed by the failure of our efforts to initiate the polymerization of styrene by a reacting mixture of C_5Cl_6 and CuCl, a failure indicating the absence of active free radicals in the reacting system.

On balance, however, there are several reasons for rejecting the complex-coupling mechanism in favor of the free radical mechanism. First, the observed activation energy is too high for the rate-determining step to be simple formation of the C_5Cl_6–CuCl complex, in view of the known ease of formation of similar complexes.[7-9] Furthermore,

(7) T. Moeller, "Inorganic Chemistry," John Wiley and Sons, Inc., New York, N. Y., 1952, ch. 18.

(8) L. J. Andrews and R. M. Keefer, *J. Am. Chem. Soc.*, **70**, 3261 (1948); **71**, 2379 (1949); R. M. Keefer, L. J. Andrews and R. E. Kepner, *ibid.*, **71**, 2381 (1949).

(9) *E.g.*, W. A. Schulze, U. S. Patent 2,386,352 (October 9, 1945); W. A. Schulze and L. C. Morris, U. S. Patent 2,386,355 (October 9, 1945); G. H. Short, U. S. Patent 2,386,360 (October 9, 1945); *C. A.*, **40**, 586 (1946).

(10) D. A. Pospekhov, *Uspekhi Khim.*, **6**, 515 (1937); *C. A.*, **31**, 8327 (1937).

runs with excess C_5Cl_6 do not produce even a transient formation of the blackish copper-containing precipitate, again arguing that reaction 1 must be a rapid equilibration which ties up an appreciable portion of the Cu(I). But if reaction 4 were rate-determining, two other problems would appear. The over-all rate would be proportional to the square of the concentration of the less abundant reactant, which is contrary to the experimental data. Furthermore, the observed pre-exponential factor is very large for the formation of an oriented transition state involving two complex molecules.

On the other hand, the E_a of 13.7 kcal. and the large pre-exponential factor seem appropriate to the monomolecular decomposition of the C_5Cl_6–CuCl complex (reaction 2). For this mechanism, with rapid complex equilibration and K_1 of moderate size (say, between 1 and 25 l. mole^{-1}), the over-all observed dependency would be essentially first order (with respect to the less abundant reactant) at reactant concentrations of about 1 M and greater, and essentially second order (first order with respect to each reactant) at reactant concentrations of the order of 0.1 M and less. This latter case conforms to our observations, both of the kinetics and of the unusual stoichiometry of the reaction. Finally, the reacting system of C_5Cl_6 and CuCl rapidly decolorizes diphenylpicrylhydrazyl, while in the absence of either reactant the color is comparatively stable (it is slowly discharged by CuCl alone). This is strong evidence for radical intermediation. In view of this, the failure of the reacting system to initiate styrene polymerization may be ascribed to the extremely high stability, due to resonance and symmetry, of the $C_5Cl_5\cdot$ radical. This radical is too inert to initiate vinyl polymerization; its stability limits it to reactions with other radicals (*e.g.*, other $C_5Cl_5\cdot$ radicals and diphenylpicrylhydrazyl).

Acknowledgment.—The authors are indebted to Drs. T. Alfrey, Jr., and R. H. Allen for helpful discussions, and to the Referees for their excellent criticism of the original manuscript.

KINETICS OF COMBUSTION OF CYANOGEN AND THE BURNING VELOCITIES OF CYANOGEN–OXYGEN–NITROGEN MIXTURES

BY EMILE RUTNER, KARL SCHELLER AND WILLIAM H. MCLAIN, JR.

Chemistry Research Laboratory, Aeronautical Research Laboratories, Wright-Patterson Air Force Base, Ohio

Received May 31, 1960

Burning velocities of cyanogen–air, and cyanogen–oxygen–nitrogen mixtures (O_2/N_2 = 30.8/69.2) were measured by the tube and balloon methods. The maximum burning velocity of dry C_2N_2–air mixtures was found to be approximately 10 cm./sec. Enrichment of the air mixtures with O_2, increased the burning velocity, as did the addition of H_2 and D_2. The results of these measurements were correlated with the Semenov–Zeldowitch–Frank–Kemmenetsky thermal theory of flame propagation, and also with the Tanford–Pease theory. In the application of the thermal theory it was found necessary to use a value of E = 39.9 kcal. for the tube data, and 35.0 kcal. for the balloon data. The observed variation of E can be related to the increase in the rate of reaction with an increase in O_2 concentration, and the subsequent closer correspondence of the actual flame temperature to the calculated one. In using the Tanford–Pease theory to correlate the data involving H_2 and D_2 it was found necessary to postulate that the effective reaction is: CO + OH → CO_2 + H. The OH producing reaction was assumed to be: O_2 + H → OH + H; while the inhibiting reactions which could account for a decrease in the effect of H_2 and D_2 with an increase in C_2N_2 concentration were assumed to be: H + C_2H_2 → HCN + CN, and H + HCN → H_2 + CN.

Introduction

Previous investigation of the slow oxidation of C_2N_2–O_2 systems by Hadow and Hinshelwood[1] and investigations of the burning velocities of lean C_2N_2–O_2–A systems by means of the bunsen burner technique[2] indicate that the acceleration of the reaction between C_2N_2 and O_2 in the presence of H_2O is consistent with the idea that the effect may be due to the influence of H_2O on the CO–O_2 reaction. A study of the burning velocities of wet and dry, lean and rich C_2N_2–air mixtures, and the burning velocities of other C_2N_2–O_2–N_2 systems was undertaken to elucidate the effect of the variation of O_2 and H_2 on the burning velocities of C_2N_2–O_2 systems. These studies were carried out utilizing the tube method of Gerstein, Levine and Wong,[3] and the rubber balloon method of Price and Potter.[4]

Experimental

Preparation of Mixtures.—Cyanogen was prepared by the thermal decomposition of AgCN under vacuum at 400°, the evolved C_2N_2 was condensed at liquid air temperature, and fractionated into breakseals.

A mass spectrographic analysis of a gaseous sample indicated that it contained traces of O_2 and N_2 but no detectable amounts of H_2O or HCN, and was 99+% C_2N_2.

Mixture of C_2N_2–O_2–N_2 were prepared by subliming desired amounts of C_2N_2 into an evacuated vessel and adding appropriate amounts of air and O_2. The gases were dried by passing them through magnesium perchlorate and Ascarite. Besides air(I), another mixture of N_2 and O_2 (30.8% O_2, 69.2% N_2)(II), was used.

Tube Method.—Burning velocities were measured by the tube method[3] and rubber balloon methods.[4] In the use

(1) H. J. Hadow and C. N. Hinshelwood, *Proc. Roy. Soc.* (*London*), A132, 375 (1931).

(2) R. N. Pease and R. S. Brokaw, *J. Am. Chem. Soc.*, 75, 1454 (1953).

(3) M. Gerstein, O. Levine and E. L. Wong, *ibid.*, 73, 418 (1951).

(4) W. T. Price and J. H. Potter, "Fourth Symposium on Combustion," The Williams & Wilkins Co., Baltimore, Md., 1953, pp. 363–368.

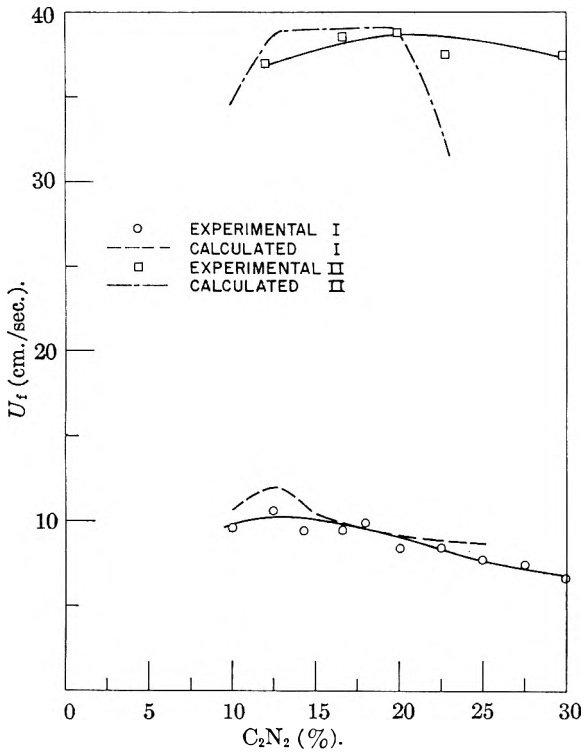

Fig. 1.—Flame velocities of C_2N_2–I(air) and C_2N_2–II–(69.2% N_2; 30.8% O_2) mixtures. Exp. curves were measured values; Calcd. curves were obtained from equation 3 with E = 39.9 kcal., for I, and E = 35.0 kcal. for II.

of the tube method a tube 27.0 mm. inside diameter and 122 cm. long was utilized which had four marks, 17.60 ± 0.01 cm. apart etched on its outside surface, the first mark being 15 cm. from the firing end. The combustion mixture was ignited with a hot wire, and the motion of flame as it proceeded down the tube was photographed with a Fairchild Oscillo-record camera. Millisecond timing marks were imprinted on the side of the film, and the spatial velocity U_s was determined from the number of timing marks between consecutive intersections of the trace of the flame front with the images of the marks on the tube. A Bell–Howell Foton camera was mounted on the oscillographic camera so that images of the flame front could be obtained simultaneously with the trace. Enlargements of the 35 mm. images were then used to determine the flame area A_f.

The flame areas, whose shapes were incomplete semi-ellipsoid, were calculated by a suitable modification of the method described by Gerstein, *et al.*,[3] and Coward and Hartwell.[5]

The burning velocity U_f is obtained from the spatial flame velocity U_s and the calculated flame area A_f in accordance with the relation

$$U_f = (U_s - U_g)(A_t/A_f) \qquad (1)$$

where A_t is the cross-sectional area of the tube and U_g is the stream velocity of the unburned mixture. It was found that U_g could be neglected in this work, since its value was small in comparison with the spatial flame velocity.

The root-mean-square deviations for the experimentally measured quantities in equation 1 were 9% for A_f and 3% for U_s.

Balloon Method.—The ballon method used was that of Price and Potter[4] modified so that samples could be run without exposure to moisture. This was done by using an electrode system consisting of a single steel tube 3.2 mm. outside diameter with an insulated iron wire 0.38 mm. diameter running down the center which protruded about 1 mm. above the tube and terminated in a sphere 0.76 mm. diameter. The tube was sealed with black wax into glass tubing connected to the vacuum system. The balloon was attached to a sleeve 10 mm. long which was friction-fitted to the electrode. The whole assembly was inclosed in a jar, constructed from two desiccator tops of 12.7 cm. diameter.

The procedure followed when making a determination was to flush the balloon several times with the combustible mixture and blow it up to a diameter of 40 to 50 mm. After this operation, the balloon was centered on the electrode and the mixture sparked by discharging a 0.01-μfd. condenser. The energy of the spark was controlled by limiting the output (5,000 to 10,000 volt) of the Hivolt Power Supply used to charge the condenser. The balloon was fired 0.45 sec. after the camera (Wollensak Fastax 16 mm.) was started, the delay time being controlled by using an Industrial Timer Corporation automatic control. During the delay time, several still shots of the balloon and desiccator top were obtained by illuminating them with a stroboscopic light. Timings were obtained from the millisecond timing marks which were imprinted on the side of the film. Eight to ten runs were made for each mixture, since the balloon had a tendency to develop asymmetrically, and such shots could not be used for data.

The data required to determine the fundamental flame velocity U_f is given by the relation

$$U_f = (dr_f/dt)(r_0^3/r_1^3) \qquad (2)$$

where r_0 is the initial radius of the balloon, r_1 is the final radius of the balloon and flame, and (dr_f/dt) is the rate of growth of the radius of the flame. All the above quantities were obtained from measurements on the film, the standard length being the diameter of the desiccator top.

In general, it can be said that in the use of both methods non-uniform propagation was observed for some ranges of composition. In the use of the balloon method, for example, it was found that C_2N_2–air mixtures could not be ignited; while mixtures of C_2N_2–oxygen–nitrogen (II) containing less than 12.0% C_2N_2 did not propagate symmetrically because of the high spark energies required to ignite them. Except in the case of 30% C_2N_2 mixtures, no reproducible value of U_f could be obtained for rich mixtures because of the blurring of the image of the wall of the balloon by brightness of the flame. Although the tube technique was used for a wider range of compositions, it could not be used for mixtures in which the ratio (O_2/N_2), was greater than in mixture II, since flames of such mixtures had a tendency to accelerate. A comparison between the tube and the balloon methods was obtained for a mixture containing 0.236 C_2N_2, 0.236 O_2, 0.528 N_2, the tube method giving a value of U_f 0.36.9 ± 1.2 cm./sec. in contrast to 37.5 ± 2.4 cm./sec. for the balloon method.

Discussion

The observed burning velocities of dry C_2N_2–air and oxygen enriched dry C_2N_2–air mixtures are depicted in Fig. 1, as a function of the cyanogen content of the mixtures. It is seen that, despite their relatively high calculated flame temperatures T_f, the maximum burning velocity of cyanogen–air mixtures (I) is small compared with that of ordinary hydrocarbon flames, which are of the order of 40 cm./sec.[3]. The low velocity may in part be attributed to the fact that the actual flame temperatures were lower than T_f because of the incomplete combustion of the cyanogen. Some evidence for incomplete combustion of cyanogen–air mixtures is presented by Berl and Barth,[6] who observed that no CO_2 was formed in moderately lean mixtures, and the observations in the present work that no carbon formed in rich, dry mixtures. Furthermore, evidence for the lack of complete combustion in oxygen enriched mixtures is given by observations of Scheller and McKnight[7] that the expansion

(5) H. Coward, F. Hartwell and E. Georgeson, *J. Chem. Soc.*, 1482 (1937).

(6) E. Berl and K. Barth, *Z physik. Chem.*, Bodenstein-Festband, 211 (1931).

(7) K. Scheller and W. E. McKnight, "Seventh Symposium on Combustion," Butterworth Sci. Publ., London, 1959, p. 369.

ratios in measurements on the flame velocities of (C_2N_2, CO, O_2, N_2) mixtures by the balloon method were in most cases less than that expected on the basis of the calculated flame temperatures.

The characteristics of these flames (*i.e.*, high T_f and low burning velocity) suggested that it might be interesting to compare the experimental data with the predictions of the Semenov–Zeldovitch–Frank–Kamenetsky[8] thermal theory of flame propagation. Their expression for the burning velocity, specialized to the case of cyanogen flames, may be written as

$$U_f = \left[\frac{2\lambda^* Z}{L\rho_0} \times \frac{RT_f^2}{E} \exp(-E/RT_f) \frac{[C_2N_2]_{eff}[O]_{eff}}{[C_2N_2]_0}\right]^{1/2} \quad (3)$$

in which

U_f	burning velocity, cm./sec.
λ^*	thermal conductivity of product gases
Z	kinetic collision number
L	heat of combustion per gram of combustible mixture including diluents
R	ideal gas constant
T_f	adiabatic flame temperature
E	activation energy for reaction between oxygen and fuel
$[O_2]_{eff}$	effective concn. of oxygen, *i.e.*, concn. in reaction zone of flame
$[C_2N_2]_0, [C_2N_2]_{eff}$	concn. of cyanogen in unburned gas and in reaction zone, resp.

The effective concentrations of fuel and oxygen appearing in equation 3 are determined from the stoichiometry of the reaction between cyanogen and oxygen, corrected for the change in temperature between the burned gas and the fresh gas and for the back diffusion of products from the burned gases. For the case of rich mixtures, for example

$$[C_2N_2]_{eff} = [([C_2N_2]_0 - [O_2]_0)(T_0/T_f)(n_0/n_f)(A/B)_f] + [O_2]_{eff}$$

$$[O_2]_{eff} = [O_2]_0(T_0/T_f)(RT_f^2/E)(n_0/n_f)(A/B)_f(1/T_0 - T_f)] \quad (4)$$

where

$[O_2]_0$	concn. of oxygen in unburned mixture
T_0	initial temp. of combustible mixture
n_0/n_f	ratio of no. of moles in fresh gas to that in product gas
$(A/B)_f = \lambda/\rho DC_p$,	determined at flame temp.
ρ	density of mixture
λ	thermal conductivity
D	diffusion coefficient
C_p	specific heat at constant pressure of mixture

Values for the thermal conductivity and diffusion coefficients were obtained from gas kinetic theory considerations[9]

D	$1.336\ (\lambda/\rho)$
λ	$1/4\ (9\gamma - 5)\eta C_v$
Θ	coefficient of viscosity
γ	specific heat ratio
C_v	specific heat at constant volume

In the rate expression used above the steric factor was allowed to be unity, since the uncertainty in the steric factor is overshadowed by the uncertainty in the temperature dependence of the transport and thermal properties of the gas at the flame temperature.[10]

(8) N. N. Semenov, *Prog. Phys. Sci.* (*U.S.S.R.*), **24**, no. 4, 433 (1940). (NACA TM 1026, 1942).

(9) J. H. Jeans, "Dynamical Theory of Gases," 4th Ed., Dover Publications.

Equilibrium flame temperatures required for the calculation of the burning velocity were determined upon the assumption that the following equilibria were obeyed on the lean side

$$CO + {}^1/_2O_2 \rightleftarrows CO \quad (5)$$

$$N_2 \rightleftarrows 2N \quad (6)$$

$$N_2 + O_2 \rightleftarrows 2NO \quad (7)$$

$$O_2 \rightleftarrows 2O \quad (8)$$

On the rich side only the cyanogen decomposition equilibrium

$$C_2N_2 \rightleftarrows 2CN \quad (9)$$

was considered, since there was no experimental evidence of carbon formation in these flames. Necessary thermodynamic data for the calculations were obtained from the tabulations of Lewis and von Elbe[11] save those for C_2N_2 and CN which were taken from the data of Rutner, McLain, Scheller[12] and Johnston, *et al.*[13] The calculated flame temperatures for both mixtures are given in Table I. Values of other molecular properties of both product and cold-gas mixtures were estimated from their composition while the value $E = 39.9$ kcal. was used for the activation for the tube data and 35 kcal. for the balloon data because these gave the best fit for the experimental curves.

Figure 1 shows the relation between U_f and composition for dry C_2N_2–air (I) and C_2N_2–oxygen–nitrogen (II) mixtures, and corresponding curves obtained from the Semenov equation. The Semenov equation gives a reasonable fit with the data obtained from mixtures I, using a value of $E = 39.9$ kcal., while the data from mixtures II required a value of 35 kcal. to obtain an approximate fit. The variation in the value of E required to fit the two sets of data can be related to the observations[6,7] that the actual flame temperatures may be low. For example, if the real flame temperature is lower than T_f, the use of T_f in equation 3 will give a high value of E, and the closer the actual temperature is to T_f, the lower the observed value of E would be. This explanation requires that the actual flame temperature approach T_f as the concentration of O_2 increases. The evidence that this requirement is fulfilled is given by the observations[6,7] noted above, and also by the following facts: An increase in O_2 concentration for a given C_2N_2 concentration increases the flame velocity, and theoretical temperatures have been observed in pure C_2N_2–O_2 mixtures.[14]

In contrast to the values of E observed for these flame reactions, the observation of James and Laffitte[15] on the variation of the induction period with temperatures for the explosion of C_2N_2–air mixtures

(10) John B. Fenn and H. F. Calcote, "Fourth Symposium on Combustion," The Williams & Wilkins Co., Baltimore, Md., 1953, p. 231.

(11) B. Lewis and G. von Elbe, "Combustion, Flames and Explosion of Gases," Academic Press, Inc., New York, N. Y., 1951.

(12) E. Rutner, W. H. McLain, Jr., and Karl Scheller, *J. Chem. Phys.*, **24**, 173 (1956).

(13) H. L. Johnston, Jack Belzer and Lydia Savedoff, TR 316-7 Cryogenic Lab., Ohio State Univ., 1953.

(14) N. Thomas, A. G. Gaydon and L. Brewer, *J. Chem. Phys.*, **20**, 369 (1952).

(15) H. James and P. Laffitte, *Compt. rend.*, **236**, 1038 (1953).

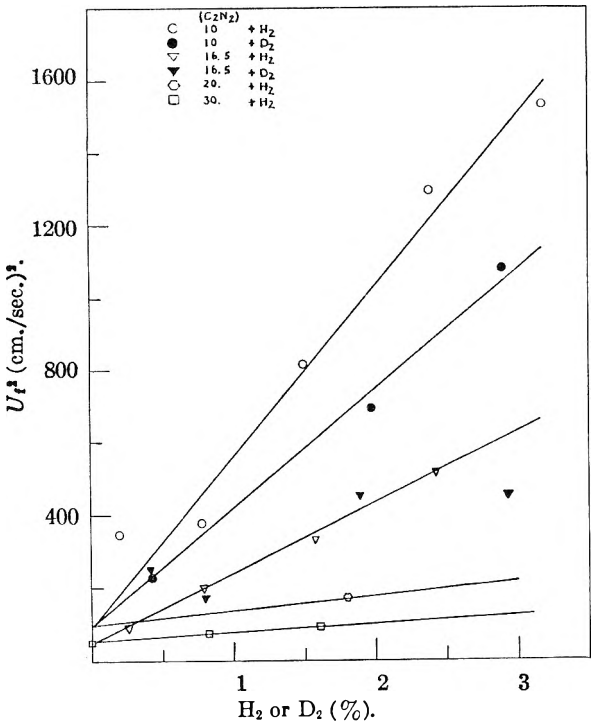

Fig. 2.—Relation between U_f^2 and H_2 or D_2 for various C_2N_2–air mixtures. See table I, note (a) for definition of (C_2N_2). Concentration of H_2 or D_2 is given as % of total gas mixture.

gave a value of $E = 66$ kcal. The observations[1] on the oxidation of C_2N_2 at 700° indicated that the C_2N_2 was oxidized to CO before an explosion took place; thus one is led to the conclusion that the value of E for the induction time observed by James and Laffitte was that for the oxidation of C_2N_2 to CO; and, therefore, at least for this reason, it may vary somewhat from the value of E obtained from flame velocities, since some CO_2 may be formed in the flames. Other contributions to divergences between the values of E obtained from the two methods arise from differences in the course of the flame reaction and the slow oxidation, and the fact that the value of E obtained from flame data depends on the nature of the temperature variations which are assumed for other parameters in equation 3.

The squares of the measured burning velocities of cyanogen–air mixtures admixed with small quantities of hydrogen or deuterium are recorded in Fig. 2. It may be observed that the effect of these additives decreases in the richer mixtures, becoming negligible at a cyanogen concentration of 30%. In the lean mixtures, the effect is similar to that observed by Brokaw and Pease[2] on their cyanogen–oxygen–argon mixtures. The squares of the burning velocities are plotted against the equilibrium concentrations of H_2O, D_2O, OH and OD in Fig. 3. In agreement with Brokaw and Pease, a correlation was found to exist between U_f^2 and the equilibrium concentrations of OH and OD. Furthermore, a correlation was also present between U_f^2 and the equilibrium H_2O and D_2O concentrations.

The equilibrium concentrations required for the graphs in Fig. 3 are recorded in Tables I and II.

TABLE I

FLAME TEMPERATURES AND EQUILIBRIUM CONCENTRATIONS OF SPECIES IN FLAMES CONTAINING H_2

C_2N_2[a]	T_f, °K.	H_2[b]	Equilibrium concn., atm. × 10^4 OH	H	H_2O	H_2
		C_2N_2–air mixtures				
10	2620	..	...	...	....	....
		0.20	9.9	3.96	11.2	0.95
		0.80	21.5	9.34	56.5	51.6
		1.50	29.7	13.4	114.0	10.8
		2.40	37.4	17.7	187.0	18.6
		3.20	41.0	21.0	252.0	28.0
12.5	2720	..	...	...	....	....
14.3	2710	..	...	...	....	....
16.7	2625	..	...	...	....	....
		0.23	1.19	13.8	3.41	8.92
		0.80	2.17	28.5	12.3	40.9
		1.58	2.24	49.6	20.7	91.7
		2.44	2.76	56.3	32.6	149.0
18.0	2550	..	...	...	....	....
20.0	2400	..	...	...	....	....
		1.80	...	...	....	....
		2.0	...	...	....	....
22.5	2280	..	...	...	....	....
25.0	2200	..	...	...	....	....
27.5	2100	..	...	...	....	....
29.5	2020	..	...	...	....	....
		0.84	...	...	....	....
		1.60	...	...	....	....
		C_2N_2–30.8% O_2 + 69.2% N_2 (II) mixtures				
16.7	3033	..	...	...	....	....
20.0	3100	..	...	...	....	....
23.0	3160	..	...	...	....	....
30.0	..	..	...	...	....	....

[a] $(C_2N_2) = \frac{100 \times (\text{atm. of } C_2N_2)}{(\text{atm. of } C_2N_2) + (\text{atm. of air})}$ or the ratio: $(C_2N_2)/(O_2)$ was constant for the series. [b] $(H_2) = \frac{100 \times (\text{atm. of } H_2)}{(\text{atm. of } H_2) + (\text{atm. of } C_2N_2) + (\text{atm. of air})}$.

They were calculated upon the assumption that the following equilibria were satisfied in addition to those postulated for reactions 5 to 8

$$CO + H_2O \rightleftarrows CO_2 + H_2 \quad (10)$$

$$H_2 \rightleftarrows 2H \quad (11)$$

$$H_2O \rightleftarrows H + OH$$

TABLE II

BURNING VELOCITIES AND EQUILIBRIUM CONCENTRATIONS OF SPECIES FOR FLAMES CONTAINING D_2

(C_2N_2)[a]	U_f, cm./sec.	D_2[b]	Equilibrium concn., atm. × 10^4 OD	D	D_2O	D_2
10	15.1	0.43	16.6	5.90	28.0	2.24
	27.3	1.97	34.8	15.1	151.0	14.7
	32.9	2.90	41.4	19.1	228.0	23.3
16.7	15.4	0.42	1.09	19.9	4.99	20.7
	12.8	.80	2.02	28.0	13.0	41.0
	21.1	1.90	2.39	46.6	25.7	113.0
	21.2	2.95	2.72	59.6	37.1	186.0

[a] $(C_2N_2) = \frac{100 \times (\text{atm. of } C_2N_2)}{(\text{atm. of } C_2N_2) + (\text{atm. of air})}$ or the ratio: $(C_2N_2)/(O_2)$ was constant for the series. [b] $(H_2) = \frac{100 \times (\text{atm. of } H_2)}{(\text{atm. of } H_2) + (\text{atm. of } C_2N_2) + (\text{atm. of air})}$.

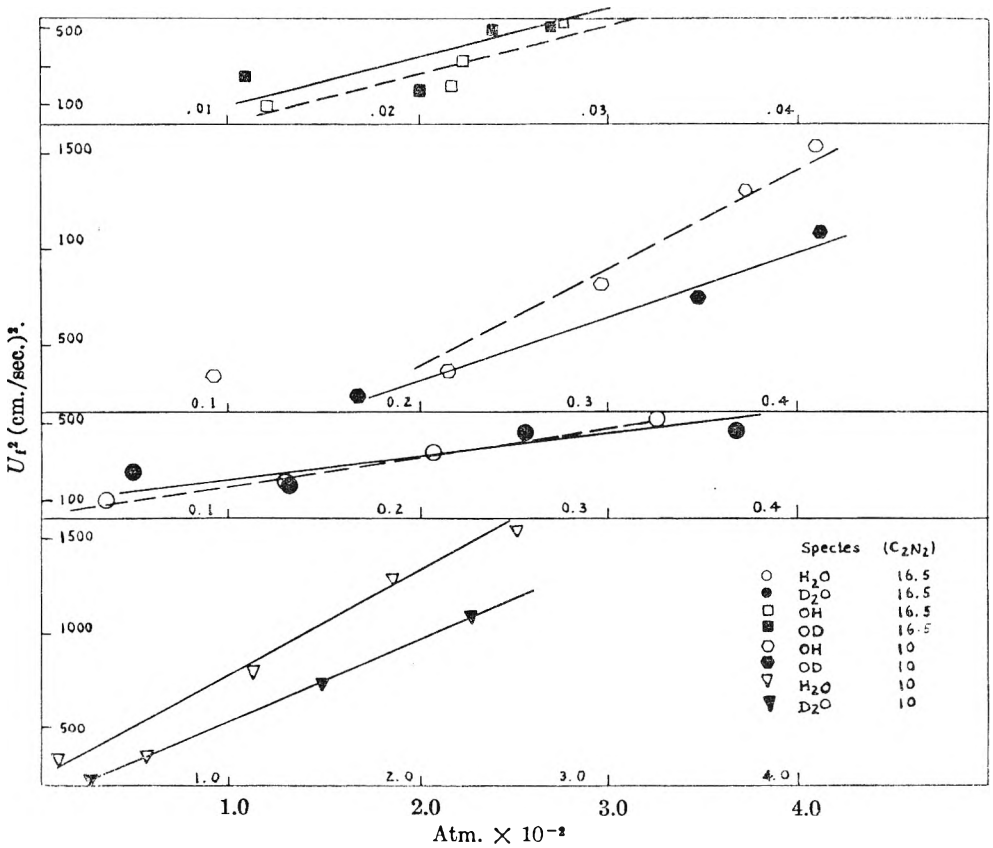

Fig. 3.—Relation between U_f^2 and equilibrium concentrations of OH, OD, H_2O and D_2O, in the flame front of C_2N_2–air mixtures. Definition of (C_2N_2) given in Table I note (a).

It was assumed, also, that the addition of H_2 (or D_2) to these mixtures in the quantities used in these experiments did not change their flame temperature significantly from that of the dry mixtures. This assumption was checked for a 10% cyanogen–air mixture to which 3% of hydrogen had been added. The calculated flame temperature differed by less than 0.5% from that of undiluted mixture. For the case of deuterium-bearing mixtures, the appropriate equilibrium constants [reactions 10 to 12] were corrected for the isotopic effect of substitution of deuterium for hydrogen. The data presented for rich mixtures, Table I, show that the effect of H_2 and D_2 additions on their burning velocity is negligible, indicating that these substances have little influence on the oxidation of cyanogen to carbon monoxide. Furthermore, it was found that CO_2 may be formed in very rich mixtures which do not contain enough oxygen to oxidize all of the cyanogen present to CO. This fact was demonstrated by igniting a sample consisting of 9.7% C_2N_2, 8.1% O_2, 79.2% N_2 and 3% H_2 in a closed vessel and analyzing the product gases in a mass spectrograph. The burned gases contained 1.4% CO_2 and 1.9% HCN, indicating that in the presence of H_2, the oxidation of CO to CO_2 and C_2N_2 to CO occurred simultaneously and competed with one another for the available oxygen. The little effect of O_2 on the rate of $C_2N_2 + H_2$ reaction even at 600°[17] makes it apparent that the products observed were the result of the flame reaction rather than any subsequent low-temperature reaction.[16]

Thus, it appears that the influence of H_2 and D_2 on the burning velocity of stoichiometric and slightly rich as well as lean cyanogen mixtures may be attributed to their accelerating effect upon the oxidation of CO. These conclusions are in contrast to those of Brokaw and Pease[2] who assumed that the addition of H_2 and D_2 to mixtures of C_2N_2–O_2–argon mixtures did not affect the combustion of the CO which was formed, although, as noted above, their results follow the Tanford–Pease[17] theory.

The accelerating influence of H_2O on the burning velocity of CO–O_2 is well established,[8,18,19] and it has been postulated that the reaction[20]

$$CO + OH \longrightarrow CO_2 + H \qquad (13)$$

is the predominant step in this process, for both C_2N_2–O_2 and CO–O_2 flames containing H_2 or H_2O. This last postulate can be tested if the flame velocity should be proportional to the square of the OH radical concentration in the flame front[20]; this relation has been found to hold for lean C_2N_2–air flames containing H_2 or D_2 (Fig. 3).

The decrease in the effect of H_2 on the flame of rich C_2N_2–air mixtures can be attributed to the

(16) N. C. Robertson and R. N. Pease, *J. Am. Chem. Soc.*, **64**, 1880 (1942).

(17) C. Tanford and R. N. Pease, Jr., *J. Chem. Phys.*, **15**, 861 (1947).

(18) E. Fiock and C. F. Marvin, Jr., *Chem. Revs.*, **21**, 367 (1937).

(19) G. A. Barskii and Ya. B. Zeldovitch, *Zhur. Fiz. Chem.*, **25**, 523 (1951).

(20) K. Scheller, "Sixth Symposium on Combustion," Reinhold Publ. Corp., New York, N. Y., 1956, p. 280.

decrease in the concentration of H atoms in the flame front by the reactions

(a) $C_2N_2 + H \longrightarrow HCN + CN$, (b) $H + CN \longrightarrow HCN$

which are similar to the effect found in halogen–hydrogen reactions.[21] The decrease in H atom concentration results in a decrease in the OH concentration, and subsequently in the decrease of the rate of reaction 13 and the flame velocity. The effect of halogens[22] in reducing the flame velocity of wet $CO–O_2$ mixtures has already been observed.

If the reaction between the OH radical and CO controls the flame propagation in moist $CO–O_2$ mixtures, a difference in effect between hydrogen and deuterium additions may be expected in view of the difference in reactivity between the OH and OD radicals. The ratio of the reaction rate constants for OH and OD may be calculated from an expression derived by Biegeleisen[23] for the effect of isotope substitution on the rate of reaction. His theoretical relation for the ratio of the reaction rates is

$$\frac{k_1}{k_2} = \frac{K_1}{K_2} \times \frac{\Pi f_T}{f^*} \left(\frac{M_1^*}{M_2^*}\right)^{1/2} \qquad (14)$$

in which the indices 1 and 2 refer to the hydrogen and deuterium isotopes, respectively, to the reactants, and * to the activated complex.

$K_1/K_2 \approx 1$ the ratio of the transmission coefficients
M^* effective mass of the activated complex along the reaction coördinate

(21) G. Hadman, H. W. Thompson and C. N. Hinshelwood, *Proc. Roy. Soc.* (*London*), **A137**, 98 (1932).

(22) E. Sterling and R. Arthur, "Third Symposium on Combustion, Flame, Explosion Phenomena," The Williams & Wilkins Co., Baltimore, Md., 1949, p. 476.

(23) J. Bigeleisen, THIS JOURNAL, **56**, 823 (1952).

and

$$f = \left(\frac{S_1}{S_2}\right) \frac{3n-6}{\Pi} \left(\frac{U_{2i}}{U_{1i}}\right) \left[\exp\left(-\frac{U_{1i}-U_{2i}}{2}\right)\right] \left[\frac{1-\exp(-U_{1i})}{1-\exp(-U_{2i})}\right] \qquad (15)$$

In expression 15, S_1/S_2 is the ratio of the symmetry numbers, and $U_i = hc\omega_i/kT$, ω_i being the vibration frequency in cm.$^{-1}$ of the appropriate normal mode. The activated complex in the reaction between CO and OH was assumed to have the form [CO–O–H]. Values for the vibration frequency for OH and OD in the activated complex were taken as those of the corresponding groups in formic acid (3570 and 2666 cm.$^{-1}$ for OH and OD, respectively[24]), yielding a value for f^* of 1.07. The ratio of the partition functions of the OH and OD radicals was calculated to be 1.02 for vibration frequencies equal to 3735.21 and 2720.9 cm.$^{-1}$ for the respective species.[25] The ratios of the symmetry numbers and the partition function for CO were both assumed to be unity. The introduction of these quantities into equation 14 gave a value for $k_{OH}/k_{OD} = 1.33$. In accordance with the square-root relation rate and burning velocity the ratio of the flame speeds of hydrogen to deuterium-containing mixtures may be expected to equal 1.15. This ratio was observed for a mixture of 10% C_2N_2 plus 3% H_2 or D_2 and air.

Acknowledgment.—The authors wish to express their appreciation to Dr. L. A. Wood for his helpful criticisms of this paper and to Dr. P. C. Colodny for aid with the calculations.

(24) G. Herzberg, "Infrared and Raman Spectra of Poly-atomic Molecules," D. Van Nostrand Co., New York, N. Y., 1945, p. 321.

(25) G. Herzberg, "Spectra of Diatomic Molecules," D. Van Nostrand Co., New York, N. Y., 1950, p. 560.

THE ISOTOPIC EXCHANGE OF FLUOROBORIC ACID WITH HYDROFLUORIC ACID

BY M. ANBAR AND S. GUTTMANN

Isotope Department, Weizmann Institute of Science, Rehovoth, Israel

Received May 31, 1960

The rate of isotopic exchange of fluorine between fluoroboric and hydrofluoric acids has been investigated. The rate of exchange $R = 4.5 \times 10^4 e^{-24,700/RT} [BF_4^-][H^+]$ l. mole^{-1} sec.$^{-1}$. The exchange was found to proceed *via* $HBF_4 \rightleftarrows HF + BF_3$, $BF_3 + H_2O \rightleftarrows HBF_3OH$ followed by rapid isotopic equilibration between BF_3OH^- and HF. The mechanism of exchange was found identical with the mechanism of hydrolysis in acid medium. The non-acid hydrolysis of BF_4^- proceeds by a SN1 mechanism with a rate constant $k = 8 \times 10^5 e^{-15,500/RT}$ sec.$^{-1}$.

The chemistry of fluoroboric acid HBF_4 has been extensively studied by Ryss, *et al.*,[1] and by Wamser[2,3] who have determined the equilibrium constants for the formation of HBF_4, HBF_3OH, $HBF_2(OH)_2$ as well as the rates of formation and hydrolysis of HBF_4 at room temperature. Wamser has pointed out that the rate of HBF_4 formation is affected by acidity though he did not present a rate law including hydrogen ion concentration. The purpose of this study was to investigate the rate of isotopic exchange of fluorine between fluoroboric and hydrofluoric acids over a range of hydrogen ion concentration and to compare it with the rates of formation and hydrolysis of fluoroboric acid over a similar range of acidity. Quantitative data on the rates of exchange and hydrolysis of fluoroborates are of importance in applying KBF_4[18] as a tracer in biological systems.[4]

(1) I. G. Ryss, M. M. Slutskaya and S. D. Palevskaya, *Dokl. S.S.S.R.*, **52**, 417 (1946); **57**, 689 (1947); *Zhur. Obshchei Khim.*, **19**, 1827, 1838 (1949); **25**, 19 (1955).

(2) C. A. Wamser, *J. Am. Chem. Soc.*, **70**, 1209 (1948).

(3) C. A. Wamser, *ibid.*, **73**, 409 (1951).

Experimental

A. Materials.—**Potassium fluoroborate** commercially available was three times recrystallized from water. Technical sodium fluoroborate was first purified from insoluble

(4) M. Anbar, S. Guttmann and Z. Lewitus, *Endocrinology*, **66**, 888 (1960).

matter by dissolving it in a minimum amount of water, then concentrated lanthanum nitrate was added in excess to remove the fluoride ions; lanthanum fluoride was separated by centrifugation and the supernatant was passed through a cation exchange column (Dowex 50, sodium form 50 mesh). The solution was next tested for traces of lanthanum by increasing the alkalinity to *p*H 9. The solution which was fluoride and lanthanum free was gravimetrically assayed for fluoroborate by precipitating both as potassium fluoroborate and nitron fluoroborate. The amount of fluoride ions present in the purified fluoroborate salts was estimated by the zirconium–alizarin[5] and ferrithiocyanate[6] methods. The amount of fluorine found in our purified KBF_4 and $NaBF_4$ in any other form than BF_4^-, was below 0.2%. This value was confirmed when KBF_4 was prepared and the amount of fluoride was determined by isotopic dilution analysis.

Carrier-free **fluoride 18** was prepared by bombarding Li_2CO_3[18] targets with 3.2 Mev. protons (20–30 microamperes) from an electrostatic Van de Graaff accelerator. The Li_2CO_3[18] was prepared by the equilibration of Li_2CO_3 with H_2O^{18} (92–96 atom % O^{18}) in a slightly acidic medium. After irradiation the targets were dissolved in 0.5 ml. of 0.1 *N* HCl. **Labelled BF_4^-** was obtained by adding a weighed amount of pure KBF_4 (50–200 mg.) to the acid solution of carrier-free LiF^{18}. The solution was heated to 100° and kept at this temperature for 2–5 minutes in order to undergo exchange. It was cooled in ice and the labelled KBF_4 was precipitated and recrystallized three times from *neutral* aqueous solution; then it was washed with ethanol and dried in a vacuum oven at 70°. Five to 10 mg. of the labelled KBF_4 was weighed and dissolved in 100 ml. of water and an aliquot of 1 ml. was taken for radioassay. To another aliquot of 1 ml., 0.5 ml. of 0.1*N* NaF was added and the fluoride ions were precipitated by $Pb(NO_3)_2$ in presence of 0.2 *N* NaCl. The PbClF precipitate was washed with 90% ethanol and radioassayed. The activity of the PbClF never exceeded 0.5% of the total activity present; this value may be considered as the upper limit of fluoride impurity in the KBF_4[18] preparations, as any exchange, hydrolysis or incomplete separation would contribute to the fluoride activity.

All other reagents used were of analytical grade.

B. Methods of Analysis. Hydrolysis of BF_4^-.—Ten-ml. of solutions of KBF_4[18] or $NaBF_4$[18] were adjusted to a certain *p*H by nitric acid, sodium acetate or sodium hydroxide, and placed in a thermostat at 25, 37, 60 or 100°. At intervals aliquotes of 1 ml. were taken, cooled and neutralized. One ml. of a solution 0.1 *N* in NaF and 0.2 *N* in NaCl was added to the solution at *p*H 3–5 and 1 ml. of 1 *N* $Pb(NO_3)_2$ was introduced to precipitate PbClF. The precipitate was centrifuged, washed with 90% ethanol and counted. When solutions of BF_4^- below 0.01 *N* were studied, one ml. of KBF_4 0.05 *N* was added as a "hold back carrier," to prevent undue adsorption of BF_4^{18-} on the precipitate. Samples were counted in a 2 inch well type NaI scintillation counter; the discriminator level was held at 400 Kev. In experiments where the effect of fluoride ion concentration on the rate of hydrolysis was studied, the initial concentration of fluoride ions was kept low in comparison with that of BF_4^-.

The rate of hydrolysis was calculated according to first-order kinetics, by plotting $\log a/(a - x)$ *vs.* t, where a is the initial concentration of BF_4^-.

Exchange of BF_4^-–F^-. 1. **Labelled BF_4^-.**—Solutions of KBF_4, or $NaBF_4$ were prepared containing known amounts of fluoride ions. The fluoride concentration chosen in these experiments was high compared with that of BF_4^-, thus there was little net change in the BF_4^- concentration due to hydrolysis.[1,2] The *p*H was adjusted and the solution was thermostated. Next a known amount of fluoride-free KBF_4[18] was added. At intervals fluoride ions were precipitated and radioassayed by the method described above.

2. **Labelled Fluoride.**—Carrier-free LiF^{18} was added to solutions containing known concentrations of BF_4^- and F^- of a known pH, which have attained hydrolytic equilibrium. Aliquots of 1 ml. were introduced into 2 ml. of 10% nitron solution. The nitron fluoroborate was separated by centrifuge, washed with 70% ethanol and counted.

The rate of exchange was calculated from

$$Rt = \frac{4[BF_4^-][F^-]}{4[BF_4^-] + [F^-]} \log \frac{A_\infty - A_0}{A_\infty - A_t}$$

where A is the activity of F^{18} at the different phases of reaction, or

$$R = \frac{4[BF_4^-][F^-]}{4[BF_4^-] + [F^-]} \times \frac{0.693}{t_{1/2}}$$

where $t_{1/2}$ was derived graphically by plotting $\log A_\infty - A_t$ *vs.* t.

Results

Isotopic Exchange of BF_4^-–F^-.—The rate of fluorine exchange between fluoroborate and fluoride ions was studied in solutions 0.01–1.0 molar in hydrogen ions. The concentrations of BF_4^- and of HF were changed in range 0.005–0.5 and 0.02–0.2 *M*, respectively. A selection of results at various temperatures is presented in Table I.

TABLE I

ISOTOPIC EXCHANGE OF FLUORINE BETWEEN BF_4^- AND HF

Temp., °C.	*p*H	$[BF_4^-]$, mole l.$^{-1}$	$[F^-]$, mole l.$^{-1}$	$t_{1/2}$, min.	R, mole l.$^{-1}$ min.$^{-1}$	$k = R/[H^+][BF_4^-]$, l. mole^{-1} min.$^{-1}$
0	1.30	0.093	0.017	1650	6.8×10^{-6}	1.4×10^{-7}
0	1.20	.099	.101	5700	9.5×10^{-6}	1.4×10^{-7}
0	1.34	.035	.015	3250	2.8×10^{-6}	1.75×10^{-7}
0	1.25	.020	.20	16400	2.4×10^{-6}	2.1×10^{-7}
25	0.28	.10	.07	35	1.15×10^{-5}	2.2×10^{-7}
25	.70	.10	.07	72	5.6×10^{-4}	2.8×10^{-7}
25	.87	.50	.07	33	1.4×10^{-4}	2.1×10^{-7}
25	.95	.2	.07	75	5.9×10^{-4}	2.6×10^{-7}
25	1.10	.088	.022	50	2.9×10^{-4}	4.1×10^{-7}
25	1.54	.42	1.034	60	3.9×10^{-4}	3.4×10^{-7}
25	1.88	.1	0.07	1340	3.0×10^{-5}	2.3×10^{-7}
37	1.08	.37	.03	5.0	4.2×10^{-3}	1.4×10^{-6}
37	1.30	.1	.1	46	1.2×10^{-3}	2.4×10^{-6}
37	1.35	.09	.2	16	7.8×10^{-4}	1.9×10^{-6}
60	0.88	.087	.033	0.7	3.0×10^{-2}	2.6×10^{-6}
60	1.1	.005	.045	12	7.7×10^{-4}	1.9×10^{-6}
60	1.3	.094	.106	4.0	1.4×10^{-2}	3.0×10^{-6}

Within the range of concentrations investigated the rate of exchange was found proportional to BF_4^- and H^+ concentrations and independent of of HF $R = k_1[H^-][BF_4^-]$. From average specific rate constants at 0, 25, 37 and 60° the activation energy of the exchange reactions was calculated $\Delta E = 24.7$ kcal./mole. The average specific rate constant in the given range of temperature is therefore $k = 4.5 \times 10^{14}\, e^{-24700/RT}$ l. mole^{-1} sec.$^{-1}$.

Hydrolysis of BF_4^-.—The rate of hydrolysis of fluoborate ions was found to be first order in BF_4^- and first order in hydrogen ion concentration in the acid region Rate $= k[H^+][BF_4^-]$ as may be seen from Table II.

TABLE II

HYDROLYSIS OF BF_4^- IN ACID SOLUTIONS AT 25°[a]

$[BF_4^-]$, mole l.$^{-1}$	$[H^-]$, mole l.$^{-1}$	$t_{1/2}$, min.	$0.693/t_{1/2} \times 10^{-3}$, min.$^{-1}$	$0.693/t_{1/2} \times 1/[H^+] \times 10^{-3}$, min.$^{-1}$
0.015	2.0	52	13.3	6.7
.017	1.0	98	7.1	7.1
.14	1.0	95	7.3	7.3
.019	0.5	201	3.45	6.9
.019	.2	490	1.41	7.0
.14	.1	870	0.8	8.0

[a] $k = 7.1 \pm 0.5 \times 10^{-3}$ mole^{-1} l. min.$^{-1}$ $= 1.18 \pm 0.08 \times 10^{-4}$ mole^{-1} l. sec.$^{-1}$.

(5) F. D. Snell and C. T. Snell, "Colorimetric Methods of Analysis," D. Van Nostrand, New York, N. Y., 1959, p. 638.

(6) R. S. Ingols, *et al.*, *Anal. Chem.*, **22**, 799 (1950).

There was found no catalytic effect of HF initially present on the rate of hydrolysis. This result is confirmed by the fact that no autocatalytic deviation from first rate law was observed. In another series of experiments bisulfate ions were added up to 0.9 M keeping the pH constant, no appreciable change of the rate of hydrolysis could be detected. Activation energy ΔE = 25.1 kcal./mole^{-1}, was derived from data at 25, 37°, ($1.23 \pm 0.05 \times 10^{-3}$ mole^{-1} l. sec.$^{-1}$), 60° (k = $1.33 \pm 0.05 \times 10^{-2}$ mole^{-1} l. sec.$^{-1}$) and at 100° ($k = 1.10 \times 10^{0}$ mole^{-1} l. sec.$^{-1}$). The specific rate constant of fluoborate hydrolysis in acid solution is therefore

$$k = 2.3 \times 10^{14}\, e^{-25,100/RT} \text{ mole}^{-1} \text{ l. sec.}^{-1}$$

In neutral and basic solutions the rate of hydrolysis is much lower and no effect of alkalinity on the rate of hydrolysis could be detected as it is shown in Table III.

TABLE III

HYDROLYSIS OF FLUOROBORATE IN NEUTRAL AND ALKALINE SOLUTIONS AT 100°[a]

[OH$^-$], mole l.$^{-1}$	[BF$_4^-$], mole l.$^{-1}$	$t_{1/2}$, min.	$0.693/t_{1/2} \times 10^{-3}$, min.$^{-1}$
2.0	0.016	167	4.2
1.0	.016	167	4.2
0.1	.020	156	4.4
10^{-8}	.010	160	4.3

[a] $k = 4.3 \times 0.1 \times 10^{-3}$ min.$^{-1}$ = $7.2 \pm 0.2\, 10^{-4}$ sec.$^{-1}$.

From measurements at 60 and at 100° the following rate constant for non acid hydrolysis of fluoroborate ion was found

$$k = 8 \times 10^{5}\, e^{-16500/RT} \text{ sec.}^{-1}$$

Discussion

Both reactions investigated, namely, the isotopic exchange between BF$_4^-$ and HF and the hydrolysis of fluoroborate ions in acid medium, follow the same rate law

$$R = k[\text{H}^+][\text{BF}_4^-]$$

It may be suggested that the isotopic exchange proceeds *via* the hydrolytic dissociation of fluoroboric acid. Consequently the acid-catalyzed hydrolysis of BF$_4^-$ will be discussed first.

The rate of hydrolysis of BF$_4^-$ may be expressed by the rate law $R_{\text{hydrolysis}} = k_h[\text{H}^+][\text{BF}_4^-]$. This rate law implies the reaction followed by a second

$$\text{BF}_4^- + \text{H}_2\text{O} \rightleftarrows \text{HBF}_4 + \text{H}_2\text{O} \qquad (1)$$

step in which HF is formed. HF may be formed from HBF$_4$ either by a dissociative process (S$_N$1)

$$\text{HBF}_4 \rightleftarrows \text{BF}_3 + \text{HF} \qquad (2)$$

followed by

$$\text{BF}_3 + \text{H}_2\text{O} \rightleftarrows \text{HBF}_3\text{OH} \qquad (2a)$$

or by a nucleophilic attack of H$_2$O on fluoroboric acid (S$_N$2)

$$\text{HBF}_4 + \text{H}_2\text{O} \rightleftarrows \text{HBF}_3\text{OH} + \text{HF} \qquad (3)$$

followed by

$$\text{HBF}_3\text{OH} + \text{H}_2\text{O} \rightleftarrows \text{BF}_3\text{OH}^- + \text{H}_3\text{O}^+ \qquad (3a)$$

Any of these reactions may be the rate-determining step; the participation of water in reaction 3 does not necessarily appear in the rate expression because its concentration remains essentially constant.

It has been shown that hydrofluoric acid as well as bisulfate ions failed to show any catalytic effect on the rate of hydrolysis; these results make a general acid catalysis rather unlikely and suggest that reaction 1 is a fast pre-equilibrium rather than a rate determining step. This assumption is supported by the relatively high energy of activation of the acid hydrolysis (~25 kcal./mole). The available experimental data on the hydrolysis of BF$_4^-$ are insufficient to decide between reaction paths (2) and (3), but some information may be gained by comparison with the reaction of fluoroborate formation.

As the equilibrium constant of BF$_4^-$ hydrolysis is unaffected by acidity,[2] the reaction of HBF$_4$ formation, namely

$$\text{BF}_3\text{OH}^- + \text{HF} \longrightarrow \text{BF}_4^- + \text{H}_2\text{O} \qquad (4)$$

must be acid catalyzed as well. It should be noted that throughout the whole range of acidities considered in this work there is no appreciable change in the concentration of HF and there are practically no fluoride ions present, therefore it is the concentration of HBF$_3$OH which increases with acidity, and reaction 5 is probably involved in the sequence of fluoroborate formation.

$$\text{H}_3\text{O}^+ + \text{BF}_3\text{OH}^- \rightleftarrows \text{HBF}_3\text{OH} + \text{H}_2\text{O} \qquad (5)$$

Once HBF$_3$OH has been formed the two alternatives are a bimolecular reaction 6

$$\text{HF} + \text{HBF}_3\text{OH} \rightleftarrows \text{HBF}_4 + \text{H}_2\text{O} \qquad (6)$$

or a fast predissociation of

$$\text{HBF}_3\text{OH} \rightleftarrows \text{H}_2\text{O} + \text{BF}_3 \qquad (7)$$

followed by

$$\text{BF}_3 + \text{HF} \longrightarrow \text{HBF}_4 \qquad (8)$$

The existence of hydrated BF$_3$ in aqueous solution as assumed in reactions 2 and 7 and its non-equivalent with the HBF$_3$OH molecule has been demonstrated by Ryss.[7]

Assuming an effective nucleophilic attack of HF on HBF$_3$OH (reaction 6) a similar interaction between HF and HBF$_4$ could be expected, leading to a bimolecular isotopic exchange. There is no experimental indication of an isotopic exchange depending on HF concentration, thus we may suggest that a bimolecular reaction between HF and HBF$_3$OH is rather unlikely. Now, if a nucleophilic attack of HF and HBF$_4$ or HBF$_3$OH seems improbable, the analogous reaction between H$_2$O and HBF$_4$ may be considered unlikely as well. The bimolecular reactions both with HBF$_4$, and HBF$_3$OH involve a five coördinated boron atom in the transition state; although such a transition state cannot be excluded, it would hardly be favored by a small boron atom shielded by negatively polarized large fluorine atoms. It is suggested, therefore, that the rate-determining step of fluoroborate hydrolysis involves a monomolecular dissociation.

The specific rate constant for the HBF$_4$ → BF$_3$ + HF reaction can only be roughly estimated. Wam-

(7) J. G. Ryss and M. M. Slutskaya, *Zhur. Obshchei Khim.*, **22**, 41 (1952).

ser found that the dissociation constant of HBF_4 is comparable with that of hydrochloric acid.[3] The dissociation constant of HCl in aqueous solution is approximately[8] 10^7, thus the specific rate constant of HBF_4 monomolecular dissociation is of the order of magnitude of 10^5 min.$^{-1}$ at 25°.

The BF_3 which is formed in the dissociative step is immediately hydrolyzed and the equilibrium $BF_3 + H_2O \rightleftarrows HBF_3OH$ is established. The equilibrium constant of this reaction ($K = 5 \times 10^6$) may be calculated from the free energies of BF_4^-, H_2O and HF[9] and from the equilibrium constant of the $BF_4 + H_2O \rightleftarrows BF_3OH^- + HF$ reaction.[2] ($K = 2.3 \times 10^{-3}$ mole l.$^{-1}$).

A specific rate constant at 25° for the reaction

$$HF + BF_3 \longrightarrow HBF_4 \ (10^{14} \text{ l. mole}^{-1} \text{ min.}^{-1})$$

can be estimated from the specific rate constant of HBF_4 hydrolysis and the equilibrium constants of the $BF_4^- + H_2O \rightleftarrows BF_3OH^- + HF$, $BF_3 + H_2O \rightleftarrows HBF_3OH$ and $HBF_3OH \rightleftarrows H^+ + BF_3OH^-$ reactions; it is then assumed that the dissociation constants of HBF_3OH and HBF_4 are comparable.

The rate of isotopic exchange between BF_4^- and HF follows the same rate law

$$R_{\text{exchange}} = k_{ex}[H^+][BF_4^-]$$

thus it may be suggested that the exchange proceeds *via* reactions 1 and 2. Yet there is an apparent discrepancy between the rate constants of the isotopic exchange and the hydrolysis reactions. At 25° we derive the values $k = 2.7 \times 10^{-2}$ and $k = 6.9 \times 10^{-3}$ l. mole^{-1} min.$^{-1}$ for the specific rate constants of the exchange and hydrolysis reactions, respectively. The energies of activation of the two reactions, on the other hand, are equal within the experimental error. The factor four between the two specific rate constants: $k_{ex}/k_h = 4$, may be accounted for if the fast isotopic equilibration $HOBF_3^- + HF^* \rightleftarrows HOBF_3^{-*} + HF$ is considered.[3] Thus for each molecule of HBF_4 undergoing hydrolysis another HBF_4 molecule is formed in which *all* four fluorine atoms are exchanged. This isotopic equilibration between BF_3OH^- and HF may be attained by successive dissociations of the type

$$HBF_3OH \rightleftarrows HBF_2OH + HF \qquad (9)$$

It may be concluded, therefore, that isotopic exchange proceeds *via* two processes; the slow hydrolysis of HBF_4 and the fast isotopic equilibrium of BF_3OH^-–HF.

Considering the non-acid hydrolysis of BF_4^- one encounters a typical SN1 (lim) mechanism[10]; there is little evidence available for the existence of a five coördinated boron atom and on the other hand both BF_3 and F^- are well established chemical species. The specific rate constants of the monomolecular dissociation of BF_4^- at 25° is slower by a factor of about 10^{10} from that of HBF_4, although its energy of activation is lower by about 9.6 kcal./mole. This points to a spectacular increase in the entropy of activation of the dissociation process on addition of a proton to the BF_4^- ion.

(8) T. Moeller, "Inorganic Chemistry," John Wiley and Sons, Inc., New York, N. Y., 1952, p. 314.

(9) W. M. Latimer, "The Oxidation States of the Elements," Prentice-Hall, Inc., New York, N. Y., 1952.

(10) F. Basolo and R. G. Pearson, "Mechanisms of Inorganic Reactions," John Wiley and Sons, Inc., New York, N. Y., 1958, p. 97.

MISCIBILITY OF METALS WITH SALTS. V. THE RUBIDIUM–RUBIDIUM HALIDE SYSTEMS

BY M. A. BREDIG AND J. W. JOHNSON

Oak Ridge National Laboratory,[1] *Chemistry Division, Oak Ridge, Tennessee*

Received May 31, 1960

The miscibility of rubidium metal with its molten halides is found to be large and, as expected, intermediate between that of potassium and cesium with their halides. A miscibility gap is absent in the RbBr–Rb system; like the other alkali metal–bromide systems, it thus deviates less from ideality than the corresponding chloride and iodide systems.

Introduction

The miscibility of the alkali metals with their halides in the molten state was shown to increase rapidly in going from the sodium systems to the potassium and cesium systems.[2] The present report covers the rubidium systems which were expected to exhibit a behavior intermediate between that of the potassium and cesium systems. One of the objectives of the present investigation was to verify the prediction that slightly smaller departure from ideality in the bromide compared with the chloride and iodide systems, as observed in the potassium[3] and sodium systems would in the case of rubidium lead to the absence of a miscibility gap in the RbBr–Rb phase diagram.

Experimental

Of the rubidium halides used, RbBr and RbI were prepared from the sulfate by double decomposition with the barium halides, recrystallization from the aqueous solution and final crystallization from the melt. The chloride was prepared from the bromide and iodide by anion exchange. The very hygroscopic fluoride was not charged to the capsule used for the thermal analysis, but was produced *in situ* by the reaction of rubidium metal with chromium difluoride. Small amounts of potassium and cesium, of a few tenths of one mole per cent., were found spectrographically to be present, but because of the similarity of these elements with rubidium are not believed to produce significant effects.

(1) Operated for the U. S. Atomic Energy Commission by the Union Carbide Corporation.

(2) M. A. Bredig and H. R. Bronstein, THIS JOURNAL, **64**, 64 (1960), and earlier papers from this Laboratory.

(3) J. W. Johnson and M. A. Bredig, *ibid.*, **62**, 604 (1958).

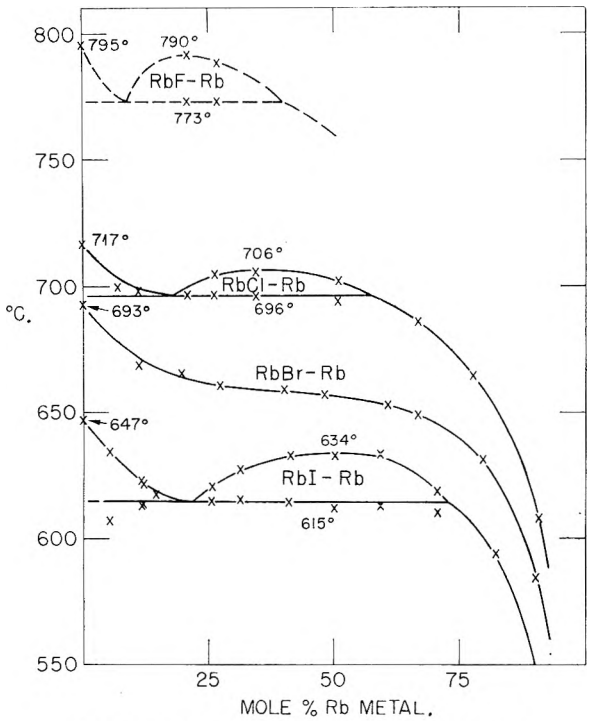

Fig. 1.—The rubidium metal–halide systems.

The technique of taking cooling curves to observe the temperature of precipitation of the second liquid phase as well as the crystallization of the halide was the same as that described previously.[3]

Results and Discussion

Table I and Fig. 1 show that the temperature–concentration area of two coexisting liquids is much smaller for the rubidium than for the potassium systems.[3] Of special interest is its complete disappearance, as expected, in the bromide system. Table II gives the compositions of the liquid phases at the monotectic and consolute temperatures. The very few tests performed in the RbF–Rb system are of an exploratory nature, merely intended to demonstrate the existence of a small area of immiscibility in the molten state. Interestingly, the consolute temperature, in all cases, lies below the melting point of the salt.

With increasing metal concentration, the depression of the melting point of the salt becomes progressively smaller than depressions calculated from the (analytical) salt concentration, N_1, and the heat of fusion of the salt, ΔH_m, by the (approximate) formula $d \ln N_1/d(1/T) = -\Delta H_m/R$ In the sodium and potassium system, this deviation has been attributed to a non-linear change in the true mole fraction of the salt caused by dimerization of the metal solute, *i.e.*, formation of a metal molecule, M_2, as an intermediate in approaching the constitution of the pure metal phase. This assumption which was useful in the interpretation of the electrical conductivity measurements[4] is also believed to be valid for the rubidium systems. It is of interest to note that no such concentration-dependent *positive* deviation from the calculated liquidus curve occurs in some other metal halide–metal systems, notably Cd–$CdCl_2$,[5] Ni–$NiCl_2$,[6] Ba–$BaCl_2$,[7] and others. Rather, monomeric dispersion of the added metal in the solution, most probably in the form of species resulting from oxidation–reduction reactions with the salts (*e.g.*, $Cd + Cd^{++} \rightarrow Cd_2^{++}$, $Ni + Ni^{++} \rightarrow 2\,Ni^{+}$, and, perhaps, $Ba + Ba^{++} \rightarrow Ba_2^{++}$ and others), can account for the results of cryoscopic and some electrical conductance measurements in those cases.

TABLE I

SOLUBILITY RELATIONS IN THE RUBIDIUM–RUBIDIUM HALIDE SYSTEMS

	Solid salt and soln.			Two liquid phases		
	Temp., °C. (±0.5)	Mole % salt (±0.1)	Monotectic Temp., °C. (±0.5)	Temp., °C. (±0.5)	Mole %, salt (±0.1)	Monotectic Temp., °C. (±0.5)
Fluoride	795	100		787	73.1	773.0
				791	79.1	773.5
	608.0	9.2		701.7	49.2	693.5
	664.3	22.2		705.7	65.5	695.4
	685.7	33.3		704.7	73.8	696.5
Chloride				...	79.4	696.4
	697.8	88.9				
	699.5	93.0				
	715.9	100				
	584.3	10.0				
	630.9	20.4				
	648.6	33.5				
	652.9	39.2		One liquid phase		
Bromide	656.9	52.0		only.		
	658.9	60.0				
	660.6	72.9				
	665.2	81.4				
	668.6	88.8				
	692.5	100				
	593.8	18.0	...	618.5	29.3	609.7
				632.7	40.6	612.4
	616.0	85.4	609.7	632.6	49.8	611.9
Iodide	621.7	88.1	613.7	632.8	58.8	614.4
	622.7	88.4	613.0	627.3	68.7	615.2
	634.0	95.6	606.4	620.5	74.3	614.9
	646.9	100	...			

TABLE II

SUMMARY OF CHARACTERISTIC COMPOSITIONS IN THE Rb–RbX SYSTEMS

X =	F	Cl	Br	I
Monotectic liquid salt phase, mole % salt	(91)	82	None	78
Monotectic liquid metal phase, mole % salt	(60)	43	None	27
Consolute composition, mole % salt	(79)	63	None	49

Acknowledgment.—The assistance of J. E. Sutherland in some of the experimental work and discussions with Professor Wm. T. Smith, Jr., Chemistry Department, University of Tennessee, are gratefully acknowledged.

(4) H. R. Bronstein and M. A. Bredig, *J. Am. Chem. Soc.*, **80**, 2077 (1958).

(5) A. H. W. Aten, *Z. physik. Chem.*, **73**, 578 (1910); K. Grjotheim F. Grönvold and J. Krogh-Moe, *J. Am. Chem. Soc.*, **77**, 5824 (1955).

(6) J. W. Johnson, Daniel Cubicciotti and C. M. Kelley, THIS JOURNAL, **62**, 1107 (1958).

(7) D. T. Petersen and J. A. Hinkebein, *ibid.*, **63**, 1360 (1959); J. A. Hinkebein, Dissertation Iowa State College, 1958; H. Schäfer and A. Niklas, *Angew. Chem.*, **64**, 611 (1952).

THE ION PAIR-QUADRUPOLE EQUILIBRIUM. TETRABUTYLAMMONIUM BROMIDE IN BENZENE–METHANOL MIXTURES[1]

BY KURT H. STERN[2] AND EDWIN A. RICHARDSON

Department of Chemistry, University of Arkansas, Fayetteville, Arkansas

Received June 2, 1960

An improved equation for the calculation of the ion pair-quadrupole equilibrium constant from dielectric data[3] is derived. An electrostatic model for the free energy is presented and compared with experiment. The continuum theory for the solvent is satisfactory for ΔF, but fails for the entropy.

We have shown recently[3] that the dielectric properties of tetrabutylammonium bromide–benzene–methanol solutions can be explained in terms of an increase in ion pair concentration (and a corresponding decrease in non-polar quadrupoles) as MeOH is added to benzene; further that the effect is most pronounced at low MeOH concentrations—no quadrupoles remain when the mole fraction MeOH exceeds 0.1—and cannot be explained in terms of an increase in solvent dielectric constant.

The purpose of the present work is to present an improved method for the calculation of the ion pair–quadrupole equilibrium constant and to discuss the thermodynamics of the process.

Equilibrium Constant.—In the original paper[4] "normal" behavior, *i.e.*, one in which no changes in the state of aggregation occur, was defined by equations 12–15 which assumed that the addition of a given amount of salt to a methanol–benzene mixture would increase the polarization as much as the same amount of salt to pure benzene. This assumption cannot be quite correct since the former solvent would produce more ion pairs for the same amount of salt. This leads us to substitute for equation 14

$$p_{123} = p_{12} + dX_3 \qquad (14')$$

where the subscripts 1,2,3 refer to the non-polar solvent, the polar molecule, and the electrolyte, respectively, and the p's are volume polarizations. On this basis an equilibrium constant for the formal equilibrium $Q \rightleftarrows 2I$ can be derived by a method quite analogous to that given previously. For $F(p)$[5] we then have

$$F(p) = dI - bI^0 \qquad (1)$$

Further, from equation 1 we have at the critical point (*i.e.*, the lowest MeOH concentration at which no quadrupoles remain)

$$F^c(p) = d^cX_3 - bI^0 \qquad (2)$$

Eliminating the term bI^0 from (1) and (2) gives

$$I = \frac{F(p) + d^cX_3 - F^c(p)}{d}$$

from which

$$K = \frac{I^2}{X_3 - I} = \frac{\left[\frac{F(p) + d^cX_3 - F^c(p)}{d}\right]^2}{X_3 - \left[\frac{F(p) + d^cX_3 - F^c(p)}{d}\right]} \qquad (3)$$

At $X_2 = X_2^c$, $F^c(p) = F(p)$ and $K \to \infty$, *i.e.*, the solute is completely dissociated into ion pairs. At $X_2 = 0$, $F(p) = 0$ and

$$K^0 = \frac{\left[\frac{d^cX_3 - F^c(p)}{d}\right]^2}{X_3 - \left[\frac{d^cX_3 - F^cp}{d}\right]}$$

The effect of changing MeOH concentration (X_2) on K at 25° is shown in Table I. All values in this paper have been recalculated on the molarity scale—from the mole fraction scale of the original paper—to facilitate comparison with the ion pair-free ion equilibrium data in the literature.

TABLE I

EFFECT OF MeOH ON $K(25°)$[a]

$X_3 \times 10^4$	K^0 ($X_2 = 0$) $\times 10^5$	K ($X = 0.005$) $\times 10^4$	K ($X_2 = 0.010$) $\times 10^3$	K ($X_2 = 0.015$) $\times 10^2$
0.5	..	5.1	..	..
1.0	5.1	5.7	4.6	..
1.5	6.2	6.6	3.7	..
2.0	8.8	7.0	3.3	2.3
2.5	5.1	5.6	2.2	1.1
3.0	..	..	3.3	1.4

[a] X_2, X_3 represent the mole fractions of MeOH, Bu_4NBr, respectively, but K values are calculated on the molarity scale. For a comparison of the dependence of K on X_3 with the mole fraction scale, *cf.*, Table VI of ref. 3.

Thermodynamics.—In Table II are listed values of K at three temperatures in pure benzene and three benzene–MeOH solutions. Each of these values has been obtained by averaging K values over all salt concentrations in Table I. The sensitivity of the equilibrium to small concentrations of MeOH is rather striking. Thus a change in dielectric constant from 2.27 ($X_2 = 0$) to 2.31 ($X_2 = 0.01$) changes K by a factor of 200. This is a far greater change than has been observed for the ion pair-free ion equilibrium. However, it is clear that the change in K cannot be attributed to a change in ϵ. Thus, for example, for pure benzene a change in temperature of 20° (25–45°) gives a $\Delta\epsilon$ of 0.035. Yet in this solvent K *increases* with a *decrease* in ϵ. The effects are thus in the opposite direction. This has also been noted for the ion pair-free ion equilibrium of Bu_4NPi in the chlorobenzenes.[6]

It is of some interest to calculate the thermodynamic functions for the process since particularly entropies give some indication of changes in the solvent. The molar entropy in pure benzene is thus 2.4/2 = 1.2 e.u. From a doubling of particles

(1) Based in part on the M.S. Thesis of E. A. Richardson.

(2) Electrochemistry Section, National Bureau of Standards, Washington 25, D. C.

(3) E. A. Richardson and K. H. Stern, *J. Am. Chem. Soc.*, **82**, 1296 (1960).

(4) For terminology and definitions this paper should be consulted.

(5) $F(p) = (p_{123} - p_{12}) - (p_{12} - p_1)$.

(6) P. H. Flaherty and K. H. Stern, *J. Am. Chem. Soc.*, **80**, 1034 (1958).

TABLE II

EQUILIBRIUM CONSTANTS FOR Q ⇄ 2I IN THE BENZENE–METHANOL SYSTEM (MOLARITY SCALE)

t (°C.)	$X_2 = 0$	$X_2 = 0.005$	$X_2 = 0.010$	$X_2 = 0.015$
25	6.3×10^{-5}	6.0×10^{-4}	3.4×10^{-3}	1.8×10^{-2}
35	9.3	6.2	2.6	1.1
45	12.6	6.6	2.4	0.9

TABLE III

THERMODYNAMIC QUANTITIES FOR THE EQUILIBRIUM Q ⇄ 2I (MOLARITY SCALE)[a]

X_2	ΔF^0_{298} (kcal.)	ΔH^0 (kcal.)	ΔS^0 (cal./°)
0.000	5.7	6.5	2.4
.005	4.4	0.8	−12
.010	3.4	−3.3	−22
.015	2.4	−7.0	−31

[a] Thermodynamic values are given for two moles of electrolyte.

alone one would expect $R \ln 2 = 1.4$ e.u. This is excellent evidence that the effect on the solvent is virtually negligible, *i.e.*, at least no *change* in solvation occurs as quadrupoles separate to ion pairs. The situation becomes strikingly different when MeOH is added. For every change in X_2 of 0.005 the entropy decreases by roughly 10 e.u. indicating the increasing solvation of ion pairs over quadrupoles. Up to a MeOH concentration of 0.015 the ion pairs do not seem to be "saturated" with MeOH since the entropy decrease shows no leveling off.

The enthalpy decrease is also fairly regular. In pure benzene a positive ΔH^0 is to be expected if only ion pair-ion pair (electrostatic) "bonds" are broken. With increasing MeOH the greater attraction of MeOH–electrolyte forces over those of MeOH–MeOH leads to an increasingly negative ΔH^0. More direct evidence for the solvation of Bu_4NBr ion pairs by MeOH has recently been obtained from infrared spectra.[7]

The continuum theory applied to the solvent will also yield an entropy decrease for the processes described without requiring a solvation model. For the ion-ion pair equilibrium this has been worked out by Denison and Ramsey.[8] Although the predicted dependence of ΔF^0 for this equilibrium on the *dielectric constant* agrees very well with experiment,[9] there have been very few tests for ΔH^0 and ΔS^0. In ethylene chloride and ethylidene chloride agreement appears to be satisfactory[8]; in the chlorobenzenes experimental entropies are about half the predicted ones.[6] In order to test the continuum theory for the higher equilibrium we write, analogous to the cycle used by Denison and Ramsey[8]

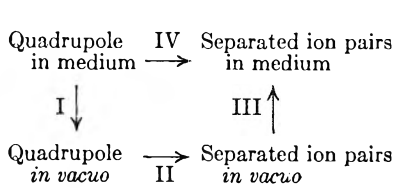

We assume, as did Denison and Ramsey, that in charging the ions they may be considered conducting spheres, but that in their interactions they behave as point charges. Since the free energy of solution for the uncharged ions is independent of distance and cancels we have omitted it. It is assumed that the ion pairs are separated to large distances. There are two distances in a quadrupole for ions of nearly equal size: r_1 = anion–cation distance, r_2 = distance between ions of like charge. a_+ and a_- are the cation and anion radii, respectively.

The work of forming a quadrupole *in vacuo*[10] and charging the four ions is

$$-\frac{4e^2}{r_1} + \frac{2e^2}{r_2} + \frac{e^2}{a_+} + \frac{e^2}{a_-}$$

and therefore the work done on the system in moving a quadrupole from the medium to a vacuum is

$$W_{\mathrm{I}} = \left(-\frac{4e^2}{r_1} + \frac{2e^2}{r_2} + \frac{e^2}{a_+} + \frac{e^2}{a_-}\right)(1 - 1/D)$$

The work of forming two ion pairs *in vacuo* from a quadrupole is

$$W_{\mathrm{II}} = 2\left(\frac{e^2}{2a_+} + \frac{e^2}{2a_-} - \frac{e^2}{r_-}\right) - \left(-\frac{4e^2}{r_1} + \frac{2e^2}{r_2} + \frac{e^2}{a_+} + \frac{e^2}{a_-}\right)$$

and

$$W_{\mathrm{III}} = 2\left(\frac{e^2}{2a_+} + \frac{e^2}{2a_-} - \frac{e^2}{r_1}\right)(1/D - 1)$$

The net process

$$W_{\mathrm{IV}} = W_{\mathrm{I}} + W_{\mathrm{II}} + W_{\mathrm{III}} = \frac{2e^2}{D}\left(\frac{1}{r_1} - \frac{1}{r_2}\right)$$

For one mole of electrolyte

$$\Delta F_{\mathrm{IV}} = \frac{Ne^2}{D}\left(\frac{1}{r_1} - \frac{1}{r_2}\right)$$

To test this model some choice of distances is necessary. r_1 should approximate the usual ion pair contact distance a. For equal anion–cation radii $r_2 = r_1\sqrt{2}$. For other size relationships a particular model must be postulated. The model used here is already somewhat simplified since in general anion–anion and cation–cation distances will not be equal. This is particularly true for rigid ions of widely different sizes. At the present stage of the theory it does not seem worthwhile to introduce too many arbitrary parameters. The theory can be used in two ways: (a) using experimental distances to calculate ΔF^0, (b) using experimental ΔF^0's to calculate distances. In either case we shall assume that the experimental ion-pair distance for Bu_4NBr[3] is valid. (a) For a square array in the quadrupole $r_1 = 2.90$ Å., $r_2 = r_1\sqrt{2} = 4.90$ Å., $\Delta F^0_{\mathrm{calc}} = 20.6$ kcal. (b) $\Delta F^0_{\mathrm{exp}}$ $(X_2 = 0) = 2.83$ kcal., $r_2 = 3.1$ Å. This calculation indicates that the assumption of a square array for the quadrupole gives quite poor agreement for ΔF^0. An examination of molecular models shows that the accommodation of the large cations in the quadrupole to an r_2 of 3.1 Å. leads to a tight but not impossible structure. As has been found previously for the ion pair case[11] it

(7) J. Bufalini and K. H. Stern, *Science*, **130**, 1249 (1959).

(8) J. T. Denison and J. B. Ramsey, *J. Am. Chem. Soc.*, **77**, 2615 (1955).

(9) *E.g.*, E. Hirsch and R. M. Fuoss, *ibid.*, **82**, 1018 (1960).

(10) G. P. Harnwell, "Principles of Electricity and Electromagnetism," 2nd Ed., McGraw-Hill Book Co., New York, N. Y., 1949, p. 48.

(11) K. H. Stern, F. H. Healey and A. E. Martell, *J. Chem. Phys.*, **19**, 1114 (1951).

would require that the anions be in contact with the nitrogen atom of the quaternary ammonium ion, the butyl groups moving out of the way to permit this. Considering the rather crude model used for the electrostatic free energy calculation the agreement must be regarded as satisfactory.

The situation is strikingly different as far as the enthalpies and entropies are concerned. A test of the continuum theory for these quantities requires no detailed model. Using experimental ΔF^0's we simply write,[8] assuming independence of ion size parameters with changing temperature

$$\Delta S^0 = \Delta F^0 \,(\mathrm{d} \ln D/\mathrm{d}T) = (\Delta F^0/T)(\mathrm{d} \ln D/\mathrm{d} \ln T)$$
$$\Delta H^0 = \Delta F^0 \,(1 + \mathrm{d} \ln D/\mathrm{d} \ln T)$$

and use the values of ΔF^0 derived from Table II. Calculated enthalpies and entropies are shown in Table IV. This is the test previously applied to the ion–ion pair equilibrium.[6]

Comparison with the experimental quantities in Table III shows that agreement is quite poor. This is particularly true of the entropy in which the trend predicted is actually the reverse of the observed one. Also the observed positive entropy in pure benzene is not accounted for by the continuum theory. Clearly the discontinuous nature of the solvent and its specific interactions with the electrolyte must be taken into account.

TABLE IV

TEST OF THE CONTINUUM THEORY[a] (25°); ΔS^0 AND ΔH^0

X_2	$\Delta S^0_{\mathrm{calc.}}$ (e.u.)	$\Delta H^0_{\mathrm{calc.}}$ (kcal.)
0.0	−4.8	4.3
.005	−3.7	3.4
.010	−2.7	2.5
.015	−2.0	1.8

[a] For all solvents d ln D/d ln T = −0.25.

Acknowledgment.—We would like to thank the National Science Foundation for the financial support of this work.

SORPTION AND MAGNETIC SUSCEPTIBILITY STUDIES ON NITRIC OXIDE–ALUMINA GEL SYSTEMS AT SEVERAL TEMPERATURES

BY AAGE SOLBAKKEN[1] AND LLOYD H. REYERSON

School of Chemistry, University of Minnesota, Minneapolis, Minnesota

Received June 13, 1960

Sorptions of nitric oxide by alumina gel were determined at 181, 192, 207 and 273°K. Magnetic susceptibility of the sorbed nitric oxide was followed by a movable magnet. A rapid physical adsorption of the nitric oxide was in each case followed by a slow chemisorption. This was definitely shown by the magnetic studies, for the susceptibility rose rapidly during the physical adsorption and then remained almost constant or fell slightly during the long period of chemisorption. Desorption of the physically sorbed nitric oxide causes the magnetic susceptibility to fall to the starting point. The slow desorption of the chemisorbed gas produces no further change in the susceptibility of the system. Here is a system exhibiting both physical and chemisorption under the same conditions. Further, the rate of chemisorption was found to be faster at lower temperatures, indicating a negative energy of activation if calculated in the usual manner. The data indicate that the transmission coefficient for the chemisorption is very low.

Introduction

Early studies in this Laboratory[2] on the magnetic susceptibility and sorption of nitrogen dioxide on alumina gel had strongly indicated that NO_2 was chemisorbed by alumina gel, and the magnetic studies indicate that aluminum nitrate was formed on the surface. More recent studies[3] on the sorption of nitric oxide on silica gel showed marked differences between the behavior of NO_2 and NO on this gel. Where the NO_2 was physically sorbed and dimerized on the gel, the NO was physically sorbed but showed definite $^2\Pi_{3/2}$ character until the surface was nearly covered with a monolayer at lower temperatures. These results suggested that the sorption of NO should be studied on alumina gel under conditions similar to those reported on silical gel. The following experiments show markedly different results from those previously reported.

Experimental

Using the same sorption and magnetic equipment as described earlier,[3] isotherm and magnetic susceptibilities were determined at 181, 192, 207 and 273°K. The alumina gel was prepared by the same identical method as in the former study.[2] Its area, as determined by the BET-nitrogen method, was found to be 368 m.²/g. In contrast, the silica gel used in the recent work[3] had an area of 562 m.²/g. The same high purity nitric oxide was sorbed and at no time during the whole investigation did the sorbed gas show any color, as reported by J. H. deBoer on work done in the laboratories of the States' Mines in Holland.[4] The very first experiments at 192°K. showed that a very different process was going on than had been previously observed. A rapid physical adsorption occurred which was followed by a very slow chemisorption. The magnetic susceptibility rose rapidly, following the physical adsorption, until the slow chemisorption began. The susceptibility then remained almost constant or fell slightly during chemisorption. This showed that the physically adsorbed gas behaved in a way similar to that adsorbed by silica gel.[3]

The chemisorption which followed was of a very different character from previous chemisorptions observed in this Laboratory. The initial rate depended on the pressure of the gas and the temperature. However, for similar pressures, the rate increased as the temperature was lowered. The rate for a given pressure and temperature declined slowly with time. If after several hours the gas pressure was reduced to zero, the physically sorbed gas quickly desorbed and the magnetic susceptibility fell to the initial value. A slow desorption of the chemisorbed gas followed with no change in magnetic susceptibility.

Because of this slow desorption, it was found desirable to warm the sample and remove all the adsorbed nitric

(1) Graduate Norwegian Fellow at the University of Minnesota from the Norwegian Institute of Technology, Trondheim, Norway.

(2) L. H. Reyerson and John Wertz, THIS JOURNAL, **53**, 234 (1949).

(3) Aage Solbakken and Lloyd H. Reyerson, *ibid.*, **63**, 1622 (1959).

(4) Personal communication from Professor J. H. deBoer.

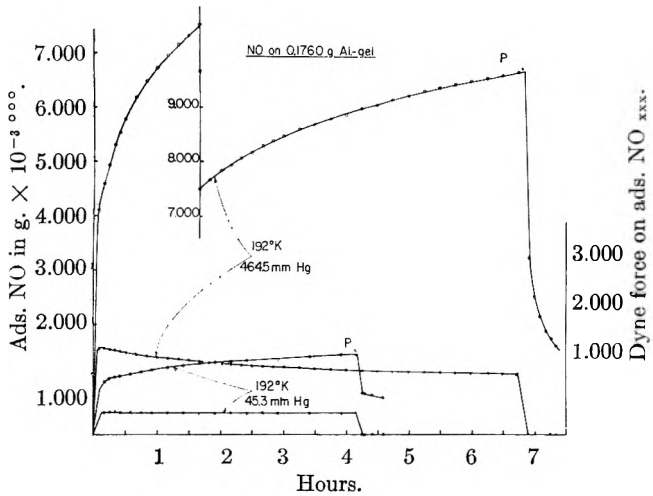

Fig. 1.

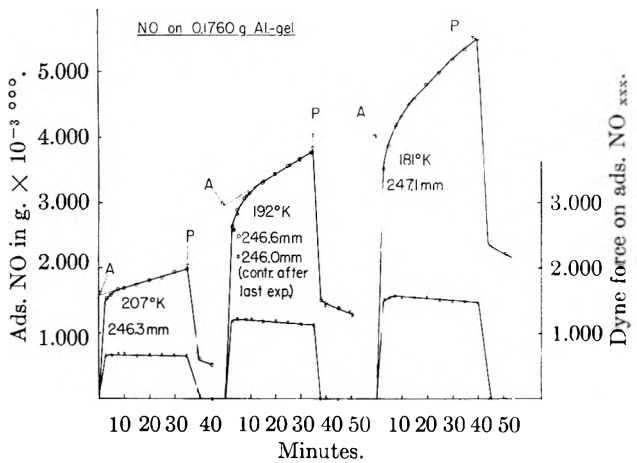

Fig. 2.

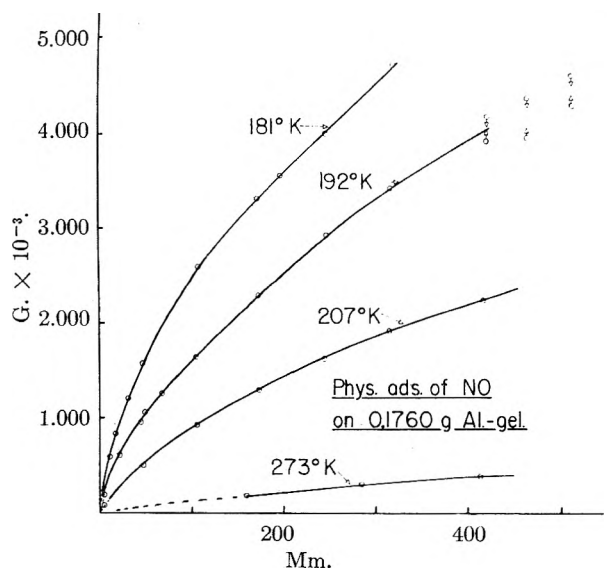

Fig. 3.

oxide before starting each new set of determinations. Thus the weight of the adsorbent was the same at the beginning of each new isotherm. The first isotherms were determined at 192°K. and those at 181, 207 and 273°K. followed. Buoyancy corrections, as well as corrections for the magnetic character of the gas present, were applied to each measurement.

Results

Physical Adsorption.—Since the NO was physically adsorbed rapidly, the equilibrium for this part of the process was reached in a couple of minutes. The chemisorption which followed gave a rate curve which was reasonably straight after the conclusion of physical adsorption. It was considered reasonable to extrapolate this curve back to zero time and use the value of this intercept for the amount of physical adsorption. Figure 1 shows the data obtained for two pressures at 192°K. The small circles show the amounts sorbed plotted against time, while the small crosses give the values of the magnetic force *vs.* time. The long, fine lines headed by arrows tie the curves for sorption with the magnetic curves for each of the two pressures. The results show that the magnetic susceptibility of the adsorbate–adsorbent system rises to a maximum and then remains almost constant or falls slightly during the slow chemisorption. At the points P the gas pressure was quickly reduced to zero and the physically adsorbed NO came off the surface rapidly, followed by a slow desorption of the chemisorbed gas. The susceptibility fell to its initial zero value during desorption of the physically adsorbed gas and then remained constant.

Figure 2 gives the adsorption–rate data as well as the magnetic susceptibility values obtained at three different temperatures using essentially the same gas pressure. These results clearly show that the rate of chemisorption rises as the temperature is lowered. Space does not permit presenting all the data obtained. The chemisorption data together with the data presented in Figs. 1–2 will be discussed in the section on chemisorption which follows. The amounts of physically adsorbed gas, obtained by the indicated extrapolated points at zero time, give the adsorption isotherms presented in Fig. 3. The scattered points at the upper end of the isotherm at 192°K. show the extremes in the accuracy that may be obtained by extrapolation of the straight line plots at higher pressures.

The isotherms for physical adsorption were all obtained at temperatures above the critical temperature for NO and show a progressive increase in the amounts adsorbed as the temperatures are lowered. The magnetic data for physical adsorption are presented in Figs. 4 and 5. It will be observed in Fig. 4 that, as reported for silica gel,[3] the physically sorbed gas at 273° has the same magnetic susceptibility as the gaseous mixture at that temperature. The points give the experimental results, while the solid line represents the calculated susceptibility of the gas at 273°K. In the lower part of Fig. 4 and for Fig. 5, the susceptibility of the first gas adsorbed follows the curve calculated for a magnetic value of 2 Bohr magnetons in the gaseous state. The lower straight lines in each case gives the susceptibility that should be observed were the gas adsorbed in the same state as in the gas phase.

As was found for silica gel, a break occurs in the curves for the observed data. Above the break

point the data gives values which definitely show that the additional adsorbed gas has the same magnetic character as that in the gas phase, while below the break point the gas shows a magnetic behavior of 2 Bohr magnetons. Table I gives the values of the amounts of NO adsorbed per cm.^{2} at the point where there is an abrupt change in the curves obtained by plotting susceptibility *vs.* amounts adsorbed. It can be noted that the number of molecules per unit area of surface which exhibit the higher magnetic property is greater for silica gel than for alumina gel. Furthermore, the number of these molecules is greater at lower temperatures. In the case of alumina gel, the largest number exhibiting the higher magnetic character was found at 207°K. and this number decreased as the temperature was lowered. It thus appears that the two surfaces act somewhat differently in physically adsorbing NO.

TABLE I

AMOUNTS OF NO ADSORBED PER UNIT AREA AT THE BREAK POINT OF THE MAGNETIC CURVES

Temp., °K.	Silica gel		Alumina gel	
	G./cm.^{2}	Molecules/cm.^{2}	G./cm.^{2}	Molecules/cm.^{2}
181	4.22×10^{-9}	0.85×10^{14}	1.31×10^{-9}	0.26×10^{14}
192	.....	.....	1.70×10^{-9}	0.34×10^{14}
193	3.66×10^{-9}	0.73×10^{14}	.....	.....
207	.....	.....	2.94×10^{-9}	0.59×10^{14}
273	0.00	0.00	0.00	0.00
293	0.00	0.00	..	..

The heats of adsorption for the physically bound NO as calculated from the isotherms of Fig. 3 by the Clausius–Clapeyron expression are given in Fig. 6. Although these calculations cannot be too accurate, the curves definitely show a change in the heats of adsorption at the same amount adsorbed as at the break point in the magnetic susceptibility curves in Figs. 4 and 5. These results are similar to those previously observed.[3]

Chemisorption.—The rates of chemisorption are calculated from tangents to the rate curves shown in Figs. 1–2 as well as to curves not shown because of space limitations, and are plotted as a function of the pressure in Fig. 7. The rates are definitely proportional to the pressures at lower values while the scattering of the points at higher pressures is due to the lack of precision in drawing the tangents to the curves because of the more rapid changes in weight. Arrow points represent two extreme tangents.

From the plots it can be seen that chemisorption proceeds faster at lower than at higher temperatures indicating a negative heat of activation if one uses the usual method for calculating chemisorption processes. By extrapolating the rates to one atmosphere of gas pressure and plotting a usual log K/T *vs.* $1/T$ one finds an enthalpy of activation $\Delta H^{\pm} = -3375$ cal./mole (assuming the change in the entropy of activation with the temperature to be negligible). From free energy considerations, the theoretical rate constants, based on two different assumptions as to initial and final states, are calculated for a transmission coefficient of unity. These results are given in Table II where they are compared to the observed experimental results. It turns out that a transmission coefficient of about

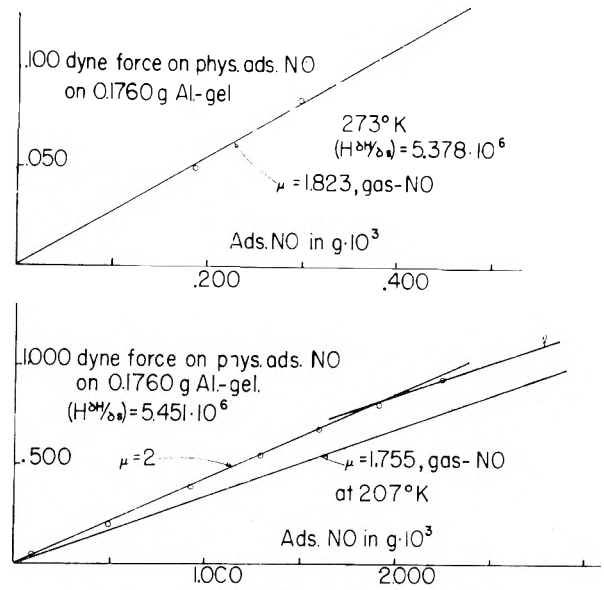

Fig. 4.

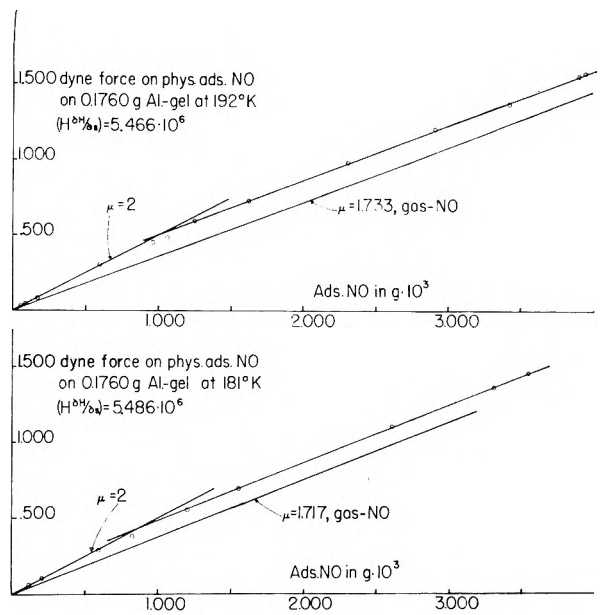

Fig. 5.

10^{-8} is required in order that the theoretical and experimental results agree reasonably well. The calculations for Table II section A were carried out on the basis of gaseous NO at one atmosphere pressure going to the activated complex of chemisorbed NO on the surface. This is the usual method adopted for the calculation of chemisorption rates.

However, the negative enthalpy of activation indicates that the mechanism involves an intermediate state. In this case the intermediate state must be the physically adsorbed NO. The isotherms of Fig. 3 permit the determination of the amounts of physically adsorbed NO at the several temperatures. The results were then used to obtain values for the rates of chemisorption at the same coverage of the surface at all of the temperatures used in the study. The rates were compared for an adsorption of 0.250 mg. of NO on the total area of the sample, *i.e.*, 64.8×10^4 cm.^{2}. Using these

TABLE II

	A: Calcd. data are based on the assumption that gaseous NO goes to the activated complex of chemisorbed NO. $\Delta H^{\ddagger} = -3{,}375$ cal./mole					B: Calcd. data are based on the assumption that the physically adsorbed NO goes to final chemisorbed NO. $\Delta H^{\ddagger} = 1.020$ cal./mole at 0.250 mg. NO adsorbed on the sample. $\theta \approx 0.1$ for 10^{14} adsorption sites/cm.^{2}				
Temp., °K.	$r^a \times 10^8$ (mole/sec.)	$\Delta S^{\ddagger}$ [b]	$K_{theor.}$ [c] $\times 10^{-8}$	$K_{exptl.}$ [d] $\times 10^3$	$\chi \times 10^8$	$r^e \times 10^9$	$\Delta S^{\ddagger}$ [f]	$K_{theor.}$ $\times 10^{-8}$	$K_{exptl.}$ $\times 10^4$	$\chi \times 10^8$
181	7.49	−43.95	11.2	6.91	0.6	1.45	−34.95	4.6	9.40	0.98
192	4.82	−44.28	5.45	4.42	0.8	0.65	−35.19	5.1	0.57	1.2
207	2.40	−45.04	2.03	2.24	1.1	0.51	−35.50	5.8	0.73	1.3
273	0.48	−46.98	0.14	0.44	3.1	0.35	−36.58	8.1	1.62	2.0

[a] Rate is extrapolated to 1 atm. pressure. [b] $\Delta S^{\ddagger} = -(S^0_{trans} + S^0_{rotation})$ at 1 atm. [c] $K_{theor.} = \frac{\kappa T}{h} e^{\Delta S^{\ddagger}/R} e^{-\Delta H^{\ddagger}/RT}$ sec.$^{-1}$ atm.$^{-1}$. [d] $K_{expt.} = \frac{rN}{As}$ sec.$^{-1}$ atm.$^{-1}$. r in moles/sec. A = area of sample 64.8 × 10^4 cm.^{2}. s = no. of sites. 10^{14} sites/cm.^{2}. [e] Rate is calculated at a coverage of 0.250 mg. NO on total sample. [f] $\Delta S^{\ddagger} = -(S^0_{trans} + S^0_{rot})$ as a two-dimensional gas at a coverage of 0.250 mg. NO on sample (84.8 × 10^4 cm.^{2}). χ = transmission coefficient.

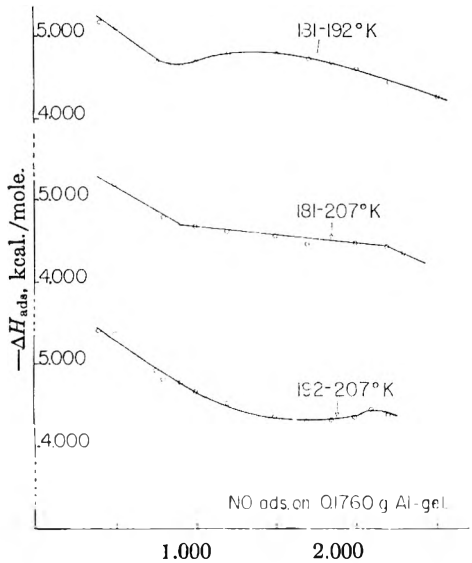

Fig. 6.

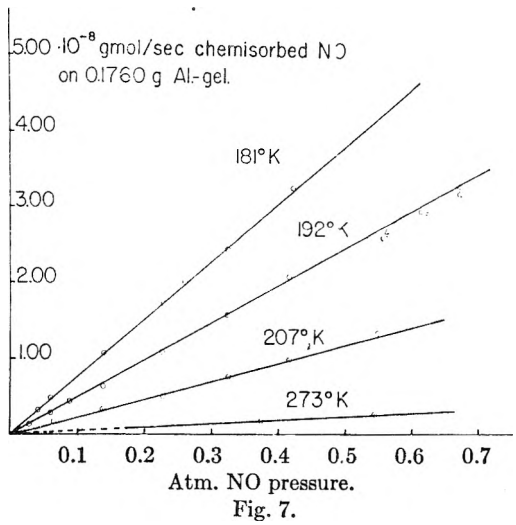

Fig. 7.

rates the log K/T *vs.* $1/T$ plot gave an enthalpy of activation of $\Delta H^{\ddagger} = 1{,}030$ cal./mole. Assuming that the physically adsorbed NO behaves as a two-dimensional gas, which has lost one degree of translational freedom, its entropy was calculated. The entropy of the activated chemisorbed complex was considered to be only vibrational entropy. Section B of Table II gives the results of such calculations. Again a transmission coefficient of about the same order of magnitude, *i.e.*, 10^{-8}, is needed to bring the experimental results in line with the theoretical rate constants.

In Fig. 8 an attempt is made to show the potential energy of the system as a function of the distance from the adsorption surface. The probable energies for the physically adsorbed state, the activated complex of the chemisorbed state and the chemisorbed state are shown on the curves. The differential enthalpies of physical adsorption, as calculated from isotherm data and shown in Fig. 6, vary between −4,000 and −5,000 cal./mole. If the value of the heat of activation for the process of the physically adsorbed NO going to the chemisorbed state, $\Delta H^* = 1{,}030$ cal./mole, be added to these values then we obtain values between −3,000 and −4,000 cal. for the potential energy of the activated complex when referred to the initial gaseous state. This is in quite good agreement with the negative heat of activation of −3,375 cal. obtained by using usual methods for calculating the chemisorption rates using the gaseous state and the clean surface as the reacting species. The agreement between the energy results obtained by considering two different mechanisms suggest the possibility that both mechanisms may be operating. The experimental results together with the theory seem to the authors to be better satisfied by the second mechanism. The following equations suggest the possible path of this chemisorption process. Gaseous molecules of NO are first physically adsorbed very rapidly by the Al_2O_3. The physically adsorbed complex then undergoes an unpairing of electrons in the Al_2O_3 yielding a covalent compound with one unpaired electron. In the final step, a second physically adsorbed NO combines rather rapidly with the intermediate compound giving the final diamagnetic product.

$$NO\cdot + Al_2O_3 \rightleftarrows \{Al_2O_3 + NO\cdot\} \quad \text{physical adsorption}$$

$$\{Al_2O_3 + NO\cdot\} \rightleftarrows \{\cdot Al_2O_3\cdot NO\cdot\} \quad \text{slow multiplicity change}$$

$$\{\cdot Al_2O_3\cdot NO\cdot\} \rightleftarrows NO{:}Al_2O_3\cdot \quad \text{covalent intermediate}$$

$$NO{:}Al_2O_3\cdot + NO\cdot \rightleftarrows NO{:}Al_2O_3{:}NO \quad \text{final product}^5$$

Discussion

It is evident that, in this study, we have an unusual example of physical adsorption and chemisorption taking place at a given solid–gas interface at the same time. Physical adsorption is rapid at 181, 192, 207 and 273°K. The magnetic susceptibility rises almost immediately to a value which is equivalent to that of NO in the excited state or that of the mixture of the two states. At the same time a slow chemisorption begins and during the whole chemisorption process, as measured in this study, there was no further appreciable change in the magnetic susceptibility of the gel with its adsorbed NO. Thus the odd electron of the chemisorbed NO must be bonding with an electron of the alumina gel. If the gas pressure of NO is quickly reduced to nearly zero the physically adsorbed gas comes off at once and the susceptibility falls to the original value for the gel. The chemisorbed NO comes off very slowly, indicating a sizable energy of activation. There is ample proof that dimerization of NO is not involved. The fact that at lower temperatures all of the NO, physically adsorbed up to nearly mono layer coverage, shows a magnetic susceptibility equivalent to 2 Bohr magnetons, suggests that the surface–NO interaction involves a total uncoupling of the spin–orbital interaction in the odd electron of NO rather than that the surface specifically adsorbs NO in the $2\pi^3/_2$ state. Since this does not happen at room temperature it would seem likely that the NO molecules are closer to the surface at the lower temperatures. If so the uncoupling forces might be perturbation forces which are very dependent upon the distance. Present knowledge of surface states makes it difficult to define actually the kinds of forces but these results suggest that such forces are strongly dependent on the temperature-dependent concentrations of electrons in certain energy levels in the surface of the solid.

Several interesting facts become evident from the chemisorption process. The process itself is slow but the rate increases as the temperature is lowered. Chemisorption is about twice as fast at 181 as at 192° K. During the long period of chemisorption the magnetic susceptibility of the Al_2O_3–NO complex either remains constant or falls slightly. This can only mean that there is a change of electron multiplicity involved as each NO molecule becomes, chemisorbed. The single odd electron of NO, in an uncoupled spin state, probably induces an unpairing of electrons in the alumina gel (Al_2O_3) to yield an intermediate covalent compound having one unpaired electron. In the final step a second NO molecule, either physically adsorbed or as a gas molecule colliding with the surface, combines rapidly with this unpaired electron to give the final diamagnetic product.

The results given in Table II show that essentially the same transmission coefficient of 10^{-8} is obtained on the basis of either assumed mechanism for the chemisorption process. This would indicate that we are dealing with a non-adiabatic reaction. In such a reaction, especially when a change in multiplicity is involved, it seems probable that the reso-

(5) The authors acknowledge with thanks the helpful suggestions of Professor Rufus Lumry.

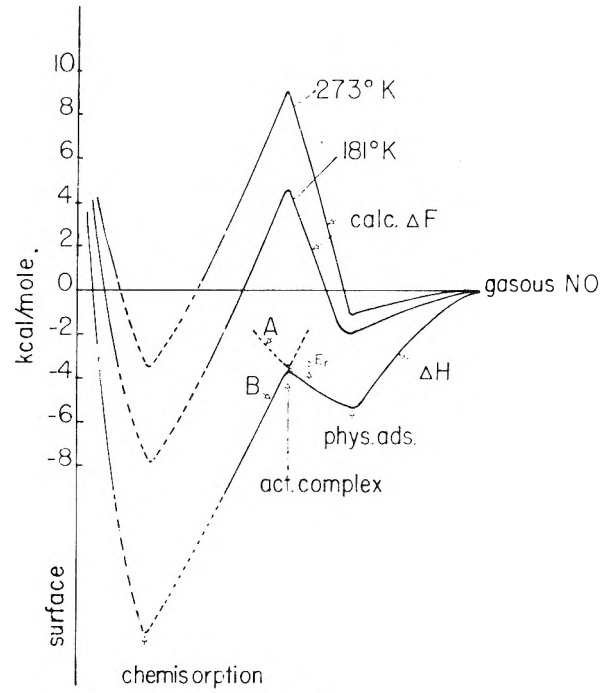

Fig. 8.

nance energy, between the reaction species on both sides of the activated complex, is low. Thus the probability of passing from one state to the other would be low in spite of the fact that the thermodynamic changes appear to be favorable. The Landau[6]–Zener[7] expressions[8] were used in these calculations. It must be remembered that the chemisorption rate is directly proportional to the pressure of the gas and the slow desorption of the chemisorbed gas tends to support this point of view.

Since there is a change in spin multiplicity, there will be no overlapping of the Hamiltonians of the system. The small resonance energy which remains seems likely to be due to perturbation forces having the character of a spin–spin and spin–orbital interaction. This makes the top of the energy curve (Fig. 8), near the activated state, very sharp and there is considerable probability that the reacting species may continue to the upper surface instead of passing over to the product side. Because of the high potential energy of the reacting complex it will not exist on the upper surface, but will fall back into the physically adsorbed state and thus will not have been chemisorbed.

In conclusion it may be said that the results of this study have shown, for the first time, that a transmission coefficient of 10^{-8} is to be found in a heterogeneous system involving the chemisorption of a gas on a solid surface. This value of 10^{-8} is one of the lowest so far found for systems having low resonance energy between the reacting species. These results should be of real interest to those working in the field of heterogeneous catalysis. Related studies are in progress in these laboratories.

(6) L. Landau, *Phys. Z. U.S.S.R.*, **1**, 88 (1932); **2**, 46 (1932).

(7) C. Zener, *Proc. Roy. Soc. (London)*, **137A**, 696 (1932); **140A**, 66 (1933).

(8) See also K. J. Laidler, "The Chemical Kinetics of Excited States," Oxford University Press, London, 1955.

A SPECTROPHOTOMETRIC STUDY OF COMPLEX FORMATION BY IRON(III) AND 2,3-DIMERCAPTO-1-PROPANOL IN ALKALINE SOLUTIONS

BY D. L. LEUSSING* AND J. P. MISLAN[1]

Department of Chemistry, University of Wisconsin, Madison, Wisconsin

Received June 13, 1960

Iron(III) and 2,3-dimercapto-1-propanol (DMP) react in alkaline solutions to form the red complex FeDMPOH. The formation constant of this species is $5 \times 10^{+30}$ as determined by competition with EDTA at 25° in 0.10 *M* ammonium chloride. The complex $FeDMP(NH_3)OH$ with a formation constant of about $7 \times 10^{+31}$ is also formed in ammoniacal solutions. In the more alkaline of those solutions studied in the present investigation (up to *p*H 11.00), the +3 valence state of iron is stable in the DMP systems. This is in contrast to the cysteinate and mercaptoacetate systems where reduction to iron(II) is accompanied by oxidation of the mercaptan to disulfide. With bidentate ligands steric factors seem to limit to two the number of sulfur atoms coördinated to an iron(III) nucleus.

The complexes formed in alkaline solutions between iron(III) and several mercaptides have been described. Intensely colored complexes are formed. With mercaptoacetate the red complex has been shown[2] to have the composition $FeOHRS_2^=$ and with cysteinate the violet color is attributed[3] to $FeOHcy_2^=$ and $Fecy_3^=$. In this latter system, however, through additional kinetic evidence it is concluded that only the complex $FeOHcy_2^=$ is formed.[4]

The reactions were studied under alkaline conditions because in acid solutions a very rapid oxidation–reduction reaction takes place in which the iron(III) is reduced to iron(II) and the mercaptide is oxidized to disulfide,[5,6] but in alkaline solutions the oxidation–reduction reaction is much slower and the equilibria are tractable. The rate of reoxidation of the ferrous complex by oxygen is very rapid and consequently this sequence of reactions serves as a catalytic path for the oxidation of the mercaptide group.[7]

The dithiols, 2,3-dimercapto-1-propanol (DMP) and 1,2-ethanedithiol (es) have been shown to form complexes having exceptionally high formation constants with some of the divalent metal ions of the first transition series.[8–10] In light of the unusual stabilities of the dithiol complexes and of the interesting reactions of the iron(III) complexes with the monomercaptides, we have undertaken an investigation of the reactions between iron(III) and DMP in alkaline solutions. Competition with ethylenediaminetetraacetate ions was used to determine the nature and stabilities of the iron(III)–DMP complexes.

Experimental

A stock solution 0.0493 *M* in ferric ammonium sulfate and 0.025 *M* in sulfuric acid was prepared and standardized against a standard potassium dichromate solution according to the usual procedure. For use, this solution was diluted two- to fivefold. Air-free stock solutions of DMP were prepared by weight as previously described.[8] An equi-molar amount of potassium hydroxide was added to each preparation to increase the rate of dissolution. The DMP solution was freshly prepared for each set of experiments. For the calculations described below the values of pK_{1a} and pK_{2a}, the proton dissociation constants of DMP, were taken to be equal to 8.69 and 10.79 as determined by the potentiometric titration of 0.0050 to 0.010 *M* DMP solutions at 25° in 0.10 *M* sodium chloride using the glass electrode to indicate the *p*H.[11] The electrode system was standardized using National Bureau of Standards buffers.

A disodium dihydrogenethylenediaminetetraacetate dihydrate solution was prepared by weight from the Fisher reagent. This was standardized against a known zinc(II) solution.[12]

Redistilled ammonia and twice distilled water were used. A Cary Model 14 Spectrophotometer was used for absorbance measurements.

Iron(III) ions and DMP molecules react rapidly in alkaline solutions to form a complex which is similar in color to that formed with mercaptoacetate. As was also observed with mercaptoacetate,[13] it was found that on injection of an iron(III) solution into an air-free DMP solution a slight amount of the iron is reduced to the ferrous state. For this reason, the extinction coefficients were determined in air-saturated solutions. Precautions must be taken with this procedure, however, because DMP is readily air oxidized to give polymeric disulfides which impart a turbidity to the solutions. It was found that satisfactory results could be obtained by adding the iron(III) solution to the buffer immediately after the DMP had been added and quickly placing the solution in an absorption cell in the spectrophotometer. In this manner readings which were stable for several minutes were obtained.

Under air-free conditions after the mixing reaction the color is very stable in contrast to the moderately rapid bleaching reactions which occur with mercaptoacetate and cysteinate. With DMP as a ligand only a 2–4% decrease was noted over a period of 48 hours in the lower *p*H range of the ammonia buffers used while no appreciable change was observed in the more alkaline solutions.

The DMP complex in potassium hydroxide solutions of DMP has an absorption maximum at 505 mμ with an extinction coefficient which is independent of *p*H. On the other hand, in going from the ammonia buffers at the lower *p*H to those at the higher *p*H, the absorption maximum shifts to 506–508 mμ and an increase in the absorbance occurs. This effect can be seen in the values calculated for the effective extinction coefficient, ϵ_{eff}, at 507 mμ given in Table I. This effective extinction coefficient is equal to the absorbance divided by the total iron in each system. Such behavior indicates the formation of a mixed complex with ammonia. The value of ϵ_{eff} at a given *p*H is independent of the total DMP of the system and this indicates that the

* To whom inquiries should be addressed at National Bureau of Standards, Washington 25, D.C.

(1) Financial assistance for this work was kindly supplied by a grant from the National Science Foundation and the Wisconsin Alumni Research Foundation.

(2) D. L. Leussing and I. M. Kolthoff, *J. Am. Chem. Soc.*, **75**, 3904 (1953).

(3) N. Tanaka, I. M. Kolthoff and W. Stricks, *J. Am. Chem. Soc.*, **77**, 1996 (1955).

(4) D. L. Leussing, J. P. Mislan and R. J. Goll, THIS JOURNAL, **64**, 1070 (1960).

(5) R. Andreasch, *Ber.*, **12**, 1391 (1879).

(6) P. Claesson, *ibid.*, **14**, 409, 412 (1881).

(7) L. J. Harris, *Biochem. J.*, **16**, 739 (1922).

(8) D. L. Leussing, *J. Am. Chem. Soc.*, **81**, 4208 (1959).

(9) D. L. Leussing and G. S. Alberts, *ibid.*, **82**, 4458 (1960).

(10) D. L. Leussing and T. N. Tischer, in press.

(11) R. C. Hansen, unpublished experiments.

(12) G. Schwarzenbach, "Die Komplexometrische Titrationen," F. Enke, Stuttgart, 1955.

(13) D. L. Leussing and L. Newman, *J. Am. Chem. Soc.*, **78**, 552 (1956).

formation of the mixed complex does not involve the loss or gain of DMP.

TABLE I

THE EFFECTIVE EXTINCTION OF IRON(III) IN ALKALINE DMP SOLUTIONS 25°, AIR-SATURATED SOLUTIONS

Buffer	Concn.[a] NH_3, moles/l.	pH	Total DMP, moles/l. $\times 10^3$	Total Fe, moles/l. $\times 10^4$	ϵ_{eff}, l. mole^{-1} cm.$^{-1}$ $\times 10^{-3}$
NH_3-NH_4C	0.0234	8.65	2.98	2.96	3.42
	.0230	8.80	2.21	2.96	3.45
	.0416	8.98	2.98	2.96	3.68
	.0416	9.00	2.21	2.96	3.61
	.0416	9.00	2.98	1.97	3.81
	.054	9.03	3.02	2.46	3.72
	.054	9.05	3.02	3.70	3.72
	.072	9.10	1.51	2.46	3.96
	.072	9.12	3.02	2.46	3.90
	.074	9.20	2.21	2.96	3.98
	.074	9.24	1.45	2.46	3.98
	.074	9.25	1.45	2.46	4.05
	.131	9.48	2.21	2.96	4.17
	.131	9.48	2.98	2.96	4.43
	.234	9.75	2.21	2.96	4.44
	.234	9.75	2.98	2.96	4.53
	.321	9.92	1.45	2.46	4.55
	.321	9.92	1.44	2.46	4.55
	.417	10.01	2.98	2.96	4.56
	.417	10.01	2.21	2.96	4.60
	1.11	10.40	2.98	1.97	4.60
	1.11	10.40	1.44	2.50	4.56
	1.11	10.40	5.00	2.96	4.58
	1.11	10.40	9.92	2.96	4.68
	1.10	10.45	2.21	2.96	4.69
	2.00	10.75	2.21	2.96	4.68
DMP	...	8.50	9.92	2.96	3.08
	...	8.62	1.10	5.92	3.04
	...	9.05	1.10	2.96	3.08
	...	10.62	1.10	5.92	3.00
	...	10.70	1.10	2.46	3.09
	...	11.00	1.10	2.96	3.10

[a] The concentration of ammonium chloride is 0.100 M in the ammonia buffers.

For an equilibrium of the type $Fe_1 + xNH_3 \rightleftarrows Fe_2$ it can be shown that $\epsilon_{eff} = \epsilon_2 - (\epsilon_{eff} - \epsilon_1)/K(NH_3)^x$ where ϵ_1 and ϵ_2 are the extinction coefficients of species 1 and 2 and K is the constant for the equilibrium. Using a value of ϵ_1 equal to $3.07 \times 10^{+3}$, it was found that in a plot of ϵ_{eff} *vs.* $(\epsilon_{eff} - \epsilon_1)/(NH_3)$ the points fall approximately along a straight line. The value of ϵ_2 is indicated to be 4.7–4.8 $\times 10^{+3}$ and that of K equal to about 14. Possibly more than one ammoniated complex exists but a large relative error exists in the difference $\epsilon_{eff} - \epsilon_1$ because of the experimental difficulties ordinarily encountered in iron(III)–mercaptide systems and, therefore, a more refined treatment of the data is not warranted.

In the competition experiments, solutions of DMP and iron(III) were prepared under air-free conditions using the sealed bottle syringe technique previously described.[2] In a typical run, the desired volume of the concentrated buffer was placed in a bottle equipped with an optical side arm. The bottle was sealed and the contents were deaerated. A given volume of the DMP solution was then injected and this was followed by injections of the air-free iron and EDTA solutions. In some runs the order of mixing was reversed and the EDTA and iron solutions were added first. This had no effect on the results. After mixing, the solutions were equilibrated in a water-bath at 25°. The experimental details and results are given in Table II.

Equilibrium in the competition experiments was attained in 3 to 6 hours depending on the conditions. After this period in the more alkaline buffers the absorbances were observed to be constant at least up to 20 hours, but in the less alkaline solutions a very slow decrease in the absorbances was observed. This decrease most likely is due to a slow reduction of the iron(III). To compensate for this, the readings from this latter period of slow change were extrapolated to zero time. The effect is slight and amounts to only a 2–3% difference in the absorbance.

In order to make accurate calculations, the amount of ferrous iron produced in the mixing reaction must be taken into account. This amount was determined at the end of a run by exposing each solution to air and immediately noting the increase in the absorbance. The increase divided by ϵ_{eff} for the particular buffer was taken as the iron(II) concentration. This figure is also given in Table II. For the calculations it was assumed that the iron(II) is present as an EDTA complex. This is justified because from the empirical relationships given[14] it is estimated that the formation constant of $FeDMP_2^{=}$ is of the order of 10^{+14} to 10^{+16} while the formation constant of Fe(II)Y[15] is $1.0 \times 10^{+14}$. From these values it is calculated that under the present conditions the EDTA complex is favored.

The concentrations of the various species were then calculated from the relationships

$$Fe(III)DMP_\Sigma = A/\epsilon_{eff}$$
$$DMP_\Sigma = DMP_t - xFeDMP_{x\Sigma} - Fe(II)$$
$$FeY_\Sigma = Fe_t - FeDMP_{x\Sigma} - Fe(II)$$
$$Y_\Sigma = Y_t - FeY_\Sigma - Fe(II)$$

where the subscript t refers to the total concentration and Σ refers to the summation, at a given pH, of the protonated, hydroxylated or ammoniated forms of the species so designated, A refers to the absorbance and Y refers to the ethylenediaminetetraacetate ion.

Apparent conditional constants were calculated for the equilibria $FeDMP_{x\Sigma} + Y_\Sigma \rightleftarrows FeY_\Sigma + xDMP_\Sigma$. Only for x equal to one were constant values obtained for the runs in each buffer. These are given in Table II under the column heated Q'. Higher values of x give greatly drifting "constants."

Using the values reported for the dissociation of the fourth proton of EDTA at 25°[16] the dissociation of the first two protons of Fe(III)Y[-15] and the values of pK_{1a} and pK_{2a} given above for DMP, values of Q'', which is equal $(FeY^-)(DMP^=)/(FeDMP_\Sigma)(Y^{-4})$, were calculated from the Q' values using the relationships

$$(FeY_\Sigma) = (1 + 2.8 \times 10^{+6}\, a_{OH} + 9.5 \times 10^{+10}\, a^2_{OH^-})(FeY^-)$$

$$(DMP_\Sigma) = \left(1 + \frac{a_H}{1.6 \times 10^{-11}} + \frac{a_H^2}{3.2 \times 10^{-20}}\right)(DMP^=)$$

and

$$(Y_\Sigma) = \left(\frac{a_H}{7.8 \times 10^{-11}} + 1\right)(Y^{-4})$$

Here, $FeDMP_\Sigma$ refers to the summation of the concentrations of the species $FeDMP(OH)_y$ and $FeDMPNH_3(OH)_y$, where y can be negative (for protonated species), zero or a positive number. The results of these calculations are given in Table III. Constants for the equilibria $FeDMP(OH)_y + Y^{-4} \rightleftarrows FeY^- + DMP^= + yOH^-$ are obtained by taking the product $[1 + 14(NH_3)]Q''$ and are given in the fifth column of Table III. This product is seen to vary approximately inversely as the activity of the hydroxide ion. This indicates that as far as the experimental accuracy allows, y can be taken to be equal to one. In the last column of Table III, values of Q, which is equal to the product $[1 + 14(NH_3)]a_{OH}Q''$, are given. This is the constant for the above reaction with y equal to one. Considering the many equilibria which must be taken into account the agreement is good. From the average value of Q equal to 2.7×10^{-6} and the value $1.3 \times 10^{+25}$ for the formation constant of FeY^-[15] the formation constant of FeDMPOH is calculated to be $5 \times 10^{+30}$. The formation constant of $FeDMP(NH_3)(OH)$ is then calculated to be 7×10^{-31}.

(14) D. L. Leussing, *Talanta*, **4**, 264 (1960).

(15) G. Schwarzenbach and J. Heller, *Helv. Chim. Acta*, **34**, 576 (1951).

(16) G. Schwarzenbach and G. Anderegg, quoted in "Stability Constants," Part 1, J. Bjerrum, G. Schwarzenbach and L. G. Sillen. Special Publication No. 6, The Chemical Society, London, 1957.

TABLE II

THE COMPETITION OF EDTA AND DMP FOR IRON(III)

T = 25°

DMP_t, $M \times 10^{+4}$	$EDTA_t$, $M \times 10^{+4}$	$Fe(III)_t$, $M \times 10^{+4}$	NH_{3t},[a] M	$A_{equil.}$, cm.$^{-1}$	Fe(II), $M \times 10^{+4}$	Fe(III) DMP_Σ, $M \times 10^{+4}$	DMP_Σ, $M \times 10^{+4}$	Y_Σ, $M \times 10^{+4}$	$Fe(III)Y_\Sigma$, $M \times 10^{+4}$	pH	Q'[c]
18.8	10.0	4.93	0.054	0.197[b]	..	0.52	18.3	5.6	4.41	9.02	28
30.1	10.0	4.93	.054	.268[b]	0.10	.71	29.3	5.8	4.12	9.02	29
37.6	10.0	4.93	.054	.308[b]	.20	.81	36.6	5.9	3.92	9.02	30
52.4	3.00	4.93	.131	1.18[b]	.50	2.85	49.0	0.92	1.58	9.39	30
65.6	3.00	4.93	.131	1.29[b]	.50	3.11	62.0	1.18	1.32	9.40	22
10.0	3.00	2.96	.321	0.315[b]	.10	0.70	9.2	0.74	2.16	9.87	38
20.0	3.00	2.96	.321	.370[b]	.30	.82	18.9	0.86	1.84	9.87	49
30.0	3.00	2.96	.321	.440[b]	.40	.97	28.6	1.01	1.59	9.87	46
8.99	10.0	4.93	1.11	.500	..	1.08	7.9	6.2	3.85	10.40	4.5[d]
18.0	10.0	4.93	1.11	.870	..	1.87	16.1	6.9	3.06	10.40	3.8[d]
11.5	10.0	4.93	1.11	.573	..	1.23	10.3	6.3	3.70	10.42	4.9
17.3	10.0	4.93	1.11	.773	..	1.66	15.6	6.7	3.27	10.42	4.6
28.9	10.0	4.93	1.11	.958	.60	2.08	26.2	7.15	2.25	10.42	4.0
43.4	10.0	4.93	1.11	1.018	1.00	2.19	40.2	7.3	1.74	10.42	4.4
10.1	3.00	2.96	1.11	0.630	0.16	1.36	8.6	1.40	1.44	10.49	6.5
20.2	3.00	2.96	1.11	.710	.40	1.53	18.3	1.57	1.03	10.49	7.8
30.4	3.00	2.96	1.11	.790	.65	1.70	28.0	1.76	0.59	10.49	5.5

[a] The concentration of ammonium chloride is 0.100 M. [b] Extrapolated to zero time. [c] Q, equals (FeY)(DMP)/(FeDMP)(Y). [d] EDTA added first.

TABLE III

THE EVALUATION OF Q FOR THE EQUILIBRIUM $FeDMPOH + Y^{-4} \rightleftarrows FeY^- + DMP^- + OH^-$

T = 25°, 0.10 M NH_4Cl

pH	NH_3, moles/l.	a_{OH} $\times 10^{+6}$	Q' av.	Q''	$Q''[1 + 14(NH_3)]$ $\times 10^{+1}$	$Q = Q''[1 + 14(NH_3)]a_{OH}$ $\times 10^{+6}$
9.02	0.054	1.05	29	1.1×10^{-1}	1.9	1.2
9.39, 9.40	.130	2.5	26	3.9×10^{-2}	1.1	2.8
9.87	.321	7.4	44	1.6×10^{-2}	0.88	6.5
10.40, 10.42	1.11	26	4.4	2.7×10^{-4}	0.045	1.2
10.49	1.11	31	6.6	3.1×10^{-4}	0.051	1.6

Discussion

The iron(III)–DMP complexes bear a close resemblance to those of the same metal ion with cysteinate and mercaptoacetate. In all of these complexes two mercaptide groups and one hydroxyl group are coördinated to the ferric ion, at least under alkaline conditions. The coördination of an ammonia molecule is in keeping with the properties of the cysteinate complexes where amine groups are also coördinated.

In view of the ease with which the divalent metal ions in the series Mn(II) to Zn(II)[10] acquire a second molecule of DMP, it is surprising that under the present experimental conditions complexes having a higher ratio of DMP to iron are not observed. It appears that a maximum coördination of of two mercaptide groups is a fundamental property of iron(III) mercaptide complexes. This may be the result of steric hindrance encountered in the coördination of the large sulfur molecules to the small iron(III) ion.

Another interesting feature is the stability of the plus three valence state of iron in the more alkaline of those DMP solutions which were studied. This stability appears to result from the fact that the equilibrium

$$2Fe(III)DMPOH + 4DMP \rightleftarrows 2Fe(II)DMP_2^- + (DMP)_2 + 2OH^-$$

lies to the left, and since the DMP–$(DMP)_2$ couple probably has about the same oxidation potential as that of mercaptoacetate–dimercaptodiacetate and cysteine–cystine, it is indicated that the complexes of trivalent iron are more stable relative to those of divalent iron with DMP as the ligand than either with cysteine or mercaptoacetate as ligands.

THE DIFFUSION COEFFICIENTS OF Pb^{210} AND Cl^{36} IN MOLTEN $PbCl_2$–KCl MIXTURES IN THE VICINITY OF THE COMPOSITION $2PbCl_2$·KCl[1]

BY GERALD PERKINS, JR., R. B. ESCUE, JAMES F. LAMB,[2] TROY H. TIDWELL[2] AND J. WAYNE WIMBERLEY[2]

Department of Chemistry, North Texas State College, Denton, Texas

Received June 15, 1960

The diffusion coefficients of Pb^{210} and Cl^{36} were measured for three compositions of $PbCl_2$–KCl mixtures: 25.2, 33.3 and 37.0 mole % KCl. The measurements were made over a temperature range of about 100° from within about 10° of the melting point. The diffusion of Cl^{36} seems to be independent of composition. The diffusion coefficient of Pb^{210}, on the other hand, varies with composition and the diffusion of this isotope seems to be particularly hindered at the composition, $2PbCl_2$·KCl.

According to many authors, the system, molten $PbCl_2$–KCl, is considered to show ambiguities in physical properties. Duke and Fleming[3] studied transport phenomena in this system and concluded that the lead is not part of a negative ion but that negative deviations in the value of the cation transference number observed in passing from pure lead chloride through progressive, intermediate compositions to pure potassium chloride are due to decreased conductance on the part of the potassium. Transference experiments by Tubandt and Reinhold[4] and X-ray crystal structure determinations by Mehmel and Nespital[5] suggest the absence of complex ions in solid $PbCl_2$–KCl mixtures. Tubandt and Reinhold found the transference number of chlorine to be equal to one in solid $2PbCl_2$·KCl. The phase diagram for the system[6] shows a congruently melting compound at the composition, $2PbCl_2$·KCl. Harrap and Heymann[7] observed no anomalous behavior in the viscosity of the system. In order to reconcile viscosity and conductance data these authors postulated the operation of a different mechanism for viscous flow which would be less sensitive to association of the ions into small complexes.

On the other hand, Lorenz and his co-workers[8] also studied transport phenomena in these mixtures and found, for some compositions, that the lead migrated out of the cathode compartment. The significance of their "transference numbers" is not clear, but their results have been taken to indicate the presence of complex ions in the melt. Bloom and Heymann[9] observed negative deviations in the value of the equivalent conductance of this system as the composition was changed. A minimum was observed in the conductance at about 50 mole % KCl for all temperatures investigated and this was attributed to the presence of the complex ion $[PbCl_3]^-$. A further, sharp minimum was observed at about 80 mole % KCl at temperatures below 650°. This second minimum did not occur above that temperature. The complex ion $[PbCl_6]^{4-}$ was postulated to explain the second minimum. Bloom and Heymann considered as anomalous the absence of a conductance minimum for the melt at the composition $2PbCl_2$·KCl (33.3 mole % KCl).

It would appear, in the light of such conflicting evidence, that the case for complex ions in this system is in considerable doubt. In order to help resolve this question an additional insight into the structure of the melt should be provided by a knowledge of the behavior of the diffusion coefficients of the lead and chlorine in the $PbCl_2$–KCl mixture in the vicinity of the composition $2PbCl_2$·KCl. This is the region in which Bloom and Heymann indicated anomalous behavior. Supplementary evidence might determine whether the observed properties should be attributed to the influence of complex aggregates and whether these are actually complex ions involving the lead and chlorine or whether they represent instead the involvement of lead along with potassium in some restriction to cation mobility. Earlier work in this Laboratory[10] showed the possibility of a restricted movement for the cation in molten $PbCl_2$ and it is possible that some similar cation interaction might restrict the movement of the potassium in $PbCl_2$–KCl mixtures. To establish this evidence the following measurements were made.

The necessary data were collected by the "capillary method" of Anderson and Saddington.[11] Active material contained within a Pyrex capillary was allowed to diffuse for a measured time into a large volume of inactive material of identical chemical composition. Conditions of the experiment were such that the solution of Fick's law for this particular case reduces to

$$\bar{C} = (8C_0/\pi^2)\exp(-\pi^2 Dt/4l^2)$$

where

$\bar{C}$ = average concn. of active material remaining in the capillary at time t
C_0 = initial concn. of active material within the capillary
D = diffusion coefficient, cm.^{2} sec.$^{-1}$
t = time, sec.
l = length of capillary, cm.

The particular conditions which lead to this simplification are discussed by Carslaw and Jaeger[12] and Anderson and Saddington.[11] The ratio $\bar{C}/C_0$

(1) The work reported in this paper is part of a continuing project initiated under a Frederick G. Cottrell grant and continued under a series of grants from the Robert A. Welch Foundation.

(2) Robert A. Welch Foundation Research Fellow.

(3) F. R. Duke and R. A. Fleming, *J. Electrochem. Soc.*, **106**, 130 (1959).

(4) C. Tubandt and H. Reinhold, *Z. Elektrochem.*, **29**, 213 (1923).

(5) M. Mehmel and W. Nespital, *Z. Kristallogr.*, **88**, 345 (1934).

(6) K. Treis, *Jahrb. Min. Beil-Bd.*, **37**, 766 (1914).

(7) B. S. Harrap and E. Heymann, *Trans. Faraaday Soc.*, **51**, 268 (1955).

(8) (a) R. Lorenz and G. Fausti, *Z. Elektrochem.*, **10**, 630 (1904); (b) R. Lorenz and W. Ruckstuhl, *Z. anorg. Chem.*, **52**, 41 (1907).

(9) H. Bloom and E. Heymann, *Proc. Roy. Soc.* (*London*), **A188**, 392 (1947).

(10) G. Perkins, Jr., R. B. Escue, J. F. Lamb and T. H. Tidwell, THIS JOURNAL, **64**, 495 (1960).

(11) K. Saddington and J. S. Anderson, *J. Chem. Soc.*, S381 (1949).

(12) H. S. Carslaw and J. C. Jaeger, "Conduction of Heat in Solids," Oxford Univ. Press, London, 1947, p. 79.

TABLE I

THE DIFFUSION COEFFICIENTS OF Pb^{210} AND Cl^{36} IN MOLTEN $PbCl_2$–KCl

Temp., °C.	D(cm.² sec.⁻¹) × 10⁵ 25.2 mole % KCl Pb^{210}		25.2 mole % KCl Cl^{36}		33.3 mole % KCl Pb^{210}		33.3 mole % KCl Cl^{36}		37.0 mole % KCl Pb^{210}		37.0 mole % KCl Cl^{36}	
448									0.58 ± 0.02		1.51 ± 0.03	
449	0.53 ± 0.06		1.40 ± 0.04									
450					0.34 ± 0.05		1.49 ± 0.03					
470			1.56	.04								
473					.61	.03	1.69	.02				
475									.67	.02	1.70	.04
490	0.76	.05	1.57	.10								
500					.80	.12	1.97	.02	.76	.03	2.10	.05
505			1.98	.06								
520									.94	.04	2.56	.04
524					.82	.08	1.95	.29				
530	0.99	.04	2.42	.11								
539	1.19	.02	2.54	.04								
550					1.10	.02	2.60	.02	1.27	.09	2.64	.12
555	1.23	.23	2.40	.02								
570	1.38	.15	2.78	.09								
575					1.50	.05	3.01	.04	1.28	.02	2.86	.04

represents the fraction of active material remaining in the capillary at the end of the experiment and is equal to the ratio of final count to initial count. This value, together with the appropriate values of t and l, will allow the calculation of D. The mechanics of the operations involved in making these various measurements, including a description of the apparatus employed, has been described in an earlier paper.[10]

Experimental

Preparation of the Mixtures.—The mixtures were made from reagent grade materials without further purification except for the removal of water. This was accomplished by heating the salts under vacuum to about 400° for a period of several hours. In the case of lead chloride the vessel was periodically flooded with hydrogen chloride to minimize hydrolysis of the salt. After melting an appropriate quantity of the lead chloride (*ca.* 2 kg.), potassium chloride in pre-calculated quantity was dissolved in the melt. A sample of the homogeneous mixture was withdrawn for the determination of system composition and for activation. In the case of the composition $2PbCl_2$·KCl the sample was not removed for activation until repeated analysis and readjustment of the potassium chloride content gave the desired composition. The samples were treated as follows.

Analysis of System Composition.—A sample of the molten mixture was withdrawn by pipet and transferred to an alundum mortar while still liquid. Upon solidification, the entire sample was pulverized and homogenized. Separate portions of this were removed for replicate analyses. For the first composition, the proportions of all three species, Pb^{++}, Cl^- and K^+, were determined and the mole per cent. KCl calculated from the results. In subsequent mixtures only a potassium analysis was performed, since this value allowed the most precise determination of the composition. The potassium was separated as the sulfate after precipitation of lead sulfate and was subsequently ignited and weighed as the sulfate. Lead was determined by precipitation as the molybdate according to Scott[13] and the chloride ion was titrated with silver nitrate.

Activation.—A portion of the material from which the final system analysis was made was transferred to a reflux flask. Water was added to dissolve the mixture and Pb^{210} and Cl^{36} were introduced into the flask in the form of crushed radon needles and HCl, respectively. Reflux was maintained until the exchange had reached equilibrium. At this point the solution was filtered while hot in order to remove the crushed glass and was then evaporated to dryness to recover the original $PbCl_2$–KCl mixture. This mixture was dried under vacuum exactly as was the pure lead chloride, then pulverized, homogenized and stored under an argon atmosphere for later use in filling the capillaries. At such time, only the amount needed for filling a particular group of capillaries was introduced into the filling furnace. This procedure was employed to minimize changes in composition which might otherwise be brought about by evaporation.

Separation and Recovery of the Isotopes.—When the capillaries were withdrawn from the immersion bath they were first allowed to cool, after which the surface was carefully scraped and cleaned of all external traces of salt. The individual capillaries were crushed and quantitatively removed to a small flask containing an aqueous mixture of nitric acid and silver nitrate. This system was refluxed for several hours until the chlorine was quantitatively precipitated as silver chloride and the lead was discharged into solution in soluble form. The mixture was filtered and washed and the filtrate diluted to a volume of 50 ml. This solution contained all the lead and was counted by standard techniques. The residue of silver chloride was next dissolved with several portions of a solution of sodium thiosulfate and the filtrate collected as it came through the filter. This solution contained all of the chloride ion. After collecting the washings, the solution was diluted to 50 ml. and counted in the same manner as the lead. The procedure for the separation of the isotopes was carefully checked for efficiency of separation and shown to give no measurable activity of unwanted isotope in either fraction and no measurable activity in the filter after the separation.

Results

The diffusion coefficients of Pb^{210} and Cl^{36} were measured at three compositions of the $PbCl_2$–KCl mixture and at several temperatures for each composition. The results are shown in Table I. The values of the diffusion coefficient are averages gathered from four trials. The average deviation is calculated from the individual values for each trial. The value given for the composition of each mixture is an average value obtained from at least three analyses.

In Fig. 1 the logarithms of these data have been plotted as a function of the reciprocal of the absolute temperature. The straight lines in the figure have been fitted to the data by the method of least squares. The equations of the lines, with standard errors indicated in parentheses, are given in Table II. Figs. 2a and 2b present a family of isotherms whose points have been calculated from the equations of Table II, while Fig. 2c gives the variation of activation energy with composition. The pertinent

(13) W. W. Scott, "Standard Methods of Chemical Analysis," Vol. I, D. Van Nostrand Co., New York, N. Y., 1939, p. 506.

area of the phase diagram has been appended to Fig. 2 for convenience.

TABLE II

EQUATIONS FOR THE DIFFUSION COEFFICIENT OF Pb^{210} AND Cl^{36} AT EACH COMPOSITION

Compn (mole % KCl)	
	D_{Pb}
25.2	$D = 5.03 \times 10^{-3} \exp(-9864 \pm 242/RT)$
33.3	$D = 2.92 \times 10^{-2} \exp(-12796 \pm 1092/RT)$
37.0	$D = 1.96 \times 10^{-3} \exp(-8405 \pm 566/RT)$
	D_{Cl}
25.2	$D = 2.34 \times 10^{-3} \exp(-7403 \pm 541/RT)$
33.3	$D = 1.44 \times 10^{-3} \exp(-6608 \pm 573/RT)$
37.0	$D = 1.31 \times 10^{-3} \exp(-6443 \pm 417/RT)$

Discussion

As in the case of pure lead chloride[10] these data show the diffusion coefficient of Cl^{36} to be greater than that of Pb^{210}. Unlike pure lead chloride, the activation energy for diffusion is greater for lead than for chlorine. It is expected that the diffusion coefficient will be given by an equation of the form

$$D = A \exp(B/RT)$$

in which

D = the diffusion coefficient
B = an activation energy for diffusion
T = absolute temperature
A = a constant

The straight line relationship between log D and $1/T$ indicated by this equation was borne out well by the data.

The results at a given temperature show changes at each composition for both the chlorine and lead. These changes seem to be progressive in the case of Cl^{36} and the activation energy shows a steady decrease as the amount of KCl in the mixture increases. This decrease may be illusory, however. The error in the data is of the order of 10% and an almost horizontal line can be drawn through the points. The range of standard error calculated by the method of least squares has been indicated by the vertical bars on the figure.

In the case of Pb^{210} the data indicate unique fluctuations in the vicinity of the composition $2PbCl_2$·KCl. Taking into account the standard error, or even increasing the range of error to 10%, the diffusion coefficients of the lead are significantly lower and the activation energy for diffusion is significantly higher at the compound composition. For both the activation energy and the diffusion coefficient the change is more pronounced on that side of the compound composition having the lower melting eutectic. While it is possible that the results could be explained by precipitation of lead chloride and potassium chloride from the melt at the lower temperatures, the measurements were made at least ten degrees above the melting point so that no change in composition of the melt should occur due to accidental solidification of one component.

The isotherms of Fig. 2 show a progressive shift toward horizontal lines. If the equations given in Table II are used to extrapolate isotherms at higher temperatures, this trend is reversed. However, in view of the conductance data gathered by Bloom and Heymann[9] and the viscosity data of Harrap and Heymann,[7] anomalous behavior is not expected at temperatures higher than about 550° so that one would expect the curves shown in Fig. 1 to approach identical slopes in the vicinity of that temperature. The limitations of the glass apparatus made measurements at temperatures above about

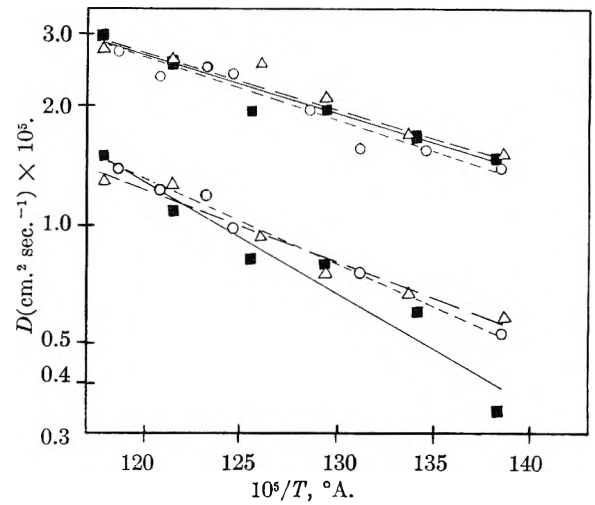

Fig. 1.—Diffusion coefficients of Cl^{36} (upper) and Pb^{210} (lower) in molten $PbCl_2$–KCl mixtures (○, 25.2 mole % KCl; ■, 33.3 mole % KCl; △, 37.0 mole % KCl).

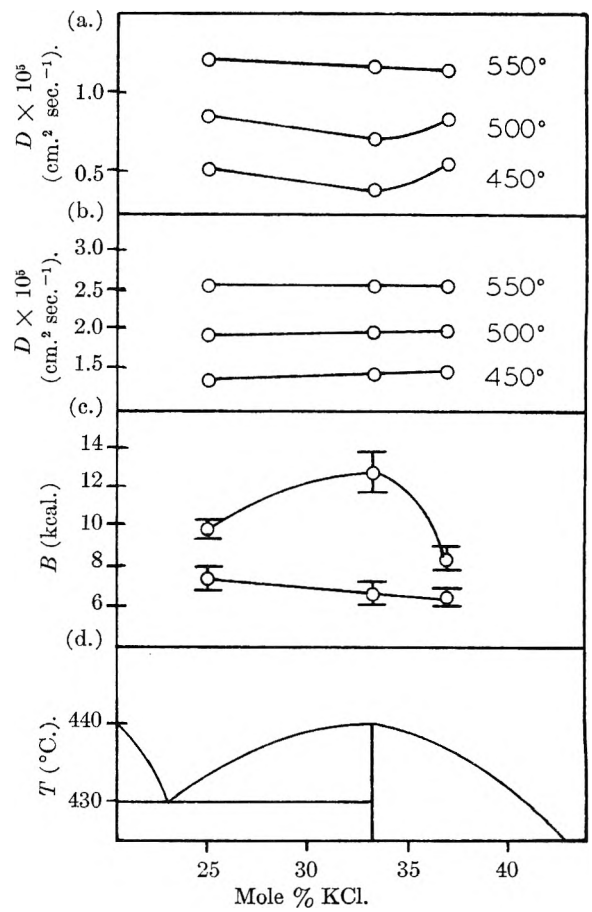

Fig. 2.—Diffusion in the system $PbCl_2$–KCl: (a) isotherms of D *vs.* composition for Pb^{210}; (b) isotherms of D *vs.* composition for Cl^{36}; (c) activation energy for diffusion *vs.* composition (upper curve) Pb^{210}; (lower curve) Cl^{36}; (d) phase diagram for region investigated.

575° impractical, and extensions to higher temperatures were not possible. We infer from Fig. 1 that the two sets of curves would resolve themselves into single lines at the upper limits of the temperature range investigated.

This work was primarily concerned with those temperatures between the melting point and the lowest temperatures used by Bloom and Heymann.[9] In this range, it seems that the lead encounters some hindrance to diffusion while the chlorine is unaffected. The lead is increasingly hindered in its diffusion as the composition approaches that of the compound $2PbCl_2 \cdot KCl$, but this hindrance becomes less as the temperature is raised.

In order to explain the inapplicability of the Stokes–Einstein equation to the pure, molten $PbCl_2$ system it was postulated that the lead was held more immobile than the chlorine.[10] This might be due to the greater mass, the influence of the greater charge in electrostatic interactions, or to other factors. It would seem that the same mechanism is operative here, since the diffusion coefficient of the lead remains smaller than that of the chlorine in $PbCl_2$–KCl mixtures. On the other hand, for the three compositions investigated, the activation energy of diffusion is greater for the lead than for the chlorine. This is contrary to the behavior of pure lead chloride. Since the activation energy of Pb^{210} varies with composition and is a maximum at that potassium content corresponding to $2PbCl_2 \cdot KCl$, it would appear that the potassium ion has an adverse influence upon the mobility of the lead in the vicinity of the compound composition. It is to be expected that this influence is mutual and that the potassium ion also encounters a hindrance to its diffusion. Such an effect has been indicated in the results of Duke and Fleming[3] and Tubandt and Reinhold.[4]

Apparently the disparity in conductance behavior at the compositions $2PbCl_2 \cdot KCl$ and $PbCl_2 \cdot 4KCl$ reported by Bloom and Heymann[9] was due to the relative differences between the melting points of the compounds and the temperatures at which the measurements were made. It is likely that a conductance minimum would also be observed at the composition $2PbCl_2 \cdot KCl$ at temperatures nearer the melting point. However, the relatively low diffusion coefficient of the lead, with its attendant low transference number, would probably moderate the decrease in conductance. Thus, the minimum at the composition $2PbCl_2 \cdot KCl$ should not be so pronounced as that at the composition $PbCl_2 \cdot 4KCl$.

More interesting here is the lack of any evidence that changes in composition influence the diffusion of the chlorine. Heretofore, explanations of the various types of behavior encountered in this system have always assumed the presence of one or more complex ions involving both the chlorine and lead. It would appear that any complexes or other aggregations which might be present at these temperatures have little or no influence on the diffusion of the chlorine but mainly involve the lead. It may be that close to the melting point the behavior is influenced more by the presence of some cation aggregation, while at higher temperatures, these cation structures may vanish and the behavior may become dependent upon the presence of the complex ions previously postulated. The trends shown by these data, however, would indicate that, at the higher temperatures, the behavior of the lead and the chlorine becomes independent of composition and this would rule out the presence of complex ions involving the lead and chlorine.

THE MUTUAL DIFFUSION OF LIGHT AND HEAVY WATER

BY L. G. LONGSWORTH

Rockefeller Institute, New York, N. Y.

Received June 22, 1960

With the aid of a new diffusion cell and Rayleigh interferometry the mutual diffusion of light and heavy water has been measured at 5, 25 and 45° over the entire range of composition. Paralleling rather closely the fluidity of H_2O–D_2O mixtures, and also the chloride ion mobility therein, the diffusion coefficient exhibits small negative departures from a linear decrease with increasing mole fraction of D_2O. The effect of temperature on diffusion in this system is compared with that of large solutes in aqueous solution.

Using a diaphragm cell Adamson and Irani[1] observed a pronounced minimum in the diffusion of light and heavy water at a mole ratio near unity. With the aid of a porous frit Baur, Garland and Stockmayer[2] were unable to confirm this result but their measurements did not indicate the slight dependence on the mole fraction that had been observed[3] with an optical method in H_2O-rich mixtures, a dependence that might be anticipated from the viscosity of D_2O and the relatively large isotope effects generally observed with deuterium. The optical results have been extended to cover the entire range of mole fractions at temperatures of 5, 25 and 45°. These measurements are reported here together with a description of a new diffusion cell that has facilitated the work.

(1) A. W. Adamson and R. R. Irani, *J. Am. Chem. Soc.*, **79**, 2967 (1957).

(2) M. E. Baur, C. W. Garland and W. H. Stockmayer, *ibid.*, **81**, 3147 (1959).

(3) L. G. Longsworth, THIS JOURNAL, **58**, 770 (1954).

Experimental

The free diffusion of an initially sharp boundary between H_2O–D_2O mixtures of different density was followed with

the aid of Rayleigh interferometry as in the previous work.[4] The diffusion cell shown in Fig. 1 was designed (a) to provide the comparison channel, essential for the formation of Rayleigh fringes, that could be filled with the denser of the two solutions, (b) to avoid the use of grease in assembly so as to be available for work with non-aqueous solvents and (c) to require less liquid than the Tiselius electrophoresis cell as adapted for diffusion studies.

In Fig. 1 the perspective is that obtained from a photograph with the camera directly in front of, and somewhat above, the cell. It consists of two stainless steel plates A and B between which is clamped the two-channel glass frame F. In the figure this frame is shown out of place to the left in order to expose the V-shaped grooves in the plate A that match the channels in the frame. A′ is a diagram of the right hand face of A, the dotted lines indicating the V-shape of the grooves and the small circle the hole that connects them at the bottom of the V. Connection between the two channels through this hole may be made, or broken, with a Teflon needle valve that is provided with an O-ring and pack nut as it passes out of the plate A. This valve is threaded into the post P and driven by the spiral gears G. One-half turn of the knob K opens, or closes, the valve. Although not visible in the figure the upper plate B is also provided with V-grooves on its underside, one of which connects with a reservoir tube T, the other with T′. These glass tubes, of 1 cm. i.d. and 18 cm. in length, fit into recesses in B that are provided with Teflon gaskets and are permanently clamped with the aid of two rods, the front one being shown at R.

At clamping pressures that avoid breakage or distortion of the glass frame F it has not been possible to prevent leakage with Teflon gaskets between F and plates A and B. Moreover, since F is removed for cleaning between experiments it was not considered practicable to clamp at temperatures at which Teflon begins to soften, as suggested by Caldwell, Hall and Babb.[5] However, gaskets cut from 0.5 mm. thick sheets of silicone rubber afford leak-proof seals at low pressure and have proved to be inert in a variety of organic liquids. The entire cell is carried by the masking plate M.

The cross section of each channel is 3 × 25 mm. and the height 40 mm. With the valve closed 12–15 ml. of the heavy liquid is introduced into the right-hand side of the assembled cell and an equal volume of light fluid in the left-hand side. A capillary glass siphon is then inserted through tube T and into the left hand channel of F, Fig. 1, so that it is out of the path of the light through the slits in the mask M and its bevelled tip is at the center of F. With the cell in the thermostat the valve is opened and siphoning at about 1 ml./minute begun, and continued until 15–18 ml. have been removed. Since the siphoning displaces the liquid junction from the valve to the level of the capillary tip, *i.e.*, through a volume of 1.5 ml., this procedure rinses the light liquid initially present in the lower half of the diffusion channel with five volumes of the heavy fluid. With slowly diffusing materials it is desirable to interrupt the siphoning at intervals to allow diffusion to occur from the stagnant film at the walls. Attempts to perfect a greaseless cell of the Antweiler type,[6] which requires a minimum of liquid since the boundary is formed without siphoning, are continuing.

The four exposures that are made during the siphoning of the final 5 ml. provide both a check on the adequacy of the rinsing and an independent value for the zero time correction. As in previous work the zero of time is taken as the time at which siphoning is stopped and the correction, Δt, actually used is the value required to minimize the deviations, from the mean, of the values for the diffusion coefficient that are obtained from each of the ten exposures as the boundary spreads. At 45° this correction was about 10 seconds, at 25°—15 seconds and at 5°—18 seconds, and in each experiment agreed, within one second, with the value obtained independently from the final pattern during siphoning.

Heavy water recovered from a previous investigation[7] was supplemented with fresh material from the Liquid Carbonic Co. and was distilled without ebullition under its own vapor pressure in an all-Pyrex still. The water recovered from a diffusion experiment was not always redistilled prior to dilution and use in a subsequent determination, however, a fact that may account for some of the density errors suggested below by the refractometric data. All densities were measured at 25° as described elsewhere[8] and the relation[9]

$$N = 9.2935\Delta d/(1 - 0.0329\Delta d)$$

used to compute the mole fraction of D_2O, the oxygen composition of all samples being assumed normal. Here

$$\Delta d = d^{25}_4 - 0.99706 = d^{25}_4 - d^{25}_4(H_2O)$$

In most experiments the density difference, $\simeq 0.012$ at 25°, was such as to give about 25 fringes and exposures during the diffusion period were timed to give a 12-fringe separation that progressed from about 1 mm. in the first pattern to not over 7 mm. in the final one. Although this concentration difference is small in terms of the number of fringes it is relatively large on the mole fraction scale and the gradients in a boundary were not Gaussian. The departures from the Gauss shape were symmetrical, however, and a diffusion coefficient reported below is the differential value at the mean concentration in the boundary.

Reference fringes bracketing those conjugate to the diffusion and reference channel are formed in each pattern by the two pairs of slits S in the mask, M of Fig. 1. These facilitate the alignment of the photographic plate in the comparator. The thermostat temperature was measured with the aid of a Pt resistance thermometer and was controlled with a contact thermometer, sensitive to 0.01°, and vacuum tube relay. In order to reduce "twinkling" of the fringes at 45° the bulk of the required heat was supplied continuously by radiation from an infrared lamp above the thermostat.

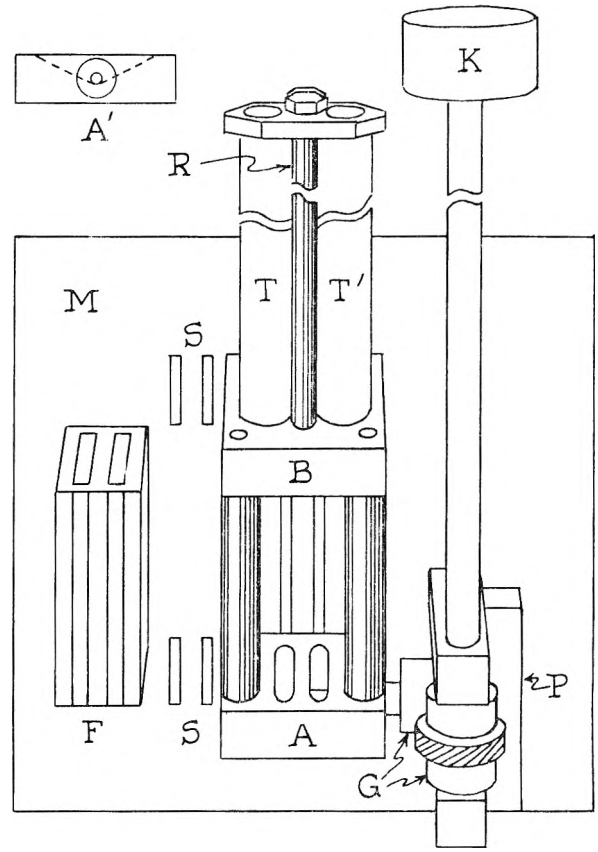

Fig. 1.—The diffusion cell.

Results

The results of all experiments are given in Table I, including the four values at 25° previously

(4) L. G. Longsworth, *J. Am. Chem. Soc.*, **74**, 4155 (1952).

(5) C. S. Caldwell, J. R. Hall and A. L. Babb, *Rev. Sci., Instr.*, **28**, 816 (1957).

(6) H. J. Antweiler, *Chemie-Ingenieur-Technik*, **24**, 284 (1952).

(7) L. G. Longsworth and D. A. MacInnes, *J. Am. Chem. Soc.*, **59**, 1666 (1937).

(8) L. G. Longsworth, *ibid.*, **59**, 1483 (1937).

(9) I. Kirshenbaum, "Physical Properties and Analysis of Heavy Water," McGraw-Hill Book Co., New York, N. Y., 1951, p. 14.

reported. In this table N is the mean mole fraction of D_2O and the diffusion coefficient D is in cm.²/sec. The data of Table I may be represented empirically as follows.

TABLE I

DIFFUSION COEFFICIENTS OF H_2O–D_2O MIXTURES

N, mean mole fraction D_2O; ΔN, mole fraction increment, D, cm.²/sec.

N	ΔN	10^5D	N	ΔN	10^5D
	25°			25°	
0.0401	0.0802	2.248	0.3982	0.0567	2.113
.0668	.1334	2.240	.4193	.1190	2.103
.0765	.1529	2.241	.5397	.1219	2.051
.0843	.1686	2.232	.6618	.1223	2.008
.1584	.3168	2.209	.7789	.1120	1.972
.2242	.1426	2.180	.8914	.1128	1.931
.2423	.0539	2.164	.9388	.1227	1.922
.3171	.0956	2.138		45°	
	5°		0.0713	0.1425	3.491
0.0456	0.0911	1.281	.0765	.1529	3.480
.1469	.1112	1.253	.1574	.1304	3.444
.2580	.1106	1.216	.2242	.1426	3.404
.3735	.1200	1.187	.2868	.1288	3.370
.4927	.1182	1.155	.4124	.1224	3.304
.6015	.0990	1.124	.5373	.1273	3.244
.7104	.1186	1.100	.6662	.1316	3.171
.8054	.1449	1.077	.7998	.1357	3.114
.9399	.1225	1.047	.9343	.1322	3.056

At 5° $10^5D = 1.295(1 - 0.2390N + 0.0375N^2) \pm 0.001$ (1)

25° $10^5D = 2.272(1 - 0.1963N + 0.0335N^2) \pm 0.003$ (2)

45° $10^5D = 3.532(1 - 0.1666N + 0.0236N^2) \pm 0.003$ (3)

The average deviation of the experimental points from the values computed with these relations is given at each temperature and is about the same as the deviation, in a given experiment, of the value for each pattern from the mean for the ten exposures. The uncertainty in D of $\simeq 0.1\%$ thus indicated is somewhat greater than that encountered with 50-fringe patterns. The higher value at 25° and $N = 0$ than that previously reported, 2.261×10^{-5}, results from the curvature in the graph of D *vs.* N revealed by the more complete coverage of the mole fraction scale in the present study.

In contrast with the diffusion coefficient the ratio of the refractive index increment, Δn, to the mole fraction difference, ΔN, exhibits no discernible dependence on N although this ratio does vary with the temperature. At a wave length of 5461 Å. the values of $10^6\,\Delta n/\Delta N$ at 5, 25 and 45° are 5338 ± 14, 4722 ± 13 and 4379 ± 18, respectively. Stokland's[9] value of 4832 at 20° and 5461 Å. falls on the curve through the points at 5, 25 and 45°. However, no simple interpolation formula for $\Delta n/\Delta N$ as a function of the temperature has been found. The average deviation from the mean at each temperature corresponds to an uncertainty of 0.07 fringe in a 25-fringe pattern or to 3×10^{-5} in the density. Since the diffusion coefficient is insensitive to density errors, and since the uncertainty in D corresponds to a smaller variation in the fringe number than 0.07, much of the variation in $\Delta n/\Delta N$ probably arises from errors in density determinations.

Discussion

Comparison of not only the signs, but also the magnitudes, of the coefficients in the relation between D and N at 25°, equation 2, with those for the fluidity[10]

$$\phi = \phi_{H_2O}(1 - 0.2232N + 0.0370N^2)$$

and with those for the chloride ion mobility[7]

$$\lambda_0(Cl^-) = 76.34(1 - 0.2126N + 0.0338N^2)$$

suggests that the diffusion behaviour of HDO is not essentially different from that of other small solutes in water. The temperature dependence of D is also typical of that of other small molecules susceptible to hydrogen bonding, *e.g.*, D_{25}/D_5 is 1.754 for HDO and 1.735 for urea,[3] both in H_2O. This ratio exceeds the fluidity quotient ϕ_{25}/ϕ_5 for water, 1.697, by 3.3% but is 3.7% less than the ratio, $298\phi_{25}/278\phi_5$, required by Stoke's relation and observed experimentally for sufficiently large solutes in water. Since the viscous flow of a pure liquid may be described as the diffusion of momentum the similarity of the flow process to the self diffusion of the liquid is emphasized by these observations. Since its physical properties differ so widely from those of hydrogen, deuterium is not a suitable isotope for the measurement of the self diffusion of liquid water. Thus the question must be left open for the present as to whether or not temperature has precisely the same effect on the self diffusion of water as on its fluidity. In pure heavy water D_{25}/D_5, from equations 1 and 2 for $N = 1$, exceeds ϕ_{25}/ϕ_5 by only 2.0%.[9]

A related problem is posed by the physiologists[11,12] who have observed that if a *porous* membrane separates water from an aqueous solution of a solute, say albumin at a concentration of c moles per liter, to which the membrane is impermeable the resulting osmotic flow is $J = KRTc$. Here K is the hydraulic permeability of the membrane as determined from the flow of water under a difference of hydrostatic pressure and *not* the diffusion permeability or "cell constant" that is obtained when the same membrane serves as the diaphragm in a diaphragm diffusion cell and is calibrated with tagged water. For example, the hydraulic permeability of a porous membrane model consisting of n right cylindrical pores per unit area, each of radius r, would be proportional to nr^4 whereas the diffusion permeability would be $\sim nr^2$. This suggests that in osmosis a real hydrostatic pressure difference equal to RTc exists across the pores of the membrane although the process is superficially an isopiestic one. A pressure difference of equal magnitude, but of opposite sign, must thus be present in the thin, unstirred diffusion layer in the solution at the membrane interface where the osmosis tends to dilute the albumin. The pressure difference across this layer arises, presumably, from the gradient in momentum transfer resulting from the disparity

(10) G. Jones and H. J. Fornwalt, *J. Chem. Phys.*, **4**, 30 (1936).

(11) A. Mauro, *Science*, **126**, 252 (1957).

(12) G. Meschia and I. Setnikar, *J. Gen. Physiol.*, **42**, 429 (1958).

in the molecular masses of water and albumin and the concentration gradient. Although similar pressure gradients exist in a freely diffusing albumin boundary no membrane is present to which the volume flow can be referred. In the true self diffusion of water no asymmetry in momentum transfer accompanies the gradient of tagged water.

Consistent with this qualitative interpretation is the experimental result that although HDO diffuses 36 times faster than albumin the activation energies for the two processes differ by less than 10%. Glasstone, Laidler and Eyring[13] have interpreted results of this type as indicating that large solute particles diffuse, not by their thermal motion into holes spontaneously arising from fluctuations in solvent density as in the diffusion of small molecules, but by self diffusion of the solvent around the macromolecule. Although small, the difference in the activation energies for the diffusion of small and large solutes exceeds, however, the errors in the diffusion measurements. Insofar as the activation energy for the diffusion of HDO approximates that for the self diffusion of H_2O the difference between this energy and the corresponding quantity for albumin suggests that the pressure gradient in the albumin boundary modifies somewhat the self diffusion of the solvent water. Thus the author prefers to visualize the flow of water around an albumin molecule in the diffusion of this solute as an osmotic flow.

Acknowledgment.—It is a pleasure to acknowledge the care with which D. A. MacInnes reviewed this manuscript and with which Emilia Jurevicius analyzed the fringe patterns. The discussion of diffusion and osmosis resulted from conversations with John G. Kirkwood. Any virtues in the interpretation are due to him. The author is responsible for the defects.

(13) S. Glasstone, K. J. Laidler and H. Eyring, "The Theory of Rate Processes," McGraw-Hill Book Co., New York, N. Y., 1941, p. 520.

INFLUENCE OF SIDE-CHAIN HYDROGEN BONDS ON THE ELASTIC PROPERTIES OF PROTEIN FIBERS AND ON THE CONFIGURATIONS OF PROTEINS IN SOLUTION[1,2]

BY HAROLD A. SCHERAGA

Department of Chemistry, Cornell University, Ithaca, New York

Received June 23, 1960

A theory has been developed to account for the effect of various chemical agents, specifically *p*H, but also salt, urea, etc., on the elastic properties of protein fibers and on the configurations of proteins in solution. In both cases hydrogen bonds between polar side-chain groups are assumed to provide stabilization of the crystalline form (*e.g.*, α-helix) compared to the amorphous form (*e.g.*, random coil) of the protein. The presence of such side-chain hydrogen bonds affects the thermodynamics of the crystalline ⇄ amorphous phase equilibrium. Equations are presented for the effect of *p*H on the equilibrium, and numerical calculations are carried out for several illustrative types of side-chain hydrogen bonds. Application of the theory to experimental data on the *p*H-dependence of the elastic properties of protein fibers or of reversible denaturation in solution may aid in the identification of the side-chain groups involved in hydrogen-bonding stabilization of the native protein

Introduction

Considerable attention has been devoted to the question of the relative stabilities of helical and randomly-coiled configurations of proteins in aqueous solutions[3-11] and in fibers.[12] While the influence of side-chain interactions and covalent cross-links on the stability has been recognized, no complete quantitative treatment of the effects of side-chain interactions on reversible changes of configuration has thus far been presented. If the side-chain polar R groups of proteins are considered to interact by hydrogen-bond formation, this being one type of interaction, it is possible to provide a quantitative treatment of the effects of *p*H and other small molecules and ions on the elastic properties of protein fibers and on reversible denaturation in solution. Various experimental results are available to indicate that some elastic mechanisms[13,14] and denaturation reactions[15-24] may involve re-

(1) This work was supported by research grant No. E-1473 from the National Institute of Allergy and Infectious Diseases of the National Institutes of Health, Public Health Service, and by grant G-6461 from the National Science Foundation.

(2) Presented at the Symposium on Secondary and Tertiary Structure in Proteins, Division of Biological Chemistry, 134th meeting of the American Chemical Society, Chicago, Illinois, September, 1958.

(3) J. A. Schellman, *Compt. rend. trav. Lab. Carlsberg, Ser. Chim.*, **29**, 223, 230 (1955).

(4) W. F. Harrington and J. A. Schellman, *ibid.*, **30**, 21 (1956).

(5) L. Peller, THIS JOURNAL, **63**, 1194, 1199 (1959).

(6) J. A. Schellman, *ibid.*, **62**, 1485 (1958).

(7) T. L. Hill, *J. Polymer Sci.*, **23**, 549 (1957); *J. Chem. Phys.*, **30**, 383 (1959).

(8) J. H. Gibbs and E. A. DiMarzio, *ibid.*, **28**, 1247 (1958); **30**, 271 (1959).

(9) B. H. Zimm and J. K. Bragg, *ibid.*, **28**, 1246 (1958); **31**, 526 (1959).

(10) S. A. Rice and A. Wada, Abstracts of the 134th meeting of the Amer. Chem. Soc., Chicago, Ill., p. 41S, Sept., 1958.

(11) S. A. Rice, A. Wada and E. P. Geiduschek, *Disc. Faraday Soc.*, **25**, 130 (1958).

(12) P. J. Flory, *J. Am. Chem. Soc.*, **78**, 5222 (1956).

(13) E. T. Dumitru, Ph.D. Thesis, Cornell University, Sept., 1957.

(14) O. K. Spurr, Jr., Ph.D. Thesis, Cornell University, Sept., 1958.

(15) J. Pace, *Biochem. J.*, **24**, 606 (1930).

(16) J. H. Northrup, *J. Gen. Physiol.*, **16**, 323 (1932).

(17) M. L. Anson and A. E. Mirsky, *ibid.*, **17**, 393 (1934).

(18) R. M. Herriott, *ibid.*, **21**, 501 (1938).

(19) A. E. Stearn, *Ergeb. Enzymforsch.*, **7**, 1 (1938).

(20) V. duVigneaud, *Cold Spring Harbor Symposium Quant. Biol.*, **6**, 275 (1938).

(21) F. H. Johnson, H. Eyring, R. Steblay, H. Chaplin, C. Huber and G. Gherardi, *J. Gen. Physiol.*, **28**, 463 (1945).

(22) M. Kunitz, *ibid.*, **32**, 241 (1948).

(23) M. A. Eisenberg and G. W. Schwert, *ibid.*, **34**, 583 (1951).

(24) F. H. Johnson, H. Eyring and M. Polissar, "The Kinetic Basis

versible processes. Since the influence of side-chain hydrogen bonds on a variety of protein reactions has previously been treated,[25-34] it is now possible to apply these considerations to reversible changes of configuration in the solid state and in solution. The theory of side-chain hydrogen bonding in proteins,[25-27,33] combined with Flory's theory of elastic mechanisms in proteins,[12] are applied here to a model for assessing the influence of various substances on elastic properties and on denaturation.

Elastic Properties[35]

Model.—A protein fiber (taken here to be of uniform cross section) is assumed to be made up of ν polypeptide chains or σ such chains in unit cross-sectional area. In the completely crystalline form the chains are assumed, *for illustrative purposes only*, to have a helical configuration[36] (*e.g.*, α-helix), to be aligned parallel to each other, and to be cross-linked by covalent bonds which do not rupture during deformation. Such cross-links can be naturally occurring ones (*e.g.*, disulfide bridges or possibly ester linkages involving side-chain amino acid residues) or synthetically introduced ones (*e.g.*, those formed by tanning with formaldehyde or benzoquinone). The number of crosslinks in the fiber will be taken as $\nu/2$, or $\nu/(2A^cL^c)$ for unit volume of the crystalline form where A^c and L^c are the cross-section and length, respectively, of the crystalline form. As pointed out by Flory,[12] a crystalline fiber which is cross-linked in this manner differs from one in which the cross-links are introduced at random when the chains have the random coil configuration. In particular, if the cross-linked helices are melted, the resulting random coils (amorphous state) will have a lower entropy than a polymer which is cross-linked in the random coil configuration. The entropy decrease, ΔS^0_X, due to the introduction of the cross-links in the crystalline form reflects the restriction on the distribution of cross-links in the randomly-coiled form. The value of ΔS^0_X, according to Flory,[12] is

$$\Delta S^0_X = -R\nu[(3/4)\ln n' + 9/4] \qquad (1)$$

where n' is the number of statistical elements (assumed here to be amino acid residues[37]) between cross-links.

Letting l' be the length of a statistical element, the length of the fiber at maximum extension, L_m, is

$$L_m = (\nu/\sigma)n'l' \qquad (2)$$

since $n'l'$ is the maximum length of one equivalent statistical chain between cross-links and ν/σ is the mean number of chains in one linear sequence throughout the length of the fiber.

We shall assume that hydrogen bonds can be formed between the polar side-chain R groups of the amino acid residues.[25] Thus, when the crystalline fiber is melted, the covalent cross-links are preserved (and contribute to ΔS^0_X of equation 1), but the side-chain hydrogen bonds as well as the peptide NH. . .OC hydrogen bonds of the backbone of the chains are ruptured. Since the hydrogen bonds rupture on melting, they make no contribution to ΔS^0_X of equation 1. Such a transformation is represented in Fig. 1. Species C, I and A, represent the crystalline (helical), intermediate, and amorphous (random coil) forms, respectively. The polypeptide chains are taken as parallel to the fiber axis in form C. The equilibrium between C and I involves the rupture of the side-chain hydrogen bonds without disturbance of the backbone hydrogen bonds. The equilibrium between I and A represents the rupture of the backbone hydrogen bonds. Because of the additional stability provided by the side-chain hydrogen bonds, form C is more stable with respect to form A than is form I. It is not implied that the sequence of events in the melting process is necessarily C → I → A. The transformation C → A is separated into these two steps merely for purposes of calculation. The model assumed here allows for reaction of the solvent with the side chains of all forms C, I and A, this point being discussed in more detail elsewhere.[39]

The elastic properties of the fiber depend on the nature of the transition from C to A. If, for example, the temperature is raised to melt the crystalline form, the fiber will shrink in length, resulting in a retractive force.[12,40,41] The contraction arises because the polypeptide molecule in the random configuration (amorphous form) has a length projected on the fiber axis, which is less than its length in the crystalline state.[42] We are concerned here primarily with the *p*H-dependence of the elastic properties, and shall assume that all the *p*H-dependence resides in the equilibrium between forms C and I because the side-chain groups can be involved in acid–base equilibria. Thus, if the *p*H is varied, the side-chain hydrogen bonds can form or rupture.[25] In this sense, the *p*H predetermines

of Molecular Biology," John Wiley and Sons, Inc., New York, N. Y., p. 234.

(25) M. Laskowski, Jr., and H. A. Scheraga, *J. Am. Chem. Soc.*, **76**, 6305 (1954).

(26) J. M. Sturtevant, M. Laskowski, Jr., T. H. Donnelly and H. A. Scheraga, *ibid.*, **77**, 6168 (1955).

(27) M. Laskowski, Jr., and H. A. Scheraga, *ibid.*, **78**, 5793 (1956).

(28) H. A. Scheraga, G. I. Loeb and M. L. Wagner, *Federation Proc.*, **15**, No. 1138 (1956).

(29) G. I. Loeb and H. A. Scheraga, THIS JOURNAL, **60**, 1633 (1956).

(30) S. Ehrenpreis, E. Sullivan and H. A. Scheraga, Abstracts of the 133rd meeting, San Francisco, California, April 1958, p. 26-C.

(31) M. Laskowski, Jr., S. Ehrenpreis, T. H. Donnelly and H. A. Scheraga, *J. Am. Chem. Soc.*, **82**, 1340 (1960).

(32) H. A. Scheraga and M. Laskowski, Jr., *Adv. in Protein Chem.*, **12**, 1 (1957).

(33) M. Laskowski, Jr., and H. A. Scheraga, Abstracts of the 124th A.C.S. meeting, p. 36C, Chicago, Ill., Sept., 1953.

(34) H. A. Scheraga, *Ann. Rev. Phys. Chem.*, **10**, 191 (1959).

(35) The notation used in this section is that of Flory.[13]

(36) The requirement of crystallinity can be met by other forms, *e.g.*, the extended β-configuration. Further, it is not necessary that the fiber be *completely* crystalline in order that this model be applicable. All that is required is partial crystallinity and preferential orientation of crystallites along the fiber axis. This requirement is met by numerous fibrous proteins and also by synthetic fibers made from globular proteins.

(37) Some discussion of this assumption has been presented elsewhere.[38]

(38) H. A. Scheraga, "Protein Structure," Academic Press, New York, N. Y., Ch. IV, in press.

(39) A. Nakajima and H. A. Scheraga, *J. Am. Chem. Soc.*, in press.

(40) P. J. Flory, *Science*, **124**, 53 (1956).

(41) P. J. Flory, *J. Cell. Comp. Physiol.*, **49**, Sup. 1, 175 (1957).

(42) An illustrative calculation to demonstrate this shrinkage has been presented elsewhere.[38]

the nature of the crystalline phase. Chemical agents, besides acid and base, can be used to fix the nature of the crystalline phase. Once the crystalline phase is defined, we can then consider the equilibrium between this particular crystalline phase C and the intermediate form I. The equilibrium between forms I and A is assumed to be independent of *p*H since it involves the rupture of hydrogen bonds between backbone NH and CO groups, neither of which dissociates or associates protons in the usual *p*H range of interest.

In the model described above, electrostatic effects have been neglected. This situation can probably be achieved experimentally by immersing the fiber in a medium of high ionic strength.

Elasticity Equation.—According to Flory[12,40,41] and Gee[43] the transformation from a crystalline to an amorphous form involves a first-order phase transition which may be characterized by eq. 3 for a fiber subject to a tensile force f. Equation 3

$$[\partial(f/T)\partial(1/T)]_P = \Delta H/\Delta L \qquad (3)$$

is an analog of the Clapeyron equation, with ΔH and ΔL being the latent heat and length changes, respectively, and T is the transition temperature. This equation pertains to the situation where both crystalline and amorphous phases coexist in equilibrium, the equilibrium force being independent of the fiber length at constant T and P. For the case of interest here, the fiber is immersed in an excess of a solvent whose *p*H can be varied. Under these conditions ΔH will contain not only the heat of fusion of the crystalline form but also the integral heat of dilution for the mixing of the amorphous phase and the solvent. When the fiber is melted in the presence of excess solvent to produce form A (which is swollen with solvent), the contributions to ΔH are assumed to be the following: (1) *a pH-dependent* part arising from the rupture of the side-chain hydrogen bonds in the transformation C→I, and (2) two *pH-independent* parts arising from the loss of crystallinity (including the rupture of the backbone hydrogen bonds) and the heat of dilution in the transformation I→A.

Integration of the Elasticity Equation.—As in the case of the Clapeyron equation, the relation between f and T at equilibrium may be obtained by integration of the differential equation 3. For this purpose it is first necessary to relate f to ΔL, the latter being equal to $L^a - L^c$ by definition. The quantity L^c is a geometrical parameter (applicable to forms C and I) which may be assumed to be essentially independent of temperature and *p*H. The quantity L^a is the length of the sample when totally amorphous and will depend on the force, the relationship between f and L^a (*i.e.*, the stress-strain relation for oriented non-crystalline fibers) having been obtained from a statistical theory by Flory.[12] The stress-strain relation for a closed system is[12]

$$= BTL^a\left(1 - \frac{L_i^3}{(L^a)^3}\right) \qquad (4)$$

where L_i is the length of the sample in the isotropic state (*i.e.*, at zero force), and

(43) G. Gee, *Quart. Rev.*, **1**, 265 (1947).

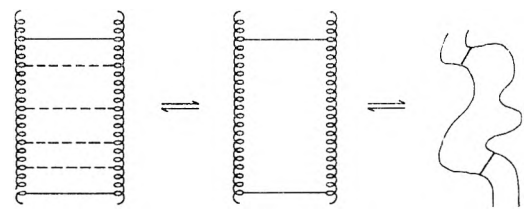

C I A

Fig. 1.—Representation of equilibria between helix and random coil forms. The solid lines represent covalent cross-links and the dashed lines side-chain hydrogen bonds. Species C, I and A are crystalline (helix), intermediate, and amorphous (random coil) forms, respectively. Forms C and A may also be regarded as native and denatured forms, respectively. In any given protein molecule the native configuration may actually consist of both helical and randomly-coiled regions, *i.e.*, the helices may not be perfect.

$$B = \frac{3k\sigma}{l'L_m} = 3k\nu n'/L_m^2 \qquad (5)$$

where k is the Boltzmann constant. It should be emphasized that equations 4 and 5 apply to an amorphous network derived by melting from a crystalline structure in which the cross-links were introduced while the polypeptide chains were ordered. Also, since only the amorphous chain units are capable of taking up numerous configurations about their single bonds, the tension may be attributed to the amorphous chains only, even when both crystalline and amorphous phases coexist in the fiber.

Substitution of equation 4 into equation 3 gives

$$(L^a - L^c)\,\mathrm{d}\left[L^a - \frac{L_i^3}{(L^a)^2}\right] = \frac{\Delta H}{B}\,\mathrm{d}\left(\frac{1}{T}\right) \qquad (6)$$

In order to integrate[12] it is assumed that B, L_i and L^c are independent of temperature and *p*H. The quantity ΔH depends on both temperature and *p*H (see below). Integrating between the limits L^c and L^a, we obtain

$$(L^a - L^c)^2\left[1 + \frac{2L_i^3}{(L^a)^2L^c}\right] = \frac{2}{B}\int_{T_m^c}^{T_m} \Delta H\,\mathrm{d}\left(\frac{1}{T}\right) \qquad (7)$$

where T_m is the melting point, or transition temperature, at a force such that the amorphous length is L^a, and T_m^c is the melting point when $L^a = L^c$. The quantity T_m^c is *p*H-dependent (see below). Substitution from equation 5 for B provides the alternative expression

$$\left[\frac{L^c - L^a}{L_m}\right]^2\left[1 + \frac{2L_i^3}{(L^a)^2\,L^c}\right] = \frac{2}{3R}\int_{T_m^c}^{T_m} \Delta h'\,\mathrm{d}\left(\frac{1}{T}\right) \qquad (8)$$

where $\Delta h'$ is the heat of fusion per mole of equivalent elastic elements, *i.e.*

$$\Delta h' = \frac{N_a\,\Delta H}{\nu n'} \qquad (9)$$

where N_a is Avogadro's number and R is the universal gas constant. For $T_m < T_m^c$ equation 8 yields two solutions,[12] L^a, one less than and the other greater than L^c. We shall consider only the solution $L^a < L^c$, since fibers invariably rupture at high extension. There are no real solutions for $T_m > T_m^c$. Thus, T_m^c appears to be a critical temperature, at any given *p*H, above which the crystalline phase cannot exist. In principle, then, equation 8 gives L^a as a function of T_m. By com-

bining this result with equation 4, it is possible to obtain the equilibrium force, f_{eq}, as a function of T_m. Such a function will indicate a monotonic increase of f_{eq} with increasing T_m at any pH. In other words, an increase in the temperature would tend to melt the crystalline regions of the fiber (enhancing the transformation from C to A). In order to maintain equilibrium between the crystalline and amorphous phases the force must be increased. At any given force, the value of T_m will be higher the higher is $\Delta h'$. Before carrying out this computation, it will be necessary to discuss the magnitude and pH dependence of $\Delta h'$ and T_m^c in the next two sections.

While equations 8 and 4 will give f_{eq} as a function of T_m, it is simpler to use an approximate equation (*merely for illustrative purposes*). Toward this end we shall consider the fiber to be subjected to a fairly large force such that $L^a >> L_i$. In this approximation, equation 4 reduces to

$$f = \frac{3kT\sigma L^a}{l'L_m} \qquad (10)$$

and equation 8 to

$$\left[\frac{L^c - L^a}{L_m}\right]^2 = \frac{2}{3R}\int_{T_m^c}^{T_m} \Delta h' \, d\left(\frac{1}{T}\right) \qquad (11)$$

Elimination of L^a/L_m between these two equations gives

$$f_{eq}/T_m = \frac{3k\sigma}{l'}\left[\frac{L^c}{L_m} \pm \sqrt{\frac{2}{3R}\int_{T_m^c}^{T_m} \Delta h' \, d\left(\frac{1}{T}\right)}\right] \qquad (12)$$

While equation 12 holds for high extensions, we shall not let the extension become too high (to avoid rupture of the fiber) and, therefore, shall consider only the lower root[12] of equation 12.

Magnitude and pH-Dependence of $\Delta h'$.—The quantity $\Delta h'$, defined in equation 9, consists of contributions $\Delta h_0'$ for the transformation I→A, and Δh_H, for the transformation C→I. In a later

$$\Delta h' = \Delta h_0' + \Delta h_H \qquad (13)$$

section we shall discuss the contribution of the heat of dilution to $\Delta h_0'$. For the present, we may assume that $\Delta h_0'$ arises only from the loss of crystallinity (including the rupture of the backbone hydrogen bonds). The quantity Δh_H depends on the heat of formation of a side-chain hydrogen bond, ΔH_{ij}°, defined previously,[25] and also on the heats of ionization of the donor and acceptor groups (see below). On the basis of thermodynamic data for aqueous urea solutions, Schellman[3] has suggested that the heat of formation of a peptide hydrogen bond is −1500 cal./mole. This is a reasonable value which we shall use for the peptide hydrogen bond. However, the side-chain hydrogen bonds, especially OH. . .O bonds, appear to have a larger negative enthalpy of formation,[44] and we shall use the higher value for the side-chain bonds. Therefore, *for illustrative purposes only*, assuming that there is one amino acid residue per statistical element,[37] $\Delta h_0' = +1500$ cal./mole. If each statistical element contained one side-chain hydrogen bond, then $\Delta h_0'$ would be augmented by Δh_H. However, there are probably fewer hydrogen bonds and we shall assume, for illustrative purposes only, that there is one side-chain hydrogen bond per chain of n' statistical elements. With this assumption the value of $\Delta h'$ is

$$\Delta h' = 1500 + \frac{\Delta h_H}{n'} \qquad (14)$$

We shall carry through the calculation by assuming that the helices in form C are perfect (except for possible small imperfections at the ends near the cross-links). However, in a real case this degree of perfection need not be achieved, *i.e.*, there may be only partial crystallinity. The influence of the side-chain hydrogen bonds on the stability of the helix, and therefore on the pH-dependence of T_m (to be computed below), will depend on the relative magnitude of the two terms on the right-hand side of equation 14, *i.e.*, the greater is the term $\Delta h_H/n'$, the greater will be the pH-dependence of T_m.

The effect of pH on the equilibrium force–temperature behavior is assumed to arise from the pH-dependent part of the $\Delta h'$ term of equation 12 (*i.e.*, from the Δh_H term of equation 14) and from the pH-dependent T_m^c. If the experiment is carried out at a pH at which the side-chain hydrogen bonds of form C are intact, then $\Delta h'$ will contain the heat of fusion of such bonds, Δh_H, and T_m^c will be correspondingly affected. If, on the other hand, the pH is such that the side-chain hydrogen bonds are ruptured, then $\Delta h'$ and T_m^c will be lower, and the transition temperature, T_m, at a given force, will also be lower. We shall, therefore, consider several different kinds of side-chain hydrogen bonding situations and show how the transition temperature at a given force varies with pH.

As a first example, we shall assume that the side-chain hydrogen bonds are all equivalent heterologous single bonds[25] between donors DH and acceptors A. As the pH is varied the donors can dissociate protons, and the acceptors can associate protons. The side-chain hydrogen bonds in form C will be ruptured when the donors are in the form D or the acceptors in the form HA, the maximum degree of hydrogen bonding occurring at a pH intermediate between the pK's of DH and HA. If attention is focussed on a given hydrogen bond between an ith donor and jth acceptor, the fraction of the molecules, x_{ij}, which will have a hydrogen bond formed will be[27]

$$x_{ij} = \frac{K_{ij}}{1 + K_{ij} + K_1/[H^+] + [H^+]/K_2} \qquad (15)$$

where K_{ij} is the equilibrium constant[25] for the formation of the ijth hydrogen bond, K_1 and K_2 are the ionization constants of the non-hydrogen bonded groups DH and HA, respectively, and $[H^+]$ is the hydrogen ion activity. By analogy with equations II-18, II-19 and II-20 of reference 27 (except that here we are considering the *pH dependence* of x_{ij}) we have

$$\Delta F^0_{obs} = \Delta F^0_{unf} + \Delta F^0_H \qquad (16)$$

$$\Delta H^0_{obs} = \Delta H^0_{unf} + \Delta H^0_H \qquad (17)$$

$$\Delta S^0_{obs} = \Delta S^0_{unf} + \Delta S^0_H \qquad (18)$$

with

$$\Delta F^0_H = -RT\sum \ln (1 - x_{ij}) \qquad (19)$$

(44) Arguments supporting a value of −6000 cal./mole for the enthalpy of formation of a side-chain hydrogen bond have been presented elsewhere.[32-34]

$$\Delta H^0_H = \sum x_{ij}\left[-\Delta H^0_{ij} + \frac{(K_1/[H^+])\Delta H_1^0 - ([H^+]/K_2)\Delta H_2^0}{1 + K_1/[H^+] + [H^+]/K_2}\right] \quad (20)$$

$$\Delta S^0_H = \frac{\Delta H^0_H - \Delta F^0_H}{T} \quad (21)$$

where ΔH^0_{ij} is the heat of formation of the ijth hydrogen bond.[44] The quantities ΔH_1^0 and ΔH_2^0 are the heats of ionization corresponding to the equilibrium constants K_1 and K_2, respectively; ΔF^0_{unf}, ΔH^0_{unf}, and ΔS^0_{unf} refer to the unfolding of the helix in the absence[3] of side-chain hydrogen bonds, and ΔF^0_{obs}, ΔH^0_{obs} and ΔS^0_{obs} refer to the process when side-chain hydrogen bonds are present. According to our illustrative assumption, we are considering a chain with only one side-chain hydrogen bond. Therefore, there will be only one term in the summations in these equations. Of course, the more terms one includes in the summations, *i.e.*, the more stabilizing hydrogen bonds there are, the greater will be the pH-dependence of T_m. The quantity Δh_H of equation 14 corresponds to ΔH^0_H of equation 20. Values of x_{ij} as a function of pH are shown in Fig. 2 for two different sets of donor and acceptor groups. This parameter is temperature dependent, as illustrated for two temperatures in Fig. 3. Corresponding values of Δh_H as a function of pH are shown in Fig. 4. The temperature dependence of Δh_H is illustrated for two temperatures in Fig. 5.

As a second example, we shall assume that the side-chain hydrogen bonds are all equivalent homologous double bonds[25] of the acetic acid dimer type. For this case (*i.e.*, an lth carboxyl group hydrogen-bonded to an mth one) x_{lm} may be approximated by the expression[27]

$$x_{lm} = \frac{K_{lm}}{1 + K_{lm} + 2K_2/[H^+] + (K_2/[H^+])^2} \quad (22)$$

The value of ΔF^0_H is

$$\Delta F^0_H = -RT\sum \ln (1 - x_{lm}) \quad (23)$$

Since the heat of ionization of non-hydrogen-bonded carboxyl groups is essentially zero, and since both the donor and acceptor groups are identical, Δh_H becomes simply

$$\Delta h_H = -x_{lm}\,\Delta H^0_{lm} \quad (24)$$

Equation 21 gives ΔS^0_H. Values of x_{lm} and Δh_H as a function of pH are shown in Fig. 6.

Evaluation of T_m^c.—We shall first evaluate T_m^c, assuming that no side-chain hydrogen bonds exist (*i.e.*, for the transformation I→A). Then the effect of the side-chain hydrogen bonds will be introduced in order to compute the pH-dependence of T_m^c. For this purpose we may write[3] for ΔF^0_{unf} of equation 16

$$\Delta F^0_{unf} = (n - 4)\Delta H^0_{res} - T(n - 1)\Delta S^0_{res} \quad (25)$$

where n is the number of amino acid residues in the chain (assumed here as equal to n', the number of statistical elements), and ΔH^0_{res} and ΔS^0_{res} are the enthalpy and entropy changes, respectively, per residue, for the unfolding of an infinitely long helix to an unstressed, *i.e.*, isotropic, random coil. If the chains are cross-linked while in the crystalline form, then the entropy of the random coil is reduced by an amount ΔS^0_X given by equation 1. In addition, at T_m^c, the entropy of the random coil is further reduced by an amount ΔS^0_{el} because the amorphous chains are under a force which is sufficiently

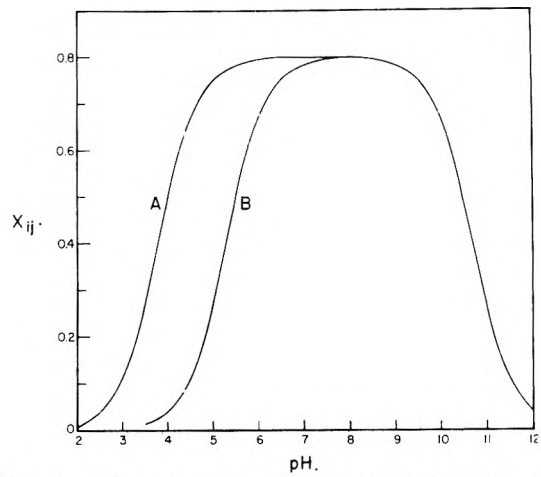

Fig. 2.—Values of x_{ij} as a function of pH at 300°K., computed from equation 15 with $K_{ij} = 4$ at 300°K. and $\Delta H°_{ij} = -6$ kcal./mole. A: tyrosyl–carboxylate ion hydrogen bond with $pK_1 = 10$ and $pK_2 = 4.5$ at 300°K. B: tyrosyl–histidine hydrogen bond with $pK_1 = 10$ and $pK_2 = 6$ at 300°K.

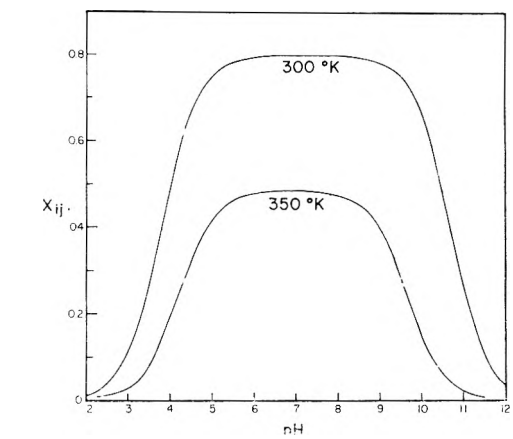

Fig. 3.—Illustration of temperature dependence of x_{ij} for tyrosyl–carboxylate ion hydrogen bonds with parameters of Fig. 2 together with $\Delta H_1^\circ = 6$ kcal./mole and $\Delta H_2^\circ = 0$.

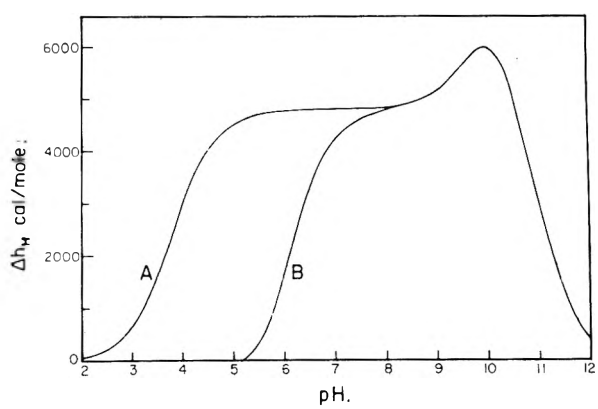

Fig. 4.—Values of Δh_H as a function of pH at 300°K., computed from equation 20 with the parameters of Figs. 2 and 3, together with $\Delta H_1^\circ = 6$ kcal./mole and $\Delta H_2^\circ = 7$ kcal./mole for the tyrosyl–histidyl hydrogen bond (B). Curve A corresponds to the tyrosyl–carboxylate ion hydrogen bond.

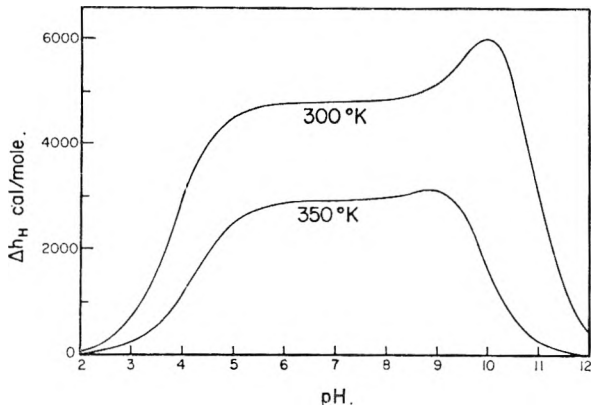

Fig. 5.—Illustration of temperature dependence of Δh_H for tyrosyl–carboxylate ion hydrogen bonds with parameters of Figs. 2 and 3.

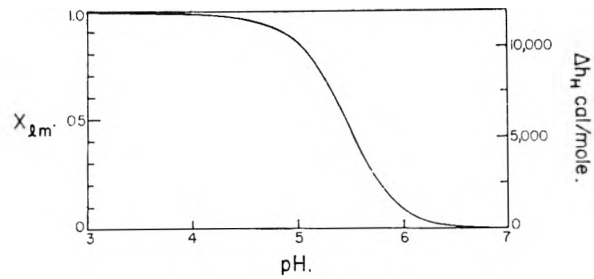

Fig. 6.—Values of x_{1m} and Δh_H as a function of pH at 300°K., computed from equations 22 and 24, respectively, for carboxyl–carboxyl acetic acid dimer-type hydrogen bonds, with $K_{1m} = 100$ and $pK_2 = 4.5$ at 300°K., $\Delta H_2^\circ = 0$, and $\Delta H_{1m}^\circ = -12$ kcal./mole.

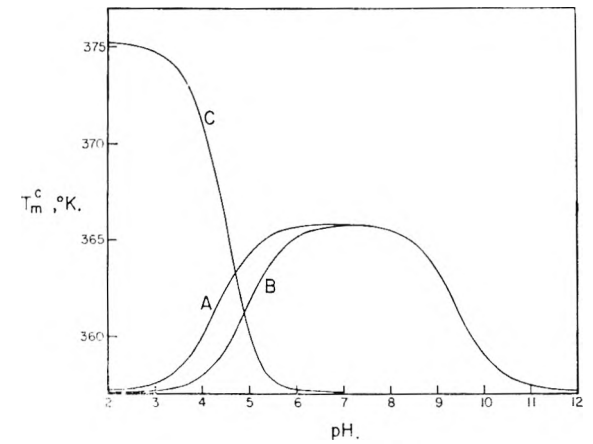

Fig. 7.—The pH dependence of T_m^c for: A, tyrosyl–carboxylate ion; B, tyrosyl–histidine; C, carboxyl–carboxyl hydrogen bonds.

large to make L^a equal to L^c. In this highly (but *not fully*) extended form, there are fewer configurations available to the chain than if it were in its isotropic form at zero force. The value of ΔS^0_{el} for high extensions, where $L_i << L^a$ and $L^a = L^c$, is approximately[12]

$$\Delta S^0_{el} = -\frac{3R\nu}{2}\left[n'\left(\frac{L^c}{L_m}\right)^2 - 1\right] \qquad (26)$$

assuming that the isotropic coil is the unperturbed coil, and that the deformation is athermal.[12] Therefore, Schellman's equation (equation 25) may be modified to take these effects into account.

$$\Delta F^0_{unf} = (n - 4)\,\Delta H^0_{res} - T\Delta S^0_0 \qquad (27)$$

where

$$\Delta S^0_0 = (n - 1)\Delta S^0_{res} + \frac{\Delta S^0_X}{\nu} + \frac{\Delta S^0_{el}}{\nu} \qquad (28)$$

Since $\Delta F^0_{unf} = 0$ at $T = T_m^c$ we obtain

$$T_m^c = \frac{(n - 4)\,\Delta H^0_{res}}{\Delta S^0_0} \qquad (29)$$

For illustrative purposes we shall take $n = 14$, $\Delta H^0_{res} = 1500$ cal./mole, $\Delta S^0_{res} = 4.2$ e.u. and $L^c/L_m = 0.41$ (the last quantity being obtained from the dimensions of the polypeptide chain in the α-helical and fully-extended forms). The resulting value of T_m^c is then 357°K. The effects of cross-linking in the crystalline state (*i.e.*, $\Delta S^0_X/\nu = -8.5$ e.u.) and of stretching of the random coil ($\Delta S^0_{el}/\nu = -4$ e.u.) on the melting temperature are shown in Table I.

TABLE I

TRANSITION TEMPERATURES FOR HELIX-RANDOM COIL TRANSITION ($n = 14$) IN THE ABSENCE OF SIDE-CHAIN HYDROGEN BONDS[a]

Nature of transformation	T_m, °K.
Non-cross-linked helix to isotropic random coil	275
Cross-linked helix to isotropic random coil	326
Cross-linked helix to stretched random coil ($L^a = L^c$)	357[b]

[a] On the basis of the model and the parameters discussed in the text. [b] This is T_m^c in the absence of side-chain hydrogen bonds.

The effects of side-chain hydrogen bonding may now be superimposed on the above results. For this purpose, assuming one side-chain hydrogen bond per chain, we may write

$$\Delta F^0_{obs} = (n - 4)\,\Delta H^0_{res} - \Delta H^0_H - T(\Delta S^0_0 + \Delta S^0_H) \qquad (30)$$

$$= (n - 4)\,\Delta H^0_{res} - T\Delta S^0_0 + \Delta F^0_H \qquad (31)$$

where $\Delta S^0_0 = 42$ e.u. according to equation 28 and ΔF^0_H is given by equation 19. Since ΔF^0_H is a function of both pH and temperature, the value of T_m^c was obtained at any given pH by solution of equation 31 (with a Burroughs 220 computing machine[45]) for $T = T_m^c$ under the condition that $\Delta F^0_{obs} = 0$. These values of T_m^c as a function of pH are shown in Fig. 7 for several types of side-chain hydrogen bonds. Similar calculations were carried out with the aid of equations 22 and 23 for homologous double bonds, and are also illustrated in Fig. 7.

Equilibrium Force–Temperature Curves.—Having evaluated $\Delta h'$ as a function of pH and temperature (from equations 14, 20 and 24, using an illustrative value of $n = n' = 14$), and T_m^c as a function of pH, it is now possible to obtain the equilibrium force–temperature curves at any particular pH with the aid of equation 12.

The geometrical parameters, L^c/L_m, σ and l', required for this computation were obtained as follows. L^c/L_m has already been shown to be 0.41 for the polypeptide chain. Since we have assumed that there is one amino acid residue per statistical element for simplicity, the value of l' is the fully extended length of an amino acid residue[46] or

(45) Programmed by Mrs. Marion Pak.

(46) R. B. Corey and L. Pauling, *Proc. Roy. Soc.* (*London*), **B141**, 10 (1953).

3.6×10^{-8} cm. A reasonable value for σ, the number of chains per cm.^{2} cross-section of the fiber, is obtained from X-ray data on poly-γ-benzyl-L-glutamate. Pauling and Corey[47] interpreted the X-ray data for this synthetic polypeptide in terms of a parallel array of α-helices with 2 helices per unit cell of cross-section 25.0 × 14.42 Å. Dividing the number of chains per unit cell by the cross-sectional area, we obtain a value of $\sigma = 5.5 \times 10^{13}$ chains per cm.^{2}. Thus, the units of f_{eq} in equation 12 will be dynes/cm.^{2}.

Computation of f_{eq} *vs.* T_m curves was carried out with a Burroughs 220 computing machine.[45] Examples of such curves are shown in Fig. 8 for tyrosyl–carboxylate ion bonds. It can be seen that f_{eq} increases with T_m at any *p*H. At *p*H 2 the side-chain hydrogen bond does not exist and Δh_H is zero (see Fig. 5); at *p*H 7 Δh_H has a high value (see Fig. 5), corresponding to a high degree of hydrogen bonding (with contributions from the heats of ionization). The curves at other *p*H's would appear similar but would be displaced from these curves. If such a fiber were immersed in a buffer at *p*H 7, then equilibrium between crystalline and amorphous phases would be established at a series of forces and temperatures along the *p*H 7 curve of Fig. 8. Consider the fiber in equilibrium at a temperature of 349°K. and a force of 3×10^7 dynes/cm.^{2}. At this *p*H the tyrosyl–carboxylate ion bonds are contributing to the stability of the crystalline form. If the *p*H is lowered to *p*H 2 and the force maintained constant at 3×10^7 dynes/cm.^{2} the tyrosyl–carboxylate ion bonds are ruptured and the crystalline phase will melt. To re-establish equilibrium at *p*H 2 at this force, the temperature must be lowered to 340°K. (the horizontal line in Fig. 8). Alternatively, equilibrium could be re-established at *p*H 2 and 349°K. if the force were increased to 5×10^7 dynes/cm. (the vertical line in Fig. 8), *i.e.*, the increased force (required to compensate for the rupture of the side-chain hydrogen bond) would tend to keep the randomly-coiled chains in an ordered array and preserve equilibrium between the two phases.

If the curves for other *p*H-values were drawn in Fig. 8, they would intersect any given line of constant force (*e.g.*, the horizontal line shown at 3×10^7 dynes/cm.^{2}) at a series of equilibrium melting temperatures T_m. The resulting values of T_m are plotted as a function of *p*H at constant force in curve A of Fig. 9 for tyrosyl–carboxylate ion hydrogen bonds. Curve B corresponds to tyrosyl–histidine bonds (see below for a discussion of curve C). It is seen that curves A and B exhibit a maximum at an intermediate *p*H, this behavior arising primarily from the corresponding *p*H-dependence of Δh_H and $T_m{}^c$ (see Figs. 4 and 7). If more than one kind of side-chain hydrogen bond were ruptured, these curves could exhibit more than one maximum. A choice of other paramters would lead to a larger or smaller dependence of T_m on *p*H. The relative magnitude of the *p*H-dependence of T_m thus provides an indication of the importance of side-chain hydrogen bonds in stabiliz-

(47) L. Pauling and R. B. Corey, *Proc. Natl. Acad. Sci., U. S.*, **37**, 241 (1951).

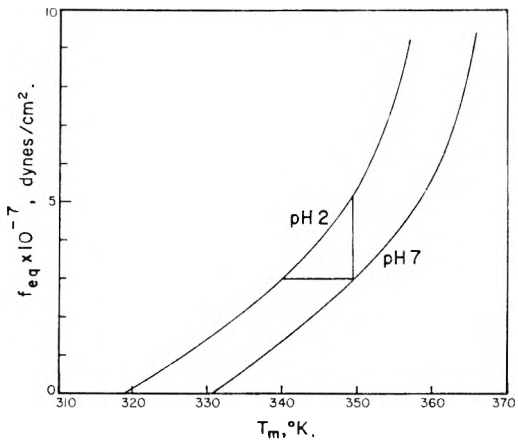

Fig. 8.—Two representative equilibrium force–temperature curves for a hypothetical fiber having side-chain tyrosyl–carboxylate ion hydrogen bonds. At *p*H 2 the side-chain bonds do not exist; at *p*H 7 there is a maximum degree of such side-chain hydrogen bonding. While these curves are drawn to $f_{eq} = 0$, it should be recalled that the approximate equation 12 is valid only at fairly high values of f_{eq}.

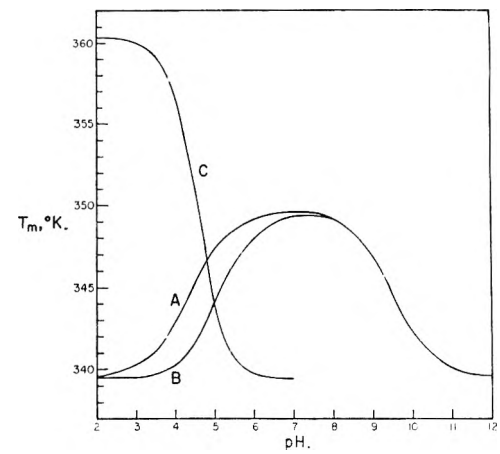

Fig. 9.—Equilibrium melting temperature as a function of *p*H for: A, tyrosyl–carboxylate ion; B, tyrosyl–histidine; and C, carboxyl–carboxyl hydrogen bonds, all at a constant force of 3×10^7 dynes/cm.^{2} for the hypothetical fiber discussed in the text.

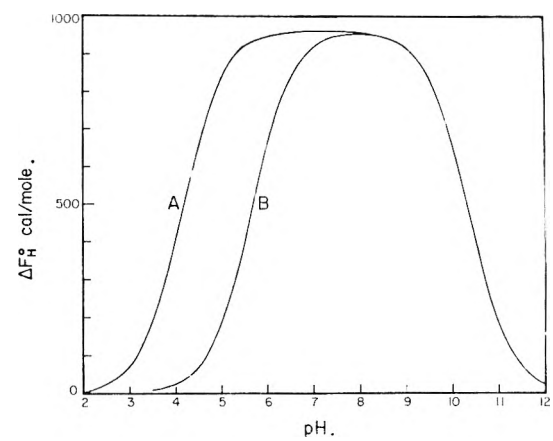

Fig. 10.—Contribution of a heterologous single hydrogen bond to ΔF_H° as a function of *p*H at 300°K., computed from equation 19, for: A, tyrosyl–carboxylate ion, and B, tyrosyl–histidine hydrogen bonds, with the parameters of Fig. 2.

ing the crystalline form. The *p*H-dependence of T_m also provides information on the *pK*'s of the donor and acceptor groups involved in side-chain hydrogen bonds in form C.

A similar calculation can be carried out for homologous double bonds, using the equations cited earlier for this type of hydrogen bond. At any given force, *e.g.*, 3×10^7 dynes/cm.^{2}, the melting temperature T_m will depend on *p*H as shown by curve C of Fig. 9. Again, the similarity in shape between this curve and those of Figs. 6 and 7 may be noted, *i.e.*, the carboxyl–carboxyl bonds exist only at low *p*H and, therefore, contribute to Δh_H and $T_m{}^c$ only at low *p*H.

Effects of Salts, Urea, Etc.—The transformations C→I and I→A involve the rupture of side-chain and backbone hydrogen bonds, respectively. If the *p*H is varied, then only the transformation C→I is affected because of the ionization of the side-chain groups, as already discussed. However, both the side-chain and backbone hydrogen bonds can be ruptured if the donor or acceptor groups can bind small ions or molecules other than protons, *e.g.*, thiocyanate ion, guanidinium ion, urea or ATP. The effect of such small ions and molecules on the formation and rupture of hydrogen bonds has already been treated.[25] As a result it has been possible to calculate the effect of these substances on the kinetics of protein denaturation.[33] Thus, the treatment presented above for the effect of *p*H on the elastic properties can easily be extended to take into account the effects of small ions and molecules. Flory[41] has given an expression for the effect of binding on the equilibrium melting temperature.

Effect of Swelling.—In applying the above considerations to experimental data account must be taken of the fact that the measurements are generally made on a network swollen with solvent, *i.e.*, on the amorphous phase mixed with solvent. Therefore, the experimental data must be corrected for the effect of swelling (*i.e.*, the contribution of the integral heat of solution to the observed heat of fusion). A treatment of the elastic properties at swelling equilibrium has been presented by Flory[12] and applied by Spurr[48] to experimental data on collagen. Theoretical treatments of this problem have also been presented by Katchalsky[49] and Prins and Hermans[50]; also a discussion of the effect of *p*H on the composition of the mixed phases has been presented by Nakajima and Scheraga.[39]

Experimental Behavior.—There are several investigations reported in the literature[51–53] on the effect of *p*H, salts, urea, etc., on the elastic properties of protein fibers. As a typical example we may cite the experiments of Lennox[52] on the effects of these substances on the shrinkage of collagen. While his data were not obtained under conditions of equilibrium between crystalline and amorphous phases, and no correction was made for swelling, nevertheless the shrinkage temperature was found to vary considerably with *p*H, and in a manner indicated by, say, curve A of Fig. 9, *i.e.*, his curves (see, *e.g.*, Figs. 7, 8 and 9 of his paper) showed a maximum, with a decrease in the shrinkage temperature at low and high *p*H. The length of the flat portion at the maximum and also the height of the maximum varied with the source of the collagen and also with the nature of added salts. In light of the theory presented herein, these variations may reflect differences in degree of side-chain hydrogen bonding caused by these additives. Presumably, an analysis of experimental data of this kind, when obtained under equilibrium conditions, and corrected for swelling, can provide information on the nature of side-chain hydrogen bonds between the polypeptide chains of which the fiber is composed. Recent experiments on ribonuclease films,[39] made under conditions of equilibrium, and corrected for swelling, seem to provide a better test of the theory than do the non-equilibrium data on collagen.[52]

The shrinkage of a muscle fiber in the presence of ATP has been interpreted by Mandelkern, *et al.*,[54] as the melting of a crystalline form, in accord with suggestions of Pryor[55] and Flory[40,41] that muscular contraction may be the result of the conversion of crystalline regions of polypeptide chains to amorphous ones. As pointed out by Mandelkern, *et al.*,[54] this is another example of the now widely observed shrinkage of fibrous proteins induced by a variety of chemical agents. In light of the model discussed herein, these agents presumably act by binding to side-chain groups and interfering with side-chain hydrogen bonding, thereby affecting[41,54] the stability of the helical or crystalline form.

Reversible Denaturation

Model.—The model represented in Fig. 1 can also serve for a theory of reversible denaturation in solution. Instead of regarding species C, I and A as sections of a fiber, we simply have to imagine a boundary to be drawn around each of these forms in order that they shall represent individual protein molecules in solution. The native protein (form C) in this idealized model is then an assembly of α-helices, cross-linked by covalent bonds and side-chain hydrogen bonds. The latter may be interchain bonds, as shown in Fig. 1, or intrachain bonds which could stabilize turns between straight segments of an α-helix. The denatured protein (form A) consists of randomly coiled chains in which the hydrogen bonds are ruptured but the covalent cross-links still persist. In an actual protein, the native form may not be completely crystalline and the reversibly denatured form may not be completely amorphous. Further, the crystalline–amorphous transition in a given case may involve only a part of the whole structure. As before, it is convenient to introduce form I for purposes of calculation of the free energy difference between forms C and A. Since we are interested here in the *p*H dependence of the standard free

(48) O. K. Spurr, Jr., Ph.D. Thesis, Cornell University, Sept., 1958.

(49) A. Katchalsky, "Conference on Contractility," Mellon Institute, Pittsburgh, Pa., Jan. 27–30, 1960, p. 22.

(50) W. Prins and J. J. Hermans, ref. 49, p. 26.

(51) E. R. Theis, *Trans. Faraday Soc.*, **B42**, 244 (1946).

(52) F. G. Lennox, *Biochim. et Biophys. Acta*, **3**, 170 (1949).

(53) W. G. Crewther and L. M. Dowling, THIS JOURNAL, **62**, 678 (1958).

(54) L. Mandelkern, A. S. Posner, A. F. Diorio and K. Laki, *Proc. Nat. Acad. of Sci.*, **45**, 814 (1959)

(55) M. G. M. Pryor, *Progr. in Biophysics*, **1**, 216 (1950).

energy change ΔF^0_{obs} for the equilibrium C⇆A we shall again assume that the free energy change for the equilibrium C⇆I is *p*H dependent whereas that for the equilibrium I⇆A is independent of *p*H. The rupture of side-chain hydrogen bonds in the former step renders the helices less stable, thus enhancing the helix-to-random coil transition. The transition from I to A is presumably the origin of the optical rotation changes observed in protein denaturation, and it is implied in our model that denaturation is regarded here as a transformation of a protein from form C to form A.

As in the case of the elastic properties, a large number of side-chain hydrogen bonds between ionizable groups will manifest itself in a significant *p*H-dependence of reversible denaturation. Further, whereas electrostatic theories of denaturation, based on the Linderstrøm-Lang model[56] for treating ionization in proteins, require symmetry about the isoelectric point, with maximum stability of the protein occurring at the isoelectric point, the hydrogen-bond theory indicates that the *p*H (or *p*H's) of maximum stability occurs in a region which depends on the *pK*'s of the donor and acceptor groups involved and needs bear no relationship to the isoelectric point. The relation between the *p*H of maximum stability and the isoelectric point thus provides a criterion to distinguish between the electrostatic and hydrogen bonding mechanisms for the *p*H-dependence of reversible denaturation. Probably experimental investigations will show that both mechanisms are operative. At any rate we shall develop here the theory for the hydrogen bonding mechanism.

Thermodynamic Formulation.—Since the reaction under consideration has been divided into two stages (see Fig. 1) we can write for the over-all standard free energy change

$$\Delta F^0_{obs} = \Delta F^0_{unf} + \Delta F^0_H \qquad (32)$$

where, according to our assumptions, ΔF^0_H is *p*H-dependent and ΔF^0_{unf} is not. This formulation is analogous to that of Fig. 4 of reference 27, and to equation 16 used for the elastic properties.

In complete analogy with the foregoing treatment of the elastic properties we can write

$$\Delta F^0_{obs} = (n - 4)\Delta H^0_{res} - T\Delta S^0_0 + \Delta F^0_H \qquad (33)$$

However, here there is no contribution ΔS^0_{el} to ΔS^0_0, since the randomly coiled form in dilute solution is assumed to be isotropic. Hence

$$\Delta S^0_0 = (n - 1)\Delta S^0_{res} + \Delta S^0_X/\nu \qquad (34)$$

where ΔS^0_X arises from the *permanent* cross-links. The value of ΔF^0_H is given by equation 19 for heterologous single bonds and by equation 23 for homologous double bonds. For illustrative purposes only, we shall use the same numerical parameters as in the treatment of the elastic properties. Obviously these can be modified for any specific protein in light of knowledge of the amino acid sequence, positions of the disulfide cross-links and postulated number of side-chain hydrogen bonds.

***p*H-Dependence.**—The contribution of a side-chain hydrogen bond to ΔF^0_H is plotted in Figs. 10 and 11 for heterologous single and homologous double bonds, respectively. According to Fig. 10, a protein having a significant number of, say, tyrosyl–histidine hydrogen bonds would show maximum stability around *p*H 8, *independent of its isoelectric point* (on this model) except insofar as electrostatic effects influence *pK*'s, a factor not considered here explicitly but which could easily have been introduced. If more than one kind of heterologous single bond were present, the curves of Fig. 10 could exhibit more than one maximum. According to Fig. 11, a protein having a significant number of carboxyl–carboxyl hydrogen bonds would be most stable at low *p*H, and would lose the stabilization of these side-chain hydrogen bonds at higher *p*H's where the carboxyl groups would be ionized. Thus, the *p*H-dependence of ΔF^0_{obs} for reversible denaturation provides a means of identifying the nature of side-chain hydrogen bonds which affect the thermodynamics of the helix-random coil tranformation.

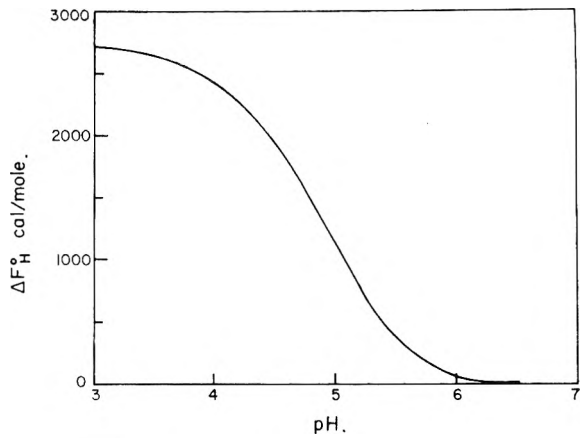

Fig. 11.—Contribution of a homologous double hydrogen bond to ΔF°_H as a function of *p*H at 300°K., computed from equation 23 for a carboxyl–carboxyl, acetic acid dimer-type hydrogen bond, with the parameters of Fig. 6.

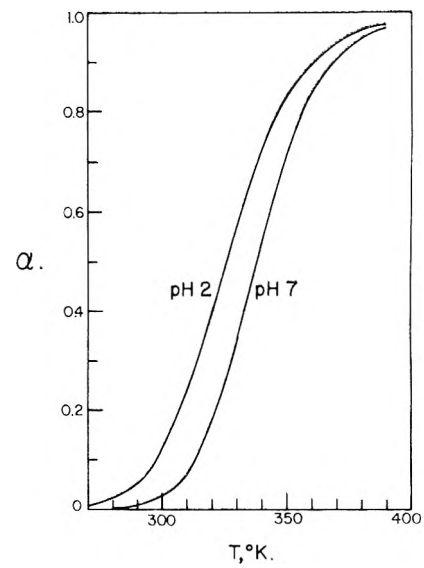

Fig. 12.—Temperature dependence of the degree of denaturation at *p*H 2 and 7 for a hypothetical protein stabilized by tyrosyl–carboxylate ion hydrogen bonds (equation 36 and the parameters of Fig. 10).

Over-all Free Energy Change.—The value of

(56) K. Linderstrøm-Lang, *Compt. rend. trav. Lab. Carlsberg*, **15**, No. 7 (1924).

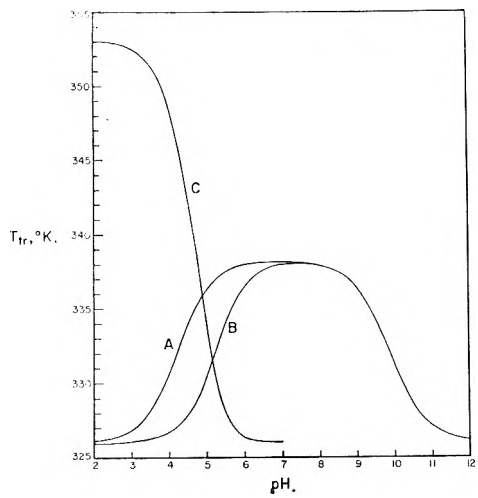

Fig. 13.—Transition temperature as a function of *p*H for a hypothetical protein stabilized by: A, tyrosyl–carboxylate ion; B, tyrosyl–histidine; and C, carboxyl–carboxyl hydrogen bonds.

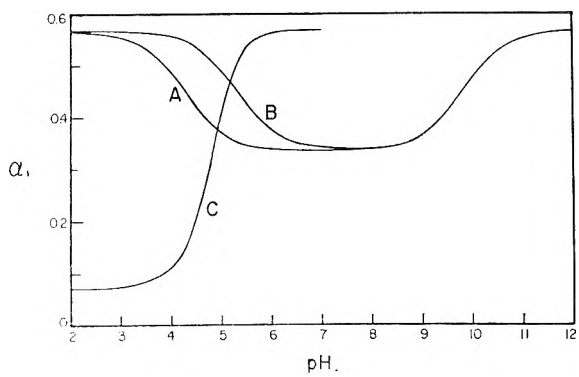

Fig. 14.—The *p*H-dependence of the degree of denaturation at 330°K. for a hypothetical protein stabilized by: A, tyrosyl–carboxylate ion; B, tyrosyl–histidine; and C, carboxyl–carboxyl hydrogen bonds.

ΔF^0_{unf} is very sensitive to the values of ΔH^0_{res} and ΔS^0_{res}, as discussed by Schellman.[3] Therefore, the values chosen here are such as to make the calculated transition temperature occur in the commonly observed range. Using the same values as in the treatment of the elastic properties, equation 33 becomes

$$\Delta F^0_{obs} = 15{,}000 - 46T + \Delta F^0_H \qquad (35)$$

It is instructive to define a parameter α as the fraction of the molecules denatured[3] (*i.e.*, in the form A) and write

$$\alpha = [1 + e^{\Delta F^0_{obs}/RT}]^{-1} \qquad (36)$$

Theoretical values of α as a function of T are plotted in Fig. 12 for a hypothetical protein stabilized by tyrosyl–carboxylate ion hydrogen bonds. Taking the transition temperature, T_{tr}, as the value of T at which $\alpha = 1/2$ (or $\Delta F^0_{obs} = 0$) at any given *p*H, the values of T_{tr} are plotted as function of *p*H in Fig. 13. Thus, it can be seen that a determination of the *p*H-dependence[57] of ΔF^0_{obs} or of T_{tr} for reversible denaturation may provide information on the kinds of side-chain hydrogen bonds which play a role in the stabilization of the native protein. Such experiments should be carried out at high ionic strength to minimize electrostatic effects.

Effect of Salts, Urea, Etc.—The remarks made in the paragraph carrying this same title in the "Elasticity" section also apply here. In other words, the above theory can be extended to account for the effect of small ions and molecules on reversible denaturation in terms of the binding of these substances to hydrogen bond donor or acceptor groups.

Experimental Behavior.—There are essentially no data in the literature on the *p*H-dependence of ΔF^0_{obs} from equilibrium studies of reversible denaturation. However, some data which may be pertinent to this discussion have been obtained by Terminiello, Bier and Nord.[58] These workers have plotted the per cent. initial enzyme activity as a function of *p*H (after incubation for various times at 100°) for trypsin, acetyltrypsin and succinyltrypsin. These proteins are presumably reversibly denatured and Figs. 2 and 3 of their paper bear a striking resemblance to Fig. 14 of this paper. Similar observations have been reported for alkaline[59] and acid[60] phosphatases. It is possible that a determination of the *p*H-dependence of ΔF^0_{obs} for the reversible denaturation of these proteins may provide information on the kinds of side-chain hydrogen bonds which play a role in the stabilization of the native protein. Preliminary results on ribonuclease[61,62] indicate that the α *vs.* T curves are similar in appearance to those of Fig. 12. However, the experimental curves[62] show a sharper transition. The experimental curve[62] of T_{tr} *vs.* *p*H (determined only between *p*H 1 and 7) is very similar to the acid branch of curve A of Fig. 13.

ADDED IN PROOF.—A discussion of the sharpness of the transition in protein denaturation will be presented in a forthcoming note.[63]

Acknowledgment.—I am indebted to Drs. P. J. Flory, M. Laskowski, Jr., G. I. Loeb and L. Mandelkern for helpful discussions and suggestions, and for reading the manuscript.

(57) Sometimes denaturation data are reported as α *vs.* *p*H at a given temperature. Such a plot is shown in Fig. 14.

(58) L. Terminiello, M. Bier and F. F. Nord, *Arch. Biochem. Biophys.*, **73**, 171 (1958).

(59) W. Cohen, M. Bier and F. F. Nord, *ibid.*, **67**, 479 (1957)—see Fig. 7.

(60) W. Cohen, M. Bier and F. F. Nord, *ibid.*, **76**, 204 (1958)—see Fig. 5.

(61) H. A. Scheraga, C. Y. Cha, C. L. Shildkraut and J. Hermans, Jr., "Amino Acids, Proteins and Cancer Biochemistry," Academic Press, New York, N. Y., 1960, p. 31.

(62) J. Hermans, Jr., and H. A. Scheraga, *J. Am. Chem. Soc.*, submitted.

(63) H. A. Scheraga, R. A. Scott, G. I. Loeb, A. Nakajima and J. Hermans, Jr., THIS JOURNAL, in press.

STUDIES ON COÖRDINATION COMPOUNDS. XIX. FORMATION CONSTANTS OF SOME METAL DERIVATIVES OF β,δ-TRIKETONES[1,2]

BY HIDEHIKO KIDO AND W. CONARD FERNELIUS

Department of Chemistry, The Pennsylvania State University, University Park, Penna.

Received June 24, 1960

The dissociation constants of 1-phenyl-1,3,5-hexanetrione and 1,5-diphenyl-1,3,5-pentanetrione have been measured in 75 volume % dioxane at 30° as well as the formation constants of complexes with uranyl, copper(II), nickel, cobalt, zinc and cadmium ions The triketones are monobasic and function as bidentate ligands.

The metal derivatives of a variety of β-diketones have been extensively studied. However, virtually nothing is known about the metal derivatives of β,δ-triketones. The present study was undertaken to gain some insight into the behavior of such compounds.

Experimental

1-Phenyl-1,3,5-hexanetrione and **1,5-diphenyl-1,3,5-pentanetrione** were kindly supplied by Drs. R. J. Light and C. R. Hauser.[3]

Techniques.—The potentiometric titrations were performed,[4] the acid dissociation constants[5] determined, and the calculations performed[6] as described previously. Tetramethylammonium hydroxide was used for all the titrations and the metal salts were perchlorates.

Results.—The results of the determinations in 75 volume % dioxane at 30° are assembled in Table I. The color of the solutions was yellow becoming more intense in basic solution, except for the uranyl ion which was definitely orange.

replaced by potassium in liquid ammonia, the pK_2 value is too great for dissociation in a partially aqueous medium. The most closely related compounds on which information is available are $CH_3COCH_2COCOCH_2COCH_3$, $pK_1 \approx 10.3$; $pK_2 \approx 13.0$, and $C_6H_5COCH_2COCOCH_2COC_6H_5$, $pK_1 \approx 11.2$; $pK_2 \approx 14.0$.[8] Thus, the second proton is held more tightly when the first is removed from I than when removed from II.

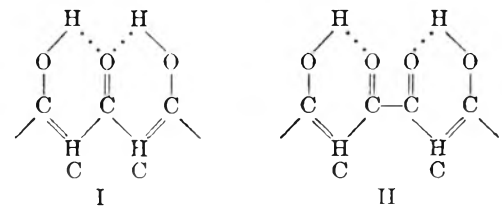

I II

In the formation of metal derivatives the usual

TABLE I

FORMATION CONSTANTS IN 75 VOLUME % DIOXANE AT 30°[a]

		log K_n							
	n =	H^+	UO_2^{++}	Be^{++}	Cu^{++}	Ni^{++}	Co^{++}	Zn^{++}	Cd^{++}
$C_6H_5COCH_2COCH_2COCH_3$	1	11.62		Yellow		9.95	9.37	9.19	7.99
		±0.03				±0.02	±0.04	±0.02	±0.03
	2		10.64	Ppt.	10.08	8.20	7.88	7.87	6.46
			±0.03		±0.05	±0.03	±0.05	±0.05	±0.03
$C_6H_5COCH_2COCH_2COC_6H_5$	1	11.90	Ppt.	Yellow		10.21	9.62	9.49	8.17
		±0.03				±0.03	±0.03	±0.03	±0.02
	2		Ppt.	Ppt.		8.89	8.51	8.54	7.84
						±0.05	±0.05	±0.06	±0.03

[a] The uncertainty in these values represents the 95% confidence limits.

Discussion

It is interesting to note that the triketones are stronger acids (tenfold or more) than the corresponding β-diketones ($CH_3COCH_2COCH_3$, 12.70, $C_6H_5COCH_2COCH_3$, 12.85 and $C_6H_5COCH_2COC_6H_5$, 13.75)[7] and that the dibenzoyl compound is the weaker acid just as dibenzoylmethane is a slightly weaker acid than benzoylacetone. Although the second proton in the triketones can be

order of stabilities is found: (a) the order of metals is $UO_2^{++} > Cu^{++} > Ni^{++} > Co^{++} > Zn^{++} > Cd^{++}$[7,9,10] and (b) the weaker acid forms the more stable derivatives.[9-11] However, the complexes of $C_6H_5COCH_2COCH_2COCH_3$ are more stable than those of $CH_3COCH_2COCH_3$ but somewhat less stable than the corresponding ones of benzoylacetone. Similarly those of $(C_6H_5COCH_2)_2CO$ are more stable than those of benzoylacetone but less stable than those of dibenzoylmethane. There is no indication that the triketones behave as other than bidentate ligands.

(1) This investigation was carried out under contract AT(30-1)-907 between The Pennsylvania State University and the U. S. Atomic Energy Commission.

(2) For XVIII of this series see H. Kido and W. C. Fernelius, *Anal. Chim. Acta*, **23**, 116 (1960).

(3) For preparation, etc., see C. R. Hauser and T. M. Harris, *J. Am. Chem. Soc.*, **80**, 6360 (1958).

(4) L. G. Van Uitert, *et al.*, *J. Am. Chem. Soc.*, **75**, 451, 457 (1953).

(5) (a) L. G. Van Uitert, *et al.*, *ibid.*, **75**, 455 (1953); (b) **76**, 5887 (1954).

(6) B. P. Block and G. H. McIntyre, Jr., *ibid.*, **75**, 5667 (1953).

(7) L. G. Van Uitert and W. C. Fernelius, *ibid.*, **75**, 2736 (1953).

(8) E. H. Holst, Ph.D. Thesis, The Pennsylvania State University, September, 1955.

(9) H. Irving and H. Rossotti, *Acta Chem. Scand.*, **10**, 72 (1956).

(10) W. C. Fernelius, *Boletín del Colegio Químicos de Puerto Rico*, **13**, 3 (1956).

(11) M. Calvin and K. W. Wilson, *J. Am. Chem. Soc.*, **67**, 2003 (1945).

THE DISPROPORTIONATION OF *p*-TOLUENESULFINIC ACID IN AQUEOUS SOLUTION

BY PAUL ALLEN, JR., AND LEO REICH[1]

Department of Chemistry and Chemical Engineering, Stevens Institute of Technology, Hoboken, New Jersey

Received June 27, 1960

A kinetic study has been made of the disproportionation of *p*-toluenesulfinic acid in water over a range of acidity and temperature; iodide ion served as a catalyst. The disproportionation has an initial unsteady state period under certain conditions and then proceeds by a reaction second order in sulfinic acid and, at low *p*H, approximately first order in hydrogen ion. A mechanism is postulated and an equation derived relating rate constant to hydrogen ion concentration. The action of iodide ion as a catalyst is discussed.

Introduction

The thermal disproportionation of sulfinic acids to sulfonic acids and thiolsulfonates has been known since the latter part of the nineteenth century.[2] However, the kinetics and mechanism of this type of reaction have not been reported in the literature.[3] Because of this, a study involving the kinetics and mechanism of the reaction in aqueous solution was undertaken.

The disproportionation occurs according to the equation

$$3RSO_2H \longrightarrow RSO_2SR + RSO_3H + H_2O \quad (1)$$

The stoichiometry of this reaction has been well established by various workers.[2,4,5] One investigator[4] found that the presence of hydroquinone or catechol had no effect on the course of the reaction, indicating that free radicals are probably not involved as intermediates. When an attempt was made to carry out the reaction in the non-polar medium, diethyl ether, very little, if any, product could be isolated.[6] However, Bredereck[3] succeeded in carrying out the disproportionation in non-aqueous media. Hilditch[7] discovered that the reaction rate could be materially increased by hydriodic acid in small amounts and others also used this acid.[7,8] The thiolsulfonates formed during the disproportionation were, in general, very insoluble in water or mixtures of alcohol and water, and usually separated as oils.

One of the main difficulties involved in a study of the thermal disproportionation of sulfinic acids is the possible existence of structural isomers of sulfinic acids and thiosulfonates. Only relatively recently has the problem of which isomers predominate been fairly well resolved.

Thiolsulfonates.—For many years, there has been discussion about the correct structure to be assigned to this class of compounds. Three formulas have been advocated

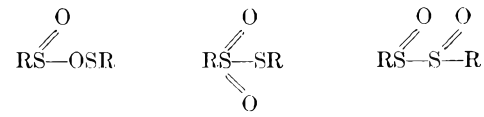

I II III

Without going into the arguments suffice it to say that the predominant chemical and optical evidence favors structure II.[8,9]

Sulfinic Acids.—The exact structure of sulfinic acids has also been a matter of controversy. Two forms may exist

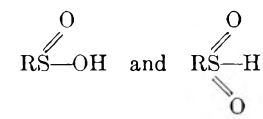

IV V

The predominance of structure IV has recently been favored on grounds of infrared and ultraviolet spectra.[10,11]

Sulfenic Acids.—In the thermal disproportionation of sulfinic acids, it has been assumed that the reaction occurs *via* an unstable intermediate sulfenic acid,[2d,6] RSOH. No free sulfenic acids have been isolated[12,13] and various attempts to prepare them have invariably led to sulfinic acids, disulfides, etc.

Despite their instability, sulfenic acids have been assumed by numerous authors as intermediates in many reactions, because only in this way has it been possible to predict the products actually obtained.[14]

In the mechanism proposed, in the present work, for the disproportionation of sulfinic acids, structures II and IV of thiolsulfonates and sulfinic acids, respectively, have been assumed as the predominant forms, and sulfenic acids have been considered to be involved as reactive intermediates.

(1) Abstracted from a thesis submitted by Leo Reich to Stevens Institute of Technology in partial fulfillment of the requirements for the degree of Doctor of Philosophy, June 1959.

(2) (a) R. Otto and O. Gruber, *Ann.*, **145**, 10 (1868); (b) C. Pauly and R. Otto, *Ber.*, **10**, 2184 (1877); (c) R. Otto, *ibid.*, **15**, 121 (1882); (d) E. Fromm and J. S. Palma, *ibid.*, **39**, 3308 (1906).

(3) During the course of this study, H. Bredereck, *et al.*, *Angew. Chem.*, **70**, 260 (1958), postulated a mechanism for such a reaction in non-aqueous media, similar to the one independently proposed in the present study, for the reaction in polar media.

(4) J. von Braun and K. Weissbach, *Ber.*, **63**, 2836 (1930).

(5) L. Horner and O. H. Basedow, *Ann.*, **612**, 108 (1958).

(6) C. S. Marvel and R. S. Johnson, *J. Org. Chem.*, **13**, 822 (1948).

(7) T. P. Hilditch, *J. Chem. Soc.*, 1091 (1910); 1091 (1911); C. M. Bere and S. Smiles, *ibid.*, 2359 (1924); J. Cymerman and J. L. Lowe, *ibid.*, 1666 (1949).

(8) S. Smiles and D. T. Gibson, *ibid.*, 176 (1924).

(9) H. Gilman, L. E. Smith and H. H. Parker, *J. Am. Chem. Soc.*, **47**, 851 (1925); L. D. Small, J. H. Bailey and C. J. Cavallito, *ibid.*, **71**, 3565 (1949); G. Leandri and A. Tundo, *Ann. Chim. (Rome)*, **47**, 575 (1957); J. Cymerman and J. B. Willis, *J. Chem. Soc.*, 1332 (1951).

(10) H. Bredereck, *et al.*, *Ber.*, **88**, 438 (1955).

(11) S. Detoni and D. Hadzi, *J. Chem. Soc.*, 3163 (1955); but see E. N. Guryanova and Y. K. Syrkin, *Zhur. fiz. Khim.*, **23**, 105 (1949).

(12) W. Autenrieth and H. Hefner, *Ber.*, **58**, 2153 (1928); T. Zincke and J. Baeumer, *Ann.*, **416**, 86 (1916); T. Zincke and K. Eismayer, *Ber.*, **51**, 751 (1918).

(13) K. Fries has reported (*Ber.*, **45**, 2965 (1912)) the isolation of one sulfenic acid, 1-anthraquinonesulfenic acid, but this has been questioned (P. N. Rylander, *J. Org. Chem.*, **21**, 1296 (1956)).

(14) (a) O. Hinsberg, *Ber.*, **36**, 107 (1903); (b) N. Kharasch, S. J. Potempa and H. L. Wehrmeister, *Chem. Revs.*, **39**, 269 (1946); also refs. 2a. 2d. 4.

Experimental

Sodium *p*-toluenesulfinate, Eastman Kodak Co., was extracted with hot benzene, dissolved in an ethanol–water mixture and heated with decolorizing carbon, Norit. After filtration and cooling, the solution deposited white crystals of sodium sulfinate dihydrate. The free acid was not prepared, but for each experiment a fresh aqueous solution of the salt was acidified with sulfuric acid to the desired *p*H. Hydriodic acid was added to supply iodide ion when desired.[15]

About 200 ml. of solution was placed in a 3-necked flask immersed in a constant temperature bath and air was removed by passing dried nitrogen into the flask above the surface of the solution. An hour was allowed for the flask to reach the bath temperature. From time to time, aliquots were removed with a pipet for analysis; the time at which the first sample was withdrawn was taken as zero time for the calculations. After the removal of a sample, nitrogen was again passed over the solution. The analysis of sulfinic acid was essentially by the method of Allen[16]; the sample was run into ice and water, made alkaline and titrated, using excess permanganate and then arsenious acid solution, about 0.05 *N*. A test showed that *p*-toluenethiolsulfonate did not interfere with the titration. The *p*H remained essentially constant during a run.

As disproportionation proceeded, thiolsulfonate settled out. To determine if it decomposed under the experimental conditions employed, thereby affecting the permanganate titration, samples of thiolsulfonate were heated at 85 and 90° with acid and iodide ion. There was no effect on permanganate up to about 35 hours of heating. On longer heating there was a slight effect, but small enough to be neglected.

TABLE I

DISPROPORTIONATION OF *p*-TOLUENESULFINIC ACID IN AQUEOUS SOLUTION

Run no.	Initial concn. of sulfinic acid, moles/l.	Temp., °C.	*p*H	Iodide concn., mg./100 ml.	k_r, l./hr. mole
1	0.070	79.9	1.05	5.7	0.34
2	.071		0.95	14.2	.46
3	.074		0.90	5.7	.37
4	.079		1.05	0.0	.065
5	.081		1.05	2.8	.33
6	.037		1.05	5.7	.35
7	.044		1.05	5.7	.36
8	.065		1.55	5.7	.090
9	.071		0.70	5.7	.43
10	.060		.30	5.7	.74
11	.060		.85	28.5	.51
12	.075		.20	5.7	.80
13[a]	.070		1.05	5.7	.32
14	.074		0.40	5.7	.66
15	.069		1.55	0.0	.00
16	.073	85.0	1.05	5.7	.36
17	.075		0.65	5.7	.56
18	.073		0.40	5.7	.83
20	.078	90.0	1.05	5.7	.44
21	.074		0.60	5.7	.81
22	.079		0.38	5.7	1.23
24	.069		1.55	5.7	0.092

[a] In run 13, 0.7 g. of sodium sulfate per 100 ml. was present.

The data obtained indicated that the reaction could best be described as second order in sulfinic acid. Plots of $1/T$ *vs.* time, t, afforded linear relationships, or linear relationships preceded by initial curvature. The second-order rate constant k_r was estimated from the linear portions of the plots, and obtained using the expression

$$1/T = 1/T_0 + Nk_rt/2V \qquad (2)$$

where T_0 = net ml. of permanganate used in titration, at zero time; T = net ml. of permanganate used in titration after the elapsed time, t; N = the normality of the permanganate solution; V = the volume of the aliquot used.

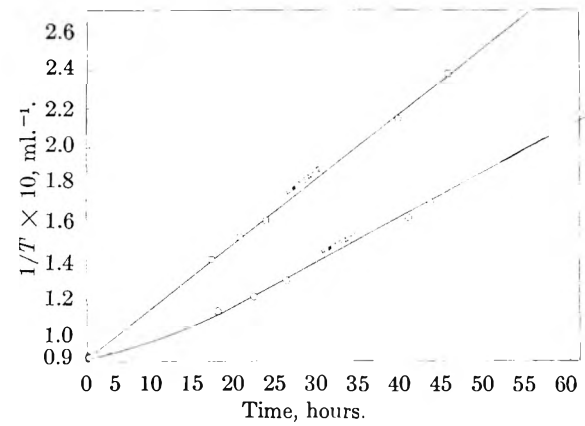

Fig. 1.—Reciprocal of net ml. of permanganate used in titration *vs.* elapsed time.

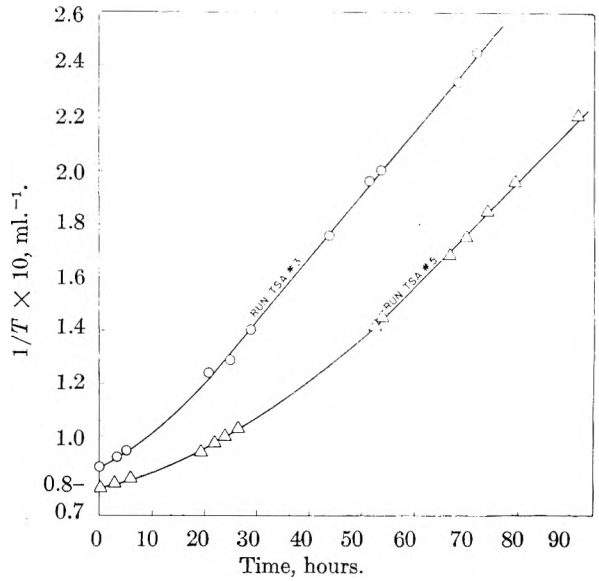

Fig. 2.—(Same as Fig. 1).

Results

The experimental results have been summarized in Table I. The table shows the effect of acidity and iodide ion concentration on the second-order rate constant at various temperatures and initial sulfinic acid concentrations.

As the *p*H decreases, the rate constant increases (the iodide ion concentration being maintained at 5.7 mg./100 ml. of solution for most of the runs). From runs 1 and 5, it can be seen that when the *p*H is kept constant (1.05), and the iodide ion concentration varied from 2.8 to 5.7 mg./100 ml., *the rate constant remains essentially constant* (0.34 and 0.33). When the iodide concentration is raised to 14.2, there is only a relatively small increase in the rate constant (runs 2 and 3), as compared with the increase in the iodide ion concentration. A still larger increase in the iodide concentration results in a still relatively small increase in the value of the rate

(15) Iodide ion was added in order to obtain reasonable reaction rates. Without it, conversions obtained were very low, even after reaction times of about one week.

(16) P. Allen, Jr., *J. Org. Chem.*, **7**, 23 (1942).

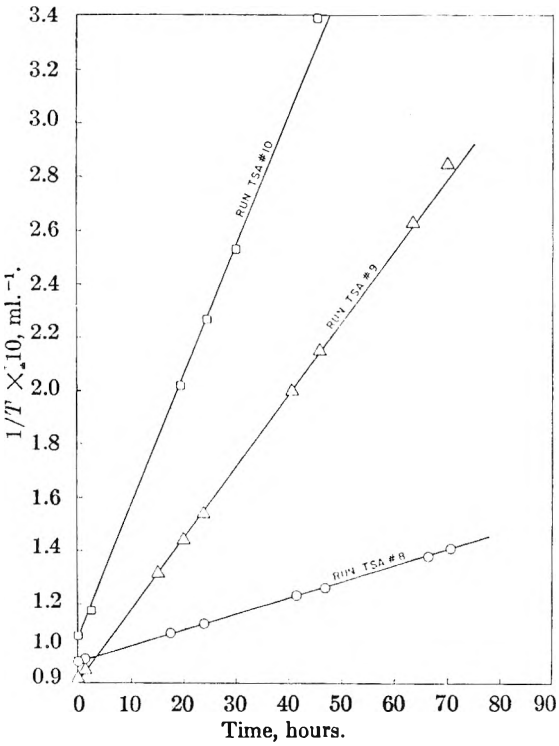

Fig. 3.—(Same as Fig. 1).

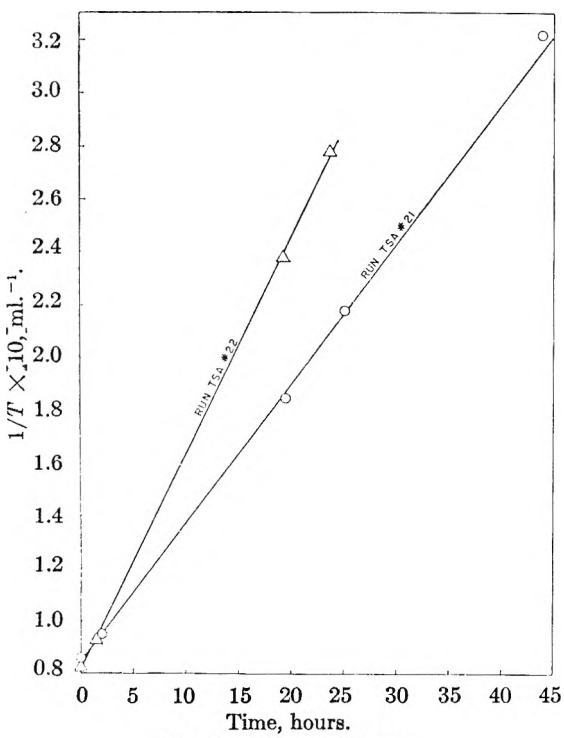

Fig. 4.—(Same as Fig. 1).

constant (runs 3 and 11); it should be noted that at these higher iodide concentrations, the *p*H's were lower and would thus contribute to a higher value of k_r. However, when no iodide ion is present (runs 4 and 15), the reaction rate is extremely slow.

In order to determine the influence of salt effects on the reaction rate, sodium sulfate was added to the reaction mixture of run 13. The effect was slight since the resulting rate constant had a value of 0.32 as compared with values of 0.34 and 0.35 (runs 1 and 6) in which no sulfate was present.

As the reaction temperature increases, the second-order reaction rate constants increase.

Some of the second-order plots show initial curvatures, Figs. 1 and 2, followed by linear relationships. However, under different experimental conditions, only linear relationships are obtained for the duration of the reaction, (Figs. 3 and 4). The diminution or disappearance of the initial curvature results from increased acidity and in some cases from an increase in the iodide ion concentration.

Discussion

The disappearance of the initial curvature in the various second-order plots indicates that there is an initial unsteady state but when conditions are favorable to the rapid establishment of a high steady-state concentration of reactive intermediates, the initial unsteady state condition and also the initial curvature vanish.

The duration of the unsteady state condition is found to depend on the iodide concentration. However, the rate constant k_r, obtained from the linear portion of the second-order plot, does not change to any great extent. Thus, when the concentration was 2.8 mg./100 ml. (run 5), the duration of the unsteady state period was about 40 hours, but when the iodide ion concentration was raised to 5.7, the duration decreased to about 15 hours (run 1). However, in both cases, the rate constant remained essentially constant (0.33 and 0.34). This indicates that at the iodide concentration employed for most of the work, 5.7 mg./100 ml., the iodide has only a small effect, if any, on any rate-determining step in the disproportionation. Thus, it is apparent that the role of the iodide ion is as a pure catalyst.[17]

It is postulated that the iodide participates in an equilibrium reaction involving the isomerization of one form of sulfinic acid to another

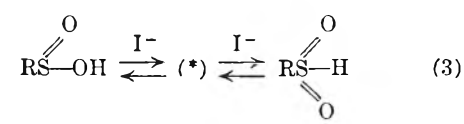

(3)

Thus, the role of the iodide is to increase the rate of attainment of this equilibrium. A low iodide concentration would mean a long unsteady state

(17) An indication that the iodide ion functions as a pure catalyst even at the higher iodide concentrations, 14.2 and 28.5, may be seen from the following treatment. Let us assume that the rate constant observed at 79.9°, k_r, may be expressed by the equation

$$k_r = (0.32 + [H^+]) \left(\frac{[H^+]}{[H^+] + K}\right)^2 f(I) \qquad (4)$$

where f(I) is assumed to be some function of the iodide ion concentration. It will later be shown that such an equation (without the f(I) term, equation 22) fits most of the data (especially at lower *p*H's) at the iodide concentration of 5.7 mg./100 ml. By utilizing the values in Table I for runs 2, 5, 6 and 11, the following values of f(I) are obtained for each of these runs, respectively, 1.49, 1.29, 1.37 and 1.45; the average value of f(I) is 1.40. If an experimental deviation of about 10% is assumed for k_r, then the deviation obtained for f(I) for the runs employing relatively high and relatively low iodide concentrations, would lie well within the experimental error. (In unpublished work in this Laboratory, on the decomposition of *n*-dodecanesulfinic acid, a variation in iodide concentration from 0.6 to 4.8 mg./100 ml., at constant *p*H, had a negligible effect on the rate constant, 2.6 to 2.4.)

period, a longer time to reach equilibrium. Absence of iodide ion should lead to an extremely slow attainment of the maximum equilibrium concentration of RS(=O)(=O)—H (structure V), resulting in a very low rate constant (runs 4, 15, 24). On the other hand, with a relatively high iodide concentration, rapid attainment of the equilibrium should result, leading to a diminution or disappearance of the unsteady state period, as observed.

The postulation of an equilibrium involving structures IV and V is made in order to account for the thiolsulfonate structure II which was the only form that could be isolated for this type of disproportionation (see the Introduction). The other form of sulfinic acid, IV, would lead to the formation of an anhydride or disulfoxide structure (I or III). The former would not be expected to form in an acidic, polar medium, and would therefore, at best, have only a transient existence. The same can be said for the latter structure, since it has never been isolated. The isomerization of one form of sulfinic acid to the other in the presence of iodide ion is attributed to the availability of electrons of the latter.

It is found that the hydrogen ion concentration affects the rate constant considerably, (Fig. 5). With increase in *p*H, the rate constant decreases; at a *p*H of 1.05, k_r is 0.34, but at *p*H 1.55 (that expected from the sulfinic acid alone), k_r is 0.09. It can be observed in Fig. 5 that at relatively low *p*H's, as the hydrogen ion concentration increases, k_r increases in a linear manner, at a particular temperature. However, this relationship does not hold at the relatively high *p*H's (greater than 1.0). Thus, it is apparent that hydrogen ions play an important role in the formation of reactive polar intermediates in the disproportionation reaction. That no salt effect is involved on changing the hydrogen ion concentration is shown by the slight influence on k_r of the addition of sodium sulfate (run 13).

The Reaction Scheme.—The following reaction mechanism is postulated

$$RS(=O)(=O)-O^- + H^+ \overset{1/K}{\rightleftharpoons}$$

$$RS(=O)(=O)-OH \underset{K_0}{\overset{I^-}{\rightleftharpoons}} (*) \underset{K'_0}{\overset{I^-}{\rightleftharpoons}} RS(=O)(=O)-H \quad (5)$$

$$RS(=O)(=O)-H \overset{K_1}{\rightleftharpoons} RS(=O)(=O)^- + H^+ \quad (6)$$

$$RS(=O)(=O)-OH + H^+ \overset{K_2}{\rightleftharpoons} RS(=O)(=O)-OH_2^+ \quad (7)$$

$$RS(=O)(=O)-OH_2^+ \overset{K_3}{\rightleftharpoons} RS{=}O^+ + H_2O \quad (8)$$

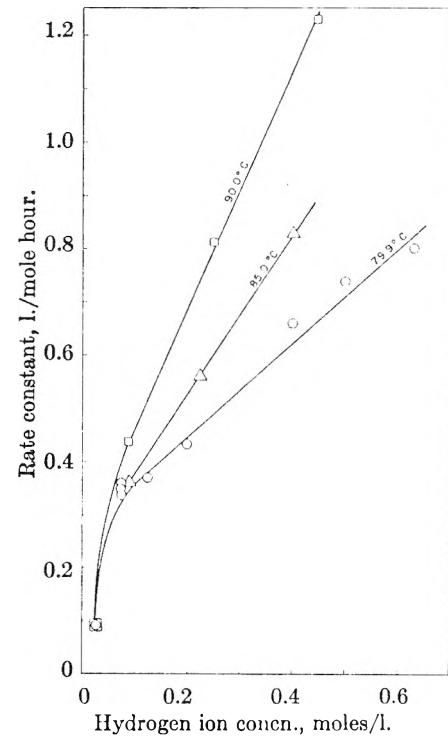

Fig. 5.—Rate constant *vs.* hydrogen ion concentration, at different temperatures and at the iodide concentration of 5.7 mg./100 ml.

$$RS{=}O^+ + RS(=O)(=O)^- \xrightarrow{k_1} [RSOSO_2R] \xrightarrow[\text{fast}]{H_2O}$$

$$RS(=O)(=O)-H + RSO_3H \quad (9)$$

$$RS{=}O^+ + RS(=O)(=O)-H \xrightarrow{k_1'} H^+ + [RSOSO_2R]$$

$$\xrightarrow[\text{fast}]{H_2O} RS(=O)(=O)-H + RSO_3H \quad (10)$$

$$RS(=O)(=O)-H + H^+ \overset{K_4}{\rightleftharpoons} RS-OH + H^+ \quad (11)$$

$$RS-OH + RS(=O)(=O)-H \xrightarrow{k_2} \left[RS(=O)(=O)-H\cdots O-SR\right]$$

$$\xrightarrow[\text{fast}]{} RS(=O)(=O)-SR + H_2O \quad (12)$$

It is assumed that the concentrations of both forms of the sulfenic acid increase until steady-state concentrations are reached, *i.e.*

$$d(RS(=O)(=O)-H)/dt = 0 \text{ and } d(RS-OH)/dt = 0 \quad (13)$$

Also, the rate of disproportionation, designated simply as Rate, can be expressed by

$$\text{Rate} = d[RSO_2SR]/dt = -1/3\, d[RSO_2H]/dt$$

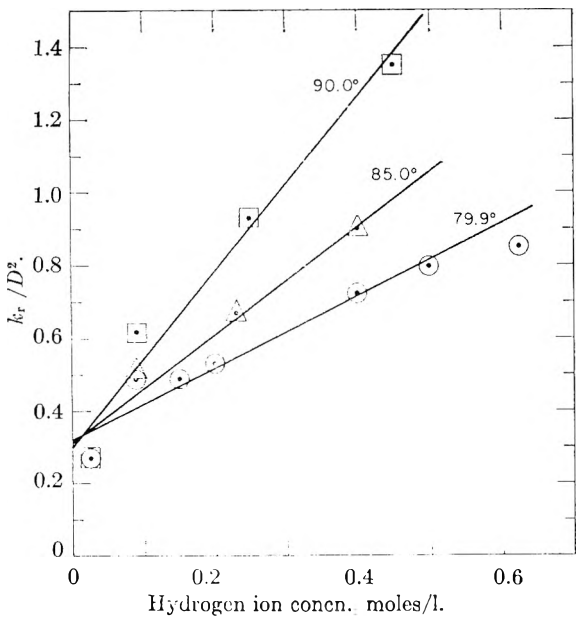

Fig. 6.—Rate constant divided by D^2 *vs.* hydrogen ion concentration.

$$= k_2\,[\mathrm{RS{-}OH}]\left[\mathrm{RS(=O)_2{-}H}\right] \qquad (14)$$

From steady-state considerations, we may also write

$$\mathrm{Rate} = k_1\,[\mathrm{RS{=}O^+}]\left[\mathrm{RS(=O)_2{-}}\right] + k_1'\,[\mathrm{RS{=}O^+}]\left[\mathrm{RS(=O)_2{-}H}\right] \qquad (15)$$

Equation 15 may be converted into

$$\mathrm{Rate} = [\mathrm{RS{=}O^+}]\left[\mathrm{RS(=O)_2{-}}\right](k_1 + k_1'[\mathrm{H^+}]) \qquad (16)$$

Letting $C_1 = k_1$, $C_2 = k_1'/K_1$, and

$C_3 = K_1K_2K_3$, which equals $\dfrac{[\mathrm{RS{=}O^+}]\left[\mathrm{RS(=O)_2{-}}\right]}{\left[\mathrm{RS{-}OH}\right]\left[\mathrm{RS(=O)_2{-}H}\right]}$

we obtain

$$\mathrm{Rate} = C_3(C_1 + C_2[\mathrm{H^+}])\left[\mathrm{RS{-}OH}\right]\left[\mathrm{RS(=O)_2{-}H}\right] \qquad (17)$$

Letting

$C_4 = K_0K_0'$, which equals $\left[\mathrm{RS(=O)_2{-}H}\right]/\left[\mathrm{RS{-}OH}\right]$

$$\mathrm{Rate} = \frac{C_3(C_1 + C_2[\mathrm{H^+}])}{C_4}\left[\mathrm{RS(=O)_2{-}H}\right]^2 \qquad (18)$$

In the experimental determination of unreacted sulfinic acid, the total sulfinic content $[RSO_2H]$ was determined by permanganate titration and must therefore be accounted for. Thus

$$[\mathrm{RSO_2H}] = \left[\mathrm{RS(=O)_2{-}H}\right] + \left[\mathrm{RS(=O)_2{-}OH}\right] + \left[\mathrm{RS(=O)_2^-}\right] + \left[\mathrm{RS(=O)_2{-}O^-}\right] = \left[\mathrm{RS(=O)_2{-}H}\right]\left(1 + \frac{1}{C_4} + \frac{K_1}{[\mathrm{H^+}]} + \frac{K}{C_4[\mathrm{H^+}]}\right) \qquad (19)$$

and hence, the expression for rate becomes

$$\mathrm{Rate} = C_3/C_4(C_1 + C_2[\mathrm{H^+}])\frac{[\mathrm{RSO_2H}]^2}{(1 + 1/C_4 + K_1/[\mathrm{H^+}] + K/C_4[\mathrm{H^+}])^2} \qquad (20)$$

Assuming C_4 has a very low value (see the Introduction), equation 14 becomes, finally

$$\mathrm{Rate} = (A + B[\mathrm{H^+}])\left(\frac{[\mathrm{H^+}]}{[\mathrm{H^+}] + K}\right)^2[\mathrm{RSO_2H}]^2 \qquad (21)$$

where

$A = \mathrm{f}(k_1) = \text{constant}$
$B = \mathrm{f}(k_1') = \text{constant}$

In the absence of iodide, the formation of structure V, equation 5, would be exceedingly slow, thereby hindering the subsequent steps, equations 9–12, resulting in a very slow reaction. With very low iodide concentration, the preceding would also be true initially, but, with time, structure V would increase toward its equilibrium value and maximum steady-state concentrations would be approached. In the presence of a relatively large concentration of iodide, the preceding steps would be expected to occur readily, leading to the rapid attainment of steady-state conditions (no initial curvature, as observed).

Since hydrogen ions influence the reaction rate, they are postulated as contributing to the formation of reactive polar intermediates, equation 7. The resulting oxonium ion could then form sulfinyl ions, equation 8. These ions have been previously postulated as intermediates in the decomposition of aryl thiolsulfonic acids.[18]

Bredereck and co-workers[3] have reported that in the disproportionation of sulfinic acids in non-aqueous media, one of the polar intermediates is a sulfinyl sulfone, which reacts further with sulfinic acid, *i.e.*, $RSOSO_2R + RSO_2H \rightarrow RSSO_2R + RSO_3H$. Their scheme does not involve sulfenic acid. However, Knoevenagel and Polack[19] found that *p*-toluenesulfinyltolylsulfone was unstable in the presence of moisture at room temperature. Because of this, and because sulfenic acid appears to be an intermediate in many other reactions involving sulfinic acids the decomposition of the postulated

(18) F. Kurzer and J. R. Powell, *J. Chem. Soc.*, 3728 (1952).
(19) F. Knoevenagel and L. Polack, *Ber.*, **41**, 3323 (1908).

sulfinyl sulfone to sulfenic acid was favored in the present mechanism.

The mechanism above distinguishes between the possible forms of thiolsulfonate. The anhydride structure was assumed as incapable of existence under the experimental conditions.[20] Also, in acidic media, the form RS-OH would be expected to predominate in equation 11. This would favor the formation of the unsymmetrical thiolsulfonate structure, II.

Application of Equation 21 to the Experimental Data.—In the general equation 21

$$k_r = (A + B[H^+]) \left(\frac{[H^+]}{[H^+] + K}\right)^2 \qquad (22)$$

and a plot of k_r *vs.* hydrogen ion concentration, Fig. 5, at constant reaction temperature and iodide concentration of 5.7 mg./100 ml., affords a linear relationship at *p*H values of 0.2 to 1.0; at values over 1.0, the linear relationship breaks down. In equation 22, at low *p*H values, the term $([H^+]/[H^+] + K)^2$ designated henceforth as D^2, is approximately constant,[21] and therefore, $k_r \approx A + B[H^+]$, and a linear relationship should be obtained as observed. At higher values, the term D^2 would not be constant and hence a curvature should appear as observed.

Approximate values of A and B may be obtained by plotting k_r/D^2 *vs.* H^+ ion concentration and drawing the best line, Fig. 6. In this manner the following were found: at 79.9°, A 0.32, B 1.0: at 85°, A 0.31, B 1.6; at 90°, A 0.30, B 2.5.

Since A and B are functions of the rate constant k_1 and k_1', respectively, they might be expected to vary with temperature. If the Arrhenius equation holds (assuming that the equilibrium constants involved do not change over the range 80–90°) a plot of log A or log B *vs.* reciprocal temperature should be linear. But the values of A given above are the same within experimental error, so it appears that the energy of activation of the step involving k_1, equation 9, is close to zero, as expected for a reaction involving oppositely charged ions. The plot of log B gives an activation energy of 22 kcal./mole for the step involving k_1', equation 10. This value compares favorably with activation energies reported for reactions between ions and neutral molecules in solution.[22]

(20) K. Fries and G. Schurman, *Ber.*, **47**, 1195 (1914).

(21) The ionization constant K of *p*-toluenesulfinic acid was taken as 0.02 (R. R. Coats and D. T. Gibson, *J. Chem. Soc.*, 442 (1940)).

(22) A. A. Frost and R. G. Pearson, "Kinetics and Mechanism," John Wiley and Son, Inc., New York, N. Y., 1953, p. 136.

ABSORPTION SPECTRA OF URANIUM(III) AND URANIUM(IV) IN $DClO_4$ SOLUTION[1]

BY DONALD COHEN AND W. T. CARNALL

Argonne National Laboratory, Argonne, Illinois

Received July 6, 1960

The absorption spectra of U(III) and U(IV) in $DClO_4$ has been observed from 0.2 to 2.6 μ. Solutions of a pure valence state were prepared and maintained by electrolytic reduction in a combination electrolysis-absorption cell. Several new bands have been discovered in the ultraviolet and near infrared regions, and their positions as well as those of the other bands in the spectra are compared with the energy levels calculated from theory.

The theoretical treatment by Jorgensen[2,3] of electron configurations corresponding to U(III) and U(IV) has resulted in the prediction of energy levels for which several of the related absorption bands in solution have not been established experimentally. In the present study the solution absorption spectra of both of these valence states and of U(VI) have been re-examined in an attempt to verify these predictions and also to resolve the differences existing in the literature with respect to the position and intensity of many of the presumably well known absorption peaks. The use of a deuterated solvent, $DClO_4$, has made possible a considerable extention of the region of investigation into the near infared as compared with the limitations imposed by working with normal aqueous solvents.[4]

Solutions of a pure valence state were prepared electrolytically in a specially designed electrolysis-absorption cell. This experimental arrangement permits the alternation of electrolysis and scanning of the absorption bands when studying a species that decomposes rapidly.

Experimental

All spectral measurements were made with a Cary Recording Spectrophotometer Model 14 at room temperature, 23 ± 2°. The wave length range of this instrument lies between 0.186 and 2.6 μ. Because of the instability of U(III) in aqueous solutions, and since electrolytic reduction at a mercury cathode was to be used for the preparation of both U(III) and U(IV), a 1 cm. quartz absorption cell was fabricated to be the center compartment of a three compartment electrolysis cell. The compartments were separated by sintered quartz discs of fine porosity (15–40 μ). Two small diameter quartz inlet tubes were fixed into the bottom of the center compartment; one for admitting nitrogen for stirring, and the other for electrical contact to the mercury cathode pool. A platinum spiral was sealed into one of the end compartments to act as the anode in the electrolysis. The other compartment was designed to connect the electrolysis cell to a reference electrode by means of an acid bridge to enable controlled-potential electrolysis. However, in the present study this feature was not used. A specially designed cell holder, made integral with the cover plate for the cell compartment, was used to position the absorption cell in the analyzing beam of the spectrophotometer.

(1) Based on work performed under the auspices of the U. S. Atomic Energy Commission.

(2) C. K. Jorgensen *Kgl. Danske. Videnskab. Selskab, Mat-fyz. Medd.*, **29** (No. 7) (1955).

(3) Ref. 2, No. 11 (1955).

(4) J. D. S. Goulden, *Spectrochim. Acta*, **14**, 657 (1959).

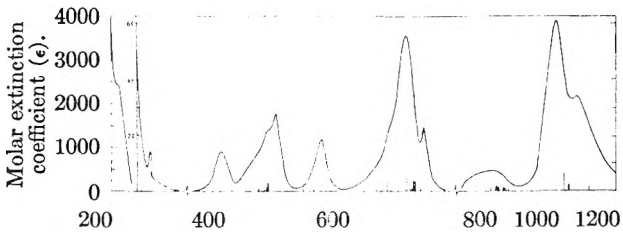

Fig. 1.—Absorption spectrum of U(IV) in 1.0 *M* $DClO_4$ showing in addition the line spectrum of U(IV) obtained by Conway.[9] The line height is proportional to the relative intensity.

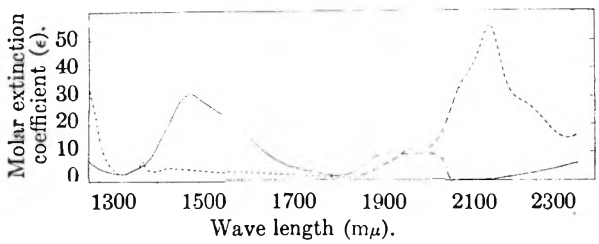

Fig. 2.—Absorption spectrum of U(III) and U(IV) in 1.0 *M* $DClO_4$ in the near infrared region. The line spectrum of U(IV) with line height proportional to relative intensity as reported by Conway[9] is also shown. ——. U(III); ———, U(IV).

The $DClO_4$ was prepared by a technique described previously[5]; solutions were made by diluting stock 12 *M* $DClO_4$ with 99.8% D_2O. The uranium stock solution was prepared by dissolving UO_3 in $DClO_4$ to yield 0.1 *M* U(VI) in 1.0 *M* $DClO_4$. Analysis of the UO_3 revealed that Mg, Si, Ca and Al constituted the main impurities, which taken together constituted less than 30 p.p.m. Possible interfering species, such as lanthanides, were below the limits of detection. This stock solution was standardized by reduction of aliquots to U(IV) on a lead reductor followed by titration with standard ceric solution. Quantitative dilutions of the standard uranium solution were electrolytically reduced and the uranium concentration checked at the end of a number of experiments by titration of the U(IV) with permanganate. Trivalent uranium concentrations were determined by air oxidation to U(IV) in the absorption cell followed by use of the spectrophotometer to establish the U(IV) concentration. Similar procedures with U(VI) in $HClO_4$ were carried out.

The absence of U(IV) peaks in the U(III) spectrum constituted the criterion for a pure U(III) solution. Although difficult, it was possible to obtain the ultraviolet spectrum of U(III) without a peak at 207.5 mμ, whereas the U(IV) maximum at this wave length has a molar extinction coefficient of 2450.

The use of a deuterated solvent made it possible to extend the region of investigation in the near infrared to *ca.* 1.88 μ, as compared to a usual cutoff at *ca.* 1.36 μ in aqueous solutions.[4] Results in the region between *ca.* 1.88 and 2.12 μ in the 1 cm. cell are uncertain because bands characteristic of the uranium ions are superimposed on the absorption due to an intense D_2O band. However, a minimum in the solvent absorption made analysis in the region *ca.* 2.12 to 2 37 μ feasible.

Most of the spectrophotometer runs were made against air as a reference. The spectral region under investigation was first scanned with pure solvent in the absorption cell, then the cell was emptied and refilled with the sample solution to be scanned over the same region. The holder masked the cell on both sides to an aperature 8 mm. wide and 12.7 mm. high. Newton and Brickwedde have pointed out the desirability of this procedure.[6] The results in the region between 1.4 and 2.4 μ were checked by running 1.5 *M* $DClO_4$ in the sample cell *vs.* the same concentration of $DClO_4$ in the reference cell to establish a base line. Then U(VI) in 1.5 *M* $DClO_4$ was added to the $DClO_4$ in the sample cell and again the base line was run. This operation was followed by reduction of the U(VI) to U(IV) or U(III).

Results and Discussion

Earlier work on the absorption spectra of U(III) and U(IV) has been summarized by Jorgensen.[2,3] Much of this work was carried out in solvents in which the uranium ions were appreciably complexed; however, it has been shown that even under these conditions the spectra may not be significantly modified in comparison to that obtained under conditions of little or no complex formation.[7,8] This is consistent with the theory that the transitions involved are between different levels within the 5f-orbital, and since this orbital lies deep, the influence of the external ligand field is minimized.

Recently Conway[9] has investigated the spectrum of U(IV) from 0.2 to 8 μ using crystals of UF_4 in a matrix of CaF_2. He has assigned term values and has estimated the intensity for each observed absorption line. In addition, the experimental data have been fitted to a system of energy levels calculated for intermediate coupling including spin-orbit and electrostatic energies but ignoring departures from spherical symmetry. In this way, parameters for these energies were evaluated, and thus the set of equations could be solved giving the frequencies of all possible transitions in the absence of significant ligand field effects. This constitutes a considerable refinement and extension of the calculations made by Jorgensen,[2] however, the method used was similar. Qualitatively, the work of Conway and Jorgensen for U(IV) gives rise to similar predictions with respect to the existence of two absorption band systems in the near infrared, indicated in crystals, but not previously proven to exist in solution. The U(III) band which Jorgensen[3] predicts should exist near 2.4 μ also lacked experimental confirmation in solution.

U(VI) System ($5f^0$).—It was found that U(VI) concentrations up to 0.05 *M* gave an exact reproduction of the reference line established by running pure $DClO_4$ *vs.* $DClO_4$ in the 1.4–2.4 μ region. The absorption spectrum of U(VI) in the visible and ultraviolet range to 200 mμ has been published previously.[10] Since U(VI) has no 5f electrons, the forbidden transitions characteristic of U(IV) and U(III) are not observed.

U(IV) System ($5f^2$).—Figures 1 and 2 show the absorption spectrum of U(IV) as determined in the present study. That portion of the spectrum between 1.88 and 2.12 μ as shown in Fig. 2, is uncertain because of intense D_2O bands which render the solution essentially black to radiation in this wave length range. The present experimental results are in good agreement with those of Jorgensen[2] for U(IV) solutions in the range 0.24–1.15 μ. The lines observed by Conway[9] for UF_4 in CaF_2 are included in Figs. 1 and 2; line height is proportional

(5) J. C. Sullivan, D. Cohen and J. C. Hindman, *J. Am. Chem. Soc.*, **79**, 3672 (1957).

(6) T. W. Newton and L. H. Brickwedde, quoted in S. E. Stephanou, J. P. Nigon and R. A. Penneman, *J. Chem. Phys.*, **21**, 42 (1953).

(7) J. J. Katz and G. T. Seaborg, "The Chemistry of the Actinide Elements," John Wiley and Sons, Inc., New York, N. Y., 1957, p. 184.

(8) C. K. Jorgensen, *Acta Chem. Scand.*, **10** (No. 9), 1503 (1956).

(9) J. G. Conway, *J. Chem. Phys.*, **31**, 1002 (1959).

(10) R. E. Connick, M. Kasha, W. H. McVey and G. E. Sheline, "The Transuranium Elements, Research Papers, National Nuclear Energy Series, Division IV," Vol. 14B, McGraw-Hill Book Co., New York, N. Y., 1949, p. 590.

to relative intensity. Table I presents the position and intensity of the band systems which we have observed for U(IV) in solution as compared to the energy levels calculated by Conway.

TABLE I

COMPARISON OF OBSERVED AND CALCULATED LEVELS IN U(IV)

Obsd. in[a] soln. ($cm.^{-1}$)	Molar extinction coeff. (ϵ) in soln.	Calcd.[9] ($cm.^{-1}$)	Term assignment[3]
		39482	$^1S_0$
40750	13.8	23330	$^3P_2$
23290	14.8	19480	$^1I_6$
20580	21.4	18503	$^3P_1$
20190	26.6	15672	$^3P_0$
18200	18.8	15664	$^1G_4$
15420	56.1	15413	$^1D_2$
14890	23.5	10922	$^3H_6$
11360	7.2	8619	$^3F_4$
9346	60.9	8574	$^3F_3$
8830	33.2	5875	$^3H_5$
6734	30.6	4031	$^3F_2$

[a] Allowed transitions found in the ultraviolet region in solution are not included in this table.

The band at 207.5 mμ has not been reported previously in the literature. Its intensity and position suggest that it must result from a LaPorte-allowed transition, presumably $5f^2$–5f6d. Similar bands in Ce(III) having $\epsilon = \sim 500$ are attributed to the 4f-5d or 4f-6s transition.[2] Thus the 207.5 mμ band is in a different class than the other bands observed at higher wave lengths which are the result of (LaPorte-forbidden) transitions within the 5f-orbital. The molar extinction coefficient for the band at 245.4 mμ was established in the present study whereas previous workers[2] had set a limiting value. Results in solution in the near infrared indicate that U(IV) begins to absorb in the 2.2–2.4 μ region. This is consistent with the existence of a broad absorption line with center at 2.42 μ found by Conway[9] in work with crystals.

Two previous studies have been cited,[2,3] as indicating the existence of a band near 1.5 μ. Dreisch and Kallscheuer[11] reported a band system near 1.53 μ in aqueous halide and sulfate solutions. However their results in the infrared and visible regions, in terms of number and position of bands as well as intensity, are in such obvious disagreement with similar studies,[12,13] that it is clear that species other than U(IV) must have been responsible for many of the bands they observed. In addition, since they were working in aqueous solutions, the band they reported near 1.53 μ must have been superimposed on an intense water band in the same region, and difficult to distinguish therefrom. In the present study we place the maximum of a U(IV) band in this region at 1.489 μ. The band observed by Rohmer, *et al.*,[14] in halide solutions at 1.43 μ was attributed by the authors as a water band. Thus

(11) T. Dreisch and O. Kallscheuer, *Z. physik. Chem.*, **B45**, 19 (1939).

(12) M. Fred and C. J. Rodden, "Analytical Chemistry of the Manhattan Project, National Nuclear Energy Series," Vol. 8, Part 1, McGraw-Hill Book Co., New York, N. Y., 1949, p. 543.

(13) J. C. Hindman, K. A. Kraus, J. J. Howland, Jr., and B. B. Cunningham, "The Transuranium Elements," ref. 12, p. 121.

(14) R. Rohmer, R. Freymann, R. Freymann, A. Chevet and P. Hamon, *Bull. soc. chim. France*, 603 (1952).

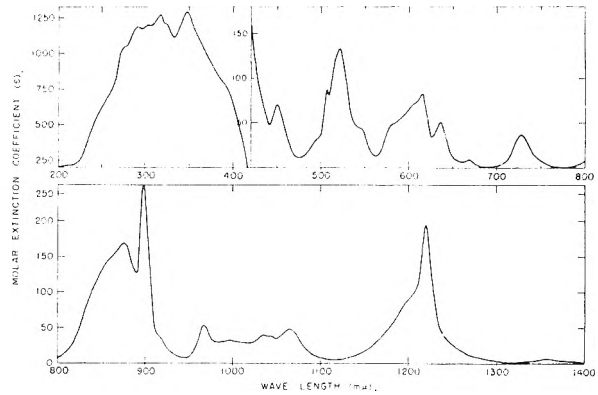

Fig. 3.—Absorption spectrum of U(III) in 1.0 *M* $DClO_4$.

the present study is the first to demonstrate clearly the existence of a U(IV) band in solution in this region.

U(III) System ($5f^3$).—Aqueous solutions of U(III) are quite unstable; U(III) reduces H_2O with the formation of U(IV) and H_2[15] ($U^{+3} \rightarrow U^{+4} + e^-$; $E^\circ = 0.61$ volt). Previous attempts to examine the solution absorption spectrum of U(III) have had to contend with the presence of significant amounts of U(IV) from which the pure U(III) spectrum was obtained by correction. The results of the present study are shown in Figs. 2 and 3. Table II compares the position of the bands observed in solution with the energy levels calculated by Jorgensen.[3] Since it was possible to alternate reduction and scanning, the solution analyzed was maintained as essentially pure U(III). Rapid analysis was particularly important in viewing the ultraviolet portion of the spectrum. The intense maxima near 320 and 350 mμ noticeably deteriorated in less than a minute. It was difficult to contend with the very rapid growth of the intense U(IV) band at 207.5 mμ; however, repeated scanning alternated with reduction with rapid stirring reduced the initial absorption in this region essentially to background.

It was found that U(III) slowly reduces ClO_4^- in agreement with the results of Lawrence.[16] The ClO_4^- was not reduced by the 3–4 v. potential used to produce U(III). Careful checking of blanks and samples revealed that no error was introduced in the ultraviolet observations due to this effect.

Selected earlier work on the solution absorption spectra of U(III) has been summarized by Jorgensen.[3] The results of the present investigation are consistent with those of Stewart[17] and Howland (as recorded in ref. 12), both of the latter obtained by reducing U(VI) to a mixture of U(III) and U(IV) by the use of zinc amalgam. However, as might be predicted, the present results are almost uniform in indicating greater molar extinction coefficients than the older studies. The extention of the area of investigation into the near infrared, made possible by the use of $DClO_4$ as a solvent, has revealed the existence of a much more intense band at 1.219 μ than had previously been reported,[17] and a new weak band at 1.356μ, and a new band at 2.187 μ.

(15) B. J. Fontana, MDDC-1453.

(16) R. W. Lawrence, *J. Am. Chem. Soc.*, **56**, 776 (1934).

(17) D. C. Stewart, ANL-4812 (Feb. 1952).

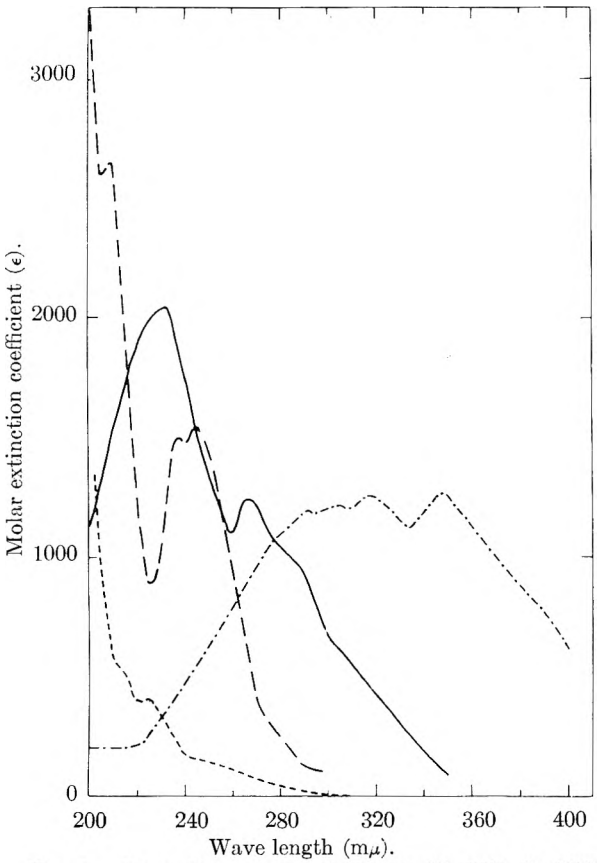

Fig. 4.—Absorption spectra of U(III), Np(III), Pu(III) and Am(III) in 1.0 *M* $HClO_4$ in the ultraviolet: -.-., U(III); ———, Np(III); — — —, Pu(III); – – – – –, Am(III).

Assuming approximate intermediate coupling of the various levels, Jorgensen[3] predicts a band near 2.44 μ and one at 1.28 μ, in addition to the numerous bands at lower wave lengths. He ascribes the visible and near infrared bands to LaPorte-forbidden transitions. The intense bands in the ultraviolet lying between 250 and 400 mμ undoubtedly correspond to the LaPorte-allowed $5f^3$–$5f^26d$ transitions. The agreement between the observed band at 1.219 μ and the one predicted in this region is reasonable; the newly discovered band at 1.356 μ may be part of this same system. The band at 2.187 μ, which is in good agreement with absorption lines at 2.2 μ found in crystals such as UF_3 in CaF_2,[18] apparently does not correspond to any of the levels predicted by Jorgensen. The band predicted to exist near 2.44 μ does find experimental confirmation in the absorption lines found in crystals of UCl_3 in $LaCl_3$,[18] but this region is beyond the limits of the present investigation in solution.

(18) J. G. Conway, private communication, April 1960.

TABLE II

COMPARISON OF OBSERVED AND CALCULATED LEVELS IN U(III)

Obsd. in[a] soln. (cm.$^{-1}$)	Molar extinction coeff. (ϵ) in soln.	Calcd.[3] (cm.$^{-1}$)	Term[3] assignment
22180	71.0	26500	$^2G_{7/2}$
19740	88.0	26300	$^4G_{11/2}$
19170	131	25100	$^2K_{13/2}$
18280	42.9	23200	$^4G_{9/2}$
16270	84.3	22200	$^2H_{11/2}$
15720	51.9	20900	$^4G_{7/2}$
14990	9.5	19700	$^2H_{9/2}$
13760	37.8	18800	$^4G_{5/2}$
11420	166	18100	$^4F_{9/2}$
11140	254	17300	$^4F_{7/2}$
10340	53.2	16600	$^4S_{3/2}$
10040	31.0	15000	$^4F_{5/2}$
9662	38.6	12600	$^4F_{3/2}$
9634	37.9	11700	$^4I_{15/2}$
9398	49.6	7800	$^4I_{13/2}$
8201	195	4100	$^4I_{11/2}$
7375	6.0		
4570	55.4		

[a] Allowed transitions found in the ultraviolet region in solution are not included in this table.

Comparison of position and intensity among the band systems in actinide elements of the same valence state[17] as well as in isoelectronic series has indicated some interesting patterns of behavior. Trivalent uranium, neptunium and plutonium all exhibit intense absorptions in the ultraviolet range ($\geq$ 200 mμ) which are attributed to LaPorte allowed transitions. As shown in Fig. 4, the position of these bands progressively shifts toward the ultraviolet with increasing Z, but the intensity, at least of the first member of the individual band systems, remains roughly constant. Intensities given in much of the earlier work on the ultraviolet region of Np and Pu are considerably less than those established in the present study.

The corresponding allowed bands for Am(III) apparently exist below 200 mμ. This progression clearly reflects an increasing difference in energy between 5f and 6d electrons.

Halpern and Harkness[19] have pointed out that differences in solvent characteristics of H_2O and D_2O can give rise to small shifts in absorption maxima. Substitution of H_2O for D_2O displaced visible bands toward higher energies for several transition elements, and similar results have been obtained for Pr(III) and Nd(III). In the present study, the visible spectra of U(III) and U(IV) were measured both in $HClO_4$ and $DClO_4$; however, no discernible changes were observed either in intensity or position of the peaks.

(19) J. Halpern and A. C. Harkness, *J. Chem. Phys.*, **31**, 1147 (1959).

A NEW TWIN HIGH-TEMPERATURE REACTION CALORIMETER. THE HEATS OF MIXING IN LIQUID SODIUM–POTASSIUM NITRATES

BY O. J. KLEPPA

Institute for the Study of Metals, University of Chicago, Chicago 37, Illinois

Received July 5, 1960

A new sensitive reaction calorimeter for work at temperatures up to 500° has been developed. The calorimeter readily permits detection of heat effects of 0.01 cal., and is suitable for precise measurements of 2 cal. and more. In its first application this apparatus has been used to determine the enthalpy of mixing in liquid sodium nitrate–potassium nitrate mixtures. From the results the following relation was derived between the molar integral enthalpy of mixing (ΔH^M) and the mole fraction of sodium nitrate (X). $\Delta H^M = -X(1 - X)\,[408.5 + 68X]$. Within the experimental error of about one per cent. this enthalpy is independent of temperature between 346 and 450°.

Introduction

A few years ago this author reported the development of a high temperature reaction calorimeter suitable for the study of heats of mixing and heats of solution in metallic liquids.[1] This apparatus has been used quite extensively for thermochemical investigation of liquid and solid alloys,[2] and has proved particularly useful for the measurement of endothermic heats of reaction generated during fairly short time intervals. In such cases the electrical calibration procedure adopted for this apparatus was at its best, since the energy released in the calibration experiment tended to compensate for most of the experimental (unknown) heat of reaction. The accuracy achieved in such experiments was of the order of ±1%. It was noted, however, that this calorimeter was less accurate for exothermic reactions, and also for endothermic and exothermic processes where the heat was generated over periods longer than a few minutes. An example of such a slow process is the mixing of two liquids with an over-all composition close to or inside a liquid miscibility gap.

Another important limitation of the earlier apparatus was its relative lack of sensitivity: in practice the smallest heat effect that could profitably be studied was of the order of 50 cal., since the random error usually was of the order of ±0.5 to 1 cal.

In view of these and other considerations it was decided to develop an improved calorimeter, designed to overcome most of the mentioned limitations. At the same time an attempt has been made to retain and improve the ease of operation which characterized the earlier apparatus. The new calorimeter is described in the present communication, which gives also a report on its first application for the measurement of heats of mixing in sodium nitrate–potassium nitrate melts. Results obtained in other applications will be presented in future communications.

Principle of Twin Calorimeter.—The new apparatus represents an adaptation for work at moderately elevated temperatures of the twin "micro" calorimeter developed by Calvét and his school.[3] The apparatus consists of two nearly identical differential calorimetric units located in two cylindrical wells in a heavy aluminum jacket. In each of these twin units a temperature difference between the calorimeter proper and the surrounding jacket gives rise to an e.m.f. in a suitably constructed 96 couple thermopile. The two thermopiles are connected in series, bucked against each other. In this manner it is assured that small drifts in the temperature of the aluminum jacket will affect the e.m.f.'s of the two thermopiles in essentially the same way, but in the opposite sense. Hence such drifts will give rise to no significant net change in the over-all output of the thermocouple system. Only one of the two calorimeters is involved in each experiment, the other one serving as a "dummy."

In the earlier apparatus the mass and heat capacity of the calorimeter proper was moderately large (~250 cal./deg.). As a result the calorimetric sensitivity was not very high, while on the other hand the rate of heat transfer between the calorimeter and the surrounding jacket was relatively low. Therefore it was convenient to operate this apparatus as a temperature rise instrument, in complete analogy with conventional room temperature calorimeters. In the new apparatus, on the other hand, the mass (and heat capacity) of the calorimeter proper has been reduced as far as possible, consistent with the requirements of design and mechanical strength. The calorimeter accordingly has a very considerable sensitivity, and a small time constant. (Half-life 5–8 minutes, the actual value depending on temperature and on the heat capacity of the substances contained in it.) These features make it convenient to operate this calorimeter as a heat flux apparatus, and to apply modern automatic equipment for recording the e.m.f. of the thermocouple system. In the present study the e.m.f. was recorded by a Brown 500 μv. recorder.

As long as no heat is generated in the calorimeters the e.m.f. is essentially zero ("apparatus zero"), with no drift. However, as soon as heat is released or absorbed in one of the calorimeters, a net e.m.f. will be observed. If the heat effect is of short duration, this e.m.f. will first rise quite fast and will then decay exponentially to a near zero value in a period of the order of 1 hour (or less). For heat effects of longer duration, this period will be correspondingly longer. The construction of the present calorimeter should permit it to be used also for reaction rate studies and for quantitative thermal analysis. However, so far such applications have not been attempted.

(1) O. J. Kleppa, THIS JOURNAL, **59**, 175 (1955).

(2) See, *e.g.*, O. J. Kleppa, *ibid.*, **60**, 842 (1956).

(3) E. Calvét and H. Prat, "Microcalorimetrie," Masson et Cie, Paris, 1956.

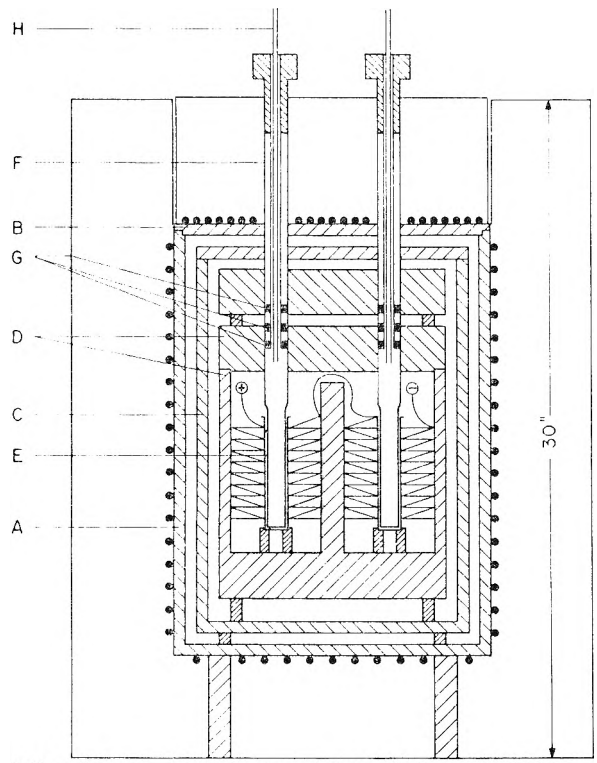

Fig. 1.—General lay-out of twin calorimeter assembly.

Since the e.m.f. generated in the thermocouple system is directly proportional to the temperature difference between the calorimeter and the surrounding jacket, it is also proportional—according to Newton's law—to the rate of heat transfer. The total area between the e.m.f.–time curve and the apparatus zero line accordingly will be proportional to the total heat effect associated with the process in the calorimeter.

The calorimeter can be calibrated either electrically or by a "drop" method, *i.e.*, an inert substance of known heat content can be dropped into the calorimeter, and the corresponding area determined.

Design of Apparatus.—The important features of the present calorimeter can best be understood by consulting Figs. 1 and 2, which give semi-schematic diagrams of the equipment. Figure 1 gives the general lay-out, while Fig. 2 shows one of the twin units in somewhat greater detail.

(a) **The Furnace.**—This is wound by means of heavy Nichrome wire on a cylindrical stainless steel core approximately 12" diameter and 20" long. The furnace has separate heating coils at the two end plates. This permits us to adjust the distribution of the load, so that temperature gradients inside the furnace can be minimized. Furnace control is by means of a chromel–alumel thermocouple, the hot junction of which is located near the heating coil. The cold junction is maintained in an ice-bath, and the e.m.f. is fed to a conventional Leeds and Northrup Micromax controller which in turn activates an auxiliary heating coil (not shown in the figure). Although it is possible to control the temperature of the top end plate separately, it was found that completely satisfactory operation could be achieved by the simpler expedient of stabilizing the power input to this heater by means of a Sola constant voltage transformer.

(b) **Heavy Shielding Assembly.**—The principal part of this shield is made from 1/2" wall steel tubing, mounted on a stainless steel base. This whole assembly is thermally insulated by means of asbestos paper, on the outside from the furnace core, on the inside from the central aluminum jacket. The shielding assembly has a dual function: (1) It serves to reduce possible longitudinal temperature gradients inside the furnace; (2) It represents a sizeable heat sink between the heating coil and the central aluminum jacket, thus contributing toward the maintenance of a constant temperature in the calorimeter assembly.[1]

(c) **Aluminum Jacket.**—This is machined from a forged section of 2S aluminum, and is about 10" in outside diameter and 12" high. Inside this block are the two cylindrical wells, each of about 4" diameter and 8" depth. The block has a removable double lid, and is mounted on a stainless steel base. In the wells are located the two twin calorimetric units.

(d) **The Calorimetric Units.**—Each of these units consists of three main parts, namely a central section which includes the calorimeter proper, a thermocouple system and an external ring assembly. The unit is built up from a stack of eight essentially identical elements, each of which contains a calorimeter component, a thermocouple component and a ring component.

The calorimeter component consists of a central lavite ring of about 1" o.d., 0.8" i.d. and 5/8" length. This ring provides support for twelve internal thermocouple junctions. Each of these junctions is enlarged by means of a rectangular piece of silver foil, of approximate dimensions 0.4" × 0.15" × 0.004".

The external junctions of the thermopile are enclosed in small sections of ceramic tubing, which in turn are lodged in suitable wells in the external ring. These rings are machined from 2S aluminum, and fit snugly inside the main aluminum jacket. Each of the eight calorimetric elements is assembled and centered by means of two circular mica spacers, and is held together by three small stainless steel bolts.

The stack of eight elements produces a central cylindrical well, about 5" long and of about 0.800" diameter. Along the inside wall of this well are found the 96 internal thermocouple junctions, distributed in a checkerboard pattern. The junctions are located by means of individual slots, and are held firmly in place by a central silver tube of 0.780" outside diameter and 0.008" wall. Electrical insulation between the thermocouple junctions and the silver tube is achieved by a double layer of mica, each layer about 0.001" thick.

Inside the silver tube there is a 60 ohm cylindrical calibration heater. The heating coil consists of nichrome ribbon (0.003" × 1/32") wound on a 0.750" o.d., 0.006" wall stainless steel core. External and internal insulation of this heater is by double layers of 0.001" mica. The windings of the heater are held in place by a thin wash of Alundum cement.

The Heats of Mixing in $NaNO_3$–KNO_3.—The parts described above may be considered to be permanent parts of the calorimeter. During actual operations other parts may be added, the nature of which will be determined by the experimental problem studied.

In the work on fused nitrates reported in the present communication a thin-walled (0.006"), closed-end, stainless steel protection tube of slightly less than 0.750" o.d. was inserted into the calorimeter cavity. This tube, which is about 24" long, provides a continuous gas-tight channel from the calorimeter proper to the external atmosphere. Its principal function is to protect the permanent parts of the calorimeter against possible contamination and damage. It can be removed for cleaning or inspection, without any further dis-assembly of the apparatus.

During the mixing experiments reported here one of the two fused salts was contained in a Pyrex test-tube of about 18 mm. outside diameter, and 5.5" length. This tube, which fits snugly inside the protection tube, is suspended, by means of two 0.010 × 1/16" nichrome ribbons, from the lowest of three heavy aluminum radiation shields. These shields are mounted on a central 1/4" diameter stainless steel supporting tube (see Fig. 1).

The second salt was contained in a Pyrex ampoule of 10 mm. diameter and about 6.5" length. This ampoule had a fine breakoff tip, and was connected to a thin walled stainless steel manipulation tube of 3/16" outside diameter. This tube fits snugly in the bore of the above-mentioned supporting tube.

The twin sample assemblies were preheated in the upper part of the protection tubes, and then inserted into the calorimeters proper. Unless quite elaborate precautions are

taken to make sure that the samples are preheated to exactly the same temperature as the calorimeters, this operation is bound to disturb the existing thermal steady state in the calorimetric system. Therefore a waiting period of about one hour usually was required before a mixing experiment could be performed.

In the present work the chemical reaction between the two salts was initiated by moving the manipulation tube down so that the ampoule tip was crushed against the bottom of the test-tube. When the ampoule was then raised for a few seconds compared to the liquid level in the test-tube, the inside melt flowed out through the ampoule orifice, and mixed with the outside melt. The draining procedure was repeated at least three times within a period of about one minute in order to achieve complete drainage from the ampoule and mixing of the two fused salts.

The breaking of the ampoule tip and the subsequent manipulation procedure generated a small but readily measureably heat effect. This was determined in separate experiments and was found to total 0.05 ± 0.03 cal. A correction of 0.05 cal. has been applied to all experimental data reported below. The uncertainty in this figure is one of the principal sources of error in the present experiments.

The salts used in the present work were Mallinckrodt A.R., and were used without further purification. Prior to the experiments the salts were dried in air at 130°.

Most experiments reported here were performed at 448 ± 2°, with a few runs also at 346 ± 0.5°. Due to somewhat unsatisfactory controller performance, (an instrument without automatic balancing was used) the temperature varied slightly from one day and one week to another. However, this seemed to have no influence on the operation of the calorimeter, indicating that the twin system functioned in a satisfactory way.

The temperature of the calorimeter was measured by means of an iron–constantan thermocouple prior to or at the conclusion of every run. The iron–constantan couple was checked every two weeks against a Bureau of Standards calibrated Pt–10%PtRh couple, and showed no significant drift.

In all measurements reported below calorimetric calibration was by the drop method: small weighed and annealed pieces of 2 mm. diameter fine gold wire (~ 99.98% Au, from Goldsmith Bros.) were dropped into the calorimeter from room temperature, and the e.m.f.–time curve was recorded. Prior to the drop the gold specimen was maintained for a period of at least 15 minutes in a well in a cylindrical copper block, the temperature of which was determined by means of a calibrated room temperature thermometer. The heat content of the gold at the calorimeter temperature T°K. was calculated from the equation recommended by Kelley[4] for 197.2 g. of Au

$$H_T - H_{298.16} = 5.66T + 0.62 \times 10^{-3}T^2 - 1743 \text{ cal.}$$

According to Kelley this equation should be correct to 0.5%.

At the very beginning of the present series of measurements a comparison was made at 450° between drop calibrations and calibrations carried out by the electrical method. The two methods agreed to within 1%.

The enthalpies of mixing in sodium–potassium nitrate melts are negative. Therefore the highest experimental precision can be achieved if the major part of the exothermic heat of mixing is compensated by an endothermic effect of known and roughly equal magnitude. This "balanced heat effect principle" is well established in micro calorimetry,[3] but was first used in high temperature reaction calorimetry by Orr, Goldberg and Hultgren.[5] A procedure based on this principle was adopted throughout the present work. In all cases the compensating endothermic effect was produced by dropping into the calorimeter from room temperature pieces of gold wire of suitable weight, soon after the start of each mixing experiment. Special precautions were taken to reduce the initial splash in the liquid. In other respects compensation drops were carried out in the same manner as calibration drops.

Results

A total of 22 mixing experiments were per-

(4) K. K. Kelley, "Contributions to the Data on Theoretical Metallurgy," Bureau of Mines Bull. #476 (1949).

(5) R. L. Orr, A. Goldberg and R. Hultgren, *Rev. Sci. Instr.*, **28**, 767 (1957).

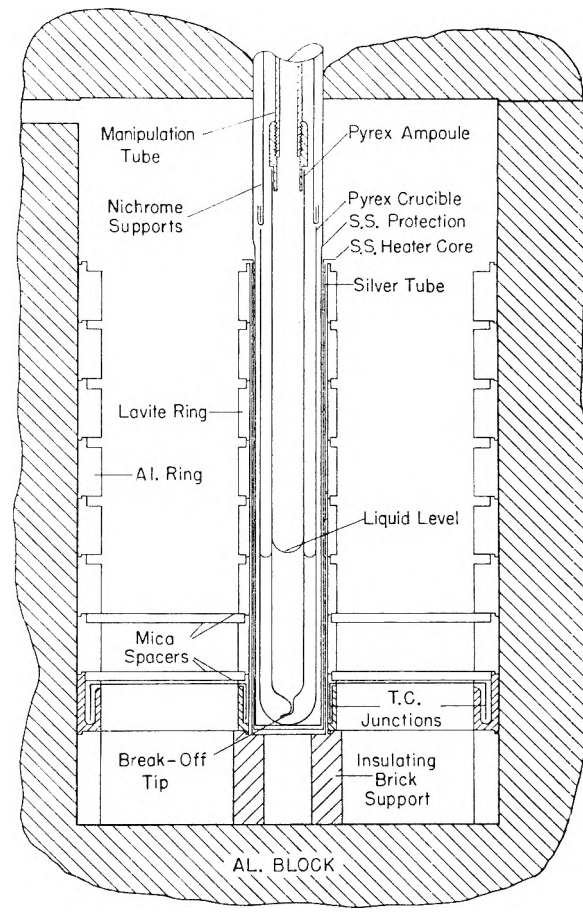

Fig. 2.—Detail of one calorimeter, and of arrangement used for heat of mixing measurements in fused nitrates.

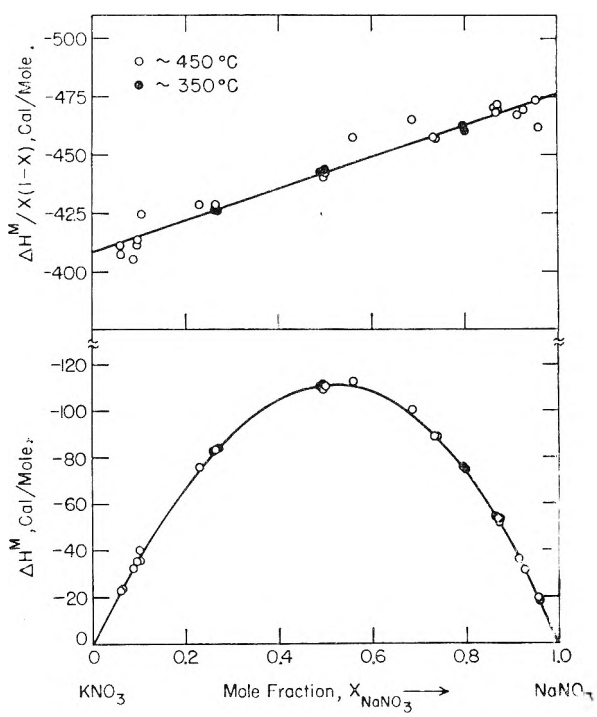

Fig. 3.—Molar integral heats of mixing (ΔH^M) in liquid sodium nitrate-potassium nitrate mixtures.

formed at 448°, with six additional runs at 346°. The range of composition covered was from about 6 to 96 mole % $NaNO_3$.

The net heat effects were measured by graphical integration of the e.m.f. *vs.* time curves in the manner outlined above. In all cases these integrations were carried out in two different ways: first by the use of a conventional polar planimeter, and then by the weighing method. In 25 out of 28 cases the results derived by these two methods agreed within 0.5% or better. The molar integral heats of mixing are recorded in Table I. This table gives also the weighed-in composition of the liquid mixture, and the total number of moles used in each experiment. The product of the number of moles and the molar integral heat of mixing is the actual heat effect associated with the mixing experiment. In the runs reported here this was between 5 and 13 cal. In most cases more than 90% of this effect was compensated by a drop of gold from room temperature into the calorimeter.

TABLE I

MOLAR INTEGRAL HEATS OF MIXING IN LIQUID $NaNO_3$–KNO_3

Compn. X_{NaNO_3}	Total moles	$-\Delta H^M$, cal./mole	Compn. X_{NaNO_3}	Total moles	$-\Delta H^M$, cal./mole
	448 ± 2°				
0.9573	0.2529	18.9	0.2643	0.1568	83.3
.9562	.2422	19.8	.2286	.1465	75.6
.9269	.2038	31.8	.1030	.2394	40.1
.9139	.1781	36.8	.0959	.2267	35.9
.8719	.2075	52.4	.0955	.2123	35.5
.8701	.2103	53.3	.0883	.2050	32.7
.8685	.2099	53.6	.06098	.2105	23.4
.8677	.2062	53.8	.05898	.2116	22.8
.7364	.1333	89.0		346 ± 0.5°	
.7344	.1321	88.9	0.7979	0.1491	74.2
.6864	.0991	100.1	.7948	.1502	75.5
.5602	.0980	112.7	.4965	.0982	110.9
.4989	.1005	110.2	.4878	.0999	110.6
.4969	.0996	110.1	.2698	.1350	83.9
			.2643	.1337	82.9

The experimental results are presented graphically in Fig. 3. In this figure are given the molar integral enthalpies of mixing, ΔH^M, as well as a plot of $\Delta H^M/X(1 - X)$ where X and $(1 - X)$ are the mole fractions of the two components. This quantity is of considerable interest in more detailed discussions of the significance of the heat of mixing data.

Unlike ΔH^M, $\Delta H^M/X(1 - X)$ is a slowly varying function of X. The intercepts of this function at $X = 1$ and $X = 0$ represent the limiting heats of solution, *i.e.*, the relative partial molal heat contents at high dilution. It will be seen that the solution of potassium nitrate into a large amount of sodium nitrate is somewhat more exothermic than the opposite process. Note also that our measurements indicate that the heat of mixing in this system is essentially independent of temperature in the considered temperature range.

From Fig. 3 we see that $\Delta H^M/X(1 - X)$ depends linearly or very nearly linearly on composition. If a linear dependence is assumed, the following expression is derived by the least squares method

$$\Delta H^M/X(1 - X) = - 408._5 - 68X_{Na} \text{ cal./mole}$$

Here X_{Na} is the mole fraction of sodium nitrate in the melt. The standard deviation of the 28 experimental points from this expression is 4.7 cal., or about 1.1%.[6]

From this expression we readily obtain the following expressions for the relative partial molal heat contents of the two components

$$\Delta\bar{H}_{KNO_3} = - X_K^2\,[544._5 - 136X_K] \text{ cal./mole}$$
$$\Delta\bar{H}_{NaNO_3} = - X_{Na}^2[340._5 + 136X_{Na}] \text{ cal./mole}$$

To the knowledge of this author there are no data available in the literature which permit a comparison of these results with earlier values. The significance of the new data will be discussed in a future communication,[7] which will report also corresponding heat of mixing information for other binary alkali nitrate systems.

Acknowledgments.—This calorimeter could not have been built without the expert craftsmanship of Mr. Paul Dolmer of the Physical Sciences Development Shop of the University of Chicago. Mr. L. Hersh carried out most of the graphical integrations and numerical evaluations. This work has been supported by the Office of Naval Research at the University of Chicago.

(6) It is possible that a slightly better fit might be obtained by introducing a parabolic term in this expression.

(7) *J. Chem. Phys.*, in press.

AN INFRARED STUDY OF SUBSTITUTION IN THE BENZENE RING

BY A. CABANA, J. L. PATENAUDE, C. SANDORFY AND P. M. G. BAVIN*

Département de Chimie, Université de Montréal, Canada, and Department of Chemistry, The University of Hull, England

Received July 8, 1960

Limited but representative series of phenol and benzonitrile derivatives (*ortho*, *meta* and *para*) were assembled and the OH and C≡N band frequencies and intensities were determined. The method of "segments" was used to evaluate the latter. Substituents are shown to divide themselves into three classes on the basis of their effect on the electronic distribution of the unperturbed ground state of the molecules, and these classes are the same as those obtained on the basis of chemical reactivity. There is, however, no complete analogy between the phenol and the benzonitrile derivatives. The observed frequencies and intensities are related to electronic distribution, and it is shown that the existence of the three groups is entirely compatible with a smooth variation of the electronic charges sent by the substituent into (*ortho*), *meta* and *para* in the series NH_2, OH, F, Cl, Br, I, CHO, C≡N, NO_2.

Introduction

The problem of benzene substitution constitutes one of the oldest problems of quantum chemistry and molecular spectroscopy. It would be very difficult to summarize all the previous literature and being fair to everybody would probably require a review paper. Most of the credit should be given to early works by Wolf and Herold,[1] Wolf and Strasser[2] and Conrad-Billroth,[3] who observed the well known fundamental regularities in the ultraviolet spectra, and to Sklar,[4] who made the first full-scale attempt to explain them.

From the chemical side, Hammett's[5] work and the introduction of his σ-factor provided a solid basis for comparative studies of spectra and chemical reactivity (see also ref. 6).

Infrared and Raman spectra of benzene derivatives have been studied by many authors (ref. 7 to 36). From the point of view of the present work, the most significant results were the relationships between infrared band frequencies and intensities of the substituent groups, and chemical reactivity as represented by Hammett's σ-factor. (See especially ref. 14 to 20.)

In the spite of the great amount of work previously done by others we decided to take up the problem again for the following reasons: (1) It was hoped that by choosing a limited but otherwise complete series of compounds (monosubstituted, *ortho*, *meta* and *para*-disubstituted) a more solid basis for future discussions could be given. Therefore, a great effort was made to secure all the necessary compounds. This was successful with the phenol derivatives but less so with the benzonitrile derivatives. (2) Two of us recently published an improved method for computing infrared intensities,[37] which is a modification of Ramsay's direct integration method.[38] It consists of dividing the band area into segments and integrating for every segment with a width parameter taken from the segment itself, applying corrections in Ramsay's manner. This method has now been applied to the case of the benzene derivatives.

Two biatomic groups, OH and C≡N, were chosen as first substituents and were combined with, as a second substituent, OH, NH_2, F, Cl, Br, I, C≡N, NO_2 and CHO. Only the stretching vibrations of the OH and C≡N groups were used. Triatomic groups were avoided because these possess two stretching vibrations and their angular dependence would make comparisons uncertain.

Experimental

The measurements were made with a Perkin–Elmer model 112 single beam, double pass spectrometer using a lithium fluoride prism.

The whole instrument was put into an atmosphere of dry nitrogen. Solutions of less than 0.001 M in CCl_4 were used for the phenol derivatives and less than 0.004 M in tetrachloroethylene for the benzonitrile derivatives. A 3 cm. cell was used. The computed spectral slit widths were less than 3 $cm.^{-1}$ in the OH region and less than 2 $cm.^{-1}$ in the C≡N region.

* I.C.I. Fellow.

(1) K. L. Wolf and W. Herold, *Z. physik. Chem.*, **B13**, 201 (1931).
(2) K. L. Wolf and O. Strasser, *ibid.*, **B21**, 389 (1933).
(3) H. Conrad-Billroth, *ibid.*, **B29**, 170 (1936).
(4) A. L. Sklar, *J. Chem. Phys.*, **10**, 135 (1942).
(5) L. P. Hammett, "Physical Organic Chemistry," McGraw–Hill Book Co., New York, N. Y., 1940, p. 184.
(6) H. H. Jaffe, *Chem. Revs.*, **53**, 191 (1953).
(7) J. Lecomte, *J. phys. radium*, **9**, 13 (1938).
(8) A. Depaigne-Delay and J. Lecomte, *ibid.*, **7**, 38 (1946).
(9) K. W. F. Kohlrausch, *Monatsh. Chem.*, **76**, 231 (1946).
(10) G. M. Barrow, *J. Chem. Phys.*, **21**, 2008 (1953).
(11) L. L. Ingraham, J. Corse, G. F. Bailey and F. Stitt, *J. Am. Chem. Soc.*, **74**, 2297 (1952).
(12) N. Fuson, M. L. Josien and E. M. Shelton, *ibid.*, **76**, 2526 (1954).
(13) J. F. Brown, *ibid.*, **77**, 6341 (1955).
(14) M. W. Skinner and H. W. Thompson, *J. Chem. Soc.*, 487 (1955).
(15) H. W. Thompson and G. Steel, *Trans. Faraday Soc.*, **52**, 1451 (1956).
(16) P. J. Stone and H. W. Thompson, *Spectrochim. Acta*, **10**, 17 (1957).
(17) H. W. Thompson, R. W. Needham and D. Jameson, *ibid.*, **9**, 208 (1957).
(18) M. R. Mander and H. W. Thompson, *Trans. Faraday Soc.*, **53**, 1402 (1957).
(19) P. J. Krueger and H. W. Thompson, *Proc. Roy. Soc. (London)*, **A243**, 143 (1958); **A250**, 22 (1959).
(20) P. Sensi and G. G. Gallo, *Gazz. chim. ital.*, **85**, 235 (1955).
(21) S. Califano and R. Moccia, *ibid.*, **87**, 805 (1957). R. Moccia and S. Califano, *ibid.*, **88**, 342 (1958).
(22) R. N. Jones, W. F. Forbes and W. A. Mueller, *Can. J. Chem.*, **35**, 504 (1957).
(23) C. Garrigou-Lagrange, J. M. Lebas and M. L. Josien, *Spectrochim. Acta*, **12**, 305 (1958).
(24) J. M. Lebas, C. Garrigou-Lagrange and M. S. Josien, *ibid.*, 225 (1959), and previous papers.
(25) L. J. Bellamy, *J. Chem. Soc.*, 2818 (1955).
(26) M. St. C. Flett, *Spectrochim. Acta*, **10**, 21 (1957).
(27) E. Lippert, *Z. Elektrochem.*, **59**, 534 (1955).
(28) E. Lippert and W. Vogel, *Z. physik. Chem.*, **9**, 133 (1956).
(29) N. S. Bayliss, A. R. H. Cole and L. H. Little, *Spectrochim. Acta*, **12**, (1959).
(30) A. W. Baker, THIS JOURNAL, **62**, 744 (1958).
(31) T. L. Brown, *ibid.*, **61**, 820 (1957).
(32) T. L. Brown, *J. Am. Chem. Soc.*, **80**, 794 (1958).
(33) D. H. Whiffen, *J. Chem. Soc.*, 1350 (1956).
(34) D. H. Whiffen, *Spectrochim. Acta*, **7**, 253 (1955).
(35) A. Stojiljkovic and D. H. Whiffen, *ibid.*, **12**, 47, 57 (1958).
(36) A. R. Katritzky and P. Simmons, *J. Chem. Soc.*, 2051 (1959).
(37) A. Cabana and C. Sandorfy, *Spectrochim. Acta*, 335 (1960).
(38) D. A. Ramsay, *J. Am. Chem. Soc.*, **74**, 72 (1952).

The following compounds were prepared by one of us (P.M.G.B.): *m*- and *p*-cyanophenol, *p*-fluorobenzonitrile, *m*- and *p*-chlorobenzonitrile, *o*-, *m*- and *p*-bromobenzonitrile, *o*-, *m*- and *p* dicyanobenzene and *p*-aminobenzonitrile.

o-Cyanophenol and *p*-nitrobenzonitrile were sent us by Dr. P. Sensi and G. G. Gallo from the research laboratories of Lepetit S.P.A., Milano, Italy. *p*-Cyanophenol came from Dr. W. V. Thorpe from the University of Birmingham, England. *o*-Iodophenol, *p*-cyanophenol, *p*-chlorobenzonitrile and *o*-dicyanobenzene were sent us from the collection of E. I. du Pont of Nemours and Company from Wilmington, Delaware, by the courtesy of du Pont of Canada limited. The other compounds were commercial products.

Before taking the spectra, the compounds were recrystallized or redistilled and their purity was checked by taking the melting or boiling points.

Results

The results are contained in Table I for phenol derivatives and Table II for benzonitrile derivatives. In the case of the *ortho* compounds, the frequencies of the intra-molecularly hydrogen bonded groups are included. In these cases the intensities were not computed as we do not know the exact proportion of free and bonded isomers. In four other cases the intensities are not given because of the very low solubility of the compounds.

TABLE I

FREQUENCIES AND INTENSITIES OF THE OH STRETCHING VIBRATION IN PHENOL DERIVATIVES

THE INTENSITIES ARE COMPUTED BY THE METHOD OF SEGMENTS. THEY ARE DIVIDED BY TWO FOR DIPHENOLS.

Substituent	*ortho* ν, cm.$^{-1}$	*ortho* ν, cm.$^{-1}$	*meta* ν, cm.$^{-1}$	*meta* $A_8\times 10^7$	*para* ν, cm.$^{-1}$	*para* $A_8\times 10^7$
None	3610.5	No band	3610.5	5.6	3610.5	5.6
NH_2	3617.7	No band	3612.4	..	3618.0	..
OH	3616.5	3567.2	3610.5	5.8	3616.7	5.7
F	No band	3590.8	3607.5	5.8	3613.5	5.4
Cl	3607.7	3544.6	3606.2	6.4	3608.8	7.0
Br	3604.0	3522.3	3604.3	6.6	3607.2	7.1
I	3600.3	3498.5	3604.0	..	3605.8	7.5
CHO	No band	3180	3604.1	6.7	3598.2	8.4
C≡N	3597.6	3555.5	3602.9	6.3	3597.5	8.1
NO_2	No band	3240	3600.5	7.7	3593.3	8.6

TABLE II

FREQUENCIES AND INTENSITIES OF THE C≡N STRETCHING VIBRATION IN BENZONITRILE DERIVATIVES

THE INTENSITIES ARE COMPUTED BY THE METHOD OF SEGMENTS. THEY ARE DIVIDED BY TWO FOR THE DICYANOBENZENES

Substituent	*ortho* ν, cm.$^{-1}$	*ortho* $A_8\times 10^8$	*meta* ν, cm.$^{-1}$	*meta* $A_8\times 10^8$	*para* ν, cm.$^{-1}$	*para* $A_8\times 10^8$
None	2231.0	6.7	2231.0	6.7	2231.0	6.7
NH_2					2223.4	32.2
OH	2233.8	..	2235.1	7.8	2229.0	18.2
	2221.2	..				
F					2233.6	7.8
Cl	2234.6	4.3	2235.1	5.3	2233.0	8.2
Br	2232.2	..	2234.5	6.1	2231.5	8.5
C≡N	2235.4	1.1	2238.3	3.6	2234.3	..
NO_2	2234.7	..	2238.5	2.9	2235.4	1.9

Intensities (A) are given in absolute units (cm.$^{-2}$ molecule^{-1} sec.$^{-1}$), using natural logarithms and were obtained by the method of segments where the band area is computed as a sum of four segments (or 8, if the band is asymmetric), each one with its own $\Delta\nu$. The reader is referred to an article by Cabana and Sandorfy[37] for more details about this method. It yields values about 10 to 15% lower and closer to reality than those obtained by integrating directly a Lorentz curve with the half width as the only width-parameter.

Stone and Thompson[16] give the frequencies and intensities of 9 compounds out of those in Table I, and Mander and Thompson[18] those of 5 compounds out of those in Table II, in the same solvent. Our frequency values agree within 1 cm.$^{-1}$ with theirs, except for phenol, *p*-cyanophenol and *p*-formylphenol, where our values are by 2.5, 3.5 and 6.2 cm.$^{-1}$ higher, respectively. The intensities were computed with different methods, but even so, in only four cases do our values differ by more than 10%, and in most cases they differ by less than 5%.

Discussion

The substituents of the benzene ring can be divided into three classes on the basis of their orienting effects. Those of the first class, such as OH and NH_2, orient a second electrophilic substitution into *ortho* or *para* and at the same time accelerate the reaction with respect to benzene itself. In the third class are those which, like NO_2, C≡N, CHO, orient a second electrophilic substitution into *meta*, slowing down the reaction. The second class has not always been so clearly distinguished. It comprises F, Cl, Br and I, which orient into *ortho* and *para* but slow down the reaction (see for example ref.[39,40]) *ortho*–*para* ratios were examined by Dewar.[41]

The Phenol Derivatives.—It appears clearly from Table III that the infrared frequencies and intensities give again three well-defined classes, and that they are the same as the ones based on chemical reactivity. This means that substituents like OH or NH_2 have one type of influence on electronic distribution in the benzene ring, NO_2, C≡N, CHO have another type of influence on it and the halogens another type again. This seems to indicate that there are certain relations in this case between the electronic distribution of the unperturbed ground state and the activation energies. It is perhaps significant in this respect that Yvan[42] found an analytical relationship between free valences and activation energies when both are computed by the Hückel method.

TABLE III

THE GENERAL TREND OF FREQUENCIES AND INTENSITIES FOR *meta* AND *para* DERIVATIVES OF PHENOL (φ STANDS FOR PHENOL)

	1st Class NH_2, OH	2nd Class (F), Cl, Br, I	3rd Class CHO, C≡N, NO_2
Frequency	$p > m = \varphi$	$\varphi > p > m$	$\varphi > m > p$
Intensity	$m > p = \varphi$	$p > m > \varphi$	$p > m > \varphi$

As early as in 1935, Wheland and Pauling[43] computed the π-electronic charge distribution in benzene derivatives using the LCAO molecular orbital method. As is well known, this type of

(39) C. K. Ingold, *Chem. Revs.*, **15**, 225 (1934).

(40) M. J. S. Dewar, "The Electronic Theory of Organic Chemistry," Oxford University Press, 1949.

(41) M. J. S. Dewar, *J. Chem. Soc.*, 463 (1949).

(42) P. Yvan, *J. chim. phys.*, **49**, 457 (1952).

(43) G. W. Wheland and L. Pauling, *J. Am. Chem. Soc.*, **57**, 2086 (1935).

calculation yields small negative charges in *ortho* and *para* and zero effective charge in meta for first class substituents and positive charges everywhere but less in *meta* for third class substituents.

So far, no calculation has been able to give the charge distribution we have to infer from the infrared data for the second class, the halogens, namely creation of positive charges everywhere but less in *ortho* and *para* than in *meta*. (R. D. Brown[44] stressed this fact.)

Looking at the data of Table I we see that for both *para* and *meta* derivatives (and the unassociated *ortho* derivatives) there is a smooth variation of the OH frequencies and intensities (in the opposite sense) if we put the halogen derivatives in what appears to be their natural place: between the other two classes. This is, of course the fact underlying the relationships found between frequencies and Hammett's σ-factor. For the *para*-derivatives the frequency varies between 3618 and 3593 and for the *meta*-derivatives between 3612 and 3600. They decrease in the order NH_2, OH, F, Cl, Br, I, CHO, C≡N, NO_2. This would correspond to a gradual decrease of electron density in the same order both in *para* and *meta*, the electron density in *meta* becoming higher than in *para* between I and CHO.

It means that the three classes are not really fundamentally different and intermediate cases (such as the one of F) are possible. The charge in *meta* varies between narrower limits than the charge in *para*, but it does vary, and in the case of the halogens it is even more affected by substitution than the charge in *ortho* and *para*. It is a challenge to quantum chemists to match the regularities discussed here by more refined calculations.

Figure 1 shows schematically how this smooth variation is compatible with the existence of the three groups and the diagrams of Fig. 2 give the charge distributions which would correspond to the observed infrared spectra on the basis of conventional ideas inspired by approximate wave mechanical calculations. (+1 or −1 represent a given amount of electronic charge thought to be about one or two hundredths of the charge of an electron.) A pattern very similar to the one in Fig. 1 was given by Pople, Bernstein and Schneider who obtained it from nuclear magnetic resonance data.[45]

The behavior of the halogens is explained by a charge distribution as on Fig. 2d.

In particular, one can explain the apparent exception of fluorine which, in *para*, raises the OH frequency but, in *meta*, lowers it with respect to phenol. All we have to suppose for this is a charge distribution in fluorobenzene shown in Fig. 2c, that is to say, negative charges still in *ortho* and *para* but positive already in *meta*.

The heightening of the OH frequency in *m*-aminophenol is explained by a charge distribution shown in Fig. 2a.

It seems that as it is usually admitted in the case of the OH group the force constant decreases regularly with increased bond polarity and that the variation of the bond dipole moment during the vibration increases regularly at the same time.

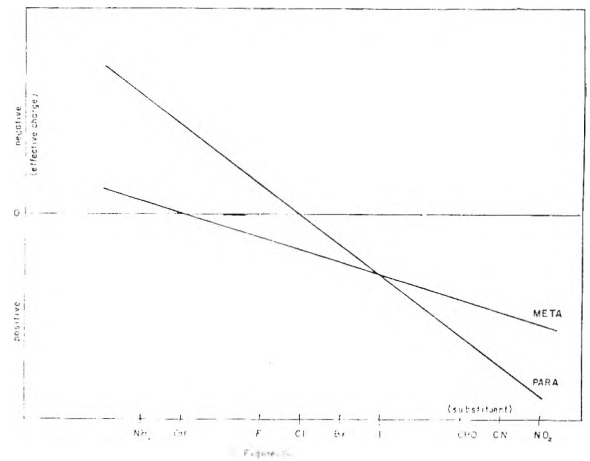

Fig. 1.—Schematic illustration showing how the smooth variation of charges is compatible with the existence of three groups of substituents. The charges are inferred from the frequencies and/or band intensities of the OH stretching vibrations.

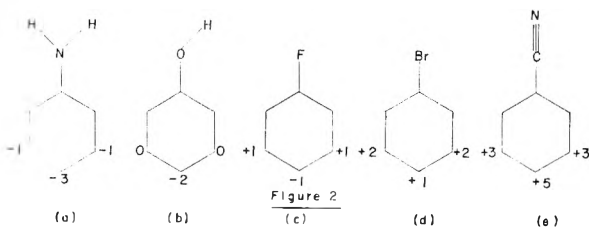

Fig. 2.—Electronic charge distributions in some monosubstituted benzene derivatives (in meta and para). The charges are inferred from the frequencies or/and intensities of the OH stretching vibrations.

Electronic charge distribution in the benzene ring is very often discussed in terms of inductive and mesomeric effects. We had no need to use these notions explicitly as the diagrams of Fig. 2 represent the resultant of both effects. We have to ask the question, however, where the high electron attracting power of the halogens corresponding to their inductive effect comes from. We suggest that it is related to digonal hybridization of the halogens, which makes them more electronegative, giving them an asymmetric lone pair which is largely responsible for the dipole moments of the halogenobenzenes.

The Benzonitrile Derivatives.—The nitrile group has a very high dipole moment, about 3.5 to 4.0 Debye. This is about twice as high as, for example, the dipole moment of a carbonyl group (see for example ref. 46). In spite of this, the intensity of the nitrile band is about 10 to 50 times lower than the intensity of an average carbonyl band. Therefore, this is a case where we have a high bond dipole which changes little during the vibration. As normally the stretching of the C≡N link would tend to increase the separation between the centroids of the positive and negative charges with electronic charge flowing toward the nitrogen atom, there must be a competing flow in the opposite direction, leaving little resultant change in dipole moment. We suggest that this is related to digonal

(44) R. D. Brown, *Quart. Rev.*, 6, 63 (1952).

(45) J. A. Pople, W. G. Schneider and H. J. Bernstein, "High-resolution Nuclear Magnetic Resonance," McGraw-Hill Book Co., New York, N. Y., 1959, p. 260.

(46) C. P. Smyth, "Dielectric Behavior and Structure," McGraw-Hill Book Co., New York, N. Y., 1955.

hybridization and the existence of an asymmetric lone pair on the nitrogen. Digonal hybridization is energetically favorable as long as it assures a stronger overlap than the unhybridized orbitals would. Thus, when the C≡N bond is stretched, the overlap diminishes and less stabilization will come from digonal hybridization. There will be a partial return to the unhybridized state with the lone pair being pulled back toward the nitrogen nucleus and the bonding electrons toward the carbon. This change would not require a change in bond angles as both p and sp bonds would give a linear arrangement. The remaining change in dipole moment would therefore be the result of a delicate equilibrium between two opposing effects which could easily be modified by a slight change in electronic distribution caused by a substituent.

This would give a qualitative explanation of the great sensitivity of the C≡N band intensity to substitution. It would also be in line with the fact that at the same time the values of the frequencies change only slightly, as this change of hybridization would only occur during the vibration and would not influence the force constant.

From Table IV it is seen that we have again three classes of substituents, the same as in the case of the phenol derivatives. There is no complete analogy, however, between the two cases as is immediately clear if we compare Tables III and IV. The one is not identical with or just the inverse of the other.

TABLE IV

THE GENERAL TREND OF FREQUENCIES AND INTENSITIES FOR *meta* AND *para* DERIVATIVES OF BENZONITRILE (N STANDS FOR BENZONITRILE)

	1st Class OH	2nd Class Cl, Br	3rd Class C≡N, NO
Frequency	$m > N > p$	$m > p > N$	$m > p > N$
Intensity	$p > m > N$	$p > N > m$	$N \gg m > p$

There is again a smooth variation of frequencies and intensities and the halogens are again between the other two classes.

Whatever the second substituent, the nitrile frequency of the *meta* isomer is always the highest. This and other anomalies show that, in the case of the nitrile group, the change in dipole moment during the vibration does not always follow the changes of the dipole moment itself from one substituent to the other, and the relation between the polarity of the bond and the force constant does not seem to be a simple one.

We conclude that qualitative explanations should not be pushed any further.

Acknowledgment.—We owe sincere thanks to all those who helped our work with samples. Their names are given in the Experimental section. We are grateful to Dr. E. K. Plyler from the U.S. National Bureau of Standards who kindly agreed to check the frequencies of our calibration bands. We are indebted to Mrs. I. R. Jegyud for helping in the preparation of the manuscript. Finally, we acknowledge financial help from the National Research Council of Canada.

GAS PHASE OXIDATION OF THE XYLENES. GENERAL KINETICS

BY FRANKLIN J. WRIGHT

Esso Research and Engineering Company, Linden, New Jersey

Received July 18, 1960

The kinetics of the slow combustion of the three xylene isomers have been studied manometrically in a quartz vessel, under static conditions at subatmospheric pressures over the temperature range from 410 to 550°, employing 1:1 to 1:20 hydrocarbon:oxygen mixtures. It was shown that $W_{max} = k.P^n$ where P is the total initial pressure, W_{max} the maximum rate developed and n is 2.8, 1.9 and 1.5 for *m*-, *o*- and *p*-xylene, respectively. Although W_{max} is affected by changes in mixture composition and temperature, the value of n is independent of these parameters. Arrhenius plots were linear between 410 and 550° and the activation energies for the over-all oxidation process were calculated to be 38, 39 and 40 kcal./mole for *o*-, *m*- and *p*-xylene, respectively. The greater ease of oxidation of *o*-xylene was ascribed to the greater reactivity of the chain branching intermediate. The lifetime of this intermediate was calculated to be 2 min. for *o*-xylene as contrasted to 20 and 17 min. for *m*- and *p*-xylene, respectively. Addition of inert gases (He, A, N_2 and SF_6) increased W_{max} thus suggesting that this rate is governed by a diffusion controlled process at the walls of the reaction vessel. Studies of the competitive oxidation of binary mixtures of the xylenes indicated that the chain propagation reactions proceed at essentially equal rates in all three oxidations and have nearly equal activation energies.

The vapor phase oxidation of hydrocarbons has been much studied in the past 30 years. Yet, in spite of their increasing use in fuels for internal combustion engines, relatively little attention has been paid to the slow combustion of the aromatic hydrocarbons.

A number of investigations of the oxidation of benzene have been reported. Fort and Hinshelwood[1] concluded that the oxidation took place by a mechanism involving chains of short length. Newitt and Burgoyne[2] studied the slow oxidation of benzene, toluene and ethylbenzene at high pressures and showed that in the case of the substituted benzenes both nuclear and side-chain oxidation occurred simultaneously whereas in the case of benzene only a single series of hydroxy intermediates preceded the breakdown of the ring. Norrish and Taylor[3] showed that the oxidation of benzene proceeded *via* a successive hydroxylation of the ring to the dihydroxy stage whereupon ring splitting and rapid degradation of the fission products ensued. Burgoyne[4] examined the oxidative behavior of benzene and a series of substituted

(1) R. Fort and C. N. Hinshelwood, *Proc. Roy. Soc. (London)*, **127A**, 218 (1930).

(2) D. M. Newitt and J. H. Burgoyne, *ibid.*, **153A**, 448 (1936).

(3) R. G. W. Norrish and G. W. Taylor, *ibid.*, **234A**, 160 (1956).

(4) J. H. Burgoyne, *ibid.*, **175A**, 539 (1940).

benzenes at normal pressures and concluded that the chain characteristics of the slow oxidation of benzene are markedly different from those of its alkyl derivatives.

A comprehensive investigation into the vapor phase oxidation of the isomeric xylenes is at present in progress in these laboratories. Some preliminary results concerning the general kinetics of the slow combustion of these compounds are presented in this paper. The xylenes were selected for study because, as well as being typical aromatics, they also exhibit striking differences in some of their combustion properties. For instance, the resistance of *o*-xylene to detonation in spark-ignited engines is markedly lower than that of the other two isomers, as indicated by the values of 13.6, 15.3 and 15.7 reported for the critical compression ratio of *o*-, *m*- and *p*-xylene (600 r.p.m., 100°F. inlet temperature).[5] Similarly the spontaneous ignition temperature of *o*-xylene is materially lower (*ca.* 60°) than that of either *m*- or *p*-xylene.[6]

Experimental

Apparatus.—A static apparatus conventional in design was used. It consisted essentially of a quartz reaction vessel of length 20 cm. and diam. 3 cm., placed horizontally in an electric furnace of large thermal inertia whose temperature could be accurately controlled to ±1°. The reaction vessel was connected to a large mixing reservoir immersed in a thermostatically controlled oil-bath maintained at 120°. The hydrocarbon–oxidant mixtures were prepared in this reservoir prior to their admission into the reaction vessel. Pressures were measured on a capillary manometer. The manometer and all connecting capillary leads to the reaction vessel were electrically heated to avoid condensation. The reaction vessel was fitted with a stopcock and could be rapidly disconnected from the rest of the apparatus and removed from the furnace.

In the part of the investigation which concerned itself with the competitive oxidation of binary mixtures of the xylenes, the amounts of each of the isomers present initially and at the end of the reaction were obtained by gas chromatography in the following manner. After cooling the reaction vessel by immersion first in cold water and then in liquid nitrogen, a small phial containing 0.25 cc. of benzene was attached to it. The contents of this phial were then transferred to the reaction vessel and the latter allowed to warm up. The walls of the reaction vessel were then carefully rinsed with the solvent and the resulting solution which contained, *inter alia*, the unconsumed xylenes was returned to the phial. This was achieved by immersing it in liquid nitrogen while at the same time the reaction vessel was gently heated by means of a heat lamp. Aliquot portions of the benzene solution were then analyzed for their xylene content by means of a Perkin–Elmer Model 154 Vapor Fractometer using a fluorene picrate column operating at 100°. In this manner the xylene concentrations could be measured with an accuracy of ±5%.

Materials.—Oxygen from a cylinder was passed over calcium chloride and phosphorus pentoxide; it was used without further purification. The xylenes were Pure Grade (99%) Phillips 66 and were further purified by vacuum distillation, the middle fraction being retained.

Results

The development of oxidation was followed by measuring the change of pressure within the reaction vessel as a function of time. The influence of temperature over the range 410 to 550°, pressure between 100 and 600 mm., dilution and surface effects on the maximum rate of oxidation attained, W_{max}, was studied using hydrocarbon:oxygen mixtures ranging in composition from 1:1 to 1:20.

(5) T. A. Boyd, *Ind. Eng. Chem.*, **26**, 1105 (1934).
(6) J. L. Jackson, *Ind. Eng. Chem.*, **43**, 2869 (1951).

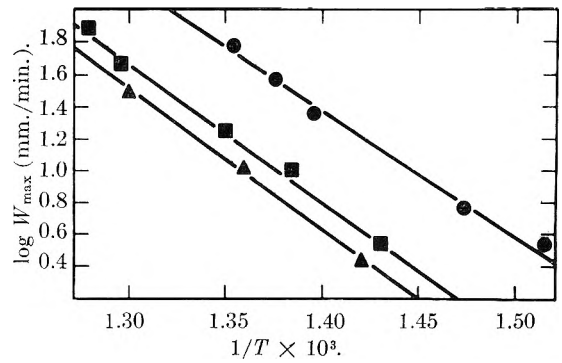

Fig. 1.—Variation of log W_{max} with $1/T$: ●, 125 mm. *o*-xylene + 375 mm. oxygen; ■, 125 mm. *m*-xylene + 375 mm. oxygen; ▲, 125 mm. *p*-xylene + 375 mm. oxygen.

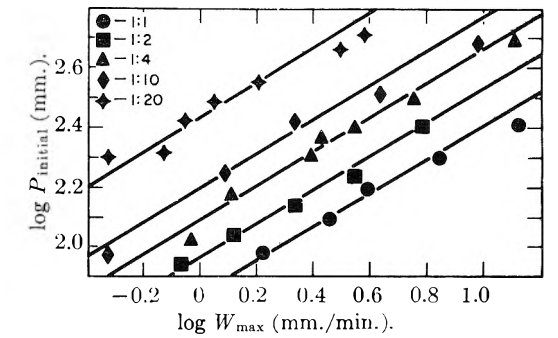

Fig. 2.—Variation of log W_{max} with log of total initial pressure for *o*-xylene:oxygen mixtures of varying compositions at 430°.

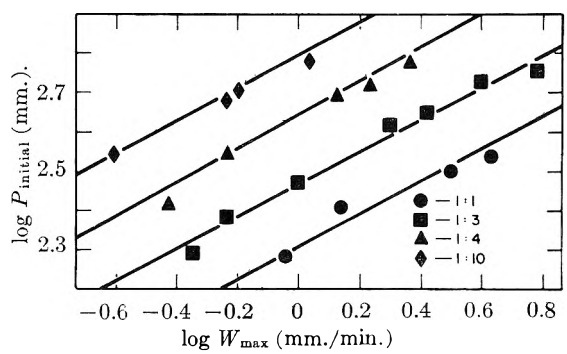

Fig. 3.—Variation of log W_{max} with log of total initial pressure for *m*-xylene:oxygen mixtures of varying composition at 430°.

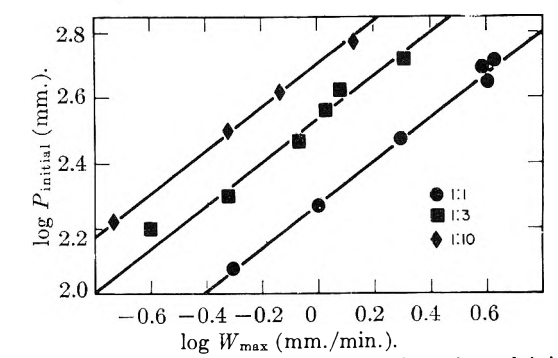

Fig. 4.—Variation of log W_{max} with log of total initial pressure for *p*-xylene:oxygen mixtures of varying composition at 430°.

The observation that at a given temperature, the final pressure increment bore a linear relationship to the initial total pressure and that the line passed

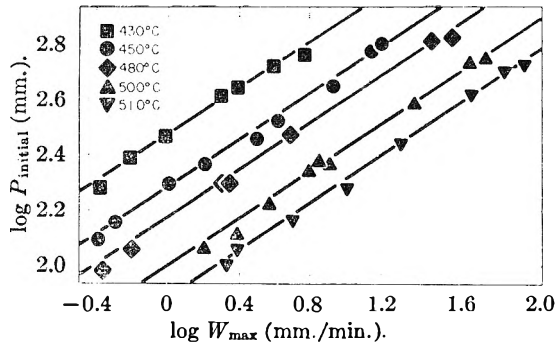

Fig. 5.—Variation of log W_{max} with log total initial pressure for a 1:3 *m*-xylene:oxygen mixture at several temperatures.

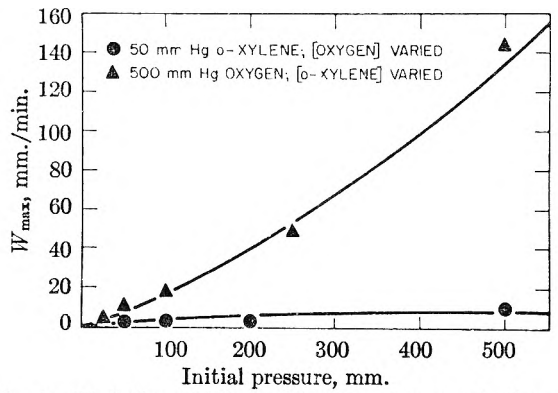

Fig. 6.—Variation of W_{max} with reactant concentrations at 430°.

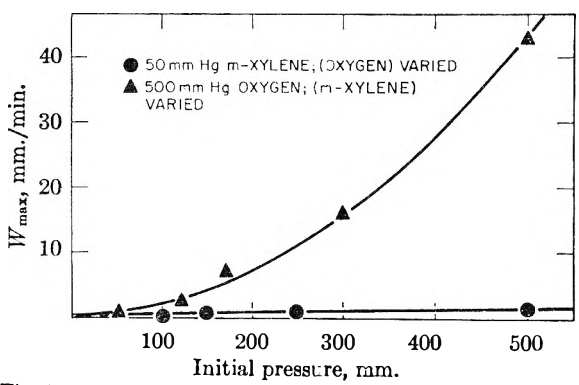

Fig. 7.—Variation of W_{max} with reactant concentrations at 430°.

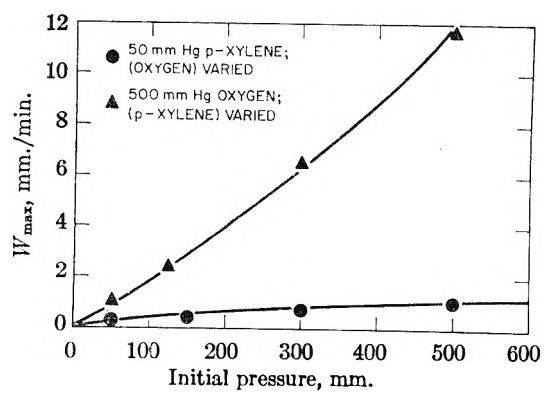

Fig. 8.—Variation of W_{max} with reactant concentrations at 430°.

through the origin of the coördinates, offered some justification for a manometric method of following the reaction rates.

The maximum rates developed, W_{max}, and the net branching factor, ϕ, were obtained from Δp–t curves. These curves generally were of the sigmoid type characteristic of degenerate branching.

Influence of Temperature.—The effect of temperature on the maximum rate of oxidation was studied using 3:1 oxygen:hydrocarbon mixtures. The concentrations of reactants were such that at 430° their total initial pressure was 500 mm. The results are shown graphically in Fig. 1 in which the logarithm of W_{max} is plotted against the reciprocal of the absolute temperature. Within the limits of experimental error, a linear relationship holds for each of the three compounds examined, and no signs of curvature indicative of an alteration of the dependence of the rate on temperature could be observed. The value of E, the activation energy for the over-all oxidation process in the temperature range 410 to 550° was found to be 38, 39 and 40 kcal./mole for *o*- m- and *p*-xylene, respectively.

If in Fig. 1 a line is drawn parallel to the ordinate, the points of intersection with the "Arrhenius Lines" give the rates at which the three hydrocarbons are oxidized under the same temperature conditions. It is thus seen that the order of relative ease of oxidation is *ortho* > *meta* > *para* and it may be concluded that the least reactive configuration is the one with the highest symmetry. These differences in the vulnerability of the three isomers to oxygen attack underscore the well-known influence of structure on oxidation reactions.[7–9]

Influence of Concentration Factors.—The effect of total and partial initial pressure of the reactants on W_{max} was examined at 430°. The maximum rate of oxidation was measured at this temperature for a number of oxygen:hydrocarbon mixtures varying in composition between 1:1 and 20:1 at total initial pressures between 50 and 600 mm. The results obtained with *o*-, *m*- and *p*-xylene are shown graphically in Figs. 2, 3 and 4, respectively. In each case, the logarithm of the total pressure is plotted against the logarithm of the maximum rate.

The linearity of these plots indicate that under these experimental conditions, W_{max} is a function of a power n of the total initial pressure. Moreover, this power appears to be independent of the stoichiometry of the reacting mixtures at least over the range studied. The values of n were found to be 1.9, 2.8 and 1.5 for *o*-, *m*- and *p*-xylene, respectively. Similar plots were obtained for a 3:1 oxygen:hydrocarbon mixture at several temperatures between 430 and 510° as illustrated by the data on *m*-xylene present in Fig. 5. All of these were found to be parallel straight lines showing clearly that over the range studied, temperature had no effect on the power index n. Although only the results

(7) C. F. Cullis and C. N. Hinshelwood, *Faraday Soc. Disc.*, **2**, 117 (1947).

(8) C. N. Hinshelwood, *J. Chem. Soc.*, 531 (1948).

(9) A. R. Ubbelohde, Six Lectures on the Basic Combustion Process, Ethyl Corporation, Detroit, 1954, 53.

obtained for *m*-xylene are shown in Fig. 5, both the *ortho* and *para* isomers were found to behave similarly.

Effect of Oxygen and Hydrocarbon Concentrations.—As can be seen from Figs. 6–8, increasing the hydrocarbon concentration results in all cases in a very marked increase in the oxidation rate. In contrast to this, the influence of oxygen is much less pronounced.

The variation of the maximum rate of pressure rise with initial pressure of reactant can be expressed by an equation of the type

$$(d(\Delta p)/dt)_{max} = k[RH]^a[O_2]^b$$

The values of the constants a and b are given in Table I.

TABLE I

ORDER OF MAXIMUM RATE OF PRESSURE RISE

	Total pressure [RH] + [O₂]	Hydrocarbon pressure a	Oxygen pressure b
m-Xylene	2.8 ± 0.2	1.9 ± 0.2	0.6 ± 0.2
o-Xylene	1.9 ± .2	1.1 ± .2	.6 ± .2
p-Xylene	1.5 ± .2	1.0 ± .2	.5 ± .2

In hydrocarbon oxidation, the occurrence of fractional orders often indicates that the rate expression should include a total pressure factor. This generally implies that chain termination is, in part at least, a diffusion-controlled wall reaction. The effect of inert gases and of the nature of the surface of the reaction vessel on the rate of reaction is in agreement with this view.

Effect of Surface and Dilution.—Substitution of the quartz reaction vessel normally used in this investigation by another quartz vessel of identical dimensions resulted in a change in the rate expressions. The results in both vessels, however, were quite reproducible and neither vessel required prolonged "aging." After treatment with organic solvents, nitric acid or after flaming, one or two runs sufficed to return the vessels to their "pretreatment" condition. No special precautions, therefore had to be taken in evacuating the vessel between runs. An isolated fact might also be reported. A coating of carbon formed by the accidental overheating of the reaction products in one of the experiments did not affect the subsequent results. All results reported here were obtained in a single reaction vessel.

The effect of inert gases was studied by the addition of He, A, N_2 and SF_6 to a mixture of 50 mm. of *p*-xylene and 150 mm. of oxygen at 425° and measuring W_{max} at successively higher pressures up to 550 mm. As shown in Fig. 9, plots of the inert gas pressure P against W_{max} were in all cases straight lines. Moreover the slopes of these lines which may be taken as a measure of the inert gas effect varied considerably depending on the nature of the diluent. Thus

	He	A	N_2	SF_6
$(dW_{max}/dP_{inert}) \times 10^4$	3.0	7.0	8.5	15.0

The implication of these variations will be discussed later.

Discussion

A detailed mechanism of the oxidation reactions cannot be deduced from rates of pressure changes alone. However, the fact that throughout the acceleration period, there was an exponential relationship between Δp and t, indicating that the reaction is autocatalytic, strongly suggests that as for most hydrocarbons,[10] the gas phase oxidation of the xylenes is a chain process involving degenerate branching. The dependence of the maximum rate on the initial pressure of oxygen and hydrocarbon rather than the instantaneous pressure at the time of attainment of this rate, implies that the rate of build up of the intermediate responsible for the delayed branching is determined by the initial conditions and that it is then this rate which in turn governs the over-all rate of reaction. The effect of the nature of the vessel and of inert gases supports this view. As Semenov[10] has pointed out, not only can the initiation and termination of the chains be affected by the walls but the branching also.

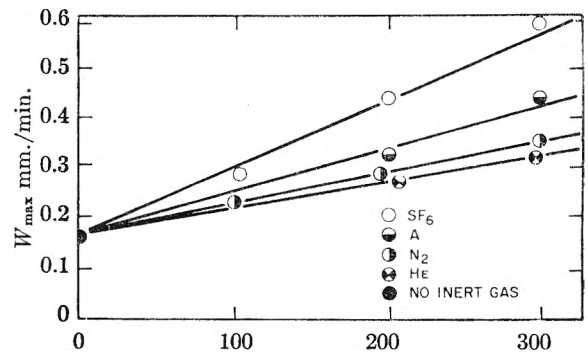

Fig. 9.—Effect of inert gases on W_{max}.

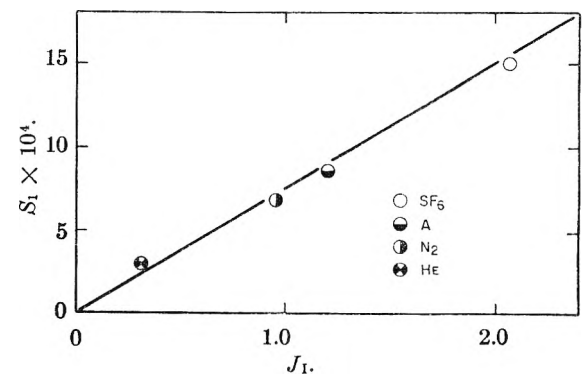

Fig. 10.—Slopes of the lines in Fig. 9 plotted against the reciprocal of the relative coefficient of diffusion.

The addition of inert gas systematically increases the maximum rate of pressure rise, W_{max}. The magnitude of this effect, however, depends very much on the nature of the diluents (Fig. 9). This suggests that one of the processes governing the rate W_{max} is determined by the rate of the diffusion controlled destruction of an active intermediate at the walls of the reaction vessel. The effect of the nature of the vessel on W_{max} is in accord with this view and further qualitative support for this suggestion was obtained in the following manner.

If the slopes S_I of the plots given in Fig. 9 are taken as a measure of the inert gas effect, then as shown by Melville[11] and Mulcahy and Ridge[12]

(10) N. N. Semenov, "Chemical Kinetics and Chain Reactions," (O.U.P., 1935).

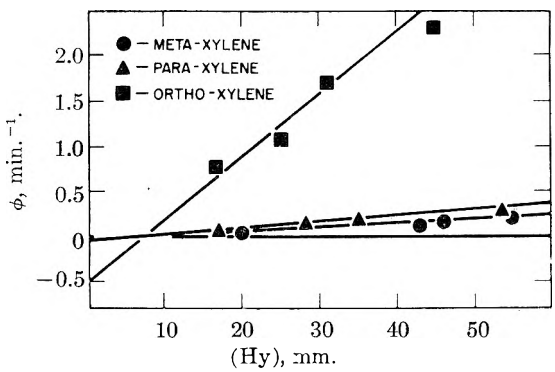

Fig. 11.—Variation of the net branching factor ϕ with hydrocarbon concentration at 430°.

$$S_I = kJ_I$$

where k is a constant and $J_I = D_{O_2}/D_I$, D_{O_2} and D_I being the coefficient of diffusion of the active intermediate into oxygen and inert gas, respectively. Values of J_I have been calculated by Ridge[13] for various inert gases. When these are plotted against the slopes S_I, as shown in Fig. 10, a straight line is obtained.

Because of the shortness of the incubation period, this parameter was not easily accessible to quantitative study. It was observed, however, that the length of the induction period was definitely reduced by the addition of inert gases. It would thus appear that chain termination at the walls is important both during and after the induction period. These observations provided no indication that a transition from one mechanism to another might occur at the end of the induction period, as suggested by Mulcahy.[14] They do, however, suggest that the effects of chain branching do not predominate over the surface effects.

For a chain reaction which proceeds by degenerate branching the net branching factor ϕ is given by

$$\phi = (2\alpha\beta\nu - 1)/\tau \qquad (2)$$

The process considered in the derivation of this equation consists of a chain reaction in which the length of the basic link is ν. A proportion, α, of the chain steps results in the production of an active intermediate, I, which has a lifetime, τ. The delayed branching originates from the new chains formed when a fraction, β, of the intermediate reacts to give two free radicals.

As suggested by Knox,[15,16] the parameters in equation 2 can be expressed in terms of concentration factors and the appropriate rate constants k_p, k_t, k_b and k_d of the four basic steps of the chain reaction, *i.e.*, propagation, termination, branching and non-branching destruction yielding inert products.

Thus, if

$$W_p = k_p[RH][X],\ W_t = k_t[X]$$
$$W_b = k_b[I],\qquad W_d = k_d[I]$$

Where [RH], [X] and [I] are, respectively, the concentrations of the hydrocarbon, chain carrier and branching intermediate.

Then $1/\tau = k_b + k_d,\ \beta = k_b/(k_d + k_b)$

$\nu = k_p[RH]/k_t$

and $\phi = 2\alpha k_p k_b[RH]/k_t - 1/\tau$

The lifetime of the intermediate I can thus be obtained from the reciprocal of the intercept of a plot of ϕ against the initial partial pressure of the hydrocarbon.

For a reaction involving branching chains, the increase in pressure, Δp, with time t, is given by an equation of the type

$$\Delta p = \frac{C}{\phi^2}(e^{\phi t} - 1)$$

where C is a constant and ϕ is the net branching factor. Thus, during the autocatalytic period of a reaction of this type, a plot of log ΔP against time should be linear once $e^{\phi t}$ is greater than unity. Moreover, the slope of such a plot is equal to the net branching factor ϕ.

Values of ϕ have been calculated in this manner for 10:1 oxygen:hydrocarbon mixtures at 430°. When these are plotted against the initial hydrocarbon concentrations, as shown in Fig. 11, a straight line is obtained for each of the three xylenes. From these, the lifetimes of the intermediate I were found to be 2, 20 and 17 minutes for *o*-, *m*- and *p*-xylene, respectively.

Thus, the lifetime of the intermediate I which plays a role in the oxidation of *o*-xylene is markedly lower, indicating a relatively greater reactivity. This is probably the reason for the greater ease of oxidation of *o*-xylene in the gas phase, a property which is reflected in the lower knock resistance of this isomer compared to the other two and in the similar trend observed in their spontaneous ignition temperatures.

The view that the effect of structure on the rate of oxidation might be related to the reactivity of the branching intermediate is further supported by the fact that the differences in the rates of initiation are probably very small since Szwarc[17] has shown that the bond strength, $D(C_6H_5CH_2{-}H)$, for *o*-, *m*- or *p*-xylene is 74, 77.5 and 75 kcal./mole, respectively, and the differences between these values are probably within the accuracy of the measurements. Also, as will be shown, there are indications that the rate of the chain propagating step is very nearly the same for the three isomers and that probably the same radical serves as the chain carrier in all three oxidations.

Because there appeared to be no convenient way of measuring the rates of chain propagating reactions directly, a competitive technique was employed to measure their relative rates. Such a technique has recently been successfully applied by Knox, Smith and Trotman-Dickenson[18,19] to the study of the oxidation of some lower molecular weight hydrocarbons such as ethane, propane and isobutane. As pointed out by these authors, in the

(11) H. W. Melville, *Trans. Faraday Soc.*, **28**, 308 (1932).
(12) M. F. R. Mulcahy and M. J. Ridge, *ibid.*, **49**, 1297 (1953).
(13) M. J. Ridge, *ibid.*, **52**, 858 (1956).
(14) M. F. R. Mulcahy, *ibid.*, **45**, 575 (1949).
(15) J. H. Knox, 7th Int. Symposium on Combustion (Butterworth, London, 1958), p. 122.
(16) J. H. Knox, *Trans. Faraday Soc.*, **55**, 1362 (1959).
(17) M. Szwarc, *Faraday Soc. Disc.*, **10**, 336 (1951).
(18) J. H. Knox, R. F. Smith and A. F. Trotman-Dickenson, 7th Int. Symposium on Combustion (Butterworth, London, 1958), p. 126.
(19) J. H. Knox, R. F. Smith and A. F. Trotman-Dickenson, *Trans. Faraday Soc.*, **54**, 1509 (1958).

oxidation of the pure hydrocarbons R_1H and R_2H, the chain propagating reactions may be written as

$$R_1H + X_1 \xrightarrow{k_{11}} X_1H + R_1 \quad (1)$$

$$R_2H + X_2 \xrightarrow{k_{22}} X_2H + R_2 \quad (2)$$

where the chain carriers X_1 and X_2 can be oxygenated radicals such as OH, HO_2, RO and RO_2. Two other reactions will furthermore occur when a mixture of such two hydrocarbons are oxidized

$$R_1H + X_2 \xrightarrow{k_{12}} X_2H + R_1 \quad (3)$$

$$R_2H + X_1 \xrightarrow{k_{21}} X_1H + R_2 \quad (4)$$

If k_1 and k_2 are defined as the over-all rate constants for the disappearance of the two hydrocarbons, it can be shown[19,20] that the ratio k_1/k_2 is related to the concentrations of each hydrocarbon present initially and at the end of the reaction in the following way

$$\frac{k_1}{k_2} = \frac{\log [R_1H] \text{ initial}/[R_1H] \text{ final}}{\log [R_2H] \text{ initial}/[R_2H] \text{ final}} \quad (5)$$

If $k_{11} \neq k_{12}$ and $k_{22} \neq k_{21}$, then in general the ratio k_1/k_2 will vary with the composition of the mixture investigated.

The ratios of the over-all rate constants, k_m/k_o and k_p/k_o, given by equation 5 have been obtained for *m*-xylene/*o*-xylene and *p*-xylene/*o*-xylene mixtures over a wide range of experimental conditions. Using 1:1 and 1:2 total hydrocarbon:oxygen mixtures, it was found that at each of the temperatures investigated in the range 400 to 500°, the ratios k_m/k_o and k_p/k_o were independent of the total initial pressure from 200 to 700 mm. and were unaffected by changes in the xylene isomers ratios from 3/1 to 1/3. At 400°

$$k_m/k_o = 1.07 \pm 0.05 \text{ and } k_p/k_o = 1.03 \pm 0.05$$

As indicated previously, a dependence of these ratios on concentration factors would be expected if $k_{11} \neq k_{12}$ and $k_{22} \neq k_{21}$. If, however, $k_{11}/k_{12} = k_{22}/k_{21}$ and in particular if X_1 and X_2 are identical so that $k_{11} \equiv k_{12}$ and $k_{22} \equiv k_{21}$, then the ratio k_1/k_2 will be independent of the ratio of the concentrations of the two hydrocarbons. The observed constancy of k_m/k_o and k_p/k_o can thus be taken as indicating not only that the reactivity of the radicals X_o, X_m and X_p are equal but that these radicals are very probably the same.

As illustrated in Figs. 12 and 13, over the range 400 to 500°, the effect of temperature on the ratios k_m/k_o and k_p/k_o is quite small. Each point on these graphs represent the mean of at least six independent determinations. The differences in activation energy $E_o - E_m$ and $E_o - E_p$ calculated from the slopes of these Arrhenius plots were found to be 0.6 ± 0.2 and 0.9 ± 0.2 kcal./mole, respectively.

From the constancy of the ratios k_m/k_o and k_p/k_o, it was concluded that the same radical X acts as the chain carrier in all three oxidations. Such constancy would also be observed if different radicals were responsible for the propagation of the chains, provided that their properties were very similar. However, in view of the sizable activation energies of between 6 and 13 kcal./mole associated with liquid phase oxidations involving ROO,[21] it might be expected that peroxy radicals formed by the reaction of oxygen with either *o*-, *m*- or *p*-xylene would also react at different rates with a given hydrocarbon. Such selectivity would lead to a dependence of k_1/k_2 on concentration factors and this is at variance with the experimental facts.

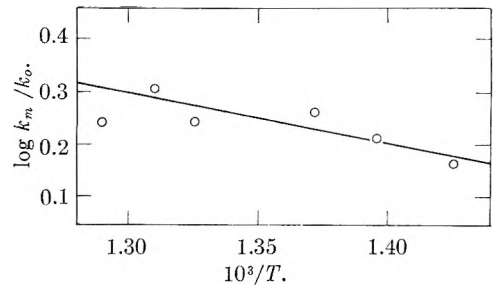

Fig. 12.—Dependence of k_m/k_o on temperature.

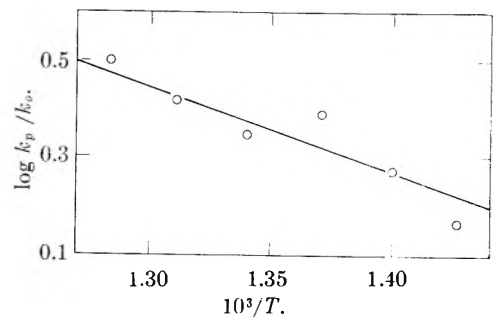

Fig. 13.—Dependence of k_p/k_o on temperature.

If all three oxidations are therefore propagated by the same radical, it must perforce be concluded that the chain carrier is either OH or HO_2. In view of the available evidence, HO_2 is favored. This radical has been suggested as the chain carrier in the oxidation of methane[22] and of other hydrocarbons above 400°[23-25] and in the gas phase oxidation of ethyl alcohol at 270°.[26] Moreover, the work of Knox, Smith and Trotman-Dickenson[18,19] on the competitive oxidation of ethane, propane and isobutane has also led them to suggest that HO_2 is probably the chain carrier in these oxidations. This conclusion was reached on the strength that the ratios of the rate constants of the chain propagating step in the oxidation of these three hydrocarbons showed remarkable constancy over a wide range of experimental conditions and also on the grounds that the HO_2 radical could satisfactorily explain the results of high temperature oxidation. The similarity between the behavior of the isomeric xylenes and that of the three paraffinic hydrocarbons strengthens the view that HO_2 could be the chain carrier. The work reported here does not

(20) W. M. Jones, *J. Chem. Phys.*, **19**, 78 (1951).

(21) L. Bateman, *Quart. Revs.*, **8**, 147 (1954).

(22) N. S. Enikolopyan, 7th Int. Symposium on Combustion (Butterworth, London, 1958), p. 157.

(23) J. W. Falconer and J. H. Knox, *Proc. Soc.* (*London*), **250A**, 493 (1959).

(24) C. N. Satterfield and R. E. Wilson, *Ind. Eng. Chem.*, **46**, 1001 (1954).

(25) D. E. Hoare and A. D. Walsh, "5th Int. Symposium on Combustion," Reinhold Publ. Corp., New York, N. Y., 1955, p. 467.

(26) C. F. Cullis and E. J. Newitt, *Proc. Roy. Soc.* (*London*), **237A**, 530 (1956).

enable any firm conclusions to be reached as to the magnitude of the activation energy of the reaction between the chain propagator X and the xylenes. The small differences which were found to exist between these activation energies are, however, in keeping with the suggestion that the chain carrier X is in fact the HO_2 radical.

While further light has been shed on the character of some of the elementary reactions which occur in the gas phase oxidation of the xylenes, it is clear that further work is still required to establish with certainty the nature of the chain carrier or of the branching intermediate. The stoichiometry of the oxidation of the xylenes is at present being obtained. In this respect, gas chromatography is proving to be a most useful tool. Such analytical information together with the kinetic details presented here should provide an adequate basis for the formulation of a satisfactory mechanism of the slow combustion of the xylenes.

NOTES

ISOTOPE EFFECT IN RECOIL TRITIUM ABSTRACTION REACTIONS WITH METHANE

By J. K. Lee, Burdon Musgrave and F. S. Rowland[1]

Department of Chemistry, University of Kansas, Lawrence, Kansas

Received April 29, 1960

An isotopic preference for the abstraction of H atoms rather than D atoms from methane has been shown by high energy tritium atoms from the nuclear reaction $He^3(n,p)H^3$. This preference has been demonstrated both intramolecularly in CH_2D_2 and intermolecularly in mixtures of CH_4 and CD_4.

The reactions of recoil tritium atoms with gaseous CH_4 have been studied thoroughly by Wolfgang, *et al.*,[2-5] and by Willard, *et al.*[6-8] It has been demonstrated that about 60% of the recoil tritium atoms react in very energetic ("hot") reactions to form CH_3T and HT in very nearly equal amounts; another 30% react to form HT by thermal reactions, or with radical scavengers if present; the remaining 10% form $CH_2T\cdot$ or other radicals, and are found either as higher molecular weight products or are scavenged along with the thermal tritium atoms. Our experiments were designed to look for isotopic preferences in the "hot" abstraction reaction. Isotope effects in recoil tritium substitution reactions have been reported previously in liquid isopropyl benzoate,[9] and in gaseous mixtures of H_2 and D_2.[10]

Gaseous mixtures of purified He^3, the appropriate isotopic methanes, and other gases when required, were sealed in Pyrex 1720 glass, and irradiated at 3×10^9 n./cm.^{2}/sec. for two days. Two separate series were prepared: one with CH_2D_2, and the other with mixtures of CH_4 and CD_4. A small amount of O_2 was always present as a radical scavenger; in several experiments, larger amounts of O_2, NO or He^4 were added.

Two (or more) aliquots of each sample were separated and analyzed for radioactive components by gas chromatography and proportional counting.[11] Relative yields of HT and DT were determined on 10′ of 13 Å. molecular sieve at −160°, while total radioactivity in hydrogen, methane and ethane was determined on silica gel at 60°. Negligible radiation-induced exchange was observed between H_2 and D_2 under similar experimental conditions.[10] The results of these runs are shown in Table I—the estimated error on each HT/DT ratio is ±0.02 unless marked. The ethane radioactivity was less than 1% of the methane radioactivity in each case. We have been unable as yet to obtain a separation of the individual monotritiated methanes by gas chromatography.

Table I

Radioactive Products of Recoil Tritium Reactions with Deuterated Methanes

Gas pressure, cm.			Specific activity	$\frac{HT + DT}{CH_2DT + CHD_2T}$
He^3	CH_2D_2	Other	HT/DT	
2.9	74.6		1.34	0.84
2.9	26.0		1.40	.83
2.9	10.2		1.42	.90
2.6	41.5	35.3 He^4	1.39	.75
2.6	25.2	51.6 He^4	1.47	.96
1.4	71.7	5.6 NO	1.19 ± 0.07	.82
1.4	48.1	29.9 O_2	1.25	.63

				Obsd. ratio		(HT + DT)/
He^3	CH_4	CD_4	Other	HT/DT	(HT/DT)/ (CH_4/CD_4)	(CH_3T + CD_3T)
1.4	33.8	39.8		1.09	1.29	0.82
1.4	55.2	18.1		3.83	1.26	.86
1.1	31.9	31.9	14.7 NO	1.27	1.27	.73
1.1	37.4	37.4	5.6 NO	1.28	1.28	.80
1.1	13.8	13.8	47.9 He^4	1.25 ± 0.07	1.25 ± 0.07	1.02
2.3	28.6	28.6	21.1 O_2	1.29	1.29	0.68
2.3	17.4	17.4	41.4 O_2	0.99 ± .03	0.99 ± .03	.47
2.3	4.3	4.3	66.6 O_2	1.03 ± .06	1.03 ± .06	.37

The isotopic preference for reaction with H rather than D in mixtures of CH_4 and CD_4 represents the combination of two effects: the relative numbers of the two molecules attacked and, once attacked, the fraction of reactions proceeding by abstraction and by substitution. The ratio of $\Sigma(HT+DT)/$

(1) Research supported by A.E.C. Contract No. AT-(11-1)-407 and by Contract No. AF-19(604)-4053 with the Geophysics Directorate of the U. S. Air Force.

(2) M. El-Sayed and R. Wolfgang, *J. Am. Chem. Soc.*, **79**, 3286 (1957).

(3) M. El-Sayed, P. Estrup and R. Wolfgang, This Journal, **62**, 1356 (1958).

(4) R. Wolfgang, *et al.*, "Second United Nations International Conference on the Peaceful Uses of Atomic Energy," Geneva, 1958, Vol. 29, 326 (1959).

(5) P. Estrup and R. Wolfgang, *J. Am. Chem. Soc.*, **82**, 2661, 2665 (1960).

(6) A. Gordus, M. Sauer and J. Willard, *ibid.*, **79**, 3284 (1957).

(7) J. Evans, J. Quinlan, M. Sauer and J. Willard, This Journal, **62**, 1351 (1958).

(8) M. Sauer and J. Willard, *ibid.*, **64**, 359 (1960).

(9) W. G. Brown and J. L. Garnett, *Intl. J. Appl. Rad. and Isotopes*, **5**, 114 (1959).

(10) J. K. Lee, Burdon Musgrave and F. S. Rowland, *J. Chem. Phys.*, **32**, 1266 (1960).

(11) See J. K. Lee, Burdon Musgrave and F. S. Rowland, *J. Am. Chem. Soc.*, **82**, 3545 (1960), for details.

$\Sigma(CH_3T+CD_3T)$ in all samples containing deuterated methanes is lower than that observed by Wolfgang, *et al.*, for CH_4, and confirmed by us in comparable experiments, leading to the conclusion that the more important factor contributing to the observed HT/DT ratios is that a larger fraction of CH_4T complexes leads to HT than of CD_4 to DT. Qualitatively, it appears that "hot" reactions with CH_4 and with CD_4 are approximately in proportion to the mole fraction of each present, although a precise measure of this proportion requires separation and assay of CH_3T and CD_3T.

The HT/DT ratios observed in the CH_2D_2 systems represent solely the relative ease of abstraction of H or D in the reaction of a recoiling tritium atom with a given methane molecule. The observed ratio, except in the presence of excess reactive scavengers, is approximately 1.4 and is hence in excellent agreement with the ratio of the C–H/C–D bond vibrational frequencies.

In each system, as the mole fraction of oxygen becomes quite large, the HT/DT ratio drops toward unity, and the ratio of total hydrogen activity to total methane activity is sharply reduced. In the presence of O_2, a large fraction of atoms will react with O_2 instead of methane, and will form HTO eventually rather than either labeled hydrogen or methane. The total observed activity in hydrogen and methane is also decreased by factors of as much as 5 of the high scavenger concentrations. The probable explanation for the change in HT/DT ratio is that tritium atoms reacting with methane in mixtures of high scavenger content have a higher average energy at the time of reaction than tritium atoms reacting in mixtures with low or zero scavenger content. This increase in average energy at reaction would tend to eliminate isotopic preferences in the abstraction reaction, and apparently also strongly favors the substitution reaction to form labeled methane *vis-à-vis* the abstraction reaction to form labeled hydrogen in "hot" reaction with methane.

NOTE ON THE FUOSS–KRAUS EQUATION FOR THE CONDUCTANCE OF SOLUTIONS CONTAINING ION-TRIPLETS

By E. C. Baughan

Chemistry Department, Royal Military College of Science, Shrivenham, Berks, England

Received May 9, 1960

Many electrolytes, particularly in solvents of low dielectric constant, show a minimum in the equivalent conductance Λ as C increases. In 1933 Fuoss and Kraus[1] explained this in terms of bilateral ion-triplet formation, thus: $MX \rightleftarrows M^+ + X'$, $MX + M^+ \rightleftarrows M_2{}^+X$, $MX + X' \rightleftarrows MX_2'$; they showed that, if certain approximations are legitimate, this explanation leads to the equation

$$\Lambda\sqrt{C} = A + BC \qquad (1)$$

where A and B are constant for a given solvent–solute system at a given temperature.

This equation has been widely applied, and most modern treatises discuss it at length. The author hopes therefore that the following simple *mathematical* consequence may prove useful.

All systems obeying equation 1 will show the *same* curve if the logarithms of Λ and C are plotted against one another, and this curve is symmetrical as log C varies about the log of the concentration C_m at which Λ has its minimum value Λ_m.

The proof is easy. From equation 1 Λ has a minimum Λ_m at a concentration C_m, and

$$\Lambda_m\sqrt{C_m} = 2BC_m = 2A \qquad (2)$$

Consider the value Λ_x of Λ at some other concentration C_x where

$$C_x = xC_m \qquad (3)$$

It may easily be shown that

$$\Lambda_x/\Lambda_m = \frac{(x+1)\sqrt{x}}{2x} \qquad (4)$$

so that a plot of log Λ against log C gives the *same* curve for all electrolytes if the points (log Λ_m, log C_m) are superposed. The proof of symmetry easily follows since

$$\frac{(x+1)\sqrt{x}}{2x} \equiv \frac{\left(\frac{1}{x}+1\right)\sqrt{\frac{1}{x}}}{2/x} \qquad (5)$$

This check on equation 1 is easy as the curve can once and for all be plotted on a transparency. And it is probably the most satisfactory way of fitting 1 to experimental data since the errors in Λ are usually proportional rather than absolute and since C is usually varied over a wide range, so that it is difficult to give due weight to both the dilute and concentrated solutions.

(1) R. M. Fuoss and C. A. Kraus, *J. Am. Chem. Soc.*, **55**, 2387 (1933).

FORMATION CONSTANTS OF 6-METHYL-3-PICOLYLAMINE WITH COPPER, NICKEL, CADMIUM AND SILVER IONS

By Harry R. Weimer[1] and W. Conard Fernelius

Department of Chemistry, the Pennsylvania State University, University Park, Penna.

Received June 24, 1960

Formation constant data for complexes of 2-picolylamine, 2-picolylmethylamine and 2-(2-amino ethyl)-pyridine with several metal ions were reported recently.[2] These data are now augmented by similar data for 6-methyl-2-picolylamine with copper, nickel, cadmium and silver ions (Table I). No values for zinc could be obtained because of precipitation. For cobalt(II) the values for both log K_1 and log K_2 varied with the value of $\bar{n}$ chosen for calculations; approximate values at 40° are 3.5 ± 0.2 and 3.0 ± 0.2.

Discussion

6-Methyl - 2 - picolylamine is a slightly stronger base than 2-picolylamine although the effect of substitution of methyl for hydrogen on the pyridyl nucleus is not as great as the effect of substitution on the primary amine group. However, the forma-

(1) Holder of a National Science Foundation Research Participation Award for the Summer of 1959.

(2) D. E. Goldberg and W. C. Fernelius, This Journal, **63**, 1246 (1959).

TABLE I

VALUES FOR THE THERMODYNAMIC QUANTITIES LOG K_n, $-\Delta F_n$, $-\Delta H_n$ AND ΔS_n INVOLVED IN THE REACTION AT 10, 20, 30 AND 40° OF SEVERAL METAL IONS WITH 6-METHYL-2-PICOLYLAMINE

$t°$, C.	H^+	Cu^{++}	Ni^{++}	Cd^{++}	Ag^+	H^+	Cu^{++}	Ni^{++}	Cd^{++}	Ag^+
			log K_1					log K_2		
10	9.18 ±0.01	7.18 ±0.01	5.05 ±0.04	4.22 ±0.05	4.40 ±0.04	2.9 ±0.1	6.03 ±0.01	3.23 ±0.04	2.84 ±0.08	3.47 ±0.07
20	9.83 ±0.01	6.95 ±0.01	4.85 ±0.02	4.09 ±0.01	4.14 ±0.08	2.9 ±0.1	5.79 ±0.01	3.05 ±0.06	2.74 ±0.05	3.46 ±0.08
30	8.70 ±0.01	6.81 ±0.01	4.71 ±0.03	4.01 ±0.06	3.97 ±0.05	2.9 ±0.1	5.65 ±0.01	3.02 ±0.05	2.69 ±0.08	3.45 ±0.09
40	8.48 ±0.01	6.69 ±0.01	4.64 ±0.01	3.89 ±0.05	3.73 ±0.04	2.9 ±0.1	5.51 ±0.01	2.85 ±0.05		3.39 ±0.11
			ΔH_1 (kcal./mole)					$-\Delta H_2$ (kcal./mole)		
10–40	9.3	6.86	5.86	4.52	9.34		7.23	4.99	−0.52	1.07
			ΔS_1 (cal./mole-deg.)					ΔS_2 (cal./mole-deg.)		
10	9.2	8.6	2.4	3.3	−12.9		2.0	−2.9	14.8	12.1
20	9.2	8.4	2.2	3.3	−12.9		1.8	−3.1	14.3	12.2
30	9.1	8.5	2.2	3.4	−12.7		2.0	−2.6	14.1	12.2
40	9.1	8.7	2.5	3.4	−12.8		2.1	−2.9	14.9	12.1

tion constant values for 6-methyl-2-picolylamine with various metal ions are significantly less than the corresponding values for 2-picolylamine. For Cu^{++} the difference between the two amines is >2 in both log K_1 and log K_2; for Ni^{++} it is >2 in log K_1, but >3 in log K_2; for Cd^{++} it is very small in log K_1 but >1 in log K_2. Further, no values for log K_3 could be measured for Cu^{++}, Ni^{++} or Cd^{++}. It is obvious that the steric effect of methyl substitution on the pyridine nucleus is much greater than substitution on the primary amine group.

The findings with Ag^+ are especially interesting. In view of the inability of both nitrogen atoms of the ethylenediamine molecule to coördinate to the same silver ion[3] it is unlikely that both nitrogens in 6-methyl-2-picolylamine coördinate to the same silver ion. The magnitude of the log K_n values supports the view that coördination is through the primary amine nitrogen rather than through the heterocyclic nitrogen.[4] However, in a plot of log K *vs.* pK_{AH} the values recorded here lie well above the line of proportionality found for simple amines. Further, the value for log K_2 is less than that for log K_1 which is unusual among silver complexes with monodentate ligands.[3]

Experimental

The preparation of solutions of metal ions as perchlorates, measurements and calculations were performed as described previously.[1] 6-Methyl-2-picolylamine (Aldrich Chemical Company, Inc.) was distilled twice at 75–75.6°, 6–7 mm. before preparing solutions.

(3) G. Schwarzenbach, B. Maissen and H. Ackermann, *Helv. Chim. Acta*, **35**, 2333 (1952); G. Schwarzenbach, H. Ackermann, B. Maissen and G. Anderegg, *ibid.*, **35**, 2337 (1952); G. Schwarzenbach, *ibid.*, **36**, 23 (1953).

(4) R. J. Bruehlmann and F. H. Verhoek, *J. Am. Chem. Soc.*, **70**, 1401 (1948).

SHOCK TUBE EXPERIMENTS ON THE PYROLYSIS OF ACETYLENE

BY GORDON B. SKINNER AND EDWARD M. SOKOLOSKI

Monsanto Chemical Company, Research and Engineering Division Research Department, Dayton, Ohio

Received June 29, 1960

Shock tube studies on the pyrolysis of acetylene have been reported by Greene, Taylor and Patterson,[1] who have also mentioned some of the earlier work on acetylene pyrolysis by other techniques. Actually, the shock tube experiments are in a class by themselves with respect to temperatures, heating times and wall effects, and comparisons with other work are difficult to make. The present paper agrees with Greene's results in some respects, and disagrees in others.

Experimental

The single-pulse shock tube described earlier[2] was used, with identical techniques and methods of calculation. As before, helium–nitrogen mixtures were used as "driver gas." Experimental temperatures were corrected for variations in temperature due to minor pressure fluctuations during the runs, and for heat effects from chemical reaction. Vapor chromatographic analyses were made for H_2, C_2H_6, C_2H_4 and C_2H_2 in all of the experiments, for C_3 and C_4 hydrocarbons in most, and for CH_4 and CO in a few.

Experiments were carried out with the gas mixtures listed in Table I. Total reaction pressures were five atmospheres, and dwell times two milliseconds. Matheson acetylene, washed with concentrated sulfuric acid and passed through an Ascarite–Drierite column, and Airco helium, nitrogen, hydrogen and argon, were used without further purification. The gas mixtures always were analyzed before reaction. A trace of vinylacetylene was found in mixture I, but none in the other mixtures since the acetylene content was lower.

Results

For mixtures 1 and 2, the chief pyrolysis products were hydrogen and vinylacetylene, although small amounts of C_2H_4, CH_4, C_3H_8 and CO also were found. Carbon was deposited in the shock tube in the higher temperature runs. The amount of acetylene decomposing increased from about 2% at 1150°K. to about 50% at 1800°K., for mixture 1.

Below about 1500°K. no hydrogen was found, and the amount of vinylacetylene produced corresponded fairly well with the acetylene which disappeared. Above 1500°K. hydrogen formed, but

(1) E. F. Greene, R. L. Taylor and W. L. Patterson, Jr., THIS JOURNAL, **62**, 238 (1958).

(2) G. B. Skinner and R. A. Ruehrwein, *ibid.*, **63**, 1736 (1959).

less than that calculated from the loss of acetylene corrected for the formation of vinylacetylene, assuming carbon to be the only product. There must therefore have been some undetected hydrocarbons present, containing (on the average) less than one atom of hydrogen per atom of carbon.

TABLE I

REACTION MIXTURE COMPOSITIONS

Mixture	Mole % of component C_2H_2	H_2	Ar
1	6.0	..	94.0
2	1.42	..	98.58
3	1.41	8.47	90.12

From the analytical data, the heating time of 2 milliseconds, the total pressure of 5 atmospheres, and the mole per cent. of Table I, rate constants for acetylene conversion to vinylacetylene, and also for total acetylene decomposition, were calculated. Comparison of the results at the two partial pressures (0.3 and 0.07 atmosphere) suggests that the reaction rates are proportional to the square of the acetylene pressure, so second-order rate constants are shown in Fig. 1.

For mixture 3, up to 3.7% of the acetylene was converted to ethylene, but this reaction is discussed in another paper.[3] Butadiene was the only other product found in significant amount. Moreover, up to 1800°K. the amounts of butadiene and ethylene found accounted fairly well for the decrease in acetylene concentration. Second-order rate constants for butadiene formation were calculated and plotted in Fig. 1, where it is seen that they lie close to those for vinylacetylene formation in the other two mixtures.

A point of difference between these results and those of Greene and co-workers is that they found considerable diacetylene and smaller amounts of vinylacetylene, while we found vinylacetylene to be the major product, with no detectable amount of diacetylene. The absence of diacetylene is not surprising at the low temperatures where no hydrogen was found, but it might be expected to form at higher temperatures. The fact that our samples were more highly diluted with argon than Greene's may have something to do with this difference in products. On the other hand, the rate constants for the conversion of acetylene to all products in Fig. 1 are in agreement with Greene's within the rather large experimental errors in both sets of data.

It seems clear that, in the range of temperatures and pressures studied, the first step in acetylene decomposition is dimerization. The subsequent steps have not been defined, but probably involve further polymerizations and condensations to produce benzene and condensed aromatic compounds which eventually may be thought of as carbon, as discussed by Gordon, Smith and McNesby.[4]

Since the rate constants for butadiene formation are close to those for vinylacetylene formation, it is likely that butadiene is formed by hydrogenation of vinylacetylene. The better material balances for mixture 3 show that butadiene is not as active a condensation intermediate as is vinylacetylene. In other words, hydrogen inhibits acetylene decomposition by converting reactive vinylacetylene to relatively unreactive butadiene.

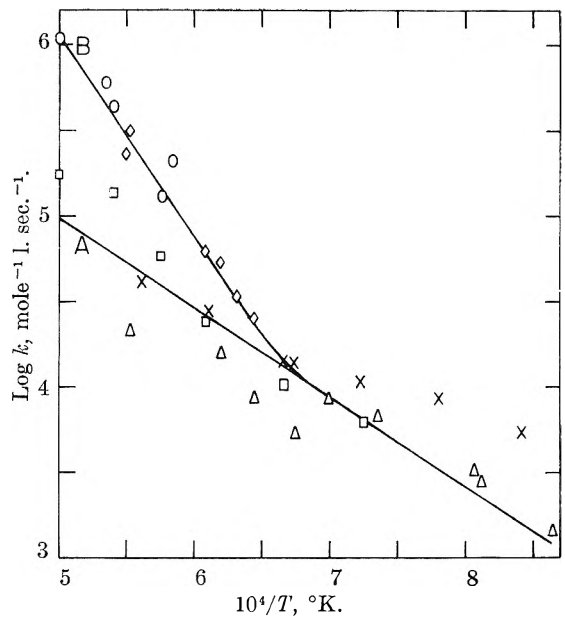

Fig. 1.—Second-order rate constants for acetylene pyrolysis: Δ, mixture 1, conversion to C_4H_4; ◇, mixture 1, conversion to all products; □, mixture 2, conversion to C_4H_6; ○, mixture 2, conversion to all products; ×, mixture 3, conversion to C_4H_6; curve A, conversion to C_4H_4; curve B, conversion to all products.

(3) G. B. Skinner and E. M. Sokoloski, THIS JOURNAL, **64**, 1028 (1960).

(4) A. S. Gordon, S. R. Smith and J. R. McNesby, "Seventh Symposium (International) on Combustion," 1959, pp. 317.

LOW TEMPERATURE HEAT CAPACITY AND ENTROPY OF BERLINITE

BY EDWARD P. EGAN, JR., AND ZACHARY T. WAKEFIELD

Division of Chemical Development, Tennessee Valley Authority, Wilson Dam, Alabama

Received July 8, 1960

Aluminum phosphates are among the compounds whose properties are of interest in connection with soil-fertilizer relationships. Presented here are the results of measurements of the heat capacity of berlinite ($AlPO_4$, the form of anhydrous aluminum phosphate stable at room temperature) over the interval 10 to 300°K., together with values derived therefrom for the entropy and enthalpy at 298.16°K.

Materials and Apparatus.—The method of preparation of berlinite was that described by Stanley.[1] Euhedral double-pyramid crystals about 1 mm. long were obtained. Their optical and X-ray properties agreed with the known data for berlinite. As the crystals contained a significant number of bubble inclusions, they were ground and washed with warm 10% HCl solution. The product, washed free of chlorides, was dried and screened to obtain a −42 +150-mesh fraction for filling the calorimeter. Spectrographic analysis showed traces of copper and silicon. The P_2O_5 content was 58.23% (stoichiometric value, 58.20%). Alumina was not determined because of the difficulty of its precise determination on this type of compound. An ignition loss of 0.04% at 500° was considered negligible.

The low temperature adiabatic vacuum calorimeter has been described.[2] Multiple vertical copper vanes, soldered

(1) J. M. Stanley, *Ind. Eng. Chem.*, **46**, 1684 (1954).

TABLE I

OBSERVED MOLAL HEAT CAPACITY OF BERLINITE, $AlPO_4$(c), CAL. DEG.$^{-1}$

T, °K.	ΔT	C_p	T, °K.	ΔT	C_p
9.42	2.08	0.034	142.11	6.06	12.03
9.64	2.50	.034	145.13	3.36	12.28
13.20	4.72	.108	148.49	6.71	12.56
13.79	4.93	.126	150.90	8.17	12.76
17.68	3.95	.308	155.09	6.50	13.09
18.82	4.71	.376	158.53	7.10	13.37
22.00	4.52	.606	161.89	7.09	13.63
23.94	4.93	.768	169.25	7.64	14.21
26.53	4.44	1.000	176.97	7.79	14.79
28.77	4.64	1.217	180.36	7.94	15.04
30.79	4.01	1.420	184.83	7.93	15.37
34.05	5.85	1.756	188.54	8.42	15.63
35.11	4.58	1.873	192.83	8.07	15.94
40.01	6.03	2.391	195.94	2.10	16.15
40.38	5.92	2.433	196.98	4.18	16.22
46.13	5.58	3.059	200.09	6.21	16.44
46.36	6.64	3.081	203.17	8.20	16.64
51.06	4.26	3.596	207.25	8.11	16.92
51.98	4.60	3.695	211.27	8.01	17.18
53.52	3.51	3.835	215.27	7.93	17.46
54.51	6.14	3.938	219.19	7.82	17.70
57.49	4.43	4.241	223.31	8.15	17.97
59.96	4.76	4.498	227.32	8.43	18.21
62.52	5.64	4.768	231.56	8.35	18.49
65.02	5.34	5.025	235.66	8.26	18.73
67.87	5.07	5.304	239.90	5.95	19.00
70.59	5.80	5.560	243.84	8.10	19.23
72.96	5.12	5.787	247.26	8.77	19.45
75.72	4.46	6.058	251.86	7.94	19.71
77.90	4.75	6.280	255.95	8.60	19.95
80.17	4.35	6.532	259.74	7.81	20.15
80.52	5.68	6.559	263.60	6.70	20.38
85.59	6.48	7.053	267.48	7.68	20.59
86.64	6.56	7.143	271.45	9.02	20.82
91.52	5.39	7.572	274.12	1.73	20.94
94.16	8.48	7.827	275.11	7.57	21.02
97.19	5.94	8.100	276.07	5.14	21.07
100.96	5.11	8.439	277.04	4.11	21.12
103.52	6.73	8.672	281.47	4.75	21.36
107.10	5.39	8.987	283.03	8.78	21.46
110.07	6.37	9.257	286.20	4.71	21.63
113.55	7.51	9.568	289.92	5.00	21.83
116.30	6.08	9.817	291.49	5.88	21.91
119.51	4.41	10.09	294.73	4.62	22.08
122.72	6.78	10.38	296.74	4.62	22.19
125.02	6.62	10.57	299.00	3.93	22.31
130.02	5.57	10.98	300.68	3.27	22.41
131.95	7.25	11.17	304.04	6.16	22.58
135.94	6.27	11.52	310.32	6.41	22.91
139.48	7.81	11.81			

at internal and external walls, were arranged so that no part of the sample was more than 2 mm. from a metal surface. One defined calorie was taken as 4.1840 abs. j.—the ice point as 273.16°K. Temperatures were read to four decimal places and were so used in the calculation of small differences; the last two places were dropped in the final tabulation of temperature.

Observations.—The observed molal heat capacities, as measured on a charge of 118.856 g. (vacuum) or 0.9746 mole of berlinite, are shown in Table I—molal thermodynamic properties at integral temperatures in Table II. The average deviation of the observed from the smoothed heat capacities was less than 0.1% except at temperatures below 30°K., where the small magnitudes impaired the accuracy.

TABLE II

MOLAL THERMODYNAMIC PROPERTIES OF BERLINITE, $AlPO_4$(c), CAL. DEG.$^{-1}$

T, °K.	C_p	S^0	$H^0 - H_0^0$
10	0.031	0.006	0.049
15	.186	.045	.548
20	.456	.132	2.098
25	.858	.275	5.336
30	1.340	.473	10.81
35	1.857	.718	18.80
40	2.393	1.001	29.42
45	2.934	1.314	42.74
50	3.473	1.651	58.76
60	4.505	2.376	98.69
70	5.505	3.147	148.8
80	6.500	3.946	208.8
90	7.454	4.768	278.6
100	8.353	5.599	357.6
110	9.250	6.438	445.7
120	10.13	7.281	542.6
130	11.00	8.126	648.3
140	11.85	8.973	762.6
150	12.69	9.820	885.3
160	13.48	10.66	1016
170	14.26	11.50	1155
180	15.02	12.34	1301
190	15.74	13.17	1455
200	16.43	14.00	1616
210	17.10	14.82	1784
220	17.75	15.63	1958
230	18.39	16.43	2139
240	19.00	17.23	2325
250	19.60	18.01	2519
260	20.17	18.79	2718
270	20.73	19.56	2922
280	21.29	20.33	3132
290	21.83	21.09	3348
300	22.37	21.83	3569
273.16	20.91	19.81	2988
298.16	22.27	21.70	3528

The entropy of crystalline berlinite at 298.16°K. is 21.70 e.u., with an estimated uncertainty interval of ±0.10 e.u. On the assumption that the solid represents the ideal state, the heat content, $H^0 - H_0^0$, at 298.16°K. is 3528 cal. mole^{-1}.

An evaluation of the entropy of the hydrated aluminum phosphate variscite ($AlPO_4 \cdot 2H_2O$) was desired also, but attempts to prepare it in pure species were fruitless. An estimated entropy of 40.5 e.u. for variscite was obtained by addition of 9.4 e.u. per mole of water[3] to the entropy of berlinite.

The calculations were made on an IBM 704 computer. As little has been reported on the application of electronic computers to heat capacity data, a brief description of the calculation, which may be termed a method of "running 30° equations," is in order.

The data were treated in overlapping 30° intervals, *e.g.*, 0–30, 10–40, 20–50°, and so on up to

(2) E. P. Egan, Jr., Z. T. Wakefield and K. L. Elmore, *J. Am. Chem. Soc.*, **73**, 5579, 5581 (1951).

(3) W. M. Latimer, *ibid.*, **73**, 1480 (1951).

280–310°K. The solution was complete in each 30° range; it involved cubic equations expressing the variations of the full calorimeter, the empty calorimeter (plus curvature correction[4]), and observed calories per mole with variation in temperature. There resulted three values of heat capacity, differing in the second or third decimal place, at each observed temperature and at each integral degree. The values were weighted according to an arbitrary weighting curve based on the normal distribution curve (a maximum of 80% at the mid-point of each 30° range and 0% at the ends). The weighted values were collected into a composite table and tabular integrations (through use of 5-point Lagrangian coefficients[5]) were made at 1° intervals for entropy and enthalpy increments. The low end of the table was filled in by plotting C_p/T against T^2 and extrapolating to 0°K.

Acknowledgment.—J. H. Christensen suggested the method of calculation. R. L. Dunn and J. W. Williard made the chemical analyses, J. P. Smith the X-ray examinations and A. W. Frazier the petrographic examinations.

(4) R. B. Scott, C. H. Meyers, R. D. Rands, Jr., F. G. Brickwedde and N. Bekkedahl, *J. Research Natl. Bur. Standards*, **35**, 39 (1945).

(5) Works Progress Administration, Mathematical Tables Project, "Tables of Lagrangian Interpolation Coefficients," Columbia University Press, New York, N. Y., 1944.

LOW TEMPERATURE HEAT CAPACITY AND ENTROPY OF POTASSIUM METAPHOSPHATE

BY EDWARD P. EGAN, JR., AND ZACHARY T. WAKEFIELD

Division of Chemical Development, Tennessee Valley Authority, Wilson Dam, Alabama

Received July 8, 1960

Potassium metaphosphate, KPO_3, commands interest as an experimental fertilizer containing two major plant-food elements in chemical combination. As part of a continuing program of determining the thermodynamic properties of compounds of interest in fertilizer technology, the heat capacity of potassium metaphosphate was measured over the interval 10 to 300°K., and values of entropy and enthalpy at 298.16°K. were derived therefrom.

Materials and Apparatus.—Potassium dihydrogen phosphate (KH_2PO_4, reagent grade) was fused in a platinum dish in a pot furnace at 875° to yield potassium metaphosphate. The melt crystallized readily when air-quenched. Six melts were required; three appeared in an optical examination to be a single crystalline phase and three contained a trace of glass. The composite sample was ground in an agate mortar and passed through a 20-mesh sieve. The product, washed three times with water and three times with acetone, was dried at 105°.

The literature contains neither optical nor X-ray powder diffraction data for KPO_3. Optical properties and interplanar spacings that were calculated from the X-ray unit-cell data of Corbridge[1] agreed with the observed data for the product described here. The optical examination showed that the euhedral crystals were repeated twins containing 10 or more crystals per unit. Spectrographic analysis showed traces of Al, Mg, Si and Na. Chemical analyses gave 39.96 and 39.87% K_2O, 60.09 and 60.05% P_2O_5 (stoichiometric values, 39.89% K_2O and 60.11% P_2O_5).

The low temperature copper adiabatic calorimeter has been described.[2] Temperatures were read to four decimal places and were so used in calculation of small temperature differences; they were rounded to two decimal places in the final tabulation. The defined calorie was taken as 4.1840 abs. j.—the ice point as 273.16°K.

TABLE I

OBSERVED MOLAL HEAT CAPACITY OF POTASSIUM METAPHOSPHATE, KPO_3(c), CAL. DEG.$^{-1}$

T, °K.	ΔT	C_p	T, °K.	ΔT	C_p
9.61	2.87	0.081	141.67	7.59	14.08
11.07	3.18	.122	144.72	7.46	14.28
14.80	4.07	.300	149.14	7.36	14.56
16.09	3.30	.386	152.50	8.09	14.77
18.33	2.90	.577	156.42	7.18	15.01
19.35	3.11	.676	160.47	7.86	15.25
21.72	3.82	.940	163.72	7.43	15.44
22.20	2.54	.998	168.05	7.30	15.70
24.52	5.19	1.302	171.06	7.25	15.88
25.26	3.53	1.406	174.89	6.36	16.09
25.76	4.21	1.478	178.44	7.50	16.29
28.86	3.60	1.947	181.78	7.42	16.47
29.92	5.59	2.115	185.87	7.36	16.68
30.35	4.93	2.181	189.32	7.66	16.86
33.13	4.92	2.640	193.16	7.22	17.06
36.11	6.79	3.142	196.05	2.18	17.20
36.20	6.75	3.154	197.44	5.23	17.28
38.36	5.51	3.518	200.17	6.05	17.41
43.03	7.02	4.282	203.06	6.02	17.55
43.09	7.00	4.288	206.38	6.39	17.71
44.15	6.05	4.461	209.04	5.94	17.83
49.40	5.61	5.294	212.52	5.89	18.00
49.87	6.66	5.368	214.94	5.87	18.11
50.45	6.54	5.455	217.96	4.99	18.26
52.98	1.52	5.822	220.34	5.82	18.37
54.28	2.99	6.014	223.13	5.35	18.49
55.41	4.84	6.178	229.46	7.32	18.78
58.05	4.56	6.537	233.06	6.49	18.95
60.83	6.00	6.920	235.71	7.24	19.08
63.19	5.73	7.231	239.51	6.41	19.23
66.53	5.40	7.650	242.70	6.74	19.38
69.02	5.92	7.933	246.08	6.74	19.51
72.06	5.67	8.269	249.40	6.67	19.66
75.04	6.12	8.599	252.78	6.66	19.78
77.84	5.89	8.913	256.04	6.60	19.92
79.40	3.41	9.079	259.41	6.59	20.05
81.29	6.66	9.285	262.79	6.91	20.19
87.72	6.21	9.928	265.96	6.52	20.32
91.46	6.60	10.25	269.09	5.70	20.45
94.06	6.46	10.48	272.45	6.45	20.58
97.61	5.71	10.78	274.68	2.87	20.65
100.37	6.16	11.02	276.42	6.08	20.74
103.47	6.01	11.27	278.55	4.88	20.81
106.66	6.42	11.53	281.27	3.62	20.92
109.62	6.29	11.76	283.82	5.65	21.02
113.21	6.68	12.05	286.47	6.78	21.13
116.28	7.05	12.29	289.45	5.62	21.23
120.00	6.91	12.58	292.43	5.14	21.34
123.44	7.26	12.83	295.05	5.57	21.44
127.03	7.14	13.07	297.74	5.49	21.54
130.81	7.48	13.33	303.61	6.23	21.76
134.18	7.39	13.57	310.01	6.57	22.01
137.84	6.31	13.83			

Observations.—The calorimeter contained 107.412 g. (vacuum) or 0.9097 mole of KPO_3. The

(1) D. E. C. Corbridge, *Acta Cryst.*, **8**, 520 (1955).

(2) E. P. Egan, Jr., Z. T. Wakefield and K. L. Elmore, *J. Am. Chem. Soc.*, **73**, 5579, 5581 (1951).

observed molal heat capacities are shown in Table I—molal thermodynamic properties at integral temperatures in Table II. The average deviation of the observed from the smoothed heat capacities was well under 0.1% except at temperatures below 20°K., where the small magnitudes impaired the accuracy.

TABLE II

MOLAL THERMODYNAMIC PROPERTIES OF POTASSIUM METAPHOSPHATE, KPO_3(c), CAL. DEG.$^{-1}$

T, °K.	C_p	S^0	$H^0 - H_0^0$
10	0.082	0.018	0.144
15	.331	.093	1.114
20	.748	.241	3.727
25	1.370	.471	8.943
30	2.128	.786	17.65
35	2.947	1.175	30.32
40	3.784	1.623	47.15
45	4.600	2.117	68.13
50	5.383	2.642	93.10
60	6.809	3.753	154.2
70	8.043	4.897	228.6
80	9.143	6.044	314.7
90	10.12	7.180	411.1
100	10.98	8.291	516.7
110	11.80	9.377	630.6
120	12.57	10.44	752.5
130	13.28	11.47	881.8
140	13.97	12.48	1018
150	14.62	13.47	1161
160	15.23	14.43	1310
170	15.81	15.37	1466
180	16.37	16.29	1626
190	16.90	17.19	1793
200	17.40	18.07	1964
210	17.88	18.93	2141
220	18.35	19.77	2322
230	18.81	20.60	2508
240	19.26	21.41	2698
250	19.68	22.20	2893
260	20.08	22.98	3092
270	20.48	23.75	3294
280	20.87	24.50	3501
290	21.25	25.24	3712
300	21.63	25.97	3926
273.16	20.60	23.98	3359
298.16	21.56	25.83	3886

The entropy of KPO_3(c) at 298.16°K. is 25.83 e.u., with an estimated uncertainty interval of ±0.10 e.u. On the assumption that the solid represents the ideal state, the heat content, $H^0 - H_0^0$, at 298.16°K. is 3886 cal. mole^{-1}. No allowance was made for possible strain introduced by the repeated twinning. The calculations were based on the simple formula weight for KPO_3, although Lamm[3] suggested that the molecular weight may be as high as 10^4 to 10^6. The calculations were made on an IBM 704 computer by a method that has been described.[4]

Acknowledgment.—J. R. Lehr and A. W. Frazier made the petrographic examination, J. P. Smith the X-ray examination and Inez Murphy the chemical analyses.

(3) O. Lamm, *Arkiv Kemi, Mineral. Geol.*, **17A**, No. 25, 27 (1944).

(4) E. P. Egan Jr., and Z. T. Wakefield, THIS JOURNAL, **65**, 1953 (1961).

INFRARED INTENSITY STUDIES OF A SERIES OF N,N-DISUBSTITUTED AMIDES

BY C. D. SCHMULBACH[1] AND RUSSELL S. DRAGO

W. A. Noyes Laboratory, University of Illinois, Urbana, Illinois

Received July 27, 1960

The heats of formation of amide–iodine complexes for a series of amides of the type $R'CON(R)_2$ have been determined in this Laboratory with the purpose of systematically studying the relative basic properties of amides.[2] A search for additional criteria to be used in establishing the relative basicity of amides led to an investigation of the integrated intensity of the amide carbonyl band. In the past, considerable success has been achieved in arriving at empirical or semi-empirical relationships between integrated intensities of a group vibration for a series of homologous compounds and a basicity or reactivity parameter indicated by σ or σ^* values for substituents.[3] It is shown that in the N,N-dimethylamide series no such correlation exists. It is further demonstrated that intensity cannot be used as a criterion for basicity in this series. A tentative explanation of the intensity data is proposed.

Experimental

Materials.—The preparation and purification of the amides and the purification of the solvent carbon tetrachloride have been described earlier.[4]

Apparatus and Procedure.—The spectra of the amides were measured on a Perkin–Elmer Model 21 double-beam spectrometer fitted with a sodium chloride prism. The slit width was allowed to vary, in accordance with a fixed slit program, from the limits of 51 μ at 1735 cm.$^{-1}$ to 59 μ at 1600 cm.$^{-1}$. The spectral slit widths, s, as computed from curves provided by Perkin–Elmer Corporation, varied only slightly from the value of 11 cm.$^{-1}$. The wave length linearity in the carbonyl region was determined using water vapor spectra. The area under the carbonyl band, 50 cm.$^{-1}$ to either side of the frequency at maximum absorbance, was calculated by the application of Simpson's rule using intervals of 2.5 cm.$^{-1}$. At least four determinations were made on samples of each compound. The values for the apparent integrated intensities of the carbonyl band were calculated. The concentration of amides was corrected for volume expansion of the solvent at elevated temperatures.[5] Values for the intensity A were calculated according to the method of Wilson and Wells.[6] Wing corrections were not applied. The half-widths in cm.$^{-1}$ are contained in Table I.

Results

The numerical results of intensity measurements are given in Table I along with results reported[7] on the primary amides.

As reported earlier,[2] the addition of iodine to a carbon tetrachloride solution of an amide gives rise to splitting of the carbonyl vibration frequency. The new peak which appears always at lower frequencies than the major band has been assigned to an amide molecule which is bound to iodine through

(1) Eastman Kodak Fellow, 1957–1958.

(2) C. D. Schmulbach and Russell S. Drago, *J. Am. Chem. Soc.*, **82**, 4484 (1960).

(3) T. L. Brown, *Chem. Revs.*, **58**, 581 (1958).

(4) R. S. Drago and C. D. Schmulbach, THIS JOURNAL, to be published.

(5) See "International Critical Tables," Vol. III, McGraw–Hill Book Co., New York, N. Y., p. 28.

(6) E. B. Wilson, Jr., and A. J. Wells, *J. Chem. Phys.*, **14**, 578 (1946).

(7) T. L. Brown, J. F. Regan, R. D. Schuetz and J. C. Sternberg, THIS JOURNAL, **63**, 1324 (1959).

TABLE I

INTEGRATED INTENSITY VALUES[a] FOR THE CARBONYL BAND OF A SERIES OF AMIDES MEASURED IN CARBON TETRACHLORIDE AT 30°

Amide		A	λ_{max} (cm.$^{-1}$)	$\Delta\nu_{1/2}$, cm.$^{-1}$
N,N-Dimethylformamide	DMF	5.78	1685	14
		5.70[b]		
N,N-Dimethylacetamide	DMA	4.78	1662	23
N,N-Dimethylpropionamide	DMP	4.22	1660	22
N,N-Dimethylbenzamide	DMB	4.51	1644	19
N,N-Diethylacetamide	DEA	3.90	1650	24
Formamide[c]		4.22	1709	15
Acetamide[c]		4.21	1678, 1702	
Propionamide[c]		3.85	1687	
Benzamide[c]		4.06	1678	21

[a] Values for integrated intensities are in units of 1×10^{-4} l. mol.$^{-1}$ cm.$^{-2}$. [b] Intensity value obtained at 50°. [c] Data from reference 7, measured in chloroform.

the carbonyl oxygen. The integrated intensity values for the complexed amide carbonyl bands were calculated by Method I described by Ramsay.[8] Since the two bands overlap, and errors in the method introduce considerable inaccuracies of the order of 30%, the data are not reported. The intensities of these bands were always much larger than those of the uncomplexed amide which had been calculated in the same fashion. The transfer of electron density in the complex from the carbonyl oxygen to the acceptor gives rise to increased importance of the ionic form in the vibrational excited state as compared to the ground state and also increases the length of the dipole in the ionic form, both resulting in larger values for integrated intensities. An increase in intensity also is reported to occur upon the addition of iodine to other solutions containing carbonyl compounds.[9]

Discussion

The intensity data (Table I) reveal several interesting effects. In the primary amides ($RCOHN_2$), it has been found[7] that there is no correlation between the carbonyl intensity and the inductive effect of the R substituent as measured by the substituent constant σ^*.[10]

A pronounced decrease in intensity is observed in propionamide compared to acetamide. It is proposed that rotational isomers exist in propionamide and the presence in one isomer of a bulky group *cis* to the carbonyl lowers the intensity. An irregular

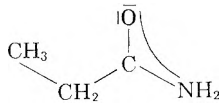

band shape indicative of rotational isomers is obtained for propionamide.[7] The same effect is indicated by our data for the intensity values for the N,N-dialkyl substituted amides. The low values obtained for DMP and DEA relative to the value for DMA are in part caused by this effect.

The decrease in intensity of DMA relative to DMF is not encountered in the primary amides (formamide and acetamide). This difference can be attributed to an internal steric interaction present in the N,N-dialkyl amides but not in the primary amides. The amides may be considered as resonance hybrids of limiting structures I and II

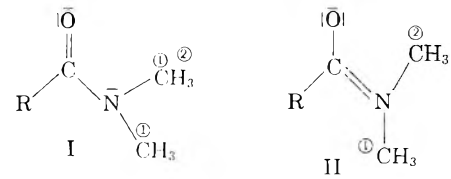

The rather sizable values of 22 and 19 kcal. calculated[11,12] for the free energy of activation necessary for reorientation around the C–N bond of DMF and DMA, respectively,[11] emphasize the rigidity of the planar O–C–N system. Both the intensity data and the entropy of formation of the DMA–I_2 complex[2] can be explained by assuming that when R is a large group it undergoes steric interaction with the CH_3 group designated as one. In the course of the normal vibration corresponding to the adsorption at 1662 cm.$^{-1}$, the carbon–oxygen bond lengthens and the C–N bond shortens.[4] This causes the $-CH_3$ groups to interact and inhibits further lengthening of the carbon–oxygen bond. The maximum value for the bond moment that may be attained is decreased for DMA and a corresponding decrease is observed in the intensity. This effect is absent in DMF, so a larger intensity is obtained than for DMA. This type of steric effect is also absent in the primary amides where a similar intensity value is obtained for both formamide and acetamide.

It is informative to compare the integrated intensity of the amide carbonyl band with the basicity of the amide toward iodine. Both the stretching of the carbon–oxygen bond and coördination to oxygen by iodine should be effected by electron donating groups and a correlation might be expected.[3] It has been demonstrated[4] that the order of basicity is approximately DMB ≈ DMA ≈ DMP > DMF. There is obviously no correlation in this series between the intensity data and the basicity of the amides. The greater inductive effect of the methyl and ethyl substituents is shown clearly in the basicity measurements.

Two possible effects, either or both of which may be operative, will be proposed to explain the differences observed between the ΔH values and the integrated intensities.

(1) Upon interaction with radiation, the DMA molecule does not have time to rearrange its methyl groups to relieve repulsions in the period of time required to undergo a vibrational transition. Upon coördination to iodine such a rearrangement can occur. A larger than expected entropy of formation of the complex indicates rearrangement does occur.

(2) The steric interactions described above to explain the intensity data are weak interactions. When a strong electron demand is made upon the

(8) D. A. Ramsay, *J. Am. Chem. Soc.*, **74**, 72 (1952).

(9) H. Yamada and K. Kozima, *ibid.*, **83**, 1543 (1960).

(10) R. W. Taft, in "Steric Effects in Organic Chemistry," M. S. Newman, Editor, John Wiley and Sons, Inc., New York, N. Y., 1956.

(11) H. S. Gutowsky and C. H. Holm, *J. Chem. Phys.*, **25**, 1228 (1956).

(12) W. D. Phillips, *ibid.*, **23**, 1363 (1955).

system, such as that involved in iodine coördination, these weak interactions have little effect on the ΔH value. These effects are slight compared to the energies of bond formation, can be overcome in part by rearrangement, and are manifested in the entropy change.[4]

This study indicates that intensity values are not reliable criteria for basicity when steric effects may be operative in the system under consideration although sometimes they have been shown[3] to parallel both basicity and reactivity in systems free from steric interactions.

Acknowledgment.—The authors gratefully acknowledge the financial support given by the Research Corporation and the very helpful discussion of the problem with Dr. T. L. Brown.

THE EFFECT OF PRESSURE ON THE RESTRICTION OF ROTATION ABOUT SINGLE BONDS

BY DONALD R. MCKELVEY AND K. R. BROWER

Department of Chemistry, New Mexico Institute of Mining and Technology, Campus Station, Socorro, New Mexico

Received June 27, 1960

Detailed calculations of the geometry and strain energy of the transition states for the racemization of a number of optically active biphenyls[1] lead to the conclusion that the chief mode of deformation is bending of the single bonds which hold the interfering groups. Since very little stretching should occur, there is no reason to expect that internal geometrical changes would produce a measurable increase in volume in the transition state. On the other hand it is likely that a significant part of the restriction of rotation arises from solvation of the polar interfering groups. It recently has been reported that the rates of racemization of biphenyls having ionic or polarized interfering groups are strongly dependent on the solvent and added salts.[2] If a considerable amount of electrostricted solvent is released during the activation process it should be possible to detect a decrease in rate with increasing pressure.

This preliminary survey reports the volume change of activation for the racemization of *d*-N-benzenesulfonyl-N-carboxymethyl-3-bromomesidine (I), *d*-N-benzenesulfonyl-N-carboxymethyl-1-amino-2,4-dimethyl-6-nitrobenzene (II) and *d*-N-benzenesulfonyl-N-carboxymethyl-1-amino-2-methylnaphthalene (III). The solvent used for I and III was dimethylformamide, whereas II was racemized in dimethylformamide, ethanol, and ethanol containing twice the amount of ammonium hydroxide required to neutralize the acid. The volume change of activation was calculated from the equation

$$-RT\,(\delta \ln k/\delta P)_T = \Delta V^*$$

in which k is the reaction rate constant.

The results are shown in Table I which lists the conditions, the rate constants in hr.$^{-1}$ at atmospheric pressure and at 1360 atm., and the volume change of activation in ml./mole. The rate constants were reproducible within 3% and the corresponding error in ΔV^* is 0.5 ml. All volume changes are very small in comparison to the molar volumes, and it seems that racemization of these compounds does not involve extensive desolvation.

TABLE I

Compd.	Solvent	T, °C.	k_0	k_P	ΔV^*
I	DMF	14.8	0.0548	0.0553	−0.2
II	DMF	50.8	.159	.166	−0.8
II	EtOH	51.5	.111	.101	1.9
II	EtOH–NH_4OH	51.5	.308	.288	2.0
III	DMF	14.5	.132	.129	0.5

Although the salt of II racemizes somewhat faster than the free acid the volume changes are essentially equal. The carboxyl group evidently does not contribute to the restriction of rotation.

Previous experiments have shown that the mesomeric effect of electron-withdrawing groups *para* to the nitrogen atom causes an increase in the rate of racemization by stabilization of the planar intermediate.[3] The same phenomenon should occur in the racemization of II, but the resulting polarization does not cause sufficient electrostriction of solvent to be reflected in the volume change of activation.

Experimental

Bromomesitylene.—The method of Smith was used.[4]

Bromonitromesitylene.—To a mixture of 14 ml. of acetic anhydride and 14 ml. of acetic acid was added 12 ml. of white fuming nitric acid at −15°. The resulting solution was added slowly to a mixture of 60 g. of bromomesitylene and 85 ml. of acetic anhydride while the temperature was maintained at −15° by addition of Dry Ice. The reaction mixture was allowed to reach room temperature and was poured into 300 ml. of water. The organic layer was diluted with ether, washed with 5% sodium hydroxide solution, dried, and distilled at a pressure of 1 mm. The fraction boiling from 120–140° was collected and crystallized from ethanol. The yield was 30 g. (41%), m.p. 51–53°; rec. m.p. 54°.

N-Benzenesulfonyl-N-carboxymethyl-3-bromomesidine.—The bromonitromesitylene was reduced, benzenesulfonylated, and carboxymethylated by a sequence of steps used in another synthesis.[5] The yield was 17 g., m.p. 218–219°. The recorded m.p. is 216.0–217.5°.[6]

N-Benzenesulfonyl-N-carboxymethyl-1-amino-2-methylnaphthalene.—The procedure of Adams and Sundstrom[3] was used with modifications described in ref. 5.

N-Benzenesulfonyl-N-carboxymethyl-1-amino-2,4-dimethyl-6-nitrobenzene.—The procedure of Adams and Gordon[7] was used with modifications described in ref. 5.

Resolution of Racemic Mixtures.—The cinchonine salts of the acids were prepared by dissolving each acid together with the stoichiometric amount of cinchonine in approximately six parts of hot ethanol. The crystals which separated after several days of refrigeration were recrystallized from ethanol, and the optically active acids were retrieved by the methods described in the preceding references. The *d*-N-benzenesulfonyl-N-carboxymethyl-3-bromomesitylene obtained in this way had $[\alpha]^{26}D$ + 27.9° in DMF whereas the reported value[6] is $[\alpha]^{29}D$ + 22.1°. The other acids had rotations in agreement with the literature values.

(1) F. H. Westheimer, *J. Chem. Phys.*, **15**, 252 (1947); K. E. Howlett, *J. Chem. Soc.*, 1055 (1960).

(2) J. E. Leffler and B. M. Graybill, THIS JOURNAL, **63**, 1457, 1461 (1959).

(3) R. Adams and K. V. Y. Sundstrom, *J. Am. Chem. Soc.*, **76**, 5474 (1954).

(4) "Organic Syntheses," Coll. Vol. II, John Wiley and Sons, Inc., New York, N. Y., 1950, p. 95.

(5) R. Adams and K. R. Brower, *J. Am. Chem. Soc.*, **78**, 663 (1956).

(6) R. Adams and M. J. Gortatowski, *ibid.*, **79**, 5525 (1957).

(7) R. Adams and J. R. Gordon, *ibid.*, **72**, 2458 (1950).

Racemization Procedure.—Solutions having initial rotations of 2–6° were heated in a constant temperature bath until the rotation had decreased by one-half. The rotations were measured with a Kern polarimeter, and the reproducibility was ±0.03°. The high pressure apparatus and sample holder already have been described.[8]

(8) K. R. Brower, *J. Am. Chem. Soc.*, **80**, 2105 (1958).

COMMUNICATIONS TO THE EDITOR

TRIMERIC BISMUTH(I): AN X-RAY DIFFRACTION STUDY OF SOLID AND MOLTEN BISMUTH(I) CHLOROALUMINATE

Sir:

This report summarizes an X-ray diffraction study of molten, polycrystalline, and monocrystalline $BiAlCl_4$ which indicates the occurrence of a trimer of bismuth atoms separated by 3.04 Å. in the configuration of an equilateral triangle.

The compound was prepared as previously described.[1] X-Ray diffraction patterns of the powder and melt were measured with monochromatized MoKα radiation in the range of $(4\pi/\lambda) \sin\theta$ less than 16. The powder pattern included diffuse as well as Bragg scattering. The patterns were interpreted, by procedures described elsewhere,[2,3] to yield the radial pair distribution functions shown in Fig. 1. The principal feature of both functions, a prominent sharp peak at about 3.0 Å. partially resolved from another at about 3.4 Å., requires the existence of a bismuth polymer. Further analysis, to be described in detail elsewhere, led to the probable configuration $(Bi_3)^{3+}$. The figure demonstrates by means of synthetic peaks that the proposed model is consistent with the observed distributions.

Single crystals of $BiAlCl_4$ have been shown[4] to be rhombohedral with space group R3c, a = 12.12 Å., α = 58° 23′, Z = 6. This cell accounts for the powder pattern of $BiAlCl_4$, thereby demonstrating the identity of the two materials. Equivalent bismuth atoms at a separation of 3 Å. can be accommodated in this cell only if related by the triad axis; thus the symmetry of the crystal also indicates the existence of a trimer.

The finding of the trimer $(Bi_3)^{3+}$ casts considerable doubt on an earlier tentative proposal,[5] based on cryoscopic and vapor pressure data, of a species $(Bi_2)^{2+}$ in the system Bi–$BiCl_3$. Recent measurements[6] of e.m.f. in molten Bi–$BiCl_3$ solutions also suggest the species $(Bi_3)^{3+}$ in this system. Additional evidence of polymer formation has been obtained[7] at this laboratory from measurements of optical absorption.

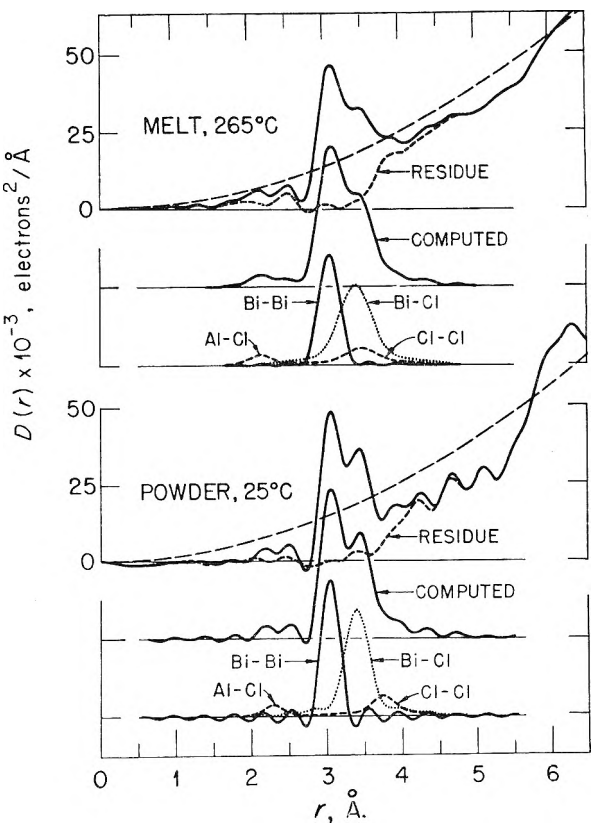

Fig. 1.—Radial pair distribution functions for $BiAlCl_4$, solid and melt, from X-ray diffraction data.

CHEMISTRY DIVISION
OAK RIDGE NATIONAL LABORATORY — H. A. LEVY
OAK RIDGE, TENNESSEE — M. A. BREDIG
OPERATED FOR THE U.S.A.E.C. — M. D. DANFORD
BY UNION CARBIDE CORPORATION — P. A. AGRON

RECEIVED OCTOBER 12, 1960

(7) C. R. Boston and G. P. Smith, Jr., personal communication, to be published.

SORPTION OF GASEOUS HYDROGEN CHLORIDE BY NYLON AND PROTEINS

Sir:

In the course of work published in 1956[1] it was noticed that when Nylon with sorbed hydrogen chloride was exposed to water vapor or liquid water, it lost its tensile strength, felt sticky to the

(1) L. H. Reyerson and L. E. Peterson, THIS JOURNAL, **60**, 1172 (1956).

(1) J. D. Corbett and R. K. McMullen, *J. Am. Chem. Soc.*, **78**, 2906 (1956).

(2) H. A. Levy, P. A. Agron and M. D. Danford, *J. Chem. Phys.*, **30**, 1486 (1959); **31**, 1458 (1959).

(3) H. A. Levy, P. A. Agron, M. A. Bredig and M. D. Danford, *Annals of the New York Academy of Sciences*, **79**, 762 (1960).

(4) H. A. Levy, P. A. Agron and R. D. Ellison, to be reported.

(5) M. A. Bredig, THIS JOURNAL, **63**, 978 (1959).

(6) L. E. Topol, S. J. Yosim and R. A. Osteryoung, Meeting American Chemical Society, New York, N. Y., 1960, division of Physical Chemistry. Abstracts p. 6-S.

touch, turned white, and became opaque. This was ascribed to hydrolysis of peptide bonds in the Nylon.[2] In contrast, no peptide bonds were hydrolyzed in the protein β-lactoglobulin when it was subjected to a similar treatment.[2] After this work had been completed, certain observations led to a reinvestigation of the phenomenon exhibited by Nylon.

Dry polycaprolactam with sorbed hydrogen chloride (about one molecule of HCl per peptide bond) was exposed to water vapor in an evacuated tube at room temperature. The Nylon slowly deliquesced; after twenty-three hours it formed a clear, extremely viscous solution. When water was added, the usual white, opaque material was formed. This was extracted thoroughly with water. In the extracts, chloride was determined by a mercurimetric method and free acid by titration in acetone.[3] The difference was within experimental error showing that no appreciable quantity of degradation products had been extracted.

In the solid residue, basic groups were determined by a modification of the methyl orange binding method of Myagkov and Pakshver.[4] The content of basic groups proved not to be appreciably different from that of the untreated polycaprolactam, suggesting a molecular weight of the order of 50,000.

These results indicated that no appreciable hydrolysis of peptide bonds in the Nylon had taken place. The breakdown of the structure of the Nylon may be attributed to the extreme solubility of Nylon in concentrated hydrochloric acid.

A detailed report of this work will appear in the *Compt. rend. trav. Lab. Carlsberg.*

(2) W. S. Hnojewyj and L. H. Reyerson, *ibid.*, **64**, 1199 (1960).

(3) K. Linderström-Lang, *Compt. rend. trav. Lab. Carlsberg*, **17**, No. 4 (1927).

(4) V. A. Myagkov and A. B. Pakshver, *Zhur. Prikl. Khim.*, **29**, 1703 (1956).

In the work reported on the sorption of dry gaseous hydrogen chloride on β-lactoglobulin,[2] the simple assumption was made that the HCl was strongly bonded to all nitrogen amine groups present in the side chains of the protein. Because of the varying character of these amine groups the bondings cannot be of equal strengths. In titration studies in aqueous and similar media, only $N_0 = 42$ out of the 57 amine groups in the side chains and N-terminal groups of this protein bind acid; for insulin (dimer of molecular weight close to 12,000) the number of such basic groups is $N_0 = 12$. If these lower values of N_0 are used, then the ratios of n/N_0 (n = the number of strongly held HCl molecules) are given in Table I.

TABLE I

Temp., °C.	Insulin Mg./g.	Insulin n	Insulin n/N_0	β-Lactoglobulin Mmoles/g.	β-Lactoglobulin n	β-Lactoglobulin n/N_0
−78.9	215	35.4	5.9	...	...	...
0	72	11.8	2.0	...	...	...
20	51	8.4	1.4	...	...	...
27	...	...	...	1.5404	57.4	1.367
30 (room temp.)	40	6.6	1.1	...	...	...
40	33.2	5 5	0.9	1.4630	54.6	1.300
60	...	...	...	1.1763	43.9	1.045

For either protein the lowest value of n/N_0 observed is close to unity as expected if the strongly bound hydrogen chloride is in chemical combination with the basic groups of the protein.

CARLSBERG LABORATORY
COPENHAGEN, VALBY, DENMARK, AND
SCHOOL OF CHEMISTRY — GORDON JOHANSEN
UNIVERSITY OF MINNESOTA — LLOYD H. REYERSON
MINNEAPOLIS 14, MINN.

RECEIVED DECEMBER 1, 1960

ADDITIONS AND CORRECTIONS

1957, Vol. 61

L. A. Girifalco and R. J. Good. A Theory for Estimation of Surface and Interfacial Energies. I. Derivation and Application to Interfacial Tension.

Page 905. Equation 23, first line, should read $\Phi = \Phi_{mb} \times \Phi_{mnb}$.

Arrigo Addamiano. The Melting Point of Cadmium Sulfide.

Page 1253–1254. The author comments: "In this note, the minimum pressure under which cadmium sulfide was observed to melt was referred to as "critical" pressure. As the adjective "critical" usually denotes physical parameters at the critical point, I should have used the more correct terminology of triple point pressure. I wish to thank Dr. J. O. Betterton, Jr., (Oak Ridge National Laboratory, Oak Ridge, Tennessee) for calling my attention to this *lapsus linguae*. My determination has been substantiated by W. E. Medcalf and R. H. Fahrig, *J. Electrochem. Soc.*, **105**, 719 (1958), who report for CdS a m.p. of approximately 1500° under a pressure of 200 atm. Also, recent vapor pressure data (H. Spandau and F. Klanberg, *Z. anorg. u. allgem. Chem.*, **295**, 309 (1958)) for CdS, in the interval 950–1175°, lead to an extrapolated value of ~ 2.3 atm. at 1475°, again in agreement with my determination.—ARRIGO ADDAMIANO.

1959, Vol. 63

P. Balestic and M. Magat. A Note on the Radiation Induced Synthesis of Lauth's Violet.

Page 977. Column 1, line 12, for "2700" read "2820."

1960, Vol. 64

Harry P. Leftin and W. Keith Hall. The Nature of the Species Responsible for the Long Wave Length Absorption Band in Acidic Solutions of Olefins.

Page 383. In Col. 1, lines 6–8 of (2), should read: ". . . $(C_6H_5)_2C{=}CHC_6H_5$, $(C_6H_5)_2C{=}C(C_6H_5)_2$, $(C_6H_5)_2C{=}CH{-}CH{=}C(C_6H_5)_2$ and, as has . . . ."

R. J. Good and L. A. Girifalco. A Theory for Estimation of Surface and Interfacial Energies. III. Estimation of Surface Energies of Solids from Contact Angle Data.

Page 561. In Col. 2, Equation 4 should read

$$\Phi = \frac{4(V_a V_b)^{1/3}}{(V_a^{1/3} + V_b^{1/3})}$$

Page 562. In Col. 2, Equation 12a should read

$$2\Phi\sqrt{\gamma_s/\gamma_l} \geqq 2 \text{ or } \gamma_l/\gamma_s \leqq \Phi^2$$

Page 563. In col. 1, line 9: for reference 13, read 14; and in the first line of footnote 12, for ref. 14 read 13.—R. J. GOOD.

O. K. Rice. The Thermodynamics of Non-uniform Systems, and the Interfacial Tension near a Critical Point.

Page 979. In col. 2, line 12, for $(\partial\Delta f/\partial c)\kappa c$ read $(\partial\Delta f/\partial c)\delta c$.—O. K. RICE.

Author Index to Volume LXIV, 1960

Subject Index to Volume LXIV, 1960

NO. 21 EPR AT WORK SERIES

HYPERFINE STRUCTURE IN ORGANIC FREE RADICALS BY EPR

(ELECTRON PARAMAGNETIC RESONANCE)

Interaction in organic free radicals of the unpaired electron with the magnetic moments of the protons frequently gives rise to well defined hyperfine structure. Often this structure permits identification of an unknown radical. One may also extract detailed information on electron wave functions from this observed hyperfine splitting.

EXAMPLE

Tetracene positive ion free radical.

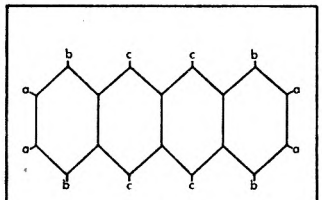

FIG. A TETRACENE

Tetracene, Figure A, when dissolved in concentrated H_2SO_4 forms a positive ion free radical, which has been investigated with EPR by Weissman and others[1]. We recently reëxamined this radical[2] using the high sensitivity Varian 100 kc EPR spectrometer. Figure B shows the total spectrum and Figure C, the seven central lines obtained with a slower scan of the DC magnetic field. The temperature was 65°C and the concentration, 10^{-4} molar.

The resonance saturates easily, and the V-4500-41A low-high power bridge was therefore necessary to permit observation at 30 db attenuation of the klystron power (0.20 mw at the sample). All lines are 60 milligauss peak-to-peak, and the line width is independent of temperature. When using 100 kc field modulation one expects resonance sidebands to occur at ± 30 milligauss from the line center, and it is felt that these sidebands determine the observed line width. Work of this type requires good magnetic field

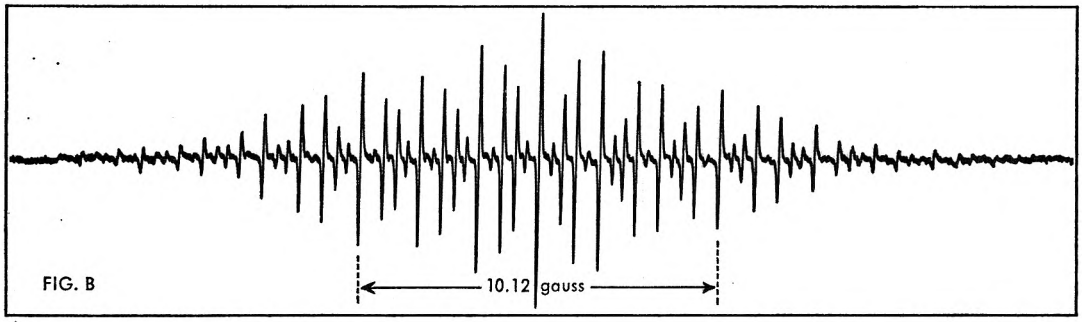

FIG. B

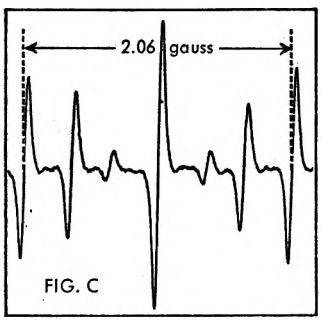

FIG. C

homogeneity and magnet power supply stability. A Varian 12" rotating magnet and regulated power supply were used.

The spectrum may readily be reconstructed. From Figure A it can be seen that there are three classes of protons, a, b and c, with four protons in each class. Four identical protons give rise to five energy levels with degeneracies of 1, 4, 6, 4, 1, and three such groups of 4 give rise to 5^3, or 125 lines with easily determined relative intensities. In fact, we find one of the splittings is within 1% of being three times another, which results in 85 lines, 81 of which can be seen in the figure. The three splittings are 1.03 gauss, 1.69 gauss, and 5.06 gauss. Calculated intensities agree closely with experimental values.

[1] *S. I. Weissman, E. DeBoer and J. J. Conradi, J. Chem. Phys. 26, 963 (1957); E. DeBoer and S. I. Weissman, J. Am. Chem. Soc. 80, 4549 (1958); A. Carrington, F. Dravnieks and M. C. R. Symons, J. Chem. Soc. 947, (1959).*

[2] *H. W. Brown and J. S. Hyde, (to be published).*

For literature which fully explains the 100 kc EPR Spectrometer and its application to basic and applied research in physics, chemistry, biology and medicine, write the Instrument Division.

VARIAN associates
PALO ALTO 52, CALIFORNIA

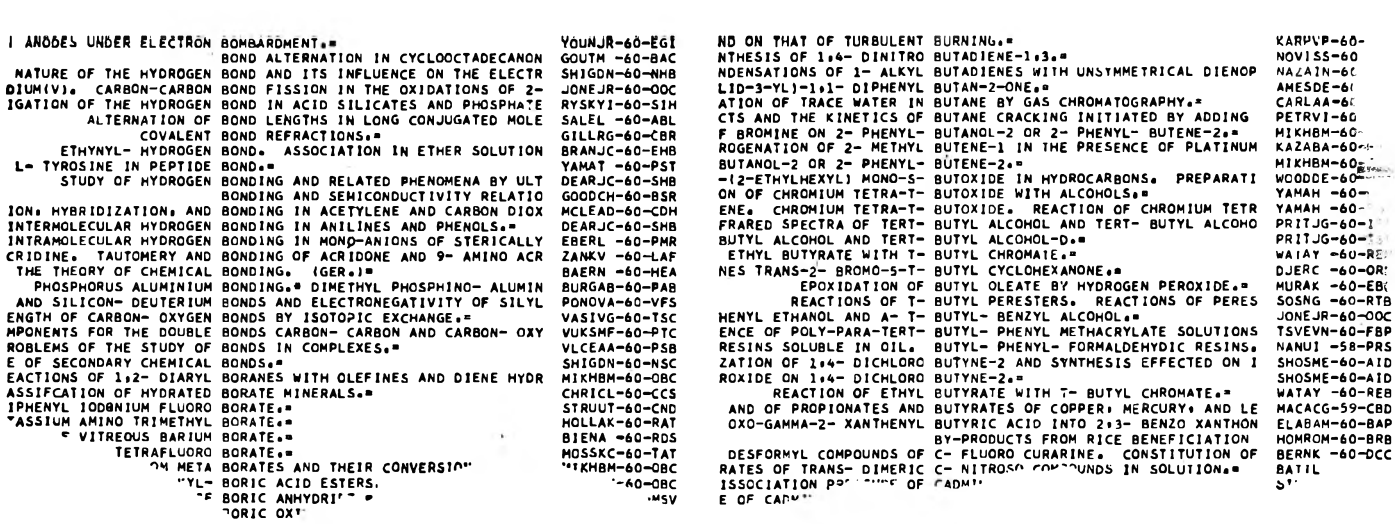

SAMPLE OF KEYWORD INDEX

announcing a new publication

CHEMICAL TITLES

the express service for increasing "current awareness" of new chemical research

● Starting in January 1961, CHEMICAL TITLES will be issued twice each month with each issue reporting approximately 3000 titles from the most recent chemical research. This service provides a current author and keyword index to selected chemical journals and is intended to fill the void between primary publication and the appearance of abstracts.

Taken from 575 journals—110 Russian—of pure and applied chemistry, these titles are listed for maximum convenience of use. The first part is a permuted title index in which keywords from each title are arranged alphabetically with each keyword in full or partial context. The second part is an alphabetical index of authors together with full titles of papers and journals in which they appear. You can find a source in a minute.

Timeliness matches ease of use. All titles are found in the listing *within two weeks of the time they are received* in the offices of The Chemical Abstracts Service, the publisher. No other index or alerting service provides such prompt and complete coverage.

Prices and discounts follow:

	Base Rate	Rate per Volume College and University	ACS Member
1st–10th subscriptions (each)	$65	$50	$50*
Additional 11th–25th subscriptions (each)	45	45	...
26th and each succeeding subscription	30	30	...

*Single subscription only

ORDER FROM: CIRCULATION DEPARTMENT • AMERICAN CHEMICAL SOCIETY
1155 SIXTEENTH STREET, N.W. • WASHINGTON 6, D.C.